PUNCHING SHEAR STRENGTH OF STEEL FIBRE REINFORCED LIGHTWEIGHT CONCRETE SLABS

by

Dimitrios D. Theodorakopoulos
(Dip.Civ.Eng. 1971, Technical University of Athens)
(M.Eng. 1976, Sheffield University)

Thesis submitted
to the
University of Sheffield
for the
degree of Doctor of Philosophy
in the
Faculty of Engineering
Department of Civil and Structural Engineering

September, 1980


FS-6
FS-19
FS-16
FS-11
FS-20

To my Dear Mother
with all my respect and love

SUMMARY

One of the problems in slab-column connections is the punching shear failure at over loads. Such failures are sudden and catastrophic,and are undesirable since they do not allow an overall yield mechanism to develop. Fibre reinforcement restrains cracking, and increases the tensile strength of concrete and bond resistance of steel reinforcement. Therefore, it should be possible to use steel fibres as shear reinforcement.

This investigation is a study of the structural behaviour of fibre reinforced lightweight concrete flat slabs in punching shear. Twenty full scale connections were tested simply supported on all four sides and loaded centrally through a column stub. The mix consisted of Lytag, sand and fly ash as partial replacement of cement. The main variables studied were the fibre volume, fibre type, column size, amount of reinforcement and concrete strength. Extensive measurements of deformations were made throughout the tests.

Fibre reinforcement reduced all the deformations of the plain concrete slab at all stages of loading. For a given serviceability criterion, the presence of fibres increased the service load of the corresponding plain concrete slab by 15-50%. Fibres also increased the post-yield ductility and energy absorption characteristics of the slabs by 125-260% and 240-270% respectively.

The presence of fibres improved the load at first crack, punching shear strength and the residual resistance after punching by about 35%, 40% and 150-400% respectively. Fibres also produced gradual punching failures and sometimes changed the mode of failure into flexure. Empirical and theoretical equations have been proposed to predict both ultimate flexural

and punching shear strength of steel fibre reinforced concrete slab-column connections and they show good agreement with data from other investigations.

It is concluded that fly-ash can be successfully used in structural lightweight concrete mixes. The addition of fibres in lightweight concrete connections reduces deformations in general, delays the formation of flexural and inclined shear cracking, and increases the service load, ultimate strength, ductility and energy absorption characteristics.

ACKNOWLEDGEMENTS

The author would like to express his sincere thanks and gratitude to Dr. R.N. Swamy, for his guidance, assistance, supervision, unfailing help and encouragement during the term of this project.

He also wishes to thank the secretarial and technical staff of the Department of Civil and Structural Engineering for their help and Mrs. J. Czerny for her well arranged accurate typing.

ο συγγραφευσ θα ηθελε να ευχαρηστηση την μητερα του καi τουσ αδελφουσ του γiαννη καi κωστα γiα την οiκονομiκη βοηθεiα καi συνεχη ενθαρρυνση κατα την δiαρκεiα αυτησ τησ εργασiασ.

CONTENTS

Page No.

Page No.

Page No.

Page No.

LIST OF FIGURES.

LIST OF TABLES

LIST OF PLATES

NOTATION

A_f	Fibre cross sectional area.
A_s	Area of tension reinforcement in each direction of the slab.
A'_s	Area of compression reinforcement in each direction of the slab.
A_e	Equivalent area of steel bars of the same weight with steel fibres.
$A_{S.F.}$	Area of fibres per unit area of a cross-section.
b	Perimeter of the loaded area of the column.
b_o	Perimeter of the critical section at $\frac{d}{2}$ from the column face (ACI)
b_d	Perimeter of the failure surface at reinforcement level.
b_p	Perimeter of the critical section at 1.5h from the column face (CP110).
b'	Width of a section.
b_1	$4r + 3\pi d$.
b_2	Width of the loaded area plus three times the depth of slab on either side of the loaded area.
d	Effective depth of the slab.
d'	Depth of compression reinforcement.
d_f	Fibre diameter.
D	Diameter of loading disc.
D_c	Density of lightweight concrete.
E_f	Elastic modulus of the fibre.
E_L	Elastic modulus of lightweight concrete.
E_N	Elastic modulus of normal weight concrete.
E_s	Elastic modulus of tension steel.
E'_s	Elastic modulus of compression steel.
f'_c	Concrete cylinder compressive strength.
f_{cu}	Concrete cube compressive strength.
f_{ct}	Concrete tensile splitting strength.
f_t	Concrete tensile strength.

f_y	Yield stress of tension reinforcement.
f_s	Stress of tension reinforcement.
f'_s	Stress of compression reinforcement.
F_c	Compression concrete force on a cross-section.
F_f	Fibre force on a cross-section.
F_s	Tension reinforcement force on a cross-section.
F'_s	Compression reinforcement force on a cross-section.
g_K	Characteristic dead load per unit area.
G_m	Shear modulus of matrix.
h	Slab overall thickness.
h_c	Diameter of the column or column head.
j	A factor equal to 0.87.
K	Constant.
k_1,k_2	Stress block parameters for normal weight concrete (CP110).
k'_1,k'_2	Stress block parameters for lightweight concrete.
K_b	Bond length coefficient of fibre.
K_L	Bond factor of fibres in lightweight concrete.
ℓ	Slab specimen length.
ℓ_o	Range of dowel action.
ℓ_1	Length of a panel in the direction of span, measured from the centres of columns.
ℓ_2	Width of a panel measured from the centres of columns.
ℓ_c	Critical fibre length.
ℓ_f	Fibre length.
ℓ_b	Length of clear span measured from face to face of columns.
ℓ_s	Distance from the column face to the line of inflection.
L	Span between centre to centre of columns.

m	Unique ultimate moment of resistance per unit width (positive).
m'	Unit moment capacity (negative).
$M(M_p, M_f)$	Unit moment capacity in a plain or fibre concrete section.
M_1, M_2, M_3 M_4	Moments of concrete, fibre, compression and tension reinforcement forces about N.A. of a cross section.
M_{ds}	Design bending moment in flat slabs defined by CP110 Code.
M_N	Total negative moment in the column strip in a flat slab (CP110).
M_o	Design bending moment in flat slabs defined by ACI Code.
M_x, M_y	Ultimate moment of resistance in the two directions.
M_u	Average ultimate moment per unit width of the slab within the base of the pyramid of failure.
N	Number of fibres in concrete volume, V.
N_1	Number of centroids per unit area of a cross-section.
N_a	Actual number of fibres at a cross-section.
P, P_1, P_2	Punching loads in Kinnunen and Nylander's theory.
q_K	Characteristic live load per unit area.
r	Side dimension of a square column.
R	Mean interfibre spacing.
S	Average spacing.
S_e	Effective spacing.
S_s	Share of shearing force due to dowel action.
v	Volume of one single fibre.
v_c	Concrete shear stress (CP110).
v_{cc}	Limiting shear stress.
v_u	Unit ultimate shear stress.
V	Shear force.
V_a	Contribution of aggregate interlock to shear resistance of a slab.

V_c	Contribution of the concrete compression zone to shear resistance of a slab.
V_d	Contribution of the dowel action to shear resistance of a slab.
V_f	Fibre percentage by volume.
V_F	Total volume of fibres in a matrix.
V_m	Matrix volume fraction.
V_{flex}	Ultimate flexural capacity calculated by the Yield line theory for plain concrete.
V_s	Contribution of fibres to shear resistance acting as shear reinforcement.
$V^F_{U.F.}$ ($V_{calc.}$)	Ultimate flexural capacity for connections with steel fibres.
V_u	Ultimate shear capacity in plain concrete.
$V^F_{u.P.}$	Ultimate shear strength in connections with steel fibres.
$V^F_{u1.p}$	Contribution of the concrete compression zone to shear strength in connections with steel fibres.
$V^F_{u2.p}$	Contribution of fibres to shear strength along the surface of failure.
$V^F_{u.p}$	Ultimate shear strength of a plain concrete slab of equal concrete strength.
$V_{u.calc.}$	Calculated shear strength for connections with steel fibres.
w	Density of concrete.
w_1	Total design load per unit area.
W_F	Weight of fibres in a slab.
z	Internal lever arm moment.
x	Neutral axis depth.

β Coefficient of effectiveness.

γ_c Factor of safety for concrete.

ε_o Concrete strain (= $\sqrt{f_{cu}}/4115$)

ε_x Strain in fibre.

ε_s Tension steel strain.

ε'_s Compression steel strain.

ε_{cu} Maximum concrete compression strain.

η Total design load per unit area.

η_o Fibre orientation factor.

η_b Bond efficiency factor.

η_L Fibre length efficiency factor.

θ Inclination of the failure surface.

λ Ratio of negative to positive unit moments (= m'/m).

μ_1, μ_2 Coefficients.

ξ_s Factor of depth of slab.

$\rho = \frac{A_s}{b'd}$ Ratio of flexural reinforcement to concrete slab section (Reinforcement ratio).

ρ'_f "Fibre reinforcement ratio".

ρ_f Equivalent reinforcement ratio for steel fibre.

σ_c Stress in the composite.

σ_f Maximum fibre stress at which fibre pull-out occurs.

σ_f^{av} Average stress in fibre.

σ_{fu} Fibre fracture stress.

σ_m Stress in matrix.

σ_{mu} Modulus of rupture of plain concrete.

σ_{cu} Ultimate tensile strength of fibre concrete.

$\sigma_{cu.shear}$	Ultimate shear strength of fibre concrete.
σ_t	Tensile strength of concrete.
τ	Average fibre-matrix bond strength.
ϕ	Reduction factor for shear equal to 0.85.
ϕ_o	V_u/V_{flex}
Δ_1	Centre deflection of slab at first crack.
Δ_2	Centre deflection at 30% of the maximum load after the maximum load is reached.

CHAPTER 1.

INTRODUCTION.

1.1 Introduction.

Concrete as the first major construction material, is being used continuously for new applications. As these applications increase, so does the effort to overcome some of its disadvantages and inherent limitations. Some of the main disadvantages and limitations of normal weight concrete are the large dead weight, the low tensile strength, and the limited ductility due to its brittle property which leads to less energy absorption and low resistance to crack control.

In recent years several developments have been taking place in the construction industry, in design techniques and in new materials.

The use of lightweight aggregates in structural concrete is a significant development in concrete construction. There is considerable evidence to show that structural lightweight concrete is a technically sound material with adequate structural properties. The trend towards lightweight concrete is because of the shortage of natural aggregates and the benefits of reduced weight, lower elastic modulus and improved thermal properties. However, lightweight concrete has disadvantages when compared with normal weight concrete, such as higher creep and shrinkage, greater deflection and lower splitting tensile strength.

One of the new developments in materials is fibre reinforced concrete. In the past twenty years or so, considerable amount of research has been carried out on fibre normal weight concrete; fibre reinforced concrete has developed from a laboratory theory into a proven construction material.

Many types of materials have been used as fibre reinforcement to brittle cement matrices, such as asbestos, glass, ceramics, polymers, etc., but the one type of fibre which has found considerable application in concrete is steel.

It is well established that the presence of fibres in normal weight concrete increases its tensile strength, ductility, energy absorption and crack control characteristics. Many investigations have shown that the presence of steel fibres in normal weight concrete beams improves their ultimate flexural strength, stiffness, ductility and resistance to cracking. Tests on beams and slab-column connections made of normal weight concrete have shown the fibre reinforcement effectiveness as shear reinforcement and the increase in their shear resistance.

The concept of reinforcing lightweight concrete with steel fibres did not receive much research attention but for the time being an extensive and very large scale research is in progress. There are no experimental data directed to the problem of fibres as shear reinforcement in lightweight concrete and no data have been reported in the technical literature. However, due to reduced modulus of elasticity and lower splitting tensile strength of the lightweight concrete the effect of adding a relatively high modulus fibre, such as steel, may be more pronounced than for normal weight concrete in both flexure and punching shear.

1.2 Purpose and Scope of the Investigation.

This investigation is carried out to study the suitability of lightweight aggregate concrete for use in slab-column connections and assess the effect of fibre reinforcement in the strength and deformation characteristics of lightweight concrete slabs and in particular to study the resistance of fibre reinforcement to punching shear.

Various mixes were cast with sand as fine aggregate and a partial replacement of cement by P.F.A. to achieve a good workable mix with a compressive strength of about 45 N/mm^2 at 28 days. The mix properties such as compressive strength, modulus of rupture, splitting tensile strength, modulus of elasticity and shrinkage with and without fibre reinforcement were studied.

Twenty full scale connections were tested simply supported on all four sides and loaded centrally through a column stub. The parameters studied were the fibre percentage, amount of tension and compression reinforcement, column size, fibre type, cube compressive strength and location of fibre reinforcement. All deformations such as deflection, rotation, steel and concrete strains of all tested slabs, were measured at various stages of loading. The ductility and energy absorption characteristics were also investigated.

Strength characteristics of the tested slabs were studied and empirical and theoretical equations were developed to evaluate both ultimate flexural and punching shear strength of slab-column connections with fibre reinforcement.

1.3 Layout of the Thesis.

In chapter 2 a general review of literature is reported about lightweight aggregate concrete, steel fibres, punching shear in conventional reinforced concrete connections with both normal and lightweight concrete and the role of fibre reinforcement in influencing the strength characteristics of beams and slab-column connections.

In chapter 3 the design of a practical workable mix with and without fibres is studied. Other fibre concrete properties are also studied and reported in this chapter. The experimental programme, test specimen details, test set up, test measurements and instrumentations are reported in Chapter 4.

Chapter 5 is devoted to the study of deformation characteristics, ductility and energy absorption capacity of tested slabs. Strength characteristics of tested slabs are reported in chapter 6. Comparisons of the effectiveness of fibre reinforcement in both normal and lightweight concrete slabs are also reported in these two chapters.

In chapter 7 a theoretical method is presented to calculate the ultimate flexural strength of fibre reinforced concrete slab-column connections. This method showed good agreement with experimental results related to flexural strength of fibre reinforced concrete slabs obtained in this investigation and by other investigators. An empirical easily-applied method to calculate the ultimate moment of resistance per unit width of fibre concrete section is also presented.

In chapter 8 the ultimate strength of plain lightweight concrete slabs, which failed in punching shear, is compared with the provisions for punching shear of various codes of practice as well as with the existing expressions for the ultimate punching strength of both normal and lightweight concrete slabs. An empirical and an approximate theoretical method are proposed to calculate the ultimate punching shear strength of fibre reinforced concrete slab-column connections. A good correlation between the test results and the predictions of this method was obtained.

In chapter 9 the limitations, general conclusions and suggestions for future work are presented.

CHAPTER 2.

REVIEW OF PAST RESEARCH.

2.1 General Introduction.

The problem of shear strength in slabs subjected to concentrated loading has received added emphasis due to its importance in connection with modern flat-slab construction, as in this, the upper and lower surfaces of the slabs are plane, and there are no beams, drop panels or column heads. It is now widely recognized that the connection between slab and column is generally the critical area as far as the strength of such a structure is concerned.

The shear failure of a slab-column connection is primarily controlled by the tensile splitting strength of concrete. The use of lightweight concrete in such connections yields a lower resistance to shear because of its lower tensile splitting strength. However, the reduced dead load of the slab made with lightweight concrete compensates its decreased capacity to shear.

The use of shear reinforcement increases the punching shear capacity of a slab-column connection by providing a means to prevent the widening and propagation of the inclined cracks. However, its effectiveness depends upon the conditions of anchorage achieved. The problem of anchorage of shear reinforcement becomes much more important in thin flat slabs and therefore there is a need for the replacement of shear reinforcement by another method. The use of steel fibres as shear reinforcement in beams has been proved to provide an increased resistance to shear, and one expects an improvement in the shear resistance of flat slab-column connections as well. In this chapter a review of the past research on lightweight concrete, and steel fibre reinforced concrete properties will be given, as well as the experimental and theoretical work on punching shear of flat slab-column connections without and with fibres.

2.2 Structural Lightweight Aggregate Concrete.

2.2.1 History and Development.

The use of concrete with natural lightweight aggregates like pumice, tuff and scoria was the first to be recognized. Some of the uses of such lightweight concrete occurred about 2,000 years ago, when the Pantheon, the Aquaduct and the Colosseum in Rome were built by the Romans. The Germans started using slag in concrete in 1822 while slag as concrete aggregate was not used in the U.S.A. until 1890 (1). In the United Kingdom foamed slag has been produced and used since 1935 (2). The production of modern lightweight aggregate started around 1917 when S.J. Hayde developed a process for heat-expansion of shales and clays to form hard lightweight material which served as aggregates in concrete having a substantial strength and low density. In the U.S.A. this aggregate was used in the construction of ships and barges after the first World War while in buildings, structural lightweight concrete was first used in the 1920's.

In the United Kingdom although the production of foamed slag started in 1935 (2), lightweight aggregates were not widely used until the 1950's when expanded clay and pulverised fuel-ash production started. In the United Kingdom, expanded clay "Anglite' concrete having a compressive strength of 31 N/mm^2 was used, in the construction of the County Laboratories building in Brentford.

Lightweight aggregate was probably first used in slab-column connections by Hognestad et al. (3) when they carried out tests on six lightweight concrete slabs, using expanded shale aggregates produced in a rotary kiln, to investigate the shear strength of lightweight concrete slabs as compared to similar slabs made with normal weight concrete. Steel fibre reinforcement was first used in lightweight concrete beams by Hannant (4).

2.2.2 Previous Research on Lightweight Aggregate Concrete in the United Kingdom.

Research on lightweight aggregate concrete, carried out after 1950, was mainly on Foamed slag, Aglite, Leca,and Lytag eaggregates which were available at that time. Research on these types of lightweight aggregates was carried out by the Building Research Station. In the 1960's extensive research on lightweight aggregates was carried out at the University of Leeds. Comprehensive research on Solite was carried out at the University of Sheffield in 1972-1974 while research on Lytag is now being carried out.

Short (5) gave a description of the properties of lightweight aggregates suitable for reinforced concrete from work carried out at the B.R.S. The main conclusions are as follows:

1. The 28-day cube strength varied from about 7.00 N/mm^2 to 31.0 N/mm^2; the dry density varied for different lightweight aggregates from about 1300 to 2000 kg/m^3.
2. Compared with gravel concrete having the same compressive strength, the tensile strength from the modulus of rupture test of lightweight aggregate was found to be generally higher.
3. The modulus of elasticity of lightweight concrete was between one-third and two-thirds of the corresponding values for gravel concrete having the same compressive strength.

4. For the same cube strength, when sand replaced the fine aggregate in the lightweight concrete, the cement content was reduced for all lightweight concretes by 13 to 25% while the dry density increased between 2 and 15%.

5. The bond strength of lightweight concrete beams was found to be half to three-quarters of the bond strength obtained with gravel concrete beams.

6. The deflection of lightweight beams was found to be 10-15% higher than the deflection of gravel concrete beams. The development of cracking was found to be more severe for lightweight concrete beams.

7. The ultimate load of beams tested was only dependent on the cube strength and percentage of steel and was not affected by the type of concrete.

Teychenne (2,6) investigated the properties of various types of lightweight aggregates with a 28-day cube strength from 17.0 N/mm^2 to 63.5 N/mm^2. The main conclusions which have been reported from his investigation are:

1. The air-dry density of lightweight aggregate concrete varies from 1120 to 2080 Kg/m^3.

2. Lightweight aggregates are capable of producing concretes with a 28 days crushing strength equal to that obtained with sand and gravel, but in some cases a higher cement content is required.

3. With a given lightweight aggregate, the main factor influencing the crushing strength is the water-cement ratio.

4. The concrete strength development up to twenty eight days is similar to that of natural aggregate concrete but there is generally a greater increase in strength at one year, particularly with Lytag.

5. The tensile splitting strength at 28 days is similar to that of normal weight concrete.

6. The modulus of elasticity increases with crushing strength. Lytag concrete has a modulus of elasticity equal to 60% of that of normal weight concrete.

7. Replacing the fine lightweight aggregate by a fine natural sand increases the density of concrete, improves slightly the workability and the crushing strength. It has little effect on the modulus of rupture and the tensile splitting strength and increases the modulus of elasticity.

The extensive research carried out in the University of Leeds on Aglite and Lytag aggregate was published in a series of papers (7,8,9). In the first paper (7) structural properties of Aglite aggregate are reported for use in reinforced and prestressed beams. Main conclusions are as follows:

1. There is no significant difference in the ultimate moments of the reinforced beams made with Aglite and gravel aggregate.

2. In beams with sintered clay concrete 20-25% greater deflection and 50% wider cracks were recorded than those of corresponding gravel concrete beams.

3. The modulus of elasticity of Aglite concrete was about 60% of that of gravel concrete.

The second paper (8) reports tests carried out on Aglite concrete to establish its tensile and compressive strengths and the behaviour and ultimate strength of reinforced beams in shear and flexure. It reported a lower tensile strength of Aglite concrete than that of gravel concrete ranging from 25-50%. At working load, the deflection of Aglite concrete beams was 40-50% greater than ordinary concrete beams. There was no difference in the ultimate moment of resistance while the shear cracking strength of Aglite concrete beams was about 75% of that of the corresponding ordinary concrete beams.

In the third series of tests (9) modulus of elasticity, modulus of rupture, shrinkage and creep properties and behaviour in flexure of Lytag concrete were determined. With respect to the compressive stress block of a Lytag concrete beam it was reported that this differed from that of a gravel concrete beam in the following respects:

a) Maximum stress did not develop until a strain of 0.3% was reached (0.2% in gravel concrete).

b) Maximum stress developed nearer the compression face.

In the University of Sheffield research was carried out on lightweight concrete using Solite lightweight aggregate made from expanded slate (10,11). The first work was carried out on the main structural properties of concrete made with this aggregate having a high early strength, which was obtained by using a very fine cement. In the second work the basic material properties and structural behaviour of 'Solite' concrete using ordinary Portland cement were studied. The main relevant conclusions are:

1. The ultimate moment of resistance of Solite concrete beams can be satisfactorily calculated by using Whitney's theory.

2. The deflection of Solite concrete beams at design load was 20-30% greater than that of the comparable gravel concrete beams.

3. Shear cracking strength of Solite concrete was found to be identical with that of comparable gravel concrete beams. Ultimate shear resistance of Solite Concrete T-beams varied between 71 and 95% of that of comparable gravel concrete T-beams.

4. The main difference in shear failure between Solite and gravel concrete lies in the fact that diagonal cracks in lightweight concrete transverse the aggregate particles as well as the matrix, whereas in gravel concrete the cracks travel round the aggregate and leave irregular and interlocked surfaces still capable of resisting further load.

In the University of Sheffield research has been carried out since 1978 on Lytag lightweight concrete. The research is still in progress. The main objects of the research are the shrinkage properties of lightweight concrete, the behaviour of limited prestressed lightweight concrete beams with and without fibres in shear and flexure, the shear capacity of T-beams, and the shear transfer in lightweight reinforced concrete with and without fibres. So far the results have shown the great potential of lightweight aggregate concrete for a wide range of structural applications; part of the results is presented in reference (12).

2.2.3 Research by Other Investigators.

There are a number of other investigations carried out in the United States of America on lightweight concrete made with lightweight aggregates available in the United States. Most of the general conclusions were similar to those observed and concluded in the United Kingdom; here only a few of the works relevant to shear resistance of lightweight concrete are discussed.

Hanson (13) reported tests on the shear capacity of lightweight concrete beams. The tests showed a good correlation between the nominal unit shear strength of the beams and the accompanying split-cylinder tensile strengths of dry concrete. It was reported that the unit shear strengths of the beams varied from 60 to 100% of that of comparable gravel concrete beams.

Ivey and Buth (14) also carried out tests on shear capacity of rectangular lightweight beams. The test results showed a reasonable correlation with Hanson's (13) results, and the average value of the ultimate stress fell 14 percent below the value predicted by Hanson's equation.

Mattock et al. (15) reported tests on shear transfer in lightweight concrete. The test specimens were of the "push-off" type; two types of lightweight aggregate were used,predominantly coated rounded lightweight aggregate and predominantly crushed angular lightweight aggregate.
The main conclusions are:

1. The shear transfer strength of lightweight concrete is less than that of gravel concrete of the same compressive strength, and is not significantly affected by the type of lightweight aggregate.
2. The coefficient of friction for gravel concrete should be multiplied by 0.75 and 0.85 for all-lightweight and sanded lightweight concrete respectively.

Experimental studies on flat slabs made with lightweight concrete will be discussed in section 2.4 of this chapter.

2.3 Fibre Reinforced Concrete.

2.3.1 Introduction.

Historically fibres have been used to reinforce brittle materials since ancient times. Straws were used to reinforce sunbaked bricks, horse hair was used to reinforce plaster, and more recently, asbestos fibres were used to reinforce Portland cement. This material known as 'asbestos cement' has found wide application for the manufacture of corrugated roofing sheets, cladding panels and pipes.

In modern times great development has been made in the production of new fibre composite materials for a wide variety of applications. Matrices which have been strengthened by means of fibre reinforcement are metals, ceramics, resins, polymers, and concrete.

Concrete as a building material has high compressive strength and is very cheap and durable; but it also possesses some well known deficiencies such as: low tensile strength, low ductility and low fracture toughness. Improvement of the tensile characteristics of concrete will make this material more economical by a reduction in the consumption of reinforcing steel, saving therefore in labour cost, and more generally will widen the field of its application. This improvement results by modification of concrete, by the inclusion of fibre reinforcement. A considerable interest in fibre reinforcement has been shown during the last twenty five years.

There is practically no limit to the type of fibres which could be used in concrete matrices except their availability, price and the satisfactory behaviour of the final product. This last factor involves characteristics of the fibres such as length, diameter, surface roughness, ease of mixing and placing, strength and stiffness. The fibres that are currently being used in concrete can be classified into two types (16). Low modulus high elongation fibres, such as nylon, polypropylene, and polyethylene, are capable of large energy absorption characteristics; they do not lead to strength improvement, but they impart toughness and resistance to impact and explosive loading. High strength, high modulus fibres such as steel, glass, asbestos and carbon, on the other hand, produce strong composites of higher strength and stiffness than the matrix itself, and to a lesser extent improved dynamic properties.

2.3.2 Fibre Strengthening Mechanisms.

The nature of a cement matrix with or without aggregates is heterogeneous and inelastic; so it makes it difficult to explain precisely how continuous or short discrete fibres reinforce the cement paste. The behaviour of fibre cement composites has been explained first by Romualdi et al. (17,18,19). The basic concept was to assume different mode of action of the steel fibre from that of conventional reinforcement. A fracture arrest approach was adopted, which indicated that for a given volume of steel fibre added,the tensile strength of the composite would increase with decreasing wire diameter and hence wire spacing. Contrary to this, normal reinforced concrete theory, does not predict any change in strength of the composite for a constant volume of steel. The geometrical spacing of fibres thus becomes a critical factor in their crack arrest mechanism. Romualdi's original tests appeared to support his theory, but Shah and Rangan (20) showed that the spacing of fibres had little influence on the first crack strength, particularly at small values of spacing. From their experimental work Shah and Rangan observed considerable improvement in ductility for fibre concrete, but the effect of wire spacing observed by them was considerably less than that predicted by Romualdi and Mandel (19).

In another approach based on a composite materials concept Swamy et al. (21) derived two equations for predicting the first crack and ultimate modulus of rupture of steel fibre reinforced concrete. The fibre reinforcing action assumed to occur through the fibre-matrix interfacial bond stress. When the composite strain exceeds the cracking strain of the matrix the latter will crack and since the fibres are stiffer than the matrix, they will deform less and as a result will exert pinching forces at the crack tips. The cracks, therefore, are prevented from propagating and the composite ultimate strength is reached when failure occurs either by fibre-matrix interface bond failure or by fibre fracture.

2.3.3 Spacing of Fibre Reinforcement.

The mechanism proposed by Romualdi and Batson (17,18) is primarily based on a geometrical fibre spacing concept, which establishes a relationship between the first crack tensile strength of the composite and fibre spacing. This mechanism predicts that the first crack strength is inversely proportional to fibre spacing for a given percentage of fibres. Romualdi and Mandel (19) then derived an expression for the geometric spacing, S, between randomly oriented, short discrete fibres.

$$S = 13.8\, d_f \sqrt{\frac{1.0}{V_f}} \quad \ldots\ldots \quad (2.1)$$

where S = average fibre spacing.

d_f = fibre diameter and

V_f = steel fibre percentage by volume.

In deriving the above equation Romualdi and Mandel (19) took into account the overlapping effect of the fibres but they assumed that the shear forces at the fibre-matrix interface are absent until the occurrence of a crack. This assumption, however, is only valid for long continuous fibres, where the shear stress distribution in the absence of a crack, extends up to half the critical length from each end of the fibre, thus leaving a major proportion of the fibre length free from any shear stresses. In the case of short fibres of length smaller than the critical fibre length, the shear stress distribution in the absence of a crack, extends along the whole length of the fibres.

Another fibre spacing formula was suggested by McKee (22) which had the form

$$S = 3\sqrt{\frac{v}{V_f}} \qquad \ldots\ldots \qquad (2.2)$$

where v = volume of one fibre.

In the derivation of the above equation the overlapping effect of fibres and bond efficiency factor have not been taken into account.

Kar and Pal (23) attempted to improve the average fibre spacing concept by introducing the bond deficiency of short fibre and the probable orientation of the fibres.. They proposed the following expression for effective fibre spacing.

$$S_e = 8.85\, d_f \sqrt{\frac{1.0}{V_f\, \eta_o\, \frac{\ell_f}{K_b d_f}\left(1 - \frac{\ell_f}{3K_b d_f}\right)}} \qquad \ldots\ldots \qquad (2.3)$$

where ℓ_f = fibre length.

η_o = average orientation factor.

K_b = bond length coefficient.

Kar and Pal related the ultimate tensile strength rather than cracking strength to the calculated effective fibre spacing, because they observed that there was only a small difference between the cracking load and the ultimate load. However, the fibre spacing concept is based on an elastic fracture mechanics criterion, which would be related to cracking strength rather than ultimate. On the other hand, the claim of Kar and Pal of no difference between the cracking load and the ultimate load is not realistic. In an actual composite there will be an increase in load at ultimate over the cracking load which depends on the amount of force that can be developed in the fibres at a crack. This force is dependent on the amount and strength of steel fibres if the bond strength is sufficient to cause the fibres to fracture. However, when final failure occurs by pulling out the fibres, the ultimate strength depends on the bond strength that can be developed.

Swamy et al. (21) derived a new "effective spacing" equation by taking into account the three basic considerations related to the transfer of stress from matrix to fibre, which are:

1. Critical fibre length.
2. Fibre-matrix interfacial bond.
3. Orientation efficiency factor for random fibres.

Bond efficiency was taken into account by introducing bond deficiency factors for both the length and diameter of fibres.

The effective spacings, S_e, are given by:

for first crack modulus of rupture

$$S_e = 27 \sqrt{\frac{d_f}{V_f \ell_f}} \quad \ldots\ldots \quad (2.4)$$

for ultimate modulus of rupture

$$S_e = 25 \sqrt{\frac{d_f}{V_f \ell_f}} \quad \ldots\ldots \quad (2.5)$$

where d_f = fibre diameter.

ℓ_f = fibre length

V_f = volume percent of fibres in matrix.

The randomness of the short fibres was taken into account by considering an orientation factor of $0.41\ \ell_f$.

Seamy et al. derived the following equations:

for the first crack composite strength

$$\sigma_c = 0.843 \quad \sigma_{mu} (1-V_f) + 2.93 \, V_f \frac{\ell_f}{d_f} \quad \ldots\ldots \qquad (2.6)$$

for the ultimate composite flexural strength,

$$\sigma_c = 0.970 \quad \sigma_{mu} (1-V_f) + 3.41 \, V_f \frac{\ell_f}{d_f} \quad \ldots\ldots \qquad (2.7)$$

where σ_c = stress in the composite.

σ_{mu} = modulus of rupture of plain concrete.

ℓ_f/d_f = aspect ratio.

V_f = fibre percentage by volume.

2.3.4 Factors Influencing the Effectiveness of Fibre Concrete.

The effectiveness of the reinforcing fibres depends on the following parameters:

1. Modular ratio (E fibre/E matrix).
2. Fibre orientation.
3. Fibre geometry - shape, length.
4. Fibre aspect ratio (length/diameter).
5. Volume content of fibres.
6. Bond strength of fibre-matrix interface.

Generally the strength of the composite increases with:

1. Increase in modular ratio.
2. Increase in fibre content.
3. Increase in aspect ratio.
4. The degree of fibre alignment with stress direction.

2.3.5 Efficiency Factors.

Critical length - Length Efficiency Factor-orientation factor.

In the case of a composite reinforced with short discontinuous fibres, the fibres cannot be directly loaded at their ends and stress is transferred into them by an average interfacial shear stress τ. The fibre stress will build up from zero to a maximum value σf in the centre point of the fibre. This means that a portion of a fibre, near its ends, will not be fully loaded and will thus be ineffective in strengthening the composite. The value of maximum fibre stress, σ_f, in the centre point of fibre, on failure of the composite, depends upon the length of the fibre; if the fibre length is long enough, the fibre tensile stress will vary from zero to the fracture stress, σ_{fu}, Fig. 2.1(a). For a fibre with length equal to a critical length, the stress σ_f will be equal to σ_{fu} only at the centre point of the fibre, Fig. 2.1(b), whereas for a short fibre the stress σf will not reach the fracture stress and fibre pull-out or debonding will occur. From equilibrium consideration it can be found that

$$\tau \quad \frac{\ell_f}{2} (\pi \, d_f) = \frac{\pi \, d_f^{\,2}}{4} \quad \sigma_f \qquad \ldots\ldots \qquad (2.8)$$

$$\therefore \quad \ell f \quad = \quad \sigma_f \, \frac{d_f}{2\tau} \qquad \ldots\ldots \qquad (2.9)$$

There is a minimum fibre length required for the fibre stress σ_f to reach fracture stress σ_{fu} without slipping occurring. This value is given by:

$$\ell_c \quad = \quad \sigma_{fu} \, \frac{d_f}{2\tau} \qquad \ldots\ldots \qquad (2.10)$$

and is termed as "critical fibre length".

For continuous fibres the basic composite mixture rule gives:

$$\sigma_c \quad = \quad \sigma_m \, V_m \quad + \quad \sigma_f \, V_f \qquad \ldots\ldots \qquad (2.11)$$

where σ_c = Composite stress.

σ_m = Matrix stress.

σ_f = Fibre stress.

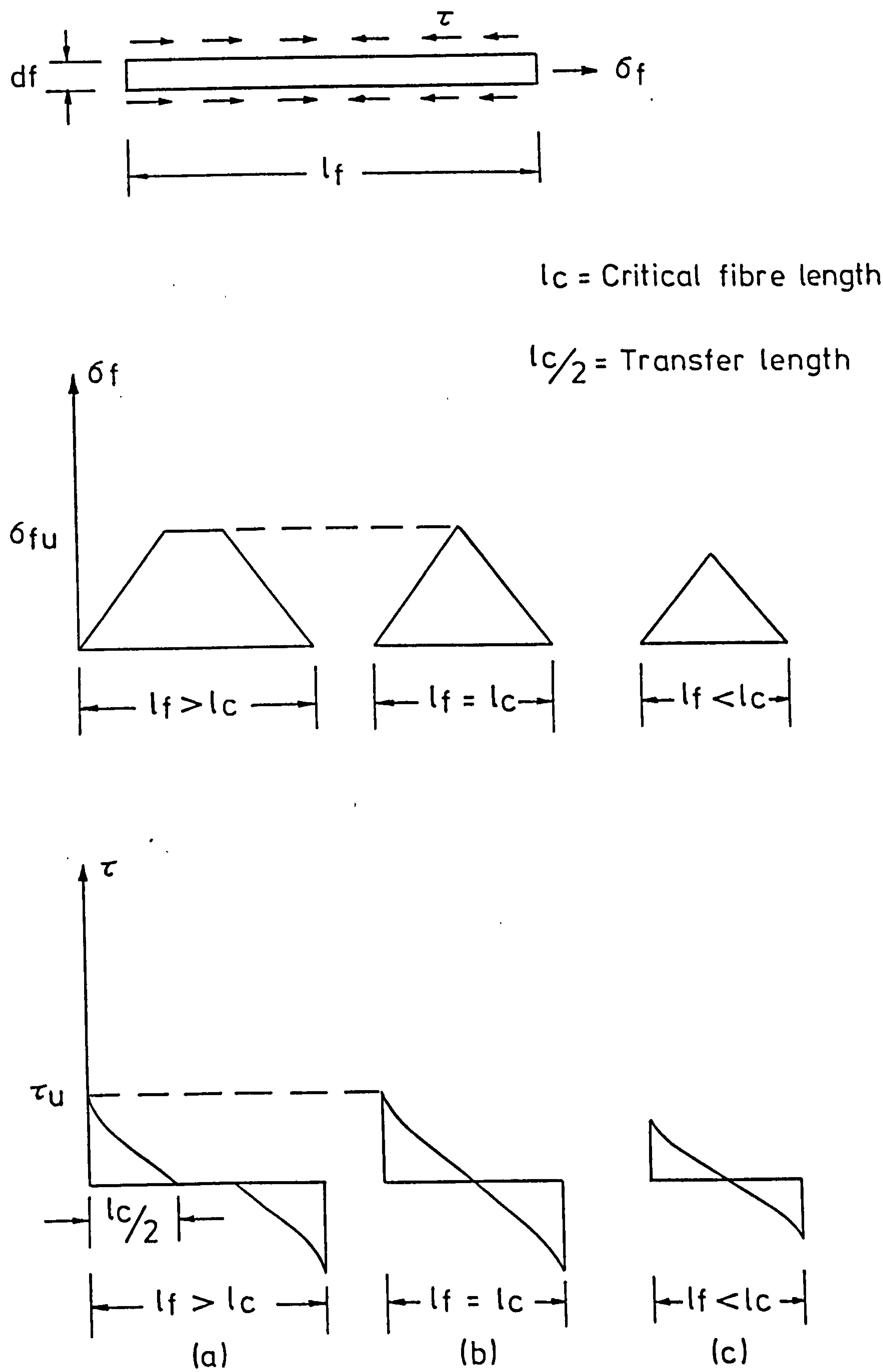

FIG. 2-1 SCHEMATIC VARIATION OF FIBRE TENSILE STRESS AND INTERFACIAL BOND STRESS

V_m = Matrix volume fraction.

V_f = Fibre volume fraction.

In considering the strength of a discontinuous fibre composite two efficiency factors must be introduced, the length efficiency factor and the orientation factor. The length efficiency factor describes the effect of the fibre length on the efficiency of the reinforcement i.e. takes into account the variation of the fibre tensile stress, σ_f along its length. The orientation factor describes the effect of fibre orientation on the composite strength. In a random orientation of short fibres in the matrix only those fibres which are parallel or almost parallel to the tensile stress direction are the most effective in strengthening the composite.

The values of length efficiency factor, η_L, and orientation factor, η_o, depend on the method of analysis used but some typical values are given below.

Cox (24) has derived the following equation for the average stress in a fibre of length ℓ_f subjected to a strain ε_x:

$$\sigma_f = E_f \ \varepsilon_x \left(1 - \frac{\tanh \beta \ell_f/2}{\beta \ell_f/2}\right) \quad \ldots\ldots \quad (2.12)$$

where E_f = Fibre Elastic Modulus

$$\beta = \left[\frac{2 \pi G_m}{E_f A_f \ln \frac{2R}{d_f}}\right]^{\frac{1}{2}}$$

where G_m = Shear Modulus of Matrix.

A_f = Fibre cross sectional area.

R = Mean interfibre spacing.

The length efficiency factor, therefore, proposed by Cox (24) is:

$$\eta_L = 1 - \frac{\tanh \beta \ell_f/2}{\beta \ell_f/2} \qquad ..... \qquad (2.13)$$

Cox proposed the following values for orientation factor, η_o.

1-D aligned $\eta_o = 1$

2-D random in plane $\eta_o = \frac{1}{3}$

3-D random $\eta_o = \frac{1}{6}$

Krenchel (25) has used a value

$$\eta_L = 1 - \frac{\ell_c}{\ell_f} \qquad ..... \qquad (2.14)$$

for the length efficiency factor, and the values of $\eta_o = 1$, $\eta_o = \frac{3}{8}$, and $\eta_o = 1/5$ for 1-D, 2-D, and 3-D respectively, for the orientation factor.

Laws (26) and Allen (27) proposed the following values for length orientation factor:

When fibre length is less than critical fibre length:

$$\eta_L = \frac{\ell_f}{2\ell_c} \qquad ..... \qquad (2.15)$$

When fibre length is greater than critical fibre length:

$$\eta_L = 1 - \frac{\ell_c}{2\ell_f} \qquad ..... \qquad (2.16)$$

Laws (26) using Krenchel's (25) values for orientation factor combined the two factors into a single efficiency factor, which was shown to be different from the product of the separate terms.

In the case of randomness in which fibres can be oriented in any direction with equal probability, a value of orientation factor of 0.41 is exact (19) and this value has been used by many authors (21,28,29,30).

The basic mixture rule can now be modified for short discontinuous fibres as follows:

$$\sigma_c = \eta_o \, \eta_L \, \sigma_f \, V_f + \sigma_m \, V_m \qquad \ldots\ldots \qquad (2.16)$$

2.3.6 Bond strength of fibre-matrix interface.

One of the most important factors influencing the properties of a fibre composite is the bond resistance between steel fibres and cementitious matrix.

The steel fibres used in composites are plain, crimped, duoform, and hooked fibres. They have either circular or rectangular cross-section, with length and aspect ratio ranging from 20 to 65 mm and from 40 to 150 respectively.

For a given fibre-matrix composite system, various indirect and direct methods can be used to determine the bond strength. In the direct methods both a single fibre model or a group of fibres embedded in a block of a matrix material can be used. The value of bond strength is calculated directly from the measured failure load. In the indirect methods a relative value of bond strength is obtained from the material properties of the composite materials.

A considerable number of researchers (31,32,33,34,36) have dealt with the bond strength by using the single and the group model. However, in an actual composite the fibres are not necessarily unidirectional. Fibres can have any direction and the interfacial bond is influenced by the neighbouring fibres. Naaman and Shah (35) carried out some tests varying, firstly the angle of orientation of the fibres with the loading direction and secondly the number of fibres being pulled out simultaneously from the same area. The results indicated a better performance for inclined single or pairs of fibres than for parallel ones. However, for groups of fibres, the pull-out load per inclined fibre at an angle of 60^{o} decreased when the number of fibres pulling out from the same area was decreased.

With steel fibres, the bond strength is a combination of adhesion, friction and mechanical interlocking. Because of this nature of the interfacial bond, the bond strength obtained by a single fibre or group of fibres parallel to the loading direction is not an accurate measure of bond strength but it is rather a measure of the anchorage bond and does not reproduce the state of stress in the matrix in the actual composite.

New methods were presented in references (36) and (37) in which both matrix and fibres are subjected to tension, the whole length of the fibre is embedded in the matrix, and testing of a single or multiple fibres in the specimens is possible.

Table 2.1 shows the bond strength values obtained by various investigations.

Indirect methods have been used, to a limited extent, to determine the interfacial bond strength in steel fibre reinforced cementitious composites.

Aveston et al., (38) calculated the interfacial bond strength from crack spacing. A value of bond strength of 6.8 N/mm^2 was obtained for continuous fibre reinforced cement paste and 6.0 to 10.6 N/mm^2 for the short fibre reinforced paste.

Swamy and Mangat (39) analyzed the results of their own flexural tests and those of other investigators, on fibre reinforced cement pastes, mortars, and concretes, by using a combined crack arrest-composite materials theory to obtain quantitative values for the bond strength in these composites at first crack and at ultimate load. The results showed that the bond stress at first crack was 3.57 N/mm^2 and 4.15 N/mm^2 at ultimate

Table 2.1 Bond Strength of steel fibre composites.

Matrix	Fibre type	Diameter and embedded length (m) (mm)		Bond Strength N/mm^2	Ref. No.
cement paste	bright high tensile wire	0.5		11.0 (35%)*	(31)
cement paste	rusty high tensile wire	0.5		10.39 (37%)*	
mortar	plain	0.38	17.5	1.24	(32)
mortar	Duoform	0.38	17.5	6.96	
mortar	looped	0.38	17.5	12.44	
cement paste	plain	0.38	17.5	2.48	
cement paste	crimped	0.79	10.2	12.89	(33)
cement paste	Duoform	0.64	22.0	3.84	
mortar	crimped	0.79	10.2	14.10	
mortar	Duoform	0.64	22.0	8.95	
mortar	plain	0.64	30.0	1.94	
mortar	plain			0.82-2.6	(34)
mortar	hooked			3.7 -5.3	
mortar	plain	0.40	12.5	2.86	(35)
mortar	plain	0.30	13.7	4.17	(36)
mortar	plain, hooked ends	0.40	21.8	4.93	
mortar	plain, weak crimped	0.35	15.2	5.25	
mortar	plain, heavy crimped	0.40	12.0	13.4	
mortar	enlarged ends	0.3x0.4	6.0	7.27	
mortar	brass coated	0.38	51.0	2.21	(37)

*Coefficient of variation.

failure. In a second paper Swamy and Mangat (120) analysed the results for individual groups of tests by using the above mentioned theory and found that bond strength, τ, ranges from 2.00 to 5.30 N/mm^2. It was shown that as the matrix changes from a mortar to a concrete matrix there is a progressive reduction in the interfacial bond strength; the bond strength increases with matrix flexural and compressive strengths, although not at the same rate.

From Table 2.1 it can be seen that there is a substantial increase in the bond strength as measured by pull-out tests on single fibres due to mechanical treatments of the fibres. However, there is only a marginal increase (40) when such treated fibres were used in actual concrete structures loaded in flexure. This is another reason not to consider that the measurement of the bond strength by means of a conventional pull-out test is an accurate one.

2.3.7 Ductility and Energy Absorption.

In practical applications, two very important factors are the ductility and energy absorption characteristics of the structure. Until recently concrete has been considered a fully brittle material, but recent research on the effect of various parameters has shown that concrete is more ductile than its constituent parts. Work by Shah and Chancra (41) has shown that the concrete ductility is a result of the progressive increase and growth of the existing microcracks.

It is generally accepted that there is a considerable increase in post cracking ductility and energy absorption characteristics of a structure imparted by the fibres. Ductility is usually determined by the ratio of deflection at ultimate load or at any specified point in the descending part of the load-deflection curve, to the deflection at first crack load, whereas energy absorption is determined by the area under load-deflection curve in flexure.

Swamy and Rao (42) reported an increase in ductility and energy absorption characteristics in 100x100x500 mm fibre concrete beam specimens, tested in flexure. This increase depends upon the type and percentage volume of fibres.

Tests on slabs (43,44) also show increases in ductility and energy absorption characteristics. Ductility was increased 2.5 times (43) when 1.74% fibre volume was used and 2.0 times (44) than that of plain concrete for 0.9% fibre volume. The corresponding increases in energy absorption were 3.5 times (43) and 4.0 times (44) that of plain concrete.

2.3.8 Durability.

Long-term stability under various environmental and exposure conditions is the most important property that needs to be established for any construction material and in particular for new materials.

The corrosion of steel fibres has been reported (45) not to cause a durability problem or a substantial change in the properties of the composite with time.

Tests reported by Edgington et al. (40) on normal weight and lightweight concrete cylinders in the uncracked state placed on three sites covering mild exposure, marine conditions and a polluted industrial atmosphere, over a period of about three years, showed that the corrosion of fibres within the concrete is unlikely to cause major problems. Steel fibre concrete also shows excellent freeze-thaw resistance, based on short-term studies (46). Obviously long-term results are necessary to establish the performance of steel fibre concrete, but considering that one of the essential properties of the fibres is to enhance the crack control characteristics of the composite, it is unlikely that such composites will be less durable than ordinary concrete.

2.3.9 Practical Applications.

Although much of the development of steel fibre cement composites has taken place in the last 15 years or so, there have been many significant applications all over the world. The following are applications referred to in published papers (16, 45, 47, 48); airfield and highway pavements, marine applications, heavy duty floors, pipes, thin wall sections, tunnel linings and strengthening rock slopes.

2.4 Reinforced Concrete Flat Slabs.

2.4.1 Introduction.

The primary function of most reinforced concrete structures is simply to carry loads safely. It seems, therefore, proper to base the design of concrete structures primarily on the load which they can carry at failure.

The development of the ultimate strength theories for design purposes, requires a good knowledge of structural behaviour. One of the sudden and dangerous failures of reinforced concrete flat slabs is the so-called punching shear failure. Since in recent years considerable progress has been made in design methods basing the safety of structures on their ultimate strength, information of the behaviour and ultimate strength of slabs failing in shear should be considered to be of great importance.

Most research on the shear strength of flat slabs both for normal and light-weight concrete, has been concerned with generation of experimental data and the development of empirical equations; only a limited number of theoretical analyses have been carried out predicting the ultimate punching strength of a flat slab-column connection. The lack of a complete theoretical model is due to the complexities of the basic three dimensional behaviour in the connection, as well as to the unknown internal shear transfer mechanism, existing in the slab before failure.

2.4.2 Some Previous Research on Normal-weight Slab-Column Connections.

Most methods of analysis for ultimate shear strength fall into two broad groups. In the first group, the strength is assumed to be governed by concrete strength, and in the second one by the flexural strength or the amount of flexural reinforcement. Further, most predict a strength varying with the ratio of the column size, r, to the slab effective depth, d.

A) Expressions dependent primarily on concrete strength.

Hognestad (49) reviewed Richart's (50) extensive series of footing tests and proposed the following equation for ultimate shearing stress:

$$\frac{V_u}{7/8\ bd} = \left[(0.035 + \frac{0.07}{\phi_o})\ f'_c + 130\ \text{psi}\right] \quad \ldots\ldots \quad (2.17)$$

where f'_c = cylinder compressive strength.

ϕ_o = V_u/V_{flex} , V_{flex} = ultimate flexural strength by yield line theory.

He recommended a critical section at the column perimeter because the final failure occurred there. He also excluded the load acting on the base of the "pyramid of rupture", assuming that this base lies at a distance d from the column perimeter. Equation 2.17 is valid when f'_c > 1800 psi (12.41 N/mm^2) and was the first attempt to recognize the dependence of shear strength on concrete compressive strength.

Elstner and Hognestad (51) tested 39 1800 mm square slabs, 150 mm thick, subdivided into nine series. Slabs were supported at the edges and loaded through a centrally loaded column stub. The main variables were concrete strength, amount of longitudinal reinforcement, column size, variations in support conditions, compression reinforcement, distribution of the tension reinforcement and shear reinforcement. They drew the following conclusions from their tests:

1. Final failure of 34 slabs was by the column punching through the slab. In most cases such punching took place after initial yielding of the reinforcement in the vicinity of the column.

2. For slabs which failed in flexure the measured ultimate strength was 10-20% greater than that predicted by the yield line theory (92), probably due to membrane action and strain hardening of the reinforcement.

3. A concentration of 50% of the tension reinforcement directly over a column did not increase the shearing strength.

4. Compression reinforcement had no effect on the ultimate shearing strength of the slabs.

5. The test results confirm the findings of the re-evaluation of Richart's (50) footing investigation, to the effect that the shearing strength is a function of concrete strength as well as of several other variables.

6. A statistical analysis of their results and those of Richart, showed that ultimate shearing stress for slabs without shear reinforcement can be expressed as:

$$\frac{V_u}{7/8\ bd} = 333\ \text{psi} + \frac{0.046}{\phi_o} f'_c \quad \ldots\ldots \qquad (2.18)$$

(imperial units)

where $b = 4r$, r = column size

f'_c = cylinder compressive strength.

$\phi_o = V_u/V_{flex}$

where the ultimate flexural strength of the slab may be computed with the aid of the yield line theory (92).

Moe (52) tested 43 1830 mm square slab-column connections, 150 mm thick, simply supported along all four edges with free lift off corners. The main variables in his tests were, the effect of holes near column faces, concentration of the tension reinforcement over the column, and the column size and shape. He analyzed his results and those of previous investigations statistically and obtained the following equation for the ultimate shearing stress:

$$\frac{V_u}{bd} = \frac{15\ (1-0.075\ r/d)\sqrt{f'_c}}{1 + \dfrac{5.25\ bd\sqrt{f'_c}}{V_{flex}}} \quad \ldots\ldots \quad (2.19)$$

(imperial units)

where b = column perimeter.

V_{flex} = ultimate flexural strength by yield line theory.

For design purposes Moe developed the following equations:

$$\frac{V_u}{bd} = (9.23 - 1.12\ \frac{r}{d})\ \sqrt{f'_c} \qquad \text{for } \frac{r}{d} \leq 3$$

$$(2.20)$$

$$\text{and } \frac{V_u}{bd} = (2.5 + 10\ \frac{d}{r})\ \sqrt{f'_c} \qquad \text{for } \frac{r}{d} > 3$$

Equation 2.19 introduces two new concepts

1. The shear strength is related to $\sqrt{f'_c}$ and not f'_c, and
2. it is dependent on the ratio of column size, r, to the effective depth, d.

Moe selected the square root expression because tensile strength is generally assumed proportional to $\sqrt{f'_c}$ and he believed that a shear failure is controlled primarily by tensile splitting strength of concrete. He also assumed a linear variation in shear strength with r/d. Since r/d values for the available test data all were between 0.75 and 3.0, he recognized that the use of eqn. 2.19 should be limited to r/d values less than 3.0. Moe's concepts form the basis for A.C.I. code of practice 318-71.

Tasker and Wyatt (53) modified Moe's equation (2.19) and proposed the following equations for ultimate shearing stress:

$$\frac{V_u}{bd} = [8.27\ (1+1.21\ \frac{d}{r}) - 5.25\ \phi_o]\ \sqrt{f'_c} \quad \ldots\ldots \quad (2.21)$$

(imperial units)

$$\text{and}\ \frac{V_u}{bd} = (2.5 + \frac{10}{1+r/d})\ \sqrt{f'_c} \quad \text{for design} \quad \ldots\ldots \quad (2.22)$$

Herzog (54) evaluated the results for 160 slabs without shear reinforcement failing in shear and proposed the following equation, for design purposes.

$$v_u = \frac{V_u}{4(r+d)d} = (2.65 + 0.00477\ \rho\ f_y)\ \sqrt{f'_c} \quad \ldots\ldots \quad (2.23)$$

where v_u = unit shearing stress which should be less or equal to $6.3\ \sqrt{f'_c}$

ρ = reinforcement ratio

f_y = yield stress of reinforcement.

B) Expressions dependent primarily on flexural effects.

Whitney (55) re-evaluated Richart's (50) and Elstner and Hognestad's (51) test results and proposed the following equation for ultimate shearing stress:

$$\frac{V_u}{4(r+d)d} = 100\ \text{psi} + 0.75\ \frac{M_u\ \sqrt{d/\ell_s}}{d^2} \quad \ldots\ldots \quad (2.24)$$

(imperial units)

where M_u is the average in two directions ultimate moment per unit width of the slab within the base of the pyramid of failure and ℓ_s is the distance from the column face to the line of inflection. This equation states that the shearing stress at a critical perimeter at a distance d/2 from the column face is a function of the ultimate moment of resistance near the column and the only influence of concrete strength is its effect on M_u.

Yitzaki (56) tested 14 slab-column specimens and proposed the following equation for the ultimate shearing stress

$$\frac{V_u}{bd} = 8\left(1 - \frac{\rho f_y}{2f'_c}\right) \frac{d}{b} \left(149.3 + 0.164\, \rho f_y\right)\left(1 + \frac{r}{2d}\right) \quad \ldots\ldots (2.25)$$

(imperial units)

where b = column perimeter.

ρ = reinforcement ratio.

f_y = reinforcement yield stress.

This equation indicates that the punching resistance depends mainly on the "reinforcement strength", ρ fy, as in the case of flexural strength. It is shown that the effect of the concrete strength on punching resistance is of the same order of magnitude as it is on the flexural strength and can be expressed by the factor $1 - \rho f_y/2 f'_c$ used in the analysis of the ultimate flexural strength of reinforced concrete members. The effect of the r/d ratio and the "reinforcement strength", ρf_y, on the punching resistance was introduced by linear independent multipliers and the constants of the equation 2.25 were evaluated from the available test data.

Blakey (57) examined available data from other investigations and proposed the following equation for shear strength:

$$V_u = \frac{2\pi\ (M_x + M_y)}{\ln \frac{r}{L} + 1.31} \text{ (imperial units)} \quad \ldots\ldots \qquad (2.26)$$

where M_x, M_y = ultimate moment of resistance in the two directions.

L = distance from column to column.

His approach does not require the calculation of a nominal shear stress.

Long (58) derived formula for predicting the punching strength of slabs at interior columns, taking into account the interaction of flexural and shear effects. He assumed two basic modes of failure. First, the flexure mode of failure, where yielding of the tension reinforcement occurs before punching, and second, the shear mode of failure, where concrete fails before tension reinforcement yields. The predicted punching load for a slab is taken to be the lesser of the two values.

$$V_u = \frac{\rho\ f_y\ d^2\ (1-0.59\ \rho\ f_y/f'_c)}{(0.2 - 0.90\ r/L)} \quad \ldots\ldots \qquad (2.27a)$$

(imperial units)

for flexure mode of failure, and

$$V_u = \frac{20\ (r+d)\ d\ (100\rho)^{0.25}\ \sqrt{f'_c}}{(0.75 + 4\ r/L)} \quad \ldots\ldots \qquad (2.27b)$$

for shear mode of failure

where L = distance from column to column.

These formulae are limited in application to isotropically reinforced square slabs which are supported on square columns.

2.4.3 Some Previous Research on Light-weight Slab-Column Connections.

Although lightweight concrete is used extensively for floor slabs, data on its shear strength are inadequate, especially in comparison to the amount of data on the strength of normal weight slabs.

Hognestad et al. (3) reproduced three normal weight concrete slabs tested and analyzed previously by Moe (52) using two different light-weight concretes for each of the three slabs. All slabs were 1800 mm square and 150 mm thick, with an effective depth of 114 mm. Their variables were the shape of column stub and slabs with openings. They concluded that the shear strength is dependent on the tensile splitting strength, f_{ct}. They expressed the ultimate shearing stress as a function of f_{ct} and modified Moe's equation as following:

$$\frac{V_u}{bd} = \frac{2.24\ (1-0.075\ r/d) f_{ct}}{1 + \dfrac{0.784\ bd\ f_{ct}}{V_{flex}}} \quad \ldots\ldots \quad (2.28)$$

This equation results from eqn. 2.19 by substituting the square root of compressive strength, $\sqrt{f'_c}$, in terms of the splitting tensile strength, f_{ct}. Experiments by Hanson (13) showed that f_{ct} equals 6.7 $\sqrt{f'_c}$

Mower and Vanderbilt (59) carried out two series of tests. In the first series most slabs were 76 mm thick, and centrally loaded through a 152 mm square column stub, 152 mm high, attached monolithically at the centre of the top side. One type of lightweight aggregate was used throughout the investigation. Their test variables in the first series were the hole pattern around the column, amount of reinforcement and concrete strength. In the second series 1200 mm square slabs were used with a column stub 127 mm high. The variables were the column size to effective depth ratio, the amount of tension reinforcement and the edge fixity. They proposed the following equation to predict the shear strength of light-weight concrete slabs.

$$\frac{V_u}{bd} = \frac{9.7(1+d/r)}{1 + \dfrac{5.25\ bd\ \sqrt{f'_c}}{V_{flex}}} \sqrt{f'_c} \quad \ldots\ldots \quad (2.29)$$

(imperial units)

Use of the compressive strength gave better agreement between computed and measured strengths than did the splitting strength.

Ivy et al. (60) tested 14 lightweight concrete slabs containing three different lightweight aggregates. Ten slabs were similar to Hognestad's et al. (3) slabs, 1830mm square, 150 mm thick with 250 mm square column stubs. The other four slabs were of larger scale, 3050 mm square, 180 mm thick, loaded through a 610 mm square column stub. They compared their results with the strengths calculated by eqn. 2.19 and found that while for specimens with perforations the measured strengths were 8% more than calculates ones, the measured strengths for specimens without perforations were 7% less than calculated ones.

2.4.4 A Review of the Theoretical Methods of Analysis for Shear Strength.

2.4.4.1 Kinnunen and Nylander.

The model developed by Kinnunen and Nylander (61) to study the shear failure of slabs without shear reinforcement was the first real attempt to establish a theoretical method of analysis. Their experimental work consisted of 60 circular slabs, 150 mm thick and 1710 mm in diameter. The slabs were subjected to load, uniformly distributed along the circumference and supported in a circular column stub. The main variables in these tests were the type and amount of flexural reinforcement and the diameter of the column stub. Three types of flexural reinforcement were used, two way reinforcement, ring reinforcement alone, and ring reinforcement in conjunction with radial reinforcement. The column stubs were 50, 150, and 300 mm in diameter.

The theoretical method of analysis was based on the mechanical model shown in Fig. 2.2. The slab outside the inclined crack was divided into sectors bounded by radial cracks, the perimeter of the slab and the

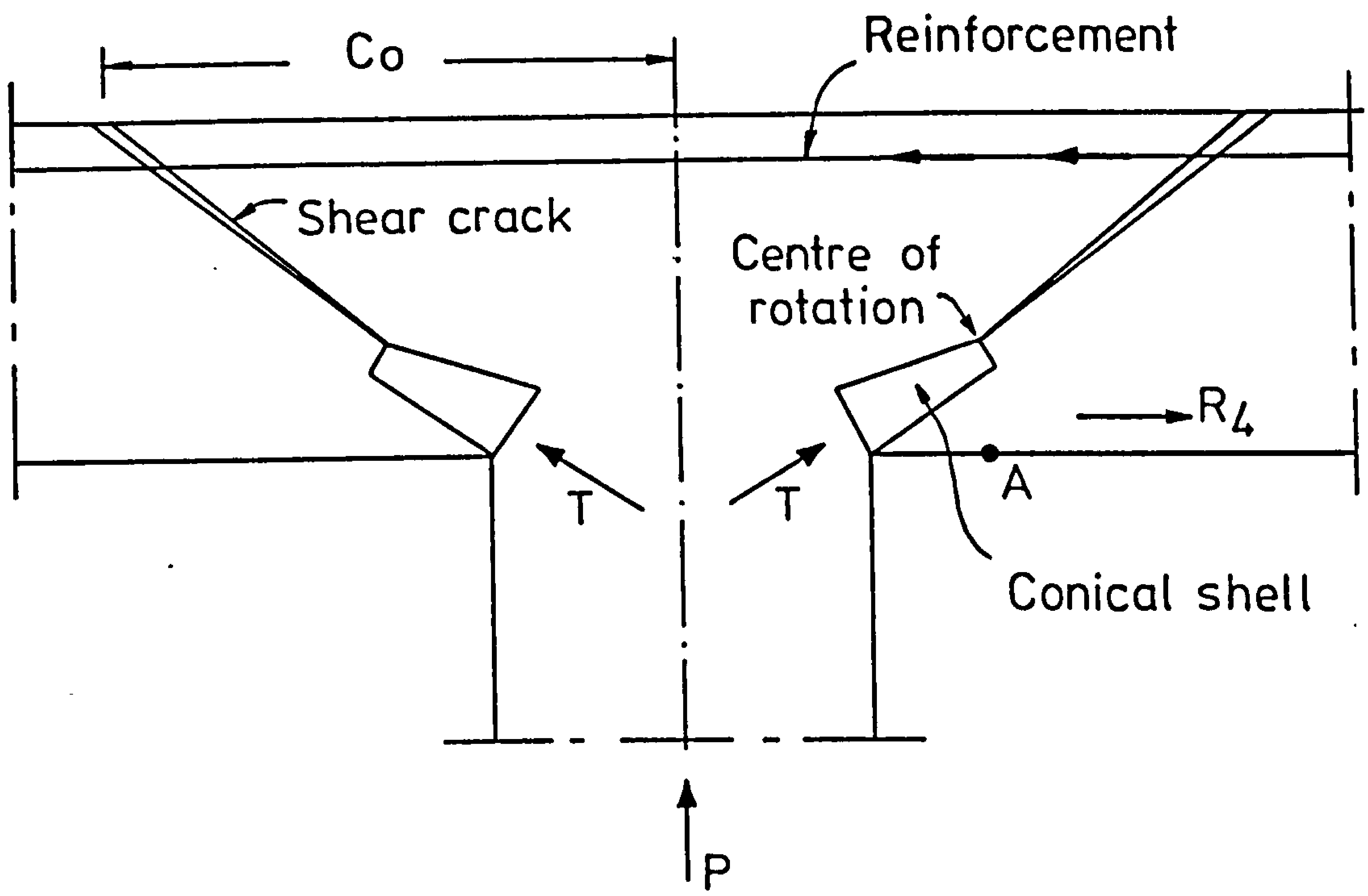

(a) Assumed geometry of connection

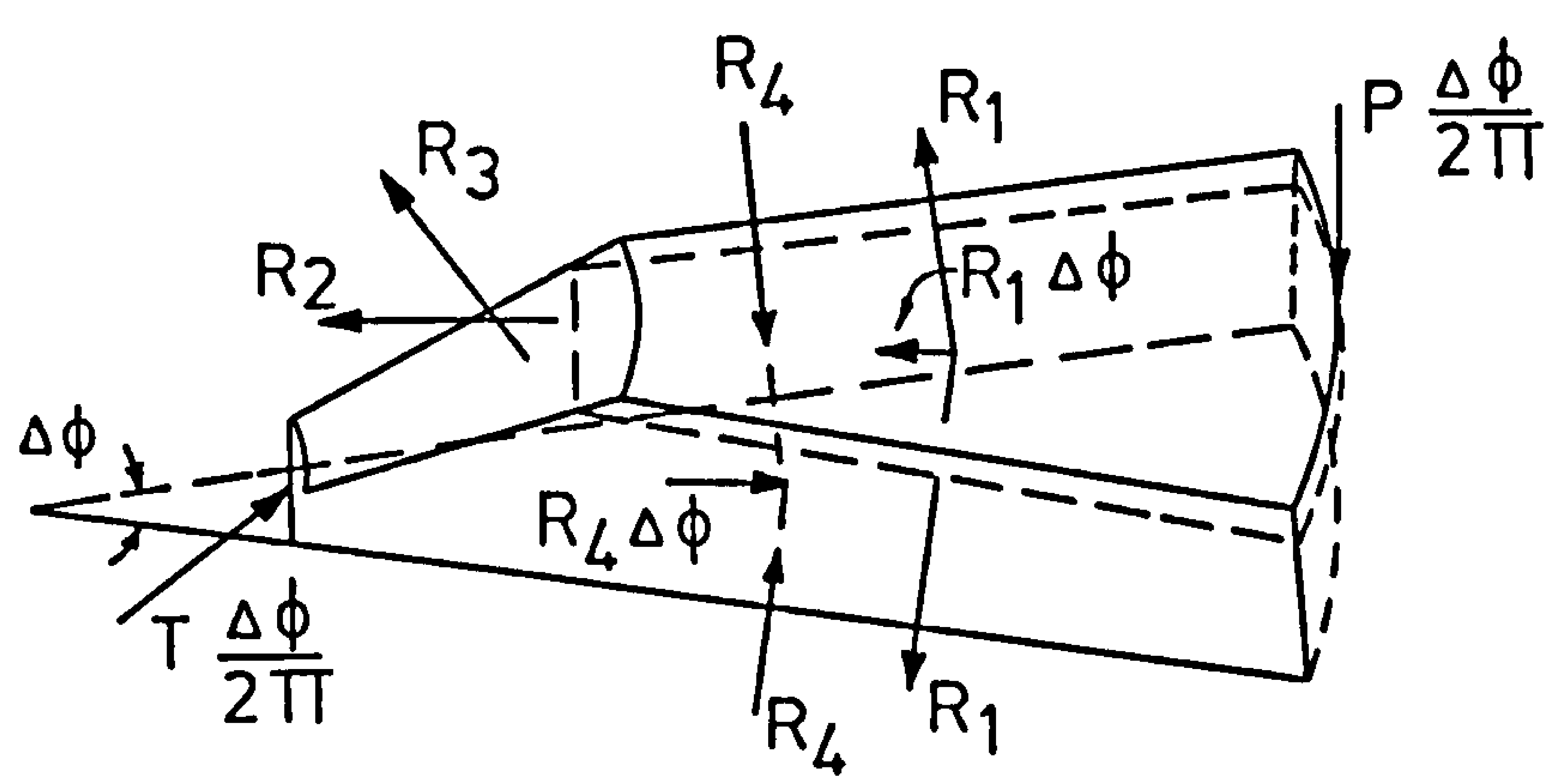

(b) Forces acting on a sector of slab

P = Applied load at the slab periphery

T = Inclined comp. force acting on the conical shell

R_1 = Resultant at right angles to radial crack of the reinforcement

R_2 = Resultant at right angles to shear crack of the reinforcement

R_3 = Resultant of shear reinforcement, if any

R_4 = Tangential resultant of the concrete compressive stresses

FIG. 2-2 MECHANICAL MODEL FROM KINNUNEN AND NYLANDER (61) inclined crack. Each sector was assumed to rotate as a rigid body about the apex of the inclined crack and to be supported on the imaginary conical shell which is in turn supported on the column. They derived expressions for the forces acting on each sector; it is supposed that these forces, except the load and reaction, are proportional to the angle of rotation of the slab. The shear strength is evaluated from the condition of equilibrium at failure. Failure occurs when the tangential strain at point A at the compressive face of the slab reaches a characteristic value. This value was determined from their test data. To use their model a depth is assumed for the inclined crack and two capacities P_1 and P_2 are calculated. P_1 is the column load given by vertical equilibrium and P_2 is the load needed to satisfy moment equilibrium about the intersection of the radial resultant of the concrete compressive force in the slab and the force in the conical shell. If P_1 does not equal P_2 a new depth for the inclined crack is selected and the process is repeated until P_1 equals P_2, The ultimate strength of slab is given by:

$$P = P_1 = P_2$$

For two-way reinforcement, Kinnunen and Nylander proposed

$$P = 1.10\ P_1 = 1.10\ P_2$$

In their tests on slabs with two-way reinforcement all measured values of ultimate load were higher than the calculated values. The difference between these values varied from 10 to 25%. This deviation can be attributed to the development of dowel forces, which are not taken into account in this theory.

2.4.4.2 <u>Kinnunen (62).</u>

The model developed by Kinnunen and Nylander (61) was later modified by Kinnunen (62) to include:

1. The effect of dowel forces.

2. The vertical component of the reinforcement forces and

3. The deviation of a two-way reinforcement pattern from polar symmetry.

2.4.4.3 Long and Bond (63).

Long and Bond (63) presented a theoretical method of analysis for the calculation of the punching load of a flat slab-column connection with two way reinforcement and no shear reinforcement. This is based on elastic thin plate theory from which the stresses in the compression zone are derived, assuming a linear distribution of stress. An octahedral shear stress criterion of failure is used to find the corresponding failure stresses. The analysis does not include the case of transfer of moment between column and slab combined with a direct punching load. The load found by this analysis was multiplied by a factor of 1.30 to take into account the dowel action effect. Tests were carried out on one-fourth scale slab-column connection and the test results were in good agreement with those predicted by their analytical method.

Examination of their theoretical analysis leads to the following critical remarks:

1. The use of the elastic theory to find the relationship between the column load and the induced bending moments means that the effect of both flexural and shear cracks is not taken into account, which may change the stress distribution and cause a redistribution in the internal tensile and compressive forces in the slab.

2. The assumption of constant shear stress distribution between neutral axis and reinforcement is questionable since the flexural cracked part of the slab does not contribute any resistance to shear.

3. Their test specimens were small and the one-fourth scale may influence the behaviour of slabs.

2.4.4.4 Long (64).

Long (64) extended the above theory, to include the case of the punching load for a slab-column connection subjected to shear and transfer moment. Shear loading and pure transfer of moment were considered separately and because the method of analysis is basically elastic these can be superimposed to apply to the general case of shear and moment transfer. A factor of 1.30 was also applied to the punching load to take into account the dowel action effect.

2.4.4.5 Nielsen et al. (65) (Plasticity theory).

Nielsen et al. (65) found the ultimate punching strength by using the theory of plasticity for concrete. They based their theoretical analysis on some basic assumptions for both concrete and steel reinforcement.

1. Concrete is considered to be a perfectly rigid-plastic material.

2. As yield condition, the modified Coulomb failure criterion was adopted i.e. the hypothesis of Coulomb together with a limitation of the tensile strength. Fig. 2.3(a).

3. The reinforcement is assumed to be capable of carrying longitudinal tensile and compressive stresses only and to be a rigid-plastic material. In Fig. 2.3(b) the stress-strain relation is shown.

The ultimate punching strength can be found as an upper bound solution, by using the work equation i.e. by equating the external work done by the load for a given failure mechanism to the internal work dissipated in the structure. They considered a failure mechanism shown in Fig.2.3(c), which consists in the punching out of a cone of concrete, while the rest of the slab remains rigid. Examination of their theoretical analysis leads to the following critical remarks:

1. The assumption about failure mechanism is a rational one and is supported by experience.

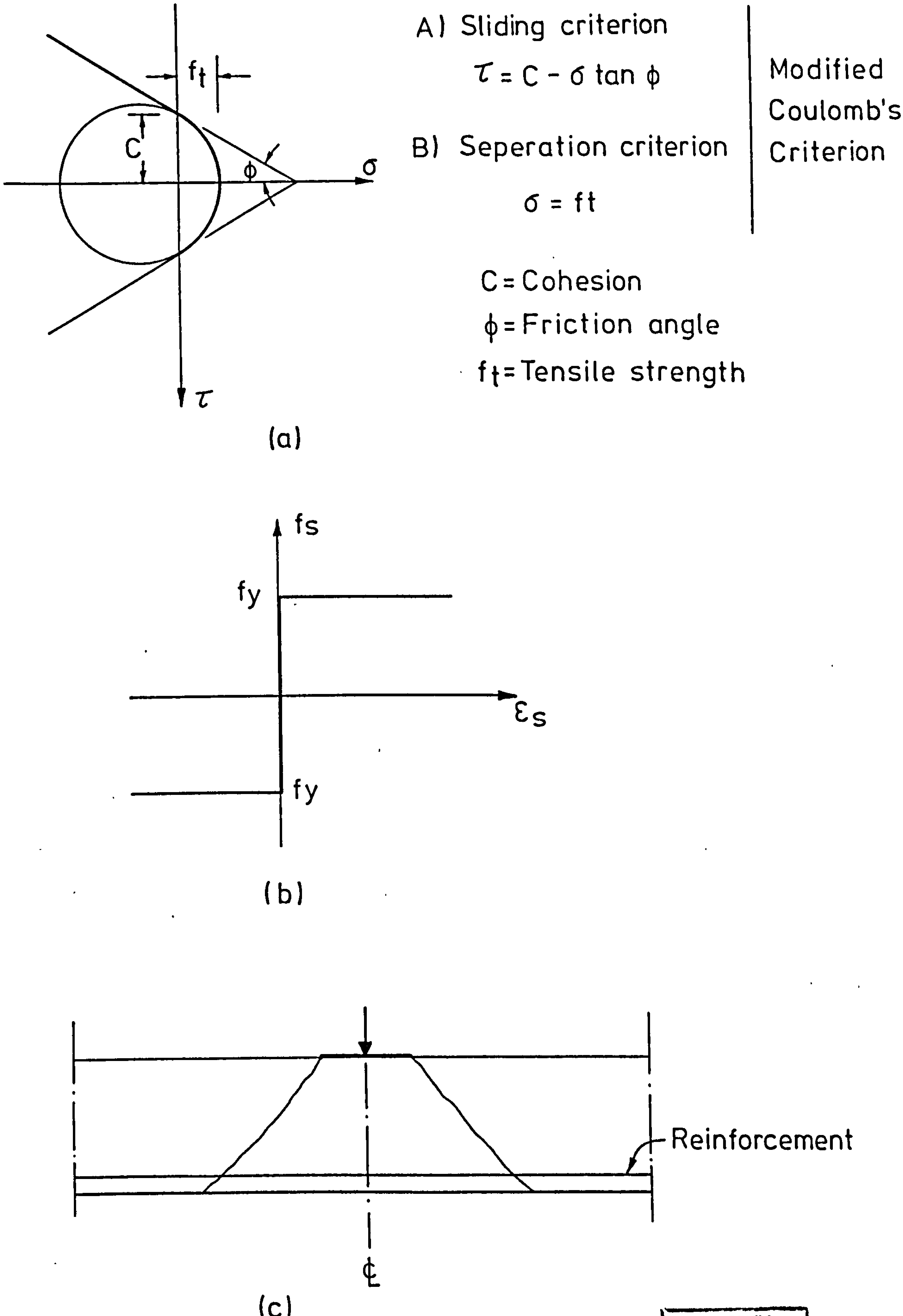

FIG. 2-3 PLASTICITY THEORY

SHEFFIELD
UNIVERSITY
LIBRARY

2. The assumption about concrete means that elastic deformations are neglected in the analysis and that unlimited ductility is implied. However, this is a drastic simplification of the behaviour of concrete since the deformation of concrete is very limited, especially in tension.

3. The assumption about reinforcement means that the dowel effect as well as the vertical component of the reinforcement force are neglected.

They produced theoretical curves for the punching load corresponding to various levels of relative tensile strength (f_t/f'_c) and made comparisons with experimental values of the punching load. From these comparisons it can be seen that the majority of the experimental ultimate loads are lower than the predicted ones. The theoretical curve more close to experimental loads is that with tensile strength of concrete equal to zero. The greater theoretical loads than experimental ones, were explained in terms of the limited deformability of the concrete which makes it highly unlikely that the compressive and tensile strength be obtained at all points of the failure surface at the instant of failure. To account for this, they introduced two effectiveness factors each one for tensile and compressive strength of concrete. They suggested an effectiveness factor for compressive strength equal to 0.835 with a coefficient of variation of 15.8%, which is the average ratio between experimental and theoretical ultimate loads; based on this value an effectiveness factor of 1/400 for the relative tensile strength (f_t/f'_c) of concrete was determined. It can be seen that the value of effectiveness factor on the tensile strength is much lower than one on the compressive strength because of the lower deformability of concrete in tension.

2.4.5 Regan's analysis (66).

Regan (66) gave emphasis to the effect of dowel forces and considered that the ultimate punching strength is given by:

$$V_u = b\, v'_c + b_d\, v'_d \quad \ldots\ldots \qquad (2.30)$$

where

b = the perimeter of the column stub.

b_d = the perimeter of the failure surface at reinforcement level.

v'_c = resistance per unit length of concrete compressive zone.

v'_d = resistance per unit length of dowel action.

Because of the uncertainties involved in the calculation of dowel forces he proposed a simpler approach. He replaced the two perimeters by a single one, so chosen that the product of its length and a unit resistance v'_c, corresponding to the value used for beams, to give a correct prediction for V_u. Empirically this is achieved by taking the critical perimeter to be located at a distance 1.75 times the effective depth from the column face. By using the value of v'_c from reference (66) the ultimate strength is given by:

$$V_u = 0.30 \left(\frac{100\, A_s\, f_{cu}}{b'd}\right)^{0.40} b_1\, d \quad \ldots\ldots \qquad (2.31)$$

where the ratio $100\, A_s/b'd$ is for the column strip and

$$b_1 = 4r + 3.5\, \pi d.$$

2.4.6 Code Specification.

A) ACI 318-71 (67) Code of Practice.

Research studied by A.C.I.-A.S.C.E. Committee 326 (68) based on Moe's (52) experimental analysis, indicated that the critical section for shear follows the periphery at the edge of the loaded area. The nominal ultimate shear stress acting on this section is a function of $\sqrt{f'_c}$, and the ratio of the side dimension of a square column to the effective depth, r/d.

$$v_u = \frac{V_u}{bd} = 4\left(1 + \frac{d}{r}\right) \sqrt{f'_c} \quad \ldots\ldots \qquad (2.32)$$

where b = $4r$ = perimeter of the column.

Furthermore, Committee 326 pointed out that the variable r/d can be taken into account by choosing a pseudocritical section, which is located at a distance d/2 from the column periphery:

$$v_u = \frac{V_u}{b_o\, d} = 4 \sqrt{f'_c} \quad \ldots\ldots \qquad (2.33)$$

where b_o = perimeter of a section at a distance d/2.

Eqn. 2.33 was considered preferable by A.C.I. Committee 318 for inclusion in the 1963 A.C.I. Code and retained in the 1971 Code (67) because of its simplicity, particularly for columns with irregular shape and for consideration of slab openings near columns.

The design shear strength at a distance d/2 is:

$$V_u = 4b_o\, d\, \phi \sqrt{f'_c}$$

where ϕ is a capacity reduction factor = 0.85 for shear.

Equation 2.32 was derived from Moe's equation 2.19 by setting the ratio $\phi_o = \frac{V_u}{V_{flex}}$ equal to unity.

When lightweight concretes are used, one of the following modifications shall apply to formula 2.33:

1. If a value of splitting tensile strength, f_{ct}, is specified, $f_{ct}/6.7$ shall be substituted for $\sqrt{f'_c}$ but the value of $f_{ct}/6.7$ shall not exceed $\sqrt{f'_c}$.

2. If a value of f_{ct} is not specified, the value of $\sqrt{f'_c}$ shall be multiplied by 0.75 for "all-lightweight" concrete and by 0.85 for "sand-lightweight" concrete.

B) CP110 Code of Practice (69).

The CP110 Code of Practice specifies a critical section for the design punching shear 1.5 times the overall depth (1.5h) from the column perimeter. The nominal shear stress is taken from Table 5 of CP110 for normal weight concrete and from Table 25 for lightweight concrete. The values of these Tables correspond to different values of compressive strength, f_{cu}, and percentage of steel reinforcement, ρ. The value of ρ to be used in Tables 5 and 25 should be taken as the average for the two directions

$$\rho = \frac{100\ A_s}{b_2\ d}$$

A_s in each direction should include all the tension reinforcement within a strip of width $b_2 = r + 6h$.

These basic shear stress values are then modified by a factor ξ_s, which is a scale factor permitting higher stresses in thinner slabs. The ξ_s values are given in Table 14 of CP110. The design shear strength is therefore given by:

$$V_u = b_p\ d\ \xi_s\ v_c \qquad \ldots\ldots \qquad (2.35)$$

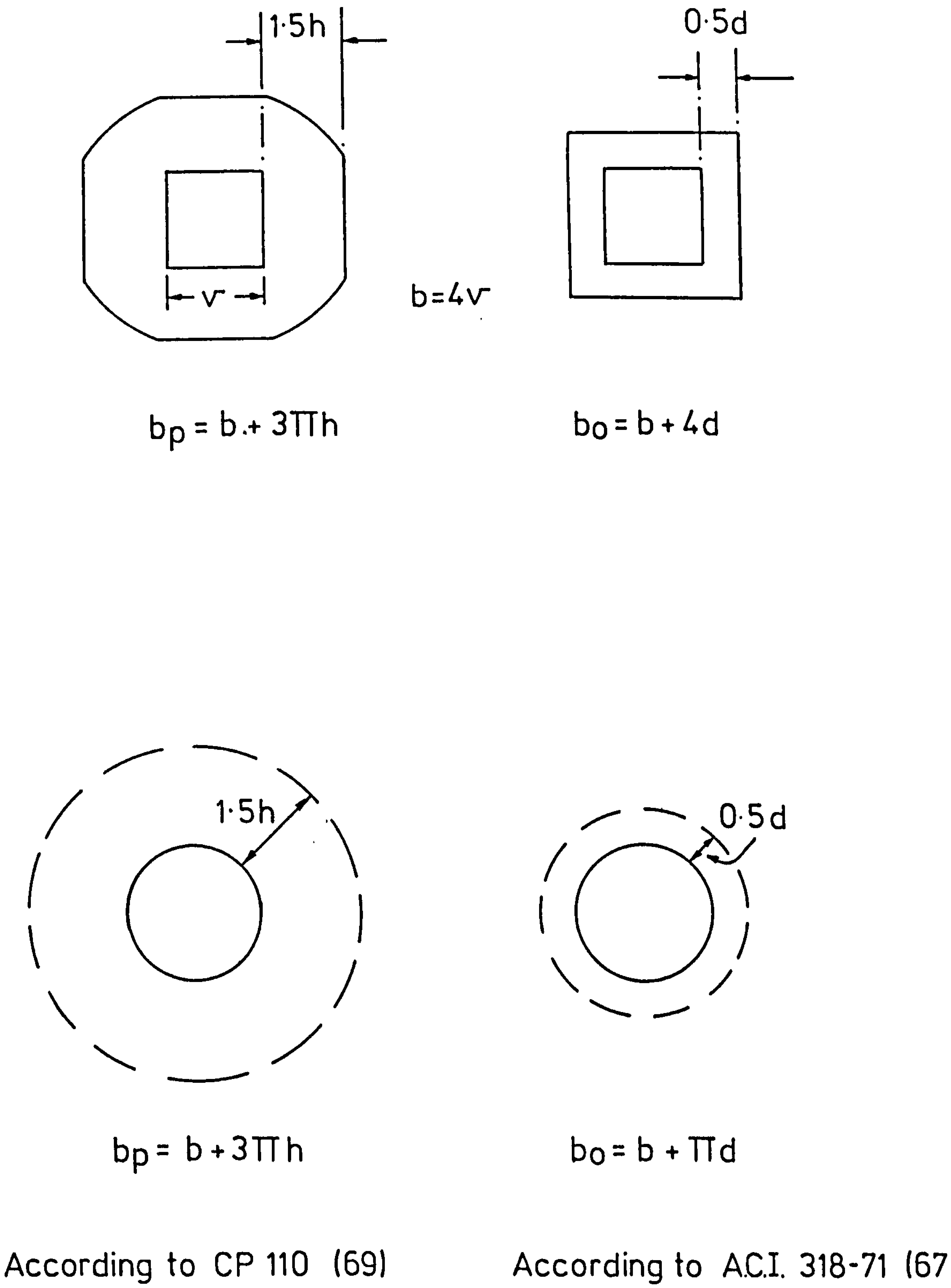

FIG. 2-4 CRITICAL PERIMETERS ACCORDING TO CP 110 AND A.C.I. 318-71

C) CEB Code provisions (118).

The CEB and ACI Code provisions for shear in slabs are similar. The Ultimate shear strength is given by:

$$V_u = b_o \; d \; f_{ct} \qquad \cdots\cdots \qquad (2.36)$$

and the design shear strength by:

$$V_u = b_o \; d \; f_{ct}/\gamma_c \qquad \cdots\cdots \qquad (2.37)$$

where b_o = punching perimeter at a distance d/2 from column face.

d = effective depth of slab.

f_{ct} = tensile stress which varies from 3.18 to 4.5 times $\sqrt{f'_c}$ depending on f'_c.

γ_c = 1.5 is the safety factor for the concrete.

Regan (70) pointed out the differences between A.C.I. 318-71 (67) and CP110 (69) Code of practice.

There are two major differences between the A.C.I. 318-71 and CP110 permissible stresses for punching. The CP110 values are much lower and are considerably influenced by the ratio of flexural reinforcement. The low values are related to the much larger perimter considered critical for punching.

The two codes' definitions of the critical perimeter, Fig. 2.4, show two differences as well. The major difference is the distance from the column to the perimeter, which is 1.5 times the overall depth of the slab in the CP110 as compared to 0.5 times the effective depth in ACI 318-71. The second difference pertains to the CP110 Code's rounded-off corners for perimeters around square columns. This seems more logical if one considers conditions at some distance from the column. CP110's large perimeter takes into account that a very considerable part of the shear force is resisted by dowel action of the flexural reinforcement of the slab, which is much more significant than in beams

From experimental evidence it can be seen that CP110's large perimeter takes better account of the geometry of a slab column connection.

2.4.7 Steel Fibres as Shear Reinforcement.

The use of steel fibres in concrete can be considered not only as a way to increase the properties of the concrete itself but as a way to replace reinforcement. Regarding the latter way the steel fibres might be used to improve the shear strength of various concrete elements, especially in the case where traditional reinforcement is difficult or impractical to place.

A limited amount of experimental data directed to the problem of fibres as shear reinforcement has been reported up to this time in the technical literature.

2.4.7.1 Shear in Beams.

Batson et al. (71) reported tests on rectangular beams. The beams were cast using a mortar mix with steel fibre contents of 0.22, 0.44, 0.88 and 1.76% by volume. The main conclusion of their investigation was that the replacement of vertical stirrups by round, flat, or crimped steel fibres provided effective reinforcement against shear failure.

Williamson and Knab (72) tested four beams 30.5 x 54.6 x 701 cm to determine the effectiveness of steel fibres in full scale structures. One beam was made without shear reinforcement, one beam with stirrups and two beams were made with 1.5% by volume steel fibre concrete, with the fibres as shear reinforcement. They found that the fibres increased the shear strength of the concrete by 39% over the beam without shear reinforcement, while the increase in shear strength for the beam with shear reinforcement was 58%. They also observed that steel fibres are not effective in preventing catastrophic shear failures in full scale beams.

Muhidin and Regan (73) reported tests on 25 simply supported I-section beams, tested under central concentrated loads. Three of the beams were without web reinforcement, four had conventional stirrups and the remaining eighteen were reinforced with Duoform fibres, with a varying percentage 0-3% by volume. Their conclusion was that the behaviour of the fibre reinforced beams was generally similar to that of equivalent members with stirrups.

La Fraugh and Moustafa (74) reported a number of results for both rectangular and T-section fibre concrete beams. Their main conclusions were that there was a dramatic improvement in ultimate capacity of beams containing steel fibres over beams without any web reinforcement; beams using steel fibres for shear reinforcement carried half as much shear as beams having the same amount of stirrups and finally the steel fibres can be used to produce beams with thinner webs resulting in overall beam weight savings.

Bahia (75) carried out a series of tests on realistic scale T-beams with and without stirrups. The main variables were, fibre content, percentage of main steel and amount of web reinforcement. The purpose of his work was to study the mechanism of shear transfer in fibre reinforced beams and the contribution of dowel action, concrete compression zone and aggregate interlock at collapse. The results showed that fibre reinforcement of 1.2% by volume increased the contribution of concrete compression flange by 70% and the combined contribution of aggregate interlock and dowel action by 114%. His study showed that fibres can be used as shear reinforcement in beams.

2.4.7.2 Investigations on Slab-Column Connections with Steel Fibres.

Seven slab-column connections were tested by Patel (76). The size of the slab specimen was taken as 1.22x1.22 m, 101 mm thick with a column stub of 203 mm in diameter in the centre. The steel fibres were flat strips 0.254x0.56 mm cross-section and 19-25.4 mm long. Two percentages 0.574% and 1.20% by volume were used. The strength of all seven specimens was controlled by flexure. The maximum column load was reported as 56.93 kN obtained by a slab without fibres, which had a tensile reinforcement ratio of 0.32% and a similar slab with 1.2% fibres replacing volume by volume the tensile steel used in the slab without fibres. Inclusion of fibres was noted to increase the load needed for visible flexural cracking of the slab. As the amount of steel fibre was increased from 0.575% to 1.2% by volume, the cracks became finer, whereas the crack pattern was observed to be almost the same. Due to the fact that only flexural failures were observed, he concluded that the fibres were effective in preventing shear type of failures.

Tests on seven specimens were reported by Lamoureaux (43). The specimens 2.08x2.08 mm, 127 mm thick were constructed identically in size and in main reinforcement to simulate the column strip of an interior panel 4.47x4.67 m of a flat-plate system. Four of the specimens were made of normal weight concrete; of these four, one was with confinement reinforcement and two were with 1.21% and 1.74% by volume steel fibres. The steel fibres were flat strips 0.254x0.56 mm of cross-section and 25.4 mm long. The three remaining specimens were made of lightweight concrete, one without confinement reinforcement, one with confinement and one with 0.91% by volume steel fibres. All seven slabs were tested to investigate the behaviour of a flat plate-column system undergoing a series of seismic motions imparted by cyclical loading. The specimens were subjected to cyclic reversed unbalanced loads placed at a distance 710 mm from the column face, the total vertical load being constant. The inclusion of fibres increased the ultimate moment of resistance of the specimen by 28.8% and 31.6%, and 33% for normal and light weight concrete respectively. Ductilities and energy absorption capacities were increased by 2.38 to 2.54 and 2.48, and 2.78 to 3.09, and 2.52 times for normal and lightweight concrete respectively. There was no increase in flexural strength when confinement reinforcement was used for both normal and light weight concrete. It was concluded that the use of randomnly oriented fibres within various concrete matrices improves considerably the overall strength characteristics of flat slab-column connections.

Criswell (77) tested four one-third scale slabs 0.635x0.635 m, 51 mm thick, with a 114 mm square column stub. Two steel reinforcement ratios of 1.04% and 1.88% with 1.0% by volume steel fibres or no fibres were used in the four slabs. The steel fibres were flat strips 0.254x0.56 mm of cross-section and 26.4 mm long. The strength of the two slabs with 1.04% steel ratio was controlled by flexure, and the two slabs with 1.88% ratio by punching. Percentage increases in strength and deflection at failure were larger for the specimens with the lower percentage of steel bars. These percentage increases were 27.2 versus 21.2% in strength and 32 versus 18% in deflection for 1.04 and 1.88% steel ratios respectively. The inclusion of fibres also improved the residual resistances remaining after punching failure. These residual resistances with 1.04 and 1.88% steel ratios were 21.4 and 29.2%, and 74.4 and 68.2% of the punching load without and with 1.0% steel fibres by volume respectively.

Ali (78) tested nineteen full-scale flat slab-column connections 1.69x1.69 mm, 125 mm thick, with a 150 mm square column slab. The main variables studied were, the fibre content, (0.6, 0.9, and 1.2% by volume), fibre type, location of fibres, percentage of compressive and tensile reinforcement and concentration of tensile reinforcement. It was reported that inclusion of fibres reduced all the deformations of the plain concrete specimens at any load stage. For a given serviceability criterion, the presence of fibres, increased the service load of the corresponding plain concrete specimen by 28-50%. Ductilities and energy absorption capacities were increased by 100% and 310% respectively for 0.9%steel fibre by volume. It was concluded that fibre reinforcement in slab-column connections can reduce deformations in general, increase first crack load, service load, ultimate strength, ductility and energy absorption characteristics, as well as change the mode of failure from punching to flexure.

2.4.8 Steel Fibres in Light-Weight Concrete.

The concept of reinforcing lightweight concrete with steel fibres has not yet received much research attention. The subject has only been touched by Hannant (79) in steel fibre reinforced lightweight beams, by Lamoureaux (43) in flat plates and studied by Sittampalam (80) in limited prestressed lightweight fibre concrete beams. However, due to the reduced modulus of elasticity and lower splitting tensile strength of the lightweight concrete, the effect of adding a relatively high modulus fibre, such as steel, may be more pronounced than for normal weight concrete in both flexural and punching shear.

2.4.9 Dowel and Membrane Effects.

2.4.9.1 Dowel Action Effect.

When an inclined crack crosses or extends along the slab reinforcement, dowel forces must be developed due to a relative movement which takes place between the levels of the reinforcing bar on either side of the crack, Fig. 2.5.

It is now generally accepted that the resistance to shear both in beams and slabs is significantly increased by the dowel forces of the tensile reinforcement. However, how much of the shear is carried by dowel action is uncertain. In most of the existing theories and empirical expressions, the effect of the dowel forces is neglected.

It is believed that the magnitude of the dowel forces is determined by many factors. Some of the most important factors are the following:

1. The tensile strength of the concrete along the splitting plane.
2. The strength properties of the reinforcing steel and especially the bending resistance of the steel bars.
3. The amount of the reinforcement, the diameter of the reinforcing bars, the distance between the reinforcing bars and the thickness of the concrete covering. For a given reinforcement ratio, the use of larger bar size will increase the stiffness of the dowels and thereby the length along the bear on the concrete, but the corresponding increase of bar spacing will produce a less uniform distribution of stress along the line of action. The two effects tend to cancel one another and therefore the reinforcement ratio can be considered to be an index of its effect on dowel action.
4. The bond between steel and concrete.
5. The direction of the reinforcing bars with reference to shear crack.

Analysis of data from tests on beams from many investigations, shows that dowel action contribution takes values ranging from 9 to 74% of the total shear resistance. The wide variation in the value of the dowel action is due to 1) the difficulty to reproduce in experiments the conditions which develop in the vicinity of a crack in a real structure, and 2) the failure to separate the individual contribution of dowel action and aggregate interlock leading to a considerable overestimation of dowel action.

Although, the smaller cover in slabs than in beams and the lack of stirrup reinforcement decrease the dowel force which can be developed in any given bar, dowel forces contribute more to shear capacity of slabs than beams, largely because the perimeter around which dowel action develops is large as compared to that of the critical compression zone. In a case of slab with two way reinforcement, Kinnunen (62) proposed that 30% of the total punching load could be attributed to the dowel action of the tensile reinforcement, whereas Moe (52) suggested that this effect contributes approximately 10% of the total punching load. Long and Bond (63) to account for dowel action used a correction factor of 1.30 applied to the theoretically found load, which means that 23% of the punching load can be attributed to this phenomenon. Anis (81) proposed a value of about 30% for dowel action effect. This value was verified by his test results in slabs designed to fail by the dowel action. Akatsuka and Seki (82) derived a formula for the dowel action effect:

$$S_s = \sigma_t \pi \ell_o (D + 2\sqrt{3}\, d + \ell_o) \quad \text{for } \phi = 30^\circ$$

where S_s = share of shearing force due to dowel action.

D = diameter of loading disc.

d = effective depth of slab.

ℓ_o = range of dowel action.

ϕ = angle of inclined crack.

σ_t = concrete tensile strength.

The addition of fibres to concrete is known to control cracking and increase the tensile strength of concrete (16), and the bond resistance

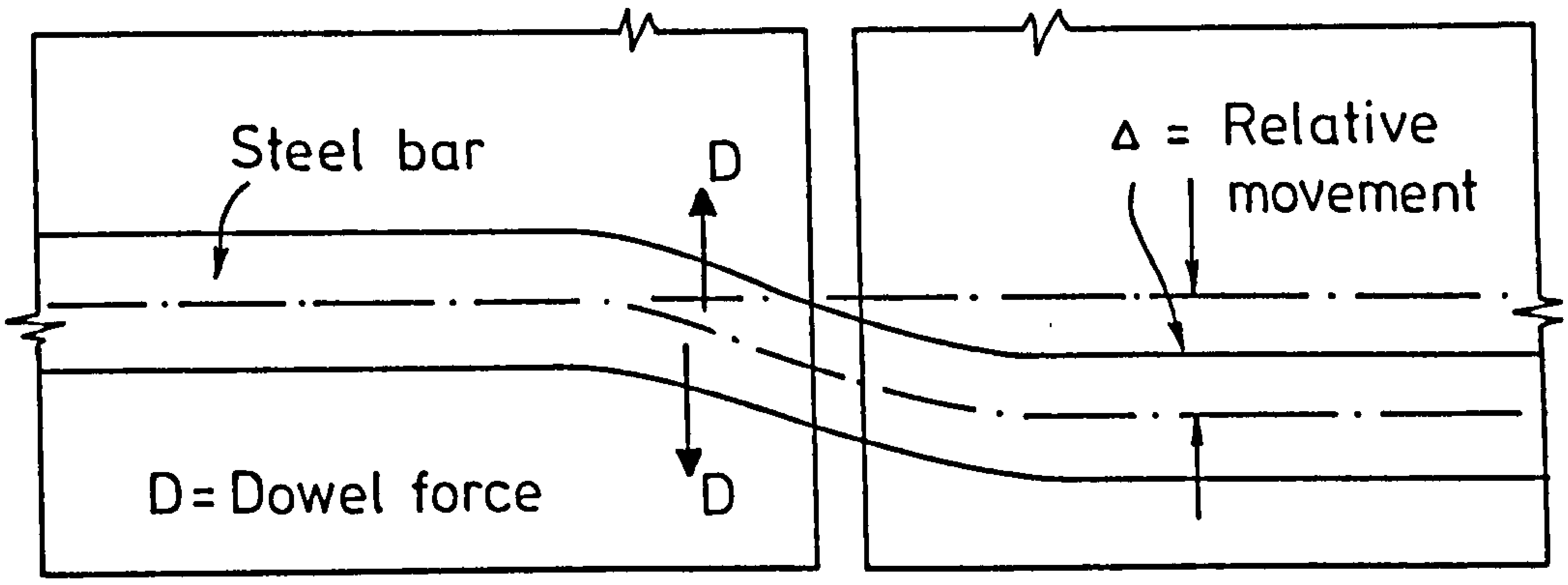

a) Dowel forces

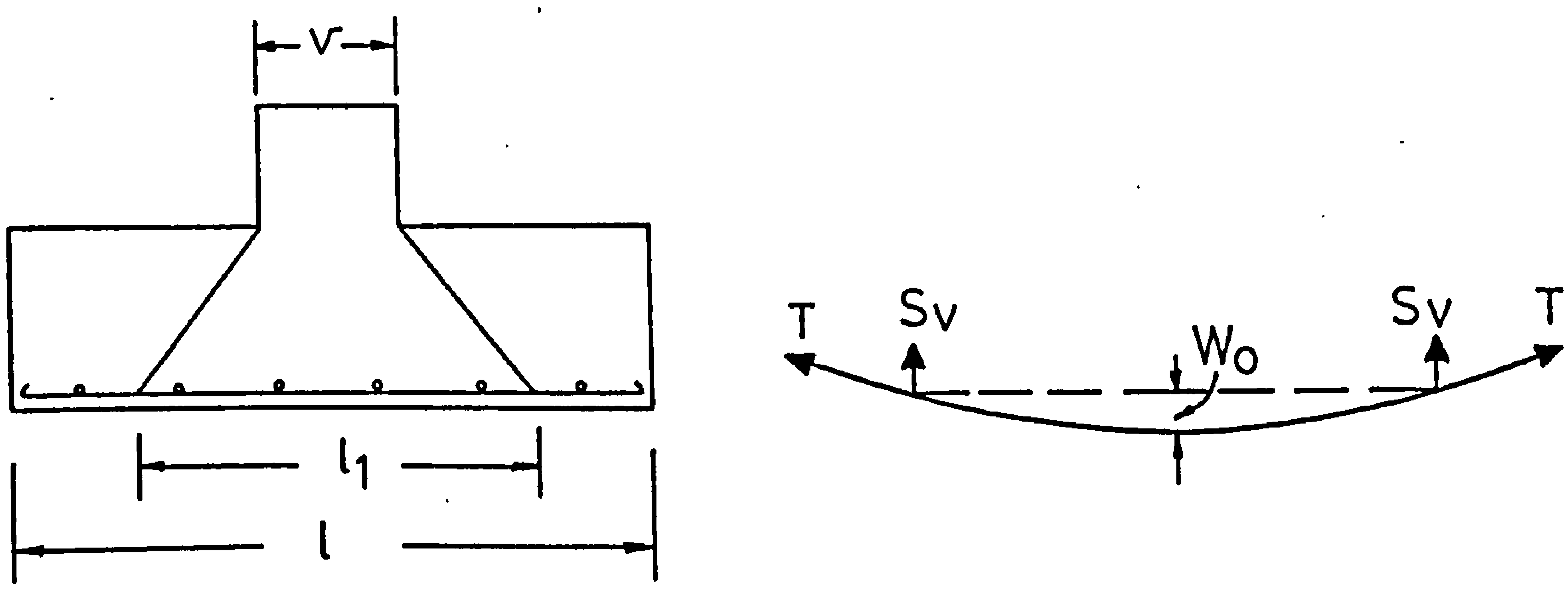

b) Membrane action of tensile reinforcement

FIG. 2-5 DOWEL AND MEMBRANE FORCES

of the reinforcement (83), and therefore an increased contribution of the dowel forces is expected. Swamy and Bahia (84) reported an increase in the ultimate dowel strength of beams due to fibres; this increase varies almost linearly with the flexural strength of the composite. Criswell (77) reported that the dowel forces in a flat slab-column connection will increase 2.5-3 times when 1% of steel fibres by volume is used. This increase was recorded for additional column movement of 2.54 mm beyond punching point. Less increase resulted when the columns were pushed further down and the fibres became unbonded. Similarly, an increase in dowel action was reported by Ali (78) at about 2 and 3 times over the plain concrete slab-column connection when 0.6 and 0.9% crimped fibres by volume were used.

2.4.9.2 Tensile Membrane Action in Simply Supported Slabs.

When a slab under load has deflected, part of the applied load is carried through extensional forces in the plane of the slab. The maximum possible value of these membrane forces may easily be obtained by assuming it to be equal to the total vertical component of the forces in the tensile reinforcement Fig. 2.5.b. Moe (52) calculates these forces by using the formula

$$S_v = 4\,T\,\frac{\omega_o}{(\ell-r)/2}$$

where ω_o = the measured centre deflection.

$T = \rho\,\ell_1\,d\,f_y$

where ℓ_1 is shown in Fig. 2.5.b.

The membrane forces were calculated, by using the above formula, for a number of slabs, but in no case exceeded 6% of the total load. Kinnunen (62) found that the vertical force due to membrane effect varies from 3 to 8%of the total load and proposed an average value of 5%.

2.4.10 Real Structures - Test Models.

Simple models of the prototype connection are usually used to obtain the ultimate punching strength; they also serve as the basis of the ultimate punching strength theories and design methods. However, these models show two major differences from real structures with reference to ultimate strength. The first difference is that a real structure can support an increased punching load due to compressive membrane actions within the slab caused by the inplane restraints. The second major difference is that, when in the models the local flexural strength is exhausted, no further shear load can be applied, whereas in a real structure increases of shear are possible due to tensile membrane action caused by the restraints.

The existence of such membrane effects in slabs with inplane restraints and subjected to concentrated load has been demonstrated by a number of investigators (85,86,87,88,89).

The load-central deflection relationship for a slab restrained against inplane movements at its boundaries is shown in Fig.2.6. In the early stages of loading the restraint against outward movement causes compressive membrane action which strengthens the slab allowing it to develop the maximum load represented by A. After the ultimate load has been reached, the supported load decreases rapidly with further deflection, due to the reduction in the compressive membrane forces and reaches point B. At that point the boundary restraints begin to resist inward movement at the edges. Beyond point B, the load is carried by the reinforcement acting as a hanging net and with further deflection, the load carried increases until the reinforcement starts to fracture at C.

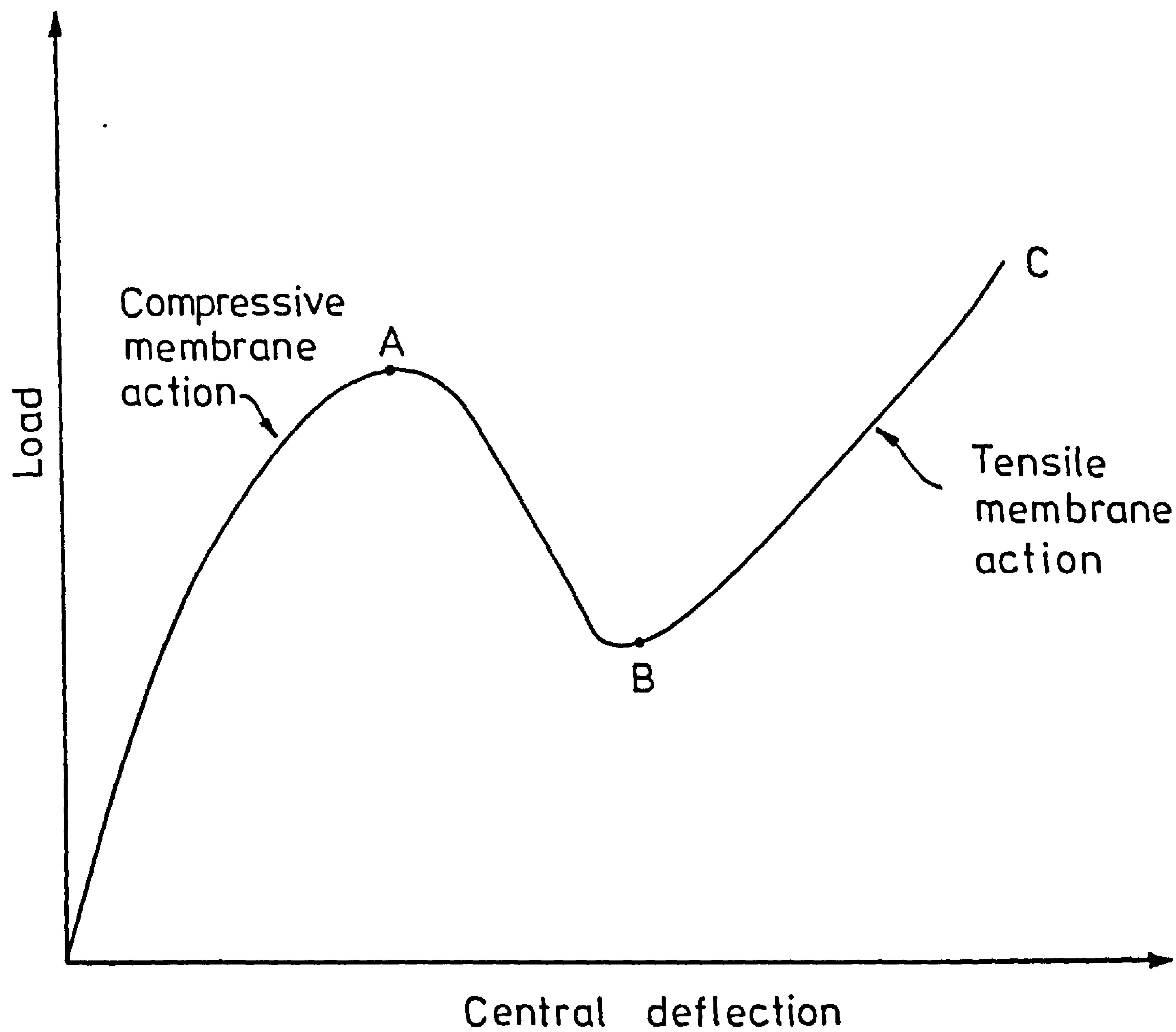

FIG. 2-6 LOAD - DEFLECTION CURVE OF SLAB WITH FULL EDGE RESTRAINT

Taylor and Hayes (86) reported that compressive membrane action increased the punching shear strength by 24-60% when the corresponding simply supported slabs were near to flexural failure at collapse, but only 0-16% when the corresponding simply supported slabs were not near to flexural failure at collapse. Lander et al. (90) found that punching failure forces obtained by test on a reinforced concrete flat slab system supported by columns of different sizes (100,200,240 and 320 mm in diameter) were of about 20% higher on average than those obtained by tests on circular reinforced concrete slabs.

CHAPTER 3.

MIX DESIGN AND MATERIAL PROPERTIES.

3.1 Introduction.

Since lightweight aggregates became available for use one of the main objects of both manufacturers and investigators has been to produce lightweight aggregate concrete of strength suitable for structural work in reinforced and prestressed concrete. There is considerable evidence to show that lightweight concrete can provide an alternative construction material to normal concrete from both economic and engineering performance points of view.

The main objective in mix design of lightweight concrete is to produce a workable mix having a minimum cement content with a density lower than that of normal concrete and with a strength similar to that found in the latter. It has been found that the compressive strength of lightweight concrete is affected by the same factors as normal concrete, the two main factors of those being the cement content and total water-cement ratio. Because of differences in the properties of various types of lightweight aggregate, separate mix designs are required for each kind of aggregate. However, in British practice the broad basis of natural-aggregate mix design has been applied to lightweight concretes (2,6). Mixes for structural lightweight concrete frequently incorporate natural sand as the fine aggregate with or without a pozzolan such as fly ash for purposes of economy and workability.

Fibre reinforced cement mortar and concrete made of natural aggregates have been shown to be practical in mixing and handling by a considerable amount of laboratory tests and field projects, but only a limited number of work has been carried out on fibre reinforced lightweight concrete showing that the effect of steel fibre addition is very similar to the effect of fibre addition to normal aggregate concrete (98,101,102).

Fibre reinforced concrete requires a considerably greater amount of fine material in the mix than plain concrete, for convenient handling and placing by current procedures and equipment. Recent research has shown that the high amount of cement content used as fine material in mix design of fibre reinforced concrete can be partially substituted by the use of fly ash.

One of the main parameters influencing the strength and workability of the fibre concrete, as in the case of plain concrete, is the water-cement ratio. Since the incorporation of fibres reduces the workability of the mix, a water reducing agent can be used so that the water-cement ratio remains the same as in plain mix and the workability reaches the required degree.

In this investigation fly ash as a substitute for cement, sand as fine aggregate, Lytag as coarse aggregate and a water reducing agent have been used. The aim was to achieve a good workable sand-lightweight concrete mix having a characteristic cube strength around 45 N/mm^2 at 28 days. Four different types of steel fibres with different shapes and aspect ratios were used with this mix. The results of various tests with and without fibre mixes were compared and some properties were measured and recorded.

3.2 Experimental Programme.

A series of preliminary tests was carried out to determine the best mix, to suit the twin demands of workability and strength. The effective water- (cement+fly ash) ratio was varied from 0.35 to 0.50. The amounts of sand, Lytag coarse aggregate and cement+fly ash were kept constant.

Then a control mix and five fibre concrete mixes were carried out to determine the effect of fibre type and percentage on various properties of fibre mixes as compared to those of the control mixes.

3.2.1 Materials.

Details of the materials used throughout the investigation are given below. In general, the same type of materials were used, although,by necessity, the materials had to be used from different deliveries.

3.2.1.1 Cement.

Ordinary Portland cement was used in this investigation. The cement was considered to comply with B.S.12 (103).

3.2.1.2 Pulverised Fly Ash (P.F.A.)

In this investigation 30% by weight of the cement was replaced by P.F.A. This amount of P.F.A. has been found to give optimum strength and elasticity properties for concrete (104).

The P.F.A. used in this work was obtained from Ferry Bridge Power Station. The chemical composition of the P.F.A. used is given in Table 3.1, and this generally complied with British Standards 3892:1965 (105) limits.

3.2.1.3 Sand.

Washed natural river sand was used throughout the investigation. The sand used was between zone 2 and 3 of B.S.882 (106) and used in the laboratory in normal concrete mixes. The sand was dried in a warm room before mixing. The results of the sieve analysis carried out and the grading curve for the sand are shown in Fig.3.1.

3.2.1.4 Coarse Aggregate.

The coarse aggregate used throughout the investigation was lightweight coarse aggregate (Lytag) of 14 mm maximum size. The Lytag grading curve is shown in Fig.3.2 and falls in the zone specified by B.S.3797 (107).

Plate 3.1 shows a picture of this aggregate. The loose bulk density and the total water absorption of the Lytag coarse aggregate, as specified by the manufacturers, were 800 Kg/m^3 and 12% respectively.

Table 3.1 Chemical Compositions of the P.F.A.

% Silica as SiO_2	56.2
% Alumina as $Al_2 O_3$	26.2
% Iron as $Fe_2 O_3$	7.3
% Titanium as $Ti_2 O_3$	1.0
% Phosphorous as P_2O_5	0.3
% Calcium as $Ca O$	1.6
% Magnesium as $Mg O$	0.7
% Sodium as $Na_2 O$	2.5
% Potassium as $K_2 O$	1.3
% Sulphur as SO_3	0.7
Loss on Ignition	2.2

Specific surface = 3690 cm^2/gm

Density = 2.17 gm/cm^2

3.2.1.5 Steel Fibres.

Five types of steel fibres were used in this investigation with equivalent diameters ranging from 0.418 to 0.760 mm, lengths ranging from 25.0 to 53 mm and with aspect ratios ranging from 50 to 100. Plate 3.2 shows all types of fibres used. The average ultimate stress of crimped, hooked and paddle fibres was determined by testing six fibres to failure using the Hounsfield W type Tensometer. The details of the fibres are shown in Table 3.2.

3.2.1.6 Steel Reinforcement.

The type of steel reinforcement used in this investigation was cold-worked ribbed bars with a specified characteristic strength of 460 N/mm^2.

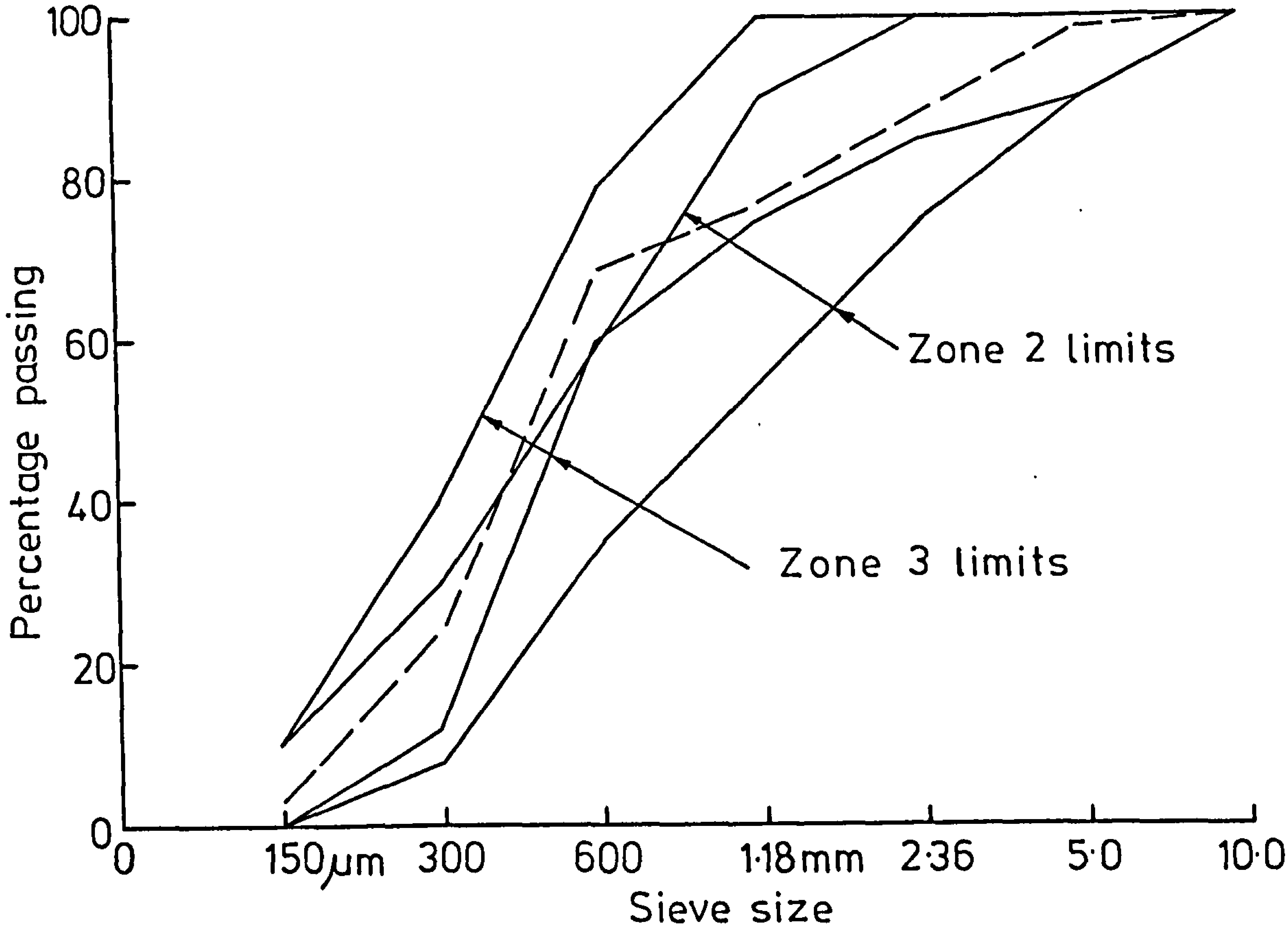

FIG. 3-1 GRADING CURVE FOR SAND

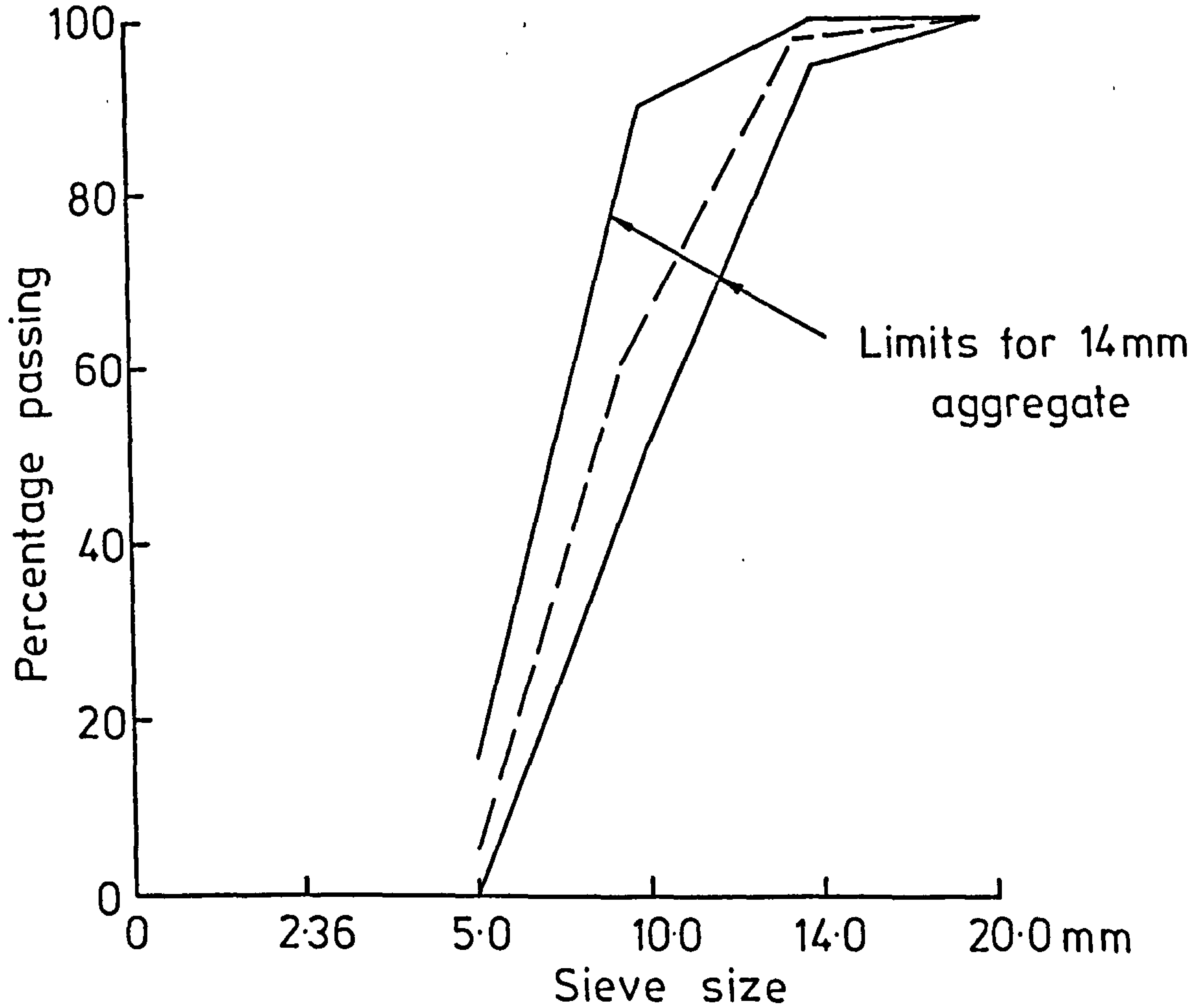

FIG. 3-2 GRADING CURVE FOR LYTAG AGGREGATE

PLATE 3-1 LYTAG AGGREGATES

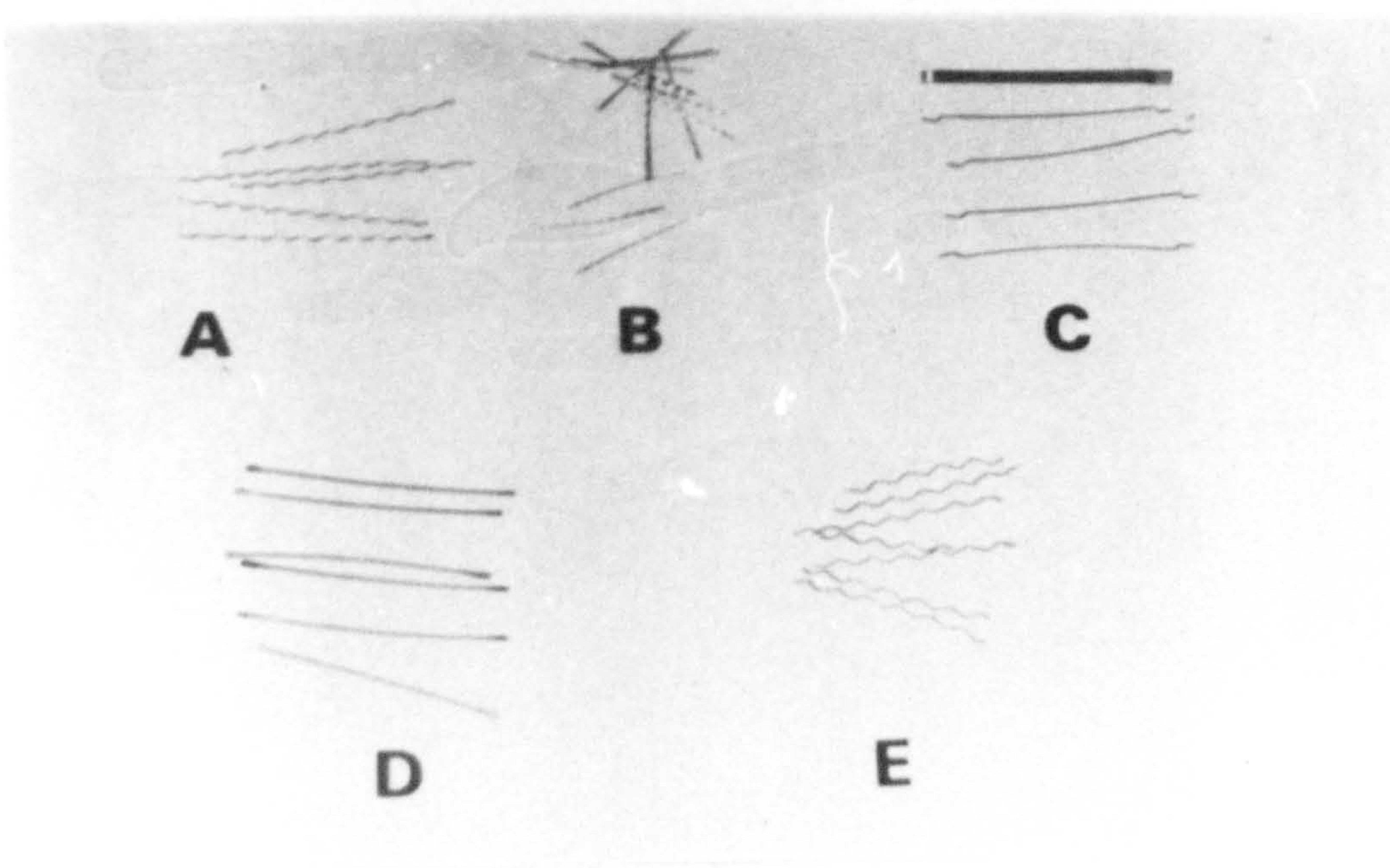

A. Crimped B. Japanese C. Hooked
D. Paddle E. Crimped

PLATE 3-2 FIBRE REINFORCEMENT

Table 3.2 Properties of the fibres.

Fibre Type	Cross Section	Length, ℓ_f mm	Equivalent Diameter, d_f mm	Aspect Ratio (ℓ_f/d_f)	Ultimate Tensile Strength N/mm^2
Crimped	Round	50	0.50	100	1820
Japanese	Rectangular	25	0.418	60	-
Hooked	Round	50	0.50	100	1100
Paddle	Elliptical	53	0.76	70	952
Crimped	Round	38	0.425	90	-

Table 3.3 Lytag-Sand-Fly Ash Mixes.

Mix*	Effective water/ cement ratio	Slump mm	Compressive strength, N/mm^2				Dry Density at 28 days Kg/m^3
			3d	7d	14d	28d	
A_1	0.35	30	29.0	41.6	49.0	52.6	1875
A_2	0.37	90	26.2	37.6	44.6	48.6	1865
A_3	0.40	160	24.2	37.0	43.2	45.3	1853
A_4	0.45	230	18.3	27.1	37.0	39.7	1846
A_5	0.50	Collapse	13.7	23.9	28.7	33.0	1837

* O.P.C.: P.F.A. : Sand: Lytag: 287: 123: 560: 696 (Kg/m^3).
Water Reducing Agent (Febflow) = 2.5 cc/1 Kg (cement + P.F.A.)

FIG. 3-3 STEEL STRESS-STRAIN CURVES

Two sizes were used, 10 mm diameter as tension reinforcement and 8 mm as compression reinforcement. Fig. 3.3 shows the stress-strain curve of each size of bar. The average ultimate stress of the 8 mm and 10 mm diameter bars was 570 N/mm^2 and 535 N/mm^2 respectively.

3.2.2 Mix Design.

The results of preliminary tests carried out to determine the mix with the required compressive strength of 45 N/mm^2 are shown in Table 3.3. The basic mix proportions used were based on manufacturer's recommendations while the water - (cement + PFA) ratio was varied from 0.35 to 0.50.

Mix A3 with a 28 days compressive strength of about 45 N/mm^2 and with a slump of 160 mm was finally selected to be used in most slabs of this investigation.

3.2.3 Mixing Procedure.

The Lytag aggregates used were partially soaked by rain or by water in the stockpile. Just before mixing the water content was determined using the "Speedy Moisture Tester" (0.% to 20% model). Thus the quantity of added water in each mix was the effective water plus 12% of the dry weight of coarse lightweight aggregate minus the water already present.

Concrete was mixed in a horizontal pan-type mixer. The materials, except fibres, were mixed for about one and a half minutes dry, water was then added and mixing continued for another two minutes until a good homogeneous mix was produced. In the case of fibre concrete, the fibres were subsequently added through a mechanical dispenser, which ensured a reasonably good fibre distribution; mixing was continued until the fibre concrete was uniform in appearance. Balling of the fibres was experienced during mixing, especially when crimped fibres were used, although not very significantly.

After mixing the concrete was poured into steel moulds, (which were covered with a thin layer of oil to prevent any bond between the mould and the concrete) in two layers and compacted using an electrical large table vibrator (3.05x120m). The specimens were left under polythene sheets in the laboratory for 24 hours, they were demoulded and stored in the laboratory under uncontrolled conditions until they were tested.

3.2.4 Size of Test Specimens and Test Procedure.

3.2.4.1 Compression Test.

For this test three cubes were used. The size of the cubes was 100x100x100 mm, and the compression test was carried out at a stress rate of 15 N/mm^2 per minute according to B.S.1881 Part 4 (108).

3.2.4.2 Flexural Test.

The flexural test was carried out on prisms and plates with a span of 400 mm under third point loading. Three prisms of 100x100x500 mm size and twelve plates of 25x100x500 mm size were tested at a stress rate of 16 N/mm^2 per minute according to B.S.1881:Part 4 (108). In the case of 25 mm thickness plates six of them were tested with cast face as tension side and six with cast face as compression side.

3.2.4.3 Splitting Test (Indirect Tensile Stress).

For this test three cylinders were used. The size of the cylinder was 100 mm diameter x 200 mm length, and the test was carried out at a stress rate of 1.50 N/mm^2 per minute according to B.S.1881:Part 4 (108).

3.2.4.4 Static Modulus of Elasticity.

The test was carried out on two 100x100x300 mm prisms according to B.S.1881 Part 4 (108). The strains were measured over a gauge length of 100 mm (middle third of the specimens) with Demec gauge, on two opposite sides of each specimen.

3.2.4.5 Unrestrained Shrinkage.

Unrestrained drying shrinkage was measured on a 100x100x300 mm prism under uncontrolled curing conditions in the laboratory. The shrinkage strains were measured over a gauge length of 100 mm with Demec gauge, on two opposite sides of the specimen.

3.3 Discussion of Test Results.

3.3.1 Properties of the Fresh Concrete Mixes.

The practical difficulties in the application of steel fibre concrete mixes are compactibility and adequate workability. The compactibility characteristics of fibre concrete differ from those of plain concrete. In the case of a plain concrete mix the workability is normally sufficient to permit compaction by vibration. However, in the case of fibre concrete mixes, it may be difficult to achieve sufficient workability to permit compaction by vibration. This may be due to the fact that there is a strong tendency for the fibres to form balls, especially with long and wavy fibres. In addition, the introduction of fibres results in the entrainment of additional air.

In these tests, a plain lightweight concrete mix of high workability was used, bearing in mind the intended incorporation of fibres. The increased workability was obtained by the direct substitution of 30% by weight of the total cement content with P.F.A. and by using a water reducing agent (Febflow). In the case of fibre concrete an increased amount of Febflow was used to obtain the desirable workability. The workability was measured by the slump and Vebe tests. Table 3.4 shows the results of these tests for the control and fibre mixes.

It can be seen from Table 3.4 that the compactibility achieved with 1.0% fibres by volume was good for structural lightweight concrete. Mix C

Table 3.4 Properties of Fresh Plain and Fibre Lightweight Concrete Mixes.

Mix*	Fibre Type	$\frac{\ell_f}{d_f}$	Fibre Percentage	Febflow cc/1 Kg (Cement P.F.A.)	Slump, mm	Vebe time, Sec.
A	-	-	0.0	2.5	160	1
B	Crimped	100	0.5	4.0	90	3
C	Crimped	100	1.0	5.5	40	7
D	Japanese	60	1.0	3.5	65	4.5
E	Hooked	100	1.0	3.5	50	5.5
F	Paddle	70	1.0	3.5	55	5.5
G	Crimped	90	1.0	4.0	70	3.5

* O.P.C: P.F.A. : Sand : Lytag : 287 : 123 : 560 : 696 (Kg/m^3)
Effective Water/(Cement+P.F.A.) ratio = 0.40

with 1% crimped fibres by volume was less workable than mixes with other types of fibres, although a greater amount of Febflow was used, because of the problem of balling of fibres due to the nature of the fibre.

3.3.2 Properties of the Hardened Concrete.

3.3.2.1 Compressive Strength.

It is established that the compressive strength of structural lightweight concrete varies similar to that of natural aggregate concrete under similar curing conditions (6,10,11,93). The development of compressive strength of plain Lytag concrete and fibre Lytag concrete is shown in Table 3.5 and Fig. 3.4. Tables 3.6 and 3.7 show the compressive strength of each mix as percentage of its 28-days strength and the compressive strength of fibre mixes as compared to that of plain concrete mix respectively. It can be seen that inclusion of 0.5% by volume crimped fibres decreased the 28-day compressive strength of plain concrete by 3.3% wheras inclusion of 1.0% by volume increased the strength by 4.0%. With 1% fibres, Japanese and paddle fibres decreased the strength by 2.4 and 5.5% respectively whereas hooked fibres increased the 28-day strength by 1.8%. Sittampalam (80) found that 1% by volume of crimped and Japanese fibres increased the 28-day strength of sand-Lytag mixes by 10.3 and 2.4% respectively. Jojagha (109) found an increase in 28-day strength of 15.2% and 3.5% with Japanese and hooked fibres respectively and a range of 3.6% decrease and 5.1% increase with paddle fibres. Richie and Al-Kayyah (101) reported that the effect of fibre inclusion on compressive strength is different for different types of fibres, and that steel fibres produced little or no increase with Lytag concrete. From Table 3.6 it can be seen that at 540 days the compressive strength was 16.1% greater than 28-day strength for plain mix and about 15% for fibre mixes, but the compressive strength of plain mix seems to

Table 3.5 Compressive Strength of Sand-Lightweight Concrete without and with fibres.

Time / Mix	Compressive Strength N/mm^2						
	1d	7d	28d	90d	180d	360d	540d
A	7.4	37.0	45.3	46.0	51.3	50.5	52.6
B	7.6	37.6	43.8	47.8	49.1	48.8	50.9
C	9.1	40.5	47.1	52.6	-	-	-
D	8.5	34.5	44.2	49.9	47.3	50.8	50.5
E	8.75	38.0	46.1	50.5	49.6	52.4	52.8
F	8.2	35.9	42.8	48.5	47.3	51.4	49.3

Table 3.6 Compressive strength at different ages as a percentage of 28 days compressive strength.

Time / Mix	1d	7d	28d	90d	180d	360d	540d
A	16.33	81.67	100	101.5	113.2	111.4	116.1
B	17.35	85.85	100	109.1	112.1	111.4	116.2
C	19.32	85.98	100	111.67	-	-	-
D	19.23	78.06	100	112.9	107.0	114.9	114.2
E	18.98	82.42	100	109.5	107.6	113.7	114.5
F	19.16	83.88	100	113.3	110.5	120.1	115.2

Table 3.7 Percentage increase of compressive strength of fibre mixes over that of plain concrete, at various ages.

Mix \ Time	1d	7d	28d	90d	180d	360d	540d
A	0.0	0.0	0.0	0.0	0.0	0.0	0.0
B	2.7	1.6	-3.3	3.9	-4.3	-3.4	-3.2
C	22.9	9.4	4.0	14.3	-	-	-
D	14.9	-6.8	-2.4	8.5	-7.8	-1.0	-3.9
E	18.2	2.7	1.8	9.8	-3.3	2.1	0.4
F	10.8	-3.0	-5.5	5.4	-7.8	0.2	-6.3

Table 3.8 Dry Density of Various Mixes (kg/m^3)

Mix \ Time	1d	7d	28d	90d	180d	360d
A	1995	1856	1830	1815	1810	1807
B	2047	1904	1875	1862	1856	1854
C	2071	1937	1911	1903	-	-
D	2066	1935	1910	1900	1896	1895
E	2062	1929	1905	1891	1884	1882
F	2049	1920	1897	1886	1880	1879

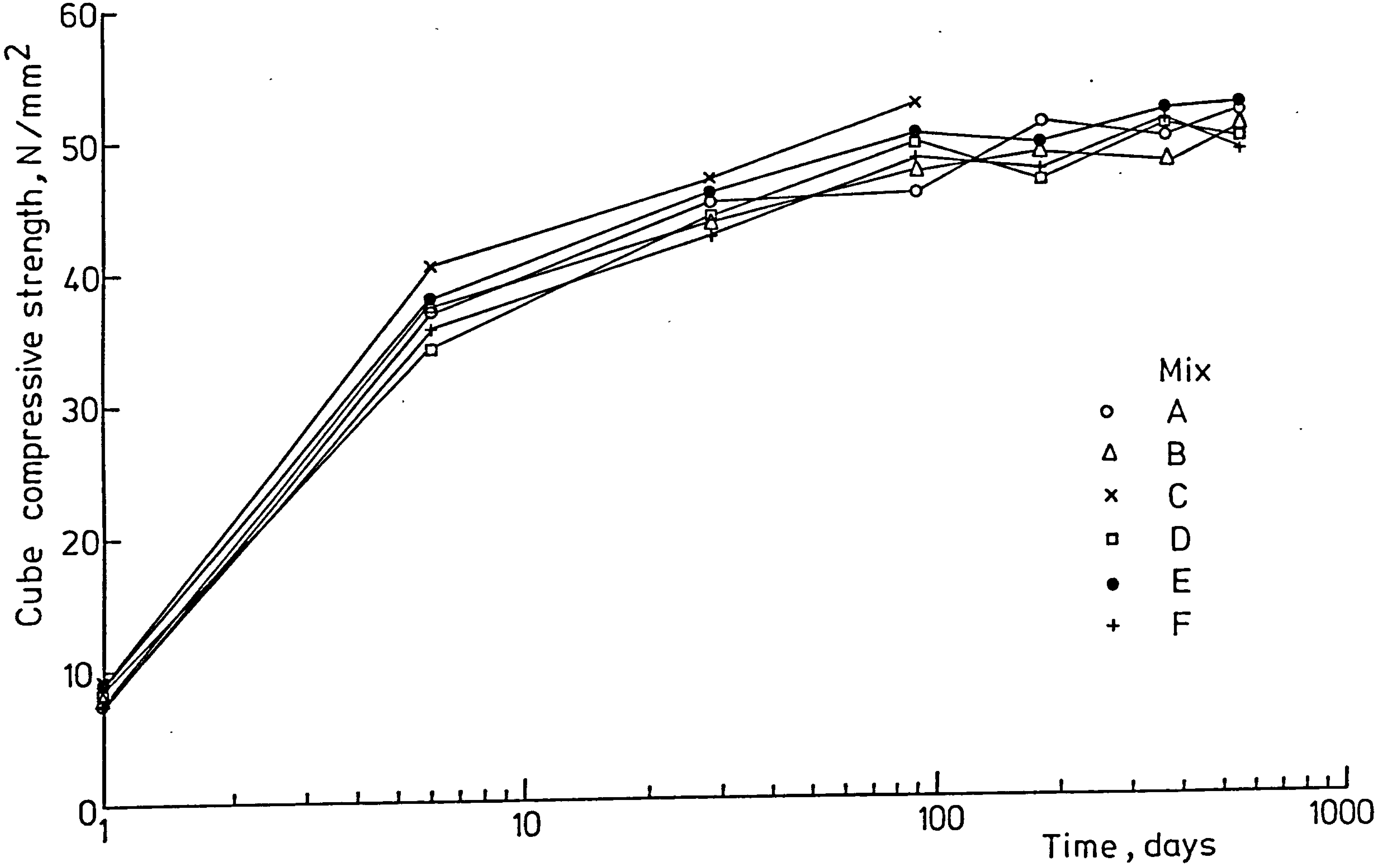

FIG. 3-4 COMPRESSIVE STRENGTH OF VARIOUS MIXES WITH TIME

stabilize after about 180 days whereas the strength of fibre mixes after 90 days. From Table 3.7 it can be seen that the one-day compressive strength of various fibre mixes is greater than that of plain mix by 10.8-22.9% with 1% fibres, whereas the 540-days strength of fibre mixes, in most cases, is less than that of plain mix.

In normal weight concrete, published results on the effect of fibre reinforcement on compressive strength seem to contradict each other. A variation range of 15% has been reported (29,75,78) in the compressive strength by using 0.6 to 1.2% by volume crimped fibres.

The presence of steel fibres enabled the cubes to keep their integrity even after failure, while plain concrete cubes disintegrated after the maximum load was reached (Plate 3.3).

From what has been discussed so far, it can be said that the effect of fibre reinforcement on compressive strength of lightweight concrete depends upon the particular type and percentage of fibre used. This effect is rather small so that there is little point in including fibres in lightweight concrete to increase the compressive strength. The compressive strength development of fibre reinforced lightweight concrete is almost similar to that of plain concrete mix. The inclusion of fibres can prevent the spalling of the unreinforced specimens and provide increased ductility in a compressive failure.

3.3.2.2 Dry Density.

Table 3.8 shows the dry density of plain and fibre lightweight concrete mixes found as an average of three 100x100x100 mm cubes. The increase in density at 28 days because of the inclusion of fibres is about 2.4% for 0.5% by volume crimped fibres and from 3.66% to 4.4% for mixes with 1% by volume (of about 4.2% by weight) fibres. It can be seen that after 180 days the density is almost constant.

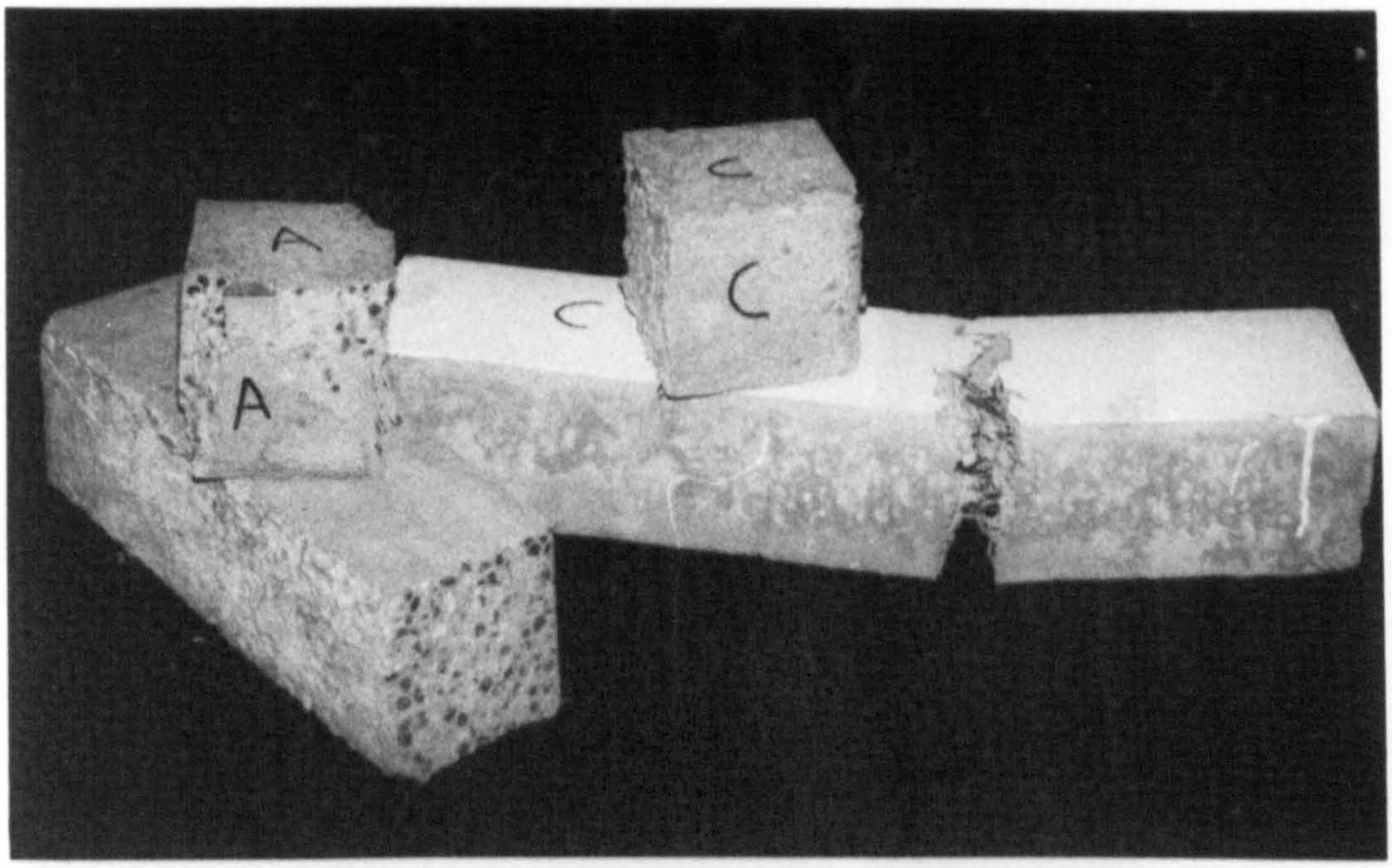

PLATE 3-3 PLAIN AND FIBRE CONCRETE CUBES AND PRISMS AFTER TESTING

3.3.2.3 Flexural Strength (Modulus of Rupture).

Tensile strength is one of the basic properties of concrete and of a large number of concrete structures. The tensile strength appears to be an important criterion of the liability to cracking in concrete structures. The tensile strength of concrete depends primarily on the tensile strength of aggregate, the tensile strength of cement paste and the aggregate matrix bond.

The values of the first crack and ultimate flexural strength of plain lightweight and fibre concrete mixes used in this investigation are shown in Table 3.9. The ultimate values are also plotted against age in Fig. 3.5. Table 3.10 shows the first crack flexural strength of various mixes as a percentage of the corresponding ultimate flexural strength at each age. Table 3.11 shows the percentage of ultimate strength, at each age, to 28-days ultimate flexural strength for each mix. Table 3.12 shows the percentage increase of ultimate and first crack flexural strengths of fibre mixes over that of plain concrete at various ages.

The ultimate flexural strength of plain sand-lightweight concrete at 28 days is 3.24 N/mm^2, less than the corresponding value of plain normal concrete of almost equal compressive strength which is 3.84 N/mm^2 (78). In lightweight concrete because of the higher aggregate-matrix bond strength the tensile strength is largely determined by the tensile strength of the lightweight aggregates which is lower than that of the gravel aggregate. The decrease in the flexural strength of lightweight relative to normal weight concrete when the concrete is dry is a feature of lightweight concrete, and is due to shrinkage (93). As the concrete dries, shrinkage stresses are set up, which may be sufficiently high to cause microcracks in the concrete. The smooth crack surfaces encountered in

Table 3.9 Ultimate and first crack flexural strength (within brackets) of sand-lightweight concrete without and with fibres.

Time / Mix	Ultimate and first crack flexural strength in N/mm^2							
	1d	3d	7d	28d	90d	180d	360d	540d
A	1.08 (1.08)	-	2.90 (2.90)	3.24 (3.24)	4.84 (4.84)	4.86 (4.86)	4.70 (4.70)	4.62 (4.62)
B	1.80 (1.60)	4.00 (3.20)	5.12 (4.42)	5.70 (4.12)	5.65 (5.20)	5.76 (5.00)	5.52 (4.74)	5.68 (5.00)
C	2.36 (2.08)	4.92 (3.96)	6.10 (4.88)	6.72 (5.56)	6.96 (5.42)	-	-	-
D	1.65 (1.65)	3.84 (3.84)	4.84 (4.68)	5.36 (5.36)	5.78 (5.78)	5.62 (5.46)	5.80 (5.40)	5.70 (5.70)
E	2.26 (1.90)	5.32 (4.52)	6.15 (4.74)	7.10 (5.44)	7.24 (5.24)	7.08 (4.74)	7.16 (5.12)	6.96 (5.86)
F	2.02 (1.72)	5.08 (4.62)	6.04 (5.12)	6.82 (5.32)	6.92 (5.76)	7.04 (5.94)	6.86 (5.12)	6.72 (5.28)

Table 3.10 % First crack flexural strength/ultimate flexural strength ratio.

Time / Mix	1d	3d	7d	28d	90d	180d	360d	540d
A	100	-	100	100	100	100	100	100
B	89	81	87	72	92	87	86	88
C	88	80	80	83	78	-	-	-
D	100	100	97	100	100	97	96	100
E	84	85	77	76	72	67	72	84
F	85	91	85	78	83	84	74	78

Table 3.11 Ultimate flexural strength at different ages as a percentage of 28 days ultimate flexural strength.

Mix \ Time	1d	3d	7d	28d	90d	180d	360d	540d
A	33.3	-	89.5	100	149.4	150.0	145.1	142.6
B	31.6	70.1	89.8	100	99.1	101.0	96.8	99.6
C	35.1	73.2	90.7	100	103.6	-	-	-
D	30.8	71.6	90.3	100	107.8	104.8	108.2	106.3
E	31.8	74.9	86.6	100	102.0	99.7	100.8	98.0
F	29.6	74.5	88.6	100	101.5	103.2	100.6	98.5

Table 3.12 Percentage increase of ultimate and first crack (within the brackets) flexural strength of fibre mixes over that of plain concrete at various ages.

Mix \ Time	1d	7d	28d	90d	180d	360d	540d
A	0.0 (0.0)	0.0 (0.0)	0.0 (0.0)	0.0 (0.0)	0.0 (0.0)	0.0 (0.0)	0.0 (0.0)
B	66.6 (48.2)	76.5 (59.4)	75.9 (27.1)	16.7 (7.4)	18.5 (2.8)	17.4 (1.0)	22.9 (8.2)
C	118.5 (92.3)	110.3 (68.3)	107.4 (71.6)	43.8 (12.0)	- -	- -	- -
D	52.7 (52.7)	66.9 (61.4)	65.4 (65.4)	19.4 (19.4)	15.6 (12.3)	23.4 (19.1)	23.4 (23.4)
E	109.2 (75.9)	112.0 (63.4)	119.1 (67.9)	49.5 (8.2)	45.6 (-2.4)	52.3 (8.9)	50.6 (26.8)
F	87.0 (59.2)	108.3 (76.5)	110.5 (64.2)	43.0 (19.0)	44.9 (22.2)	45.9 (8.9)	45.5 (14.3)

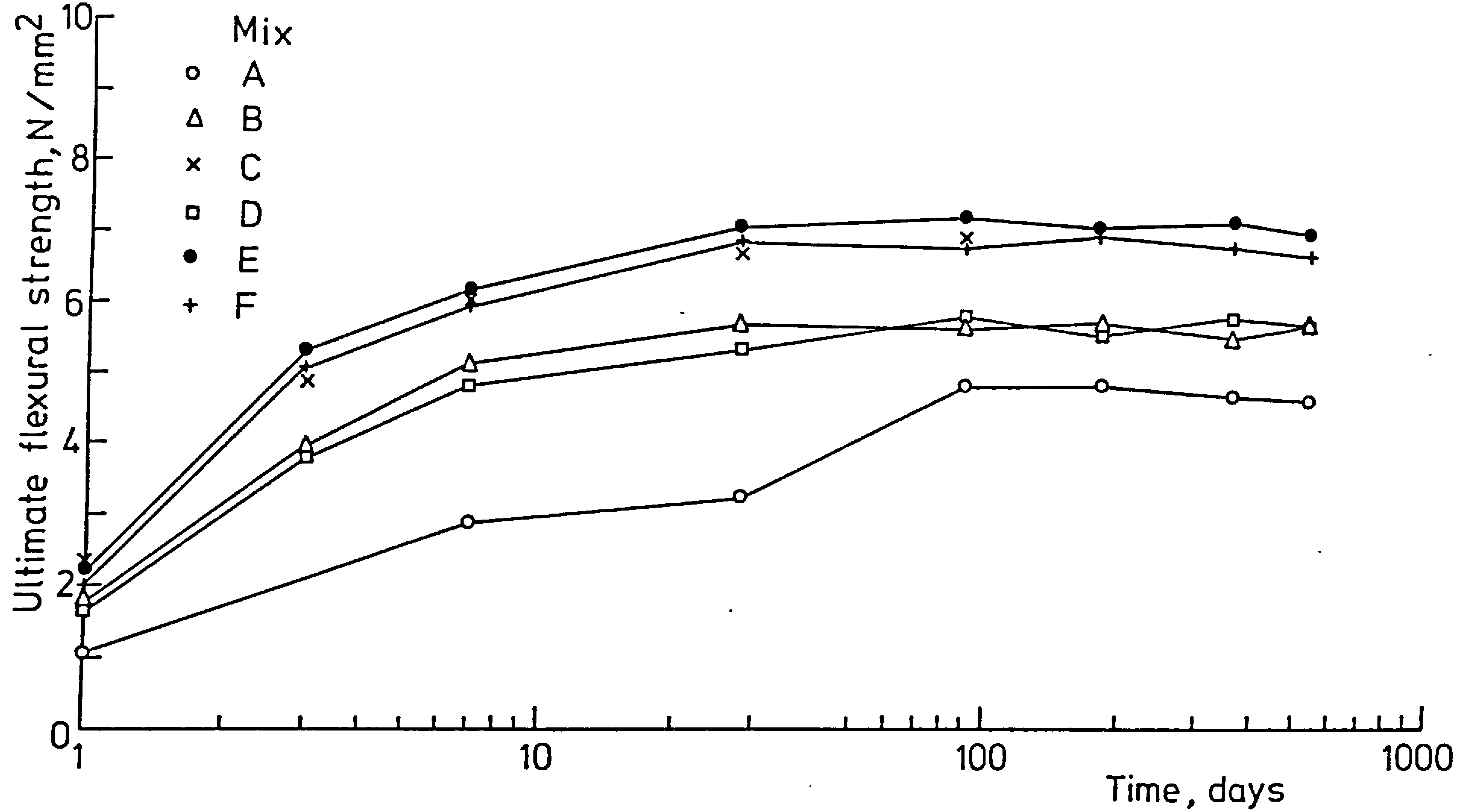

FIG. 3-5 ULTIMATE FLEXURAL STRENGTH OF VARIOUS MIXES WITH TIME

lightweight aggregate concrete suggest the possibility of these cracks forming through the aggregates particles, while this is most unlikely to happen with good gravel aggregates. On the other hand, the tensile strength under continuous moist conditions for lightweight and normal concrete of equal compressive strength is approximately the same (2).

From Table 3.11 it can be seen that there is a significant increase in 90 days flexural strength of plain lightweight concrete over the strength at 28 days, of about 49.4%. The corresponding increase at 540 days is 42.6%. This increase in the case of 'Solite' lightweight concrete of 41 N/mm^2 and 52 N/mm^2 compressive strength (11) at 540 days was about 105% and 65% respectively for specimens cured under uncontrolled laboratory conditions.

The first crack strength was difficult to detect by visual inspection for the plain specimens; the failure was always brittle and the crack was through the lightweight aggregates (Plate 3.3).

It is known that the relationship between the splitting tensile strength or the modulus of rupture and the compressive strength of concrete approximately follows the expression:

$$\sigma_{mu} \text{ or } f_{ct} = K \sqrt{f_{cu}} \qquad (3.1)$$

where σ_{mu} is the modulus of rupture in N/mm^2

f_{ct} is the splitting tensile strength in N/mm^2

f_{cu} is the cube strength in N/mm^2

and K is a constant.

Orangun (93) found that K is equal to 0.67 for Lytag lightweight concrete. Equation (3.1) with K = 0.67 overestimates the 28 days flexural strength by 39.2%. The value of K suggested by Orangun was the average of both the moist and dry specimens and obviously this value underestimates the strength in the first case and overestimates in the second case, respectively.

With fibre reinforcement, the flexural strength is influenced by the geometry of the fibre (110), the size and shape of aggregate and the volume fraction (45). From Table 3.12 it can be seen that there is a considerable increase in ultimate flexural strength at 28 days due to addition of fibres. The percentage increase was 75.9 for mix B with 0.5% crimped fibres and 107.4 for mix C with 1.0% crimped fibres by volume. Mix D with Japanese fibres showed a lower percentage increase because of their shorter length (25 mm) while mixes E and F with 1.0% hooked and paddle fibres showed similar behaviour as mix C with crimped fibres. Sittampalan (80) found a 75-100% increase in flexural strength at 28 days with crimped and Japanese fibres while Jojagha (109) found 43.5%, 101.7% and 86.1% increases at 28 days with Japanese, hooked and paddle fibres respectively. The corresponding increase for normal weight concrete of almost equal compressive strength was about 70% with 0.9% crimped fibres (78). With fibre reinforcement there is also, in most cases, a distinct first cracking strength. From Table 3.10 it can be seen that the first crack strength - ultimate flexural strength ratio was higher for mix B with 0.5% fibres than that of mix C with 1.0% crimped fibres because of the smaller number of fibres bridging the cracks. Japanese fibres (mix D) showed no increase in strength after cracking in some cases and almost negligible in other cases. Joyahga (109) reported no increase at all in strength after cracking with Japanese fibres while Sittampalan (80) found 36% increase, which is rather a big increase for such small length fibres. In mix D with Japanese fibres no more cracks were developed after the first crack, which eventually progressed to failure. This is due again to 25 mm length of fibres, which is not enough to allow bond resistance to be developed and pull-out starts as the crack occurs. With crimped, hooked and paddle fibres the situation was different.

After the first crack, several other cracks developed and the specimen failed either at the position of the first crack or at the position of a crack formed later. Fibre concrete mixes showed a high degree of ductility before failure; fibre pullout started as ultimate strength was reached. As it may be seen from Table 3.12 the first crack flexural strength of fibre mixes is higher than the flexural strength of lightweight concrete without fibre reinforcement.

From Table 3.11 it can be seen that the development of the flexural strength of fibre mixes with time is similar to that of unreinforced mix only up to 28 days. After 28 days there is not any considerable effect of fibre reinforcement on flexural strength. An increase of about 6.3% and a decrease of about 2.0% with 1% Japanese and hooked fibres respectively was observed in 540 days flexural strength over the strength at 28 days. For normal weight fibre reinforced concrete Stavrides (30) reported an increase of about 3.6% with 1% crimped fibres at 180 days while Al-Taan (29) reported a decrease of 14% with 1.0% crimped fibres at 570 days.

Table 3.13 shows the effect of specimen thickness on flexural strength. Because of the small thickness of the specimens there was no increase in the flexural strength once the cracking occurred although the failure of fibre specimens was a ductile one. The results showed an increase in flexural strength when the thickness of the specimen was reduced from 100 mm to 25 mm. When the specimens were tested with cast face as tension face, this increase was much lower than that obtained when specimens were tested with other face as tension face. This was because the cast face is an area of weakness for the specimen and no perfect compaction can be achieved, especially when fibres are used. This explains the lower percentage increases of fibre mixes relative to that of plain concrete (column 6).

Table 3.13 Influence of specimen thickness on flexural strength.

Mix	Cube Strength N/mm^2	Flexural Strength (100x100 x500 mm) N/mm^2	Flexural Strength 25x100x500mm N/mm^2 Tension face		% increase $\frac{(4)}{(3)}$	% increase $\frac{(5)}{(3)}$
			Cast face	Other face		
(1)	(2)	(3)	(4)	(5)	(6)	(7)
A	43.7	3.45	3.85	4.10	11.59	18.84
C	44.5	6.48	6.80	7.92	4.94	22.2
D	43.8	5.43	6.62	7.44	21.92	37.0
E	48.3	6.60	6.94	8.52	5.15	29.09
F	46.7	6.75	7.24	8.45	7.26	25.18

NOTE: These specimens, 100x100x500 mm (3 prisms) and 25x100x500 mm (12 plates) were cast separately for each mix to determine the influence of depth of specimen on flexural strength.

On the other hand, the fibre mixes showed higher increases relative to plain mix,(for example, 29.09% for hooked fibres as compared to 18.84 for plain concrete mix when other face was used as tension face), probably because of the two dimensional distribution of fibres in the 25 mm thick specimen. Swamy and Stavrides (104) reported an increase in flexural strength of 1.0% normal weight fibre concrete of about 20% when specimen thickness was reduced from 250 mm to 100 mm. Increases in flexural strength of about 20% and 15% were reported (111) for plain normal weight and fibre concrete respectively when specimens thickness was reduced from 100 mm to 25 mm.

3.3.2.4 Splitting Tensile Strength.

The split-cylinder test is another method to measure the tensile strength of concrete. This test appears to have some important advantages over the flexural test as a measure of tension (13). In the flexural test the outer fibres of the specimen, which sustain the maximum stress, are sensitive to moisture changes, especially in lightweight concrete, while the maximum tensile stresses in the splitting test are applied to the interior of the cylinder. A similar effect results from local defects such as large pieces of aggregate near the surface. In the case of the split-cylinder test, the tensile stress is distributed over a large diameter area of the cylinder and thus stress concentrations from specimen defects or other causes could be reduced by plasticity.

The values of the first crack and ultimate splitting tensile strength of plain lightweight and fibre concrete mixes used in this investigation are shown in Table 3.14. The ultimate values are also plotted against age in Fig. 3.6. Table 3.15 shows the first crack splitting strength of various mixes as a percentage of the corresponding ultimate splitting tensile strength

Table 3.14 Ultimate and first crack splitting strength (within brackets) of sand-lightweight concrete without and with fibres.

Time / Mix	Ultimate and first crack tensile splitting strength, N/mm^2							
	1d	3d	7d	28d	90d	180d	360d	540d
A	0.64 (0.64)	-	2.62 (2.62)	3.02 (3.02)	3.10 (3.10)	3.05 (3.05)	3.40 (3.40)	3.46 (3.46)
B	1.15 (1.10)	2.18 (2.01)	3.53 (3.17)	3.97 (3.62)	4.02 (3.58)	4.08 (3.75)	4.08 (3.67)	4.29 (3.81)
C	1.22 (1.11)	2.56 (2.15)	3.82 (3.40)	4.66 (3.96)	4.80 (3.89)	-	-	-
D	1.05 (1.05)	2.29 (2.24)	3.46 (3.18)	3.83 (3.52)	4.13 (3.72)	4.18 (3.97)	4.32 (3.97)	4.24 (3.86)
E	1.02 (0.95)	2.08 (1.87)	3.34 2.97)	4.12 (3.34)	4.56 (3.88)	4.42 (3.67)	4.48 (3.58)	4.66 (3.54)
F	1.18 (1.06)	2.27 (2.11)	3.57 (2.93)	4.36 (3.49)	4.48 (3.45)	4.56 (3.88)	4.72 (4.06)	4.69 (3.85)

Table 3.15 % First crack splitting strength/Ultimate tensile splitting strength ratio.

Time / Mix	1d	3d	7d	28d	90d	180d	360d	540d
A	100	-	100	100	100	100	100	100
B	96	92	90	91	89	92	90	89
C	91	84	89	85	81	-	-	-
D	100	98	92	92	90	95	92	91
E	93	90	89	81	85	83	80	76
F	90	93	82	80	77	85	86	82

Table 3.16 Ultimate splitting tensile strength of different ages as a percentage of 28 days strength.

Mix \ Time	1d	3d	7d	28d	90d	180d	360d	540d
A	21.2	-	86.8	100	102.6	100.9	112.6	114.6
B	29.0	54.9	88.9	100	101.3	102.8	102.8	108.1
C	26.2	54.9	82.0	100	103.0	-	-	-
D	27.4	59.8	90.3	100	107.8	109.1	112.8	110.7
E	24.8	50.5	81.1	100	110.7	107.3	108.7	113.0
F	27.1	52.1	81.9	100	102.8	104.6	108.3	107.6

Table 3.17 Percentage increase of ultimate splitting tensile strength of fibre mixes over that of plain concrete at various ages.

Mix \ Time	1d	7d	28d	90d	180d	360d	540d
A	0.0	0.0	0.0	0.0	0.0	0.0	0.0
B	79.7	34.7	31.5	29.7	33.8	20.0	24.0
C	90.1	45.8	54.3	54.8	-	-	-
D	64.1	32.1	26.8	33.2	37.1	27.1	22.6
E	59.4	27.5	36.4	47.1	44.9	31.8	34.7
F	84.4	36.6	44.4	44.5	49.5	38.8	35.5

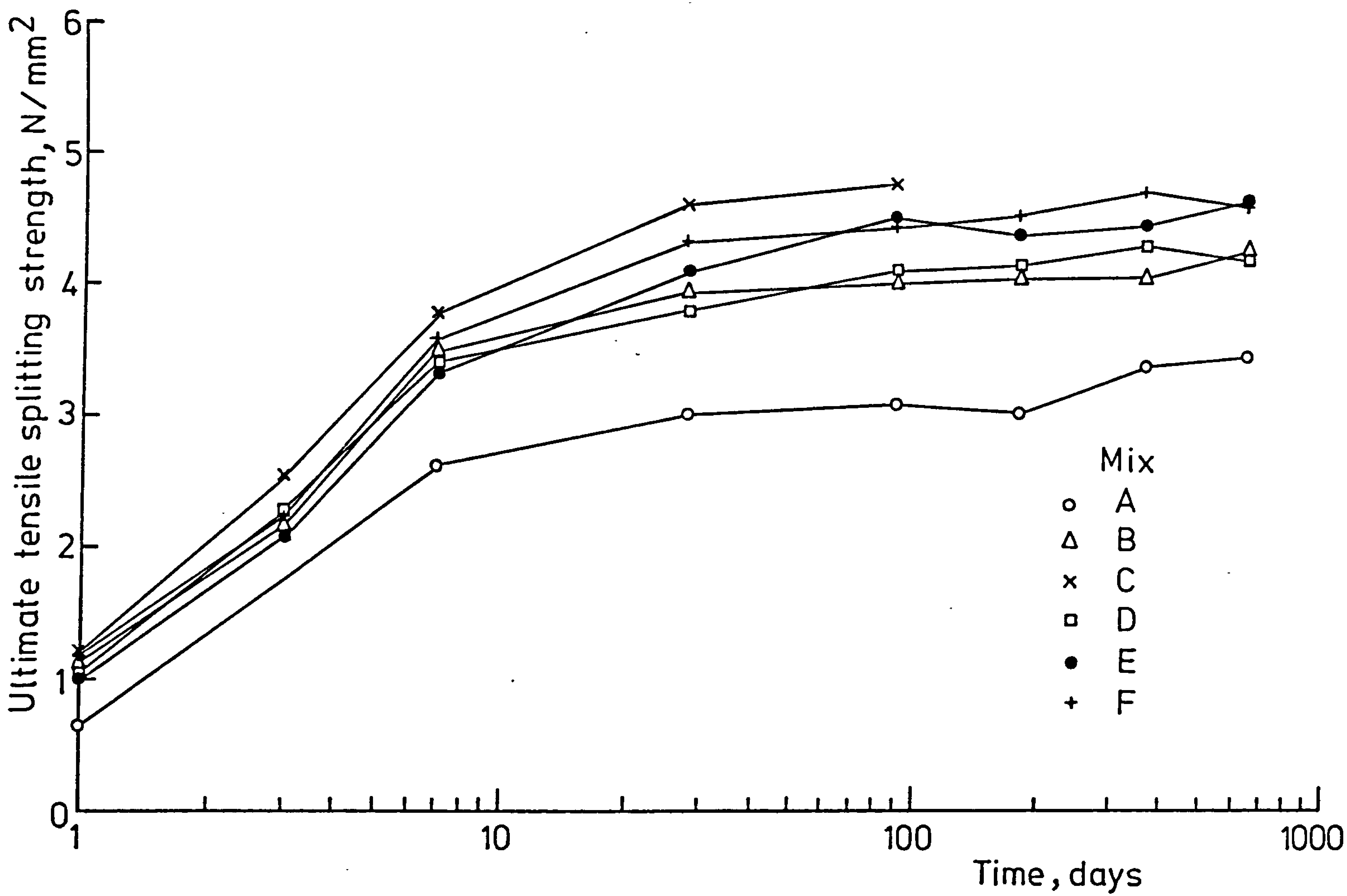

FIG. 3-6 ULTIMATE TENSILE SPLITTING STRENGTH OF VARIOUS MIXES WITH TIME

at each age. Table 3.16 shows the percentage of ultimate tensile strength at each age, to 28 days ultimate strength for each mix. Table 3.17 shows the percentage increase of ultimate splitting strength of fibre mixes over that of plain concrete at various ages.

The ultimate splitting tensile strength of plain sand-lightweight concrete (Mix A) at 28 days is 3.02 N/mm^2, less than the corresponding value of plain normal concrete of almost equal compressive strength, which is 3.33 N/mm^2 (78), because the splitting strength, as the flexural strength, is largely dependent on the tensile strength of aggregates.

From Table 3.16 it can be seen that there is no significant increase in the splitting sgrength (Mix A) up to 180 days over that at 28 days, but there is an increase of about 14.6% at 540 days, which is much less than the corresponding increase (42.6%) for the flexural strength. The increase in strength of 'Solite' lightweight concrete at 430 days over 28 days strength was about 33% under uncontrolled laboratory conditions.

The plain lightweight concrete cylinders failed suddenly and were split into separate halves through an approximate plane located on or near to the loaded line. This failure plane passed directly through nearly all pieces of lightweight aggregate as shown in Plate 3.4. This mode of failure is the common case in all lightweight cylinders regardless of the compressive strength while in the normal weight concrete the failure surface travels round the aggregates and only in concretes with very high compressive strengths the failure plane passes through a limited number of aggregate particles.

The relationship between the splitting tensile strength and the compressive strength of lightweight concrete is given by equation 3.1 where the constant K has a value of 0.42 (93). Equation 3.1 with K = 0.42 under-estimates the 28 days splitting tensile strength by 6.3%. The ratio of the ultimate splitting tensile strength over flexural strength at 28 days is

3.02/3.24 = 0.93 while Sattampalan found this ratio equal to 1.03 for all-cement sand-Lytag eoncrete. This ratio in the case of Solite lightweight concrete of 41 and 52 N/mm^2 compressive strength (11) was 1.01 and 0.79 respectively for specimens cured under uncontrolled laboratory conditions.

With fibre reinforcement, the mode of failure of specimens was changed; the specimens merely cracked at failure without any sign of collapse or separation as shown in Plate 3.4. With all the types of fibres used in this investigation there was a distinct first cracking strength. The crack was initiated in the plane of loading and occupied a considerable part of diameter length (Fig.3.7(a)). After that, the specimen could still resist an increased load until the crack propagated up to the ends of the diameter. The load at this stage was considered to be the ultimate load. A gradual drop in the load was observed with simultaneous spalling of the concrete at points A and B in Fig. 3.7(c) after the ultimate load had been reached, and finally the specimen was fully disrupted. However, in some cases, the drop in the load was stopped and an increasing load was resisted while the plywood strips were inserted in the cylinder as shown in Fig. 3.7(d) and Plate 3.5. The increased load resisted in these cases does not truly represent a splitting strength because after the compressive failure at point A and B in Fig. 3.7(c), the specimen starts to work in compression. From this observation, it can be said that one must be very careful when testing cylinders with fibre concrete for measuring the splitting tensile strength.

From Table 3.17 it can be seen that there is an increase in the splitting tensile strength due to addition of fibres. The percentage increase, at 28 days, is 31.5 and 54.3 for mix B with 0.5% crimped fibres and mix C with 1.0% crimped fibres respectively. The percentage increase varied from 26.8 to 54.3 for various types of fibres used. These increases in the splitting

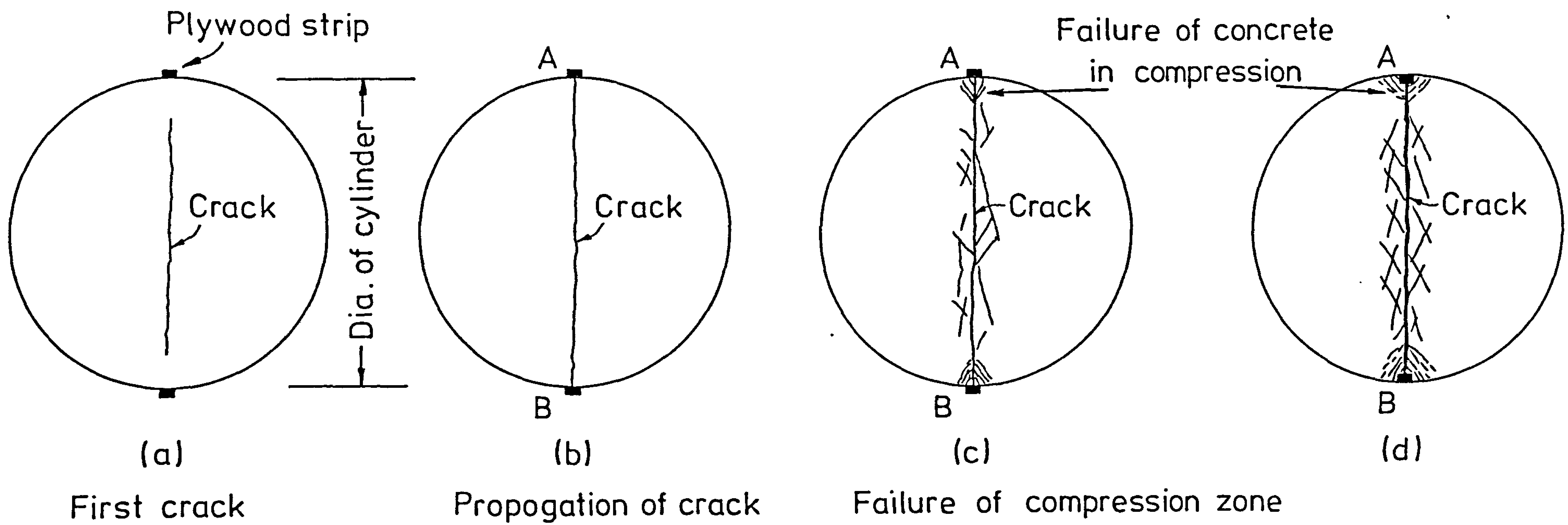

FIG. 3-7 FAILURE OF THE FIBRE CONCRETE CYLINDER SPECIMEN

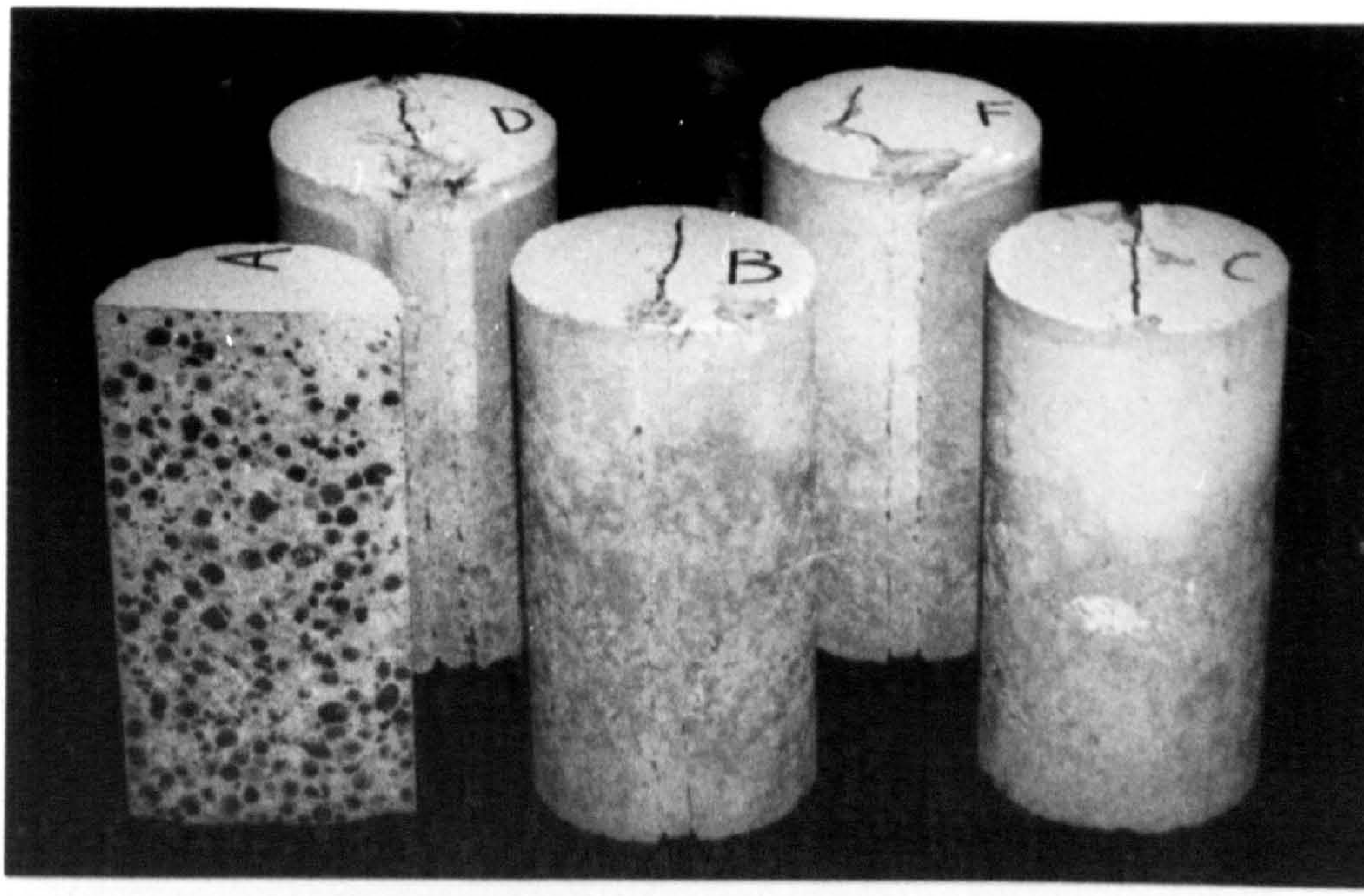

PLATE 3-4 PLAIN AND FIBRE CONCRETE CYLINDERS AFTER TESTING

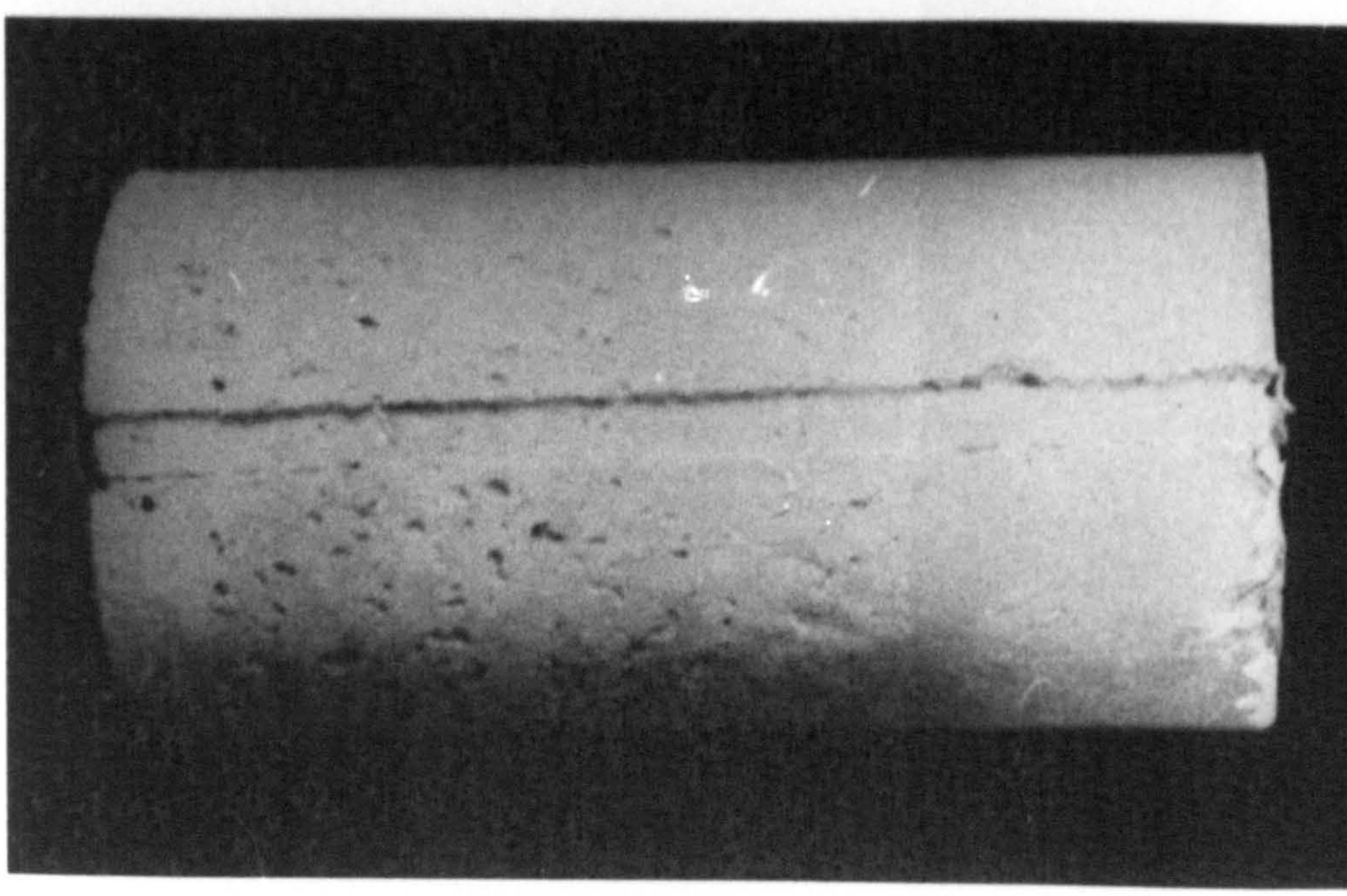

PLATE 3-5 FIBRE CONCRETE CYLINDER AFTER TESTING

FIG. 3-8 RELATIONSHIP BETWEEN SPLITTING TENSILE AND FLEXURAL STRENGTH OF FIBRE MIXES

strength of fibre mixes were lower than those found in the flexural strength (Table 3.12). The explanation for this could be that after cracking has occurred in the cylinder, the ability of the fibres to bridge the crack cannot fully be utilized because of the premature failure of the edges of the diameter in compression (Fig.3.7(c)), as happens in a flexural test. The first crack strength over ultimate splitting strength ratios shown in Table 3.15 are higher than those obtained from the flexural test, probably for the same reason.

From Table 3.16 it can be seen that the development of the splitting tensile strength of fibre mixes with time is similar to that of the unreinforced mix. The ratio of the ultimate splitting strength at 540 days to the value at 28 days for mixes D, E and F had an average value of about 1.10.

The test results of this investigation from 1 day to 540 days yielded ratios of the ultimate splitting tensile strength over flexural strength for plain concrete, ranging from 0.59 to 0.93 with an average ratio of 0.74. This average ratio in the case of Solite lightweight concrete (11) was 0.76. With fibre reinforcement, this ratio ranged from 0.56 at 1 day to 0.72 at 540 days with an average value of about 0.64. Fig.3.8 shows the relationship between splitting tensile and flexural strength of different fibre mixes at various ages. The straight lines in Fig.3.8 pass through the origin of the axes and the point represented by the average values of tensile splitting and flexural strengths.

3.3.2.5 Modulus of Elasticity.

The elastic modulus is primarily dependent on the strength and density of concrete. It is also influenced by the volume and modulus of the aggregate and to a lesser extent by the conditions of curing age, mix properties and type of cement. It is therefore expected that the values of modulus of elasticity (E) of lightweight concrete to be lower than that of normal weight concrete having the same compressive strength.

Table 3.18 shows the values of modulus of elasticity of various mixes. The E-value for plain mix at 28 days is 17.35 kN/mm^2 almost half of the corresponding value of normal weight concrete of almost equal compressive strength which was 33.29 kN/mm^2 (78). For structurel lightweight concrete the elastic modulus can be expressed as: (94)

$$E_L = K W^2 \sqrt{f_{cu}} \quad \ldots\ldots \tag{3.2}$$

where E_L is the modulus of elasticity in kN/mm^2

W is the density of concrete in Kg/m^3

f_{cu} is the cube strength of concrete in N/mm^2

K is a constant having a value of 0.97×10^{-6}.

Application of equation (3.2) gives a value of E equal to 21.86 kN/mm^2 which is 25.9% higher than that found in this investigation. The difference might be due to the fact that constant K was calculated from tests of Solite concrete. The percentage increase of E at 540 days over that at 28 days was 10.6, while Bandyopadhyay (11) and Teychenne (6) reported values of about 8% at 540 days and 17% at 360 days respectively.

The addition of steel fibres in concrete yields a higher modulus of elasticity although the increase is not expected to be so much as in the case of flexural strength since the reinforcing action is different. Table 3.19 shows the percentage increase of modulus of elasticity of fibre mixes over that of plain concrete at various ages. It can be seen that a maximum increase of about 12% was achieved at 28 days when 1.0% by volume fibres was used, this increase being around 20% at 450 days. Ritchie (101) reported an E-value for plain lightweight concrete of about 16.75 kN/mm^2 at 28 days and an increase of about 3.2% when 0.6% steel fibres by volume

Table 3.18 Modulus of Elasticity of Sand-lightweight concrete without and with fibres.

Mix \ Time	Modulus of Elasticity, KN/mm^2							% increase at 540d over 28d
	3d	7d	28d	90d	180d	360d	540d	
A	10.84	16.35	17.35	16.6	17.25	18.9	19.2	10.6
B	12.47	16.45	17.15	17.50	17.84	19.85	20.54	19.8
C	12.85	17.60	19.37	20.34	-	-	-	-
D	12.35	17.64	18.86	19.92	20.20	21.32	21.86	15.9
E	12.67	17.20	19.25	19.85	20.72	22.08	22.85	18.7
F	12.90	17.85	19.52	20.75	21.0	21.82	23.00	17.9

Table 3.19 Percentage increase of Modulus of Elasticity of fibre mixes over that of plain concrete at various ages.

Mix \ Time	3d	7d	28d	90d	180d	360d	540d
A	0	0	0	0	0	0	0
B	15	1	-1	5	4	5	7
C	19	8	12	22	-	-	-
D	14	8	9	20	17	13	16
E	17	5	11	20	20	17	21
F	19	9	12	25	22	15	22

were used. For normal weight concrete the corresponding increase was 18.2% (78) and 20.6% (75) when 0.9% and 1.2% crimped fibres respectively were used, while Al Taan (29) reported increases of about 0.8% and 6% when 0.5% and 1.0% fibres were used respectively. From Table 3.18 it can be seen that modulus of elasticity increases with age. The average increase of mixes D, E and F at 540 days relative to E-value at 28 days was 17.5%, which is higher than that of plain mix A. Al-Taan (29) reported that for normal weight concrete this increase was about 25% at 765 days.

3.3.2.6 Unrestrained Shrinkage.

The results of the free shrinkage tests are shown in Fig. 3.9. These results confirm that the presence of fibres restrains the shrinkage movements of the unreinforced matrix (109, 111). The shrinkage of mixes B and C with 0.5% and 1% crimped fibres by volume was 88.2% and 83% respectively of that of unreinforced mix at 90 days. Japanese fibres (Mix D) with a shrinkage value of 77% of that of mix A showed a better effect in restraining shrinkage movements than hooked and paddle fibres with a shrinkage value of 82.3% and 86% respectively at 90 days. This can be explained in terms of smaller size of the Japanese fibres. Because of their smaller size, the number of fibres for a given fibre volume is greater than the number of crimped, hooked and paddle fibre, which means that Japanese fibre is more effective in restraining shrinkage movement. The effect of 1% crimped fibres in lightweight concrete is greater than that found for normal fibre concrete (111). This is because since in lightweight concrete the weaker and less stiff aggregates impose less restraint in the cement paste than that of dense aggregates in normal weight concrete, it is expected that the effect of addition of fibres, acting as stiff aggregates, should be more pronounced in lightweight concrete than in normal weight concrete.

FIG. 3-9 SHRINKAGE OF VARIOUS MIXES

From Fig. 3.9 it can be seen that the presence of fibres tended to stabilize the shrinkage movements slightly earlier.

3.3.3 Strength Results of Specimens Cast with Slabs.

The compressive, flexural and splitting tensile strengths of specimens cast and tested with each slab connection are shown in Table 3.21. The mix designs used in slabs FS-16, FS-17 and FS-18 with characteristic compressive strengths 35 N/mm^2, 60 N/mm^2 and $20/mm^2$ respectively, were obtained from information already available in the department. The mix proportions for these strengths are shown in Table 3.20.

Table 3.20

Characteristic Strength N/mm^2	Cement kg/m^3	Sand kg/m^3	Lytag kg/m^3	Eff. Water kg/m^3
20	200	740	696	180
35	320	634	696	175
60	470	500	696	180

The distribution of compressive, flexural and splitting tensile strengths for both plain and fibre concrete is represented graphically by histograms (Fig. 3.10). The number of plain concrete specimens is twelve (three specimens for each plain concrete slab, FS-1, FS-8, FS-10 and FS-19). The number of fibre concrete specimens is twenty four (three specimens for each fibre concrete slab with 1% by volume crimped fibres). In Fig. 3.11 the ultimate flexural and splitting tensile strengths are plotted against compressive strength of 1.0% by volume crimped fibre mixes to see the scatter of test results. The straight lines in this figure pass through the origin of axes and the point represented by the average values of two variables.

Table 3.21 Results of Slab-Connections.

Slab Number	% Fibre Volume	Fibre Type	Compressive Strength N/mm^2	Flexural Strength N/mm^2	Splitting Tens. Strength N/mm^2
FS-1	0.0	-	44.20	3.24	2.85
FS-2	0.5	Crimped	42.50	6.04	4.06
FS-3	1.0	Crimped	44.56	6.15	4.36
FS-4	1.0	Crimped	46.67	6.19	4.52
FS-5	1.0	Crimped	47.50	6.80	4.86
FS-6	1.0	Crimped	44.60	6.52	4.42
FS-7	1.0	Crimped	45.80	6.78	4.56
FS-8	0.0	-	45.83	3.20	2.95
FS-9	1.0	Crimped	44.50	6.56	4.37
FS-10	0.0	-	45.50	3.46	3.12
FS-11	1.0	Crimped	42.80	6.38	4.75
FS-12	1.0	Japanese	45.10	5.20	3.79
FS-13	1.0	Hooked	41.85	6.95	4.36
FS-14	1.0	Paddle	43.73	6.62	4.50
FS-15*	1.0	Crimped	39.05	6.47	-
FS-16	1.0	Paddle	34.9	6.19	-
FS-17	1.0	Paddle	58.56	6.79	-
FS-18	1.0	Paddle	17.75	3.93	-
FS-19	0.0	-	43.12	3.52	2.82
FS-20	1.0	Crimped	46.30	6.72	4.38

*6 mm Lytag aggregates were used as coarse aggregates in specimen FS-15.

FIG. 3-10 DISTRIBUTION OF PLAIN AND FIBRE CONCRETE STRENGTHS

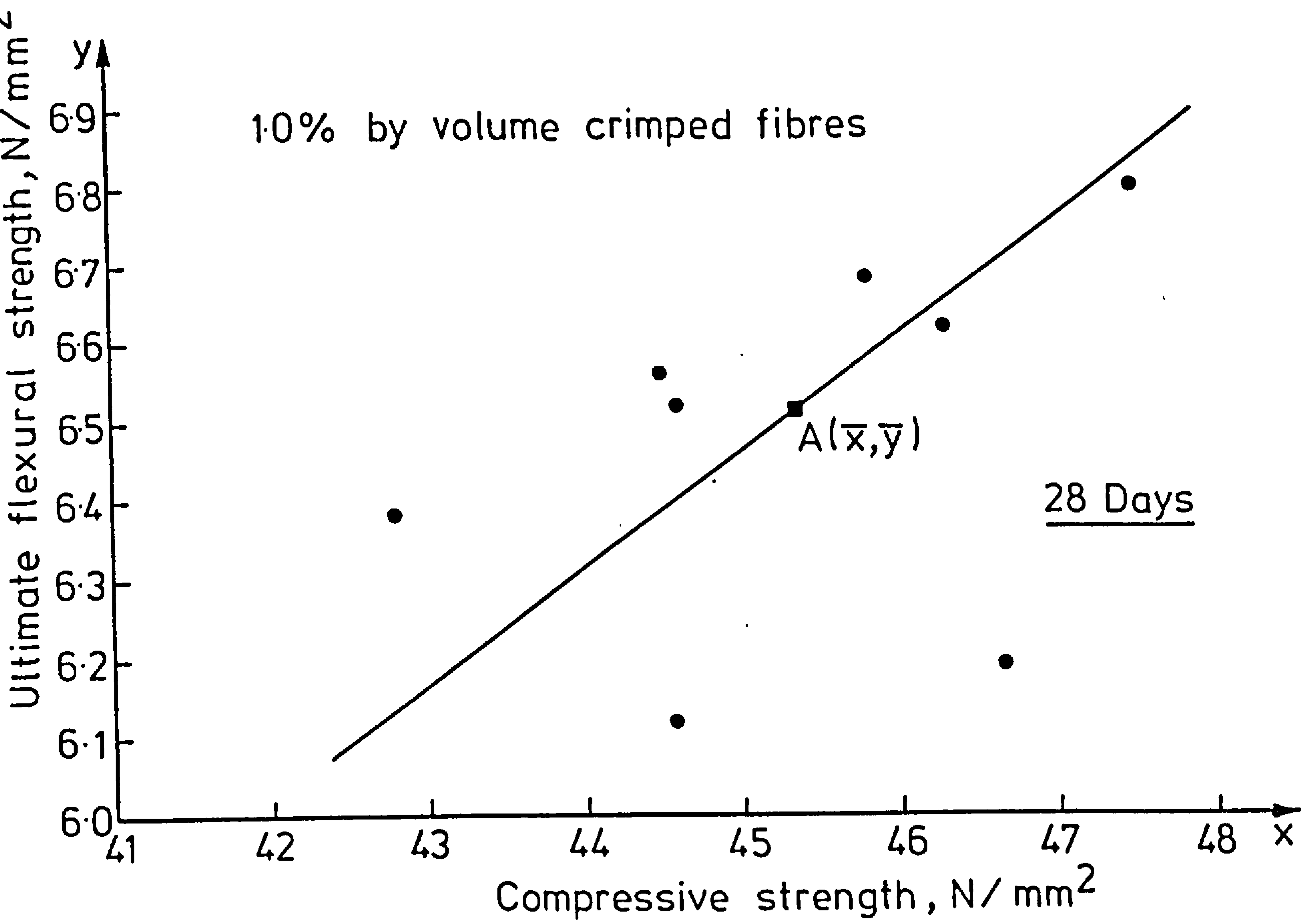

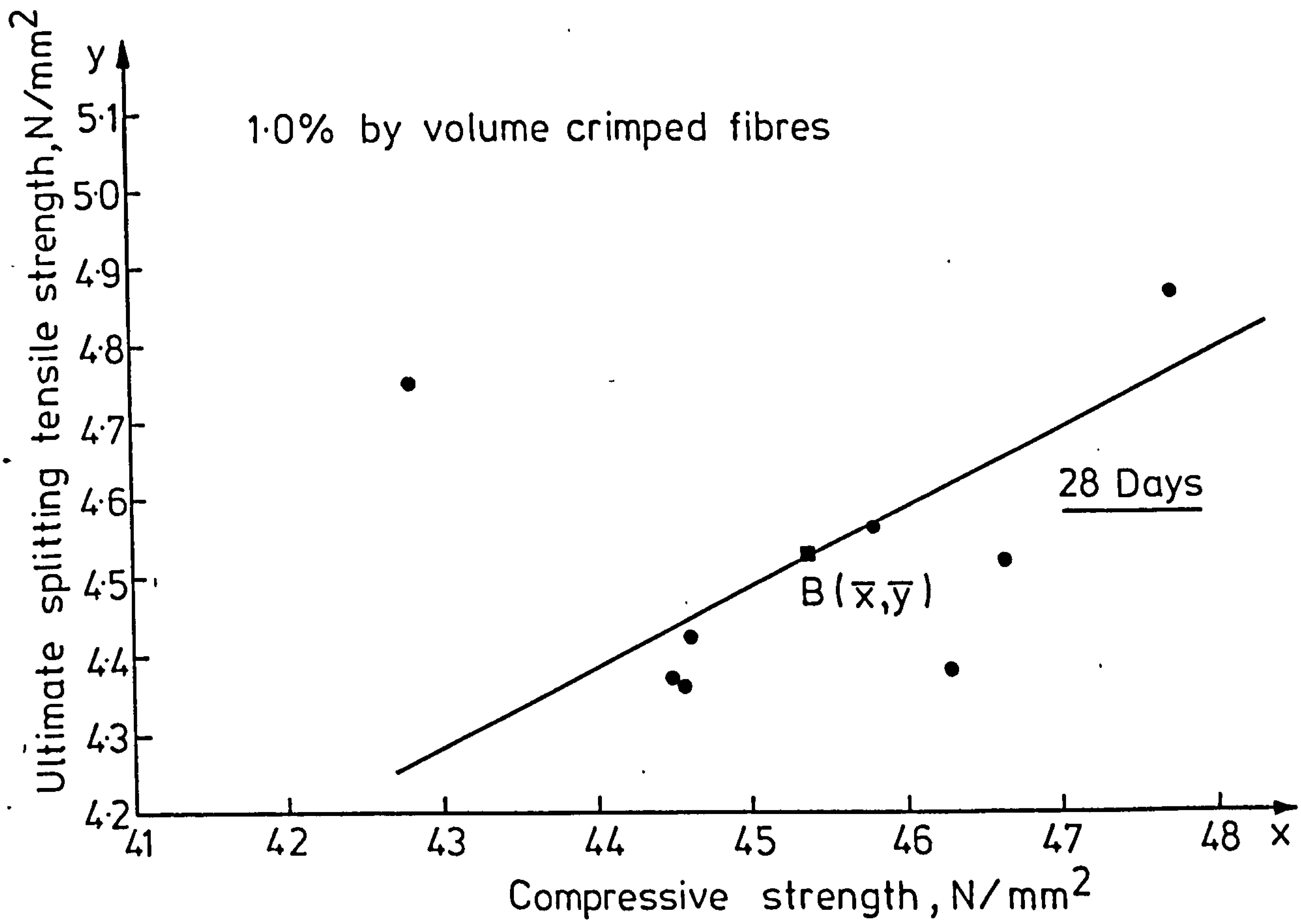

FIG. 3-11 SCATTER OF TEST RESULTS

From Fig. 3.10 it can be seen that there is a very small increase in the compressive strength results of the fibre mix. This increase is too small and could be attributed either to the presence of fibres or to chance. Swamy and Stavrides (112) in a statistical analysis of thirty six specimens each of plain and fibre normal concrete made from one mix found that the increase observed in the compressive strength of the fibre mix was too great to be attributed to chance. Fibre concrete flexural and splitting strength results showed larger standard deviations than corresponding plain concrete results while fibre concrete compressive strength results had a smaller standard deviation than in plain concrete. In general, it is expected that the fibre concrete results must have larger standard deviations than those in plain concrete results and this can be explained in terms of the possibility of different fibre distribution under identical conditions.

3.4 Conclusions.

Based on the results obtained in this investigation the following conclusions can be drawn:

1. Fly ash replacement of cement can be successfully carried out with lightweight aggregates and such mixes can be designed for any strength range. For mixes used in this study, strengths of 33 to 52.6 N/mm^2 were obtained at 28 days. All these mixes had a high degree of workability.

2. Fibres can be introduced and successfully incorporated in lightweight aggregate concrete mixes. The workability of fibre concrete mixes was improved by the use of fly ash and of a water reducing agent, thus easing the compaction problems of fibre concrete.

3. Inclusion of fibres affected compressive strength only slightly. The maximum increase at 28 days was 4.0% and the lower reduction was 5.5%. The increase of compressive strength of fibre concrete mixes from 28 days to 18 months was of about 15% as compared to 16.1% of the unreinforced lightweight

concrete mix. The inclusion of fibres prevented the spalling of the unreinforced specimens.

4. The density of plain lightweight concrete was 1830 Kg/m^3 at 28 days while the average density of 1% by volume fibre concrete mixes was about 1906 Kg/m^3.

5. The flexural strength of plain lightweight concrete mix was increased by about 49.4% from 28 days to 90 days, this increase being about 42.6% at 540 days. With 0.5% by volume crimped fibres the ultimate flexural strength was increased by 75.9% at 28 days while with 1% fibre reinforcement of various types this increase ranged from 65.4 to 11 9.1%. The first crack flexural strength was increased by 64.2 - 71.6% over that of plain concrete at 28 days. The increase in ultimate flexural strength depends upon the type of fibre used. There is little increase in flexural strength from 28 to 540 days for fibre mixes.

Reducing the depth of test specimen from 100 mm to 25 mm increased the ultimate flexural strength by about 19% for plain concrete and 22-37% for fibre concrete.

6. The splitting tensile strength of lightweight concrete was lower than the flexural strength either with fibres or without fibres. With 0.5% by volume crimped fibres the ultimate splitting strength was increased by 31.5% at 28 days, while with 1.0% fibre reinforcement of various types this increase ranged from 26.8 to 54.3%. The increase of the splitting strength from 28 to 540 days was 14.6% for plain mix and ranged from 7.6 to 10.7% for 1% fibre reinforcement mixes.

In a split-cylinder test with fibre concrete, the ultimate splitting tensile strength is not governed by the pull-out resistance of the fibres, as in the case of the flexural test, because of the premature failure in compression of the edges of the diameter where the load is applied.

7. The unreinforced concrete specimens for both flexural and split-cylinder tests had a brittle mode of failure as usual but with fibre reinforcement the mode of failure was changed, and the specimens showed a high degree of ductility before failure.

8. With 1.0% by volume fibre reinforcement the increase of modulus of elasticity ranged from 9-12% at 28 days, this increase being higher at 540 days. An increase of 10.6% of modulus of elasticity was achieved from 28 to 540 days for plain concrete while this increase ranged from 15.9-19.8% with fibre reinforcement.

9. Fibre reinforcement restrains the shrinkage movement of the unreinforced matrix. Japanese fibres of 25 mm length were more effective in controlling shrinkage strains than fibres of 50 mm length.

CHAPTER 4.

DESIGN OF THE EXPERIMENTAL INVESTIGATION.

4.1 Introduction.

A literature study of the strength and behaviour of plain concrete slab-column connections reveals that a number of experimental studies has been carried out by several investigators. The results from these studies have provided a lot of information regarding shear strength and behaviour of the slabs. The analysis of these results yielded methods for calculating the shear strength of slab-column connections, which involve either approximate theoretical solutions, often including experimental constants, or semi-empirical expressions based on statistical analysis undertaken by the investigators. Although a complete understanding and a general analytical solution of this problem has been precluded by the problems arising from the complexity of the stress distributions near the column, the nonlinearity and nonhomogeneity of the highly stressed and cracked reinforced concrete at the critical sections, and the large number of parameters which possibly influence the strength and behaviour of connections, the experimentally obtained results have led to design procedures which are simple in concept and easy to apply and have been proven to give safe, economical and satisfactory structures.

So far no mention has been made of any comparison between plain lightweight reinforced concrete slab-column connections and connections made with a combination of fibres and steel bars. The main difference between concrete reinforced with short discontinuous fibres and conventional steel bars is the fact that whereas reinforcing bars are aligned along the direction of stress the fibres usually have a three dimensional configuration.

The test programme reported in this study was designed to investigate the effect of fibre reinforcement on the strength and deformation characteristics of lightweight concrete slab-column connections.

4.2 Prototype and Model Scale.

The prototype selected in this investigation is a flat-plate structure with a column spacing of 4.0 m centre to centre in both directions (Fig. 4.1). The overall slab depth is 125 mm, with an average effective depth of 100 mm. The slab is supported on 100, 150 or 200 mm square columns and was adequately overdesigned for shear failures to occur during testing procedure. The allowable design live load for the prototype, may be found from the flexural capacity of the connection area by using the design provisions and moment distributions for the slab according to CP110 (69) and A.C.I. code of practice (67) and the assumed geometry and dimensions.

The connection specimens tested in this investigation are one to one full-scale models of the prototype connection and adjacent slab areas. Any possible size effects are thus avoided. This also avoids the possible distortion of the relative shear and flexural strengths resulting from the usually higher-than-normal ratio of tensile to compressive strength common with the small aggregate concrete often necessary with small-scale models.

4.3 Test Specimens.

All slab specimens tested in this investigation were 1800 mm square with an overall thickness of 125 mm and having a square column stub 250 mm high cast monolithically at the centre of the slab (Fig.4.2). The slab specimens were reinforced with Tor Steel bars of 10 mm and 8 mm in diameter distributed across the section. Details and dimensions of the slabs are presented in Fig. 4.2. All slabs were simply supported along all four edges with the corners free to lift, and were loaded through the column stub.

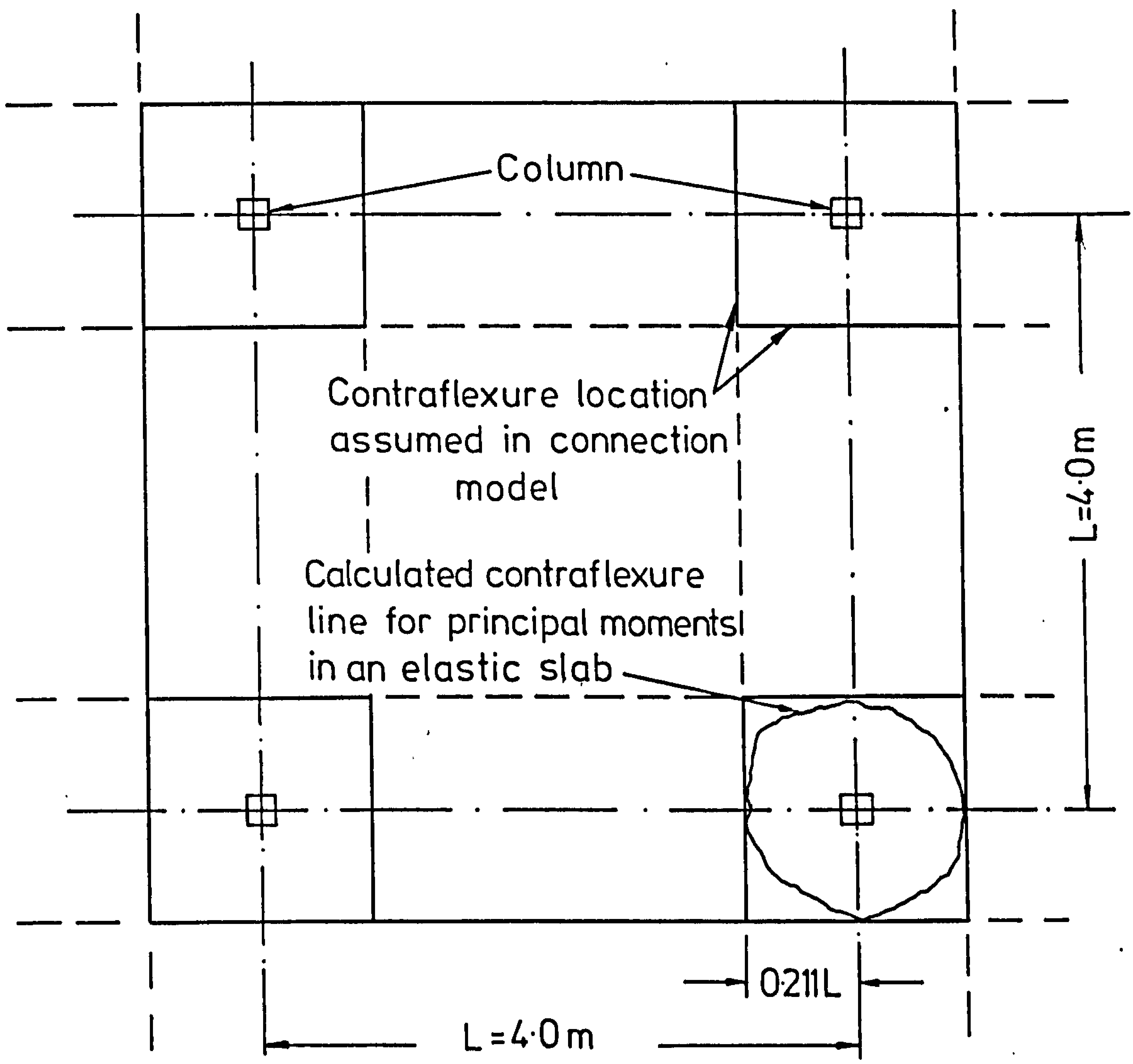

FIG.4·1 PLAN VIEW OF SLAB SYSTEM SHOWING LOCATION OF CONTRAFLEXURE LINES

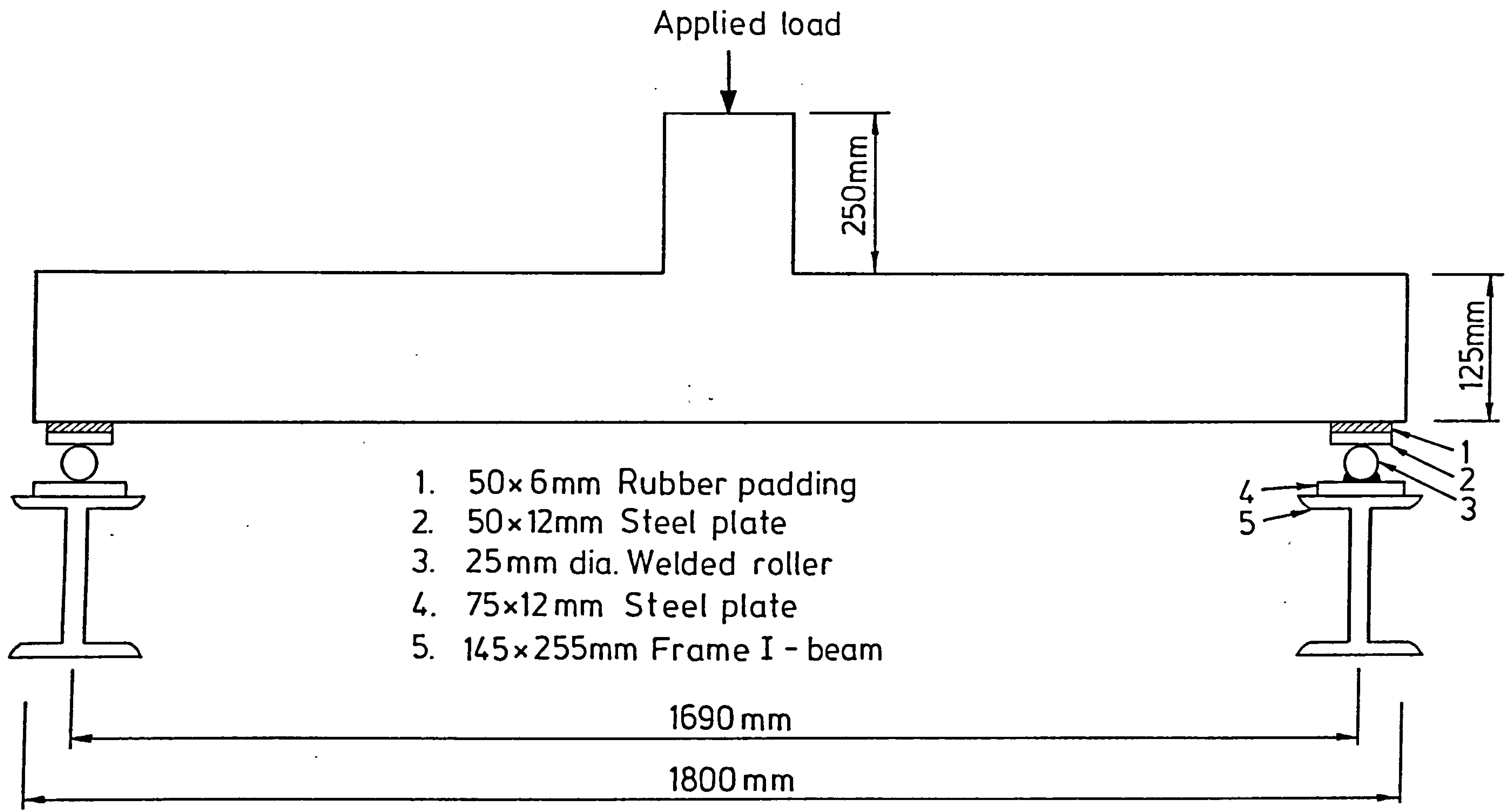

FIG. 4·2 TEST SLAB SPECIMEN AND SUPPORT DETAILS

The supports were positioned at 55 mm in from the edges of the slabs giving spans of approximately 1690 mm. The detail of the slab support is shown in Fig. 4.2. The selected size of the slab specimens is supposed to represent, with good approximation, the region of negative bending around an interior supporting column of the prototype system and inside the line of contra-flexure, which is the line of zero radial moment obtained from an elastic analysis of the prototype structure subject to uniform loading. The square shape of the test specimens was chosen for obvious practical reasons because it would be impossible to support the slab if it extended only to contraflexure line.

The location and shape of the contraflexure line are not constant in a reinforced concrete slab system. Cracking of the slab produces changes in the relative stiffness of various sections and directions. Redistribution of moments takes place in the slab system, causing changes in the location of the contraflexure line. The model used does not include this effect. Despite this, the strengths observed with the use of the isolated connection models are thought to be very close to the strengths of the connection in an actual slab system.

4.4 Test Variables and Experimental Programme.

The experimental test programme for this investigation is shown in Table 4.1. The programme is divided into five series and the most important variables studied in each series are:

1. Series 1: The steel fibre percentage by volume varying from 0.0 to 1.0%.
2. Series 2: The reduction of both tensile and compressive reinforcement and fibres location (Slab FS-20).
3. Series 3: The column size variation for both plain reinforced and fibre reinforced lightweight concrete.

Table 4.1 Slab details.

Series Number	Series Detail	Slab Number	Reinforcement: Tensile Reinforcement	Reinforcement: Compressive Reinforcement	Steel Fibre Type	Steel fibre percentage by volume	Column size, mm	Cube compressive strength, N/mm^2
1	Steel Fibre percentage by volume	FS-1	12-10mm	7-8mm	-	0.0	150	44.20
		FS-2	12-10mm	7-8mm	Crimped	0.5	150	42.50
		FS-3	12-10mm	7-8mm	Crimped	1.0	150	44.56
2	Reinforcement Reduction	FS-4	12-10mm	-	Crimped	1.0	150	46.67
		FS-5	8-10mm	7-8mm	Crimped	1.0	150	47.50
		FS-6	8-10mm	-	Crimped	1.0	150	44.60
		FS-7	8-10mm	3-8mm	Crimped	1.0	150	45.80
		FS-19	8-10mm	7-8mm	-	0.0	150	43.10
		FS-20	8-10mm	-	Crimped	1.0	150	46.30
3	Square Column Size	FS-8	12-10mm	7-8mm	-	0.0	100	45.80
		FS-9	12-10mm	7-8mm	Crimped	1.0	100	44.50
		FS-10	12-10mm	7-8mm	-	0.0	200	45.5
		FS-11	12-10mm	7-8mm	Crimped	1.0	200	42.80
4	Steel Fibre Type	FS-12	12-10mm	7-8mm	Japanese	1.0	150	45.10
		FS-13	12-10mm	7-8mm	Hooked	1.0	150	41.85
		FS-14	12-10mm	7-8mm	Paddle	1.0	150	43.73
		FS-15	12-10mm	7-8mm	Crimped*	1.0	150	39.05
5	Cube Comp. Strength	FS-16	12-10mm	7-8mm	Paddle	1.0	150	34.9
		FS-17	12-10mm	7-8mm	Paddle	1.0	150	58.56
		FS-18	12-10mm	7-8mm	Paddle	1.0	150	17.75

*Length = 38 mm Diameter = 0425 mm.

NOTE: Fibres were distributed only for 550 mm from slab centre except in slab FS-20, where they were distributed for the whole specimen.

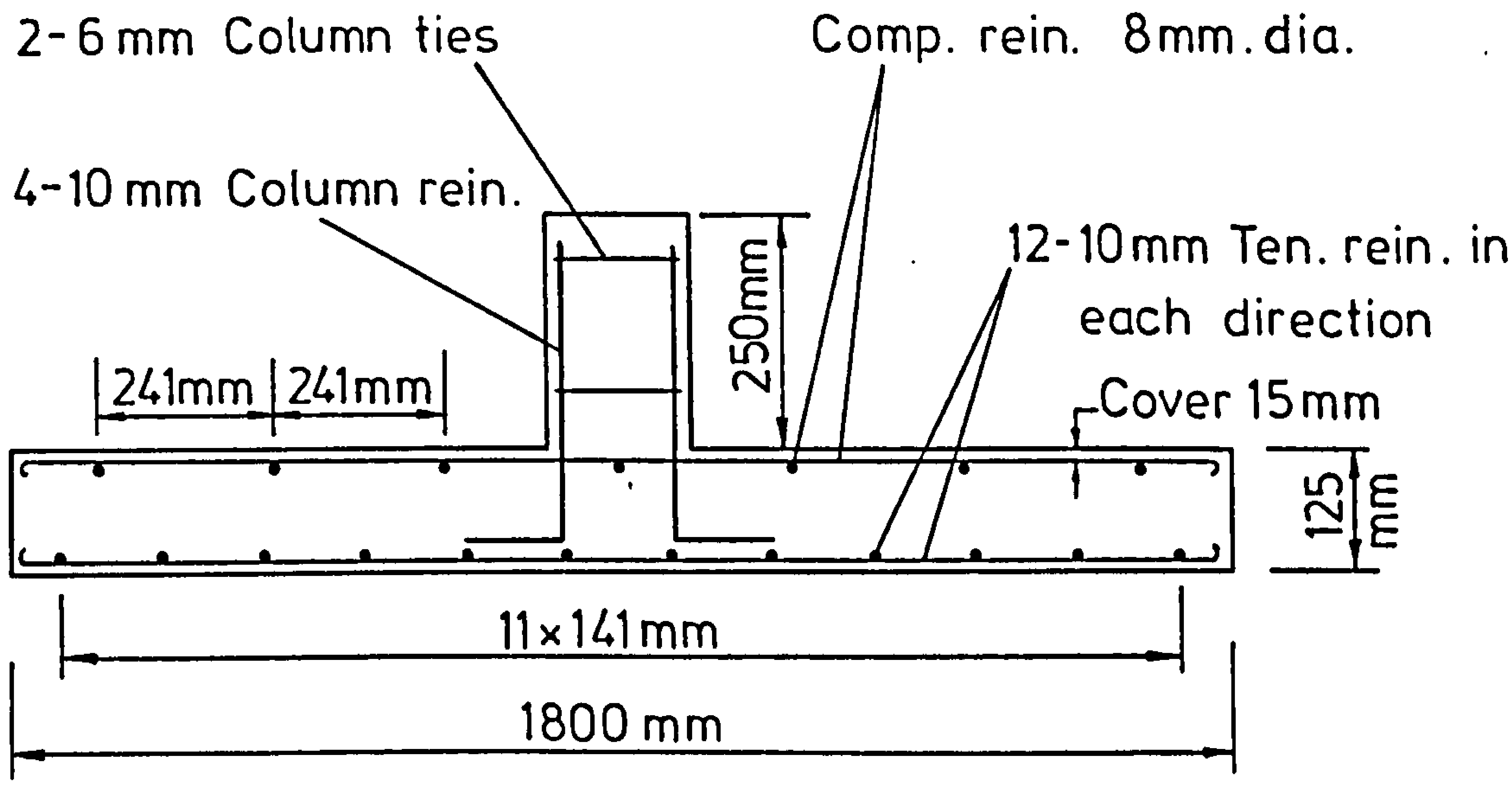

FIG. 4-3 TYPICAL ARRANGEMENT OF STEEL BARS IN SLABS WITH 12-10mm TEN. REIN.

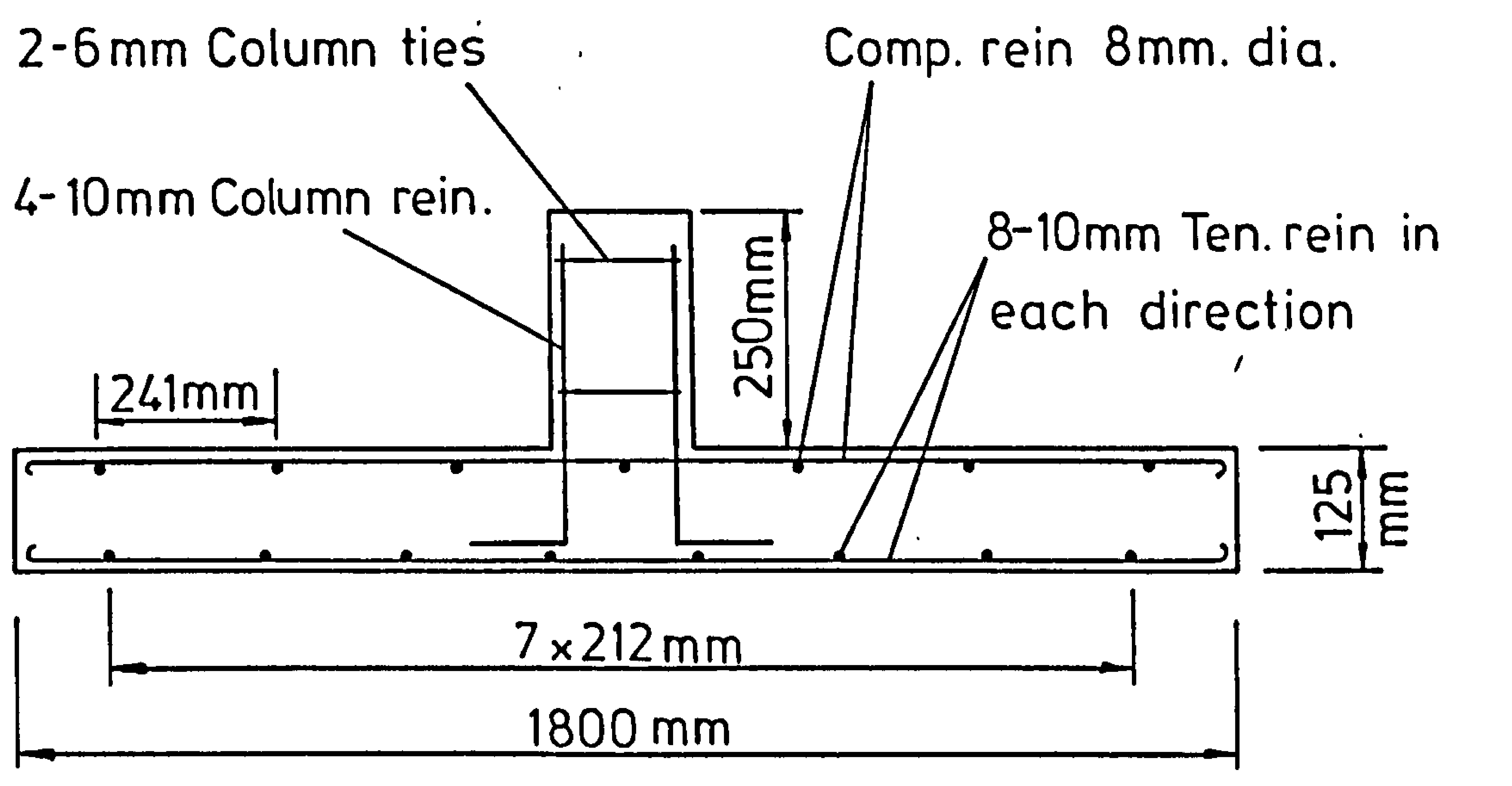

FIG. 4-4 TYPICAL ARRANGEMENT OF STEEL BARS IN SLABS WITH 8-10mm TEN. REIN.

4. Series 4: The steel fibre type at constant fibre volume (1%).

5. Series 5: The cube compressive strength variation with a given type of steel fibre (Paddle fibres).

The steel fibres were distributed within a square 1100x1100mm in the central area of slab, except for the slab FS-20 where they were distributed for the whole specimen.

Figs. 4.3 and 4.4 show a typical arrangement of the reinforcement in the test slabs.

The specimens and the corresponding tests are designated as follows

a) The letters FS indicate the test slab.

b) Numbers 1 to 20 indicate the test slab number.

c) 0.5% and 1.0% indicate the amount of steel fibre percentage by volume in the slab.

4.5 Flexural Design Load (at Ultimate L.S.) and Punching Shear Load According to CP110 (69).

4.5.1 Flexural Design Load (at Ultimate L.S.) of Slab.

Data:

$d = 100$ mm (effective depth)

$r = 150$ mm (column size)

$A_s = 12\text{-}10$ mm in each direction $= 942\ \text{mm}^2$

$$\rho = \frac{A_s}{bd} = \frac{940}{1690 \times 100} = 0.005574$$

$f_y = 460\ \text{N/mm}^2$

$f_{cu} = 45\ \text{N/mm}^2$ (Assumed)

$h = 125$ mm

According to CP110 (Clause 3.3.5.3) the design formula for calculating the ultimate moment of resistance is:

$$M_N = (0.87\, f_y)\, A_s\, Z \qquad \ldots\ldots \qquad (4.1)$$

where $Z = (1 - \frac{1.1 \times f_y A_s}{f_{cu} bd}) d$ ..... (4.2)

$\therefore$ $Z = 93.732$ mm

and $M_N = 35.336$ kN.m/1.69 m width

$\therefore$ $M_N = 20.909$ kN.m/m width

or $M_N = 41.818$ kN.m/2 m width.

This is the moment in the column strip.

The total moment in a panel in a given direction is related with the moment in the column strip with the expression

$$M_{ds} = \frac{M_N}{0.46} \qquad ..... \qquad (4.3)$$

according to the values given in Table 18 of the CP110 and shown in Fig.4.5 for slabs without drops. The moment M_{ds} is given by

$$M_{ds} = \frac{\eta \ell_1}{8} (\ell_2 - \frac{2h_c}{3}) \qquad ..... \qquad (4.4)$$

where $\eta = 1.4\, g_K + 1.6\, q_K$ ..... (4.5)

h_c = the diameter of the column head

g_K = dead load

q_K = live load.

In the case of a square column of size r,

$$\frac{\pi h_c^2}{4} = r^2 \quad \text{or} \quad h_c = 1.13\, r$$

From equation 4.3

$$M_{ds} = \frac{41.818}{0.46} = 90.909 \text{ kN.m}$$

and by substituting $\ell_1 = 4.0$ m, $\ell_2 = 4.0$ m, $M_{ds} = 90.909$ kN.m and $h_c = 1.13 \times 0.15 = 0.1693$ m in equation 4.4:

$\therefore$ $\eta = 12.033$ kN/m^2

The flexural load at ultimate limit state is equal to

$$\eta \ell_1 \ell_2 = 12.033 x 4.0 x 4.0 = \underline{\underline{192.53 \text{ KN.}}}$$

Assuming a value of 1900 Kg/m^3 for the weight of reinforced lightweight concrete, g_K is equal to

$$g_K = 0.125 \times 1900 = 237.5 \text{ kg/m}^2 = 2.33 \text{ KN/m}^2$$

and therefore $q_K = \dfrac{\eta - 1.4\, g_K}{1.6} = \dfrac{12.033 - 1.4x2.33}{1.6} = 5.482 \text{ KN/m}^2$

The service load per unit area is equal to $g_K + q_K = 2.33 + 5.482 = 7.812$ KN/m^2 and service load is equal to 7.812x4x4 = <u>125 KN.</u>

4.5.2 Punching Shear Load (at Ultimate L.S.) of Slab.

The critical section for calculating shear load is shown in Fig.4.6(a) and it is equal to b_p = 2x150+2x150+3πx125 = 1778 mm.

The punching shear load is given by:

$$V = b_p \times d \times v \quad \text{where } v = \xi_s \times v_c \qquad \ldots \quad (4.6)$$

where ξ_s = 1.30 for h = 150 mm or less (Table 14 of CP110)

and v_c is obtained from Table 25 of CP110.

The value of ρ to be used in Table 25 includes all the tension reinforcement within a strip of width b_2 = r+2x(3h) = 900 mm. As shown in Fig.4.6(b) there are 6 steel bars within this strip and hence

$$\rho = \frac{100x6x78.5}{900x900} = 0.5233$$

From Table 25, for = 0.5233 and $f_{cu} \geq 40$ N/mm^2 by interpolation

$$v_c = 0.44746 \text{ N/mm}^2$$

$$\therefore \; V = 1778 \times 100 \times 1.30 \times 0.44746 = \underline{\underline{103.42 \text{ KN.}}}$$

All the values of flexural design load, service load and punching shear load obtained according to CP110 for slabs FS-1, FS-8, FS-10 and FS-19 are given in Table 4.2.

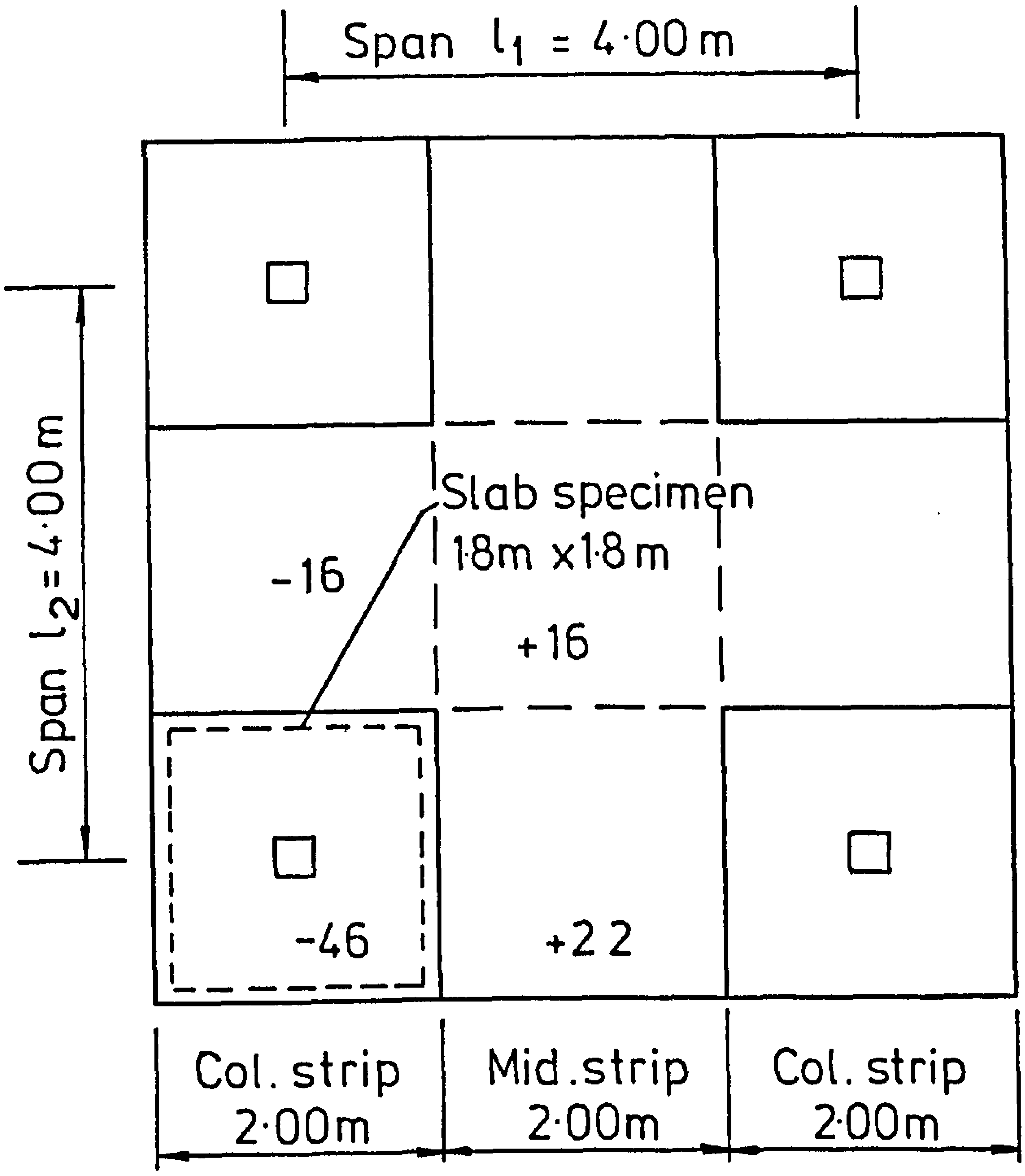

FIG. 4-5 MOMENTS IN FLAT SLABS IN PERCENTAGES OF Mds
(WITHOUT DROPS, INTERIOR PANEL)

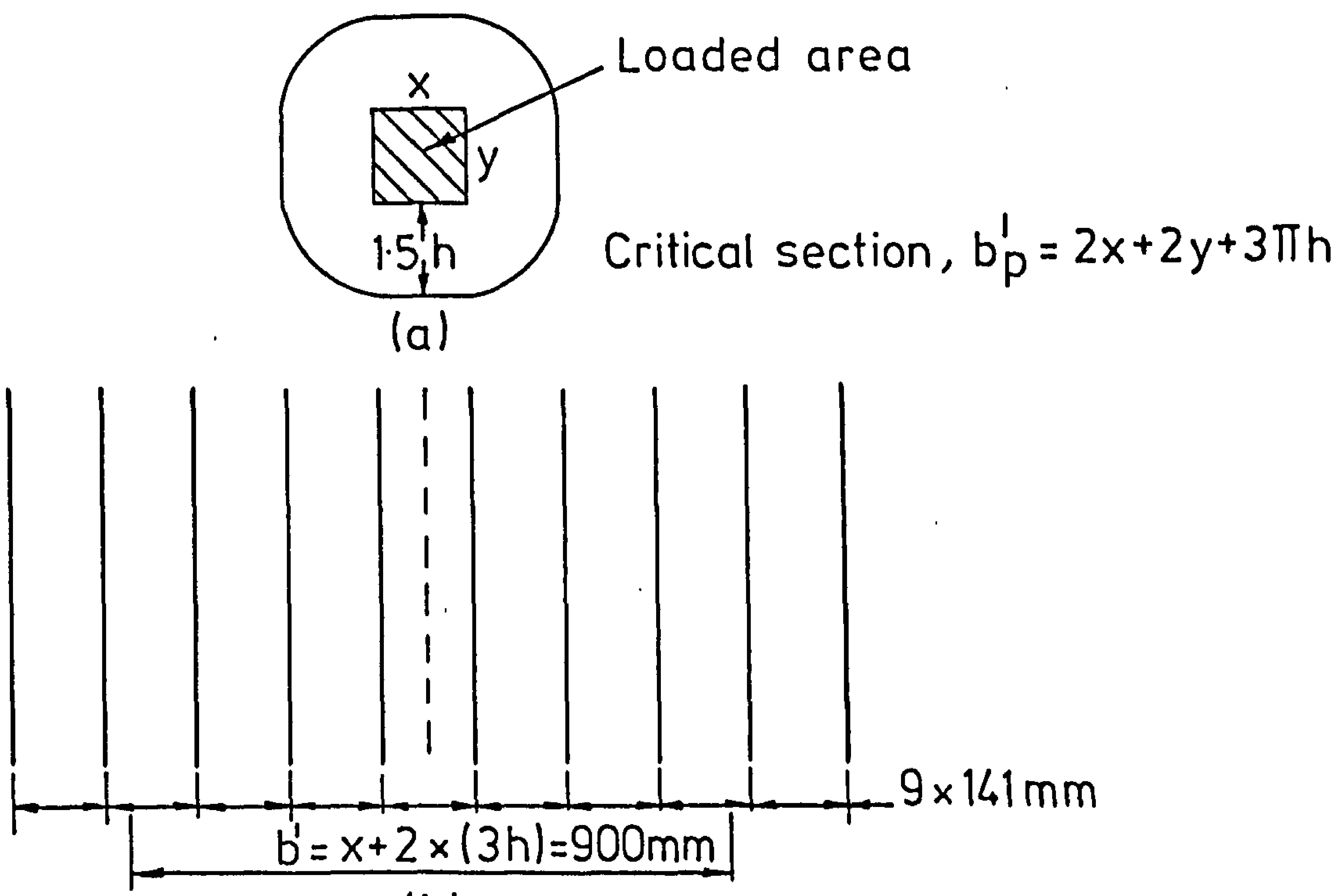

FIG. 4-6 CP 110 PROVISIONS FOR PUNCHING SHEAR

4.6 Flexural Design Load (at Ultimate L.S.) and Punching Shear Load According to A.C.I. code of practice (68).

4.6.1 Flexural Design Load (at Ultimate L.S.) of Slab.

According to A.C.I. code the moment of resistance is given by

$M'_N \quad = \quad A_s\, f_y\, jd = 12 \times 78.5 \times 460 \times 0.87 \times 100 = 37.699$ kN.m/1.69 m width

or $M'_N \quad = \quad 44.614$ kN.m/2m width = 44.614 kN.m/column stip width.

The total design moment in a panel in a given direction is given by:

$$M_o = \frac{w_1\, \ell_1\, \ell_n^{\,2}}{8} \qquad \ldots \quad (4.7)$$

where w_1 = total design load per unit area.

ℓ_n = clear span from face to face of columns

Moment M_o is related with M_N as follows

$$M_o = \frac{M_N{}'}{0.65\text{x}0.75} = \frac{44.614}{0.65\text{x } 0.75} = 91.516 \text{ kN.m}$$

Equation 4.7 gives

$$w_1 = \frac{8\ M_o}{\ell_1\ \ \ell_n^{\,2}} = \frac{8 \times 91.516}{40 \times 3.85^2} = 12.348 \text{ kN/m}^2$$

The flexural design load is equal to

$$w_1 \ell_1 \ell_2 = 12.348\text{x}4.0\text{x}4.0 = 197.57 \text{ kN.}$$

4.6.2 Punching Shear Load (at Ultimate L.S.) of Slab.

The critical section for calculating shear load is located at a distance d/2 from column faces and it is equal to

$$b_o = 4(r+d) = 4(150+100) = 1000\text{mm}$$

The design punching shear load is given by:

$$V = b_o \times d \times \phi \times (0.85 \times 4\sqrt{f_c{}'})$$

where ϕ = reduction factor for shear strength = 0.85.

Table 4.2 Design flexural load and punching load according to CP110 (69) and A.C.I. Codes (68).

Slab Number	h (mm)	d (mm)	r (mm)	ρ	f_{cu} N/mm^2	$f'_c = 0.79 f_{cu}$ N/mm^2	CP110 Design Flexural Load (kN)	CP110 Service Load (kN)	CP110 Design Shear Load (kN)	A.C.I. Design Flexural Load (kN)	A.C.I. Design Shear Load (kN)	$\frac{(12)}{(10)}$	$\frac{(11)}{(8)}$
1	2	3	4	5	6	7	8	9	10	11	12	13	14
FS-1	125	100	150	0.005574	44.20	34.92	192.53	125.0	103.42	197.57	141.77	1.371	1.026
FS-8	125	100	100	0.005574	45.8	36.18	188.85	122.69	93.81	192.54	115.46	1.231	1.020
FS-10	125	100	200	0.005574	45.5	35.95	196.30	127.34	113.14	202.81	172.62	1.527	1.033
FS-19	125	100	150	0.003716	43.1	34.05	130.10	85.97	79.35	131.71	140.00	1.764	1.012
										Average of ratios		1.473	1.023

$0.85x4\sqrt{f_c'}$ = permissible shear stress for sand-lightweight concrete.

Finally V = 141.77 KN.

All the values of flexural design load and punching shear load obtained according to A.C.I. code for slabs FS-1, FS-8, FS-10 and FS-19 are given in Table 4.2. From this Table it can be seen that CP110 is conservative compared to the A.C.I. code by about 47.3% in relation to shear (column 13) and 2.3% in relation to flexure (column 14).

4.7 Fabrication and Curing.

The specimens were cast in a mould consisting of 25 mm thickness plywood base and steel sides. The column forms were made of 25 mm thickness plywood. After the mould was oiled lightly, the slab reinforcement was placed and then the column steel was fixed. The concrete cover of 15 mm for the tensile reinforcement was obrained by welding chairs to the slab reinforcement. The concrete cover of 15 mm for the compressive reinforcement was obtained by fixing the reinforcement in the column ties and in the lifting hooks and by using high chairs which were placed along the edges of the specimens to eliminate their effect on the shearing strength. Four lifting hooks were fixed in the tensile reinforcement to facilitate the handling of the slab.

A removable 15 mm thick plywood form was used around the column area as temporary form for the steel fibre concrete placed at a distance of 550 mm from the centre of the slab.

The concrete was mixed in five batches (two fibre mixes and three plain concrete mixes) of 0.1 m^3 each using a horizontal pan-type mixer. The materials, except fibres were mixed for about one and a half minute in dry, water was then added and mixing continued for another two minutes. In the case of fibre concrete a mechanical dispenser was used to distribute the steel fibres into the concrete mixer. Casting of the slabs was accompanied by casting of three 150x150x150 mm cubes, three 500x100x100 mm prisms and three 200 mm in height and 100 mm in diameter cylinders. After casting,the concrete of the slabs and control specimens was compacted by using an electrical large table vibrator (3.05 x 1.20 m) consisting of three units external vibrators.

The following sequence was used in placing the two fibre concrete mixes in the central area and the three mixes of plain concrete in the outside area.

1. The first batch of fibre concrete was placed under and immediately around the column inside the temporary forms.

2. The second and third batches of plain concrete were placed in the area outside the forms, and the slab was then vibrated for two minutes.

3. The fourth batch of fibre concrete was again placed inside the temporary forms and the slab was vibrated for one minute and then the temporary forms were removed.

4. The fifth batch of plain concrete was placed in the required area outside of the previous location of temporary forms and the slab was vibrated just enough to remove all air bubbles.

5. The column stub was filled by plain concrete and vibrated mechanically by using a steel rod. Then the surfaces were well finished using a steel trowel.

Curing of the slabs and control specimens took place under uncontrolled laboratory conditions. After casting the slab and control specimens were covered with a polythene sheet. The column stub and control specimens were demoulded at 24 hours whereas the slab was demoulded after four days and remained under polythene sheet for a further 18 to 20 days. From this time to testing at 28 days the slabs were stored uncovered in the laboratory ready for installation in the testing rig and instrumentation.

4.8 Instrumentation.

Three basic types of measurements were taken during all of the slab tests. These are deflections, strains and rotations.

4.8.1 Deflections.

Deflections were measured by means of dial gauges of 0.01 mm accuracy and 25 mm travel. A maximum of ten dial gauges were used to measure vertical displacements at points D_1 to D_{10} in both lateral and diagonal directions. One more, at point D_{11}, was used at one corner of the slab to record the vertical lift off. Details of the dial gauge positions are shown in Figs. 4.7(a) and (b).

4.8.2 Strains.

Concrete strain readings were measured using a 100 mm Demec gauge on the compression and tension sides of the slab in both lateral and diagonal directions. A maximum of twenty eight readings were taken for each side including radial and tangential concrete strains. Typical Demec point layouts are shown in Figs. 4.7(a) and (b), and Plate 4.1.

Strains on the tensile and compressive steel were measured by means of 10 mm gauge length electrical resistance strain gauges having a gauge factor of 2.08 and a resistance of 120 ohms. All steel strain measurements were recorded manually using the automatic selector Type 1542 and the strain gauge apparatus Type 1516 as shown in Plate 4.2. A typical steel strain gauge layout is shown in Figs. 4.8(a) and (b).

4.8.3 Rotations.

Rotation measurements, at various locations on the compression side of the slab, were derived from slope changes using a Hilger and Watts clinometer capable of reading to 1min of arc (0.29×10^{-3} rads). Each clinometer point consisted of 12 mm diameter steel ball glued to a 12 mm steel washer, 150 mm centre to centre. The locations of rotation measurement are presented in Fig.4.7 (b) and Plate 4.1.

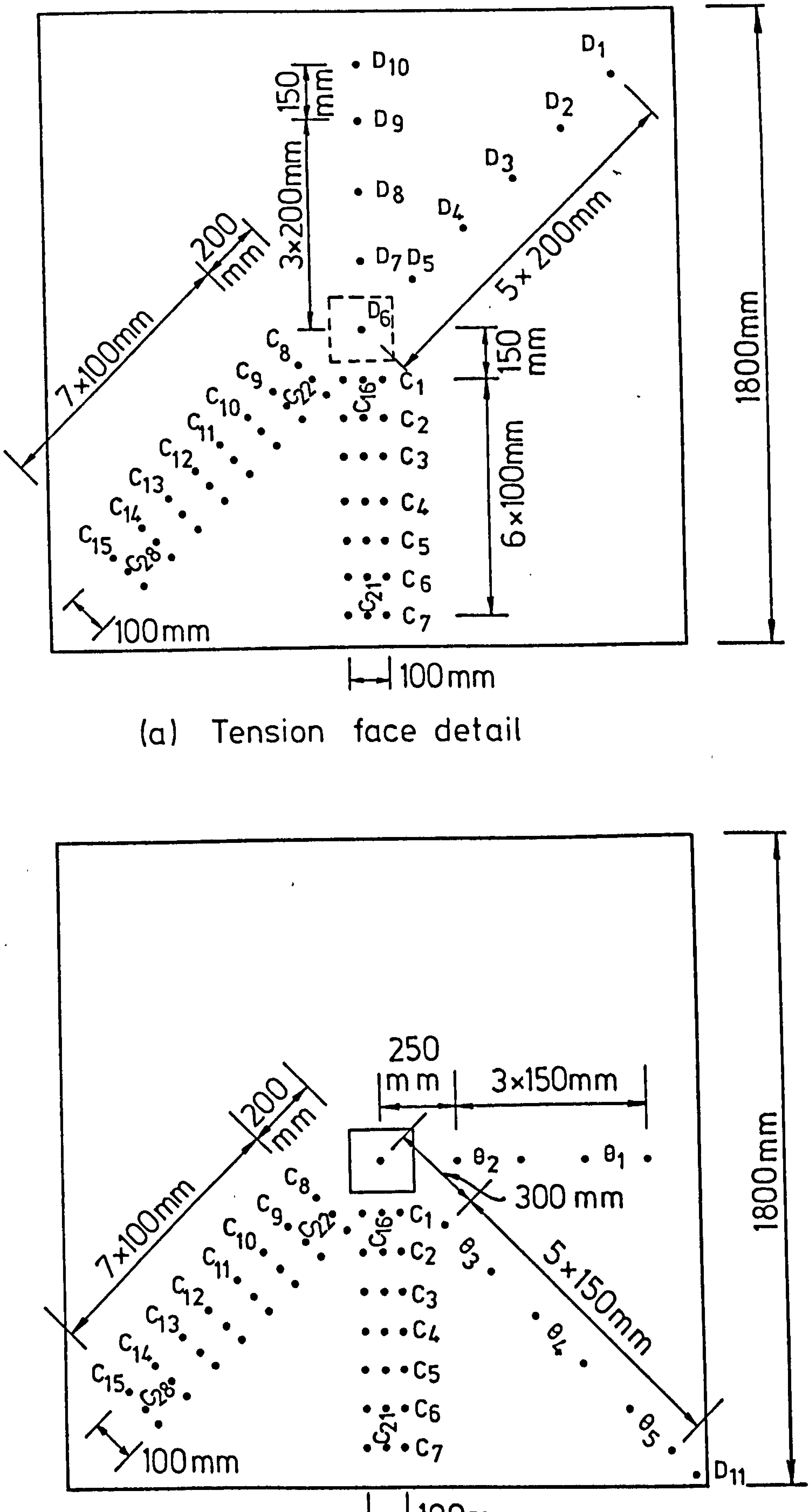

(a) Tension face detail

(b) Compression face detail

FIG. 4-7 TEST SPECIMEN FACE DETAIL

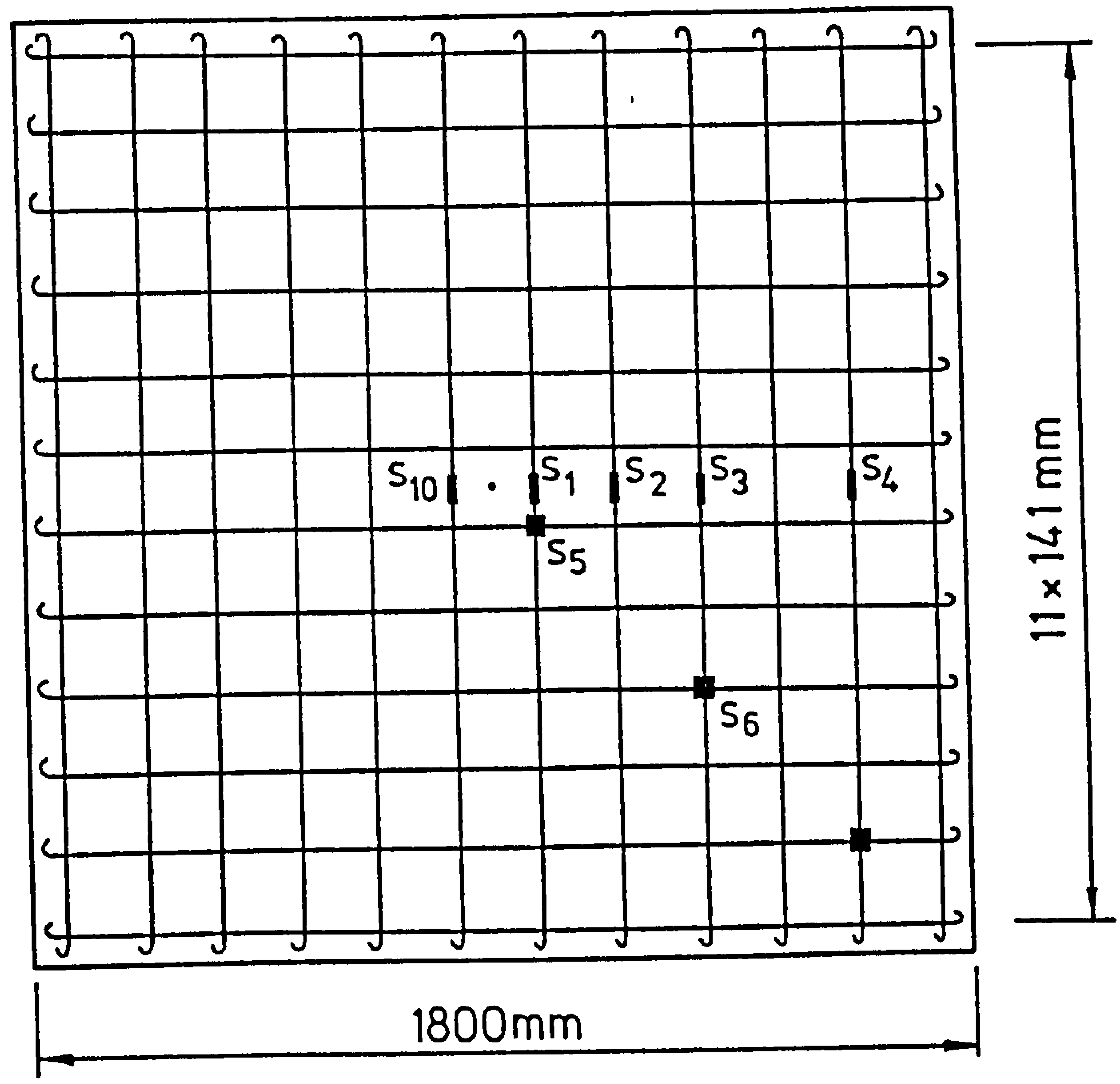

(a) Tensile reinforcement

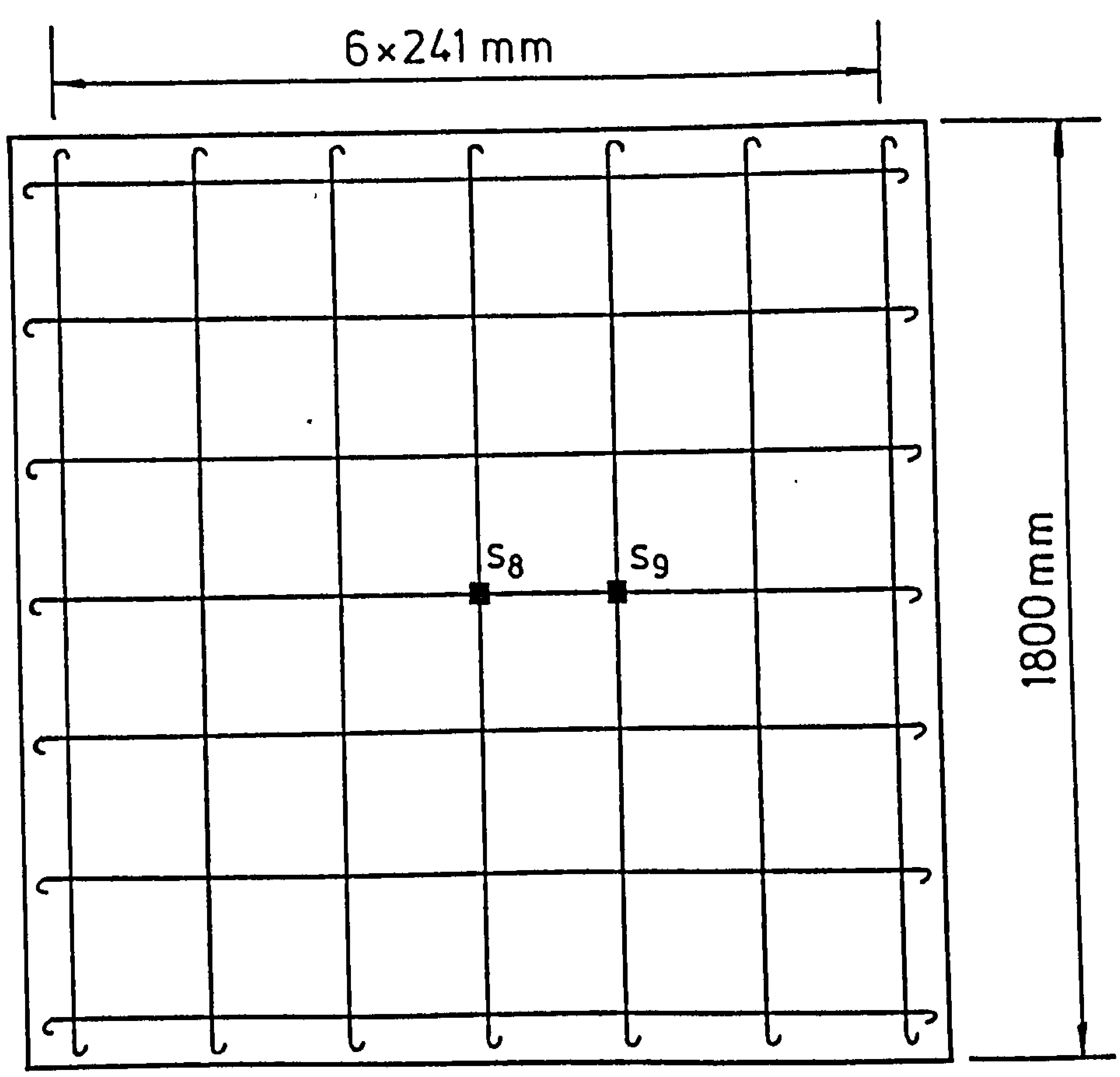

(b) Compressive reinforcement

FIG.4-8. TYPICAL STRAIN GAUGE POSITIONS ON REINFORCEMENT

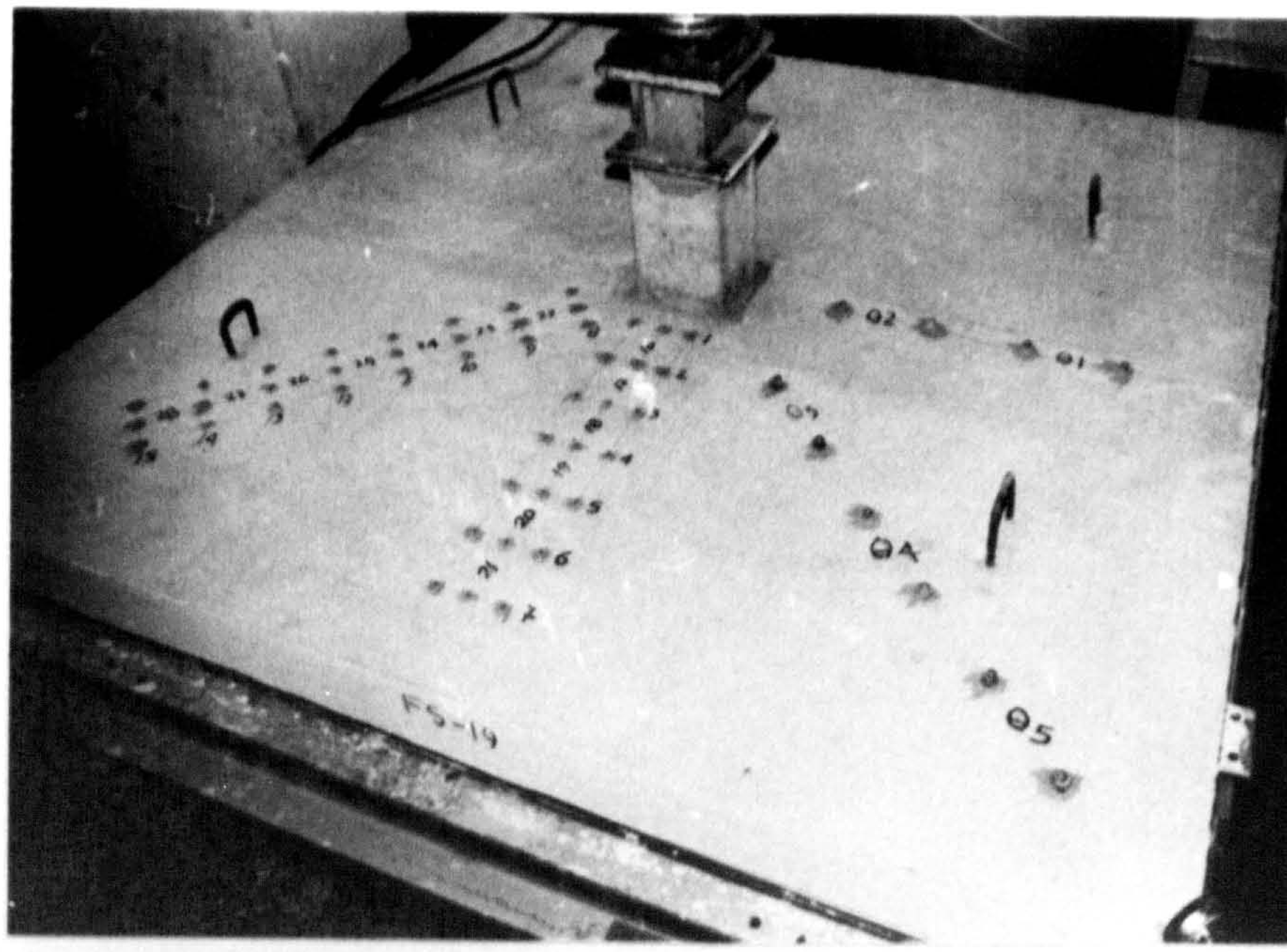

PLATE 4-1 SLAB TEST SPECIMEN COMPRESSION FACE DETAIL

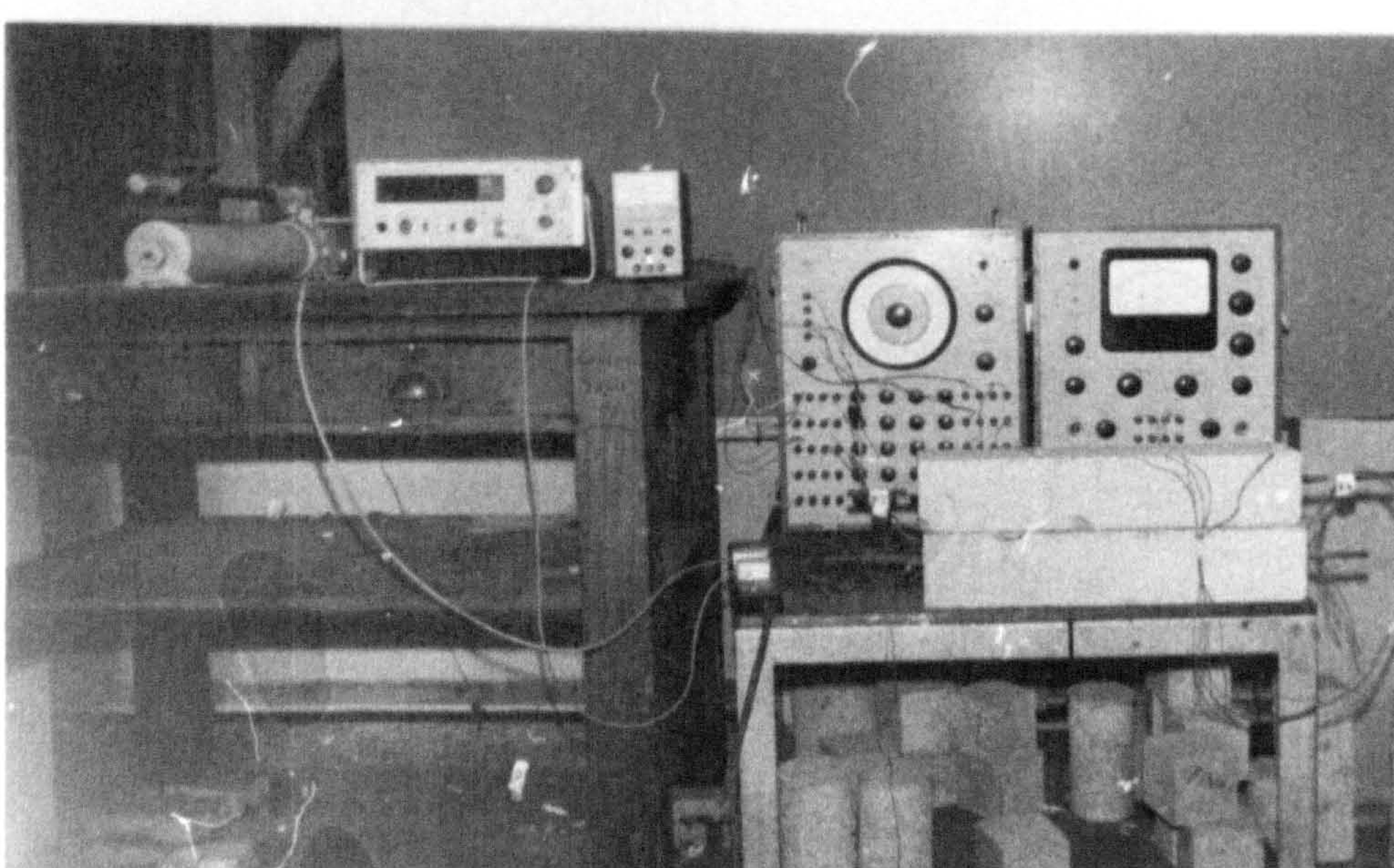

PLATE 4-2 LOAD AND STEEL STRAIN TEST DEVICE

4.9 Loading Device and Testing Procedure.

A hydraulic testing device capable of producing a static load up to 50 Tons was used for all the tests. A calibrated load cell was used for the load transmission and it was of a H500 type, 50 Tons capacity operating on 10 volts. The load cell was placed on a base plate, which in turn was placed on 12 mm thick steel plate having the same size of the column stub and fixed with 1:1 sand and cement mortar.

At the beginning of each test zero readings were taken for all the instruments, and then loading was started. The load was applied during about one minute in increments of approximately 15.0 KN until failure. For each load increment readings of all gauges were taken and cracks were detected and marked. Because of the numerous readings taken at each load increment each loading stage took from 15 to 20 minutes to complete. This rather long duration caused a drop in load by the time all readings were taken, the drop being greater in the final stages of loading with a maximum of about 4%. During and after testing photographs of the slabs were taken.

CHAPTER 5.

DEFORMATION CHARACTERISTICS OF TESTED SLABS.

5.1 Introduction.

The deformation and cracking characteristics of structural lightweight concrete members are important in design. Because of the lower modulus of elasticity of lightweight aggregate concrete, the deflection of lightweight concrete slabs will be greater than that of normal weight concrete slabs. Also, for a given load, other deformations such as strains in concrete and reinforcement are likely to be greater. For reinforced concrete flat plates and flat slabs there is a number of ways to reduce deformations, such as thickening the slab or increasing the flexural reinforcement.

In the tests reported here an attempt has been made to reduce deformations by using fibre reinforcement in slab column connections. This chapter deals with the results of the experiments carried out in this investigation on twenty slab-column connections. The behaviour of the specimens during testing is discussed in relation to cracking patterns,deflection, rotation, steel strain and concrete strain.

5.2 General Behaviour of the Slabs and Crack Patterns.

The deformations of all tested slabs were all very small in the elastic stage of loading until the first crack appeared, then they increased steadily and then rapidly, as cracking propagated on the tension side of the specimen and yielding of the reinforcement approached.

In the plain concrete slabs, the first visible crack occurred on the tension side in both directions and around the column stub at about 18-19% of the maximum load for slabs FS-1, FS-8 and FS-10 with a tension steel reinforcement ratio equal to 0.5574% and at about 16% of the maximum load for slab FS-19 with a lower tension steel reinforcement ratio equal to

0.3716%. These percentages are in agreement with the results from tests on normal weight concrete slabs reported by Ali (78) and Anis (81). The presence of fibre reinforcement increased the first crack load by about 30-45% but the first crack to maximum load ratio was about the same as in plain concrete slabs. Plate 5.1 shows the first crack position for various slabs with and without fibre reinforcement.

As loading continued on both plain and fibre concrete slabs the cracks started to propagate radially, first in the lateral direction towards the edge of the slabs at about 20% of the maximum load and then in the diagonal direction at about 30% of the maximum load. Ali (76) reported that in normal weight concrete slabs the cracking in the diagonal direction occurred before that in the lateral direction. Plate 5.2 and 5.3 show the developed cracks during testing in slabs FS-1 (V_f = 0.0%) and FS-2 (V_f = 0.5%) respectively. These radial cracks reached the edge of the slabs and then appeared in the vertical face of the slabs. The load at which the radial cracks appears in the vertical face of slab was about 30-40% of the ultimate load; the cracks which appeared first were located within a region at a distance 250 mm from the middle of the vertical face of the slab. The cracks in this region were almost vertical and propagated for only one or two steps of loading after their appearance. The other cracks in the vertical face of slab were initially vertical and then propagated continuously with incrasing load at an angle with horizontal ranging from 60^o to 70^o. (Pl.5.4). In plain concrete slabs the side cracks did not reach the upper slab edge but they did reach in most fibre concrete slabs especially in those which failed in flexure. Plate 5.5 shows the side crack patterns of slabs FS-7 and FS-17 which failed in flexure. It can be seen that the side cracks located at the position of the yield lines propagated almost horizontally during the late stages of loading before failure occurred.

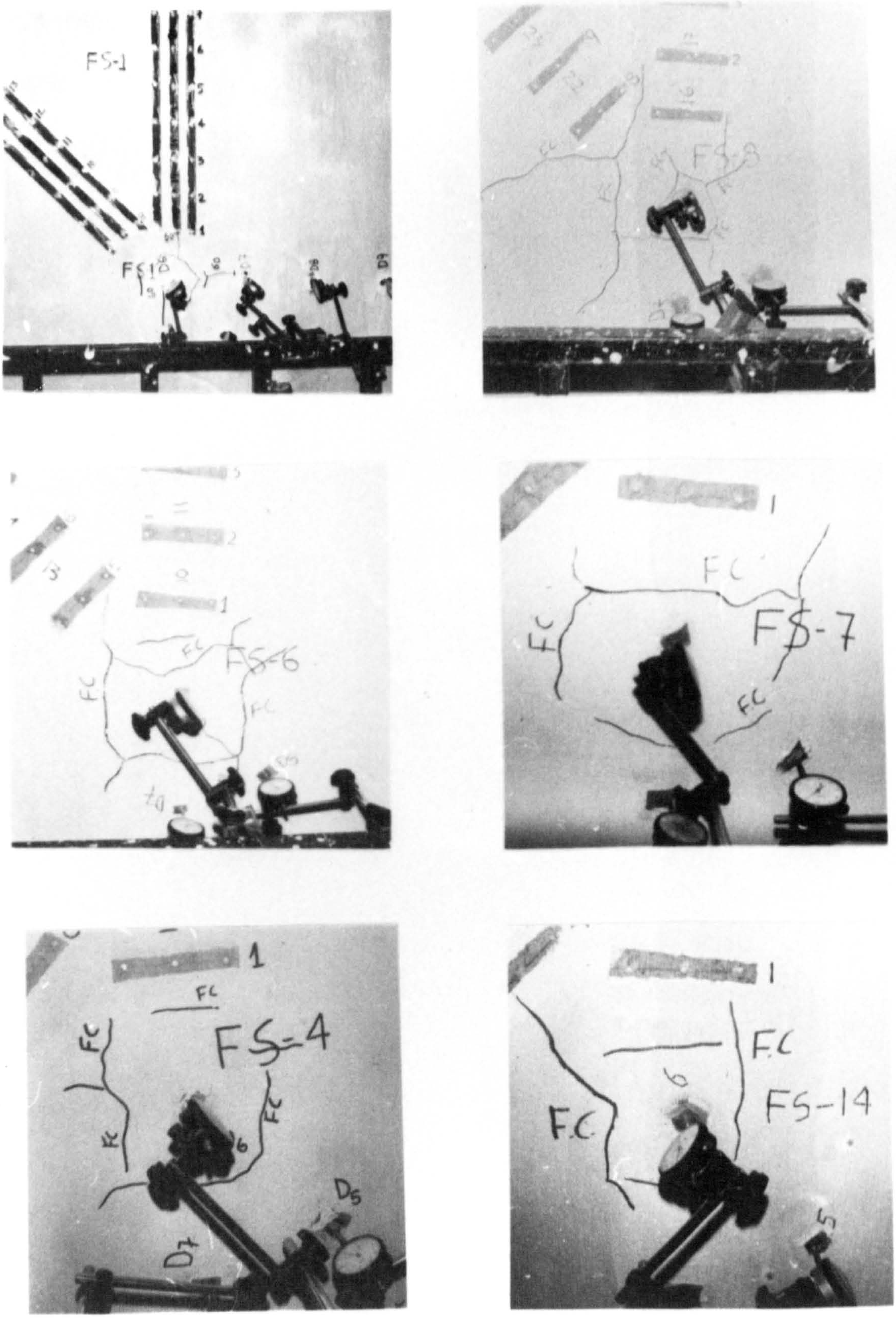

PLATE 5-1 FIRST TENSION CRACK IN SLABS WITH AND WITHOUT FIBRE REINFORCEMENT

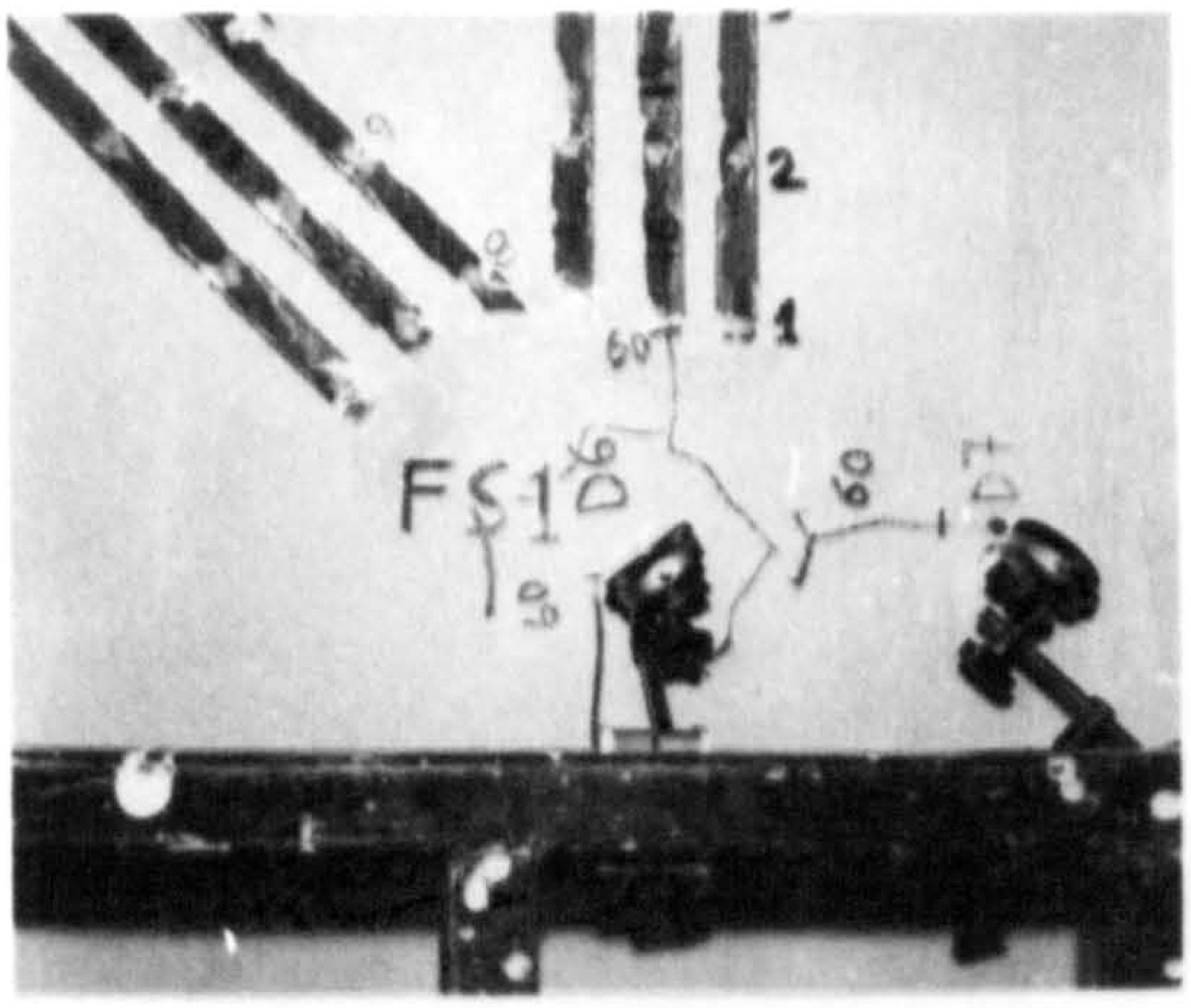

(a) At first crack

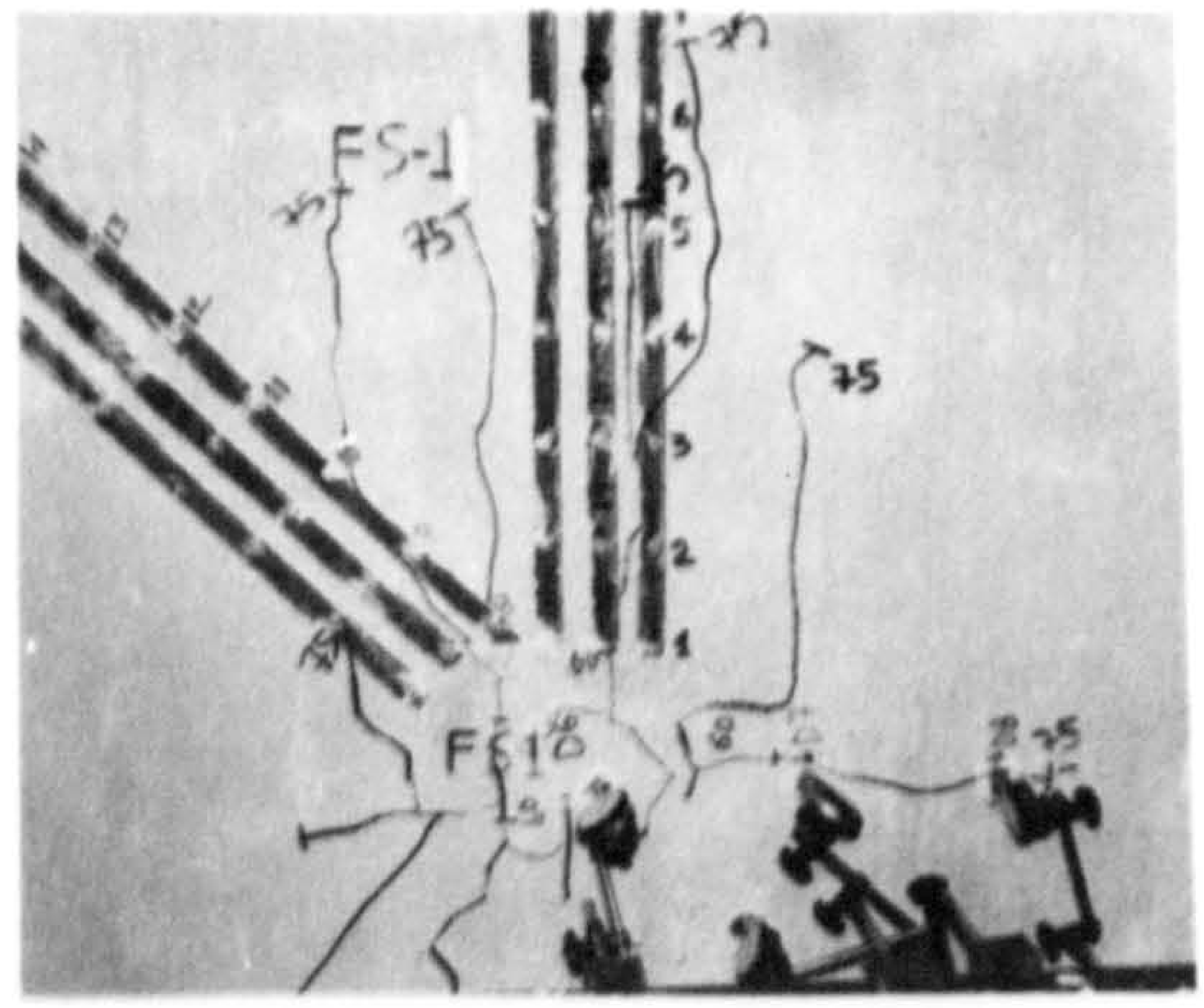

(b) After first crack (propogation in lateral direction)

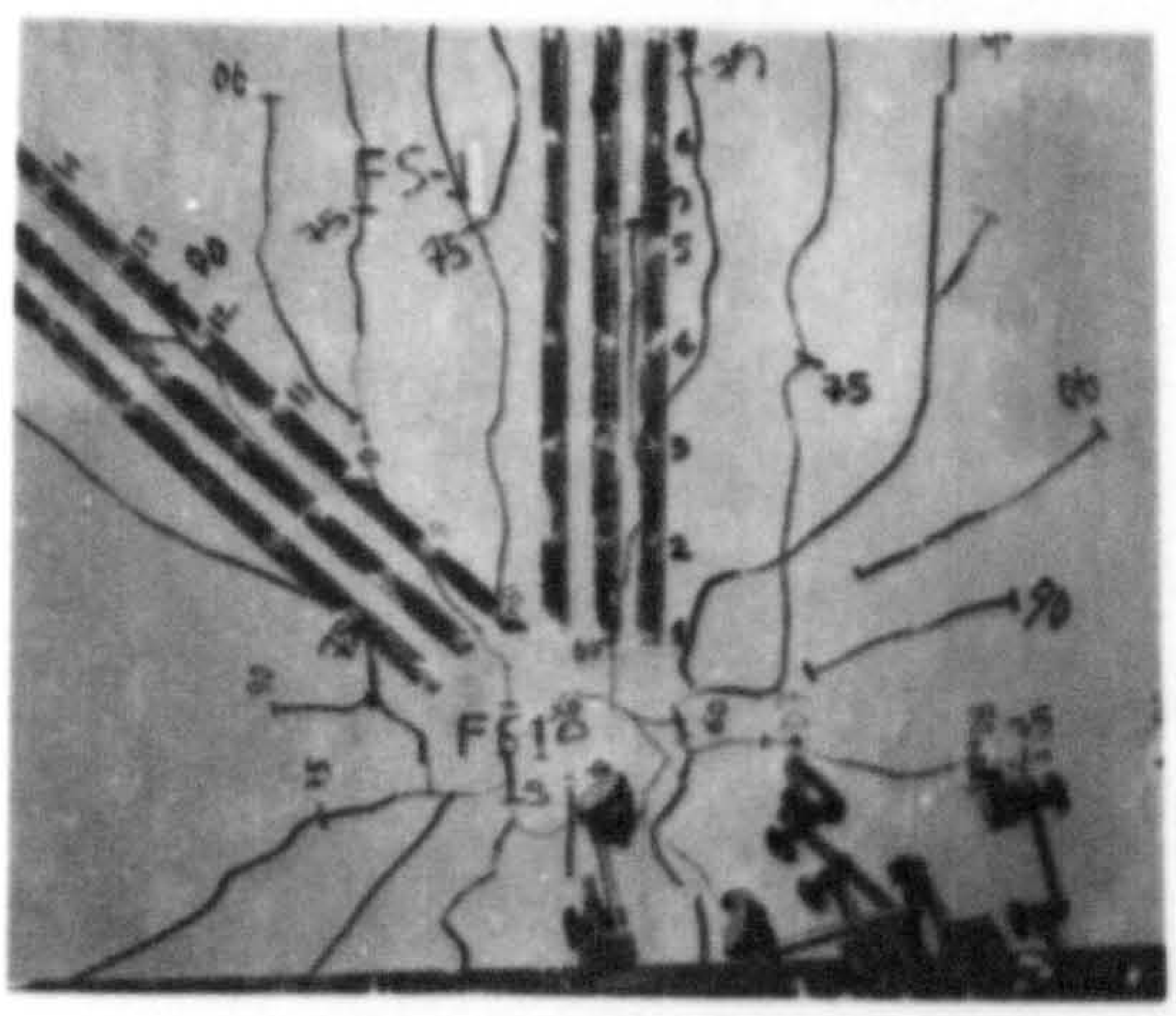

(c) Propogation in diagonal direction

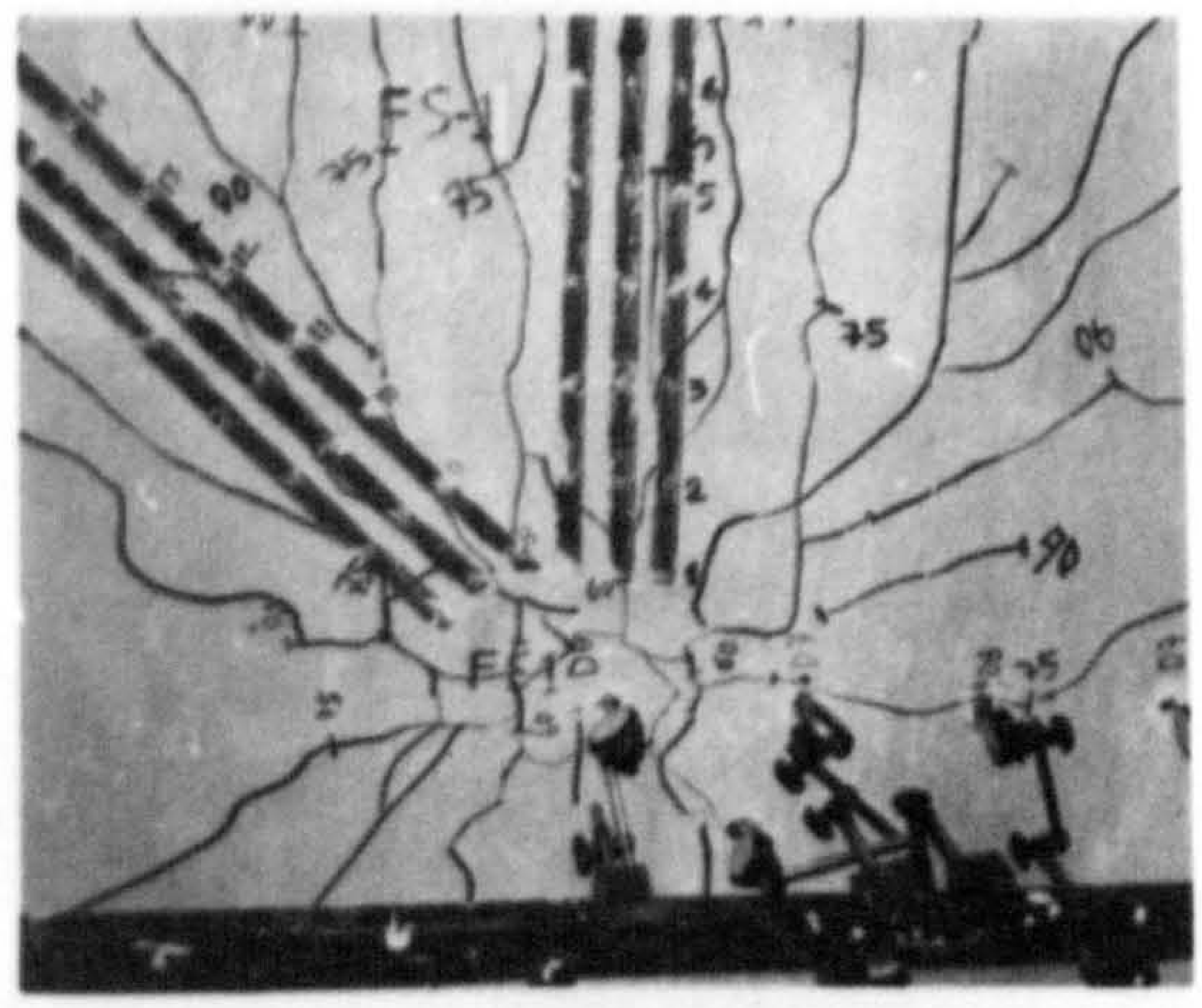

(d) At service load

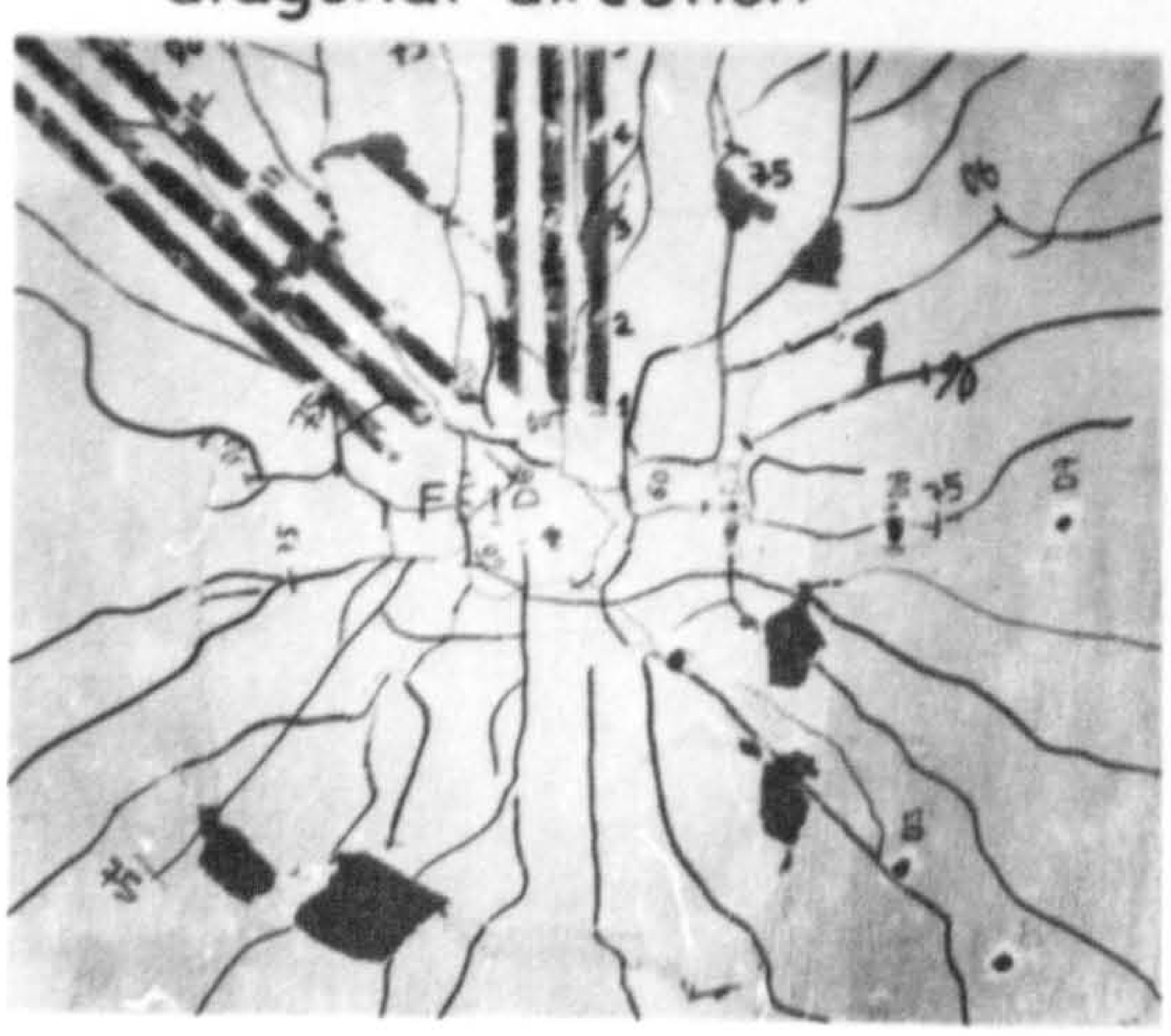

(e) Cracks before complete punching

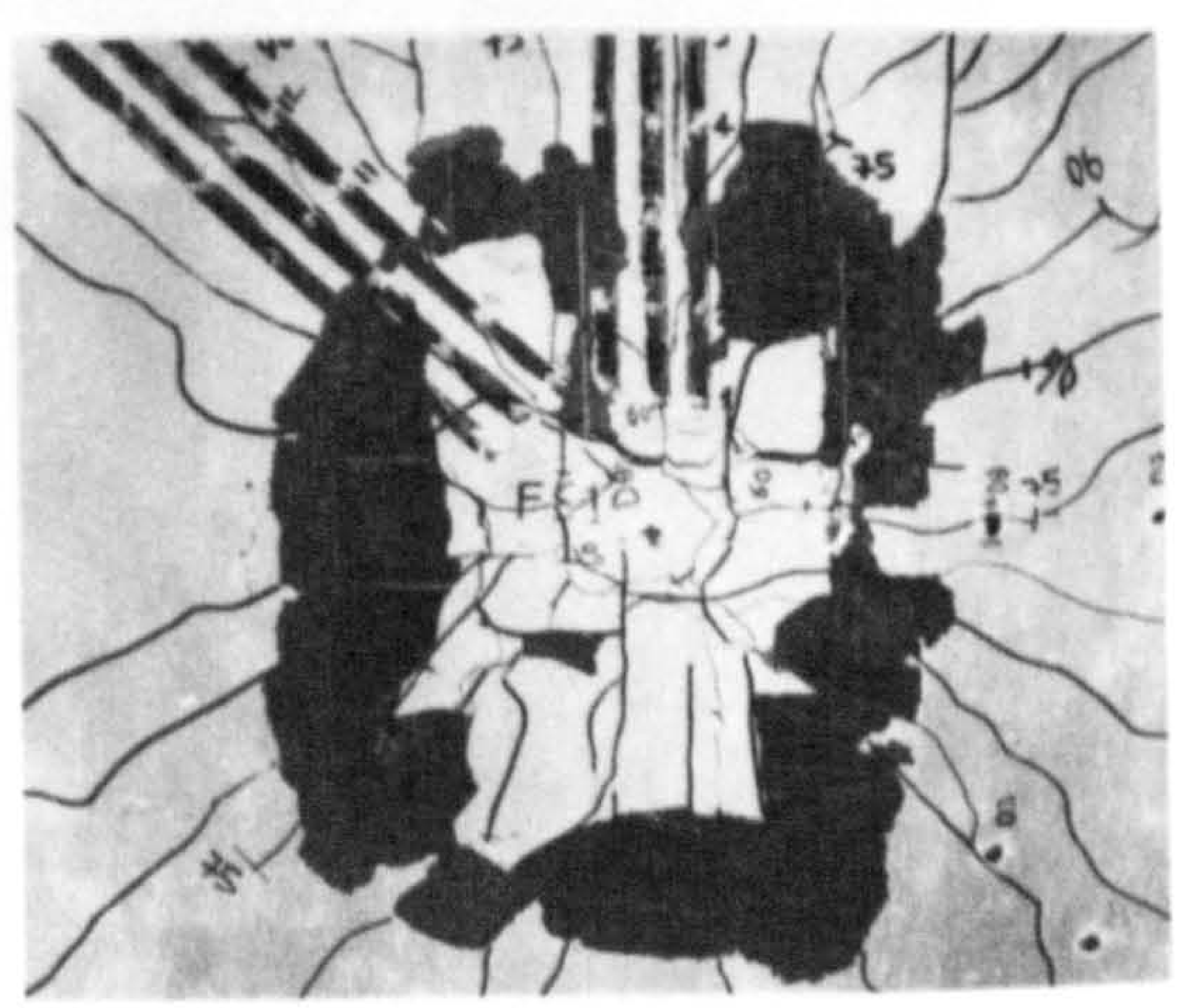

(f) After complete punching

PLATE 5-2 CRACK DEVELOPMENT IN SLAB FS-1 ($V_f = 0\%$) DURING TEST

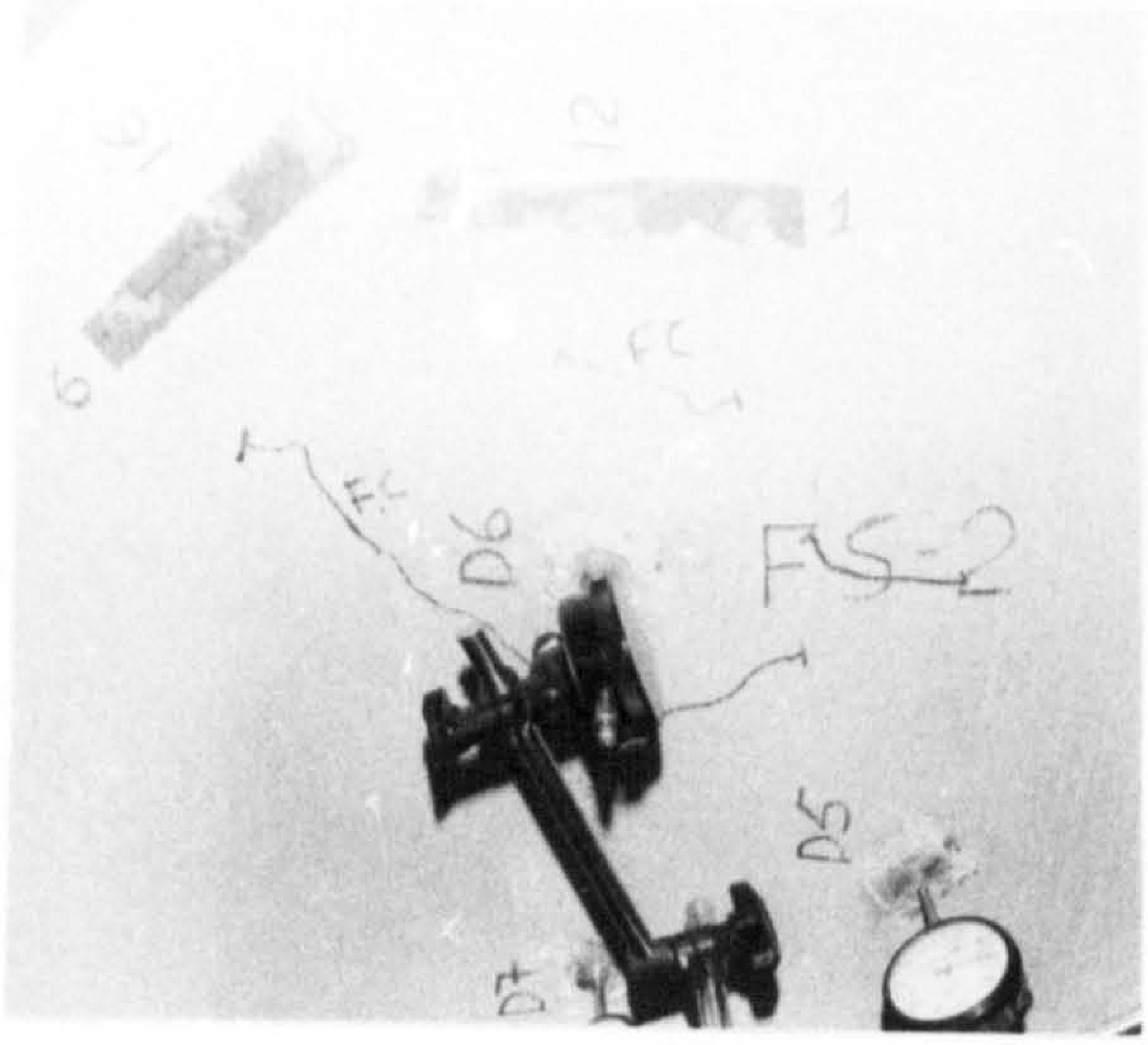

(a) At first crack

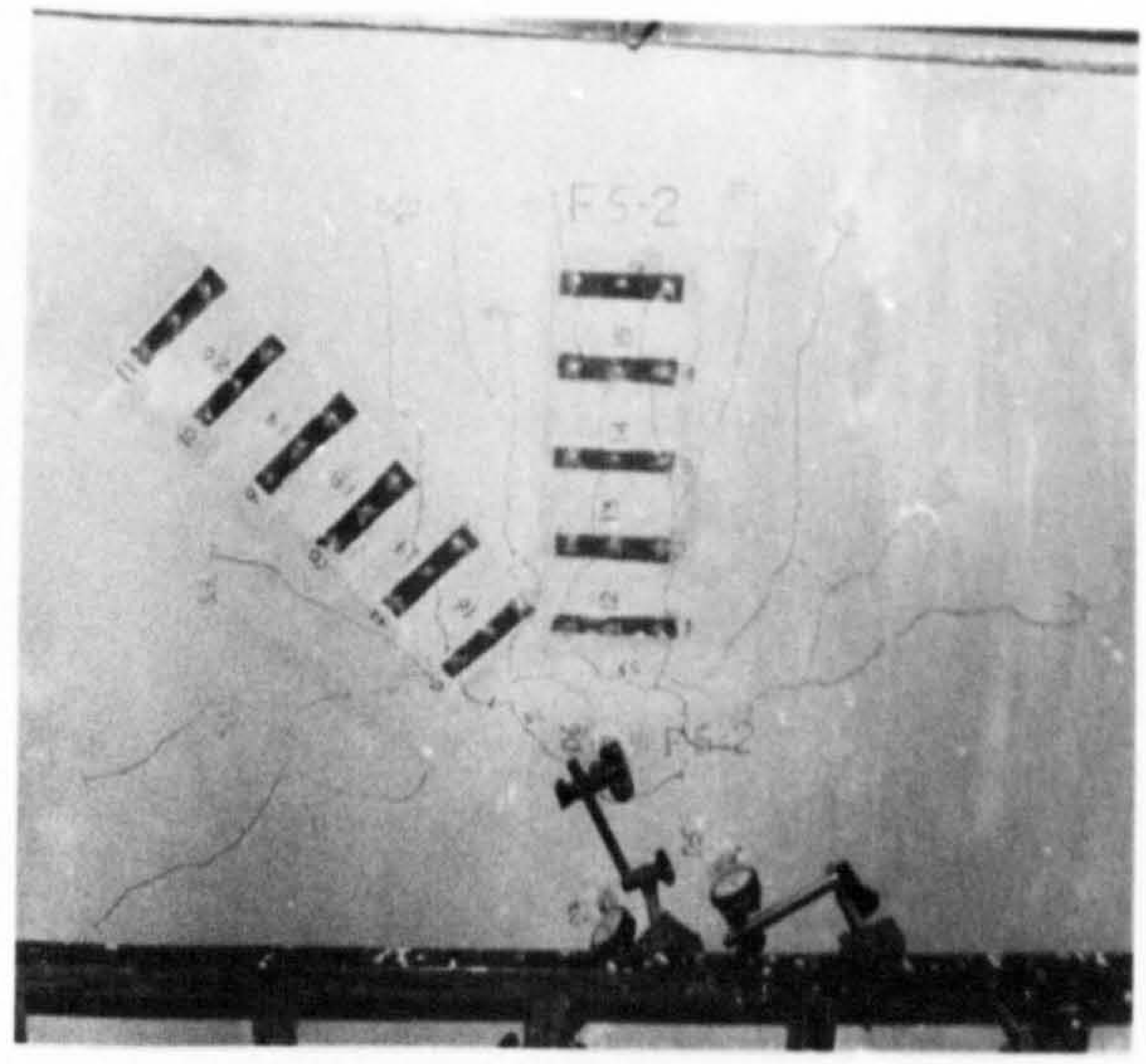

(b) After first crack

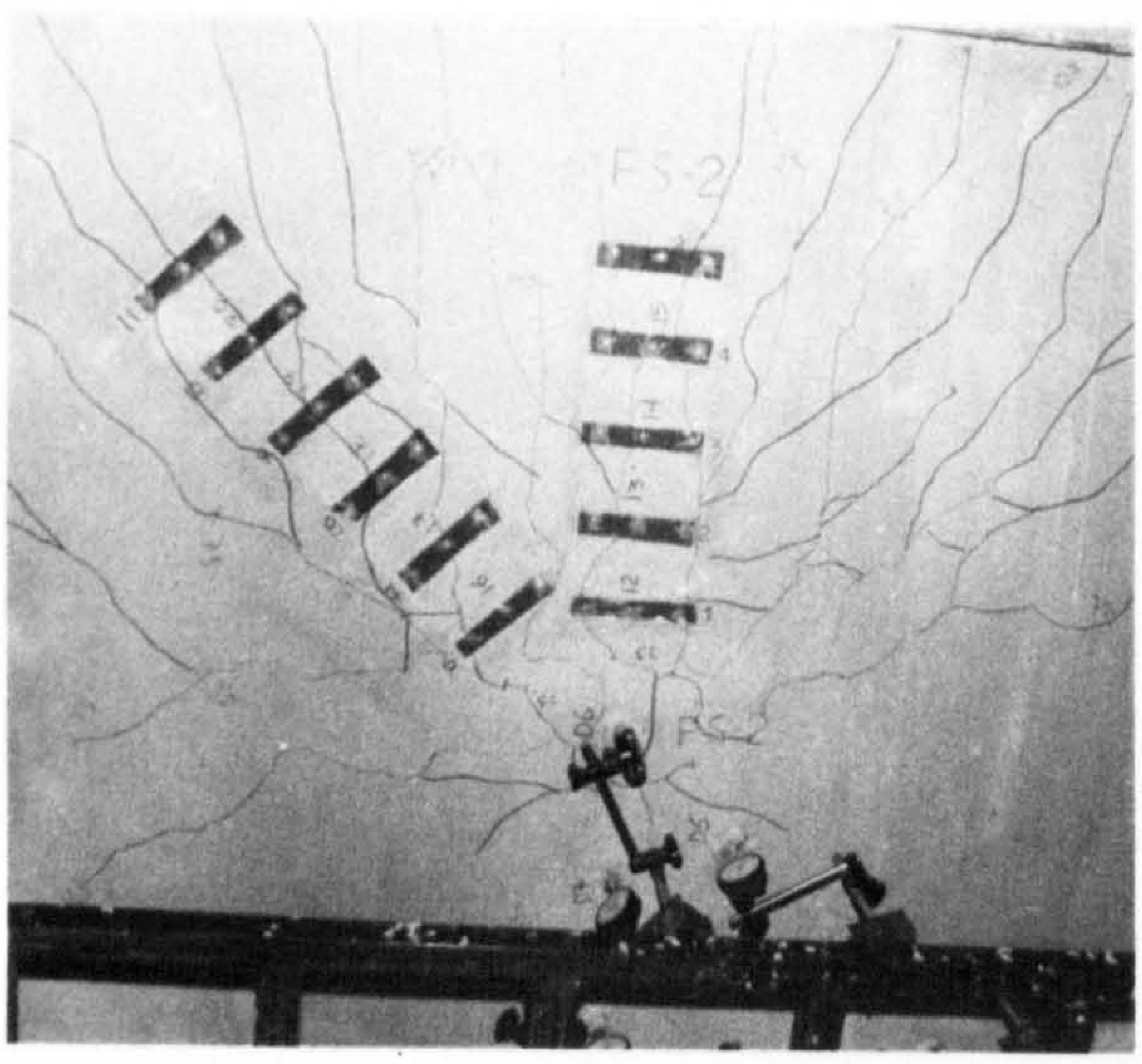

(a) At service load

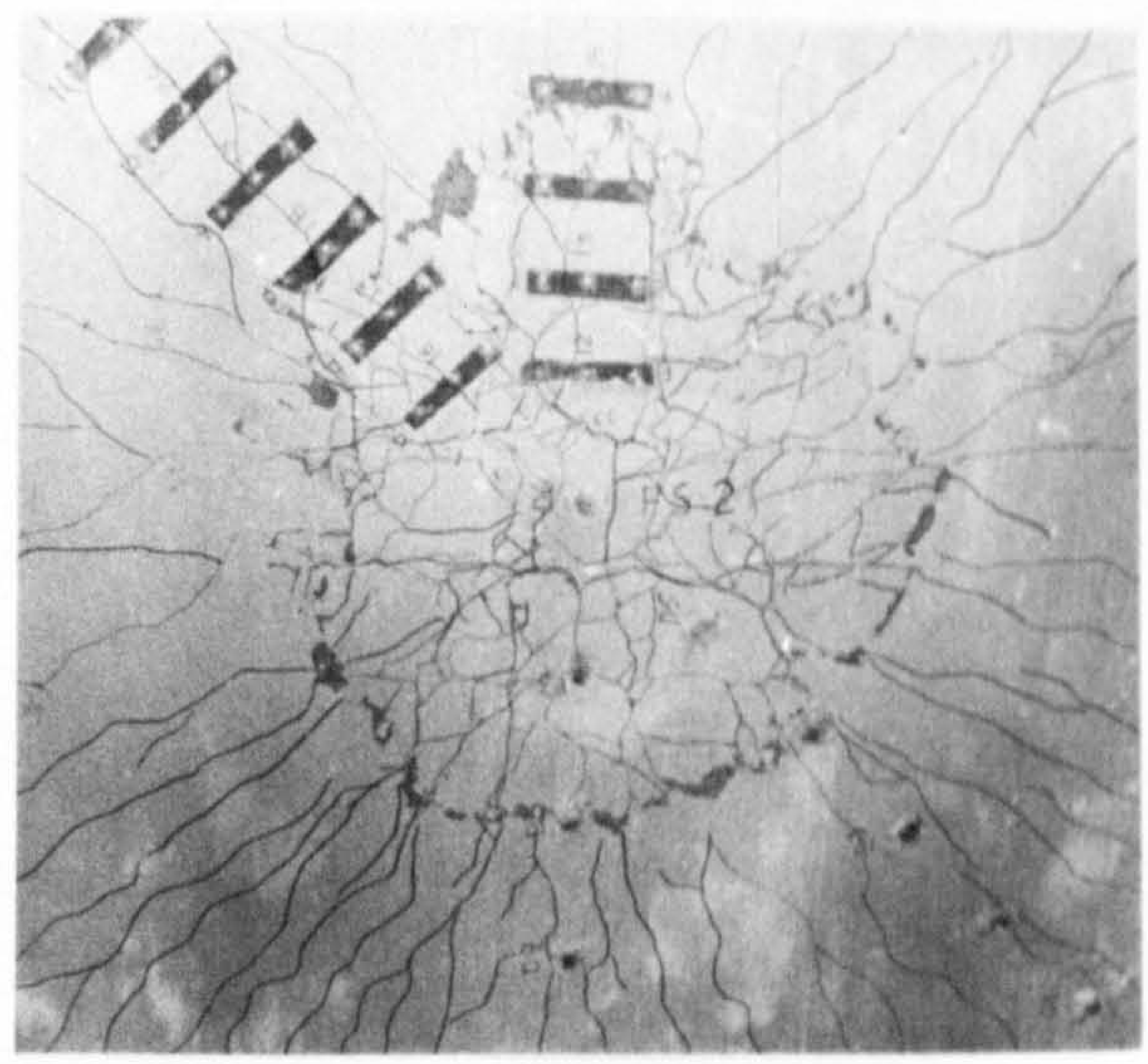

(d) At failure load

PLATE 5-3 CRACK DEVELOPMENT IN SLAB FS-2 (V_f =0·5%)

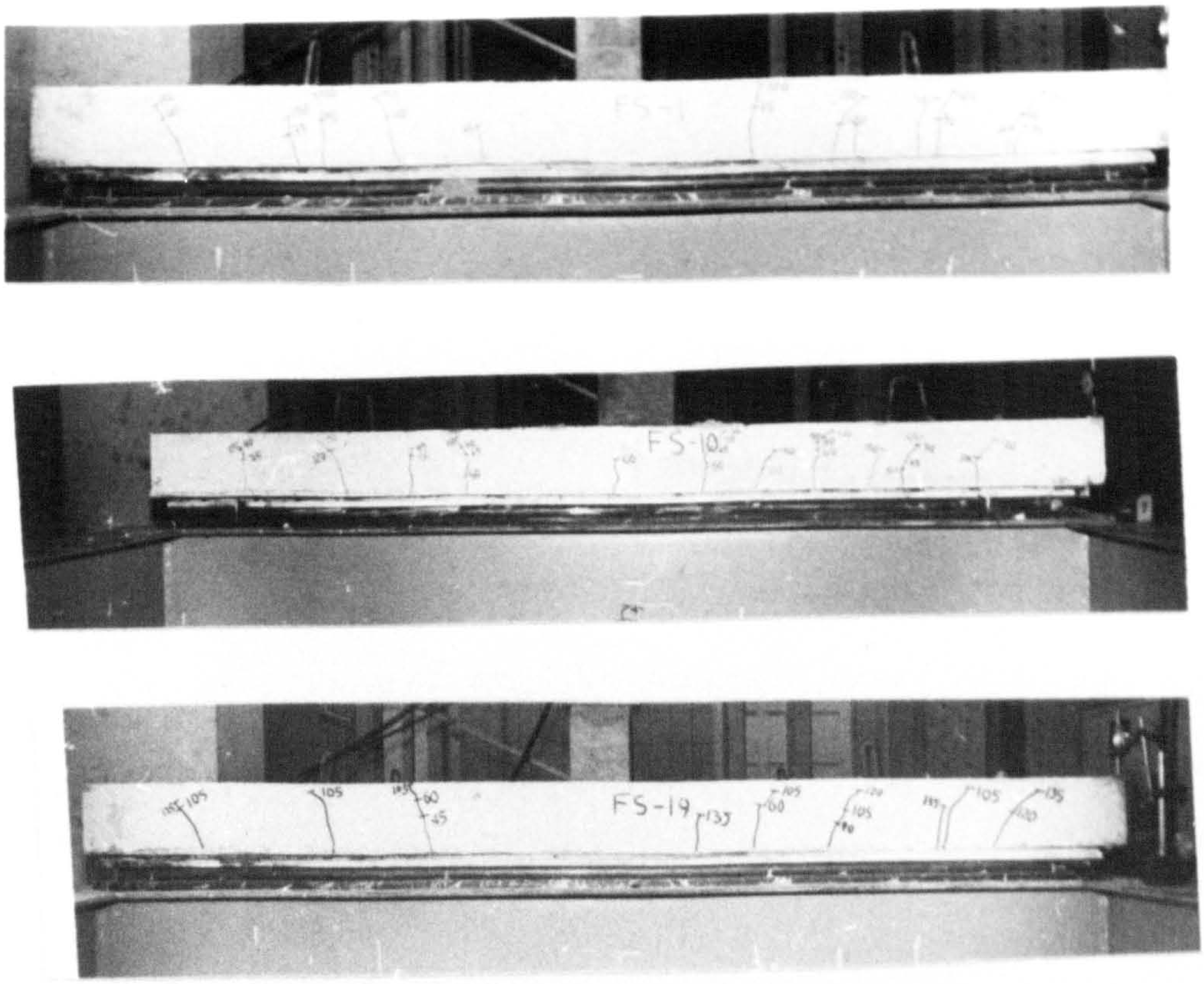

(a) Plain concrete slabs

(b) Fibre concrete slabs

PLATE 5·4 SIDE CRACK PATTERNS FOR VARIOUS SLABS FAILING IN PUNCHING SHEAR

The crack patterns of fibre concrete slabs failing in punching shear were observed to be about the same as for slabs without steel fibres, except that in the former, the cracks were much finer and more in number than in the corresponding plain concrete slab connections. The cracks were widening with increasing load until failure occurred. In the plain concrete slab connections, the punching failure was complete and sudden. In the fibre concrete slab connections which failed in punching shear the failure was gradual, and the punching perimeter was bigger. More details and photographs at failure are discussed in Chapter 6.

All plain concrete slabs and those fibre concrete slabs which failed in punching shear had no cracks on the compression surface at all except the punching line in the immediate vicinity of column faces.

The addition of fibre reinforcement in slabs FS-6, FS-7, FS-11 and FS-17 enabled the slabs to fail in flexure instead of punching shear. These fibre concrete slabs failed in flexure first and then they failed in punching as loading continued. The crack patterns in these slabs on both compression and tension sides were quite different from those in slabs failing in punching. The crack patterns on the compression face of the slabs failing in flexure were circular with different diameters all occurring around the column stub. Plate 5.6(A) shows this crack pattern for slab FS-17 which failed in flexure. The crack patterns on the tension surface can be considered to be a combination of flexural and punching crack failures as can be seen from Plate 5.6(B) since the slabs failed in punching after their flexural failure. It was noted that the average location of yield lines from the corners of the slabs was about (0.259 $(\ell-r)$ for slabs FS-6 and FS-7 (ρ = 0.3716%) and 0.311 $(\ell-r)$ for slabs FS-11 and FS-17 (ρ=0.5574%) while the theoretical value for plain concrete slabs predicted by yield line

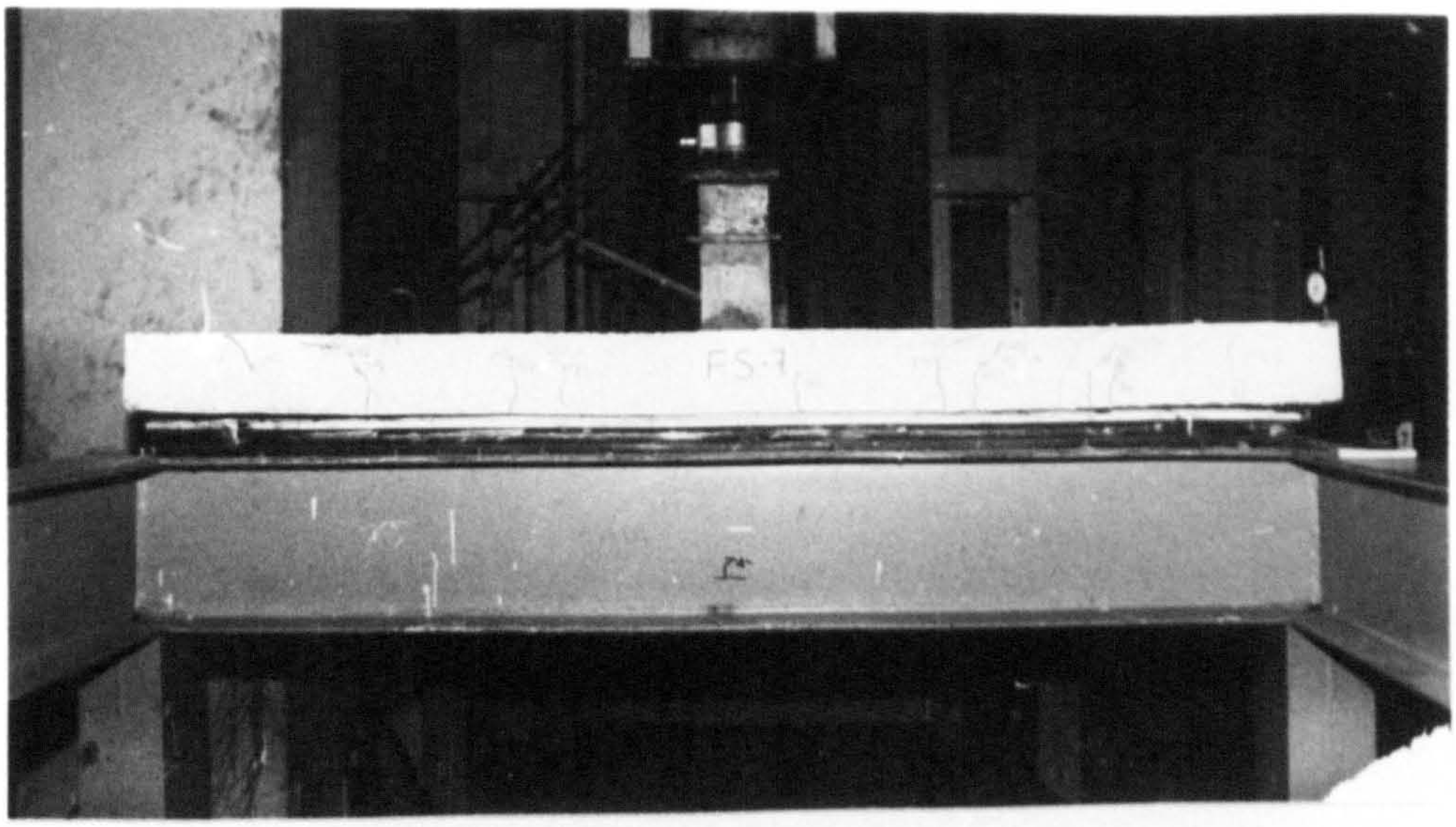

(a) Slab FS-7 ($V_f = 1\%$, $\rho = 0{\cdot}3716\%$)

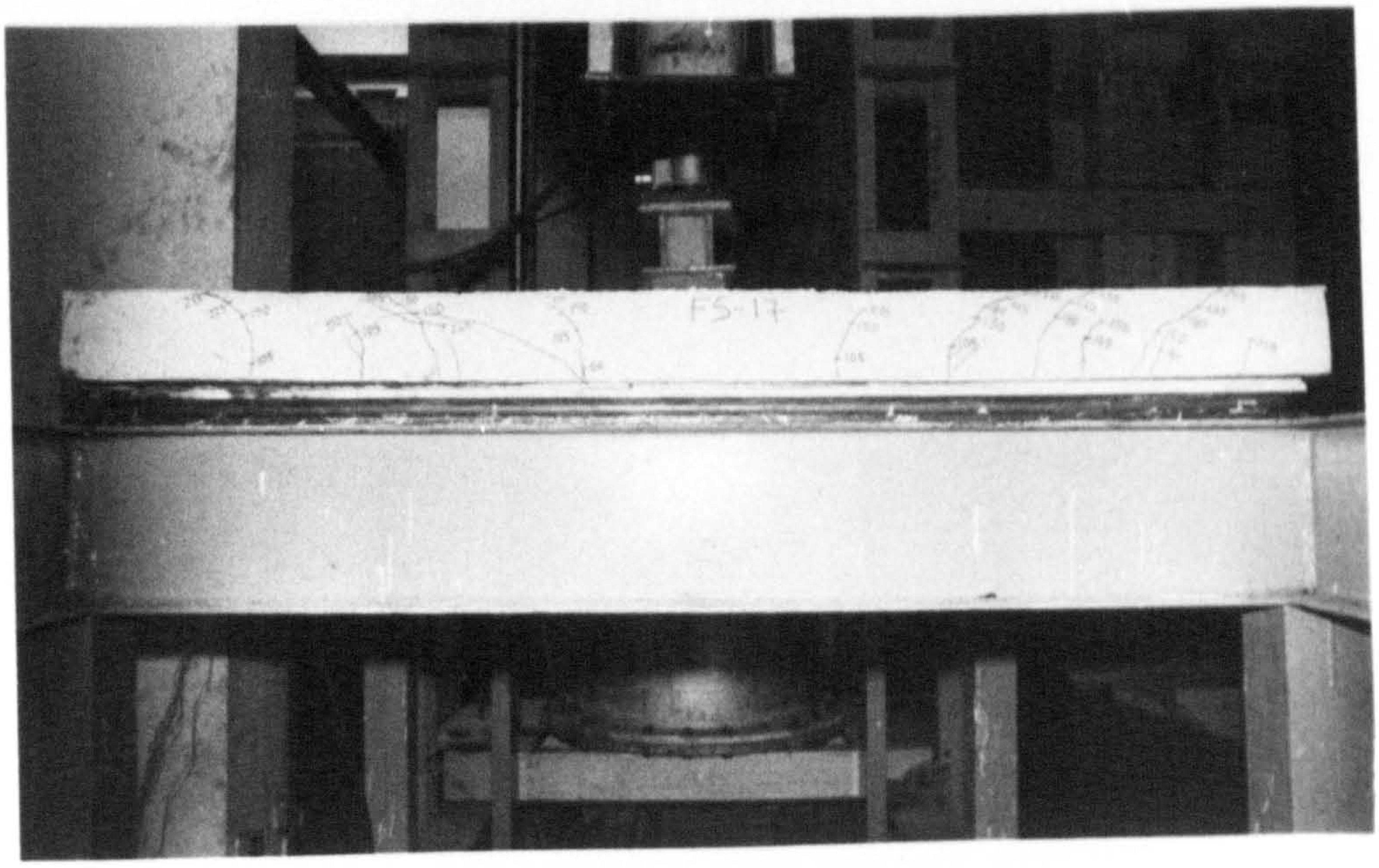

(b) Slab FS-17 ($V_f = 1\%$, $\rho = 0{\cdot}5574\%$)

PLATE 5-5 SIDE CRACK PATTERNS FOR FIBRE CONCRETE SLABS FAILING IN FLEXURE

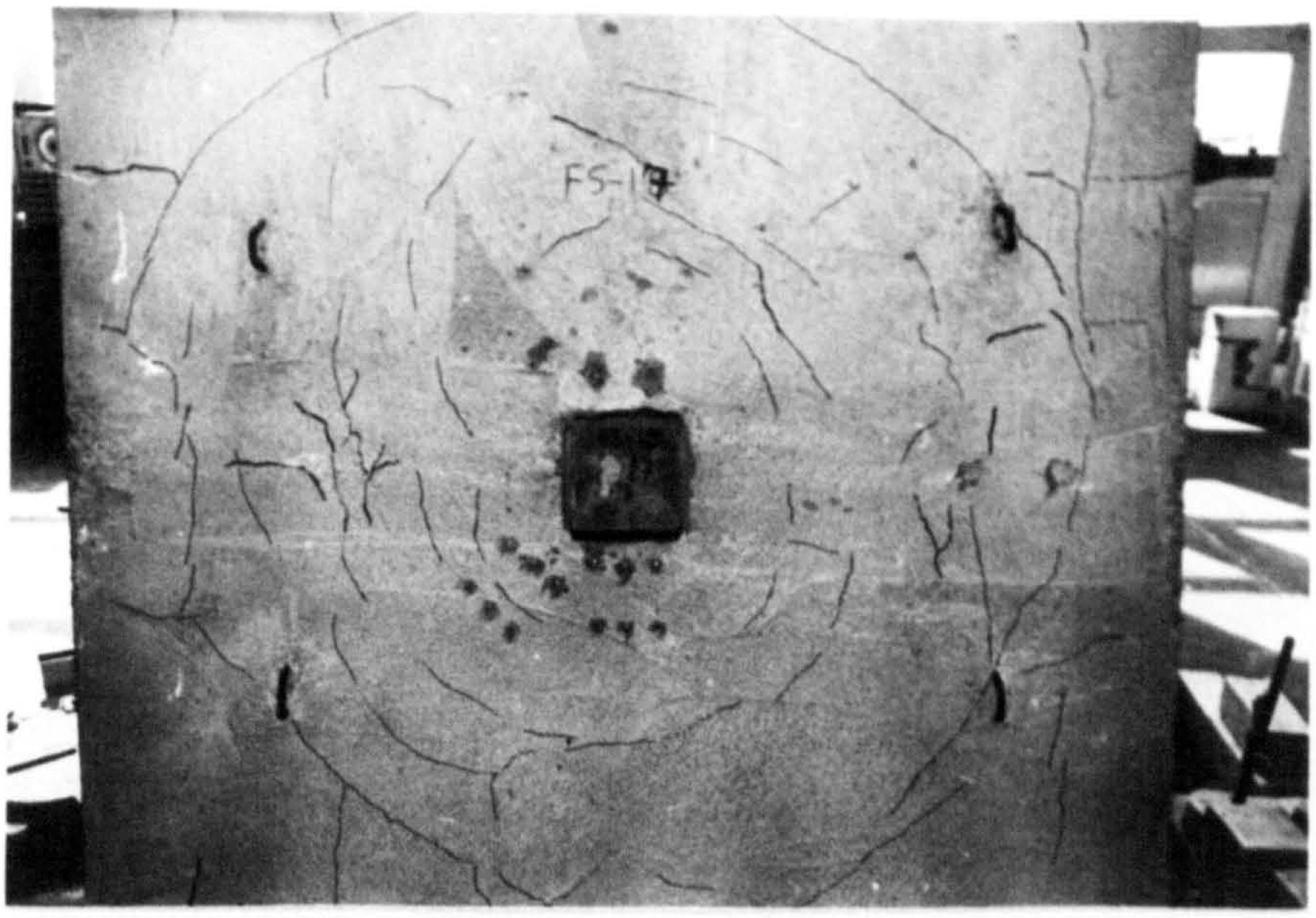

(a) Failure cracks at compression surface of slab FS-17 ($V_f = 1\%$) failing in flexure

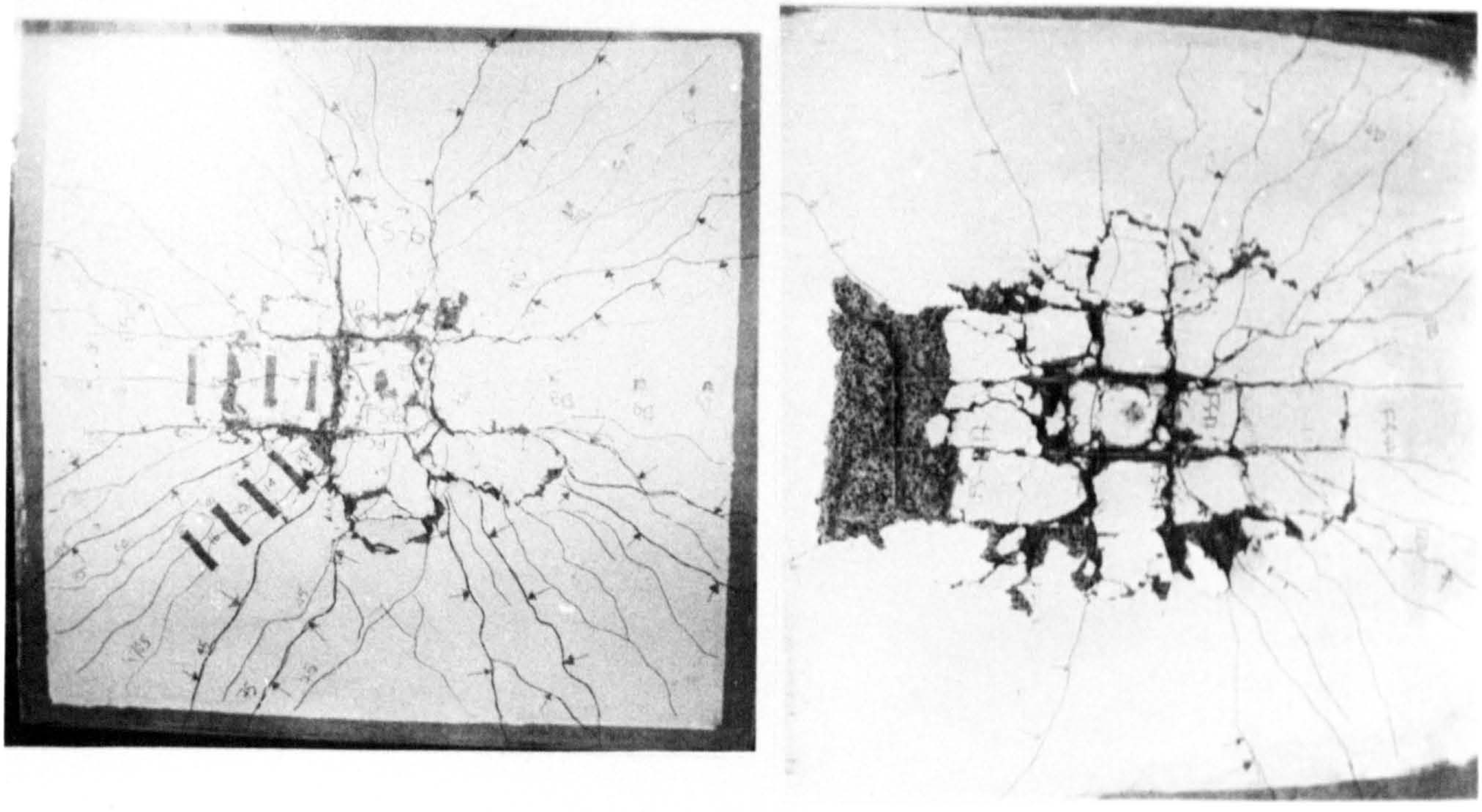

(b) Actual yield line pattern and failure cracks at tension surface of slabs FS-6 and FS-17 failing in flexure

PLATE 5-6 CRACK PATTERNS FOR SLABS FAILING IN FLEXURE theory is 0.293 (ℓ-r) (82). The yield lines for the more heavily reinforced slabs (ρ=0.557 4%) were much finer, than the yield lines in more slightly reinforced slabs (ρ=0.3716%).

5.3 Deformation Characteristics Under Load.

In this section, the deflections, rotations, steel strains and concrete strains measured in all tested slabs are presented. To obtain a clear picture of the effect of various variables studied in this investigation on the deformation characteristics, the slabs have been separated into groups as shown in Table 5.1. Each group in Table 5.1 contains slabs, which differ from one another by one variable. For example, group 1 contains the slabs FS-1, FS-2 and FS-3 with 0.0, 0.5 and 1.0% by volume crimped fibres respectively.

5.4 Load-Deflection Relationships.

The deflection of each test slab was measured along both lateral and diagonal directions on the tension side of the slab by means of dial gauges. Observed values of the deflection at the centres of the test slabs are plotted in Fig.5.1 as a function of the applied load. The first crack load, service load according to CP110 (69) code of practice as well as the load at which the tension reinforcement near the centre of the slab started yielding are marked in these figures. The maximum deflection for all slab specimens at first crack load, service load, yield load are listed in Table 5.2. This Table also shows the relation of the deflections at these loads and the maximum load deflections. In Fig.5.1 (group 1) the load-centre deflection curves of normal weight concrete slabs S-1 (V_f=0.0%) and S-3 (V_f=0.9%) from reference (78) are also plotted.

From Fig.5.1 some critical events in the load-deflection behaviour of both plain and fibre concrete slabs can be seen. Initially, the slab was

Table 5.1 Division of tested slabs into Groups.

Group number	Slab number	Remarks (Variables in each Group)
Group 1	FS-1, FS-2, FS-3	Fibre Percentage for slabs with r/d = 1.0
Group 2	FS-3, FS-4	Comp. Reinforcement
Group 3	FS-3, FS-5	Tension Reinforcement
Group 4	FS-4, FS-6	Tension Reinforcement
Group 5	FS-5, FS-6, FS-7, FS-19	Comp. Reinforcement
Group 6	FS-1, FS-8, FS-10, FS-19	Column size and Tension Reinf. (Plain concrete slabs)
Group 7	FS-3, FS-9, FS-11	Column size (Fibre concrete slabs)
Group 8	FS-1, FS-3, FS-12, FS-13, FS-14, FS-15	Fibre Type
Group 9	FS-8, FS-9	Fibre Percentage (r/d = 1.0)
Group 10	FS-10, FS-11	Fibre Percentage (r/d = 2.0
Group 11	FS-14, FS-16, FS-17, FS-18	Cube Compr. Strength (Fibre concrete slabs)
Group 12	FS-6, FS-20	Location of fibre reinforcement

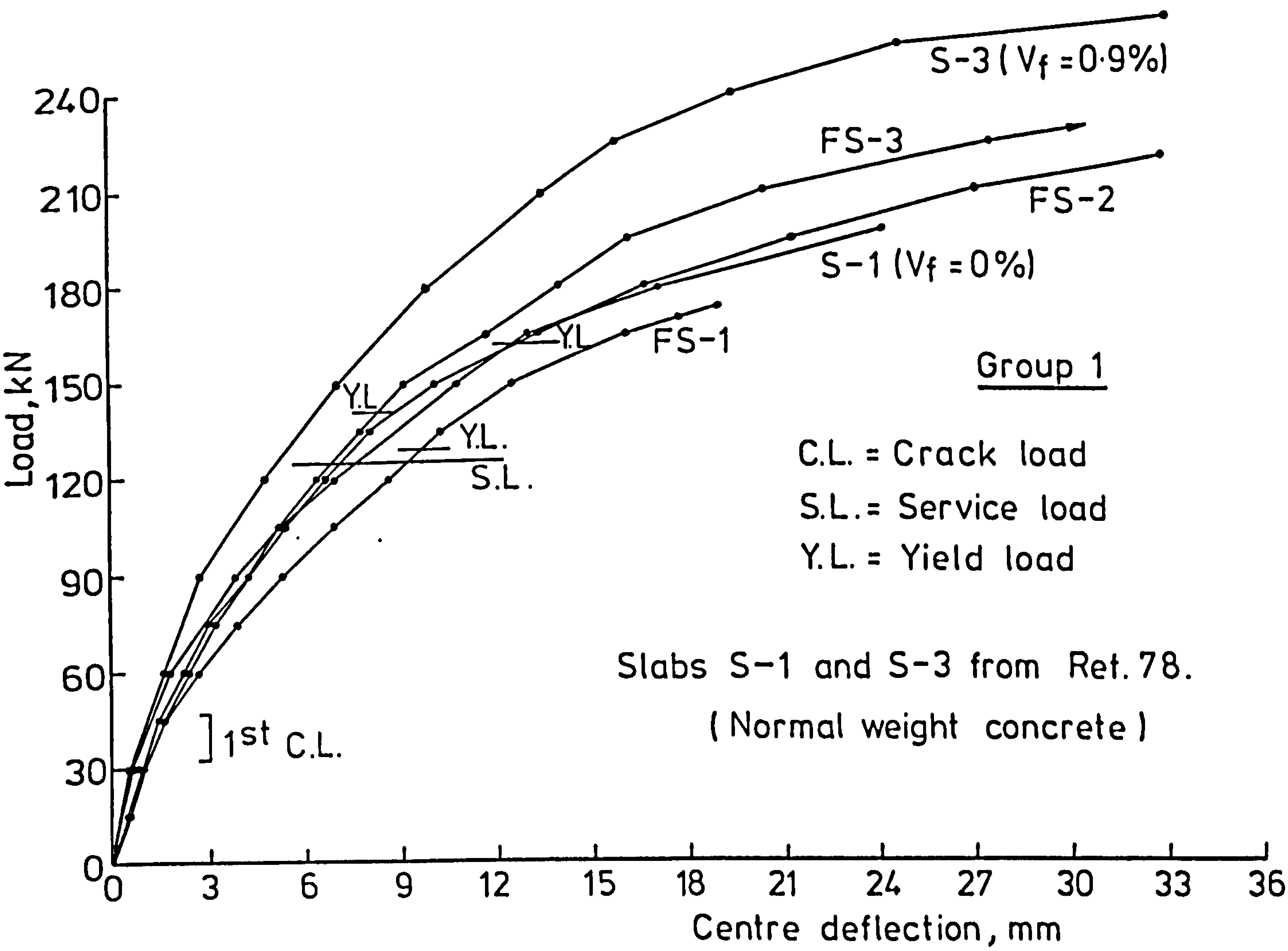

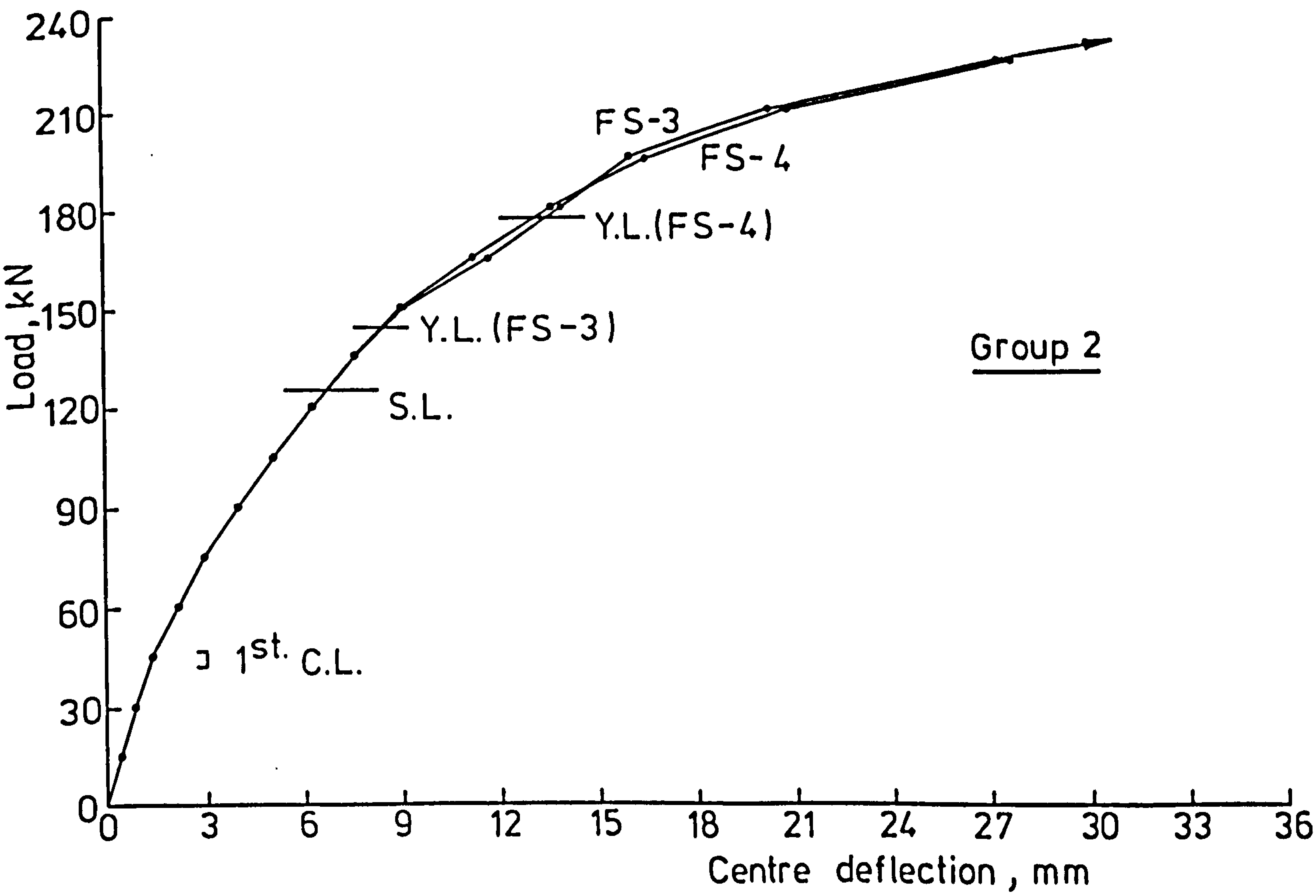

FIG. 5-1 LOAD - DEFLECTION CURVES

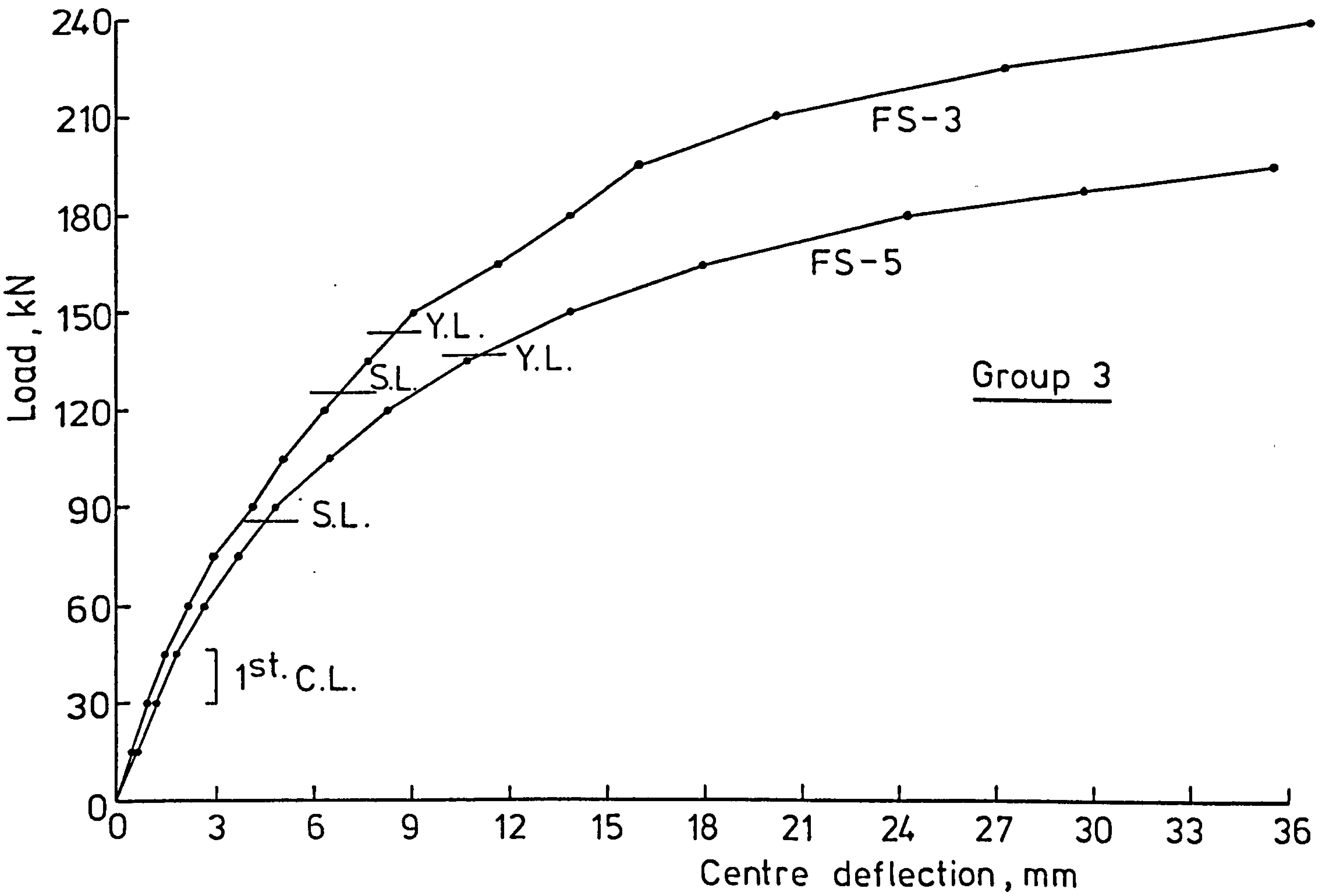

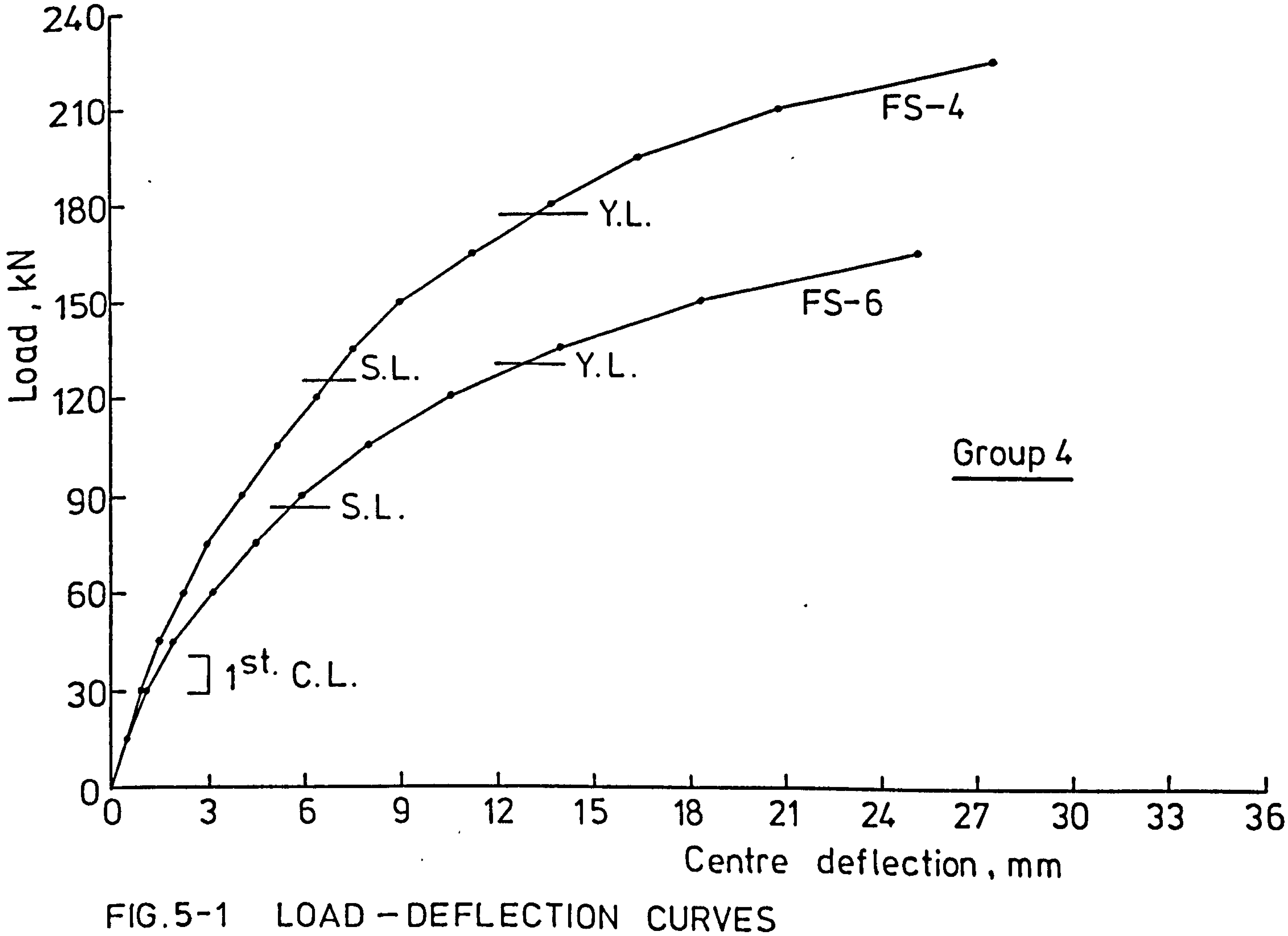

FIG.5-1 LOAD – DEFLECTION CURVES

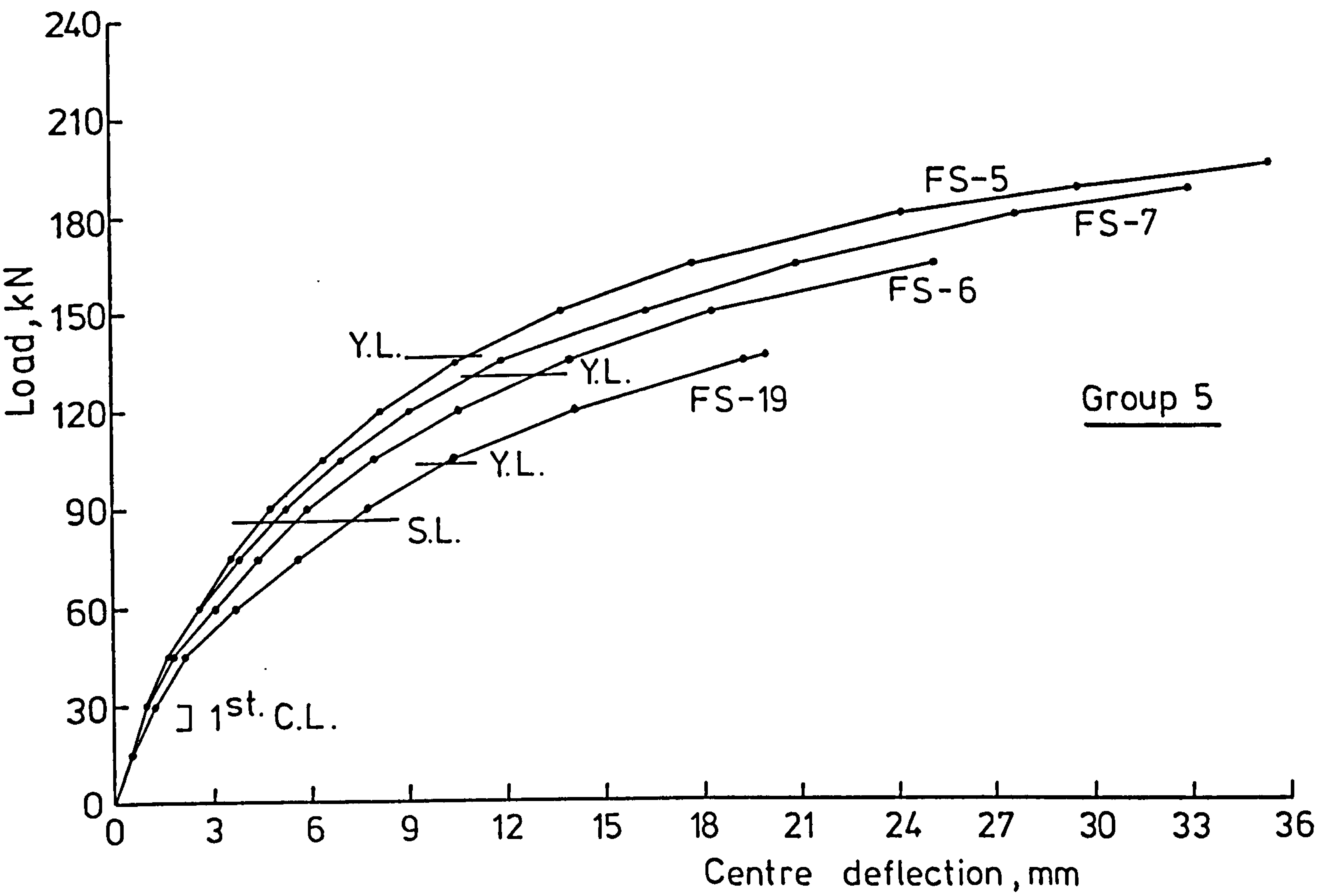

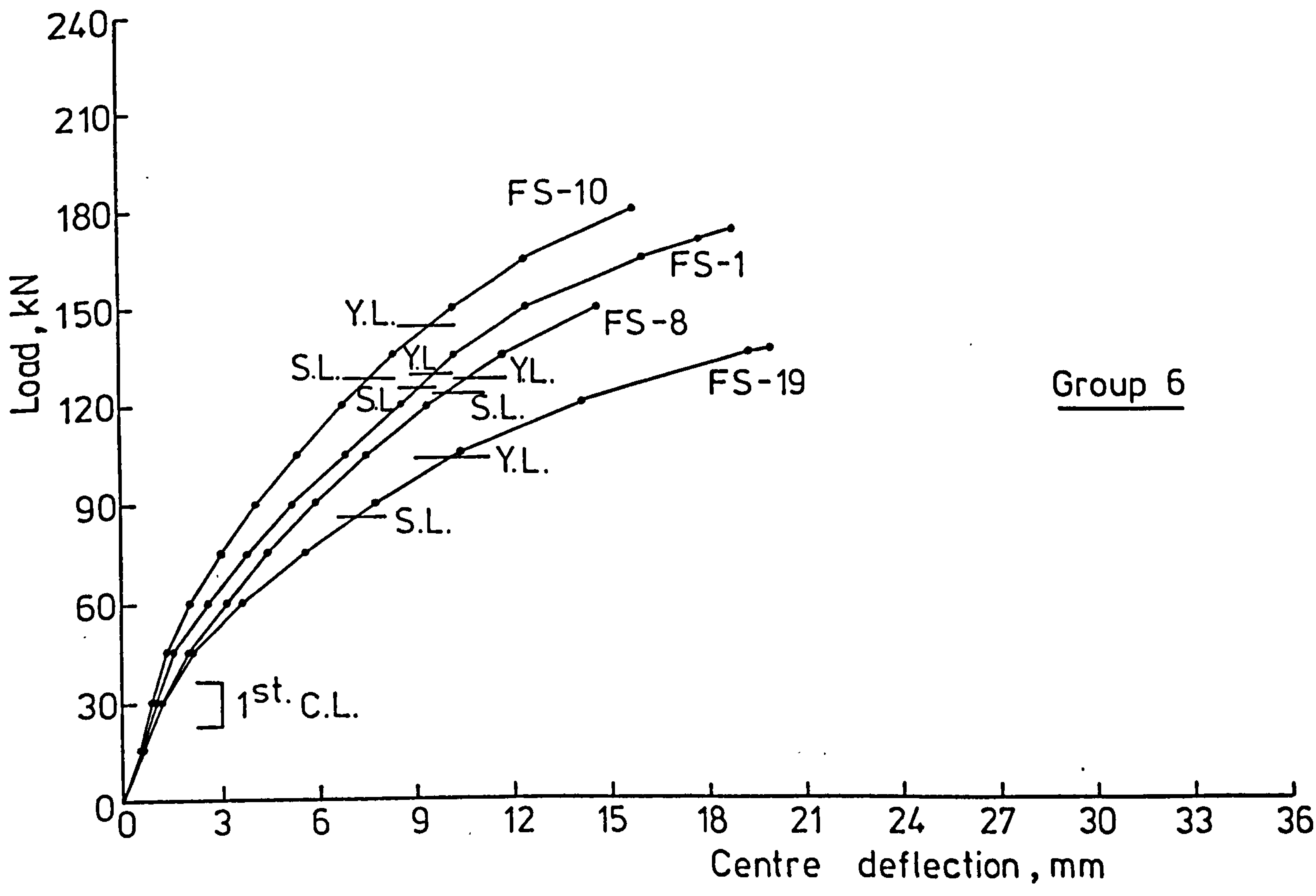

FIG. 5-1 LOAD – DEFLECTION CURVES

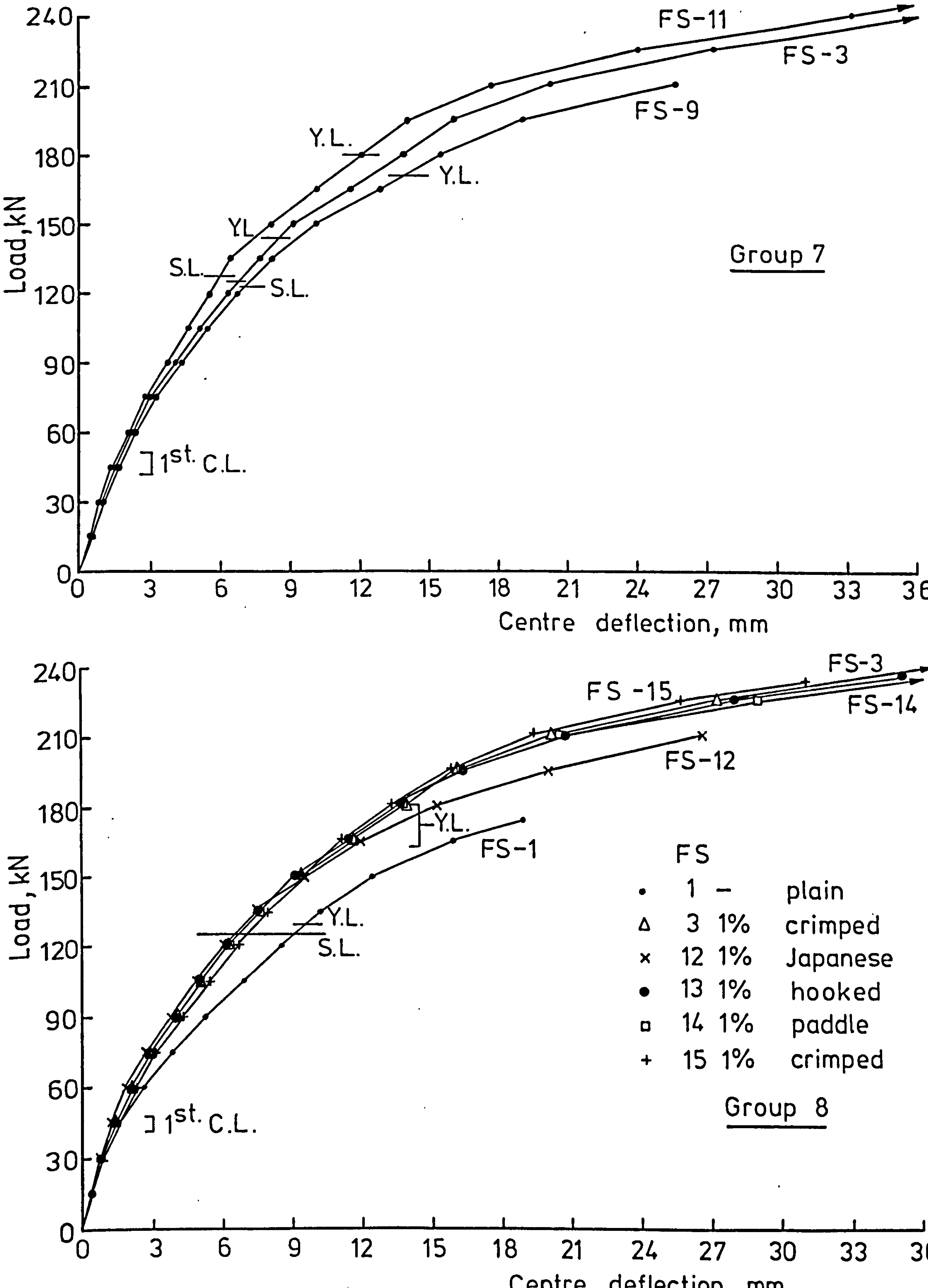

FIG. 5-1 LOAD – DEFLECTION CURVES

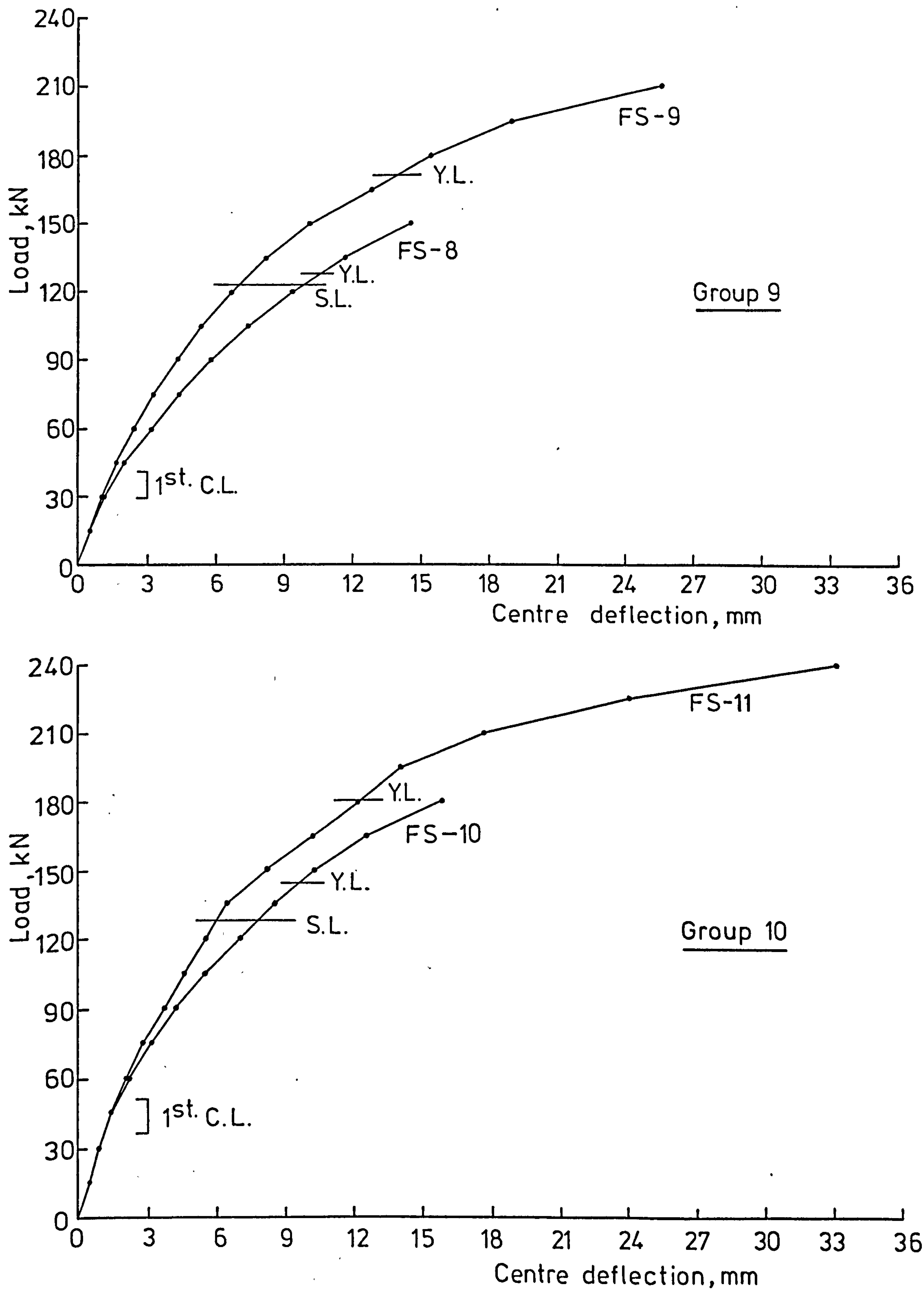

FIG. 5-1 LOAD – DEFLECTION CURVES

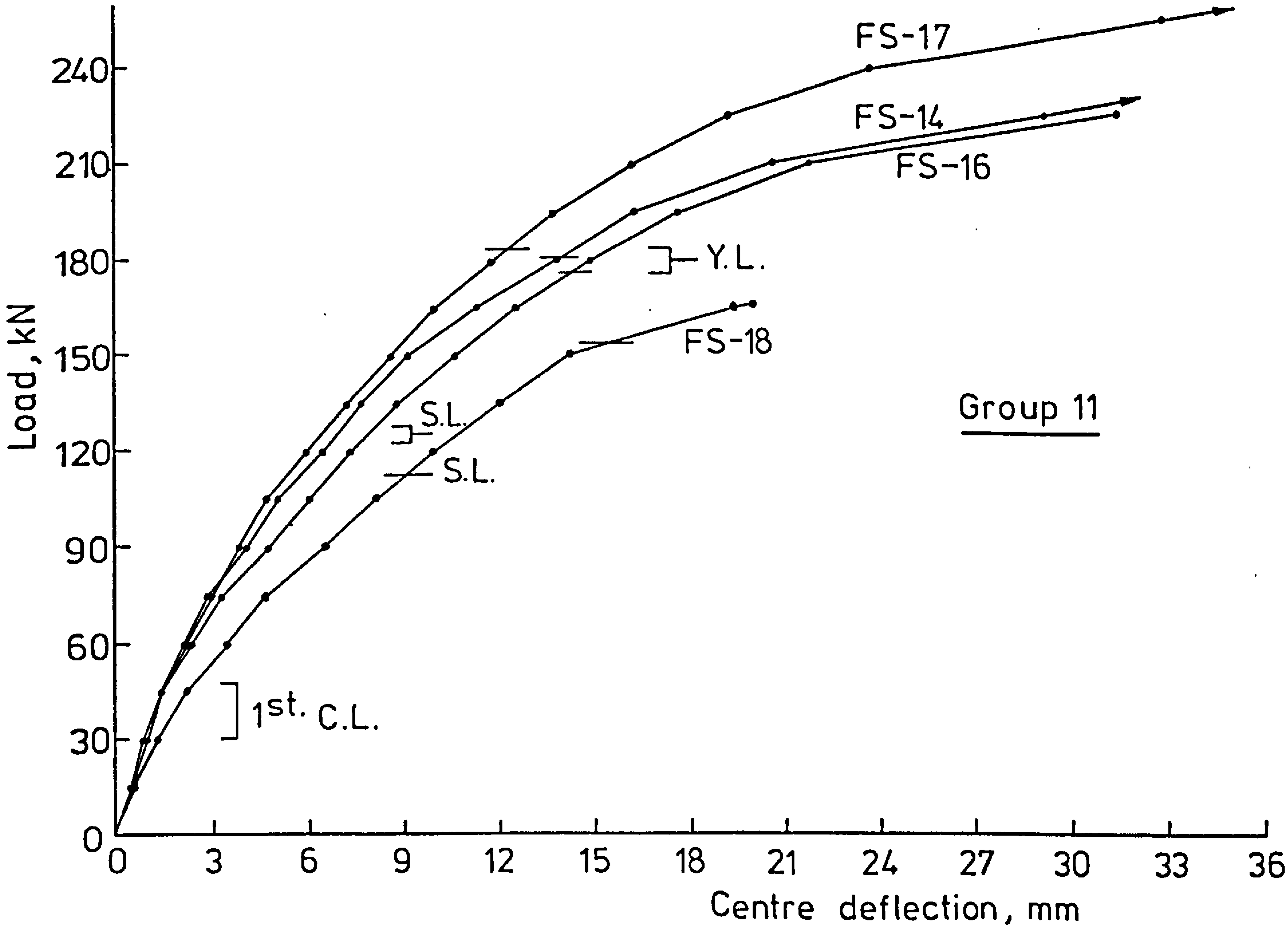

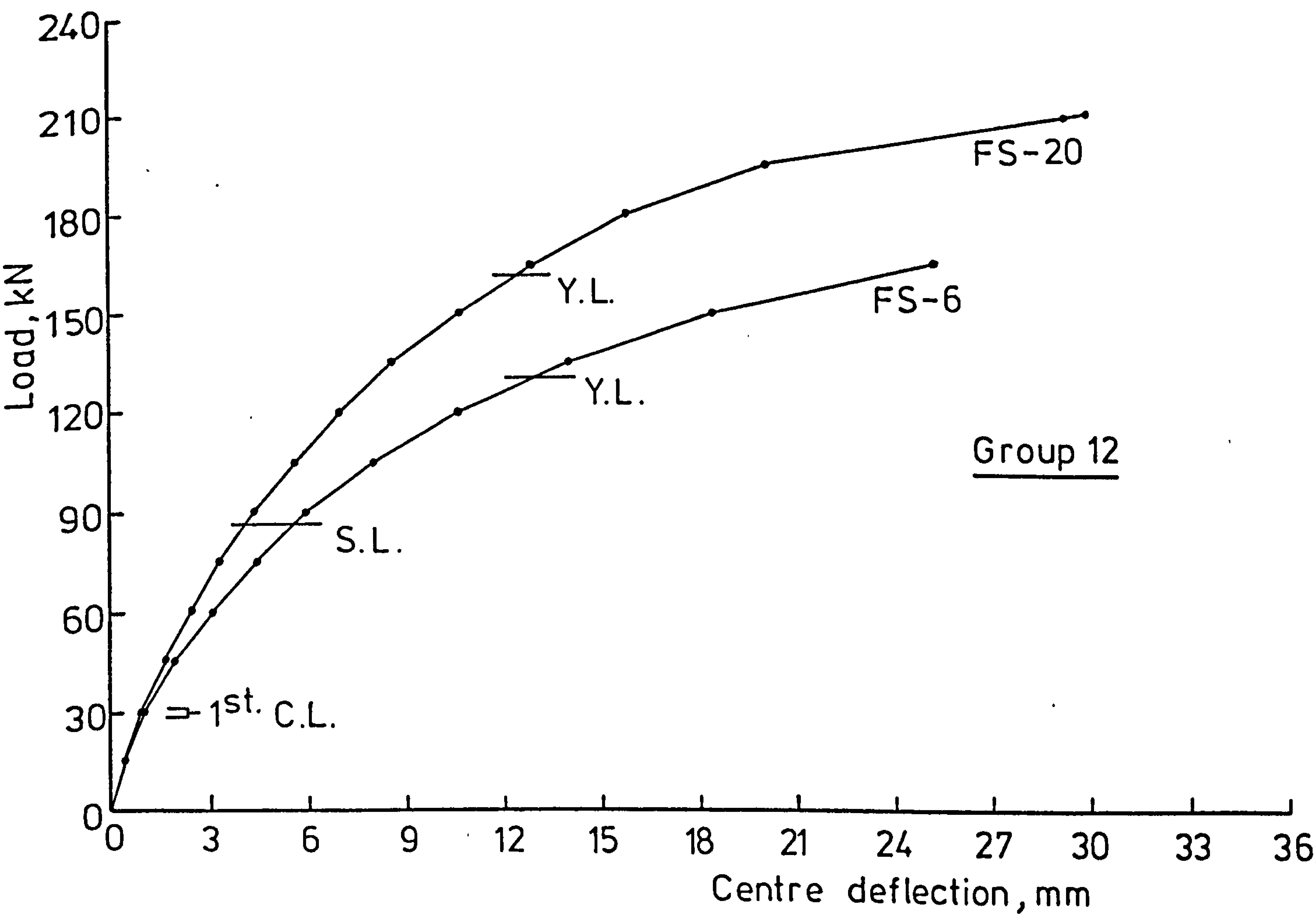

FIG. 5-1 LOAD-DEFLECTION CURVES

uncracked and quite stiff. A significant decrease in the stiffness accompanied cracking of the slab, and a second decrease began with the start of yielding of the reinforcement. The load-deflection curve became nearly horizontal, especially in the more lightly reinforced slabs, as yielding of the reinforcement extended throughout the slab. The transitions between these three stages were gradual because of the gradual spread of both cracking and yielding throughout the slab.

Since the first crack was determined visually using a magnifying glass, while the load was increased gradually, the values of the load at which the first crack appeared are not so reliable. The first crack load is different from one slab to another and therefore no direct comparison in the deflection as well as in the other deformations can be made. From test data, it was noted, that the reduction in the centre deflection of fibre concrete slabs at a load equal to first crack load of the corresponding plain concrete slabs was around 10%. This rather low effect of fibre reinforcement on deflection at the early stages of loading is due to the fact that increase in the modulus of elasticity of concrete due to presence of fibres and therefore the increase in the stiffness of the slab is marginal.

The load-deflection curves show that the presence of fibre reinforcement causes substantial reductions in the centre deflections.

The effect of fibre reinforcement on centre deflections at service load and maximum load is discussed below.

5.4.1 Deflection Characteristics at Service Load.

Table 5.2 (column 9) shows the deflection of all test slabs at service load (CP110) as well as its ratio to deflection at maximum load (column 10). In fibre concrete slabs the steel fibre effect was neglected in calculating the service load. The service load of plain concrete slabs is different

Table 5.2 Deflections characteristics of test slabs.

Series Number	Series Detail	Slab Number	Fibre Type and Percentage	First Crack Load: Load in kN	First Crack Load: Deflection in mm	First Crack Load: $\frac{(6)}{(15)}$ %	Service Load (CP110): Load in kN	Service Load (CP110): Deflection in mm	Service Load (CP110): $\frac{(9)}{(15)}$ %	Yield Load: Load in kN	Yield Load: Deflection in mm	Yield Load: $\frac{(12)}{(15)}$ %	Ultimate Load: Load in kN	Ultimate Load: Deflection in mm	$\frac{\text{Max.Load Deflection}}{\text{Span lencth}}$ %
1	2	3	4	5	6	7	8	9	10	11	12	13	14	15	16
1	Fibre Percentage	FS-1	– 0.0	32.0	1.22	6.3	125.0	9.15	48.2	129.0	9.75	51.13	173.5	19.0	1.12
		FS-2	Crimped 0.5	42.5	1.42	4.2	125.0	7.20	21.8	162.0	12.60	38.2	225.0	33.0*	1.95
		FS-3	Crimped 1.0	46.8	1.50	4.1	125.0	6.80	18.5	144.0	8.40	22.9	247.4	36.75*	2.17
2	Reinforcement Reduction	FS-4	Crimped 1.0	40.9	1.24	4.3	125.0	6.80	24.5	177.0	13.05	47.0	224.4	27.5	1.64
		FS-5	Crimped 1.0	30.0	1.23	3.4	85.97	4.50	12.6	136.5	10.80	30.3	198.1	35.70*	2.11
		FS-6	Crimped 1.0	29.0	1.12	4.3	85.97	5.55	21.9	130.5	12.75	50.3	174.5	25.35*	1.50
		FS-7	Crimped 1.0	30.0	1.20	3.6	85.97	4.80	14.5	130.0	11.00	33.2	192.4	33.15	1.96
		FS-19	– 0.0	22.5	1.00	5.1	85.97	7.05	35.3	103.5	10.20	51.0	136.5	20.00	1.18
		FS-20	Crimped 1.0	31.5	1.03	3.3	85.97	4.05	13.5	162	12.45	41.5	211.0	30.00	1.78

Table 5.2 (Continued)

				First Crack Load			Service Load (CP110)			Yield Load			Ultimate Load		
1	2	3	4	5	6	7	8	9	10	11	12	13	14	15	16
3	Column Size	FS-8	- 0.0	29.0	1.15	7.8	122.69	9.85	67.0	127.5	10.70	72.8	150.3	14.70	0.87
		FS-9	Crimped 1.0	41.4	1.35	5.3	122.69	7.05	27.5	171.0	14.00	54.6	216.6	25.65	1.52
		FS-10	- 0.0	36.0	1.26	7.5	127.34	7.80	48.6	144.0	9.40	59.8	191.4	16.05*	0.95
		FS-11	Crimped 1.0	48.9	1.52	3.6	127.34	6.00	14.6	180	12.15	29.6	259.8	41.00*	2.43
4	Fibre Type	FS-12	Japanese 1.0	42.5	1.20	4.5	125.0	6.60	24.7	162.5	13.10	49.1	217.5	26.70*	1.58
		FS-13	Hooked 1.0	44.0	1.30	3.8	125.0	6.75	19.7	178.5	13.35	40.0	235.7	34.25	2.03
		FS-14	Paddle 1.0	45.5	1.50	3.8	125.0	6.70	17.2	180.5	13.80	35.4	239.5	39.00	2.31
		FS-15+	Crimped 1.0	41.0	1.50	4.8	125.0	7.10	22.8	172.5	12.15	38.9	238.0	31.20*	1.85
5	Cube Compressive Strength	FS-16	Paddle 1.0	42.5	1.35	4.3	122.7	7.80	24.8	175.5	14.25	45.2	227.8	31.5	1.86
		FS-17	Paddle 1.0	47.5	1.70	3.7	126.9	6.50	14.4	184.0	12.30	27.0	268.4	45.60	2.70
		FS-18	Paddle 1.0	30.5	1.35	6.7	112.7	9.0	45.0	153.0	15.15	75.8	166.0	20.00	1.18

NOTE:-
1) In calculating service load (CP110) steel fibre effect was neglected.
2) +Slab FS-15, 6 mm Lytag aggregates, fibres $\ell_f/d_f = 90$.
3) *Indicates readings at 94 to 97% of the maximum load.
4) SLABS FS-6, FS-7, FS-11 and FS-17 failed in flexure.

for each of plain concrete slabs depending mainly upon the tension reinforcement ratio and the column size.

Table 5.3 (column 4) shows the ratio between deflection of the fibre slabs and deflection of the corresponding plain concrete slabs at service load. From this Table it can be seen that the centre deflection in slab FS-3 was reduced by 25.7% at service load when fibre content increased to 1.0% by volume. Ali (78) reported that the reduction in the centre deflection in normal weight concrete slabs was 31% and 22% when 0.9% by volume crimped fibres were used in the whole slab and around the column stub (3.5xh from column faces) respectively. The use of different fibre type in slabs FS-12, FS-13, FS-14 and FS-15 caused almost the same reduction in the centre deflection.

The reduction in the centre deflection was 28.4% and 23.1% when 1.0% by volume crimped fibres were used in slabs with 100 and 200 mm column size respectively.

The reduction of the flexural reinforcement in slab FS-5 caused a higher reduction in the centre deflection as compared to that of slab FS-19, equal to 36.2% when 1.0% by volume crimped fibres were used.

The centre deflection load was not affected when compressive reinforcement was reduced by 100% in slab FS-4 (ρ=0.5574%) when compared with deflection of slab FS-3 with full compressive reinforcement, but it was affected when the compressive reinforcement was reduced in the slabs FS-6 and FS-7 with a tension reinforcement ratio equal to 0.3716%.

The use of 1.0% by volume crimped fibres in the whole slab (slab FS-20), although without compressive reinforcement, caused a higher reduction in centre deflection when compared with slab FS-5 with compressive reinforcement and fibres located at 5.5 times the effective depth from column faces. (Table 5.3, column 4).

5.4.2 Deflection Characteristics near Ultimate Load of Plain Concrete Slabs.

From Fig.5.1 and Table 5.2 (column 15) it can be seen that the centre deflection of fibre concrete slabs at failure load was almost twice of that of the corresponding plain concrete slabs. This is because the presence of fibre reinforcement caused a considerable increase in ultimate load of the plain concrete slabs and therefore deflections were measured and different load level. So, for comparison purposes the effect of fibres on centre deflection is considered at a load very close to ultimate load of the corresponding concrete slabs. Table 5.3 (column 8) shows the ratio between deflection of the fibre concrete slabs at a load near the ultimate load of plain concrete slabs. It can be seen that the reduction in the centre-deflection at this load level, due to presence of fibres, was, in general higher than that at service load level. Smaller reductions were observed only in slabs FS-2 with 0.5% by volume crimped fibres and FS-12 with 1% by volume, 25 mm long, Japanese fibres. This could be explained in terms of extensive debonding of steel fibres at this load level, because of the small fibre percentage in slab FS-2 and small fibre length in slab FS-12.

The reduction in the centre deflection due to presence of fibres seems to be, as in the case of the reduction at service load, dependent upon 1) the tension reinforcement ratio being higher for slabs with a lower reinforcement ratio, 2) upon the compressive reinforcement but only in slabs with $\rho = 0.3716\%$ and 3) upon the location of fibre reinforcement.

5.4.3 Comparison Deflection Between Lightweight and Normal Weight Concrete Slabs.

One of the factors which has to be allowed for in the use of lightweight concrete in structural elements is the increased deflection which may result when compared with normal weight concrete.

Table 5.3 Comparison of deformation characteristics between fibre and corresponding plain concrete slabs at service load and near ultimate load of plain concrete slabs.

% Tension Reinforcement Ratio	Column size, r, in mm		% Deformation of fibre concrete slabs/Deformation of the corresponding plain concrete slab							
			At Service Load (S.L.) (CP110)				Near Ultimate Load (N.U.L.) of plain concrete slabs			
		FS-1	S.L. = 125.0 KN				N.U.L. = 165.0 KN			
			Deflection	Rotation	Tension Steel Strain	Con. Compr. Strain	Deflection	Rotation	Tension Steel Strain	Con. Compr. Strain
1	2	3	4	5	6	7	8	9	10	11
ρ = 0.5574	150	FS-2/FS-1	78.7	81.2	65.8	84.0	83.2	80.9	59.2	88.2
		FS-3/FS-1	74.3	76.5	63.3	74.1	72.8	73.1	84.2	78.5
		FS-4/FS-1	74.1	78.1	44.3	70.4	70.1	73.9	42.8	71.1
		FS-12/FS-1	72.1	82.8	49.4	70.4	74.8	73.9	59.2	74.8
		FS-13/FS-1	73.8	75.0	44.3	67.9	71.02	71.3	40.8	67.4
		FS-14/FS-1	73.2	73.4	40.5	67.9	70.1	72.4	40.1	65.9
		FS-15/FS-1	77.6	73.4	45.6	70.4	69.8	72.6	45.4	74.1
	100	FS-8	S.L. = 122.69 KN				N.U.L. = 135.0 KN			
		FS-9/FS-8	71.6	70.8	49.4	71.1	70.5	69.4	45.0	70.9
	200	FS-10	S.L. = 127.34 KN				N.U.L. = 180 KN			
		FS-11/FS-10	76.9	72.4	56.9	71.6	76.0	70.9	56.6	75.5
ρ = 0.3716	150	FS-19	S.L. = 85.97 KN				N.U.L. = 135.0 KN			
		FS-5/FS-19	63.8	63.0	60.0	76.0	54.3	60.4	51.3	69.0
		FS-6/FS-19	78.7	77.7	58.2	86.0	72.1	72.7	59.4	81.0
		FS-7/FS-19	68.0	66.6	58.2	78.0	61.9	65.5	59.4	69.0
		FS-20/FS-19	57.4	48.1	38.2	62.0	45.0	44.6	31.9	58.2

The load-deflection curves of two normal weight concrete slabs (78) with and without fibres are shown in Fig.5.1 (group 1). The deflections of the Lytag slab (FS-1) were about 25% higher than that of gravel slab (S-1). However, the addition of fibres to Lytag slabs FS-2 (V_f = 0.0%) and FS-3 (V_f = 1.0%) reduced the deflections to values similar to, or slightly less than, those of the normal weight concrete slab (V_f = 0.0%). From Fig.5.1 (group 1) it can be seen that at early stages of loading the deflection of normal weight concrete slab S-1 was lower even than that of lightweight concrete slab FS-3 with 1.0% by volume crimped fibres, because the addition of fibres hardly increases the modulus of elasticity of lightweight concrete. However at later stages of loading where extensive flexural cracking occurs, the deflection of plain normal weight concrete slab S-1 was higher than that of fibre lightweight concrete slab FS-3, and this is due to ability of fibres of reducing cracking in the tensile zone and lowering the neutral axis.

It can be concluded that the addition of steel fibres to reinforced lightweight concrete slabs can reduce deflections to values similar to, or slightly less than, those of the plain normal weight concrete slabs.

5.4.4 Other Deflection Comparisons.

The first crack centre-deflection compared to the maximum load deflection for all four plain lightweight concrete slabs which failed in punching shear varied from 5.1 to 7.8%. This ratio varied from 3.3 to 4.8% when 1.0% fibre reinforcement was used. These values were almost of the same order as those reported by Ali (78) being 4.05% and 4.41-5.25% for plain and fibre normal weight concrete respectively.

The failure deflections with the span of the connection specimen slabs are also compared in Table 5.2 (column 16). The plain concrete slab FS-1 failed at a deflection of 1.12% of the span length while Ali (78) reported such a value equal to 1.43% in a comparable normal weight concrete slab. This percentage increased to 2.17 in slab FS-3 when 1.0% by volume crimped fibres were used which is almost equal to that of comparable normal weight fibre concrete slabs (78).

Figs. 5.2A, B and C show the load-deflection curves at different positions along lateral and diagonal directions for slabs FS-1, FS-8, FS-7 and FS-14. From these figures it can be seen that the deflections measured in lateral and diagonal directions at points of equal distance from the slab centre were almost of the same magnitude. The deflection at point D_1 was initially increased up to a certain value and subsequently decreased because of the lifting off corners. The deflections at points D_2 and D_{10} located at distances far away from the slab centre showed a decrease rate of increase after a certain load, which might probably be due to formation of inclined cracking.

The measured deflections at different distances for slab FS-1 are compared with the centre deflection in both lateral and diagonal directions in Fig.5.3. These data for all test slabs are shown in Table 5.4 but only in lateral direction since, as it was mentioned before, the deflections in diagonal direction were of the same magnitude as in lateral direction. From Table 5.4 it can be seen that the deflections measured at D_8, which is almost at quarterspan, were about of 70% of the centre deflection which is in agreement with Ali (78) 69.75%.

The slab corners lifted off the supports at a rate which varied from 18 to 25% of the downward centre deflection in plain concrete wlabs which is in agreement with Ali's (78) 17-29% and Criswell's (25) 25% for normal weight concrete slabs. This percentage was, in general, reduced when fibre reinforcement was used in the slab column connections. For example,

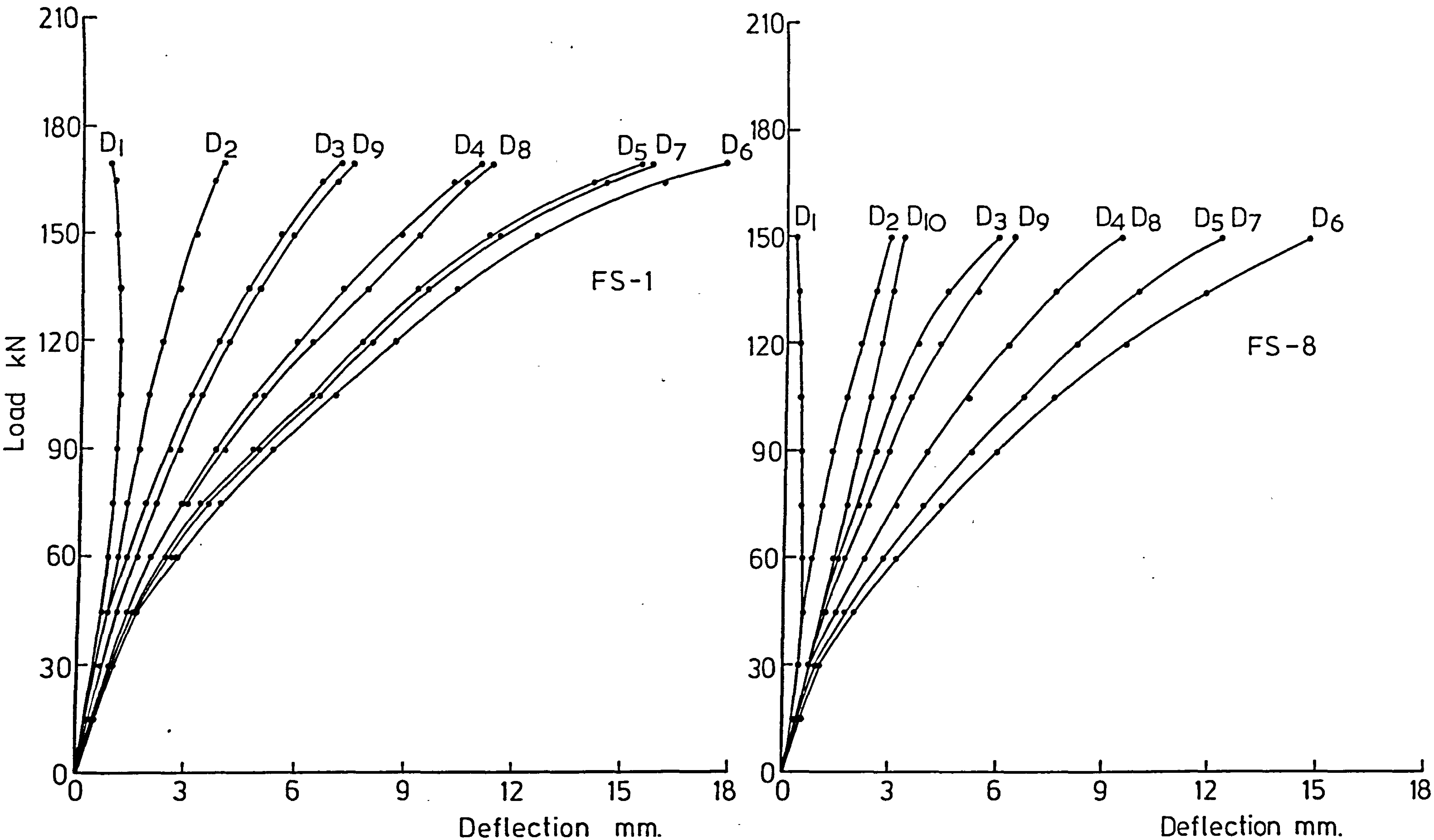

FIG. 5-2 A LOAD - DEFLECTION CURVES FOR PLAIN CONCRETE SLABS

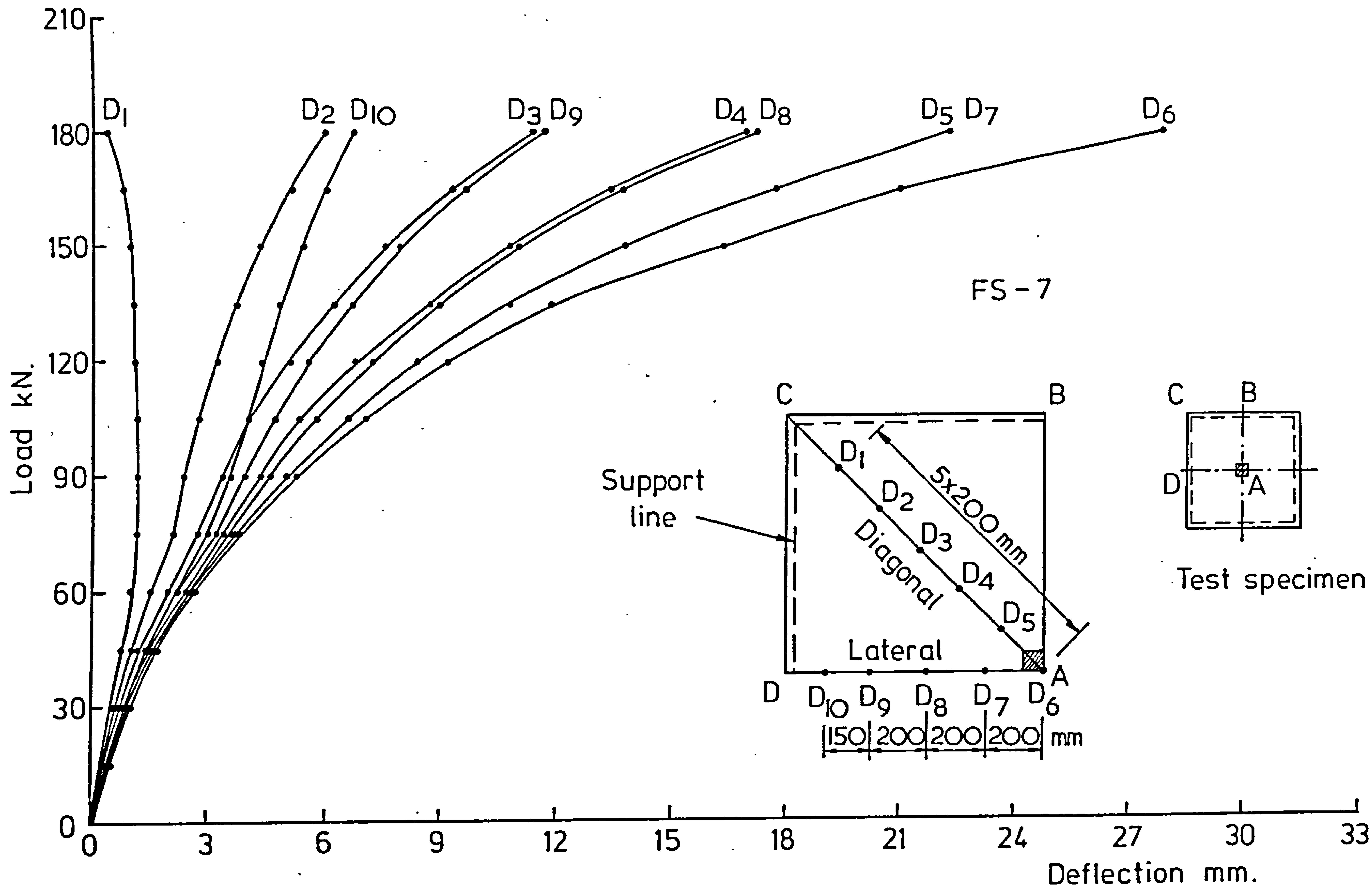

FIG.5-2 B LOAD DEFLECTION CURVES FOR SLAB FS-7 ($V_f = 1\%$)

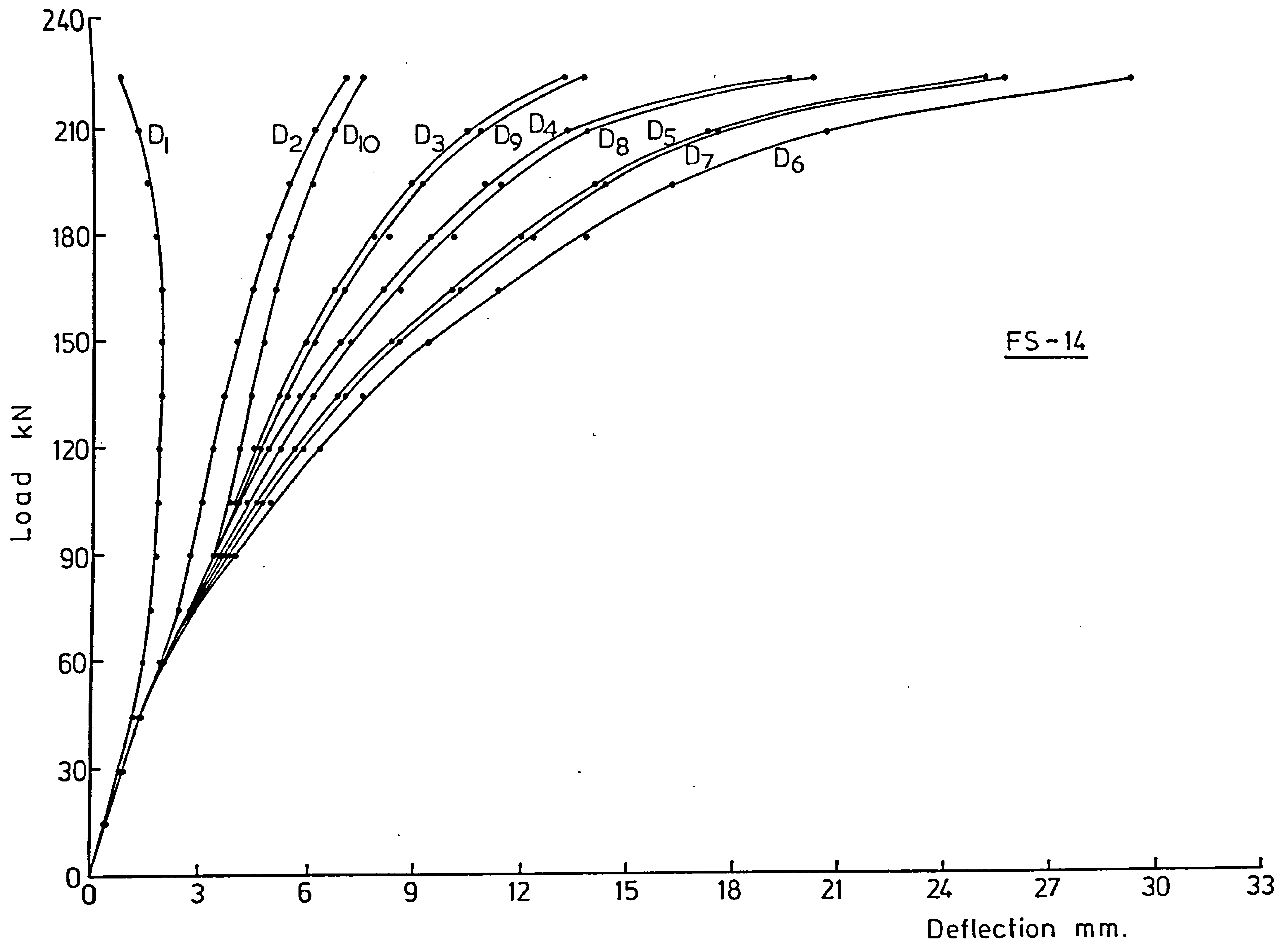

FIG. 5·2C LOAD - DEFLECTION CURVES FOR SLAB FS-14 ($V_f = 1\%$)

Table 5.4 Comparison of deflections in lateral direction.

Slab Number	Fibre Type and Percentage	Deflection at D_7*/Centre Deflection	Deflection at D_8*/Centre Deflection	Deflection at D_9*/Centre Deflection	Corner Liftoff Deflection/ Centre Deflection
1	2	3	4	5	6
FS-1	- 0.0	0.90	0.71	0.50	0.25
FS-2	Crimped 0.5	0.90	0.69	0.48	0.21
FS-3	Crimped 1.0	0.88	0.68	0.42	0.18
FS-4	Crimped 1.0	0.89	0.67	0.45	0.17
FS-5	Crimped 1.0	0.89	0.70	0.46	0.15
FS-6	Crimped 1.0	0.90	0.69	0.41	0.14
FS-7	Crimped 1.0	0.88	0.68	0.48	0.16
FS-8	- 0.0	0.87	0.66	0.45	0.18
FS-9	Crimped 1.0	0.83	0.63	0.44	0.19
FS-10	- 1.0	0.95	0.79	0.54	0.20
FS-11	Crimped 1.0	0.92	0.67	0.48	0.18
FS-12	Japanese 1.0	0.88	0.65	0.44	0.19
FS-13	Hooked 1.0	0.89	0.69	0.51	0.18
FS-14	Paddle 1.0	0.89	0.73	0.55	0.18
FS-15	Crimped 1.0	0.88	0.70	0.50	0.17
FS-16	Paddle 1.0	0.90	0.68	0.48	0.20
FS-17	Paddle 1.0	0.92	0.71	0.52	0.17
FS-18	Paddle 1.0	0.86	0.71	0.47	0.22
FS-19	- 0.0	0.91	0.70	0.45	0.19
FS-20	Paddle 1.0	0.89	0.70	0.43	0.17

*Dial gauge numbers refer to Fig. 4.7.

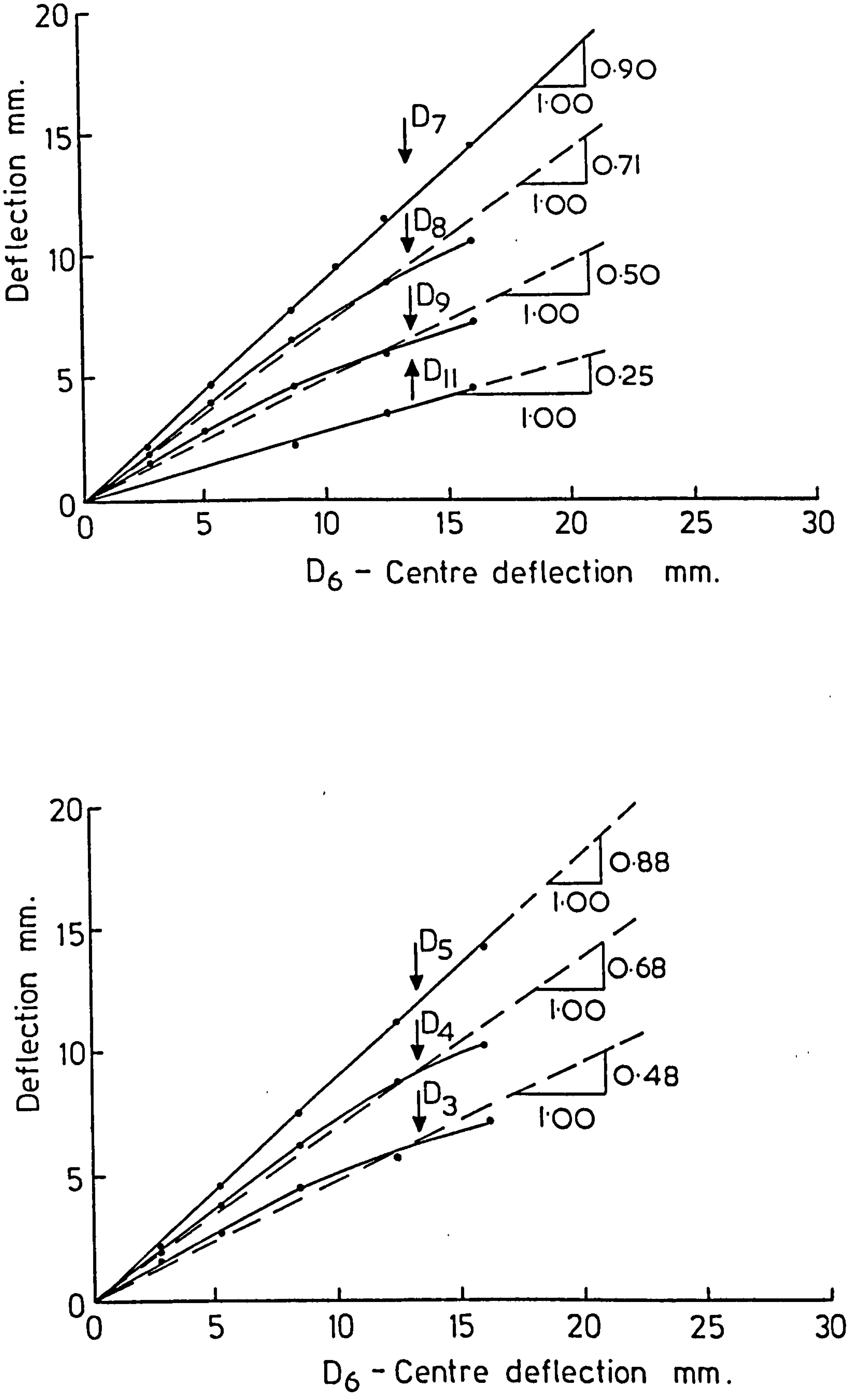

FIG.5-3 DEFLECTIONS COMPARISON FOR SLAB FS-1
IN LATERAL AND DIAGONAL DIRECTIONS

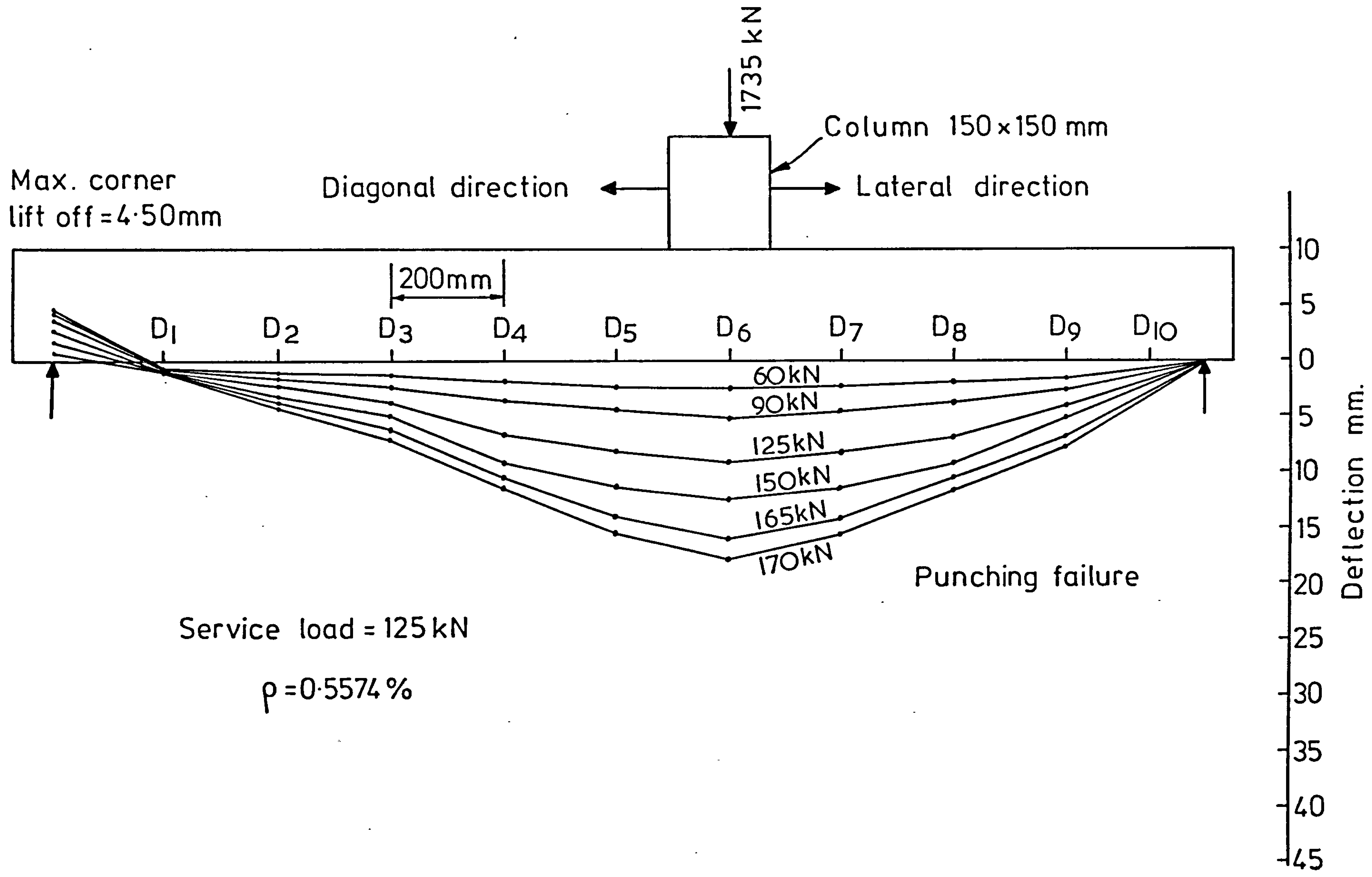

FIG. 5-4 A LOAD – DEFLECTION DISTRIBUTION FOR SLAB FS-1 (V_f = 0%)

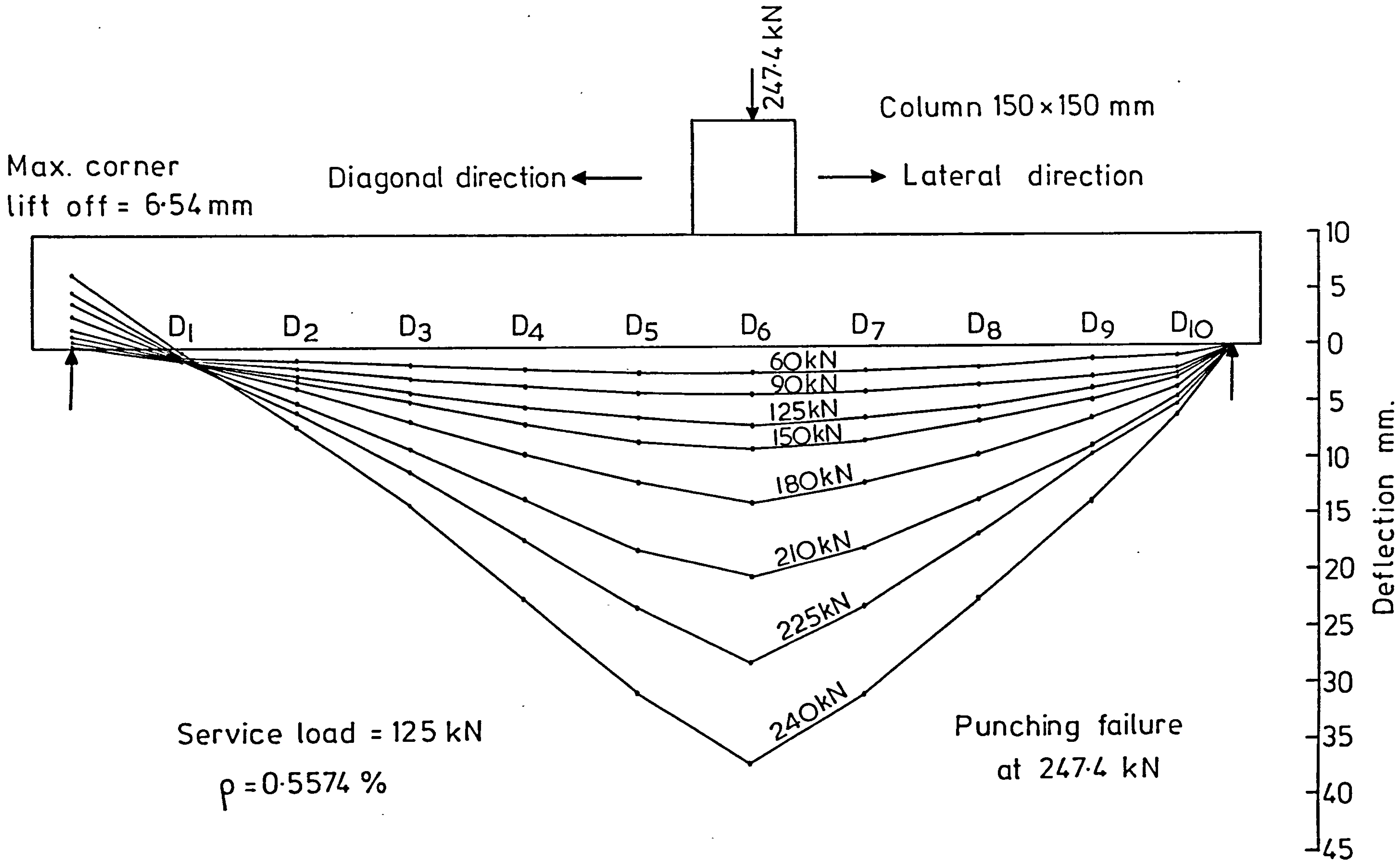

FIG. 5-4 B LOAD – DEFLECTION DISTRIBUTION FOR SLAB FS-3 ($V_f = 1\%$)

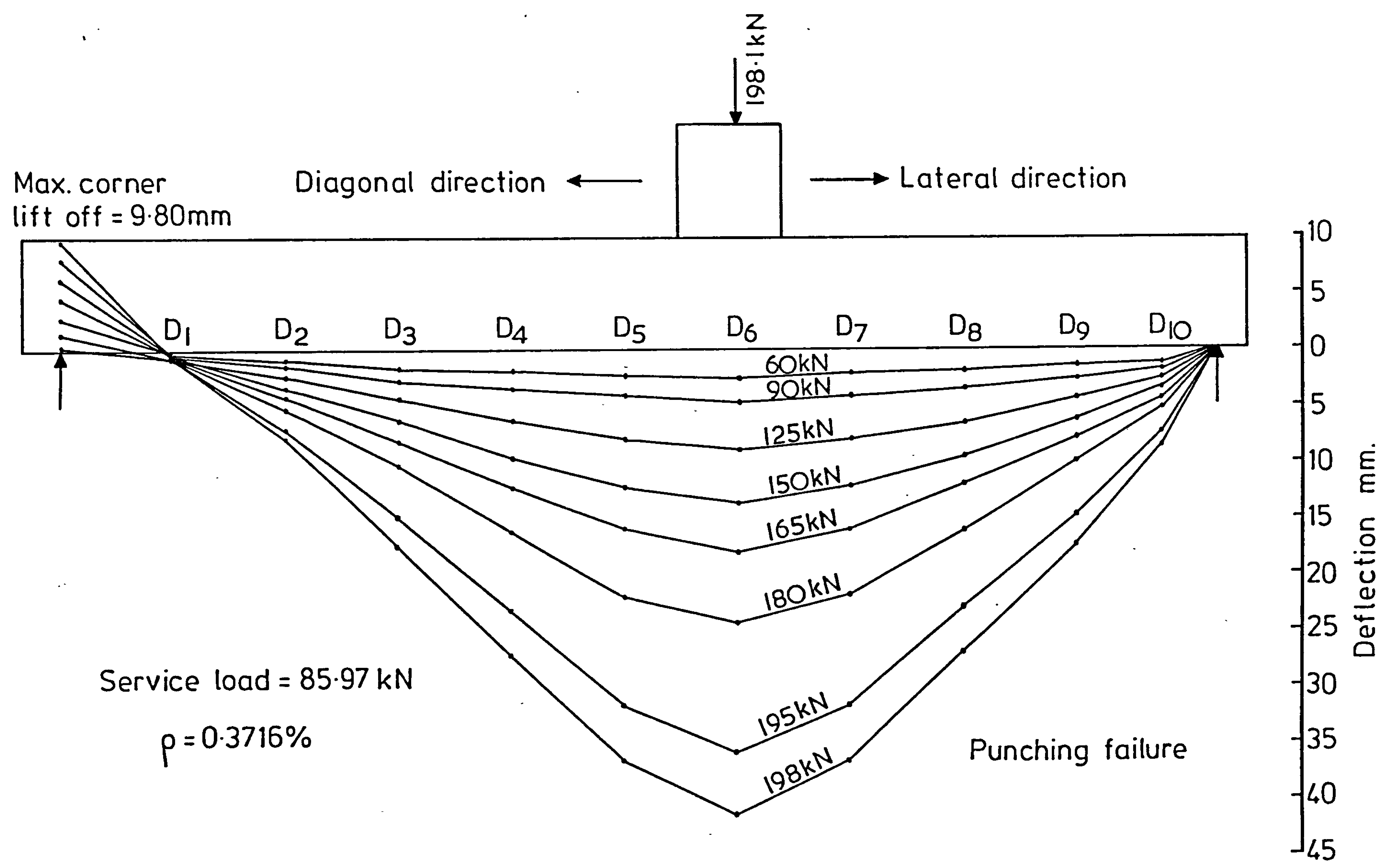

FIG. 5-4 C LOAD-DEFLECTION DISTRIBUTION FOR SLAB FS-5 (V_f = 1 %)

this percentage was reduced from 25% in plain concrete slab FS-1 to 18% in fibre concrete slab FS-3.

To obtain a picture of the deflected shape of the slab, the load-deflection curves for slabs FS-1, FS-3 and FS-7 are shown in Figs. 5.4A, B and C respectively. It can be seen that the deflected shape is almost linear in the area of slab outside the punching cone which occurred at a distance 300-350 mm from the slab centre.

5.5 Load-Rotation Relationships.

Slab rotations were measured at several positions in the compressive face of each test slab as shown in Fig.4.7. The maximum rotation, θ_1, for all test slabs are plotted in Fig.5.5 as a function of the applied load. The rotations at all locations of slabs FS-1, FS-2 and FS-3 are shown in Fig.5.6. The maximum rotation, θ_1, for all slab specimens was measured at first crack, service load, and near maximum failure load and are listed in Table 5.5. Slab rotations were small at the elastic stage as loading was applied, then they decreased steadily after the first crack on continued loading.

The maximum rotation θ_1, in all slabs, occurred at the far end of the column stub, in lateral direction. This rotation and the others were, in general, reduced drastically when steel fibre reinforcement was used in the slab-column connections.

5.5.1 Rotation Characteristics at and above Service Load.

Table 5.3 shows the ratio between rotation of the fibre concrete slabs and rotation of the corresponding plain concrete slabs both at service load (column 5) and at a load near the ultimate load of plain concrete slabs (column 9). From this Table it can be seen that the maximum rotation in slab FS-3 was reduced by 23.5 and 26.9% at service load and near the ultimate

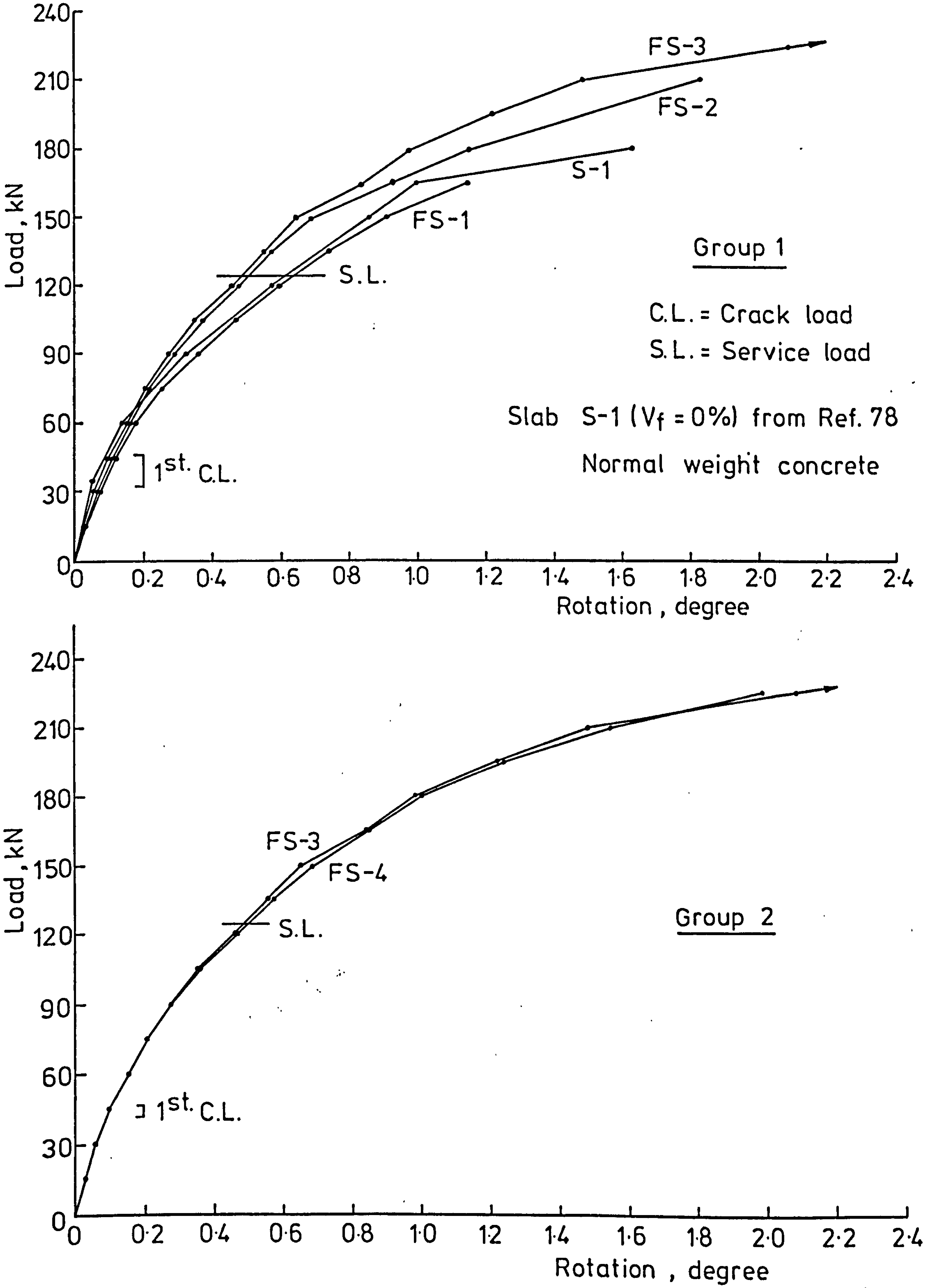

FIG. 5-5 LOAD-ROTATION CURVES FOR θ_1 MAXIMUM

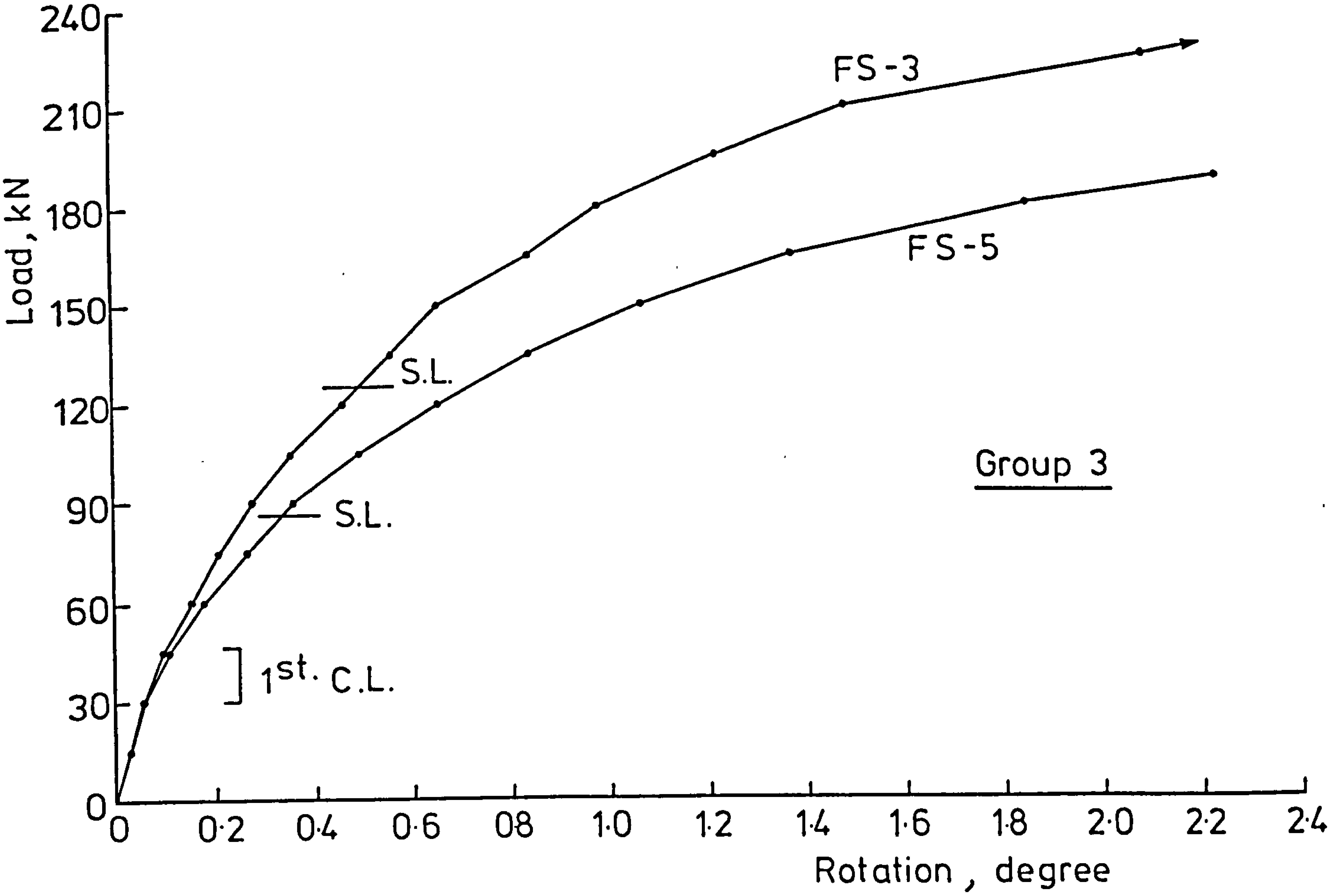

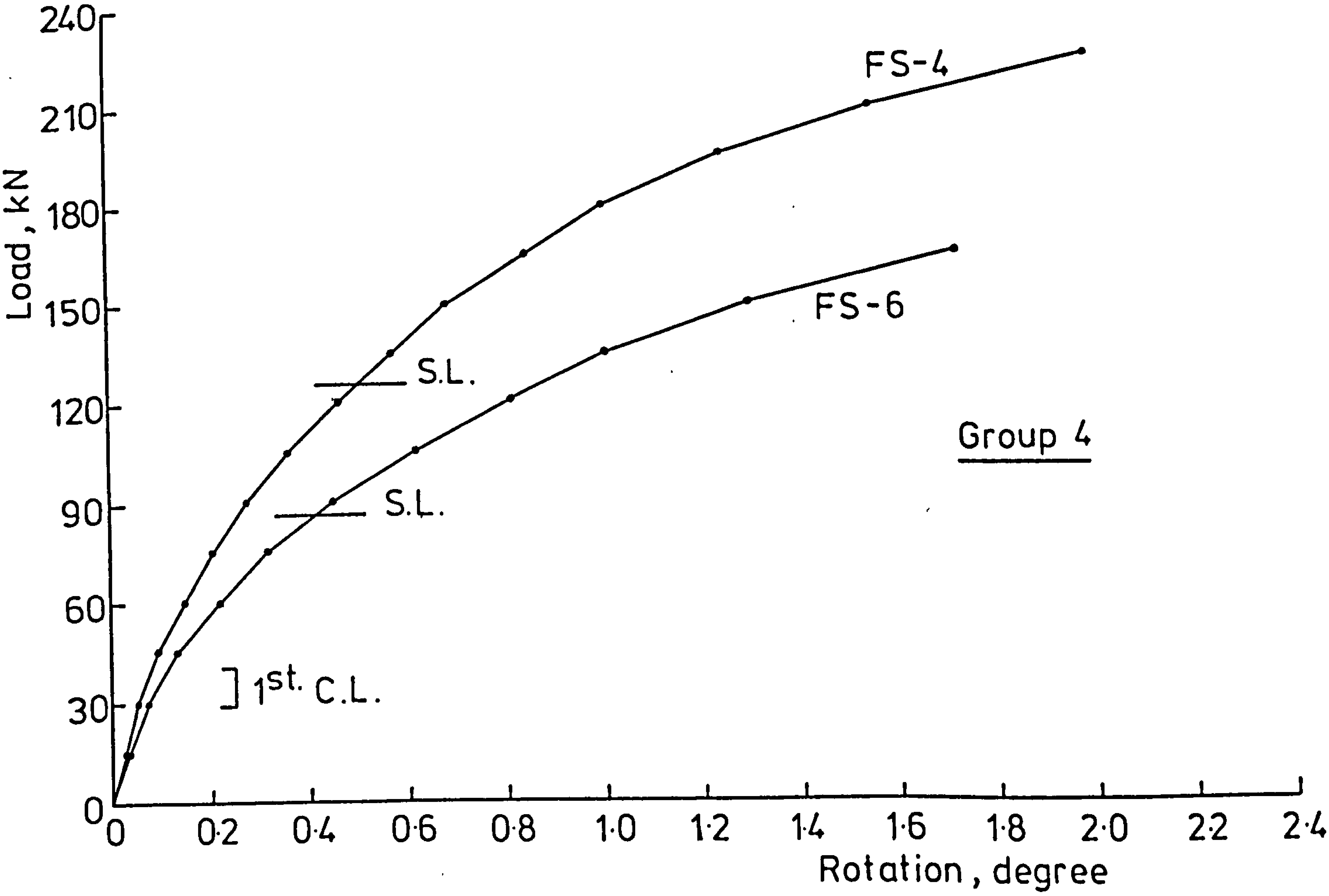

FIG. 5-5 LOAD – ROTATION CURVES FOR θ_1 MAXIMUM

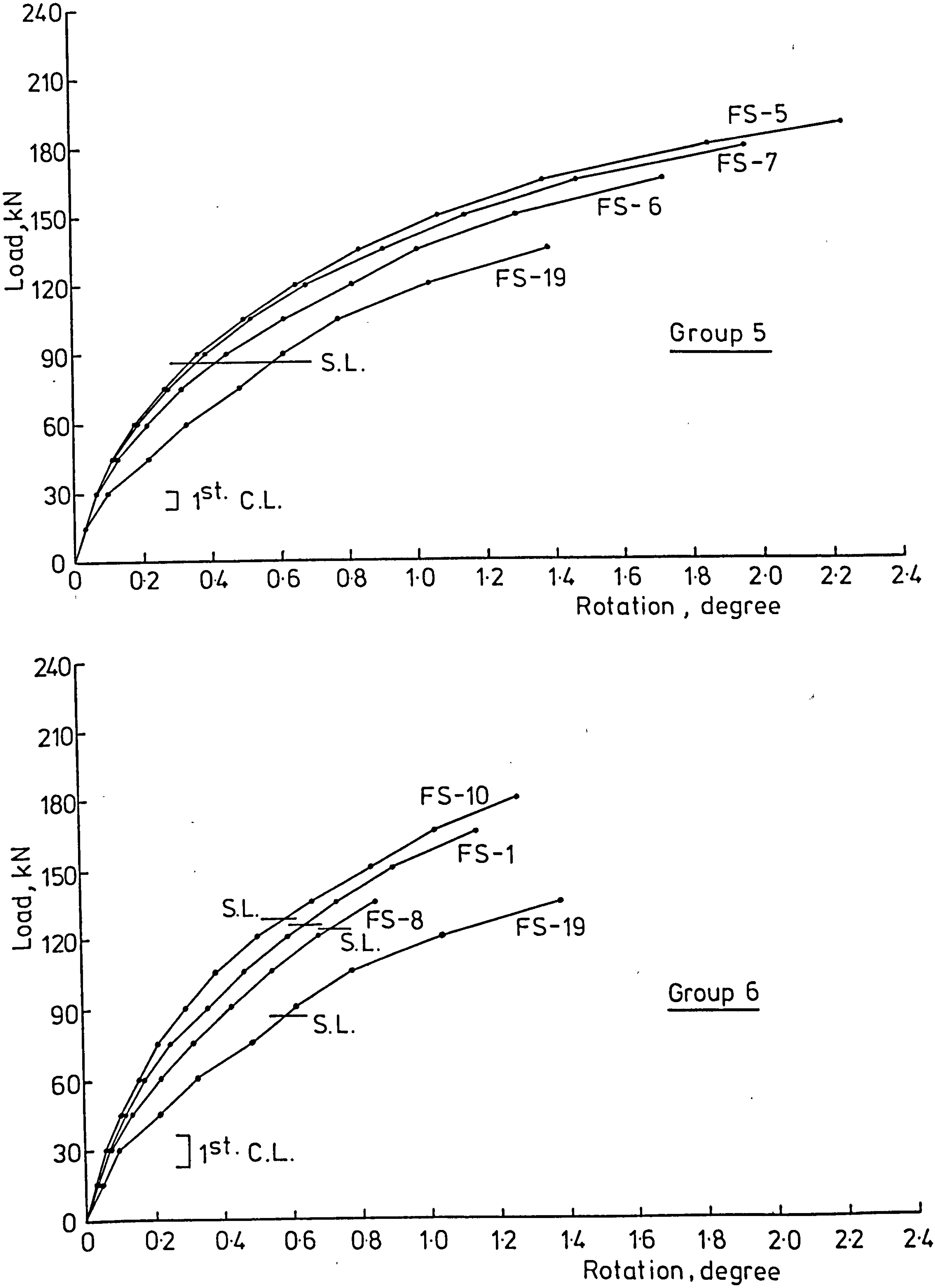

FIG. 5-5 LOAD-ROTATION CURVES FOR θ_1 MAXIMUM

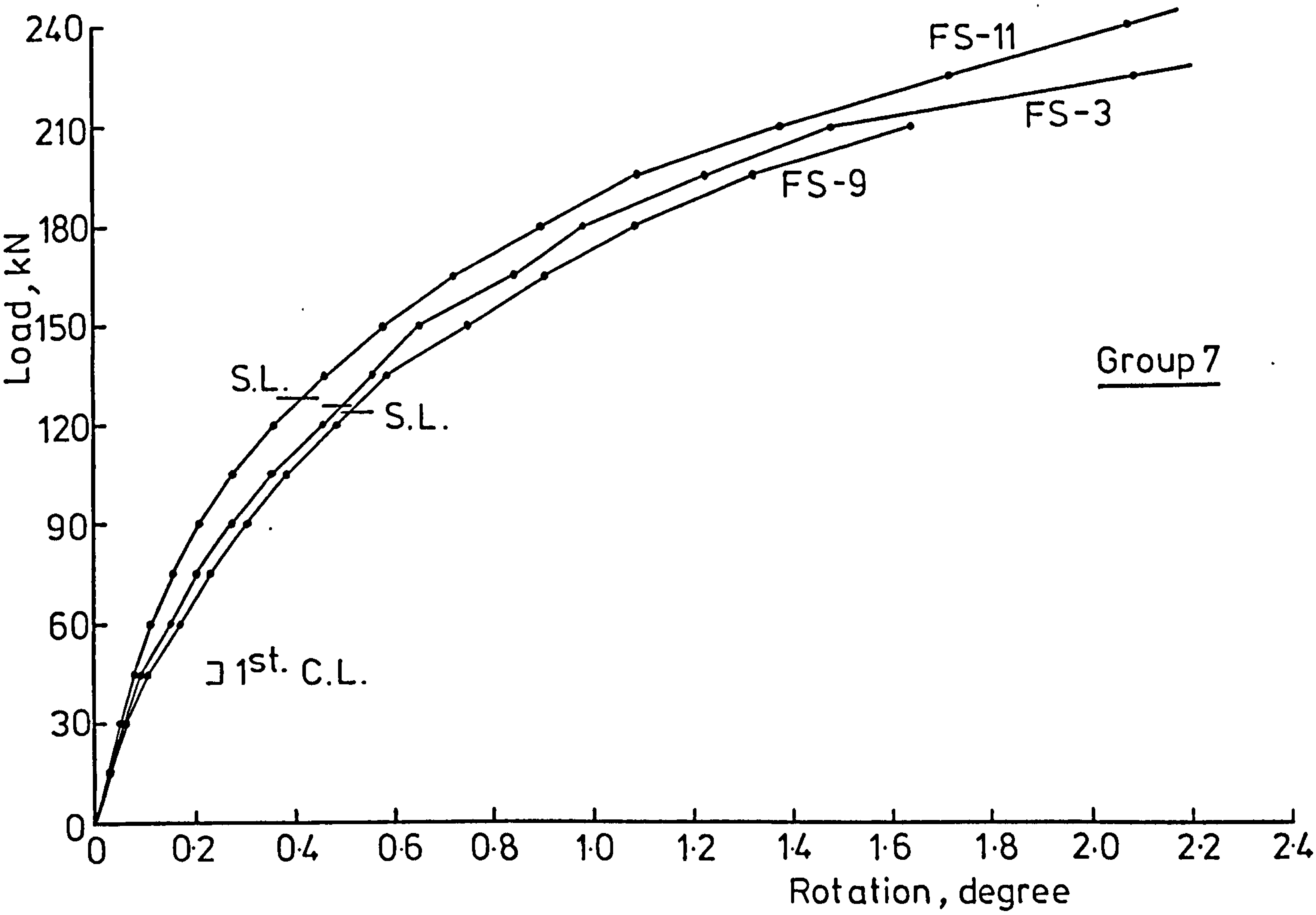

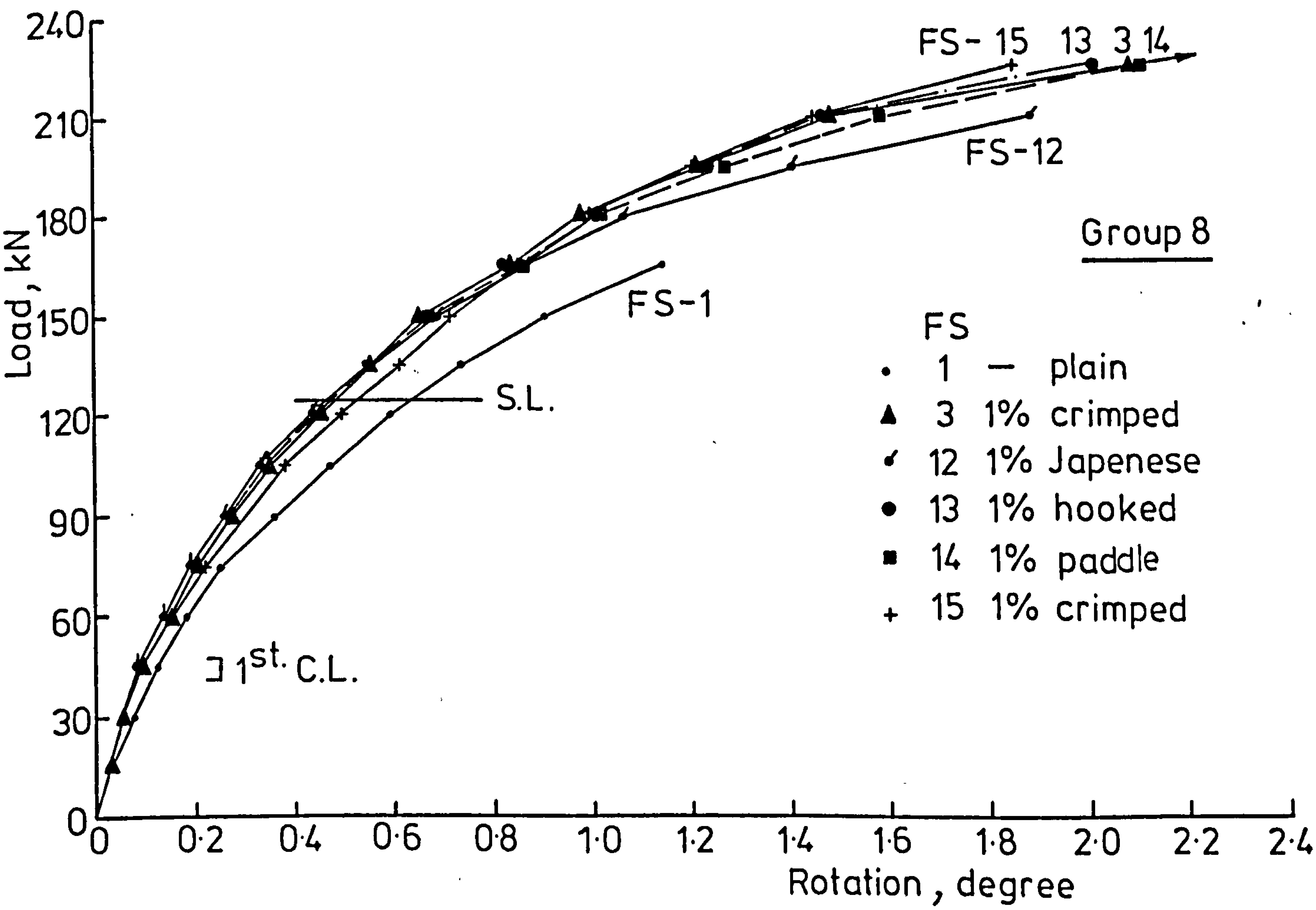

FIG. 5-5 LOAD-ROTATION CURVES FOR θ_1 MAXIMUM

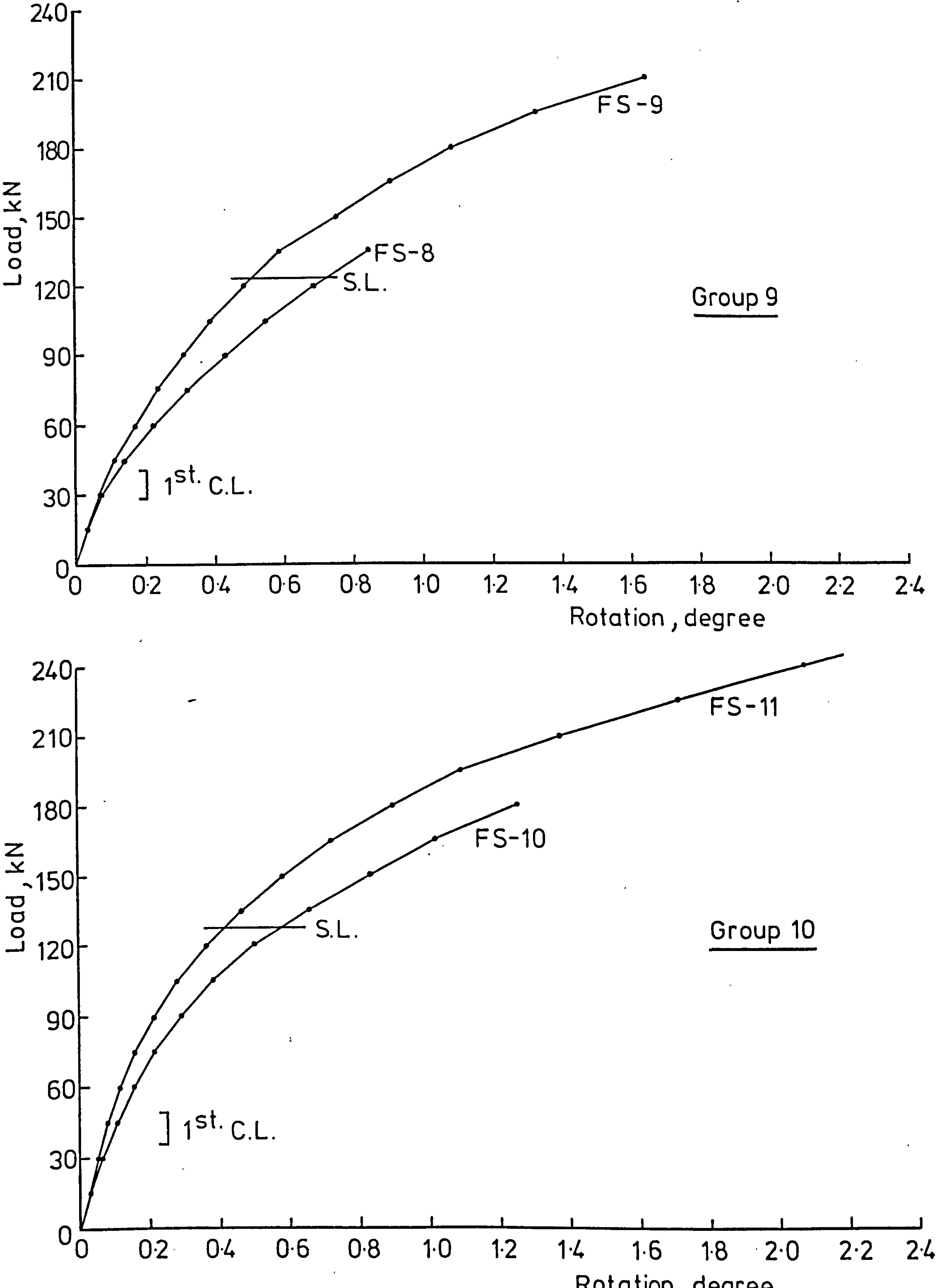

FIG. 5-5 LOAD-ROTATION CURVES FOR θ_1 MAXIMUM

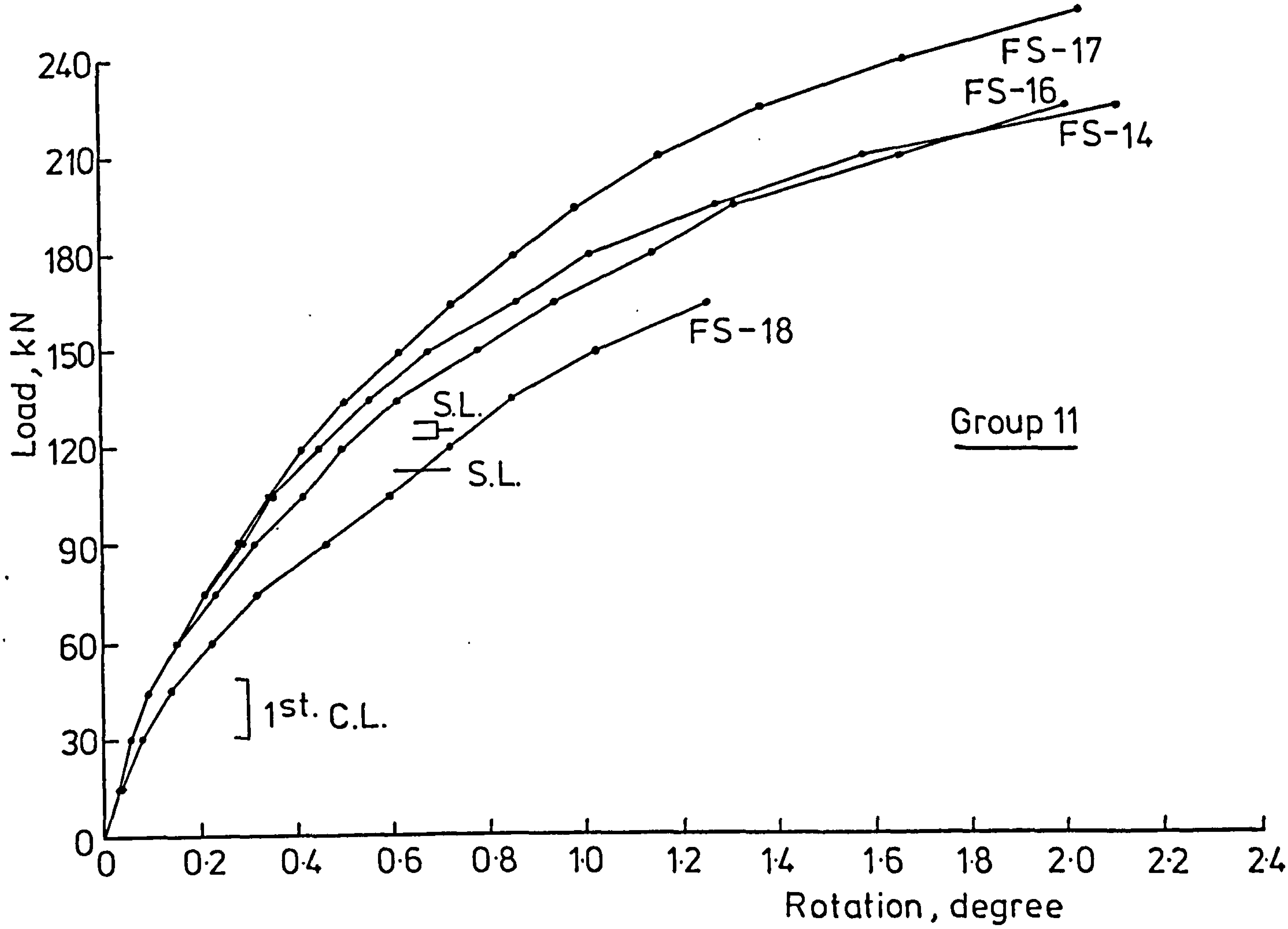

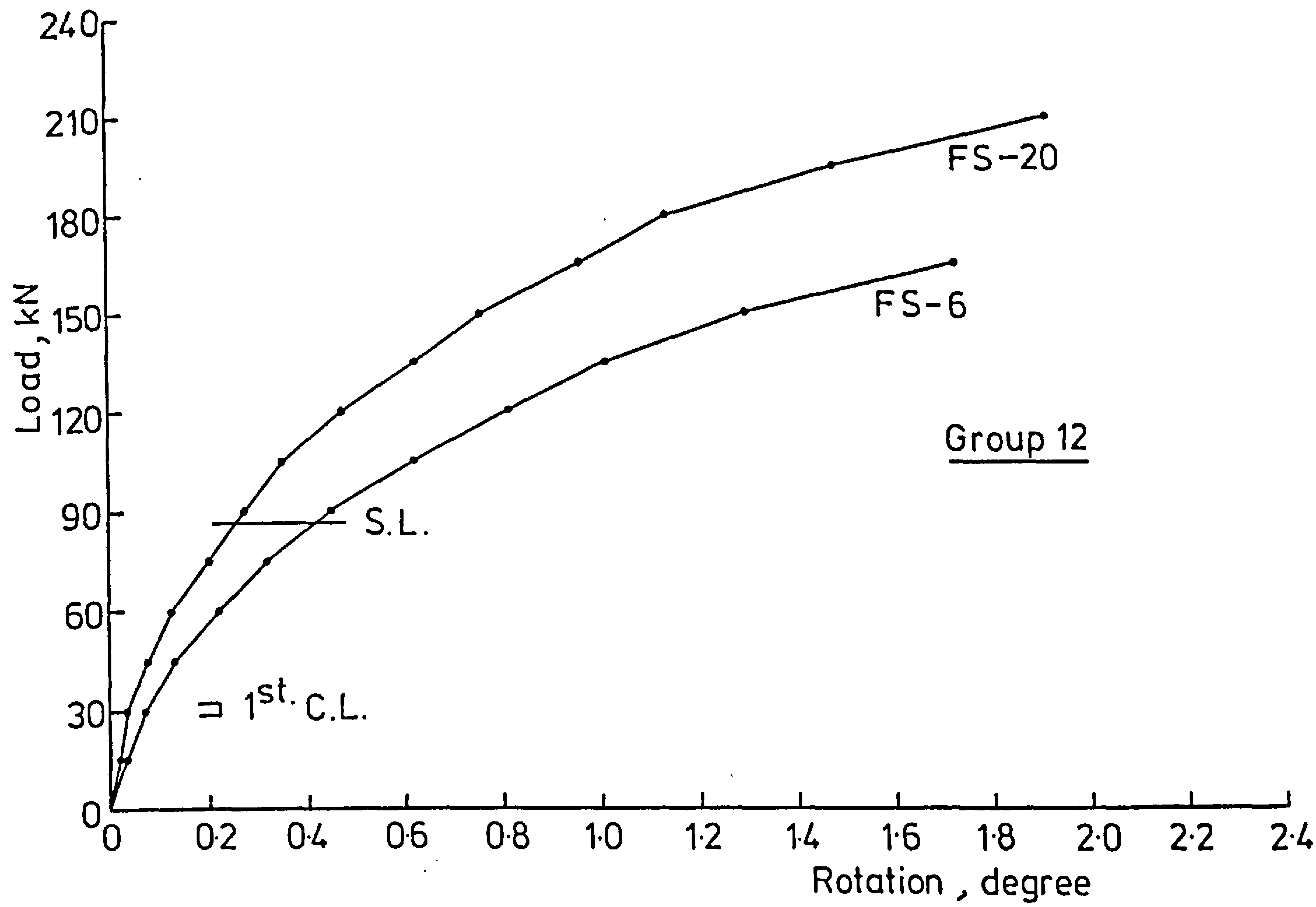

FIG. 5-5 LOAD-ROTATION CURVES FOR θ_1 MAXIMUM

Table 5.5 Deformation characteristics of test slab.

				Deformation at First Crack				Deformation at Service Load				Deformation at Max. Load			
Series Number	Series Detail	Slab Number	Fibre Type and Percentage	Load in KN	Max. Rotation in degree	Max. Tension steel strain $\times 10^{-6}$	Max. Comp. Concrete strain $\times 10^{-6}$	Load in KN	Max. Rotation in degree	Max. Tension steel strain $\times 10^{-6}$	Max. Comp. Concrete strain $\times 10^{-6}$	Load in KN	Max. Rotation in degree*	Max. Tension steel strain $\times 10^{-6}$ **	Max. Comp. Concrete strain $\times 10^{-6}$ *
1	2	3	4	5	6	7	8	9	10	11	12	13	14	15	16
1	Fibre Percentage	FS-1	– 0.0	32.0	0.08	400	260	125.0	0.64	3950	1620	173.5	1.15	7600	2700
		FS-2	Crimped 0.5	42.5	0.10	400	340	125.0	0.52	2600	1360	225.0	1.85	10500	4240
		FS-3	Crimped 1.0	46.8	0.10	600	280	125.0	0.49	2500	1200	247.4	2.6	11750	5140
2	Reinforcement Reduction	FS-4	Crimped 1.0	40.9	0.085	300	240	125.0	0.50	1750	1140	224.4	2.0	9400	3740
		FS-5	Crimped 1.0	30.0	0.06	250	180	85.97	0.34	1650	760	198.1	2.25	9600	4700
		FS-6	Crimped 1.0	29.0	0.065	250	200	85.97	0.42	1600	860	174.5	1.73	7500	3220
		FS-7	Crimped 1.0	30.0	0.060	250	160	85.97	0.36	1600	780	192.4	1.96	11000	3240
		FS-19	– 0.0	22.5	0.060	350	180	85.97	0.54	2740	1000	136.5	1.39	8000	2320
		FS-20	Crimped 0.0	31.5	0.040	200	160	85.97	0.26	1050	620	211.0	1.92	13000	3920

Table 5.5 (Continued)

				Deformation at First Crack				Deformation at Service Load				Deformation at Max. Load			
1	2	3	4	5	6	7	8	9	10	11	12	13	14	15	16
3	Column Size	FS-8	- 0.0	29.0	0.07	400	300	122.69	0.72	3850	1940	150.3	0.85	5000	2300
		FS-9	Crimped 1.0	41.4	0.10	300	280	122.69	0.51	1900	1380	216.6	1.65	9250	3740
		FS-10	- 0.0	36.0	0.08	320	240	127.34	0.58	3250	1200	191.4	1.27	7600	2120
		FS-11	Crimped 1.0	48.9	0.09	400	220	127.34	0.42	1850	860	259.8	2.51	7250	4400
4	Fibre Type	FS-12	Japanese 1.0	42.5	0.08	270	250	125.0	0.53	1950	1140	217.5	1.90	7800	3700
		FS-13	Hooked 1.0	44.0	0.09	300	260	125.0	0.48	1750	1100	235.7	2.03	9000	4200
		FS-14	Paddle 1.0	45.5	0.09	280	260	125.0	0.47	1600	1100	239.5	2.12	6600	3960
		FS-15	Crimped 1.0	41.0	0.07	350	280	125.0	0.47	1800	1200	238.0	1.86	9700	4060
5	Cube Compressive Strength	FS-16	Paddle 1.0	42.4	0.08	280	220	122.7	0.53	1500	1100	227.8	2.02	9600	3780
		FS-17	Paddle 1.0	47.5	0.09	200	240	126.9	0.46	1600	1060	268.4	2.05	11000	5000
		FS-18	Paddle 1.0	30.5	0.08	270	220	112.7	0.67	2400	1660	166.0	1.26	5300	3920

NOTE:- 1) In calculating service load (CP110) steel fibre effect was neglected.
2) Slab FS-15, 6 mm Lytag aggregates, fibres $\ell_f/d_f = 90$.
3) *Indicates readings at 90 to 97% of the maximum load.
4) ** Indicates readings at 85 to 95% of the maximum load.

load of plain concrete slab FS-1 respectively, when fibre content increased to 1.0% by volume. Ali (78) reported that the reduction in the maximum rotation in normal weight concrete slabs was 35 and 38% near service load and maximum load respectively when 0.9% by volume crimped fibres were used around the column stub.

The use of different fibre type in slabs FS-12, FS-13, FS-14 and FS-15 caused almost the same reductions in the maximum rotation. The reduction in the rotation was 29.2 and 27.6% at service load when 1.0% by volume crimped fibres were used in slabs FS-9 and FS-11 with 100 and 200 mm column size respectively.

The use of 1.0% by volume crimped fibres in slabs FS-5 (ρ=0.3716%) caused a higher reduction in rotation (equal to 37% at service load) than that caused by fibres in slabs with ρ = 0.5574%, i.e. the effect of fibres in reducing the maximum rotation is more pronounced in the more lightly reinforced slabs.

The rotation at both service and near ultimate load was not affected when compressive reinforcement was reduced by 100% in slab FS-4 (ρ=0.5574%) when compared with rotation of slab FS-3 with full compressive reinforcement, but it was affected when the compressive reinforcement was reduced in the slabs FS-6 and FS-7 with a tension reinforcement ratio equal to 0.3716%.

The use of 1.0% by volume crimped fibres in the whole slab (slab FS-20) caused even higher reduction in rotation when compared with slabs FS-5, FS-6 and FS-7 where fibres are located around the column stub (Table 5.3).

The maximum rotation was decreased with increasing cube compressive strength in slabs FS-18, FS-16, FS-14 and FS-17 all with 1.0% by volume paddle fibres as can be seen from Table 5.5 and Fig. 5.5 (group 11).

From Fig. 5.6 it can be seen that all rotations for each individual slab were close enough in value especially at early stages of loading; the

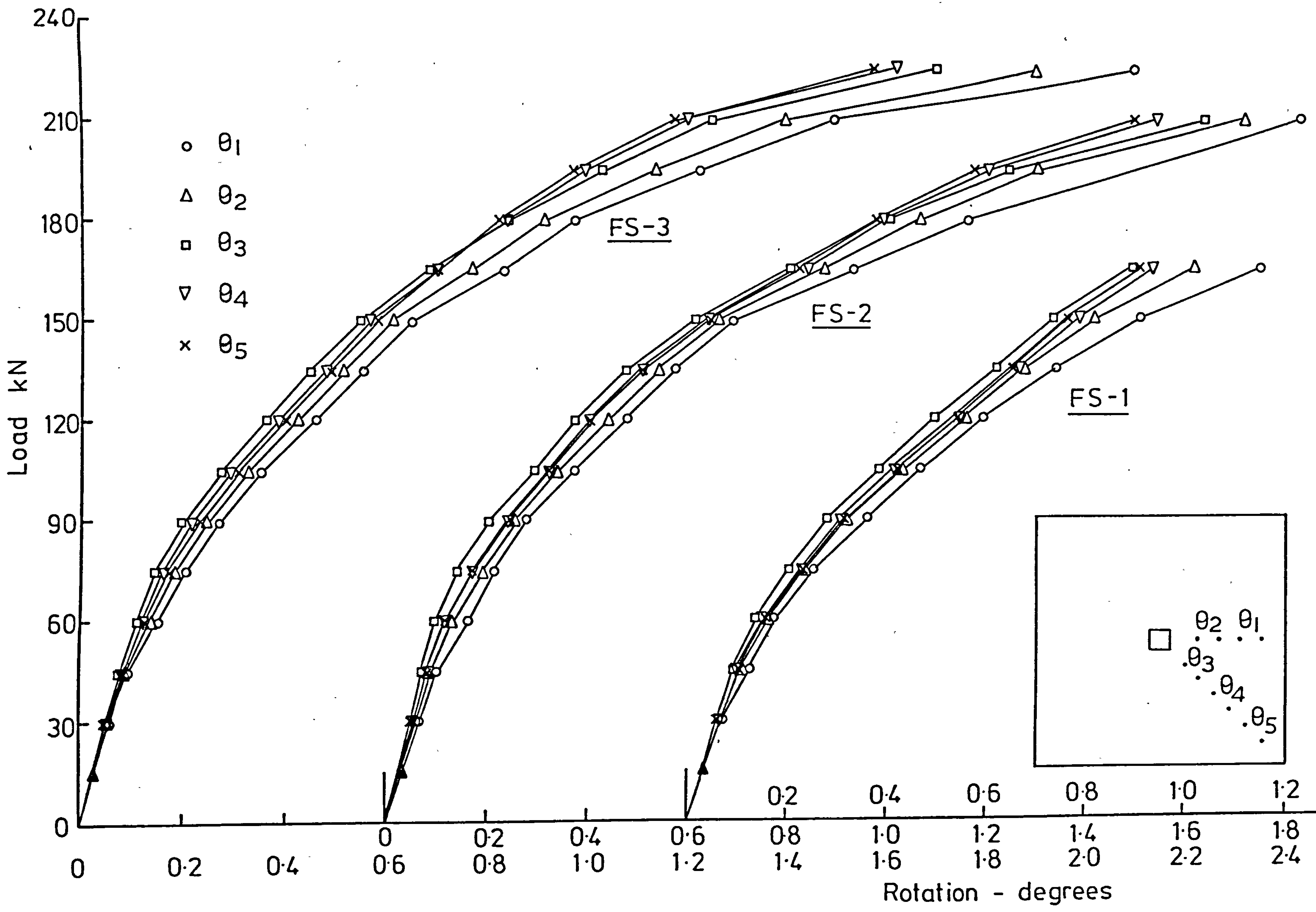

FIG. 5·6 LOAD-ROTATION CURVES FOR SLABS FS1-FS3 ($V_f = 0-1\%$)

difference in value was increased as loading continued till failure. It can also be seen, for example in slab FS-3, that while at the early stages of loading the order of magnitude for the rotation was $\theta_1>\theta_2>\theta_5>\theta_4>\theta_3$, it changed to $\theta_1>\theta_2>\theta_3>\theta_4>\theta_5$ as loading continued because the rotations θ_4 and θ_5 are affected by the lift off corner of the slab.

From Table 5.3 it can be seen that the reduction of rotation of plain concrete slabs due to presence of fibres was almost of the same magnitude to reduction in maximum deflection.

5.5.2 Comparison of Rotation Between Lightweight and Normal Weight Concrete Slabs.

The load-maximum rotation curve of a comparable normal weight plain concrete slab S-1 (78) is shown in Figs. 5.5 (group 1). The rotation of this slab was about 5% lower than that of the plain lightweight concrete slab FS-1. Since the addition of 1.0% fibre reinforcement in lightweight concrete slabs reduced the rotation by about 25% it can be concluded that the rotation of fibre lightweight concrete slabs is about 20% lower than that of normal weight concrete slab. This reduction is referred to stages of loading above service load, where extensive cracking occurred in slabs and fibres act as a crack arresting mechanism. From Fig. 5.5 (group 1) it can be seen that at early stages of loading the rotation in slab S-1 (plain normal weight) is less than that of slab FS-3 (fibre lightweight concrete) because the addition of fibres in slab FS-3 hardly increases the modulus of elasticity of lightweight concrete and therefore the stiffness of the slab.

5.6 Load-Steel Strain Relationships.

5.6.1 Compressive Steel.

Figs. 5.7A and B show the compressive steel strains measured at the centre of the slabs. From these figures it can be seen that the steel

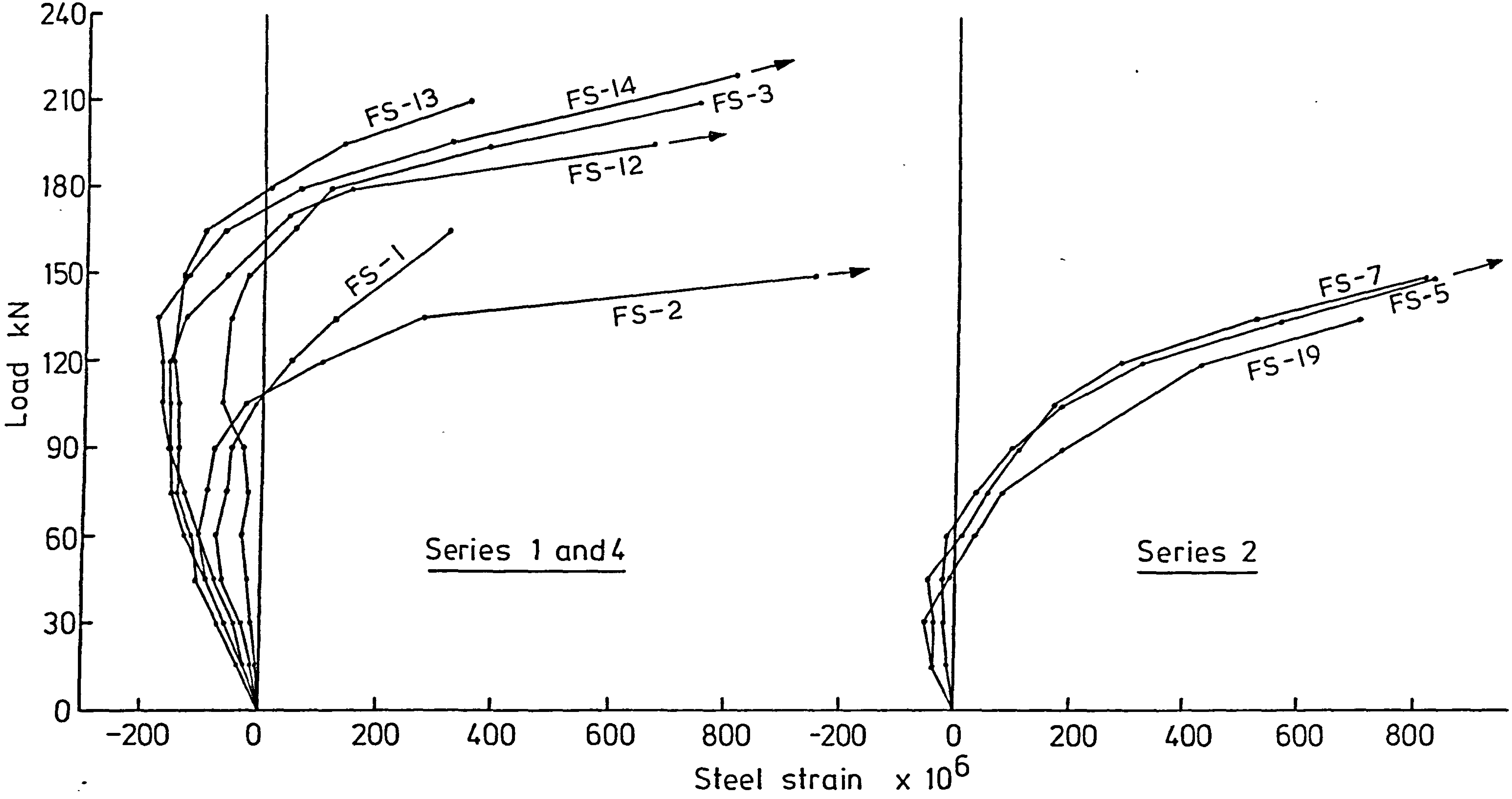

FIG.5-7A LOAD-MAX. COMPRESSION STEEL STRAIN CURVES AT CENTRE OF SPAN

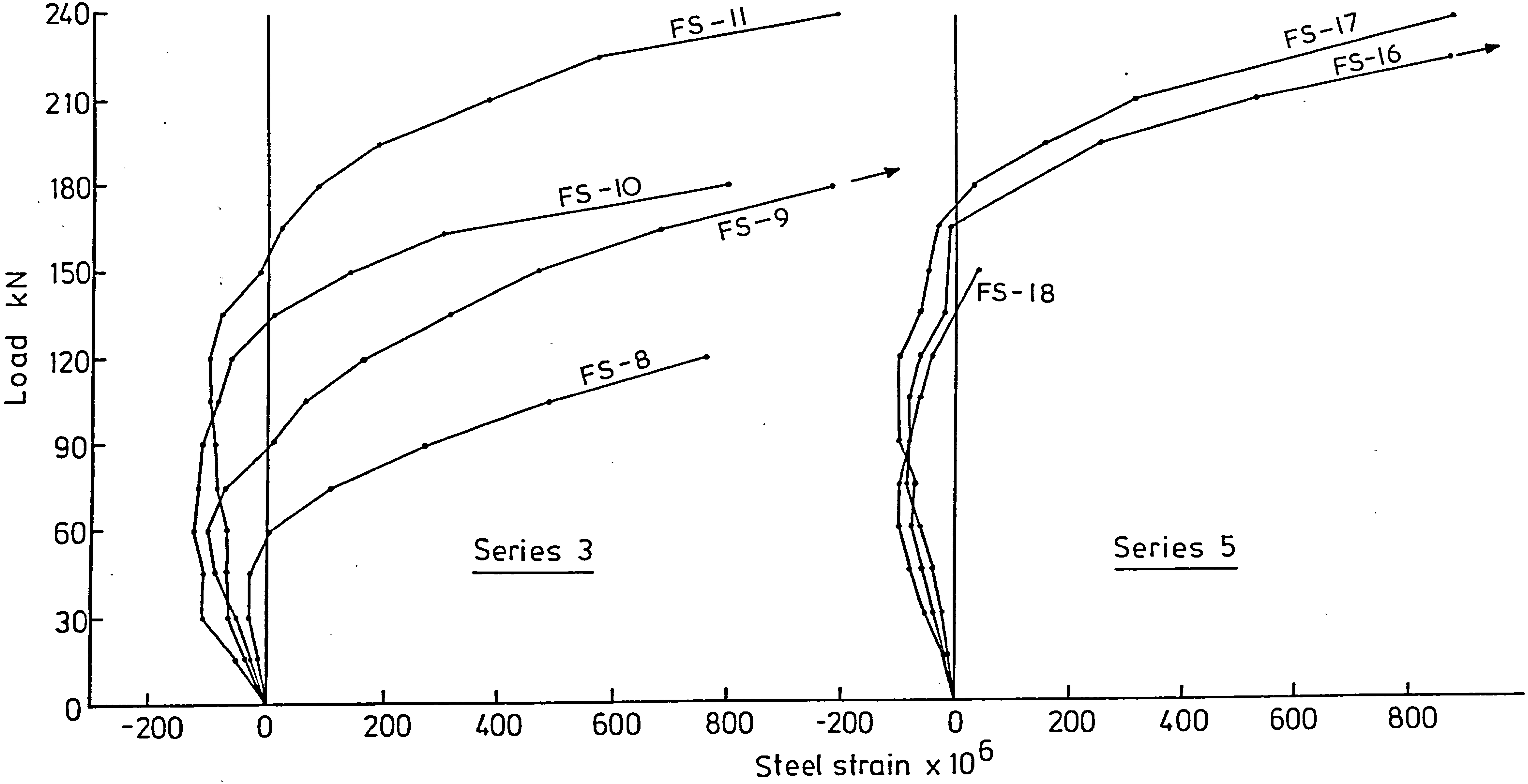

FIG. 5-7B LOAD - MAX. COMPRESSION STEEL STRAIN CURVES AT CENTRE OF SPAN strains in the compression reinforcement were initially compressive and gradually changed into tension with further increase in load, which means that the reinforcement started acting in tension. From test data it was noted that none of the compression reinforcement reached their yield strains.

From Figs. 5.7A and B it can be seen that the load at which the strain in the compressive reinforcement changed from compression to tension was higher in fibre concrete slabs than in corresponding plain concrete slabs, indicating the effect of fibre reinforcement in preventing the upward movement of neutral axis.

5.6.2 Tension Steel.

The strain gauge locations on the tension flexural reinforcement were previously shown in Fig.4.8. The tension steel strains near the centre were measured for all slabs and plotted in Figs. 5.8 as a function of the applied load. The tension steel strain for all slab specimens at first crack load, service load and near maximum failure load are listed in Table 5.5.

The tension steel strain was very small at the elastic stage of loading until the first crack appeared, then it increased steadily and then rapidly as yielding approached. From Fig.5.8 it can be seen that the tension steel strain reduced drastically when fibre reinforcement was used in the slab-column connections.

5.6.2.1 Tension Steel Strain Characteristics at and above Service Load.

It was mentioned previously that the steel strains for all slab specimens were very small at the elastic stage. Therefore the steel strain characteristics will be discussed at and above service load because of their importance. Table 5.3 shows the ratio between tension steel strain of

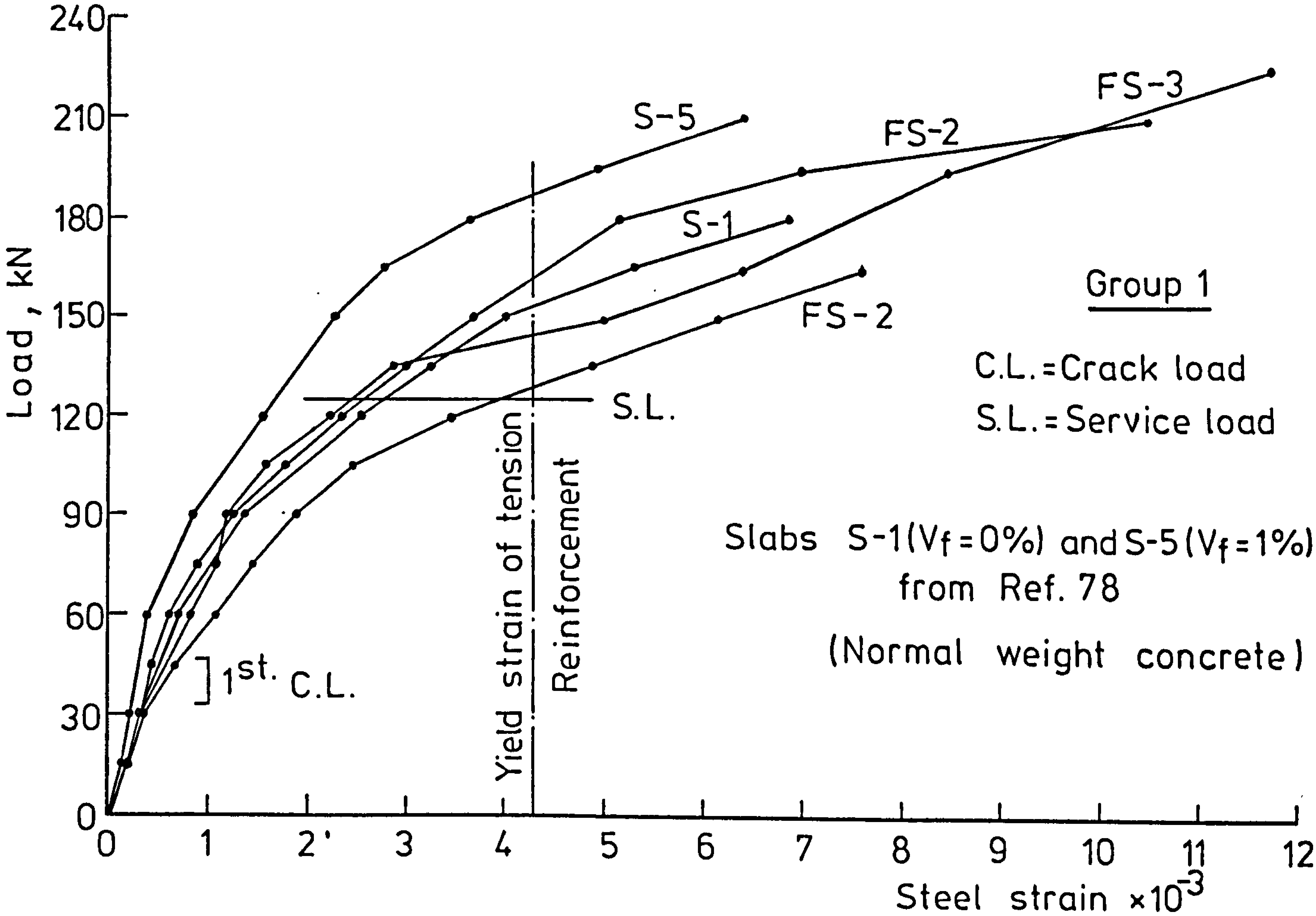

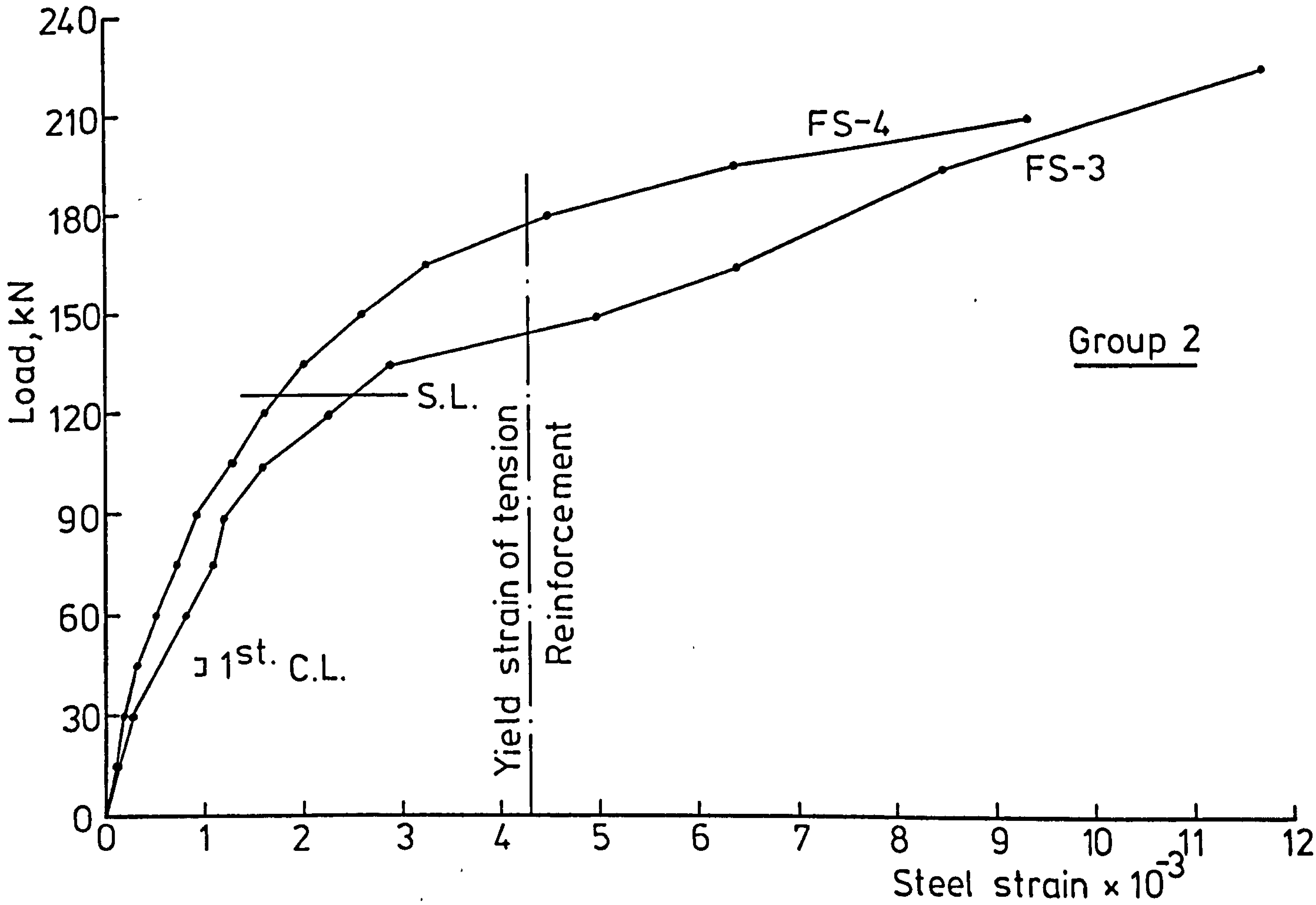

FIG. 5-8 LOAD-TENSION STEEL STRAIN CURVES NEAR CENTRE OF SPAN

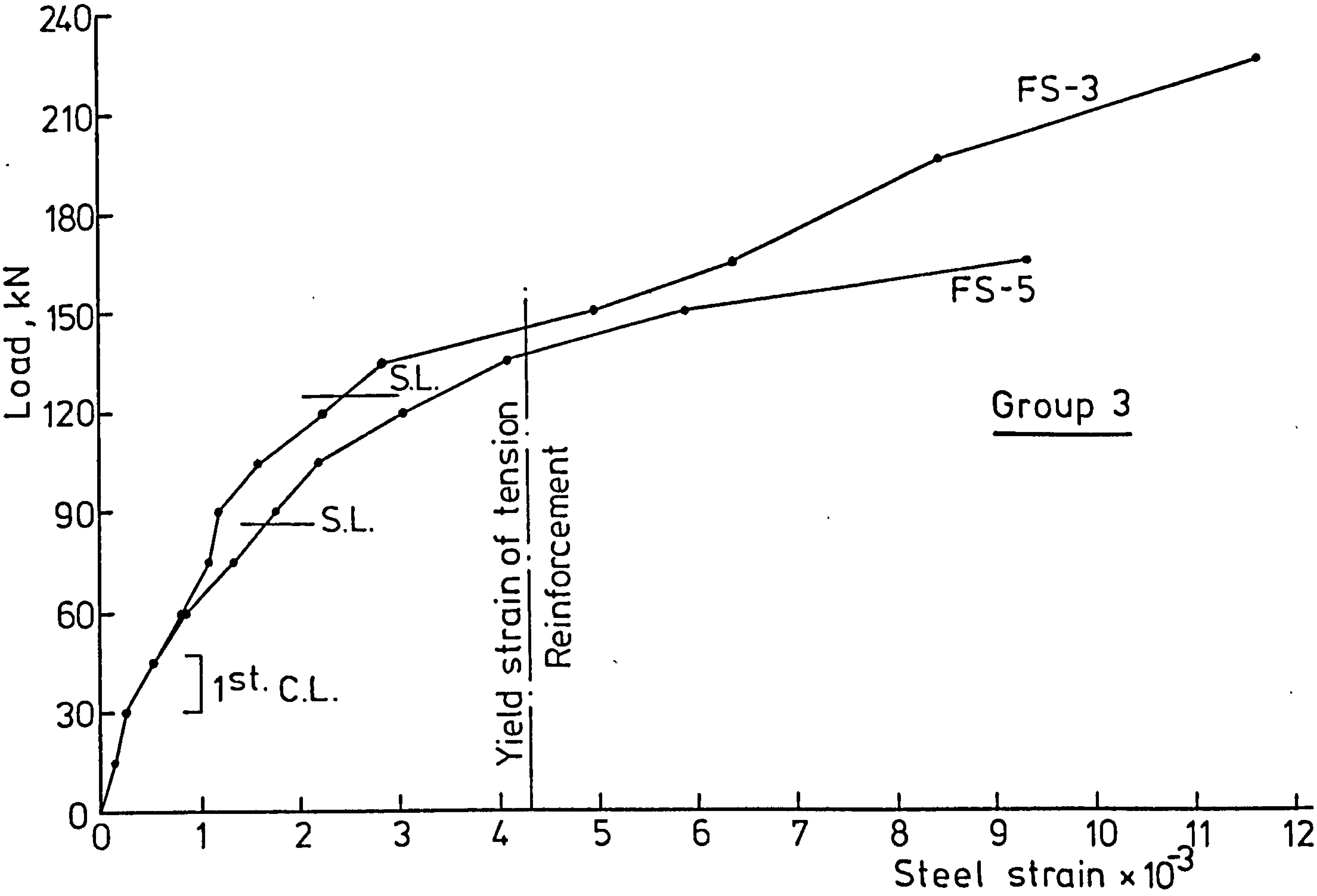

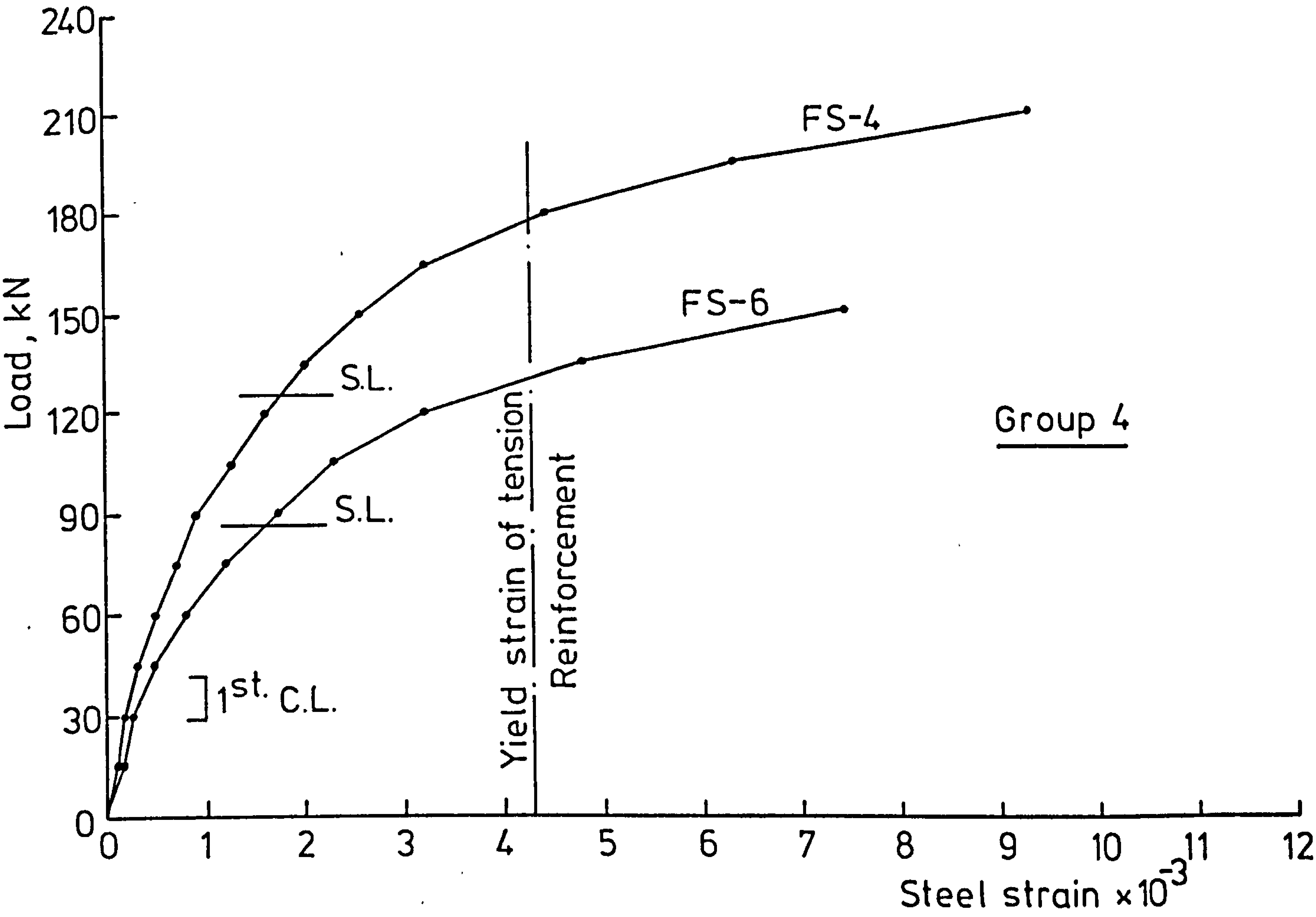

FIG. 5-8 LOAD – TENSION STEEL STRAIN CURVES NEAR CENTRE OF SPAN

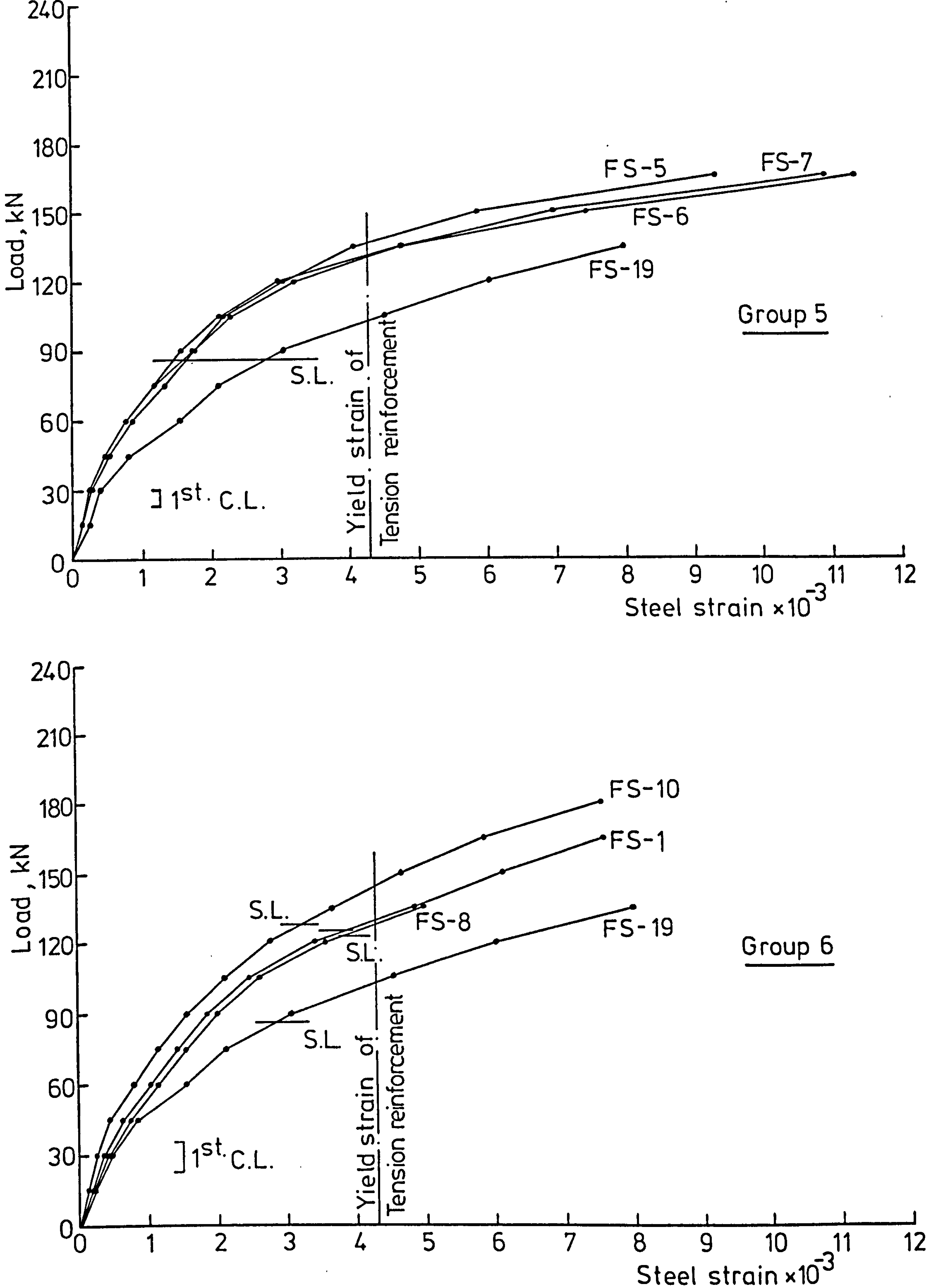

FIG. 5-8 LOAD-TENSION STEEL STRAIN CURVES NEAR CENTRE OF SPAN

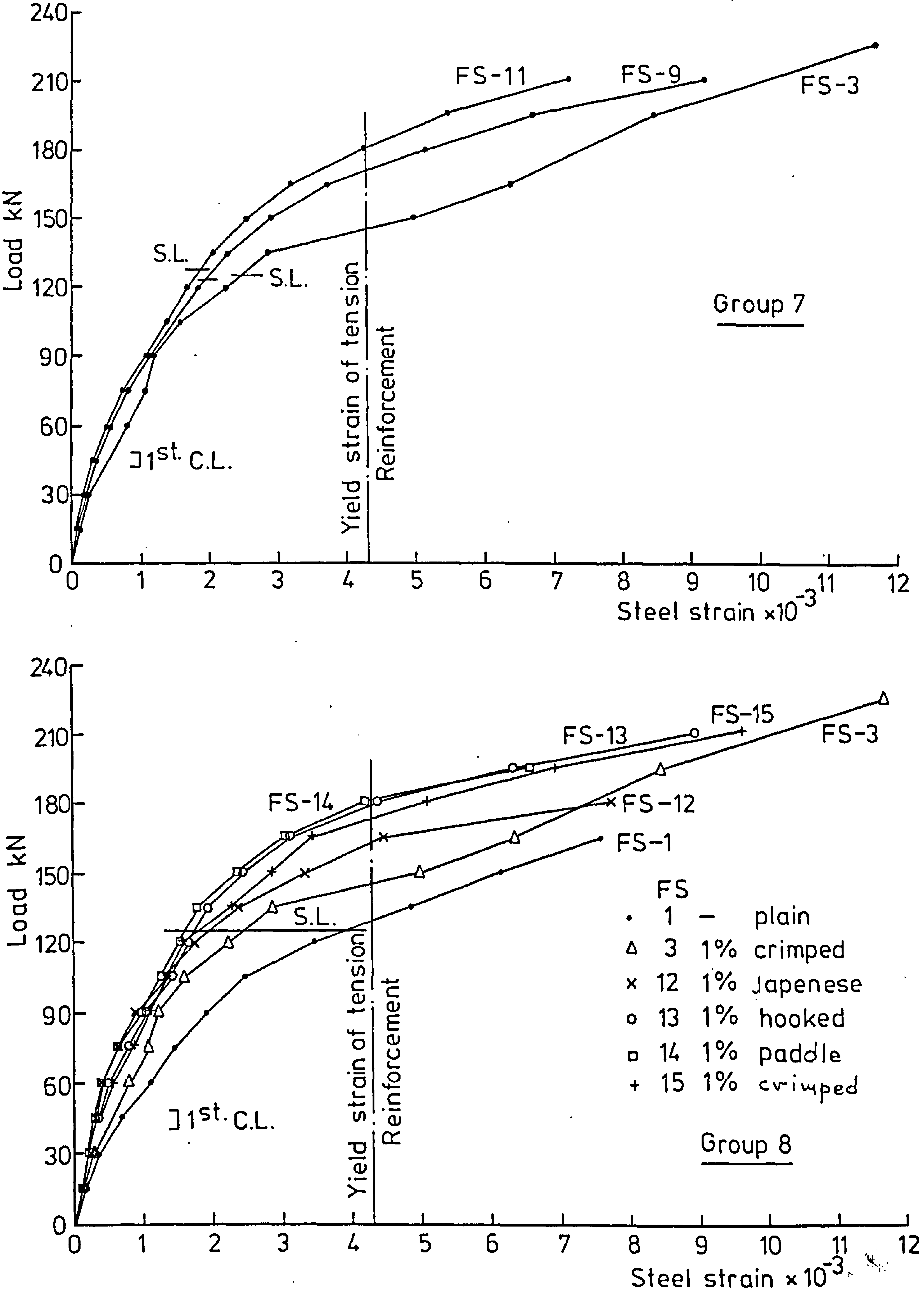

FIG. 5-8 LOAD – TENSION STEEL STRAIN CURVES NEAR CENTRE OF SPAN

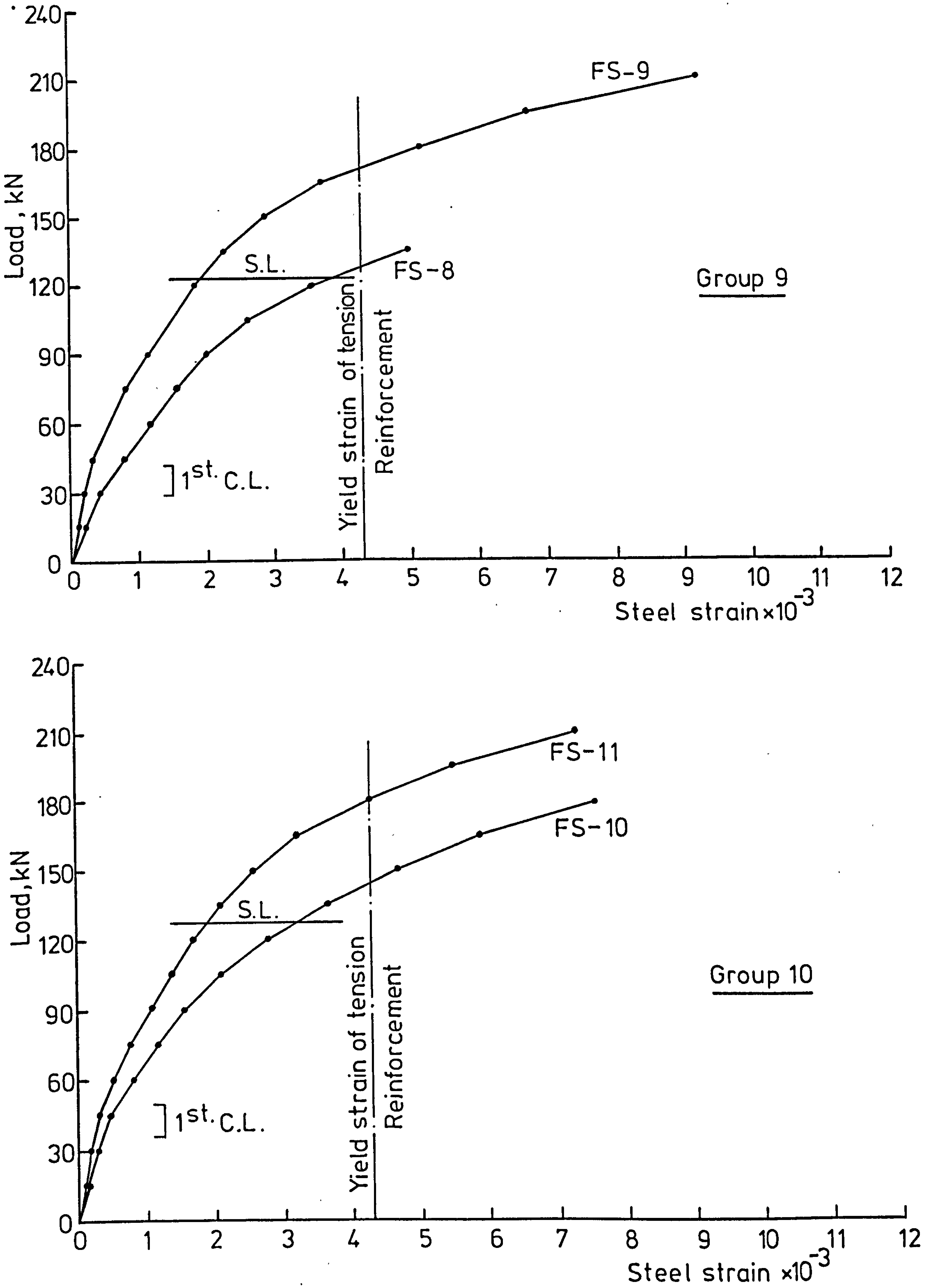

FIG. 5-8 LOAD — TENSION STEEL STRAIN CURVES NEAR CENTRE OF SPAN

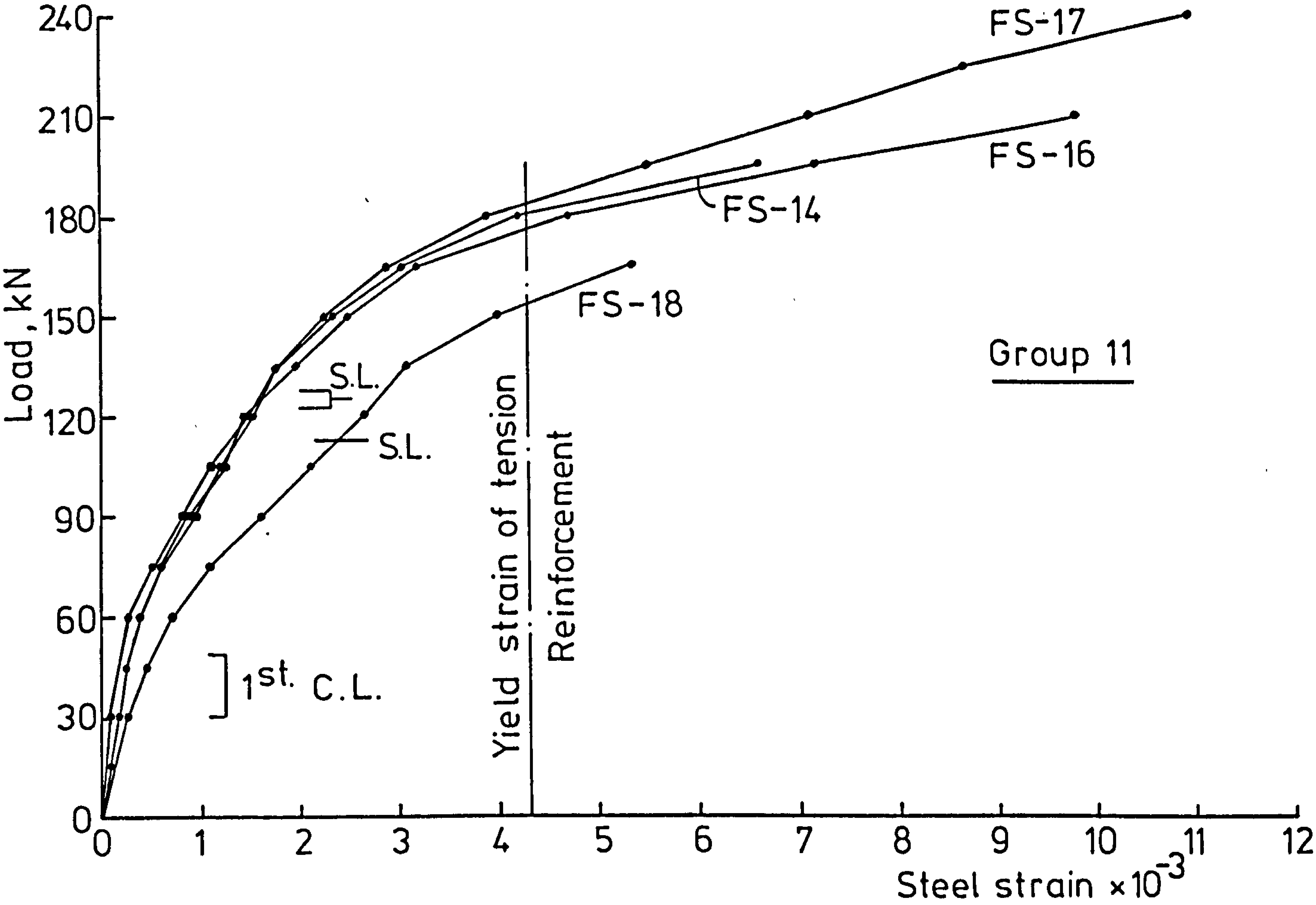

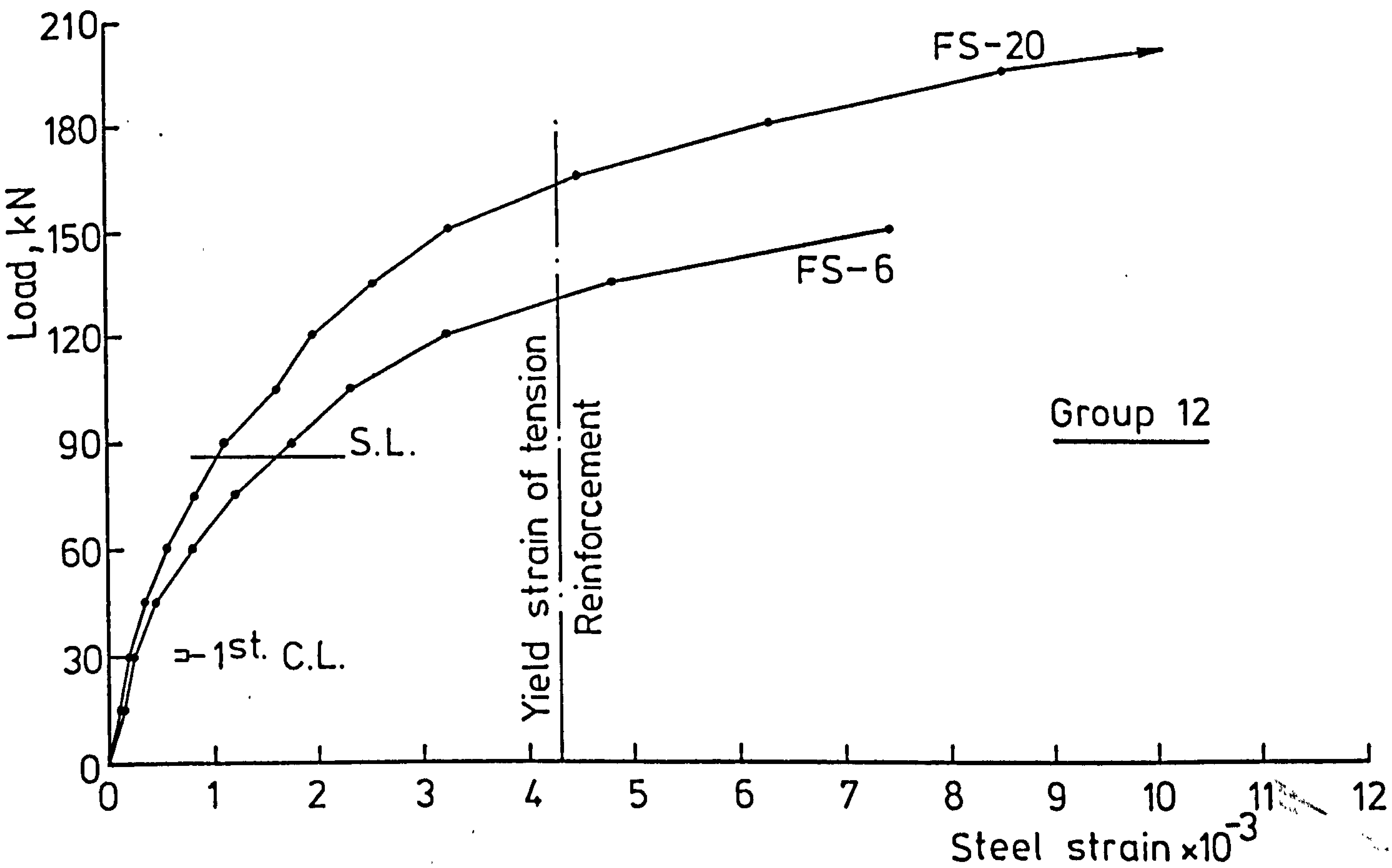

FIG. 5-8 LOAD - TENSION STEEL STRAIN CURVES NEAR CENTRE OF SPAN

the corresponding plain concrete slabs both at service load (column 6) and at a load near the ultimate load of plain concrete slabs (column 10). From this Table it can be seen that the tension steel strain near the centre of the slab reduced by about 55-60% when 1.0% by volume crimped, hooked and paddle fibres were used in slabs FS-4, FS-13 and FS-14 respectively (ρ=0.5574%). This reduction in the tension steel strain was about 55 and 45% when 1.0% by volume crimped fibres were used in slabs FS-9 and FS-11 with 100 and 200 mm column size respectively. Ali (78) reported a 48% reduction in steel strain when 0.9% by volume crimped fibres were used in normal weight concrete slabs.

The use of 1.0% by volume crimped fibres in slab FS-5 (ρ= 0.3716%) reduced the tension steel strain of the slab FS-19 by 40 and 48.7% at service load and near ultimate load respectively. These percentages were smaller when the compression reinforcement was reduced in slabs FS-6 and FS-7. The use of 1.0% by volume crimped fibres in the whole slab (slab FS-20) caused even higher reduction in the tension steel strain compared with slabs FS-5, FS-6 and FS-7 where fibres are located around the column stub.

The tension steel strain was decreased with increasing cube compressive strength in slabs FS-18, FS-16, FS-14 and FS-17 all with 1.0% by volume paddle fibres as can be seen from Table 5.5 and Figs. 5.8 (group 11).

From Table 5.3 it can be seen that the reduction of maximum tension steel strain of plain concrete slabs due to presence of fibres was higher than the reduction in centre deflection and maximum rotation.

The load-tension steel strain distribution curves for slabs FS-1 and FS-13 in both lateral and diagonal directions are shown in Fig.5.9. From this figure it can be seen that the presence of fibres reduced not

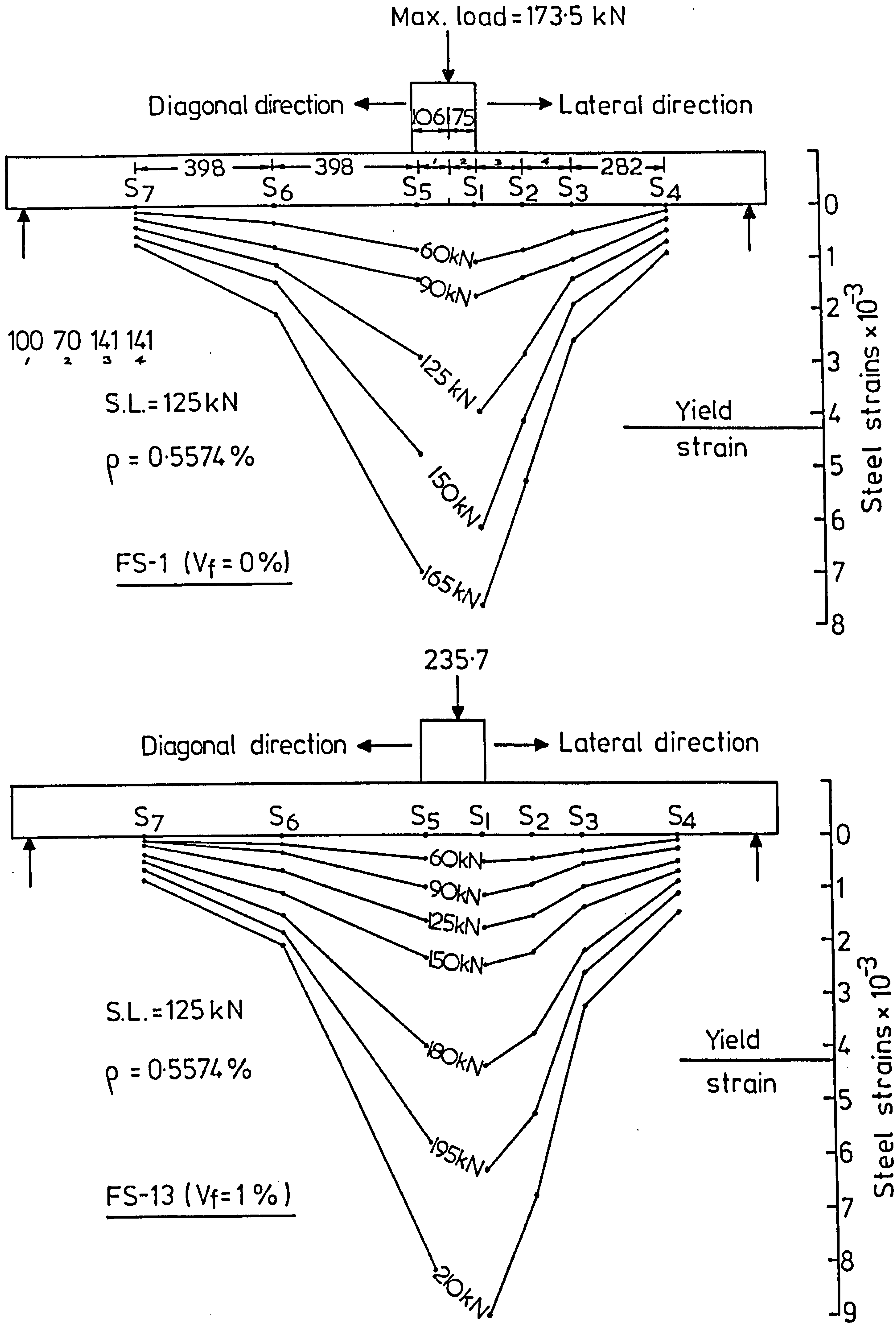

FIG.5·9 LOAD-TENSION STEEL STRAIN DISTRIBUTION FOR SLABS FS-1 AND FS-13

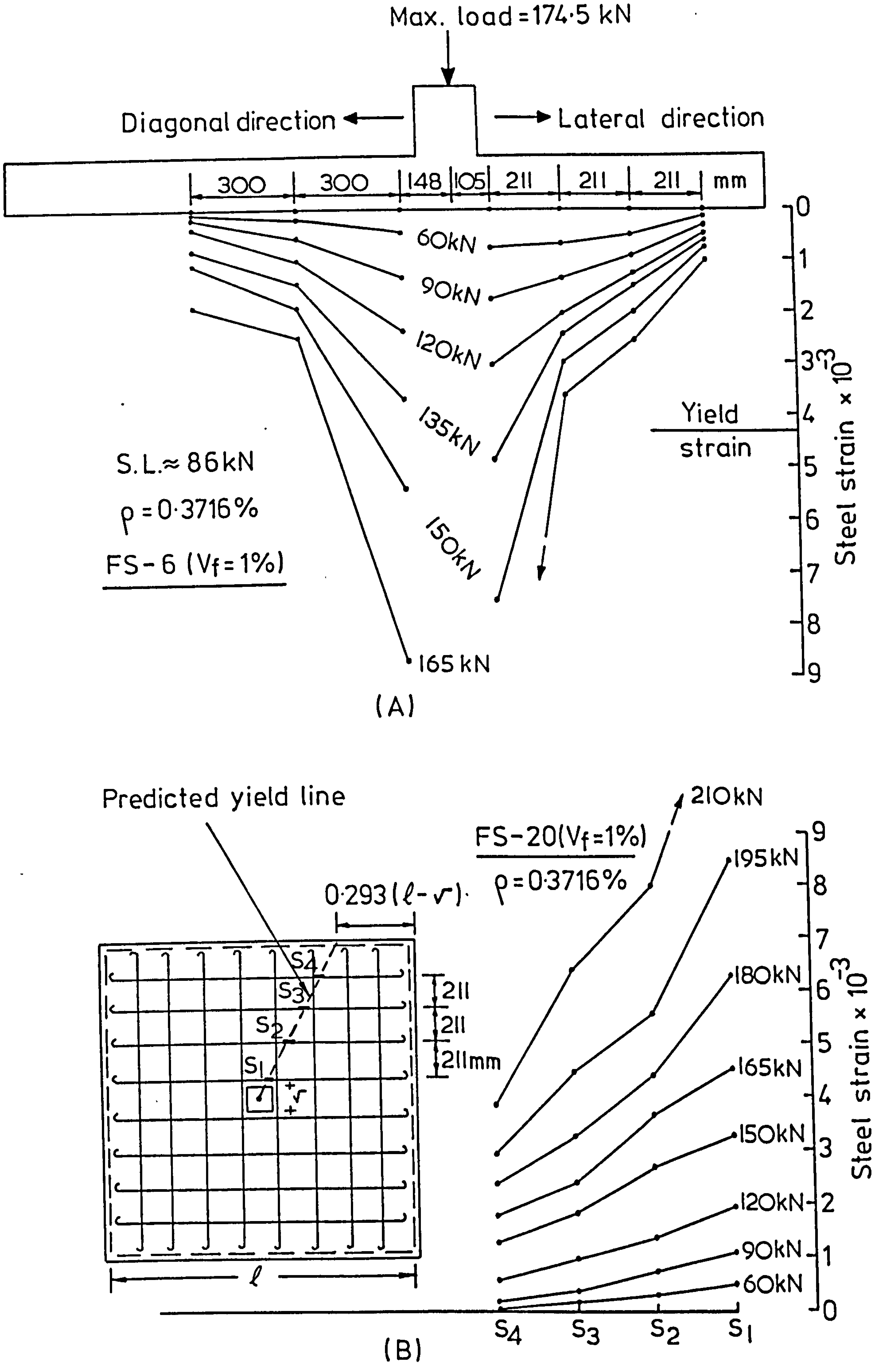

FIG.5-10 LOAD-TENSION STEEL STRAIN DISTRIBUTION FOR SLABS FS-6 AND FS-20

only the steel strain near the centre of the slab but also the steel strains at different locations. It can also be seen that the steel strain in lateral direction was higher than the steel strain in diagonal direction measured on the same bar.

Fig.5.10(A) shows the load-tension steel strain distribution curves for slab FS-6. Although this slab failed in flexure the steel strains in both lateral and diagonal directions were still below the yield strain except those measured near the centre of the slab. This is due to the fact that in a slab under concentrated load and with corners free to lift-off, the reinforcement yielding propagates along the 'yield line' located at an intermediate position between lateral and diagonal directions. Fig.5.10(B) shows how the reinforcement yielding propagates in slab FS-20 when strains were measured at positions located along the yield line predicted by yield line theory (92).

5.6.3 Comparison of Tension Steel Strain Between Lightweight and Normal Weight Concrete Slabs.

The load-tension steel strain curves of two normal weight concrete slabs (78) with and without fibres are shown for comparison purposes in Fig.5.8 (group 1). The tension steel strains of Lytag slab FS-1 (V_f=0.0%) at service load were about 45% higher than those of gravel slab S-1 (V_f=0.0%). However, the addition of fibre reinforcement to the light-weight concrete slabs FS-2 and FS-3 reduced the tension steel strains to values slightly less than those of the gravel concrete slab S-1 (V_f=0.0%).

5.7 Load-Concrete Strain Relationship.

Concrete strains were taken at different positions on the compressive and tensile sides of each slab as shown previously in Fig. 4.7. The maximum compression concrete strain for all slabs was measured and plotted in Figs. 5.11 as a function of the applied load. The maximum compression

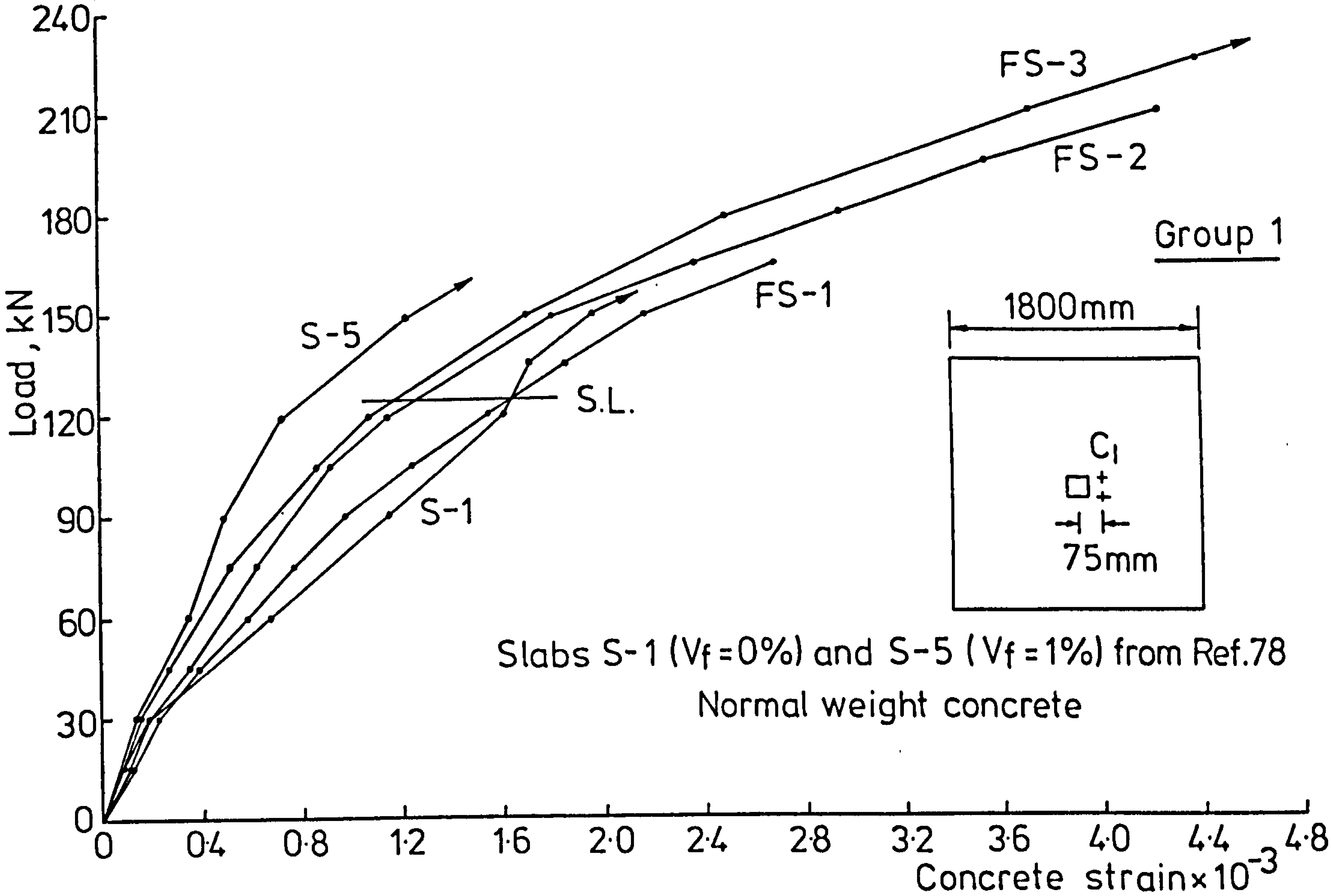

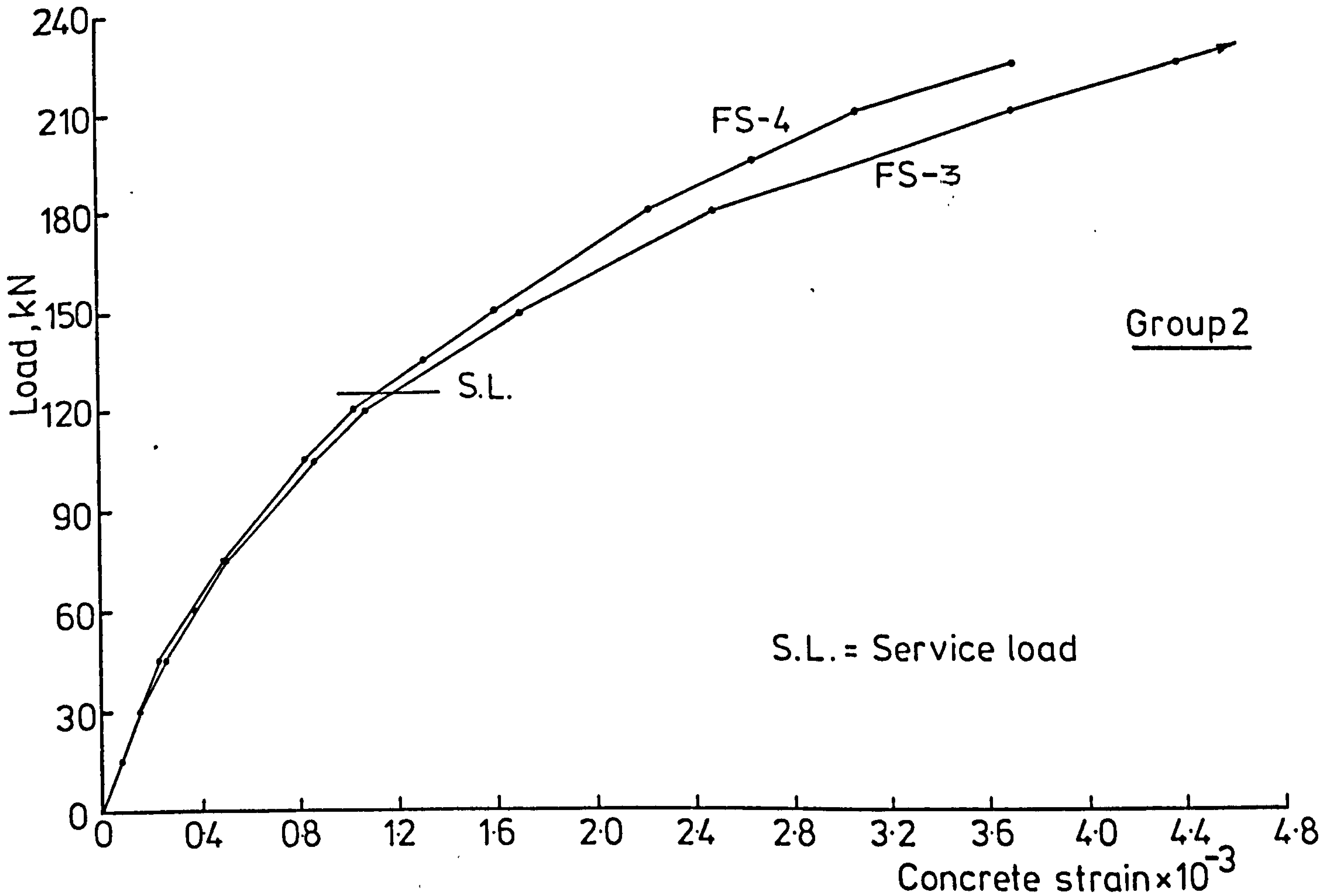

FIG. 5-11 LOAD - COMPRESSION CONCRETE STRAIN CURVES AT C_1 MAX.

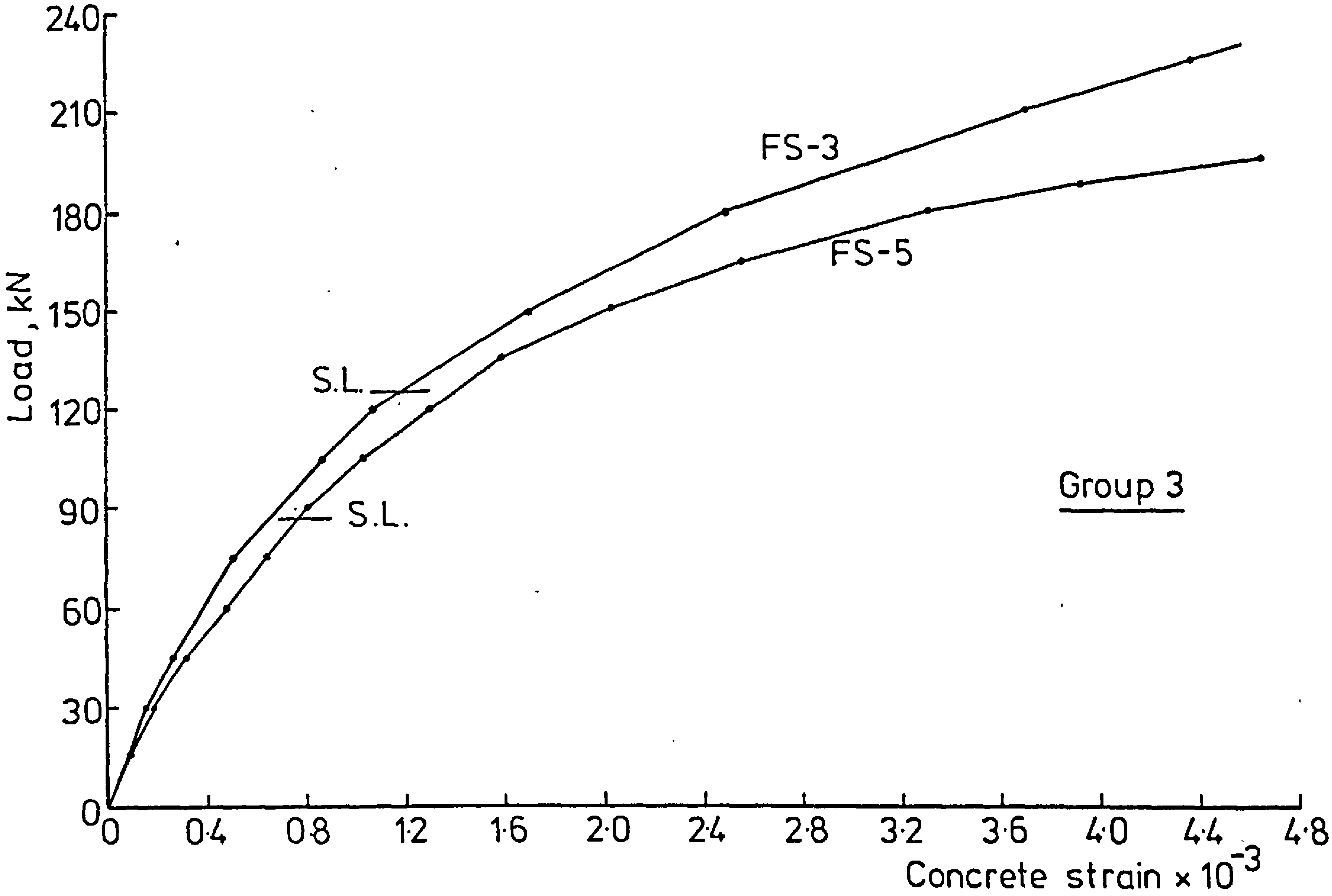

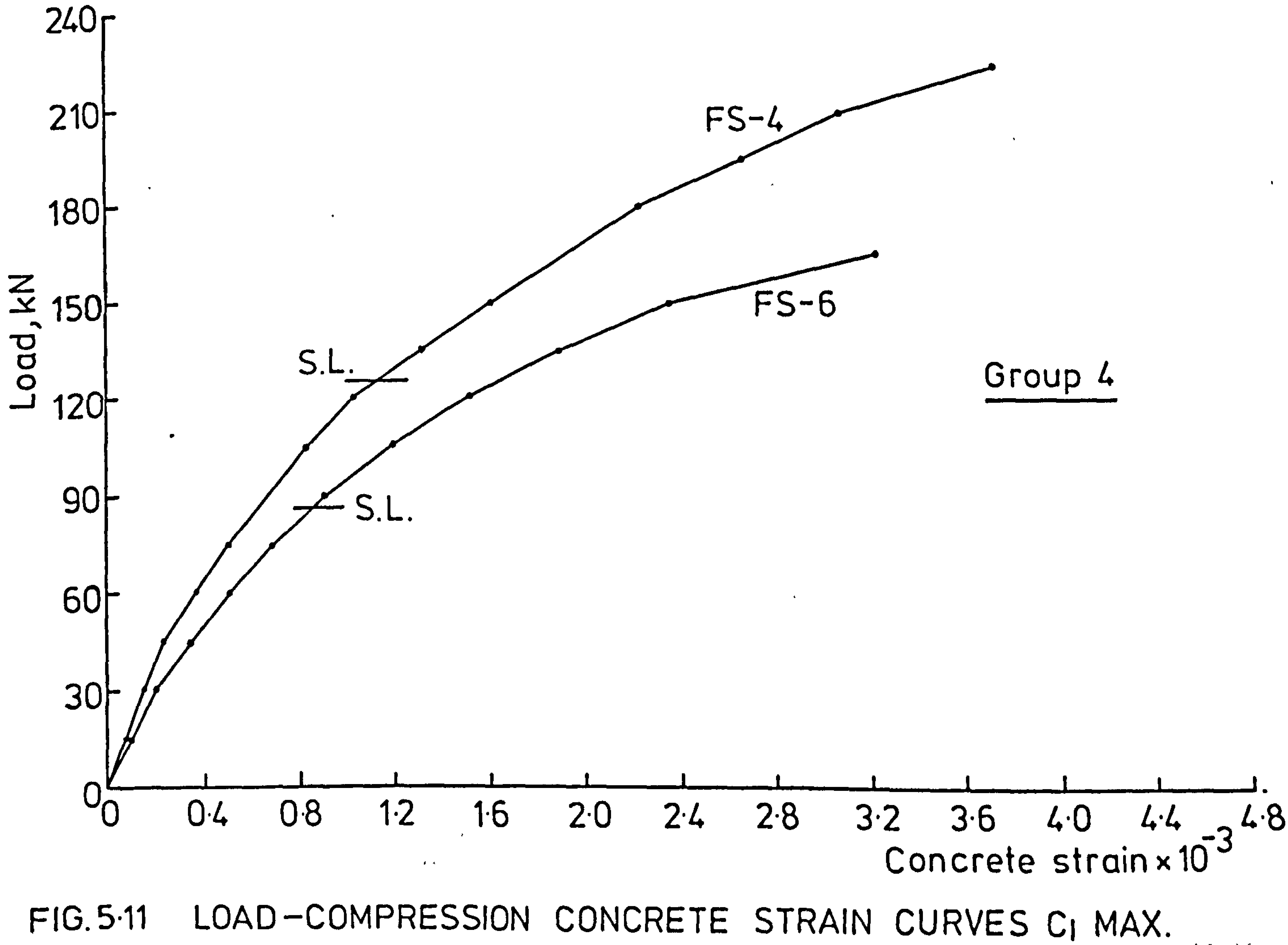

FIG. 5.11 LOAD-COMPRESSION CONCRETE STRAIN CURVES C_1 MAX.

FIG. 5-11 LOAD – COMPRESSION CONCRETE STRAIN CURVES AT C_l MAX.

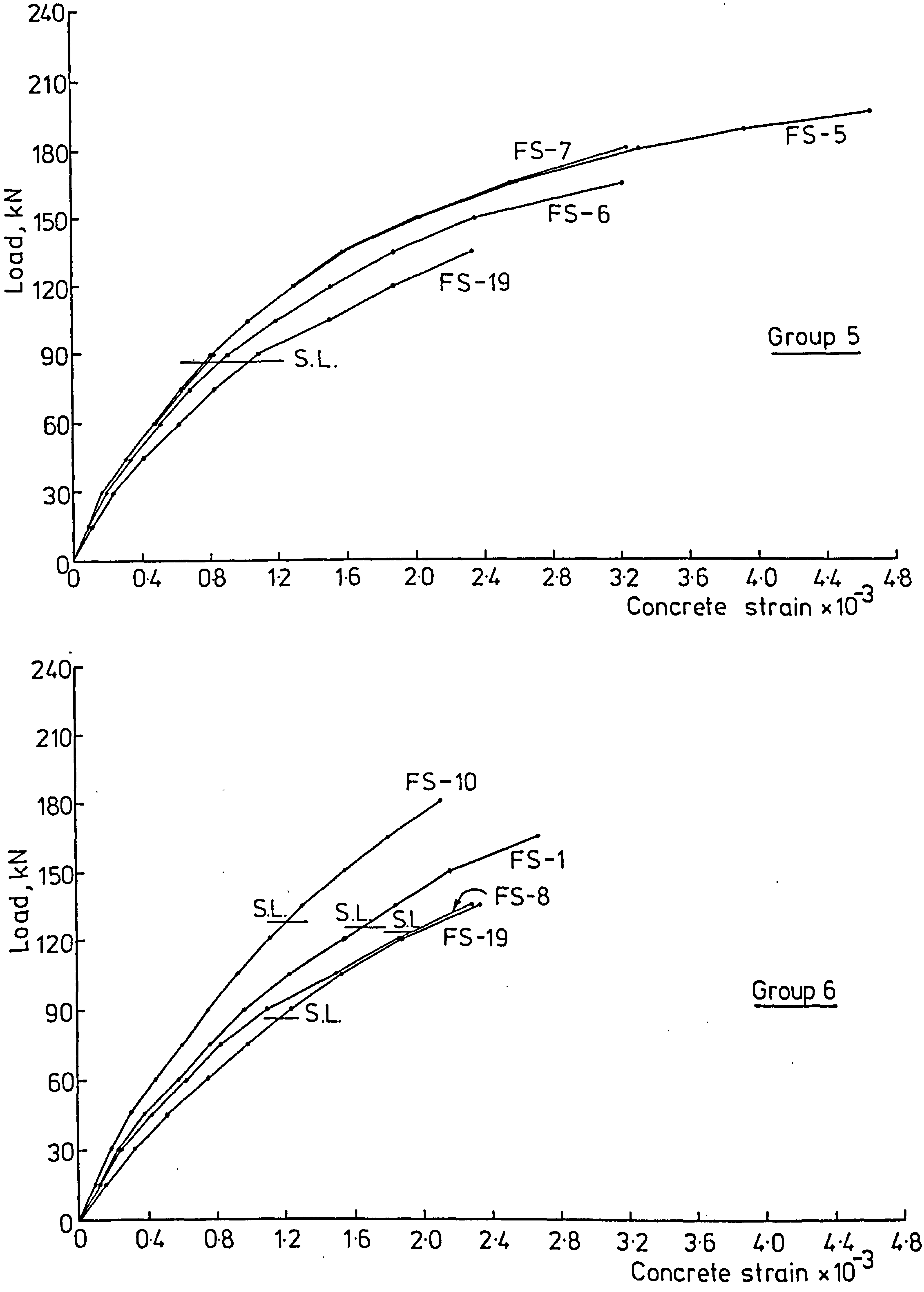

FIG. 5-11 LOAD-COMPRESSION CONCRETE STRAIN CURVES AT C_1 MAX.

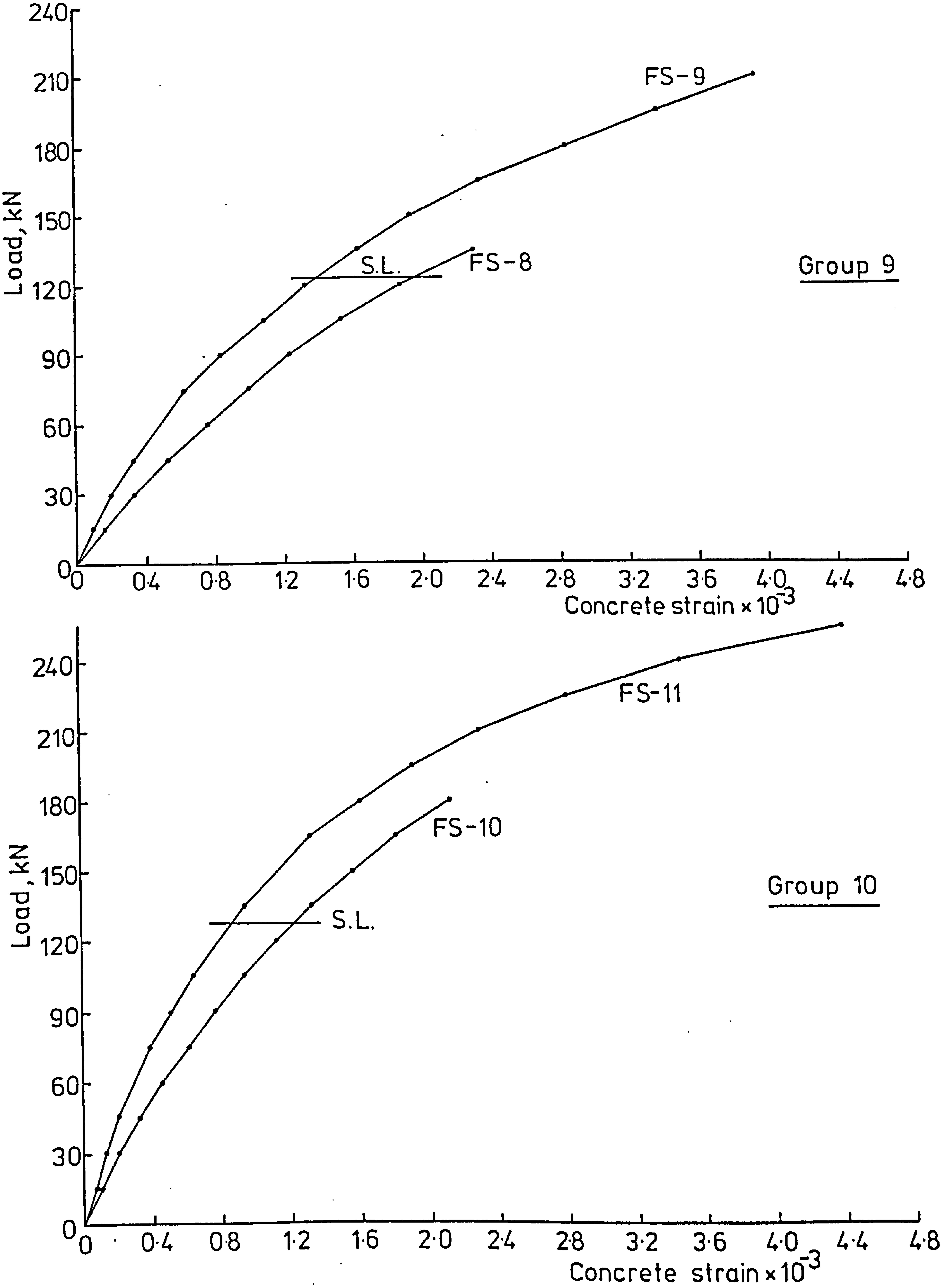

FIG.5-11 LOAD-COMPRESSION CONCRETE STRAIN CURVES AT C_1 MAX

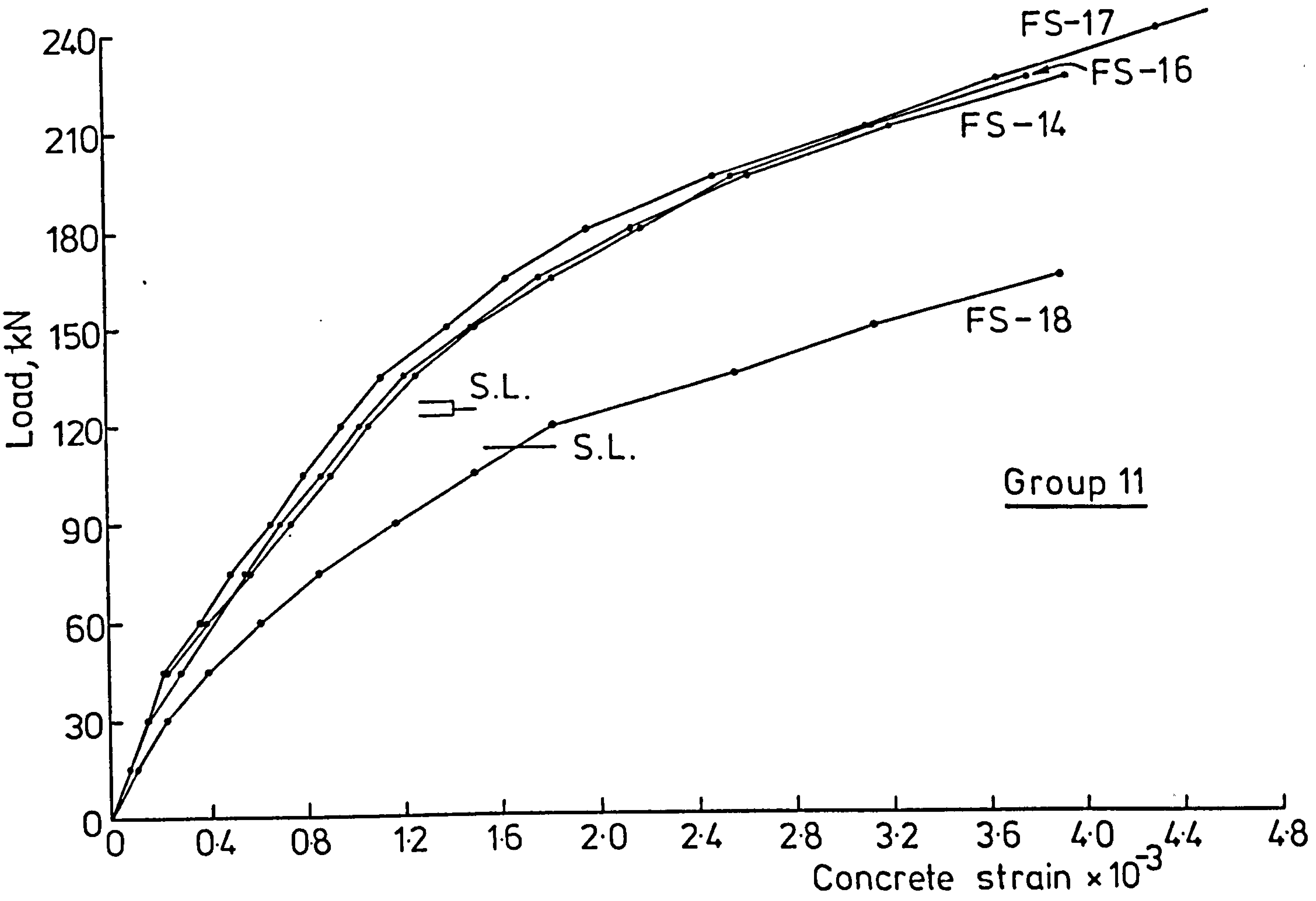

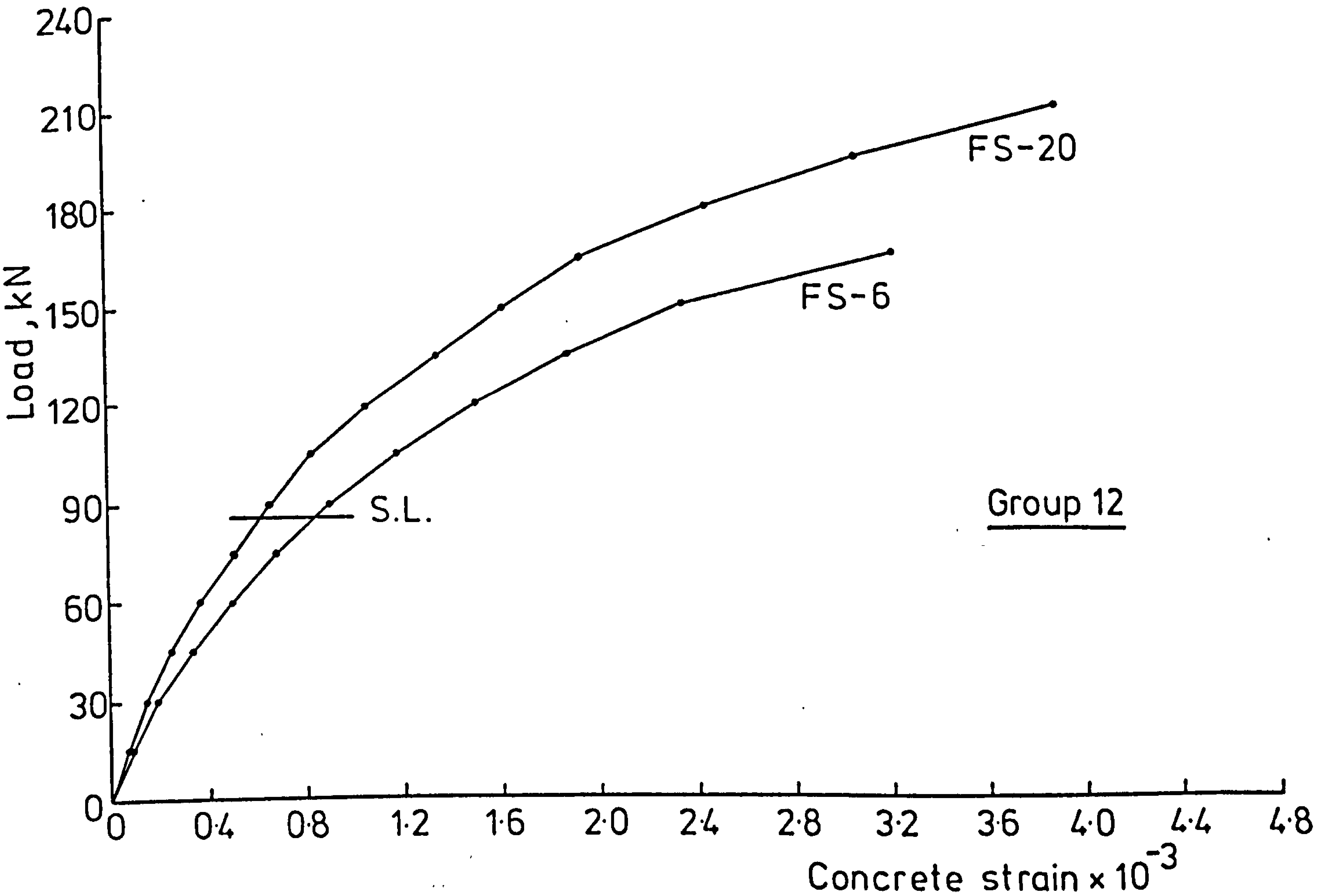

FIG. 5-11 LOAD-COMPRESSION CONCRETE STRAIN CURVES AT C_l MAX.

strains at first crack load, service load and maximum load are listed in Table 5.5.

The compression concrete strains were very small in the elastic stage of loading until the first crack appeared, then they increased steadily as loading continued. From Table 5.5 (column 16) it can be seen that the maximum compression strain in all plain concrete slabs failing in punching shear was lower than the maximum allowable value of 0.0035 given by CP110 (69) at a load varying from 90 to 97% of the maximum load. This concrete strain, however, was generally higher than the limiting value of 0.0035 in the case of fibre concrete slabs. The maximum compression concrete strain was increased by an average about 20% over that limit value when 1.0% by volume reinforcement was used in slab-column connections with ρ value equal to 0.5574%. Ali (78) reported similar increases in concrete compression strain when steel fibres were used in normal weight concrete slab connections.

The tension concrete strains in both lateral and diagonal direction were very small until the first crack appeared. The maximum value of tension concrete strain at first crack was about 0.0003.

It can be concluded that the presence of fibres in the compression zone enabled the concrete to reach higher strains than those in the corresponding plain concrete slabs.

5.7.1 Compression Concrete strain at and Above Service Load.

Table 5.3 shows the ratio between compression concrete strain of the fibre concrete slabs and rotation of the corresponding plain concrete slabs both at service load (column 7) and at a load near the ultimate load of plain concrete slabs (column 11). From this Table it can be seen that the compression concrete strain in slab FS-3 was reduced by 25.9 and 21.5%

at service load and near the ultimate load respectively when fibre content increased to 1.0% by volume. Ali (78) reported that the reduction in the compression concrete strain in normal weight concrete slabs was about 50% when 0.9% by volume crimped fibres were used around the column stub.

The use of different fibre type in slabs FS-12, FS-13, FS-14 and FS-15 reduced the concrete strain by about 25-35%. The reduction in concrete strain was about 25-30% at and above service load when 1.0% by volume crimped fibres were used in slabs FS-9 and FS-11 with 100 and 200 mm column size respectively.

The use of fibre reinforcement in slab FS-5 (ρ= 0.3716%) caused almost the same reduction in concrete strain as in the case of fibre concrete slabs with ρ = 0.5574%. The reduction of the compressive reinforcement hardly affects the concrete strain in the more heavily slabs (ρ=0.5574%) but it does in the slabs with ρ = 0.3716% as can be seen from Table 5.3.

The use of 1.0% by volume crimped fibres in the whole slab (Slab FS-20) caused even higher reduction in concrete strain as it compared with slabs FS-5, FS-6 and FS-7 where fibres are located around the column stub.

From Fig.5.11 (group 11) it can be seen that the concrete compression strain was much higher in slab FS-18 with cube compressive strength equal to 18 N/mm^2 than in slabs FS-16, FS-14 and FS-17 with compressive strengths varying from 35 to 58 N/mm^2.

5.7.2 Concrete Strains Comparison.

To obtain a clear picture of the distribution of concrete strains measured at different locations on the compressive side of slabs, the load-concrete strain distributions curves for slabs FS-1 (V_f=0.0%) and FS-3 (V_f=1.0%) were plotted at 30 KN intervals in both lateral and diagonal

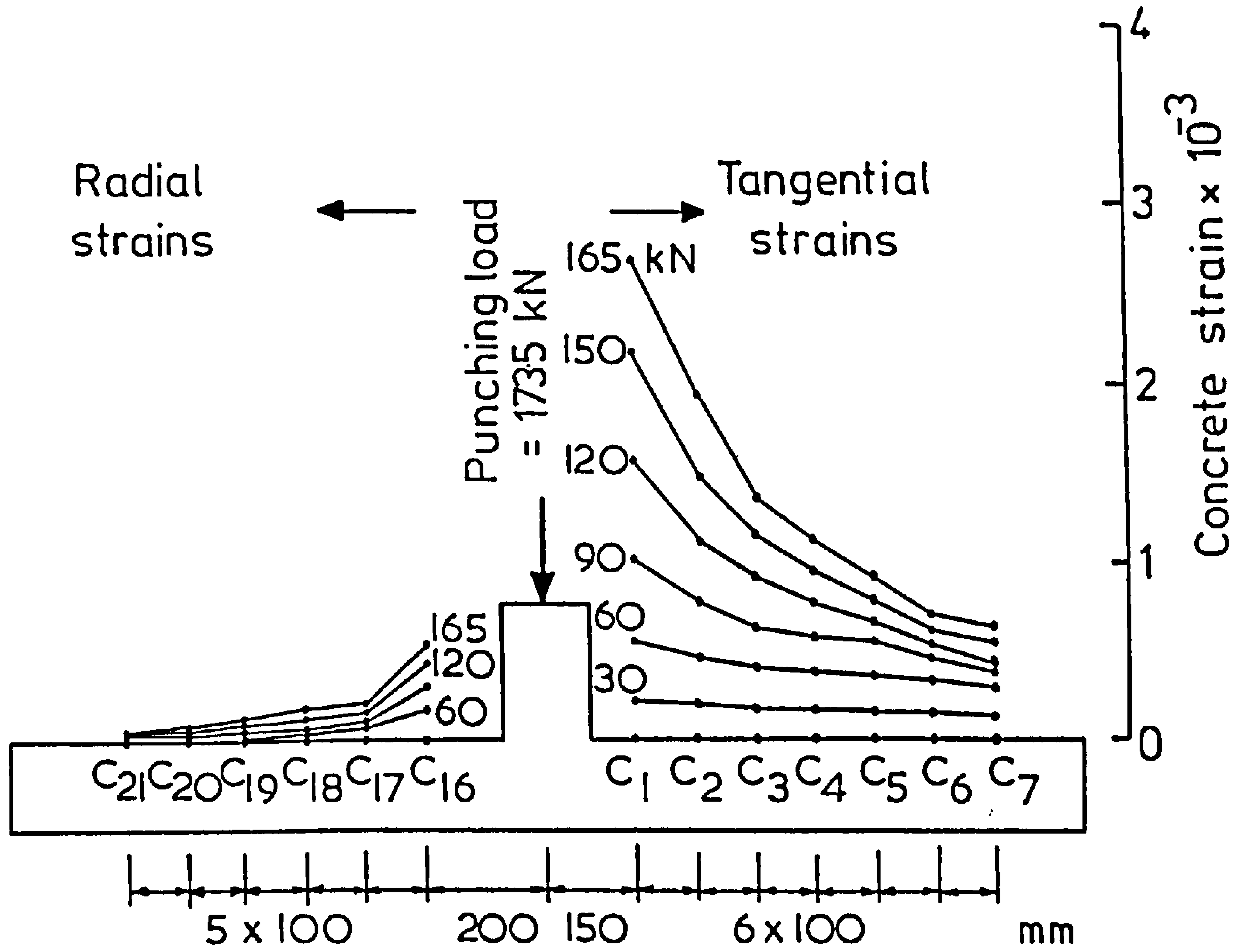

FIG. 5-12 A CONCRETE COMPRESSION STRAINS DISTRIBUTION FOR SLAB FS-1 (V_f = 0%) IN LATERAL DIRECTION

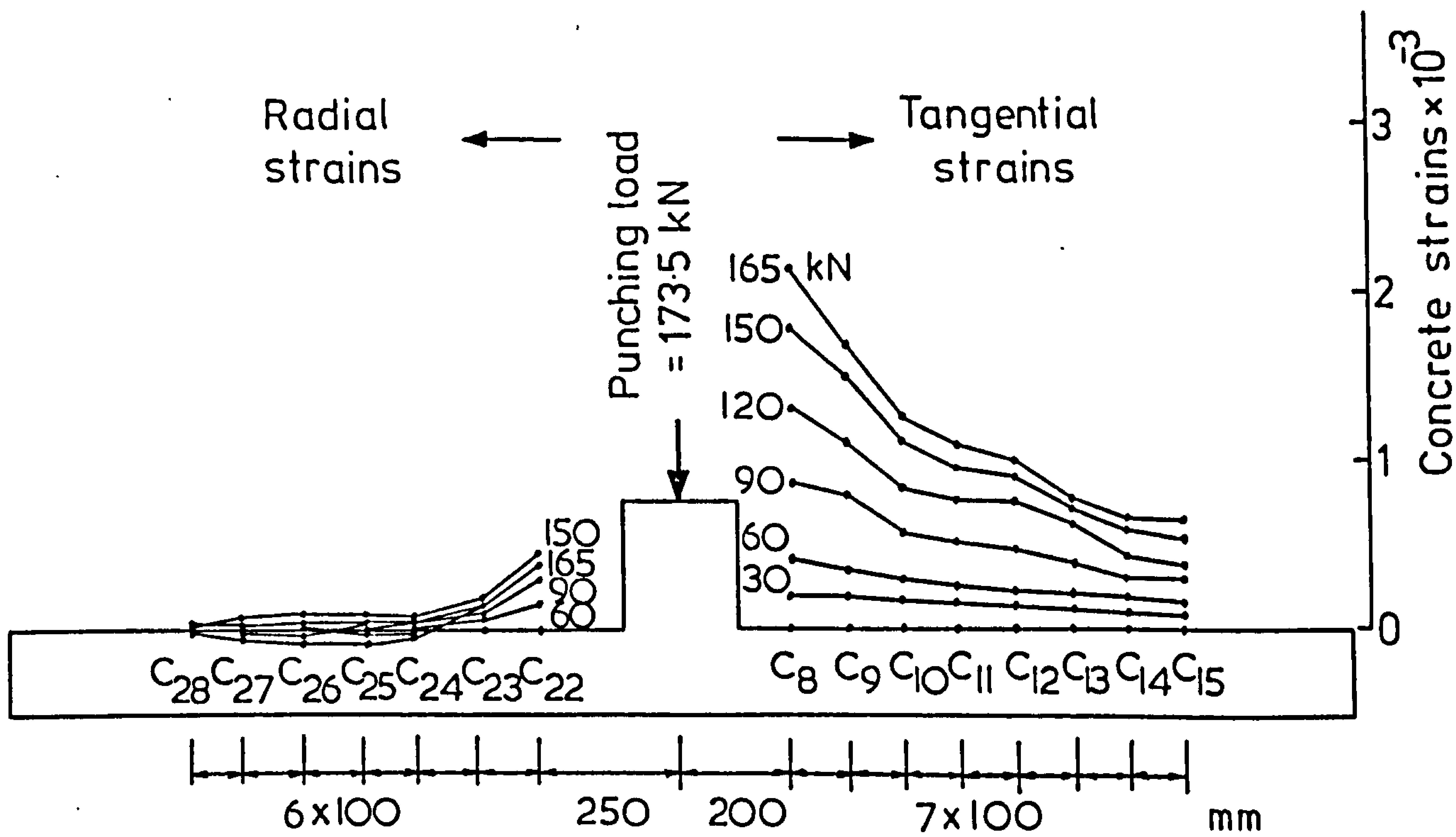

FIG. 5-12 B CONCRETE COMPRESSION STRAINS DISTRIBUTION FOR SLAB FS-1 (V_f = 0%) IN DIAGONAL DIRECTION

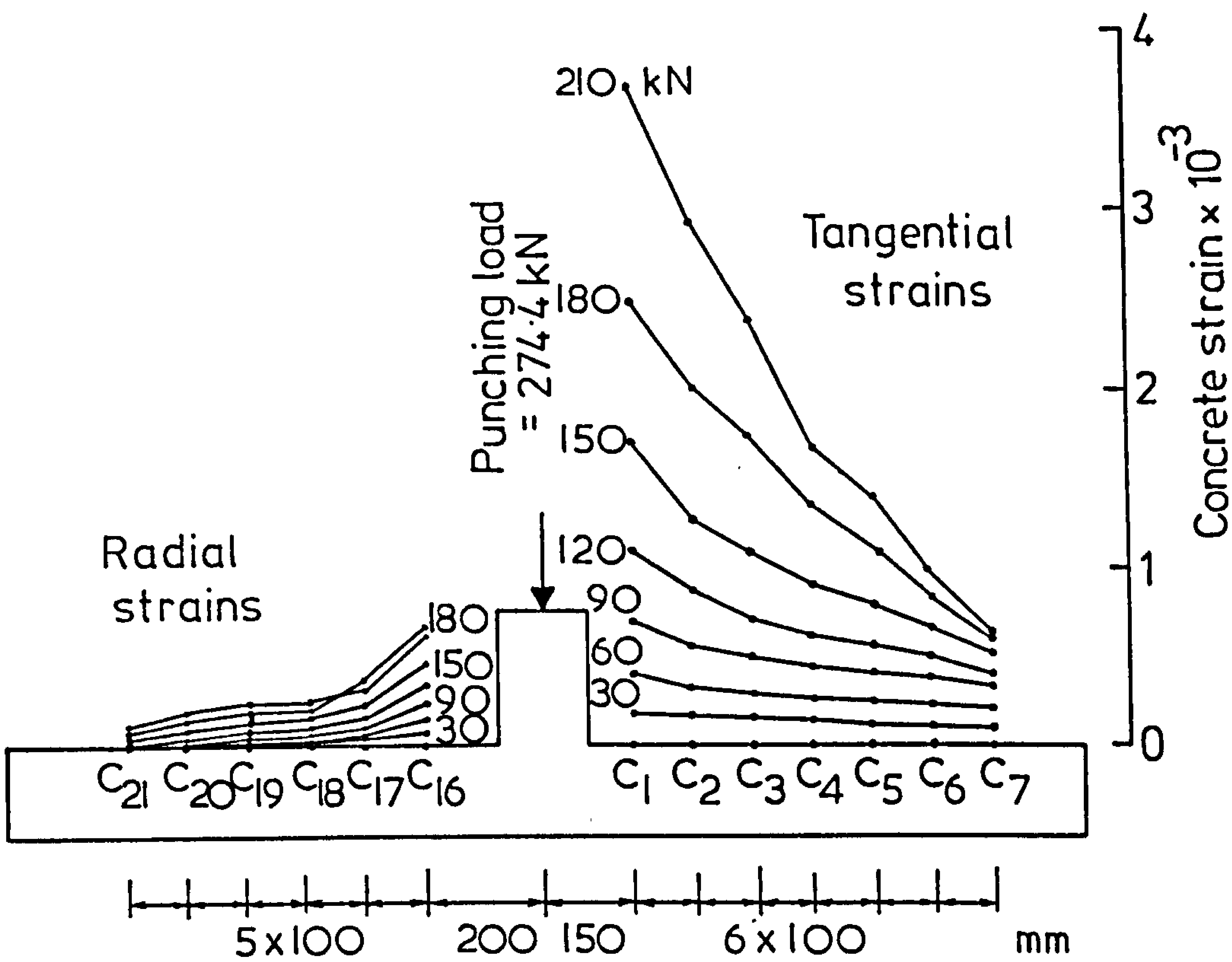

FIG. 5-13A CONCRETE COMPRESSION STRAINS DISTRIBUTION FOR SLAB FS-3 ($V_f = 1\%$) IN LATERAL DIRECTION

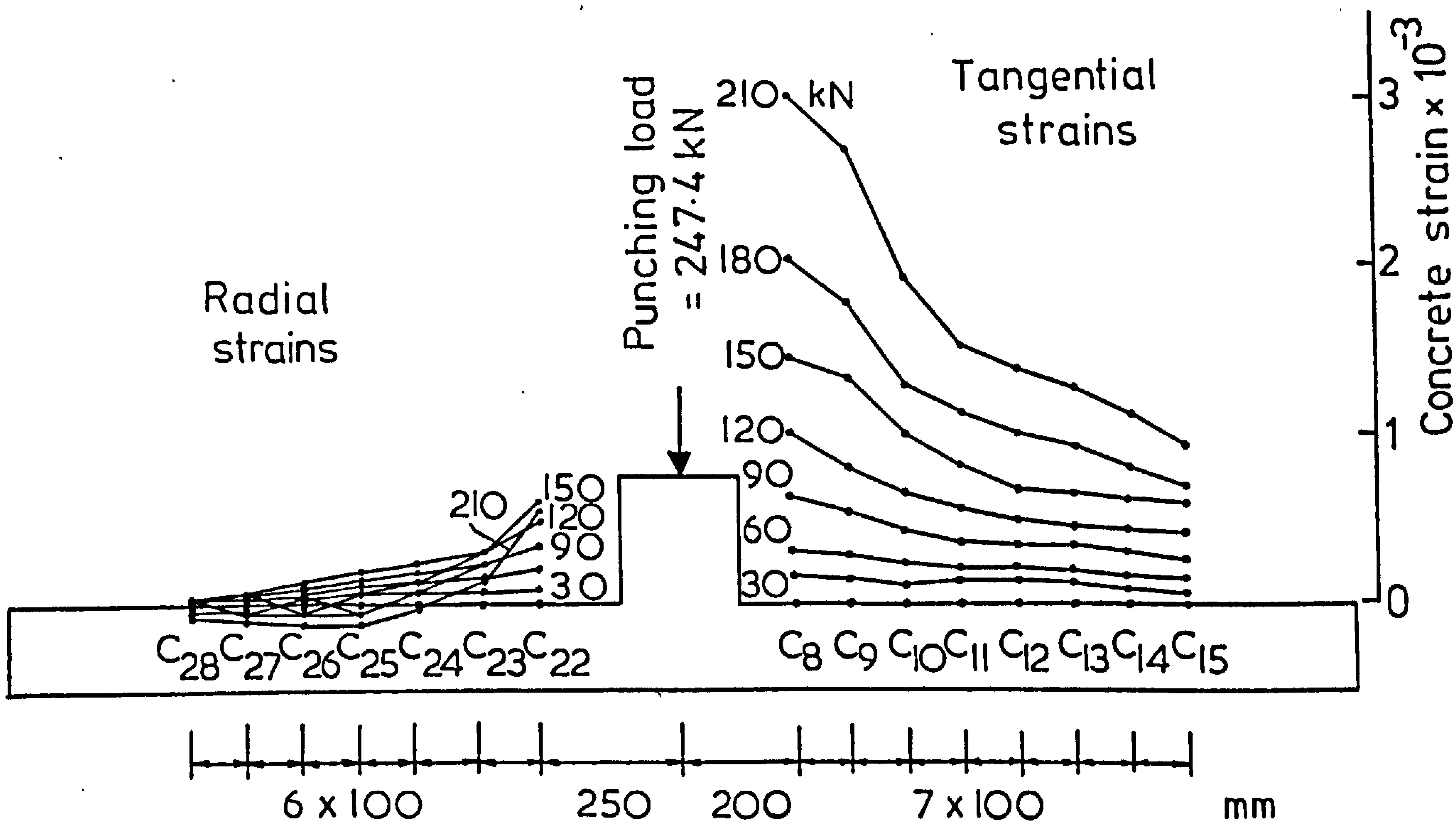

FIG. 5-13 B CONCRETE COMPRESSION STRAINS DISTRIBUTION FOR SLAB FS-3 ($V_f = 1\%$) IN DIAGONAL DIRECTION

directions in Figs. 5.12A to 5.13B. From these figures it can be seen that the addition of fibres in slab-column connections reduced the compression concrete strains at any location in both lateral and diagonal directions. It can also be seen that the ratio between the maximum tangential compression strain (C_1) and radial compression strain (C_{16}) of the lateral direction varied from 5 in slab FS-1 to 6 in slab FS-3. These ratios were about the same in the diagonal direction as can be seen from Figs. 5.12B and 5.13B.

The load-concrete strains curves measured at any location on the compressive side of the slab FS-9 are shown in Figs. 5.14 and 5.15. From Fig.5.14 it can be seen that the tangential (transverse) concrete strain in both lateral and diagonal directions decreased with increasing distance from the slab centre; however, the rate of decrease in strain with increasing distance from the slab centre was higher in the lateral direction than that in the diagonal direction. It can also be seen that all tangential strains were compressive and continuously increased with increasing load.

The distribution of radial strains in both lateral and diagonal directions was different from that of tangential strains as can be seen from Fig.5.15. Initially, most of them were compressive and increased with increasing load. But after a certain load these radial strains decreased or even changed to tensile strains. It can be seen that the radial compressive strain decreased and converted into tensile one at sections located in the diagonal direction. The load at which the radial compressive strain started to decrease could be related to the inclined diagonal tension cracking developed in the critical section of the slab (see Chapter 6).

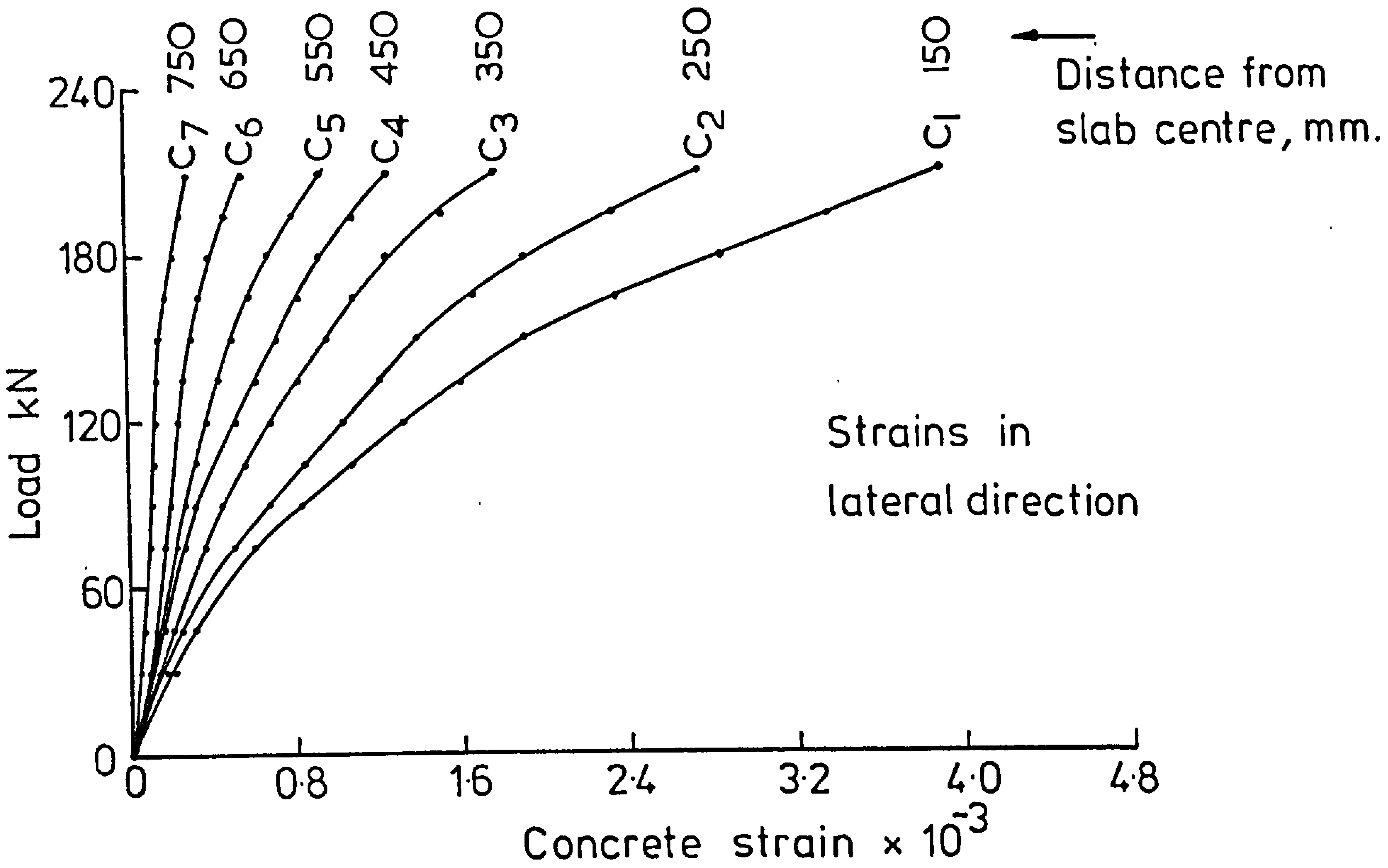

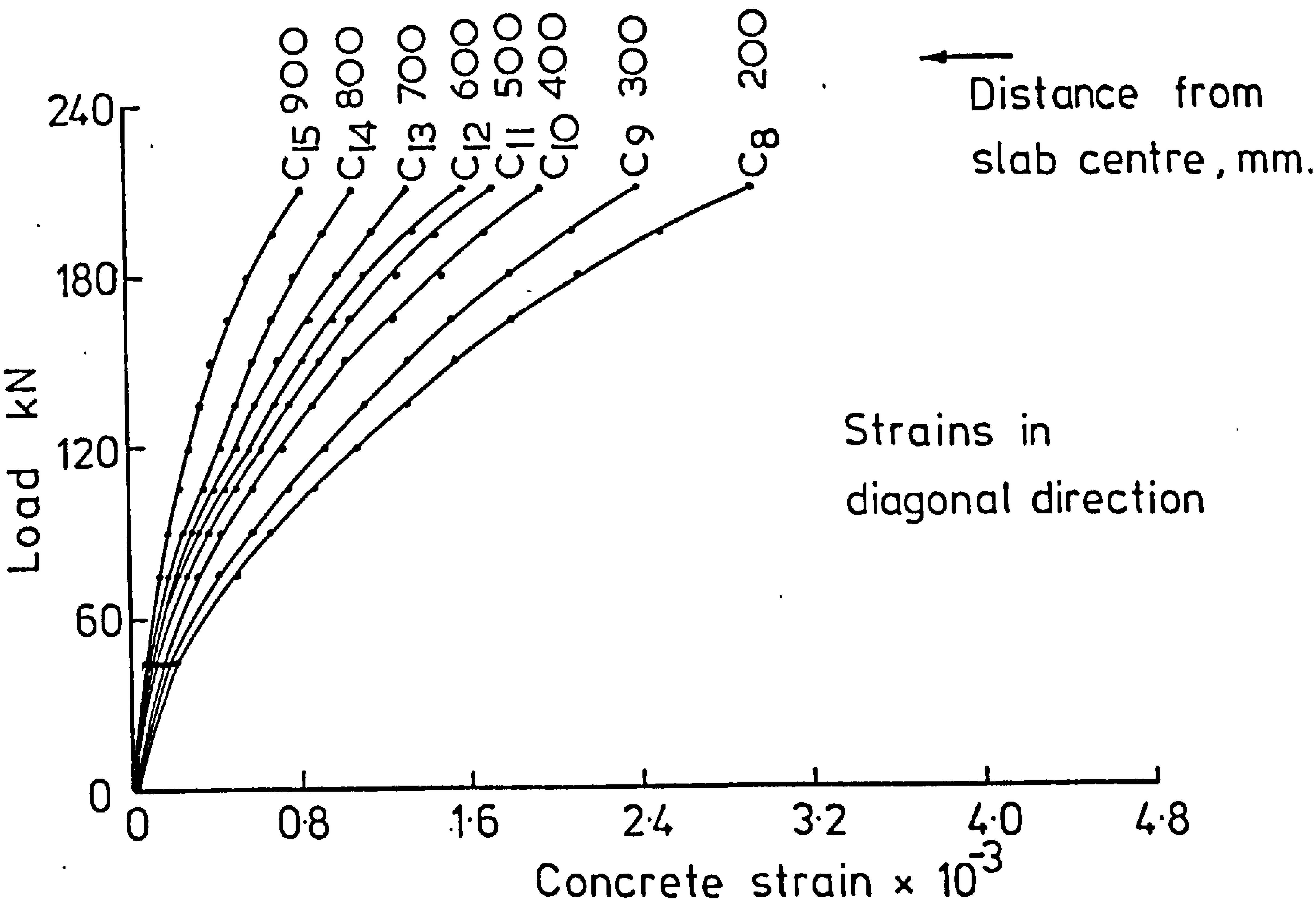

FIG. 5·14 CONCRETE COMPRESSION TANGENTIAL STRAINS FOR SLAB FS-9 ($V_f = 1\%$)

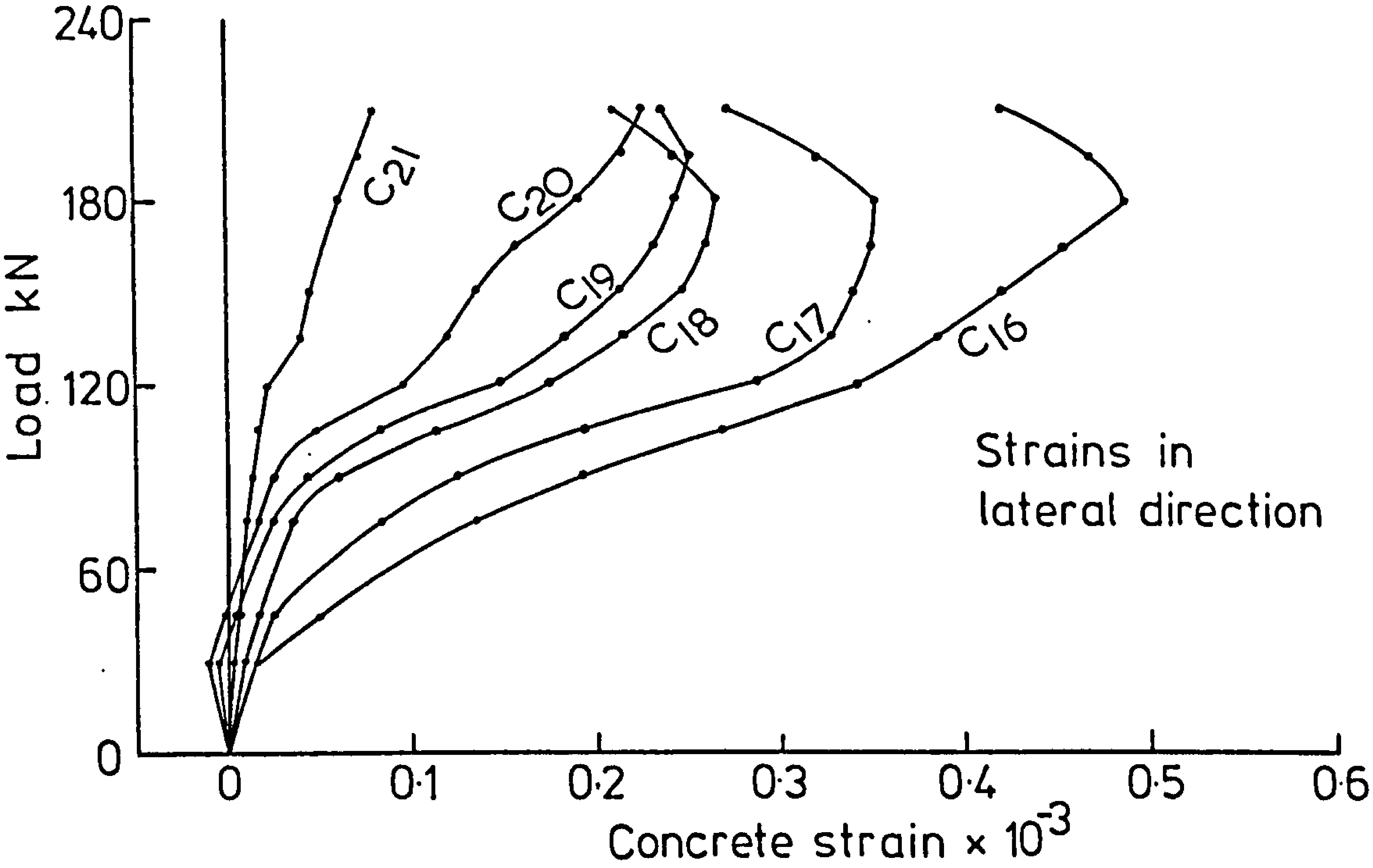

Gauge No's refer to FIG. 4·7

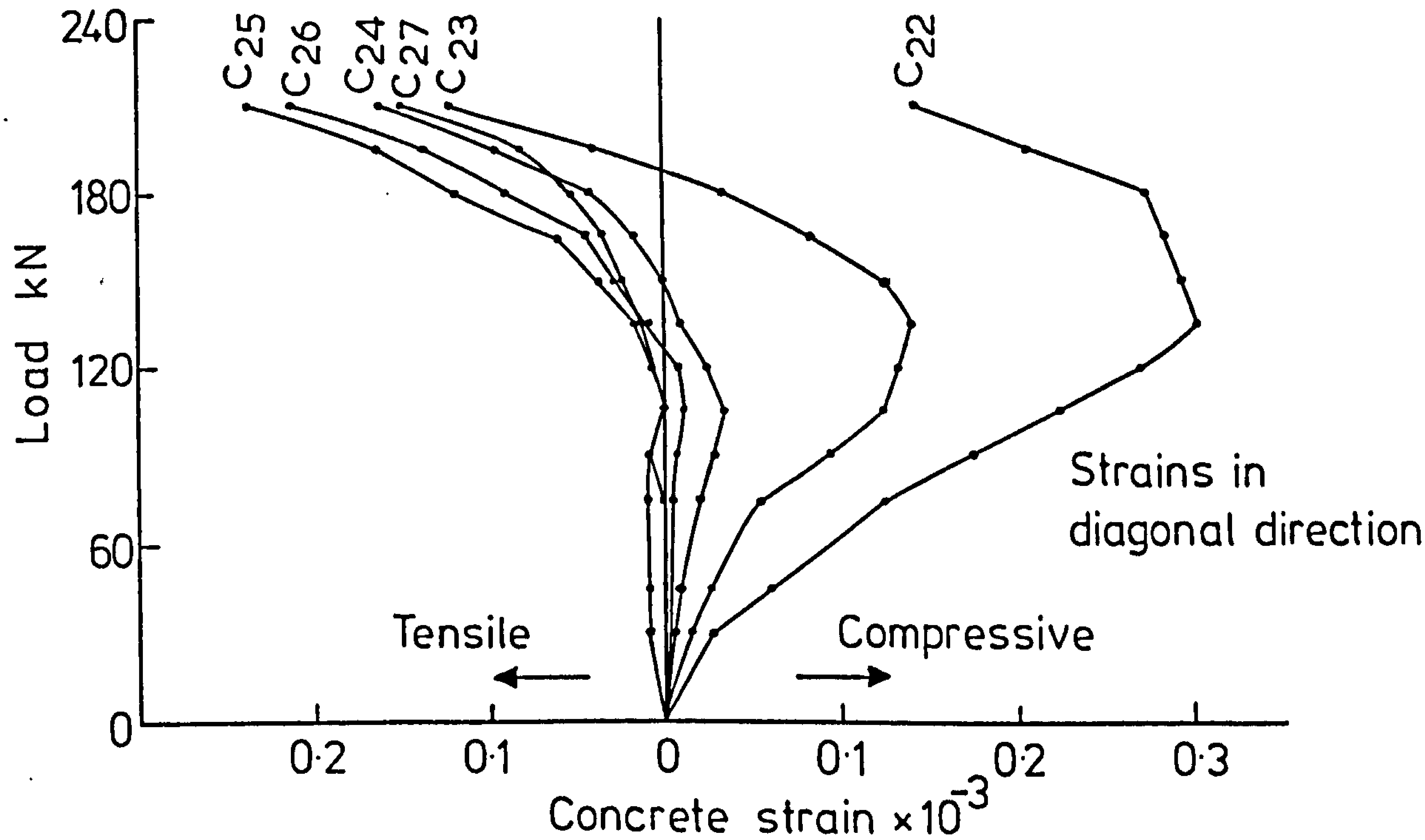

FIG. 5·15 CONCRETE COMPRESSION RADIAL STRAINS FOR SLAB FS-9 ($V_f = 1\%$)

5.7.3 Comparison Concrete Strain Between Lightweight and Normal Weight Concrete Slabs.

The load-maximum compression concrete curves of two normal weight concrete slabs S-1 (V_f=0.0%) and S-5 (V_f=1.0%) from reference 78 are shown in Fig.5.11 (group 1). From this Figure it can be seen that there is no significant difference in concrete strain between plain normal weight and plain lightweight concrete slabs.

5.8 Ductilities and Energy Absorptions.

As it was mentioned previously the addition of fibre reinforcement in slab-column connections increased the deflections at failure, which leads to better ductilities and energy absorption characteristics. Fig.5.16 shows the complete load-centre deflection curves for some of the test slabs.

The ultimate ductility, as determined by the ratio of centre deflection at 30% of the maximum load (after reaching the maximum load) to first crack deflection of a slab is shown in Fig.5.17. The value of 30% of the maximum load was chosen to take into account the tensile membrane action of the flexural reinforcing bars in plain concrete slabs after failure. Ali (78) used such a value equal to 25% of the maximum load which is the residual resistance after failure in his normal weight plain concrete slabs. The ultimate ductilities for some test slabs are listed in Table 5.6. It can be seen that ductility was increased by 125 to 158% when 1.0% by volume steel fibres were used around the column stub in slabs with ρ = 0.5574%. The presence of fibres in the whole slab specimen (slab FS-20) increasedthe ductility over that of the corresponding plain concrete

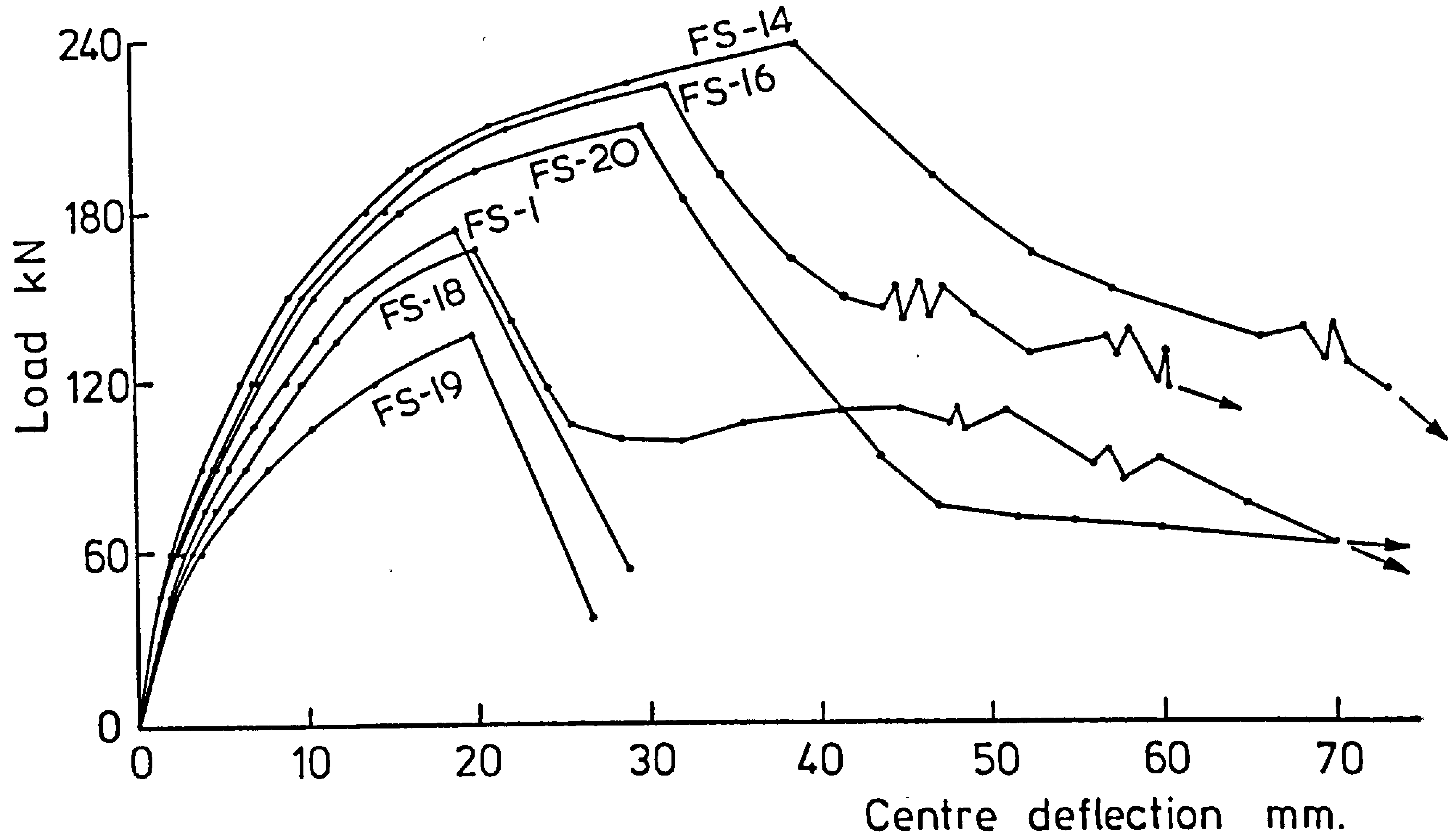

FIG. 5·16 LOAD-DEFLECTION CURVES AT CENTRE OF SPAN

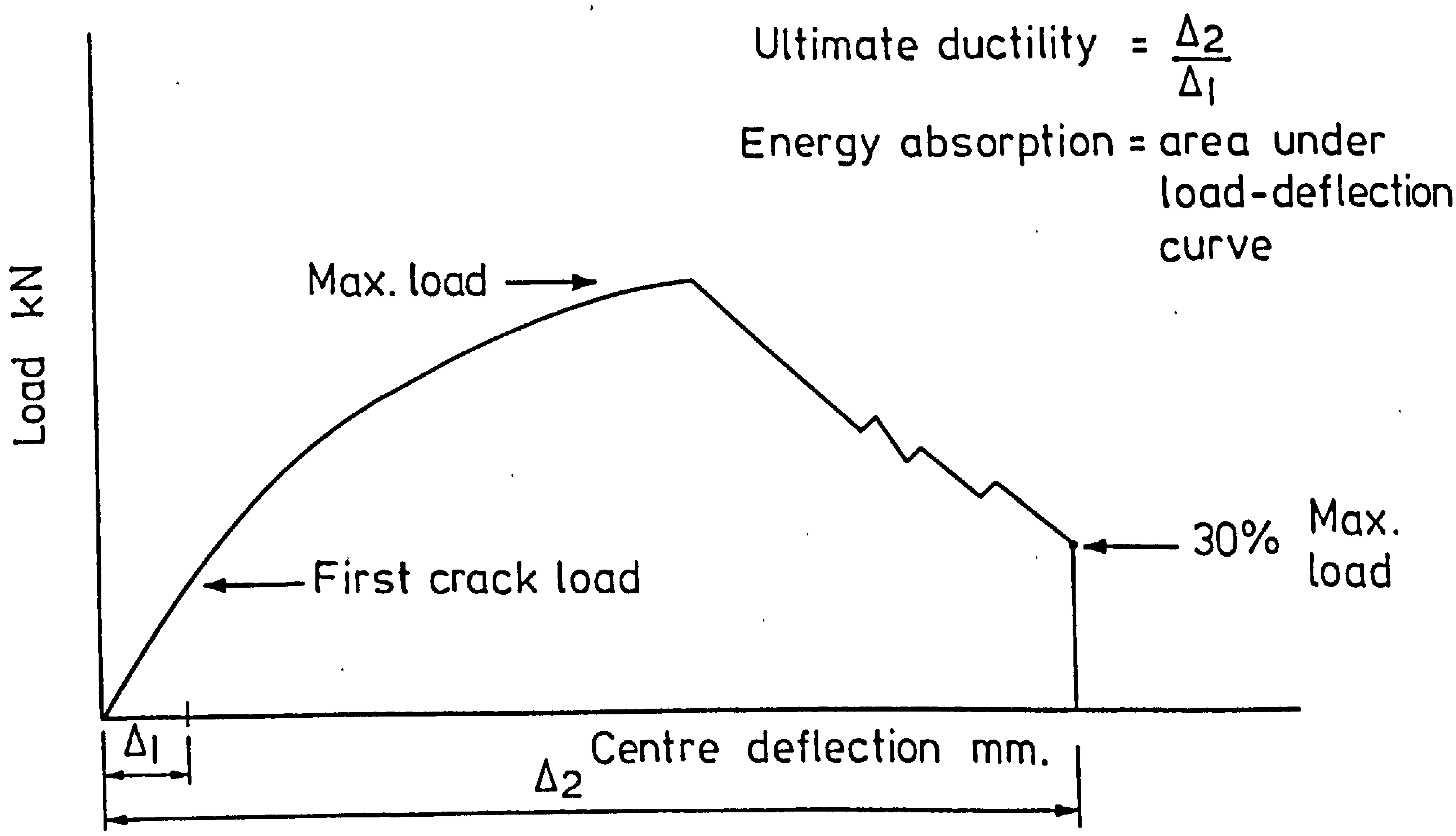

FIG. 5-17 DETERMINING THE ULTIMATE DUCTILITY AND ENERGY ABSORPTION CAPACITY

Table 5.6 Observed Relative Ductility and Energy absorption of Test specimens.

% Tension Reinforcement Ratio	Slab Number	Steel Fibre Type	Fibre Percentage	Cube Compress. Strength in N/mm^2	Ultimate Ductility (Deflection at 30% of Max Load/ First crack deflection)	% Increase in ultimate ductility over that of plain concrete	Energy Absorption in KN. mm	% Increase in energy absorption over that of plain concrete
	1	2	3	4	5	6	7	8
0.5574	FS-1	-	0.0	44.20	23.5	0.0	3300	0.0
	FS-14	Paddle	1.0	43.73	53.0	125.0	11130	237.3
	FS-16	Paddle	1.0	34.9	60.7	158.3	10400	215.5
	FS-18	Paddle	1.0	17.75	53.7	128.5	6550	98.5
0.3716	FS-19	-	0.0	43.10	21.2	0.0	2400	0.0
	FS-20*	Crimped	1.0	46.30	76.7	261.8	8860	269.2

*Fibres for the whole slab specimen.

slab (FS-19) by about 260%. Ali (78) reported increases in ductility by about 90 and 115% in normal weight concrete slabs with 0.9 and 1.2% by volume crimped fibres respectively.

The energy absorption capacity, as determined by the area under load-deflection curve at 30% of the maximum load (after reaching the maximum load) is shown in Fig.5.17. The energy absorption capacities for some test slabs are listed in Table 5.6. From this Table it can be seen that the presence of 1.0% fibre reinforcement increased the energy absorption capacity by about 237% in slab FS-14. Smaller increases were observed in slabs FS-16 and FS-18 when the cube compressive strength reduced to 34.9 and 17.75 N/mm^2 respectively. The presence of fibres in the whole slab specimen (slab FS-20) increased the energy absorption capacity over that of the corresponding plain concrete slab (FS-19) by about 270%. Ali (78) reported that the energy absorption capacity was increased by about 310% when 0.9% by volume crimped fibres were used in normal weight concrete slabs. From Table 5.6 (column 7) it can be seen that the energy absorption capacity in both plain and fibre concrete slabs of comparable cube compressive strength was higher in more heavily reinforced slabs. The ultimate ductility and energy absorption capacity results show the unique advantage of the fibre reinforcement in improving the failure behaviour of slab-column connections.

5.9 Conclusions.

Based on the results presented in this chapter the following conclusions can be drawn:

1. The presence of fibre reinforcement delays the formation of first crack as well as the development of tensile cracking. Cracking in the lateral direction started before that in the diagonal direction while in

normal weight concrete slabs cracking in the diagonal direction occurred before that in the lateral direction (78). The cracks started at about 20% and 30% of the maximum load in the lateral and diagonal direction respectively in both plain and fibre concrete slabs.

2. The radial cracks appeared first in the vertical side of the slab at about 30-40% of the ultimate load; they were initially almost vertical, then inclined at an angle 60-70^{o} to horizontal and, in slabs failing in flexure or in punching but at an ultimate load close to flexural strength, they propagated almost horizontally. The side cracks reached the upper edge of the slab only in slabs failing in flexure or in slabs failing in punching at a load close to flexural strength.

3. The crack patterns were generally observed to be about the same for the fibre concrete slabs which failed in punching as for the plain concrete slabs, except that in the former, the cracks were much finer and more in number than in the corresponding plain concrete slab.

4. All slabs which failed in punching shear had no cracks at all on the compression surface and the punching lines formed immediately in the vicinity of the column faces.

5. The addition of fibre reinforcement in some slab-column connections enabled the slabs to fail first in flexure and then in punching as the loading continued. The crack patterns in these slabs on both compression and tension surfaces were quite different from those failing in punching.

6. The location of yield lines in fibre concrete slabs is very close to the location of yield lines predicted by the yield line theory for plain concrete slabs. The yield lines were more close to slab corners in more slightly reinforced slabs (ρ=0.3716%) than in more heavily reinforced slabs (ρ=0.5574%).

7. The presence of the fibre reinforcement substantially reduced all the deformations of the plain concrete slab connection at all stages of loading. The reduction in deformations was more pronounced at higher stages of loading.

8. The reductions in deflection, rotation, steel strain and compression concrete strain at service load (CP110) were about 25.5, 23.5, 55 and 26% when 1.0% by volume crimped fibres were used in slab column connection with ρ = 0.5574%. The corresponding reductions in the case of normal weight concrete slabs with 0.9% by volume crimped fibres were about 25, 35, 48 and 48% respectively (78).

9. The reduction in deformations when different fibre types were used in slab connections was about the same as for crimped fibres.

10. The effectiveness of 1.0% by volume crimped fibres in reducing the deformations of slab-column connections seems to be independent from the size of the column stub.

11. Higher reductions in deformations due to addition of fibres were observed in the more slightly reinforced concrete slabs (ρ=0.3716%) than those in the more heavily reinforced slabs (ρ=0.5574%).

12. The effectiveness of fibre reinforcement in reducing deformations is more pronounced when they were used in the whole slab specimen instead of using them around the column stub.

13. The effect of compression reinforcement reduction was higher in more slightly reinforced slabs (ρ=0.3716%) than in more heavily reinforced slabs (ρ=0.5574%).

14. The first crack deflection to maximum load deflection ratio was reduced by about 50% due to presence of fibres. The maximum load deflection to span specimen length ratio increased from 1.12 to 2.17% as fibre content increased from 0.0 to 1.0% by volume.

15. The presence of fibres in slab-column connection can confine the compression zone in the slab and enable the concrete to reach higher strains than those in the corresponding plain concrete slab connections.

16. The addition of fibre reinforcement in slab-column connections increased about twice the deflections at failure, which leads to better ductilities and energy absorption characteristics. The ultimate ductility was increased about 125-158% and about 260% when fibre reinforcement was used around the column stub and in the whole slab specimen respectively. The corresponding increases in ultimate energy absorption were about 237 and 270% respectively. Almost similar increases in ductility and energy absorption characteristics were reported by Ali (78) when fibre reinforcement was used in normal weight concrete slabs.

17. The presence of fibre reinforcement in lightweight concrete slab connections can reduce the values of all deformations to similar or less values than those for plain normal weight concrete slabs.

CHAPTER 6.

STRENGTH CHARACTERISTICS OF TESTED SLABS.

6.1 Introduction.

One of the main practical problems for slab-column connections in reinforced flat slabs and flat plates is the avoidance of punching shear failures at over loads. Such failures, which are usually sudden and catastrophic in nature, are undesirable since they do not allow an overall yield line mechanism to develop before punching.

It has been confirmed by previous research on slab-column connections that the punching shear resistance can be increased by thickening the slab, increasing the flexural reinforcement near the column, increasing the size of the column, increasing the concrete strength and by providing suitable shear reinforcement in the form of vertical links, bent-up bars or any other type of reinforcement inside the critical zone around the column.

This chapter deals with the strength characteristics of the specimens tested in this investigation. It will be shown that the punching shear strength of slab-column connections can be improved by the addition of short, discrete steel fibres uniformly dispersed and randomly oriented in the concrete matrix.

6.2 Strength Characteristics.

In this section first crack load, service load, inclined cracking load, yield load, maximum failure load, residual resistances remaining after failure and reinforcement displacement load were recorded in all twenty slabs. The obtained data are presented and discussed here.

6.2.1 Load at First Tensile Crack.

The load at first tensile crack was determined in this investigation visually using a magnifying glass while the applied load was increased gradually. Load at first crack for all slab specimens is shown in Table 6.1 (column 5).

In the plain lightweight concrete slab FS-1, the first crack occurred when the applied load reached 32 kN, while the first crack load for a similar plain normal weight concrete slab was 35 kN (78). The first crack load in slabs FS-2 with 0.5% crimped fibres and FS-3 with 1.0% crimped fibres by volume occurred when the applied loads reached 42.5 and 46.8 kN respectively. These loads represent an increase in first crack load of slabs with fibres of about 32.8 and 46.2% over that of plain lightweight concrete as can be seen in Table 6.2 (column 4). The increases in the first crack load in the case of normal weight concrete were of about 23.1, 62.6, 51.7% when 0.6, 0.9 and 1.2% crimped fibres by volume respectively were used (78). From Table 6.1 (column 11) it can be seen that although the first crack load increased in slabs FS-2 and FS-3 by 32.8 and 46.2% respectively due to the addition of fibres there was only a small increase in the ratio of the first crack load to the maximum load from 18.4% for plain concrete slab FS-1 to 18.9% for fibre concrete slabs FS-2 and FS-3.

From Table 6.2 it can be seen that the increase in the first crack load due to addition of different types of fibres (slabs FS-12, FS-13, FS-14 and FS-15) over that of slab FS-1, varied from 28.2 to 42.2% depending upon the particular type of fibre used, while the ratios of the first crack load to the maximum loads varied from 17.2 to 19.5% (Table 6.1, column 11).

The increase in the first crack load due to addition of 1.0% crimped fibres by volume over that of the corresponding plain concrete slabs was 42.7 and 35.8%when 100 mm and 200 mm square column stubs were used respectively (Table 6.2).

From Table 6.1 it can be seen that the tensile flexural reinforcement reduction does affect the first crack load for both plain (slab FS-19) and

Table 6.1 Strength characteristics of tested slabs.

Series Number	Series Detail	Slab Number	Steel Fibre Type and Percentage by Volume	First Crack Load in KN	Shear Cracking Load in KN	Yield Load in KN	Maximum Load in KN	Residual Resistance in KN	Reinf. Displacement in KN	First Crack Load / Maximum Load %	Shear Crack.Load / Maximum Load %	Yield Load / Maximum Load %	Residual Res. / Maximum Load %	Reinf. Disp.Load / Maximum Load %
1	2	3	4	5	6	7	8	9	10	11	12	13	14	15
1	Steel fibre percentage by Volume	FS-1	- 0.0	32.0	105	129.0	173.5	53.5	53.5	18.4	60.5	74.4	30.8	30.6
		FS-2	Crimped 0.5	42.5	120	162.0	225.0	142.6	92.7	18.9	53.3	72.0	63.4	41.2
		FS-3	Crimped 1.0	46.8	135	144.0	247.4	200.9	122.5	18.9	54.6	58.2	81.2	49.5
2	Reinforcement Reduction	FS-4	Crimped 1.0	40.9	120	177.0	224.4	172.1	120.6	18.2	53.5	78.9	76.7	53.7
		FS-5	Crimped 1.0	30.0	105	136.0	198.1	167	90.5	15.1	53.0	68.9	84.3	45.7
		FS-6	Crimped 1.0	29.0	90	131.0	174.5	169.3	-	16.6	51.6	74.8	97	-
		FS-7	Crimped 1.0	30.0	105	130.0	192.4	183.2	-	15.6	54.6	67.6	95.2	-
		FS-19	- 0.0	22.5	75	104.0	136.5	35.7	35.7	16.5	54.9	75.8	26.2	26.2
		FS-20	Crimped 1.0	31.5	105	162.0	211.0	183.1	94.4	14.9	49.7	76.8	86.8	44.7

Table 6.1 (Continued)

1	2	3	4	5	6	7	8	9	10	11	12	13	14	15
3	Square Column size	FS-8	– 0.0	29.0	75	128.0	150.3	49.2	49.2	19.3	49.9	84.8	32.6	32.6
		FS-9	Crimped 1.0	41.4	105	171.0	216.6	163.1	98.4	19.1	48.5	78.9	75.3	45.4
		FS-10	– 0.0	36.0	120	144.0	191.4	59.5	59.5	18.8	62.3	75.2	31.1	31.1
		FS-11	Crimped 1.0	48.9	135	180.0	259.8	244.0	148.5	18.8	52.2	69.3	93.9	57.2
4	Steel Fibre Type	FS-12	Japanese 1.0	42.5	135	163.0	217.5	155.5	105.6	19.5	62.1	74.7	71.5	48.6
		FS-13	Hooked 1.0	44.0	120	178.0	235.5	173.9	117.2	18.7	50.9	75.7	73.8	49.7
		FS-14	Paddle 1.0	45.5	135	180.5	239.5	193.3	138.4	19.0	56.4	75.4	80.7	57.8
		FS-15*	Crimped** 1.0	41.0	135	172.5	238.0	179.9	110.2	17.2	50.4	72.5	75.6	46.3
5	Cube Comp. Strength	FS-16	Paddle 1.0	42.4	120	175.5	227.8	191.5	145.5	18.6	52.7	77.0	84.0	63.8
		FS-17	Paddle 1.0	47.5	135	184	268.4	257.2	133	17.7	50.3	68.6	95.8	49.6
		FS-18	Paddle 1.0	30.5	75	153	166.0	140.5	101.5	18.4	45.2	92.2	84.6	61.2

*6.0 mm Lytag aggregates ** $\ell_f/d_f = 90$

NOTE:- Fibres were distributed only for 550 mm from slab centre except in slab FS-20, where they were distributed for the whole specimen.

- Slabs FS-6, FS-7, FS-11 and FS-17 failed in flexure.

Table 6.2 Percentage increase of various loads of fibre concrete slabs over corresponding loads of plain concrete slabs.

% Tension Reinf. Ratio, ρ	Column size, r, in mm	Slabs ratios	First Crack Load	Shear Crack. Load	Yield Load	Maximum Load	Resid. Resistance	Reinf. Displacement Load
1	2	3	4	5	6	7	8	9
$\rho = 0.5574$	150	FS-2 / FS-1	32.8	14.3	25.6	29.7	166.5	73.3
		FS-3 / FS-1	46.2	28.6	11.6	42.6	275.5	129.0
		FS-4 / FS-1	27.8	14.3	37.21	29.3	121.7	125.4
		FS-12 / FS-1	32.8	28.6	26.4	25.4	190.6	97.4
		FS-13 / FS-1	37.5	14.3	38.8	35.7	225.0	119.0
		FS-14 / FS-1	42.2	28.6	39.9	38.0	261.3	158.7
		FS-15* / FS-1	28.2	28.6	33.7	37.2	236.3	106.0
	100	FS-9 / FS-8	42.7	40.0	33.6	44.1	231.5	100.0
	200	FS-11 / FS-10	35.8	12.5	25.0	35.5	310.0	149.6
$\rho = 0.3716$	150	FS-5 / FS-19	33.3	40.0	30.8	45.1	367.8	153.5
		FS-6 / FS-19	28.8	20.0	26.0	27.8	374.2	-
		FS-7 / FS-19	33.3	40.0	25.0	41.0	413.2	-
		FS-20 / FS-19	40.0	40.0	55.8	54.6	413.1	164.4

*6 mm Lytag aggregates.

NOTE: Slabs FS-6, FS-7, FS-11 and FS-17 failed in flexure.

fibre concrete slabs (FS-5, FS-6, FS-7 and FS-20). In the case of normal weight concrete Ali (78) found that the reinforcement reduction did not effect the first crack load. The first crack load for slab FS-19 was 22.5 kN and varied from 29 to 31.5 kN for slabs with 1.0% fibre reinforcement; that means an increase in the first crack load due to addition of fibres from 28.8 to 40% as can be seen from Table 6.2. The lower value (28.8%) is for slab FS-6 without any compression reinforcement while the higher value (40%) is for slab FS-20 without compression reinforcement but with the fibres distributed in the whole specimen. From Table 6.1 it can be seen that the ratios of first crack load to the maximum load for slabs with tension reinforcement reduction varied from 14.9 to 16.6%, which are less than the ratios for slabs with tension ρ value equal to 0.5574%.

The use of different compressive strength in slabs with 1.0% by volume paddle fibres gave first crack load over maximum load ratios ranged from 17.7 to 18.6%. The value 17.7% is for slab FS-17 which failed in flexure; this value is almost of the same order as the values for slabs failing in punching and this is because the flexure failure load is believed to be very close to punching shear load.

From what is presented here it can be said that the plain lightweight concrete slabs had their first crack load to maximum load ratios ranged from 16.5 to 19.3% which is in agreement with Ali (78) and Anis (81); this ratio was almost of the same order in the case of fibre lightweight concrete slabs.

The increase in first crack load due to addition of 1.0% fibres ranged from 27.8 to 46.2% and seems to be dependent upon the fibre type, column size and the tension reinforcement ratio, ρ.

6.2.2 Shear Cracking Load.

As a rule it is not possible to determine the shear cracks in a slab and to find a completely unique value of the shear cracking load, i.e. the

FIG. 6-1 CONCRETE RADIAL COMPRESSION STRAINS IN DIAGONAL DIRECTION FOR SLABS FS-10 ($V_f = 0\%$) AND FS-11 ($V_f = 1\%$)

load at which the shear cracks begin to open up. Several methods have been used to find a realistic experimental technique in which the shear cracking load could be obtained. Moe (52) tested slabs provided with square holes at some distances from the circumference of column. Kinnunen and Nylander (61) and Anis (81) detected the inclined shear cracks using strain gauges immersed in the concrete during casting around the column faces. In other methods the shear cracking load was estimated on the basis of the crack pattern in the slab and the strain in the ring type flexural reinforcement (61), the strain in the compression steel reinforcement (78) and the concrete compression strain (81). In this section the shear cracking load is obtained by studying the concrete strains measured in the compression face of the slabs.

The use of this method to obtain the shear cracking load instead of using the method based on compression steel strains measurements could be justified by the fact that inclined shear cracking occurs in concrete and therefore its presence affects first the concrete deformations. On the other hand, the compression steel strain methods would require measurements at positions just above the top of shear cracking otherwise the shear cracking load would be overestimated.

The concrete strains in the compression face of slabs were measured tangentially and radially at different distances from the column face in both lateral and diagonal directions (Fig.4.7(b)). As was reported in Chapter 5 the radial strain in both directions increases with the applied load but as the loading continued the strain, in general, started decreasing; the load at which this decrease occurs is lower for strains in sections at some distance from column face (strains C24, C25, C26, Fig.5.15) than that for strains at sections near the column face (strains C22, C23, Fig.5.15).

This was observed in all tested slabs and is shown in Fig.6.1 where the radial concrete strains in diagonal direction for slabs FS-10 (V_f=0.0%) and FS-11 (V_f=1.0%) are plotted. It should be noted that the concrete radial strains, for example for slab FS-11, from C24 to C28 were changed to tensile strain, the maximum tensile strain being at section C26. The load at which the radial strain starts to decrease can be related to the inclined shear cracking developed in the critical section of the slab. As the inclined crack of the slab forms a redistribution of the forces will occur and the compressive force of the concrete will be transmitted towards the tensile reinforcement (Fig.6.1) causing a reduction in the radial strain, first at sections away from column face and then at sections near the column face. Therefore, the load at which the radial strains C24 to C27 in diagonal strains start decreasing can be considered as the shear cracking load. The fact that the reduction of the radial strain occurs first in the diagonal direction and not in the lateral direction is an indication that the shear cracking forms near the corners of the column stub, where a concentration of stresses exists and then propagates laterally in the plane of the slab.

Table 6.1 shows the corresponding shear cracking load (column 6) and the shear cracking load to maximum load ratio (column 12) for all tested slabs. This ratio varied from 49.9 to 62.3%for plain concrete slabs, which is in agreement with the 45 to 75% reported by Kinnunen and Nylander (61) and with the 48 to 65% reported by Criswell (114). Table 6.2 (column 5) shows the increase in the shear cracking load due to addition of fibre reinforcement over that of plain lightweight concrete slabs. This increase was 28.6% for slabs with 150 mm column stub, 0.5574% reinforcement ratio and 1.0% by volume crimped, Japanese and paddle fibres (slabs FS-3, FS-12, FS-14 and FS-15) and 14.3% for slab FS-13 with 1.0% by volume hooked fibres. The lower value in the increase of the shear cracking load in the slab FS-13 with hooked fibres as compared with those obtained in slabs with other fibre type could be explained in terms of the load increment during the test. The load increment was 15 KN and therefore the shear cracking load obtained in various slabs by studying the concrete strains measured in the compression face of the slabs cannot be considered to be the precise value but a rounded value to the nearest 15 KN.

The increase in the shear cracking load ranged from 12.5 to 40% for slabs with 1.0% by volume crimped fibres but with different column stub, and was 40% for slabs with 1.0% by volume crimped fibres with reduced reinforcement (slabs FS-5, FS-7 and FS-20). The reduction in the compression reinforcement for slabs FS-4 and FS-6 caused a lower increase in the shear cracking slabs than that in slabs FS-3 and FS-5 respectively.

It can be concluded that the presence of steel fibres in a slab-column connection can delay the formation of the inclined shear cracking and this delay appears to be dependent upon the fibre percentage, the column stub and the amount of reduction in both compression and tension reinforcement.

6.2.3 Service Load Based on Deformation Criteria.

It has been shown (Chapter 5) that the presence of fibre reinforcement in slab-column connections reduces the deflections as well as other deformations. In this section the increase in the service load of the fibre concrete slabs is presented if the maximum deflection, rotation, concrete and steel strain at the service load of the corresponding plain concrete slabs are accepted as the criteria of serviceability. Table 6.3 shows this increase in the service load for slabs with 0.5574% tension

Table 6.3 Service loads based on deformation criteria.

% Tens. Reinf. Ratio	Column size, r, in mm	Slab Number	Fibre Type and Percentage by Volume	Deflection in mm	Service Load in kN	% increase in service load	Rotation in degree	Service Load in kN	% increase in service load	Concrete strain x 10^{-5}	Service Load in kN	% increase in service load	Steel Strain x 10^{-5}	Service Load in kN	% increase in service load
1	2	3	4	5	6	7	8	9	10	11	12	13	14	15	16
ρ = 0.5574	150	FS-1	- 0.0	9.15	125.0	0	0.64	125.0	0	162	125.0	0	3950	125.0	0
		FS-2	Crimped 0.5	9.15	147.0	17.6	0.64	147.0	17.6	162	142.5	14	3950	156.0	24.8
		FS-3	Crimped 1.0	9.15	150.0	20.0	0.64	150.0	20.0	162	147.0	17.6	3950	142.0	13.6
		FS-12	Japanese 1.0	9.15	1480	18.4	0.64	144.0	15.2	162	148.5	18.8	3950	157.5	26.0
		FS-13	Hooked 1.0	9.15	151.5	21.2	0.64	145.5	16.4	162	154.5	23.6	3950	174.0	39.2
		FS-14	Paddle 1.0	9.15	150.0	20.0	0.64	147.0	17.6	162	156.0	24.8	3950	177.0	41.6
		FS-15	Crimped 1.0	9.15	146.5	17.2	0.64	138.0	10.4	162	147.0	17.6	3950	169.5	35.6
	100	FS-8	- 0.0	9.85	122.7	0	0.72	122.7	0	194	122.7	0	3850	122.7	0
		FS-9	Crimped 1.0	9.85	147.0	19.8	0.72	147.0	19.8	194	150	22.6	3850	166.5	35.7
	200	FS-10	- 0.0	7.80	127.35	0	0.58	127.35	0	120	127.35	0	3250	127.35	0
		FS-11	Crimped 2.0	7.80	147.0	15.4	0.58	150	17.8	120	155.0	21.7	3250	165.0	29.6
ρ = 0.3716	150	FS-19	- 0.0	7.05	85.97	0	0.54	85.97	0	100	85.97	0	2750	85.97	0
		FS-5	Crimped 1.0	7.05	111.0	29.1	0.54	109.5	27.4	100	103.5	20.4	2750	114	32.6
		FS-6	Crimped 1.0	7.05	99.0	15.2	0.54	99.0	15.2	100	95	10.5	2750	115.5	34.3
		FS-7	Crimped 1.0	7.05	106	23.3	0.54	108	25.6	100	103.5	20.4	2750	112	30.3
		FS-20	Crimped 1.0	7.05	121.5	41.3	0.54	127.5	48.3	100	116	34.9	2750	139.5	62.2

NOTE: Service load for plain concrete slabs according to CP110.

reinforcement ratio and different column stub and for slabs with 0.3716% tension reinforcement ratio.

From Table 6.3 it can be seen that the presence of fibres can, for a given serviceability criterion, increase the service load that a slab-column connection can carry. The service load for fibre concrete slabs with $r = 150$ mm, $\rho = 0.5574\%$, $V_f = 1.0\%$ by volume and different fibre type was increased by 15 to 40% beyond that of a plain concrete slab depending upon the type of serviceability criterion, while for normal weight fibre concrete slabs Ali (78) reported increases varying from 25 to 50% but with the fibres distributed over the whole specimen.

The change in the column size gave no significant differences in the increase of service lond when 1.0% crimped fibres were used. In general, it can be said that the fibre concrete slabs with $\rho = 0.5574\%$ had a 20% increase in service load when deflection, rotation and concrete strain were used as a serviceability criterion and 35% in the case of steel strain as a serviceability criterion.

The reduction in the tension reinforcement ($\rho = 0.3716\%$) caused a greater increase in the service load for slab with 1.0% by volume crimped fibres, (slab FS-5), beyond that of corresponding plain lightweight concrete slab (FS-19) than that of slab FS-3 (ρ=0.5574%). This might be due to the fact that the effect of fibre reinforcement in reducing all the deformations of the plain concrete slab is more pronounced in slabs with low tension reinforcement ratio. The use of fibres over the whole specimen in slab FS-20, although no compression reinforcement was used, caused a considerable increase in the service load varying from 34.9 to 62.2% beyond that of slab FS-19.

6.2.4 Yield Load.

It has been shown in Chapter 5 that the strain gauge placed on the reinforcement near the column face showed little strain until the slab began to crack, then indicated a steady increase until yielding was reached. The load at which yielding of tension reinforcement for all tested slabs was reached was noted and listed in Table 6.1 (column 7).

The yield load for plain concrete slab FS-1 was 129 kN while it varied from 144 to 180.5 kN for slabs with 1.0% fibre reinforcement of different type. These values are lower than the yield load values for normal weight concrete slabs by about 16 and 12% for plain and fibre concrete respectively (78). The reinforcement yielding for all tested specimens occurred between 60% and 90% of the corresponding maximum failure load. From Table 6.2 (column 6) the effect of fibre reinforcement can be seen in delaying the reinforcement yielding. The load at which the reinforcement yielding occurred, increased by 30-45% over that of the corresponding plain concrete slab when 1.0% by volume fibres were used, the higher increase corresponding to slabs with the lower reinforcement ratio ($\rho = 0.3716\%$). The use of fibres over the whole specimen in slab FS-20, although no compression reinforcement was used, gave a 54.6% increase in the yield load over that of slab FS-19, which is twice the increase of slab FS-6 where the fibres were distributed around the column at about 5.5 times the slab effective depth.

6.2.5 Load at Maximum Strength.

All the loads at maximum strength for slabs tested in this investigation are shown in Table 6.1 (column 8). Table 6.2 (column 7) shows the increase in ultimate strength of fibre concrete slabs over that of plain lightweight concrete slabs.

The plain concrete slab FS-1 with $\rho = 0.5574\%$ and $r = 150$ mm failed in punching shear at 173.5 kN. The corresponding slab made with normal weight concrete (78) failed in punching shear as well at 197.7 kN, thus giving a lightweight/normal weight punching shear strength ratio equal to 0.878 (= 173.5/197.7), which is higher than 0.85 and 0.80 ratios suggested by ACI (67) and CP110 (69) Code of practice respectively. The ultimate punching shear strength of slabs FS-2 and FS-3 was increased by 29.7 and 42.6% when 0.5 and 1.0% by volume crimped fibres were used respectively (Table 6.2). In the case of normal weight concrete Criswell (77) reported a 21% increase in ultimate punching shear strength due to addition of 1.0% by volume fibres having an aspect ratio equal to 60, while Ali (78) reported increases of 23.2, 33.0 and 42.1% when 0.6, 0.9, and 1.2% by volume crimped fibres respectively were used. As can be seen the addition of relatively high modulus steel fibres in concrete slabs made with lightweight concrete having a reduced modulus of elasticity and lower splitting tensile strength yields a little higher increase in punching shear strength than that for normal weight concrete slabs.

The steel fibre type affected the maximum strengths in general. The increase in punching shear strength was 25.4% in slab FS-12 with 1.0% by volume Japanese fibres of 25 mm length and varied from 35.7 to 38% with hooked (FS-13) and paddle (FS-14) fibres of 50 mm length. In slab FS-15 with 1.0% crimped fibres of 38 mm length, although 6 mm Lytag aggregates were used as coarse aggregates, the increase in punching shear strength was similar to that obtained by other fibre types (Table 6.2). The higher increase in punching shear strength was obtained when crimped fibres of 50 mm length were used in slab FS-3.

The punching shear strength in slab FS-4 without compression reinforcement increased by 29.3% over that of plain concrete slab FS-1 and decreased by 9% when compared with the ultimate strength of slab FS-3. Ali (78) reported a decrease of about 3% in ultimate strength of fibre concrete slabs when the compression reinforcement reduced from 7 of 8 mm bars to 3 bars placed in the middle half of the slab. Elstner and Hognestand (51) reported that no strength increases resulted from the use of compression reinforcement in plain normal weight concrete slabs. However, it is believed, especially for under-reinforced slabs, that the use of compression reinforcement increases the depth of the concrete compression block and it can also carry shear locally at the top of a shear crack, thus leading to an increased punching shear capacity.

The use of a 100 mm square column stub in slabs FS-8 and FS-9 resulted in an increase in ultimate punching shear strength due to addition of 1.0% crimped fibres of about 44%, which is a little higher than that found for slabs with a 150 mm square column stub. When 1.0% by volume crimped fibres were used in the slab FS-11 having a 200 mm square column stub, the mode of failure was changed from punching shear of the corresponding plain concrete slab, FS-10, to flexure, the increase in the ultimate strength due to addition of fibres being 35.5% (Table 6.2).

In the case of a 33% reduced tension reinforcement ($\rho = 0.3716\%$) the addition of 1.0% by volume crimped fibres in slab FS-5 gave a 45.1% increase in punching shear strength over that of the corresponding plain lightweight concrete slab FS-19. The reduction of the compression reinforcement in slabs FS-6 and FS-7 allowed the slabs to fail in flexure instead of punching shear and gave 27.8 and 41% increase in the maximum strength respectively when compared with slab FS-19, due to addition of 1.0% fibre reinforcement. The use of fibre reinforcement over the whole specimen in slab FS-20 as compared to slab FS-6, both without compression

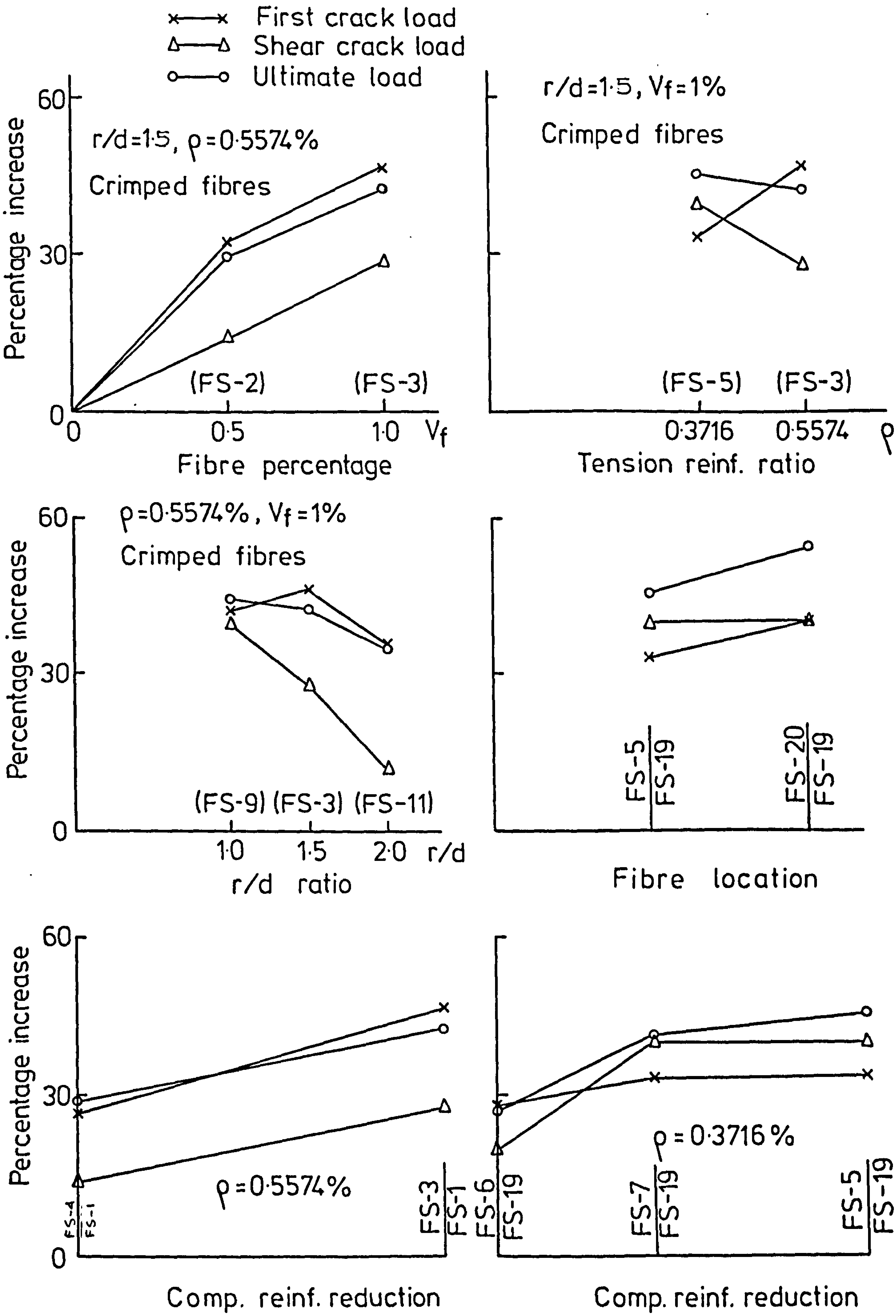

FIG. 6-2 PERCENTAGE INCREASE OF VARIOUS LOADS OF FIBRE CONCRETE SLABS OVER CORRESPONDING LOADS OF PLAIN CONCRETE SLABS

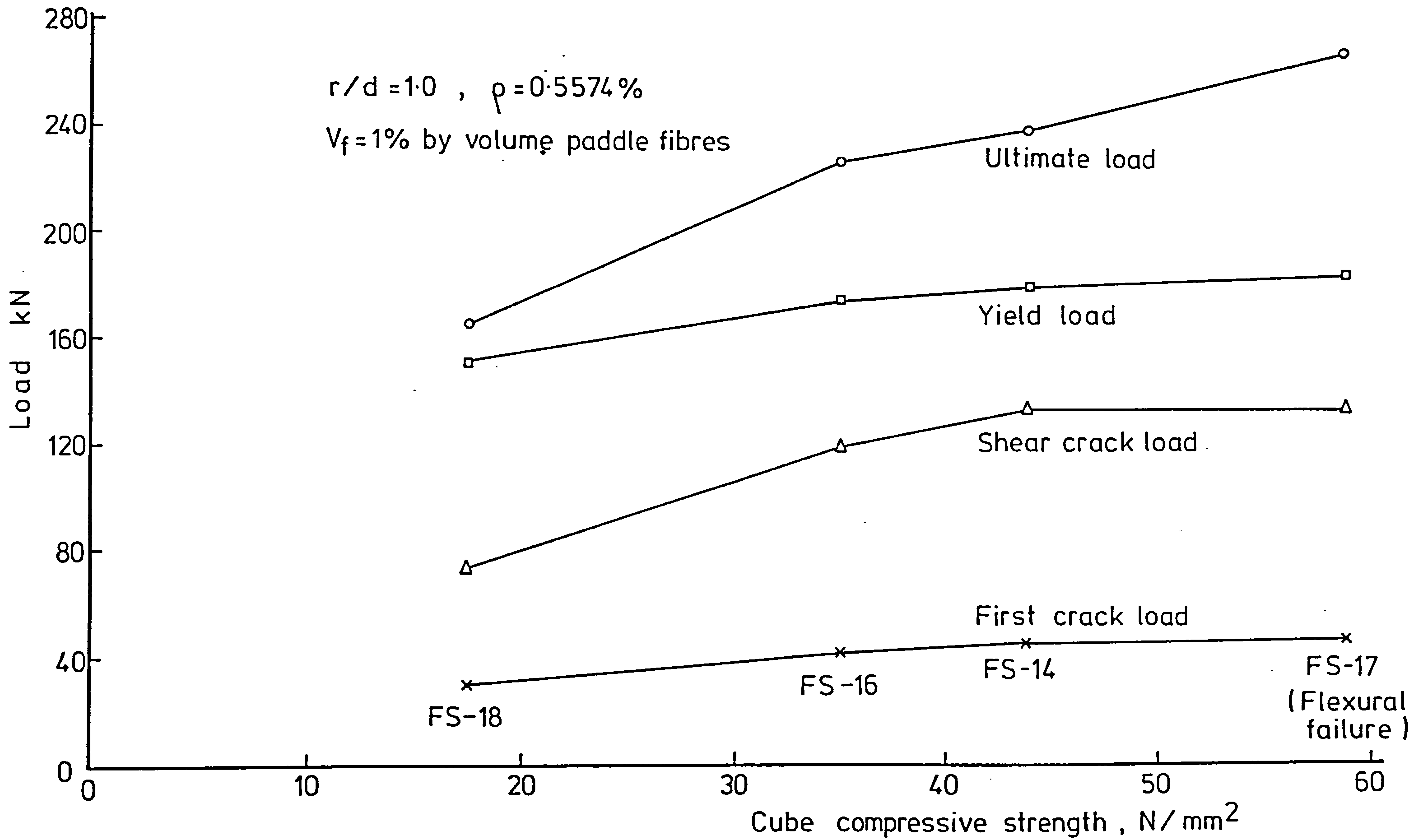

FIG. 6-3 STRENGTH CHARACTERISTICS OF FIBRE CONCRETE SLABS WITH DIFFERENT COMPRESSIVE STRENGTH

reinforcement, allowed the slab to increase its flexural capacity and eventually to fail in punching shear at a load 54.6% higher than that of slab FS-19. Ali (78) reported that for slabs with $\rho = 0.5574\%$ there was no considerable difference in the ultimate punching shear strength when the fibres were used either over the whole specimen or only around the column stub. The increase in ultimate strength obtained in slab FS-20 as compared to that of slab FS-6 might probably be due to the fact that the distribution of fibres over the whole specimen is more severe for slabs with a lower tension reinforcement ratio ($\rho = 0.3716\%$).

From the ultimate strengths obtained for slabs FS-14, FS-16, FS-17 and FS-18 with 1.0% by volume paddle fibres and different compressive strengths (Table 6.1, column 8) it can be said that the ultimate strength of fibre concrete slabs depends on the concrete compressive strength as in the plain concrete slabs. The use of 1.0% paddle fibres in slab FS-18 with compressive strength equal to 17.75 N/mm^2 allowed the slab to fail in punching shear at 166.0 kN, which is close to 173.5 kN punching shear load of plain concrete slab FS-1 with compressive strength equal to 44.2 N/mm^2. The slab FS-17 with a compressive strength equal to 58.56 N/mm^2 failed in flexure. Fig.6.2 shows the percentage increase of various loads of fibre concrete slabs over the corresponding loads of plain concrete slabs. Fig.6.3 shows the strength characteristics of fibre concrete slabs with different compressive strength.

From what is discussed here it can be said that the presence of fibres increases the ultimate strength of slabs and can change the mode of failure from punching shear to flexure.

6.2.6 Residual Resistance and Reinforcement Displacement Load

The sudden drop in resistance and the loss of continuity associated with punching shear failure permitted the slabs to rebound almost towards their original position. Some slab resistance survived after punching failure, which was supported by the tensile membrane action (dowel forces) of the flexural reinforcing bars in the case of plain concrete and by the combined action of dowel forces and of the fibres bridging the inclined cracks in the case of fibre concrete. The residual resistance for all tested slabs as well as its ratio to the maximum load is shown in Table 6.1 (columns 9 and 14 respectively). It was observed that the residual resistance in plain concrete slabs (FS-1, FS-8, FS-10 and FS-19) varied from 26.2 to 32.6% of their maximum load, which is in agreement with Criswell's 25% (114), Ali's 24.8% (78) and Long's 30% (64) for normal weight concrete slabs. Slabs FS-2 (V_f = 0.5%) and FS-3 (V_f = 1.0%) had their residual resistance at 63.4 and 81.4% of their corresponding maximum loads, against 75.2% for normal weight fibre concrete slab with 0.9% by volume crimped fibres reported by Ali (78). In general, it can be said that fibre concrete slabs failing in punching shear had their residual resistance at 71.5-86.8% of their maximum loads (Table 6.1 column 14). The fibre concrete slabs which failed in flexure (FS-6, FS-7, FS-11 and FS-17) had their residual resistance at 93.9-97% of their maximum load, which is in agreement with Ali's 97% (78) for normal weight concrete slabs.

Table 6.2 (column 8) shows the increase in the residual resistance of fibre concrete slabs over that of plain lightweight concrete slabs; it can be seen that this increase varied from 121.7 to 275.5% for slabs with V_f = 1.0% and ρ = 0.5574% and from 367.8 to 413.1% for slabs with V_f = 1.0% and ρ = 0.3716%. This rather high increase in the residual resistance of fibre concrete slabs can be attributed, as mentioned before, not only to the increased tensile membrane action of the flexural reinforcement due to addition of fibres but also to the fact that at the moment of failure the ability of fibres to bridge the inclined cracking has not been fully utilized because of the premature failure in the compression zone of the slab.

In the plain concrete slabs immediately after punching shear failure occurred and as loading continued, the reinforcement started to be displaced and moved from its original embedded position; then load decreased by steps when fracture of reinforcing bars occurred and the slab collapsed completely. In the fibre concrete slabs immediately after punching shear failure and as loading continued the columns were pushed down, with the fibres becoming more and more debonded while the load decreased gradually until a value, where the fibres were completely debonded and the reinforcement started to be displaced. In the fibre concrete slabs, which failed in flexure and as the loading continued, the columns were punched through the slab and then the load decreased as in the case of slabs which failed in punching shear. The load at which the reinforcement displacement started for all tested slabs as well as its ratio to the maximum load is shown in Table 6.1 (columns 10 and 15 respectively). The reinforcement displacement load to maximum load ratio for fibre concrete slabs with 1.0% fibre reinforcement varied from 44.7 to 61.2% while this ratio varied from 43.1 to 69.5% for normal weight fibre concrete slabs with 0.9% fibre reinforcement (78).

Table 6.2 (column 9) shows the increase in the reinforcement displacement load of fibre concrete slabs over that of plain lightweight concrete slabs. It can be seen that this increase was 73.3% and 129% for slabs FS-2 and FS-3 with 0.5 and 1.0% by volume of crimped fibres respectively. With 1.0% fibre reinforcement the increase in the reinforcement displacement

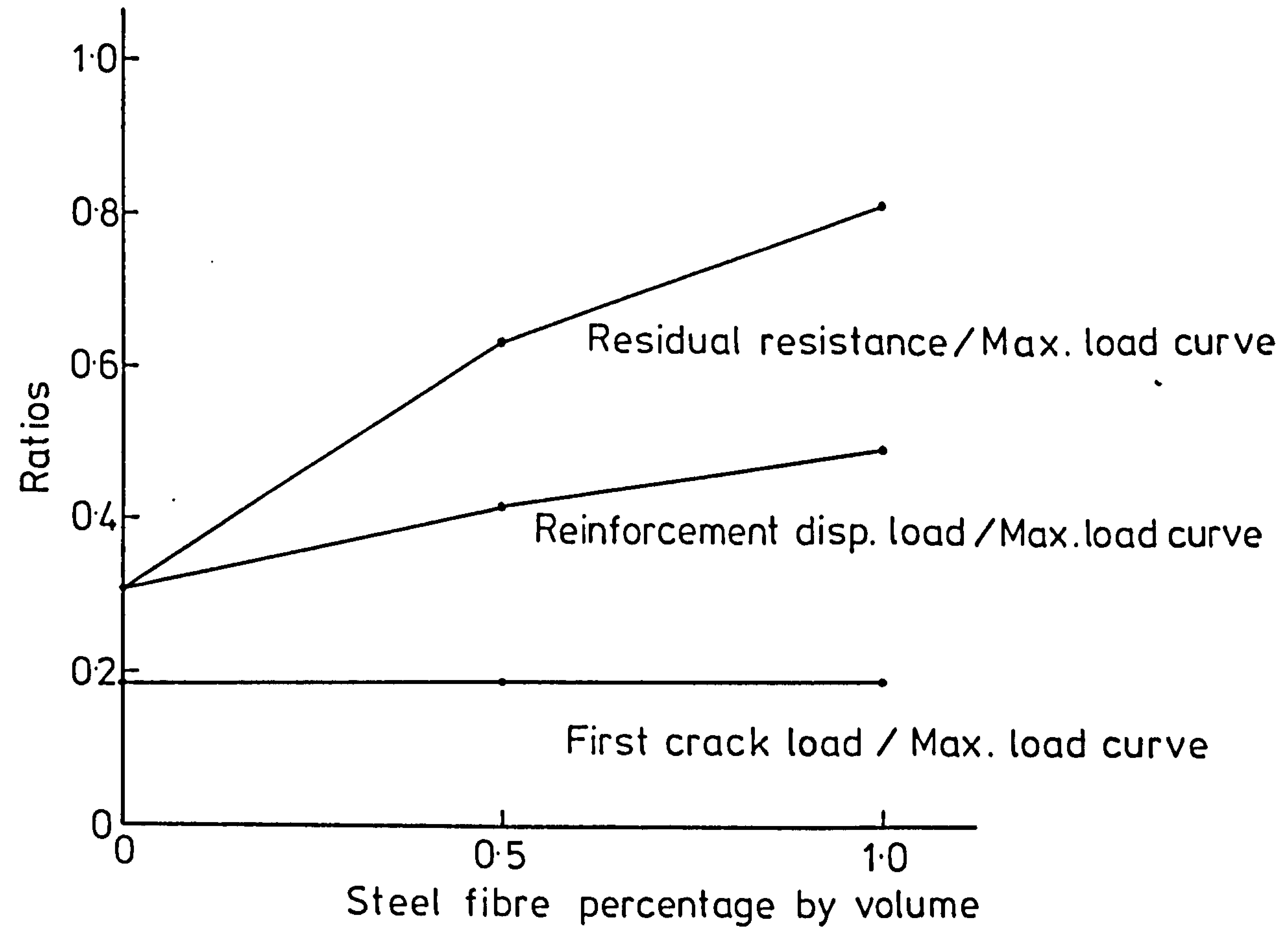

FIG. 6-4 RATIOS - STEEL FIBRE PERCENTAGE CURVES FOR SLABS FS-1 TO FS-3

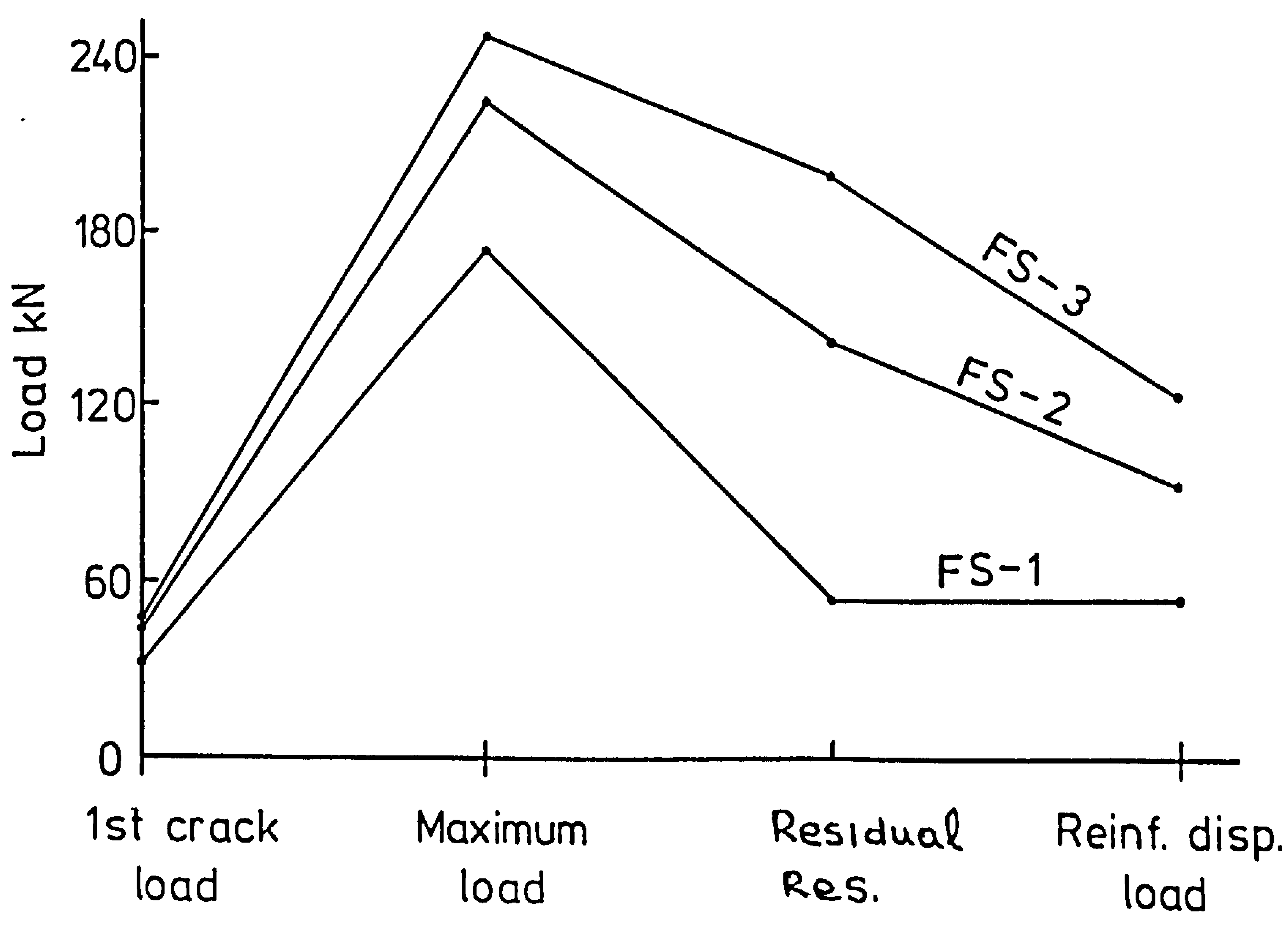

FIG. 6-5 TEST RESULTS COMPARISON

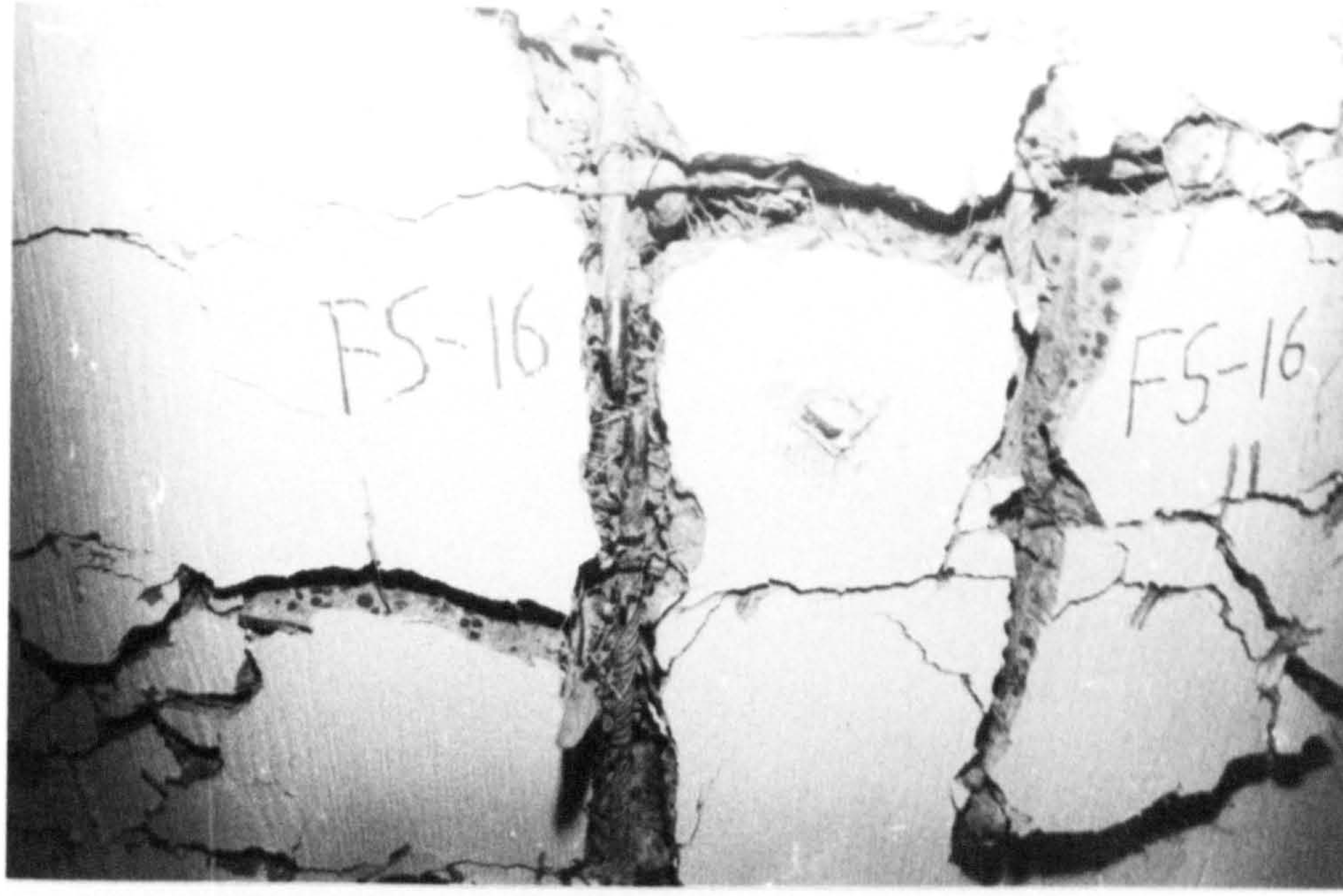

(a) Slab FS-16 (Punching shear failure)

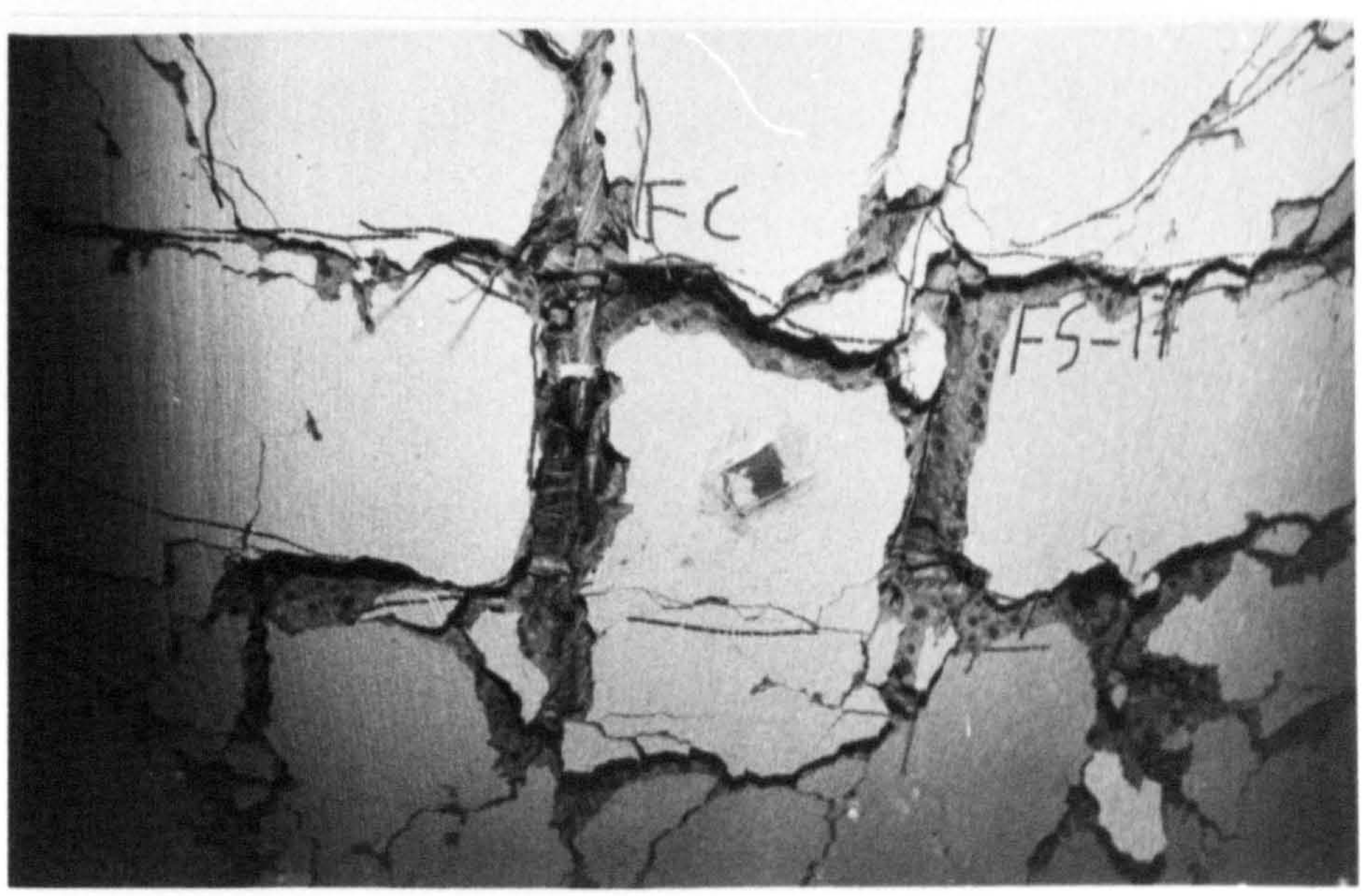

(b) Slab FS-17 (Flexure failure)

PLATE 6-1 REINFORCEMENT DISPLACEMENT AND CUTTING IN SLABS FS-16 AND FS-17 (V_f = 1% PADDLE FIBRES) load over that of plain concrete slabs varied from 97.4 to 158.7% and from 153.5 to 164.4% for reinforcement ratios 0.5574 and 0.3716% respectively.

The residual resistances and reinforcement displacement loads for slabs FS-1, FS-2 and FS-3 are plotted in Figs. 6.4 and 6.5.

Plate 6.1 shows the steel fibre presence in slab FS-16 which failed in punching shear and slab FS-17 which failed in flexure, and the cutting of reinforcing bars after reinforcement displacement started.

6.3 The Failure Surface.

The plain lightweight concrete slabs tested in this investigation failed suddenly in punching shear along a surface formed by inclined cracks in the immediate vicinity of the column. The failure surface had a shape approximating the surface of a truncated cone spreading out from the column, with an average distance of 2.38h, 1.90h, 2.48h and 1.94h from the column face at the tension surface for slabs FS-1, FS-8, FS-10 and FS-19 respectively, which implies angles of the failure surface varied from 22° to 28° (Table 6.4). This is in agreement with data reported by other investigators (52, 61, 78, 82, 113) for normal weight concrete slabs. Pl.6.2 shows the complete punching failure observed in plain concrete slabs FS-1, FS-8 and FS-10.

The use of 0.5% and 1.0% by volume crimped fibres in slabs FS-2 and FS-3 increased the average distance of the failure surface from the column face at the tension surface to 2.47h and 2.58h respectively, implying a decrease in the angle of failure surface to 22° for slab FS-2 and 21° for slab FS-3 as compared to 23° for plain lightweight concrete slab FS-1.

All observed data concerning the punching location and angle of failure surface are shown in Table 6.4. As can be seen from this Table the use of 1.0% fibre reinforcement reduced the angle of failure surface of the corresponding plain concrete slabs by a maximum of 3°. The angle of failure

Table 6.4 Observed failure surface and angle of test specimens.

Series Number	Slab Number	Column size, r, in mm	Compression Reinf. / Tension Reinf.	Steel Fibre Type and Percentage by Volume	Cube Compress. Strength N/mm^2	Maximum Load in KN	CP110's and ACI's shear section from col. face	Exper. shear section from column face	Punching failure angle
1	2	3	4	5	6	7	8	9	10
1	FS-1	150	7-8 mm 12-10mm	- 0.0	44.20	173.5	1.5h 0.5d	2.38h	23^o
	FS-2	150	7-8 mm 12-10mm	Crimped 0.5	42.50	225.0	1.5h 0.5d	2.47h	22^o
	FS-3	150	7-8 mm 12-10mm	Crimped 1.0	44.56	247.4	1.5h 0.5h	2.58h	21^o
2	FS-4	150	- 12-10mm	Crimped 1.0	46.67	224.4	1.5h 0.5d	2.32h	23^o
	FS-5	150	7-8mm 8-10mm	Crimped 1.0	47.50	198.1	1.5h 0.5d	2.20h	24^o
	FS-6	150	- 8-10mm	Crimped 1.0	44.60	174.5	- -	-	-
	FS-7	150	3-8 mm 8-10mm	Crimped 1.0	45.80	192.4	- -	-	-
	FS-19	150	7-8 mm 8-10mm	- 0.0	43.10	136.5	1.5h 0.5d	1.94h	27^o
	FS-20	150	- 8-10mm	Crimped 1.0	46.30	211.0	1.5h 0.5d	1.97h	27^o
3	FS-8	100	7-8 mm 12-10mm	- 0.0	45.80	150.3	1.5h 0.5d	1.90h	28^o
	FS-9	100	7-8 mm 12-10mm	Crimped 1.0	44.50	216.6	1.5h 0.5h	2.03h	26^o
	FS-10	200	7-8 mm 12-10mm	- 0.0	45.50	191.4	1.5h 0.5d	2.48h	22^o
	FS-11	200	7-8mm 12-10mm	Crimped 1.0	42.80	259.8	- -	-	-
4	FS-12	150	7-8 mm 12-10mm	Japanese 1.0	45.10	217.5	1.5h 0.5d	2.70h	20^o
	FS-13	150	7-8 mm 12-10mm	Hooked 1.0	41.85	235.5	1.5h 0.5d	2.40h	23^o
	FS-14	150	7-8 mm 12-10mm	Paddle 1.0	43.73	239.5	1.5h 0.5d	2.60h	21^o
	FS-15*	150	7-8 mm 12-10mm	Crimped** 1.0	39.05	238.0	1.5h 0.5d	2.11h	25^o
5	FS-16	150	7-8mm 12-10mm	Paddle 1.0	34.9	227.8	1.5h 0.5d	1.86h	28^o
	FS-17	150	7-8 mm 12-10mm	Paddle 1.0	58.56	268.4	- -	-	-
	FS-18	150	7-8 mm 12-10mm	Paddle 1.0	17.75	166.0	1.5h 0.5d	1.16h	41^o

*6.6 mm Lytag aggregates, ** ℓ_f/d_f = 90.

NOTE: Slabs FS-6, FS-7, FS-11 and FS-17 failed in flexure.

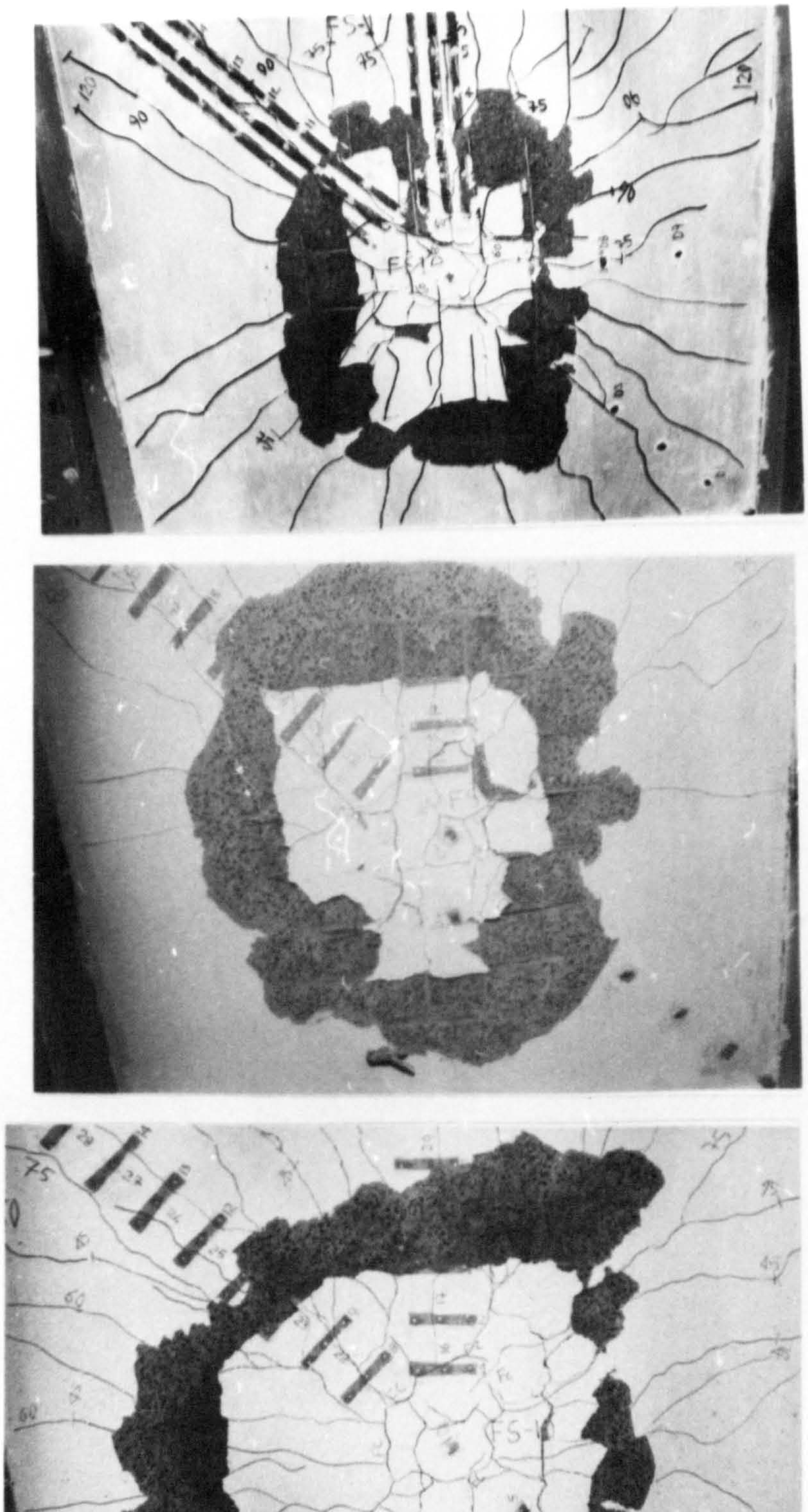

PLATE 6-2 COMPLETE PUNCHING FAILURE FOR PLAIN LIGHTWEIGHT CONCRETE SLABS FS-1, FS-8 AND FS-10

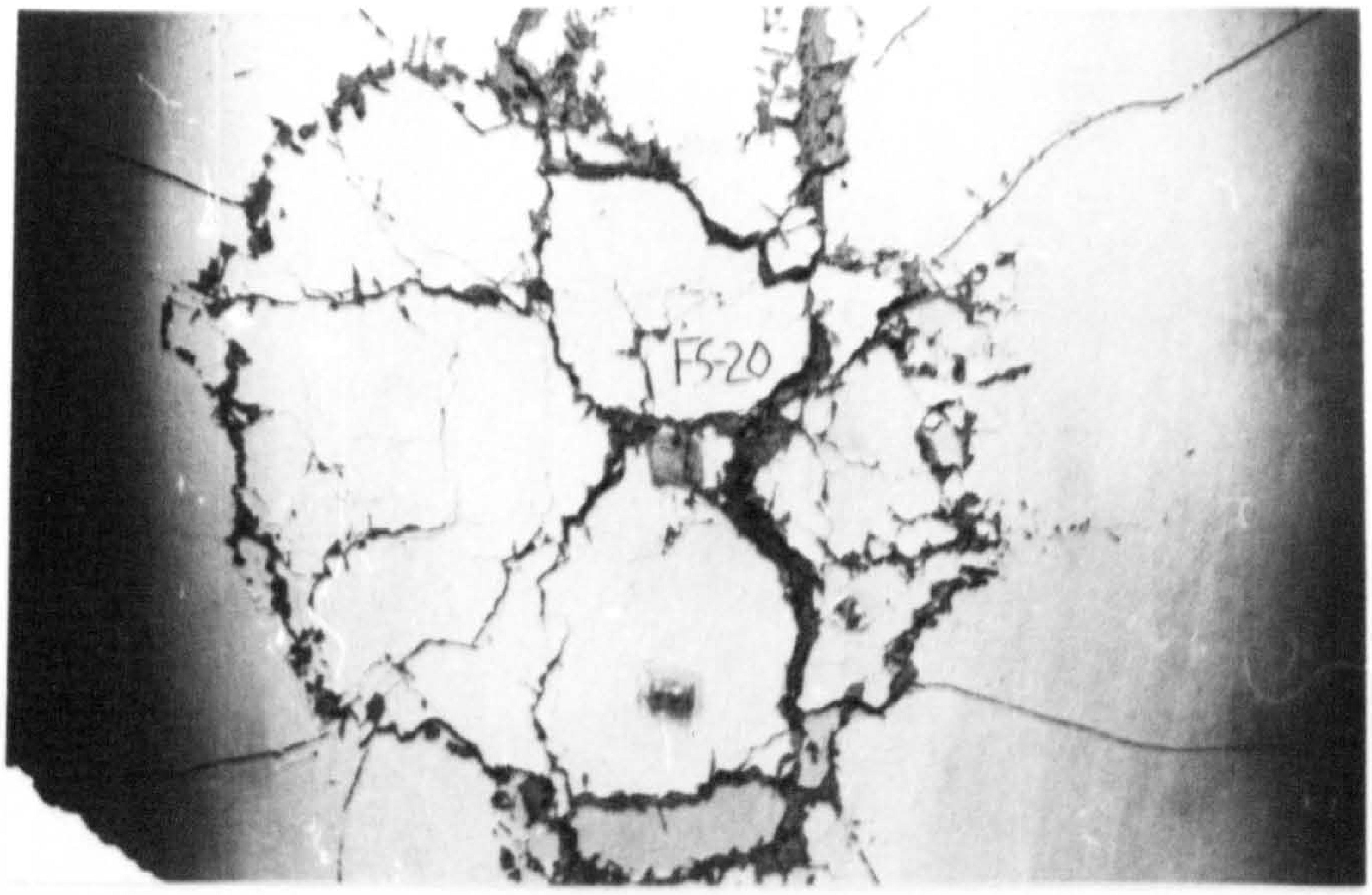

(a) Irregular punching periphery

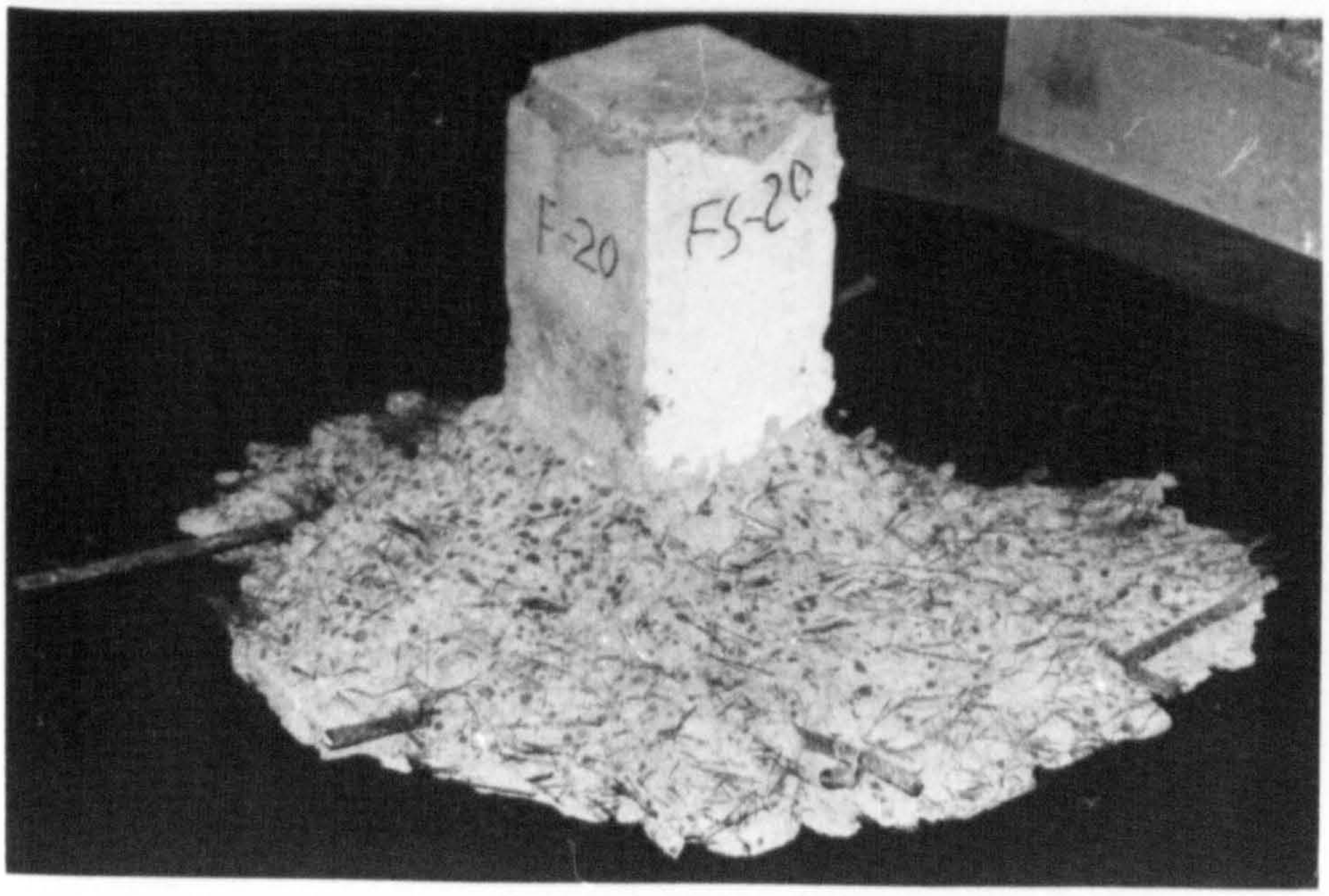

(b) Column and failure cone

PLATE 6-3 PUNCHING FAILURE SURFACE FOR SLAB FS-20

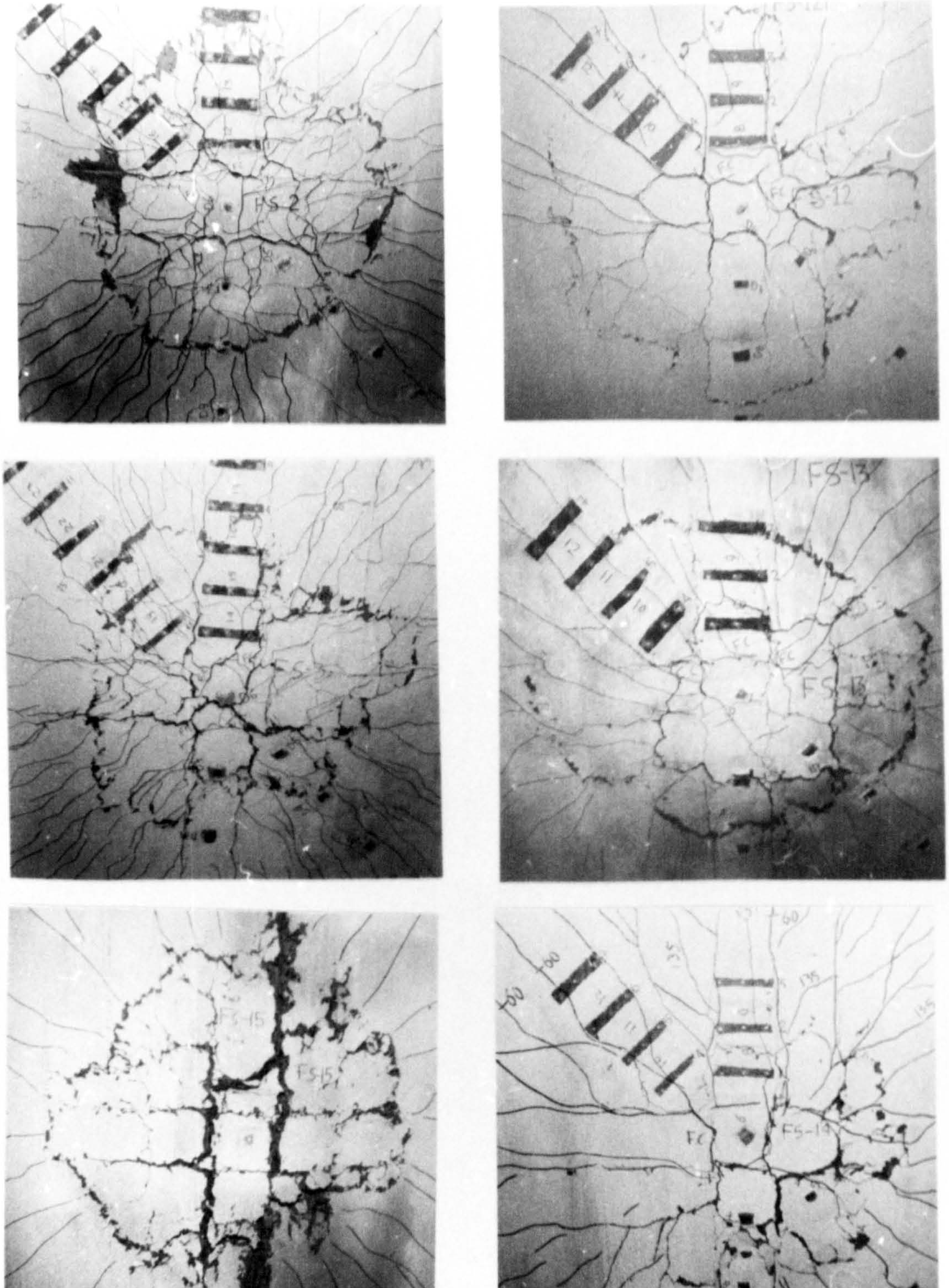

(a) Gradual complete punching failure of slabs FS-2, FS-3 and FS-15

(b) Gradual incomplete punching failure of slabs FS-12, FS-13 and FS-14

PLATE 6-4 FAILURE PHOTOGRAPHS FOR SLABS WITH FIBRE REINFORCEMENT FAILING IN PUNCHING SHEAR

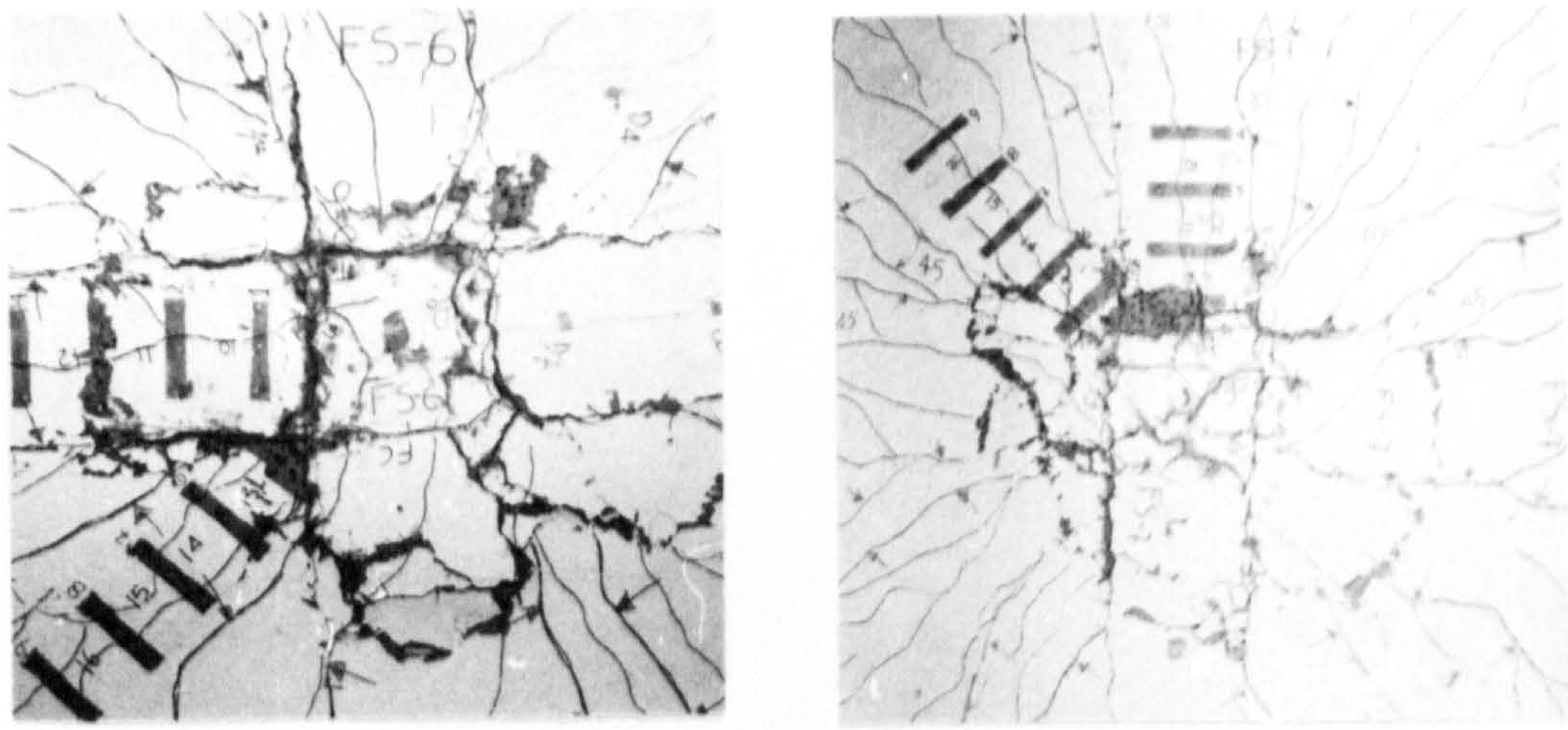

(a) Incomplete failure surface of slabs FS-6 and FS-7

($\rho = 0.3716\%$)

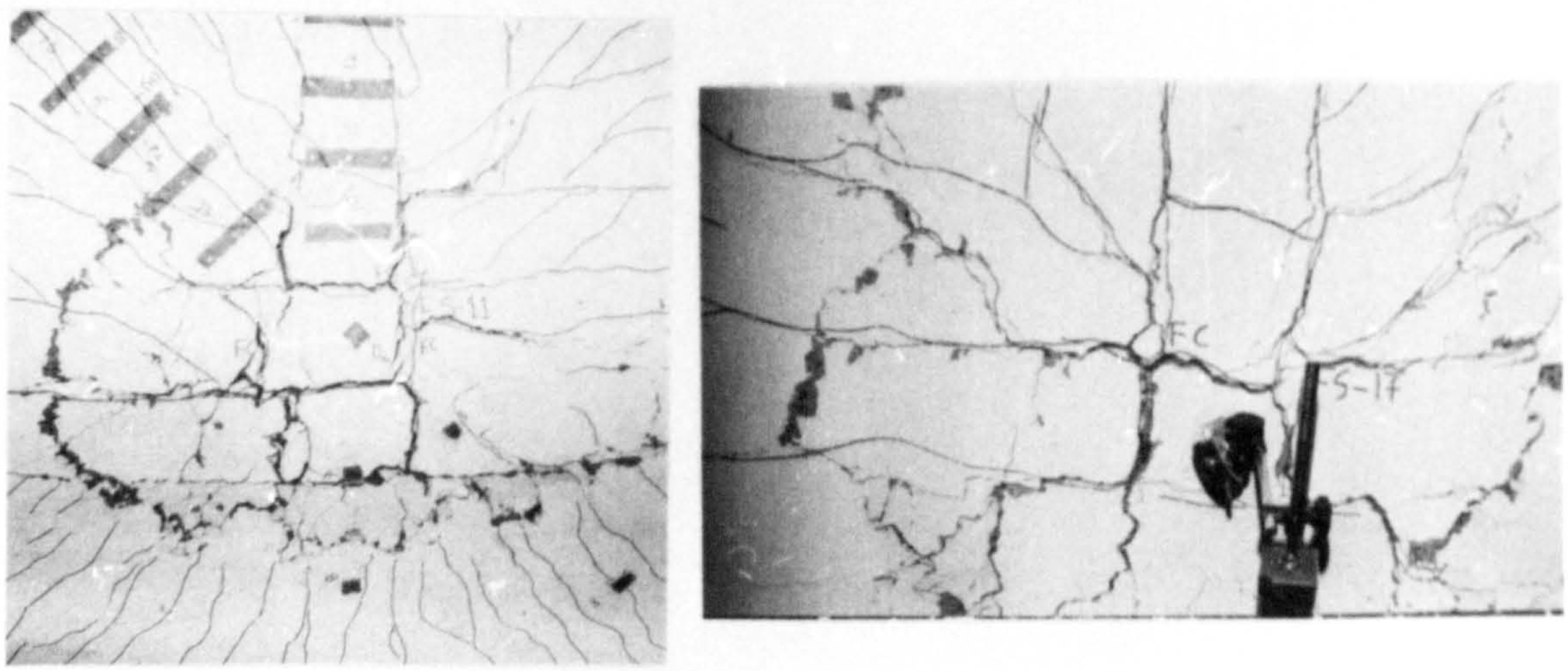

(b) Incomplete failure surface of slabs FS-11 and FS-17

($\rho = 0.5574\%$)

PLATE 6-5 FAILURE PHOTOGRAPHS FOR SLABS WITH FIBRE REINFORCEMENT FAILING IN FLEXURE

(a) Punching line in slab FS-16 failing in shear

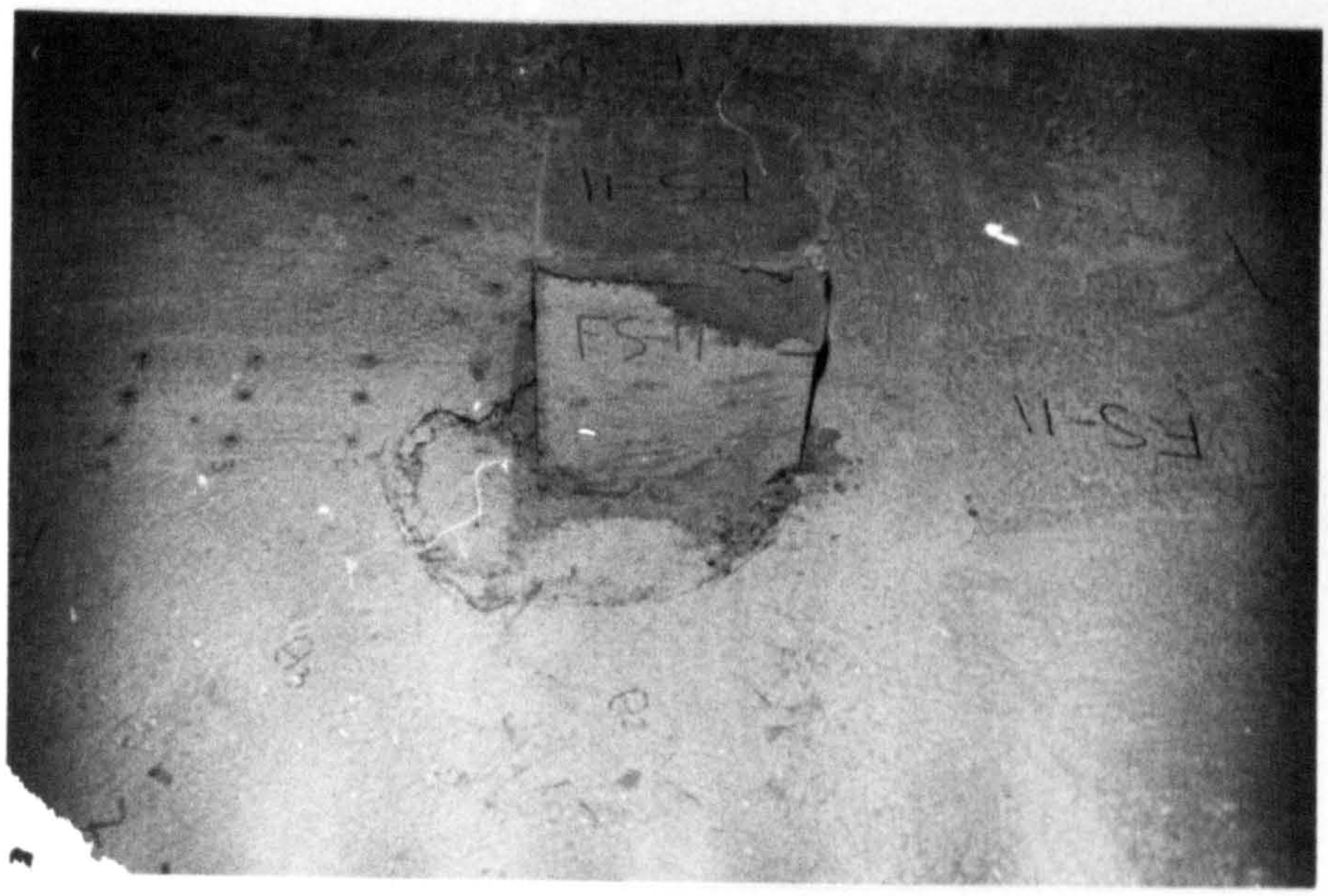

(b) Column punching in slab FS-11 after failure in flexure

PLATE 6-6 PUNCHING LINES IN SLABS FS-16 AND FS-11 for slab FS-8 is 41°, and this rather high value may probably be due to the low compressive strength (17.75 N/mm^2) used in this slab.

The fibre concrete slabs, which failed in punching shear, had their failure surface in the form of truncated cone as the plain concrete slabs. Plate 6.3(B) shows the punching failure surface for slab FS-20.

From plates 6.3(A) and 6.4 it can be seen that the failure surfaces were quite irregular in most slabs with fibre reinforcement. This conflicts with the observations reported by Ali (78) for normal weight fibre concrete slabs where the punching shear shape was either a circular or an elliptical one. The punching failure for slabs with steel fibres was gradual but the process of punching was incomplete in some slabs. Plate 6.4(A) shows some slabs with a complete punching line at the tension surface and Plate 6.4(B) slabs with an incomplete punching line.

Plate 6.5 shows the punching line at tension surface of all four fibre concrete slabs which failed in flexure and then as loading continued the column punched through the slab. As can be seen the punching line was incomplete in all four slabs.

All the plain or fibre concrete slabs which failed in punching shear had the punching lines on the compression face directly in the vicinity of the column faces and showed no sign of concrete crushing except for slab FS-16 as can be seen in Plate 6.6(A). In the slabs which failed in flexure and then the column punched through the slab as loading continued, the punching lines on the compression face were also directly in the vicinity of the column faces except for slab FS-11 where the punching line deviated from the column perimeter (Plate 6.6(B)).

6.4 Conclusions.

Based on the results presented in this chapter the following conclusions can be drawn.

1. The first crack load improved by 30-45% when 1.0% by volume fibre reinforcement was used in lightweight concrete slabs. The ratio of the first crack load to maximum load for both plain and fibre concrete slabs was about 19% and 16% for 0.5574% and 0.3716% tension reinforcement ratios respectively.

2. The presence of steel fibres in a slab-column connection can delay the formation of the inclined shear cracking; this delay appears to be increased with increasing fibre percentage, decreasing column size and decreasing tension reinforcement. The ratio of the shear cracking load to maximum load varied from about 45 to 62% which is in agreement with data reported by other investigators.

3. The presence of fibre reinforcement increased the service load by 15-40% beyond that of plain concrete slabs depending upon the type of serviceability criterion used. When fibres were used over the whole specimen a higher increase in service load was obtained.

4. The reinforcement yielding in most of the tested slabs occurred at about 75% of the corresponding maximum load. The use of 1.0% by volume of fibre reinforcement increased the yield load by 30-45% beyond that of plain concrete slabs. When fibres were used over the whole specimen a 55% increase in yield load was obtained.

5. The ultimate punching shear strength increased by 29.7 and 42.6% when 0.5 and 1.0% by volume of crimped fibres were used in slabs with a 0.5574% reinforcement ratio. The increase in ultimate punching strength varied from 25.4 to 38% when different fibre types were used depending upon the particular fibre type used. The improvement in ultimate punching strength was about 44% when a 100 mm column stub was used. The use of a 200 mm square column stub allowed the slab to fail in flexure instead of punching

shear giving an increase in ultimate load of about 35%. When 1.0% by volume of crimped fibres were used in slabs with a 33% tensile reinforcement reduction the ultimate pjnching load increased by about 45%. When fibres were used over the whole specimen a 55% increase in punching strength was obtained.

The reduction of the compression reinforcement decreased the ultimate strength of fibres and changed the mode of failure from punching shear to flexure in the slabs with a lower tension reinforcement ratio. The use of different compressive strength in fibre concrete slabs yielded different values for ultimate load given that the addition of fibres does not improve the compressive strength of concrete and the punching strength depends primarily on the resistance of compression zone.

Generally speaking, the inclusion of fibre reinforcement in concrete matrix can increase the ultimate punching shear strength of concrete slabs and sometimes will change the mode of failure from punching shear to flexure.

6. The residual resistance after punching shear failure and the reinforcement displacement load for plain concrete slab specimens varied from 26 to 32% of the maximum load. This residual resistance improved by 200-275% and 400% because of the addition of 1.0% fibre reinforcement for slabs with 0.5574 and 0.3716% tensile reinforcement ratios respectively, the corresponding increases in the reinforcement displacement load being 100-150% and around 150% respectively.

7. In the case of fibre concrete, the residual resistance varied from 70-85% and 94-97% of the maximum load for slabs failing in punching shear and flexure respectively.

All punching failures resulted in truncated cone shaped surfaces, starting from the column faces at the compression surface of the slab and extended outwards to give sections at the tension surface varying from 1.90h to 2.48h for plain concrete specimens implying angles of the failure surfaces from 22° to 28°. In fibre concrete slabs the punching perimeter was bigger resulting in a decrease in the angle of surface by a maximum of 3°.

8. In the plain concrete slabs, the punching failure was complete and sudden. In fibre concrete slabs, the punching shear failure was gradual and sometimes incomplete. The failure surfaces in most fibre concrete slabs were quite irregular while in the plain concrete slabs the perimeter at the tension surface tended to be square.

9. The test results reported in this chapter showed that lightweight concrete can be used as a structural material in plain concrete flat slab-column connections; the ultimate punching shear strength obtained was about 87% of that of comparable plain normal weight concrete connections. The use of fibre reinforcement in lightweight concrete slabs as shear reinforcement is very promising as in the case of normal weight concrete (78). The difference between the types of concrete materials is one of magnitude of various load characteristics and not of fundamental difference in behaviour.

CHAPTER 7.

ULTIMATE FLEXURAL STRENGTH ANALYSIS OF SLABS.

7.1 Introduction.

In a slab-column connection, punching shear failure or flexural failure will occur under vertical loads depending primarily on the amount of tensile reinforcement. In this chapter an attempt is made to apply the yield line theory to determine the flexural strength of fibre reinforced concrete flat slabs. The test results obtained in this investigation and from various authors will be used to verify the proposed analysis.

The yield line theory pioneered by Johansen (91) is an ultimate load theory for ultimate flexural strength and is based on assumed collapse mechanism and plastic properties of under reinforced slabs. The assumed collapse mechanism is defined by a pattern of yield lines along which the reinforcement has yielded. The location of yield lines depends upon the shape, loading and edge conditions of the slabs.

7.2 Yield Line Theory Concept.

Consider a reinforced concrete slab loaded to failure. Initially it behaves elastically, until the concrete cracks on the tension face. More load causes some redistribution of moments from more to less cracked regions but the reinforcement yields first in the area of maximum elastic moment in the centre of the slab. This first yielding does not cause failure, or even any considerable change in the behaviour of the slab. Further loading causes yielding in the adjacent zones and in this way 'yield lines' are propagated from the centre, Fig.7.1(a). With further loading the region of yielding spreads gradually until the yield lines reach the boundary of the slab Fig.7.1(b). They cannot propagate further and therefore the slab is

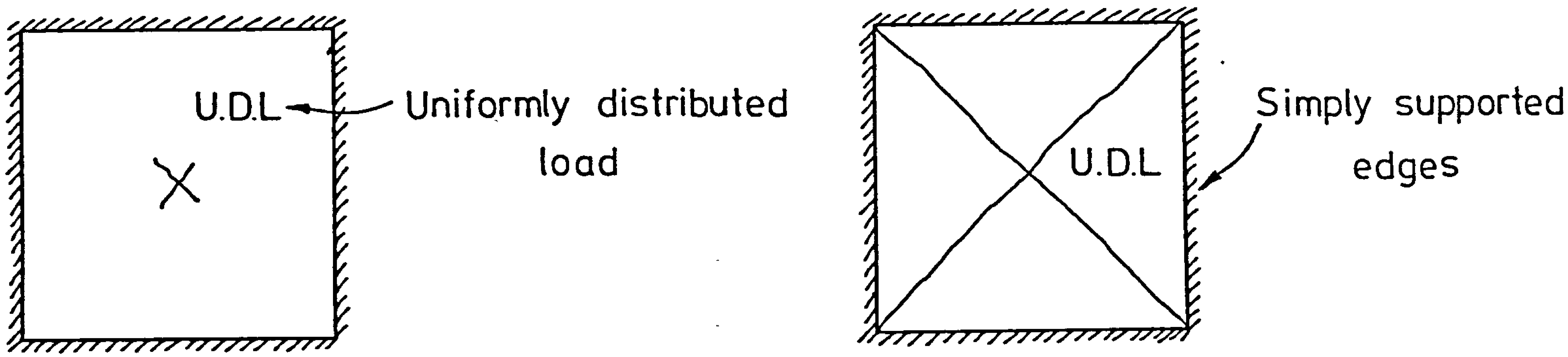

(a) Initial formation of yield lines (b) Diagonal yield lines

FIG.7-1 FORMATION OF YIELD LINES

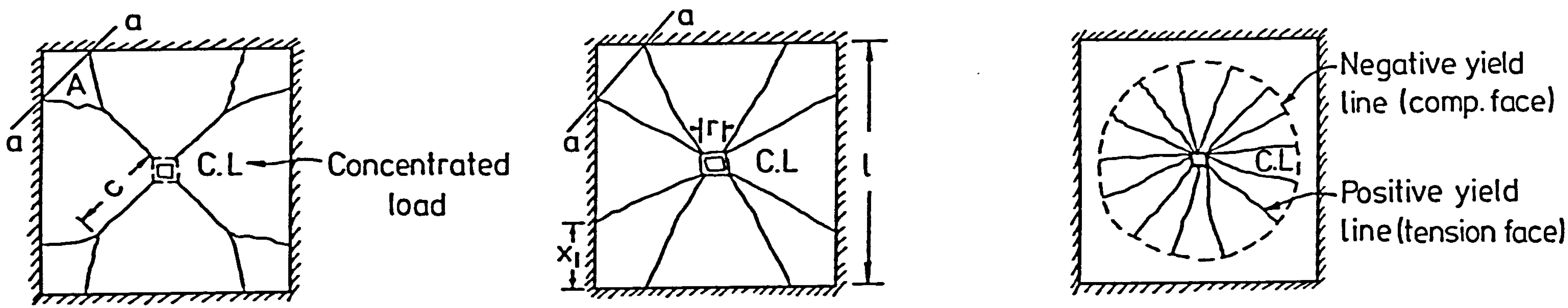

(a) (b)

Y – Shaped yield line patterns

(c)

Circular fan pattern

FIG 7-2 YIELD LINE PATTERNS

carrying its maximum load. At that stage the slab is considered to have been transformed into a mechanism.

The basic assumption of rigid plastic theories, of which yield line theory is an example, is that curvatures along the yield lines are much greater than those in the adjacent slab elements where deformations are assumed elastic and therefore negligible in comparison with plastic ones. In the yield line method the forces in the slab elements are not determined and the solutions obtained are upper bound.

In the application of yield line theory the method of calculating the ultimate strength of a slab to a given type of loading, is to investigate the various possible collapse mechanisms and to ensure that the selected one will produce the most critical collapse load. Once a yield line pattern has been assumed there are two methods of solution available, the virtual work method and the equilibrium method. In the virtual work method the relation between the applied loads and the strength of a slab can be found by equating the work done by the external loads due to a given hypothetical displacement with the internal dissipation of energy in the yield lines. In the equilibrium method a knowledge of shear forces acting at the junction of yield lines and boundaries of slab is required and solutions are therefore more difficult to obtain. Full details of the application of the yield line theory to slabs, are given in Reference 22.

7.3 Yield line Patterns.

1. Y-shaped yield line pattern.

In Fig.7.1(b) it has been assumed that yield lines enter the corner between two intersecting supported sides. This is the case when the corners are tied down. If the corners are not tied down, a new yield line pattern will appear, leaving a new slab part A, Fig.7.2(a), rotating as a lever about the axis a-a. This part is referred to as a corner lever. The corner lever appears because the Y-shaped yield pattern is more dangerous than the single yield line pattern.

In the case of a simply supported slab with corners free to lift off, under concentrated load, the yield line pattern is shown in Fig.7.2(a). By applying the principle of virtual work it can be found that the most critical yield line pattern is for c equal to zero Fig.7.2(b). In this case the ultimate flexural strength of the slab is given by the following equation: (Appendix A).

$$V_{flex} = 8\,m\,\left(\frac{1}{1-r/\ell} - 3+2\sqrt{2}\right) \quad \ldots\ldots \quad (7.1)$$

where V_{flex} = ultimate flexural strength of the slab.

m = the ultimate flexural moment per unit width.

r = column size.

ℓ = slab span.

The value of x_1 (Fig.7.2(b)) which gives this minimum load is:

$$x_1 = \left(1 - \frac{\sqrt{2}}{2}\right)(\ell-r) = 0.293\,(\ell-r) \quad \ldots\ldots \quad (7.2)$$

2. Circular fan pattern.

In the case of concentrated loads a yield line pattern shown in Fig. 7.2(c) is possible which consists of a curved negative yield line from which an infinite number of positive yield lines approach the load in a radial direction. By using the principle of virtual work the ultimate flexural strength is given by:

$$V_{flex.} = 2\,\pi\,(m+m') \quad \ldots\ldots \quad (7.3)$$

where m = the ultimate flexural moment per unit width (positive)

m' = the ultimate flexural moment per unit width (negative)

Table 7.1 Values of V_{flex} obtained from Eqn. 7.1 and 7.4.

λ	Equation 7.1	Equation 7.4
0	7.406 m	6.28 m
0.10	7.406 m	6.908 m
0.15	7.406 m	7.222 m
0.1788	7.406 m	7.406 m
0.20	7.406 m	7.536 m
0.30	7.406 m	8.164 m
0.40	7.406 m	8.792 m

By putting $m'/m = \lambda$

$$V_{flex} = 2\pi(\lambda+1)\ m \qquad \ldots\ldots \qquad (7.4)$$

The ultimate flexural strength of a slab is considered to be the lesser of the two values obtained from equations (7.1) and (7.4) and as can be seen it depends primarily upon the value of parameter λ.

For values of $r = 150$ mm, $\ell = 1.69$ m, used in this investigation. Table 7.1 shows the values of the ultimate flexural load obtained for the two possible yield line patterns, for various values of λ.

From Table 7.1 it can be seen that for values of λ up to 0.1788 the circular fan mechanism is the critical one and the ultimate flexural strength is given by Eqn. (7.4), and for values of λ greater than 0.1788 the ultimate flexural strength is given by Eqn. (7.1) which corresponds to Y-shaped yield line mechanism.

7.4 Fibre Efficiency and Ultimate Tensile Strength of Concrete.

In chapter 2 the notions of fibre orientation factor, η_o, and length efficiency factor, η_L, as well as the critical fibre length, ℓ_c, were discussed. The critical fibre length is given by

$$\ell_c = \sigma_{fu} \frac{d_f}{2\tau} \qquad \ldots\ldots \qquad (7.5)$$

where σ_{fu} = Fibre fracture stress.

d_f = Fibre diameter.

τ = Interfacial shear stress.

In chapter 2 the values of η_o and η_L proposed by various investigators, and the basic composite mixture rule in the case of discontinuous fibres were also discussed. The composite mixture rule with small discontinuous fibres gives:

$$\sigma_c = \eta_o\ \eta_L\ \sigma_{fu} V_f + \sigma_m V_m \qquad \ldots\ldots \qquad (7.6)$$

Equation 7.6 is dependent only upon the properties and volume fractions of the constituents, and is independent of the state of stress to which the composite is subjected. Swamy and Mangat (39) used this equation to estimate the ultimate modulus of rupture of fibre cement composites, while other investigators used it to estimate the ultimate tensile strength by neglecting the contribution of matrix after cracking occurs (29,30). In fibre concrete composites the modulus of rupture can be up to three times the direct tensile strength even though, according to elastic theory they are nominally a measure of the same value. This discrepancy can be attributed to the fact that the post-cracking stress-strain curve on the tension side of a fibre concrete beam is very different from that in compression and, as a result, conventional beam theory is inadequate. The presence of fibres in the tension zone develops a quasi-plastic behaviour of fibre concrete beam as a result of fibre pull-out after matrix cracking. Thus, the values of modulus of rupture of fibre concretes based on elastic theory, are not real values nor are they representative of tensile strengths. The real quantities are the forces in the individual fibres spanning cracks and these are integrated, averaged and divided by the beam cross-sectional area to give a quantity known as the average tensile stress in the composite. This is the same convenient quantity as if measured in a direct tensile test after matrix cracking and should not be confused with the modulus of rupture of an elastic material (122). In what follows, the force per unit area of a section carried by the fibres, which is equivalent to the post-cracking tensile strength in direct tension, is found to be used as the contribution of fibres in the tensile zone in concrete sections.

In the cracked region of the stress-strain curve, the ultimate tensile strength of the composite will be given by:

$$\sigma_{cu} = \eta_o \eta_L \sigma_{fu} V_f \quad \ldots\ldots \quad (7.7)$$

where σ_{cu} = Ultimate composite strength.

This means that after cracking of the matrix the fibres will take up all the applied stress.

In this investigation a value of orientation factor of 0.41 (19) is used, which has been used by many authors (29,30,39). Law's (26) expressions for the length efficiency factor are also used, given by

$$\eta_L = \frac{\ell_f}{2\ell_c} \quad \ldots\ldots \quad (7.8)$$

when $\ell_f < \ell_c$ or by

$$\eta_L = 1 - \frac{\ell_c}{2\ell_f} \quad \ldots\ldots \quad (7.9)$$

when $\ell_f > \ell_c$

Using the value of ℓ_c from eqn. (7.5) the value of η_L is given by:

for $\ell_f < \ell_c$

$$\eta_L = \frac{\tau}{\sigma_{fu}} \frac{\ell_f}{d_f} \quad \ldots\ldots \quad (7.10)$$

for $\ell_f > \ell_c$

$$\eta_L = 1 - \frac{\sigma_{fu}}{4\tau} \frac{d_f}{\ell_f} \quad \ldots\ldots \quad (7.11)$$

A value is now needed for bond strength, τ, to be applied in Eqn. (7.10) or (7.11) and (7.7) to calculate the ultimate tensile strength of fibre concrete, σ_{cu}; it would be more appropriate to use interfacial bond strength value based on flexural tests than that obtained by means of pull out tests, since σ_{cu} is to be used for flexural analysis of the tested slabs. A basic value for τ of 4.15 N/mm^2 proposed by Swamy and Mangat (39) is chosen and for any particular type of fibre used in this investigation, a bond efficiency factor is applied. The selected value for τ of 4.15 N/mm^2 is valid for normal weight concrete. Since there is evidence (93) that the bond stress between steel bars and Lytag lightweight concrete is about 75 to 85% of that of normal weight concrete a factor K_L equal to 0.85 is applied to the basic value of fibre bond stress of 4.15 N/mm^2, to be used in this investigation.

Table 7.2 shows the value of bond efficiency factor assigned for the fibres used in this investigation and the corresponding value of bond strength for each fibre type, based on the selected value of 4.15 N/mm^2, which can be said to be the bond strength for smooth fibres.

The modulus of rupture results, for all the fibre types, obtained in this investigation and those obtained from Ref. 78 were analyzed using the method proposed by Swamy and Magnat (39), and the bond stress values for each fibre type are shown in Table 7.3. It can be seen that the proposed values for fibre bond strength calculated by using the bond efficiency factors from Table 7.2 are close enough to those predicted by Swamy's and Magnat's method (39). The bond efficiency factor for each fibre type is an arbitrarily assigned factor, depending on fibre shape; however, for crimped and hooked fibres the values assigned for the bond efficiency factor have been successfully used by many investigators.

7.4.1 Calculated Values of Critical Length and Composite Ultimate Tensile Strength.

The critical fibre length for each type of fibre can be calculated from Eqn. (7.5) by using values for σ_{fu} (fibre fracture stress) from Table 3.1 (Chapter 3) and values for τ from Table 7.2. The calculated values of critical fibre length are shown in Table 7.4. From this Table it can be seen that the fibre length is less than critical fibre length.

Table 7.2 Bond Strength for various fibres.

Fibre type	Fibre diameter, length mm	Bond Eff. factor η_b	Bond factor for Lb.Wb. K_L	Bond Strength, τ N/mm^2
Crimped	0.50x50	1.20	0.85	0.85 x 4.15 x 1.20 = 4.233
Japanese	0.42x25	1.00	0.85	0.85 x 4.15 x 1.00 = 3.527
Hooked	0.50x50	1.15	0.85	0.85 x 4.15 x 1.15 = 4.06
Paddle	0.76x53	1.65	0.85	0.85 x 4.15 x 1.65 = 5.82
Crimped	0.425x38.0	1.20	0.85	0.85 x 4.15 x 1.2 = 4.233

Table 7.3 Comparison of proposed values of τ and those obtained from modulus of rupture tests based on Swamy's theory (39)

Number of Results	Concrete	Fibre type	Proposed value of τ N/mm^2	Value of τ from modulus of rupture tests N/mm^2
9	Normal weight	Crimped	4.15x1.2=4.98	4.53
3	Normal weight	Hooked	4.15x1.15=4.77	5.13
8	Lightweight	Crimped	4.233	4.11
3	Lightweight	Japanese	3.527	4.37
3	Lightweight	Hooked	4.06	4.50
5	Lightweight	Paddle	5.82	6.08

Table 7.4 Critical fibre length values.

Fibre type	d_f mm	τ N/mm^2	σ_{cu} N/mm^2	ℓ_c mm	
Crimped	0.50	4.233	1820	107.5	$\ell_f < \ell_c$
Hooked	0.50	4.06	1100	67.75	$\ell_f < \ell_c$
Paddle	0.76	5.82	950	62.00	$\ell_f < \ell_c$

The length efficiency factor for $\ell_f < \ell_c$ is given by Eqn. (7.8) and therefore Eqn. (7.7) combined with Eqn. (7.5) gives:

$$\sigma_{cu} = \eta_o \left(\frac{\ell_f}{2\ell_c}\right) \left(\frac{2\tau}{d_f}\ell_c\right) V_f \qquad \text{or}$$

$$\sigma_{cu} = \eta_o \; \tau \; \frac{\ell_f}{d_f} \; V_f \qquad \ldots\ldots \qquad (7.12)$$

The ultimate tensile strength of concrete with 1% fibres by volume is now calculated for each type of fibre by using Eqn. (7.12).

1.	Crimped	$\sigma_{cu} = 0.41 \times 4.233 \times 100 \times 1\%$	$= 1.736$ N/mm^2
2.	Japanese	$\sigma_{cu} = 0.41 \times 3.257 \times 60 \times 1\%$	$= 0.801$ N/mm^2
3.	Hooked	$\sigma_{cu} = 0.41 \times 4.06 \times 100 \times 1\%$	$= 1.665$ N/mm^2
4	Paddle	$\sigma_{cu} = 0.41 \times 5.82 \times 70 \times 1\%$	$= 1.670$ N/mm^2
5.	Crimped	$\sigma_{cu} = 0.41 \times 4.233 \times 90 \times 1\%$	$= 1.562$ N/mm^2

7.5 Stress-strain Characteristics of Fibre Concrete in Compression.

For plain concrete the stress-strain curve in compression (Fig. 7.3) in general consists of two parts. In the ascending part, the stress increases with strain at a decreasing rate up to a strain varying from 0.0016 to 0.0025. In the descending part, the curve turns over and after a brief transition, stress decreases more or less linearly with strain until the concrete is completely disrupted. In the case of lightweight concrete the ascending part will exhibit elastic behaviour up to about 80% of the peak stress (94) with a lower value of modulus of elasticity as compared to normal weight concrete. The descending part will generally be shorter and steeper than that of normal weight concrete. The CP110 code of practice (69) uses the idealized part shown in Fig.7.3 for the descending part of stress-strain curve up to a strain of 0.0035 without a distinction in the type of concrete.

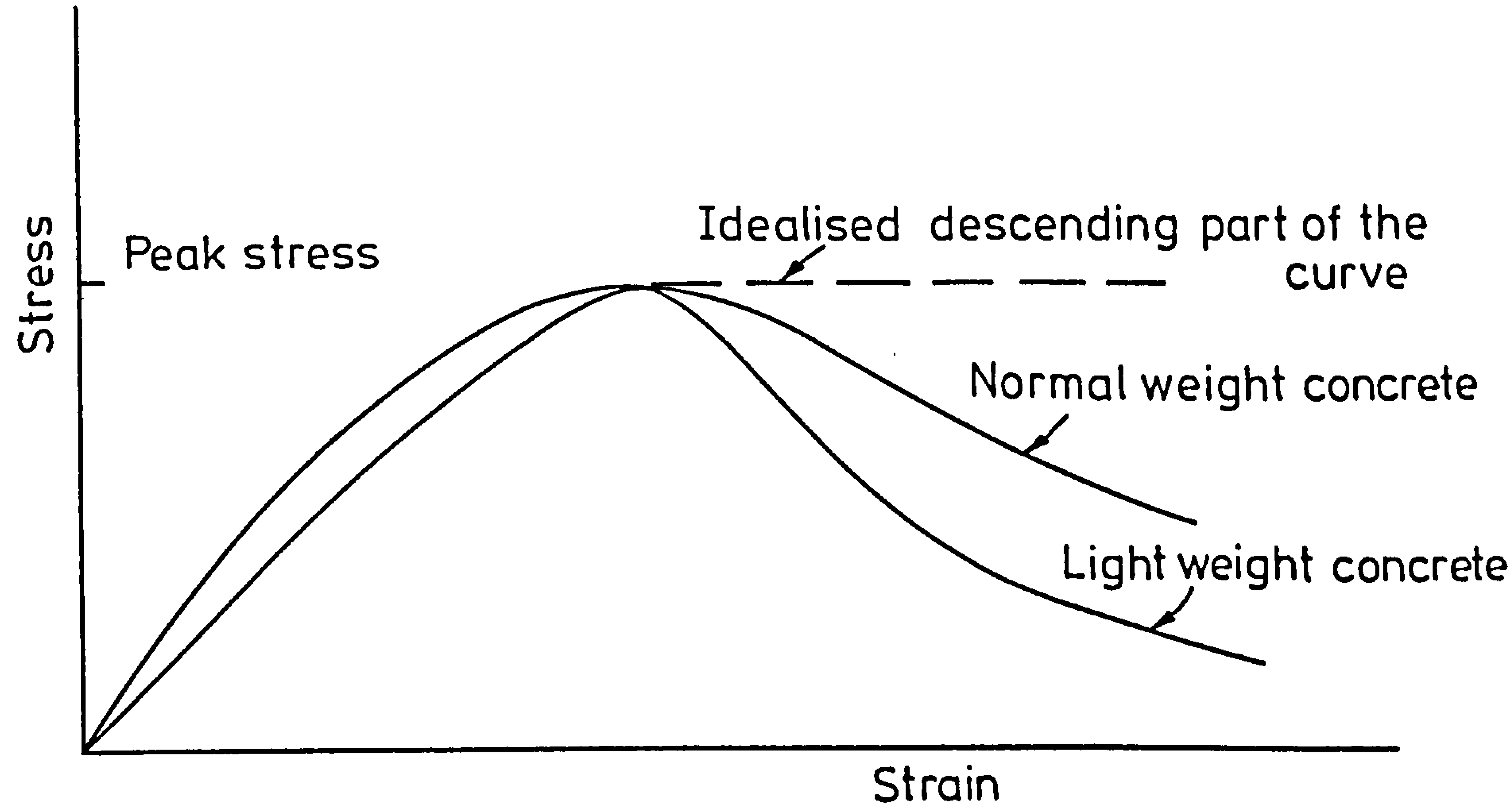

FIG. 7·3 SCHEMATIC STRESS-STRAIN CURVE OF PLAIN CONCRETE IN COMPRESSION

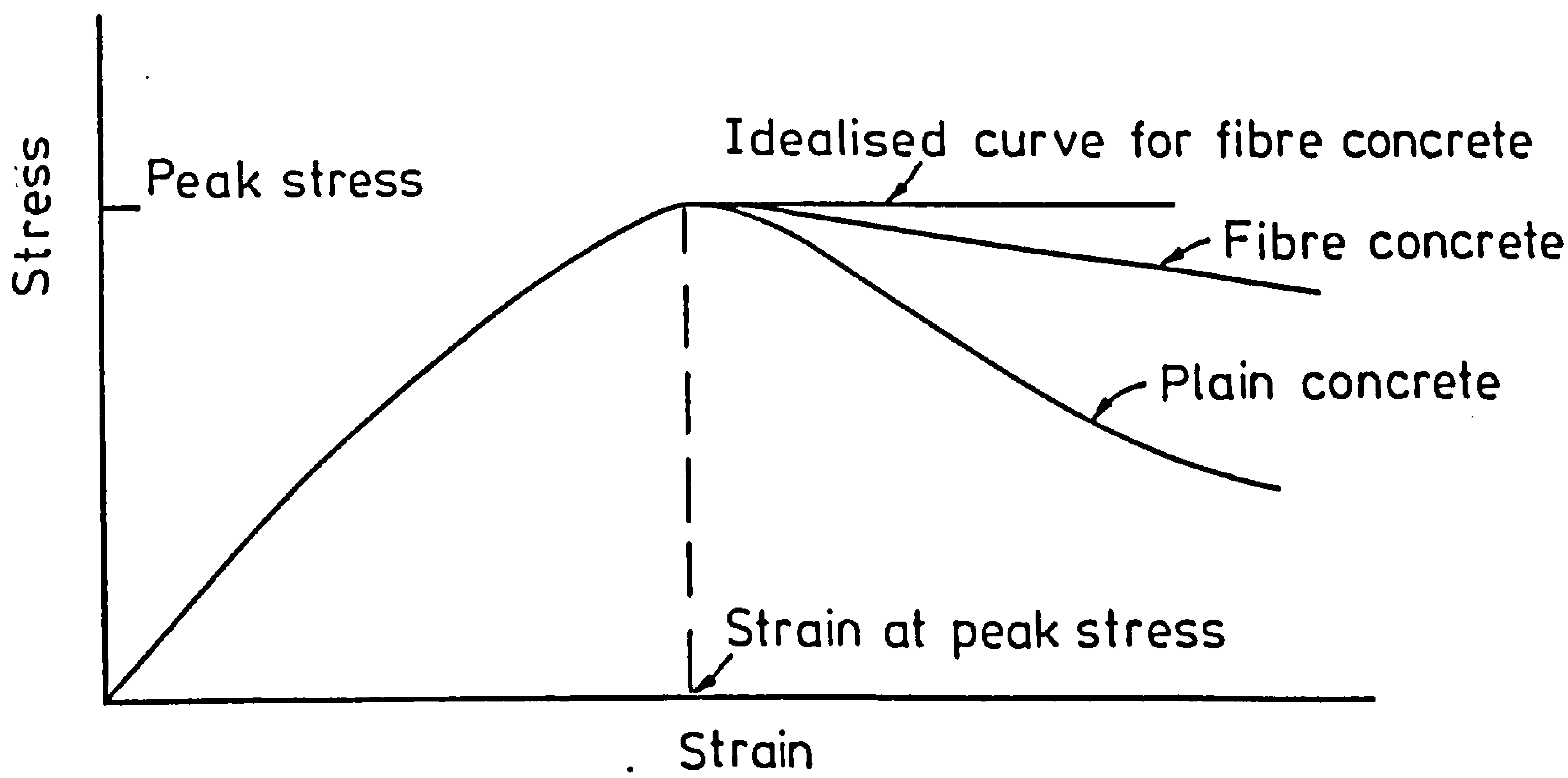

FIG. 7·4 SCHEMATIC STRESS-STRAIN CURVES OF PLAIN AND FIBRE CONCRETE IN COMPRESSION

In the case of fibre concrete, the stres-strain behaviour for the ascending part is similar to that of plain concrete, the peak stress value and corresponding strain value being comparable to those of plain concrete. Hughes and Fattuhi (95) found a 3% decrease in strain at peak stress in fibre reinforced concrete while Al-Noori (96) and Shah et al. (97) reported 9% and 3% increases respectively, in strain at peak stress in fibre reinforced concrete as compared to that of plain normal concrete. An increase in the strain at peak stress at about 25% was also reported (98) in the case of steel fibre light weight concrete, the peak stress being the same. However, in the descending part of the stress-strain curve the situation is slightly different (Fig.7.4). In this part, the transition zone is much longer than for plain concrete. The descending part of fibre reinforced concrete specimens was observed to be nearly horizontal for a majority of the cases (100). This second stage could be idealized as a horizontal line with constant stress and an ultimate strain greater than 0.0035, which is the CP110 ultimate strain for plain concrete. The value of strain of 0.0035 for plain concrete, which is considered to be a measurement of ductility, is in most cases the strain corresponding to a stress between 70-90% of the peak stress, on the descending part of the curve. Savvas (99) reported an average increase of about 28% in strain, at a stress 70-90% of peak stress, in the case of fibre reinforced concrete, as compared to corresponding value of plain concrete, by studying the stress-strain curves from references (95), (96), (97). Considering that 0.0035 is a realistic value of strain for plain concrete, the ultimate strain of fibre reinforced concrete becomes equal to $1.28 \times 0.0035 = 0.0045$.

7.6 <u>Ultimate Flexural Strength Analysis.</u>

In the application of yield line theory a calculation of the ultimate moment of resistance per unit width of the slab is necessary. In this investigation the fibres have been placed at a distance 550 mm from the centre of the slab; that means that along a yield line there are two different moments of resistance, one corresponding to the region of fibre reinforced concrete and one to the region of plain concrete, and, therefore, a unique ultimate moment of resistance must be calculated. In the Appendix A this unique moment of resistance is calculated when the two individual moments are known.

In this section the ultimate moment of resistance per unit width of the slab for both plain and fibre concrete sections is calculated.

7.6.1 Assumptions.

1. The strains in the concrete and the reinforcing steel are directly proportional to the distances from the neutral axis at which the strain is zero, Fig.7.5(a).

2. Concrete does not carry any tension in conventional concrete sections, but does in the case of fibre reinforced sections. The actual stress block in the tension zones in the case of fibre concrete is shown in Fig.7.5(b). The fibres will contribute to the strength over the height z, where z is the crack height. The strain at the level z is equal to cracking strain of concrete. Above the level z the contribution in the strength is due to elastic and uncracked concrete. For the sake of simplification without any loss in accuracy, the tensile contribution of the steel fibres is assumed to be represented by a rectangular stress block as shown in Fig.7.5 (c), the value of stress being equal to σ_{cu} (Section 7.4.1). Such a rectangular stress block in the tension zone has been successfully used by many authors (29), (3)), (99). This rectangular stress block is extended up to the neutral axis depth because the distance of level z from the neutral axis is very small when compared with the neutral axis depth.

3. The ultimate flexural strength of the section is reached when the concrete strain at the extreme compression fibre reaches a specified value ε_{cu}. The value of ε_{cu} for normal weight concrete according to CP110 (69) is 0.0035. For light weight concrete the maximum compressive strain must be limited to the value appropriate for the light weight concrete mix. Since values of compressive strain of about 0.0030 were observed in the plain concrete slabs tested in this investigation which failed in punching shear, the limiting value of 0.0035 is used for light weight concrete also in this analysis. For fibre concrete sections a higher value of ε_{cu} is assigned equal to 0.0045 as was explained in section 7.5.

4. At failure, the distribution of plain normal weight concrete compressive stresses is defined by an idealized stress-strain curve. The stress-strain curve for normal concrete in compression recommended by CP110 (69) after setting all the partial safety factors equal to 1.0 is shown in Fig.7.6. This curve is assumed parabolic up to a strain given by $\varepsilon_o = \sqrt{f_{cu}}/4115$ with a maximum stress equal to $0.67 \times f_{cu}$. The maximum stress remains constant until a concrete strain of 0.0035 is reached. The initial slope of the parabolic part is $E_N = 5.5\sqrt{f_{cu}}$, corresponding to the modulus of elasticity value. However, for light weight concrete having a density, D_c, between 1400 to 2300 kg/m^3, this value of modulus of elasticity should be multiplied by $(\frac{D_c}{2300})^2$ (69), and therefore the initial slope of the stress-strain curve becomes $E_L = E_N (\frac{D_c}{2300})^2$ (Fig.7.6), the rectangular part of the stress-strain curve being unchanged.

For an actual structural member, the compressive strength which must be used in the calculations is a fraction of that measured by crushing tests on cylinders or cubes of the same concrete, to account for differences in stress flow, which depends upon the geometry of the structural member and differences due to a stratification of the concrete in the member as cast.

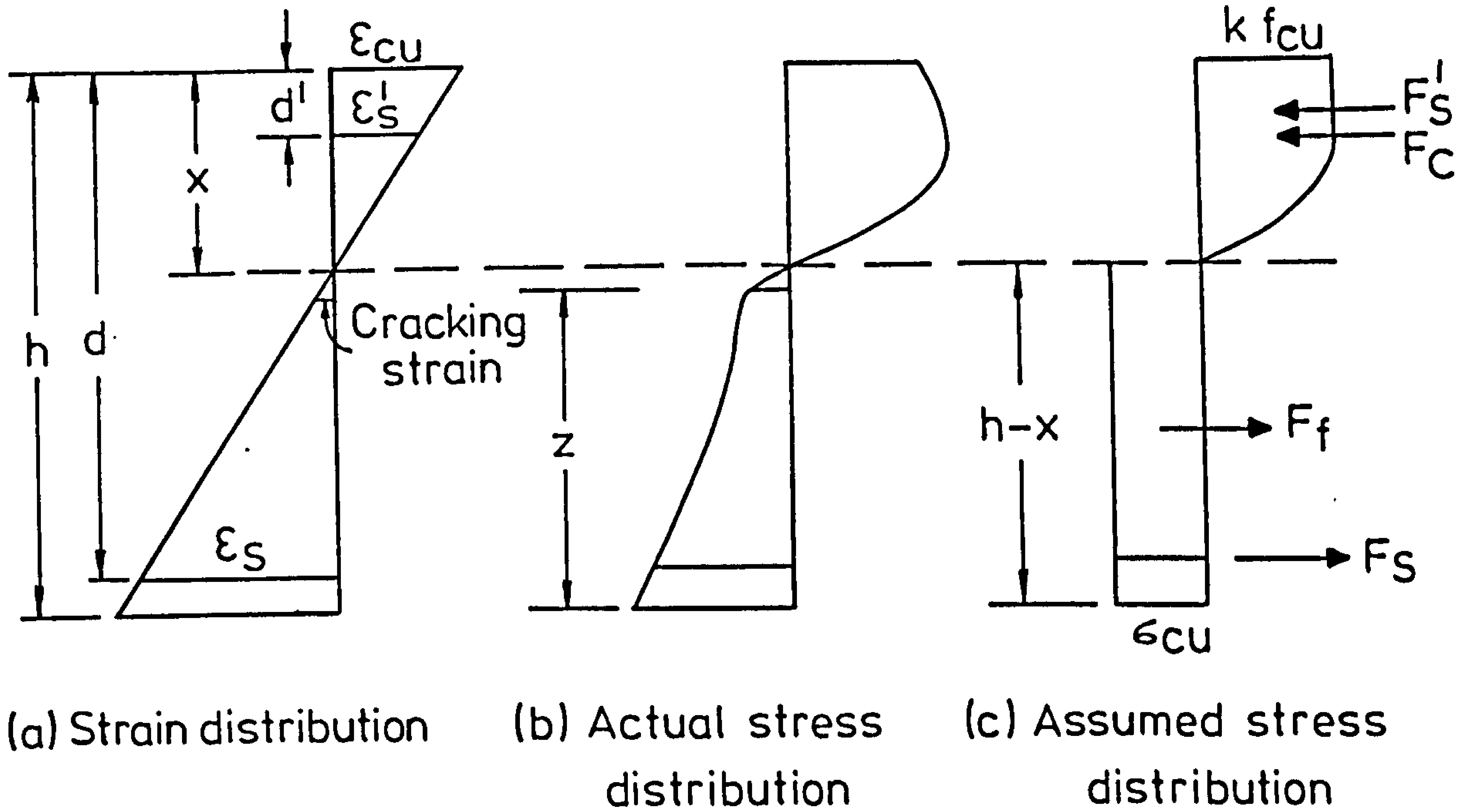

FIG. 7·5 STRAIN AND STRESS DISTRIBUTION

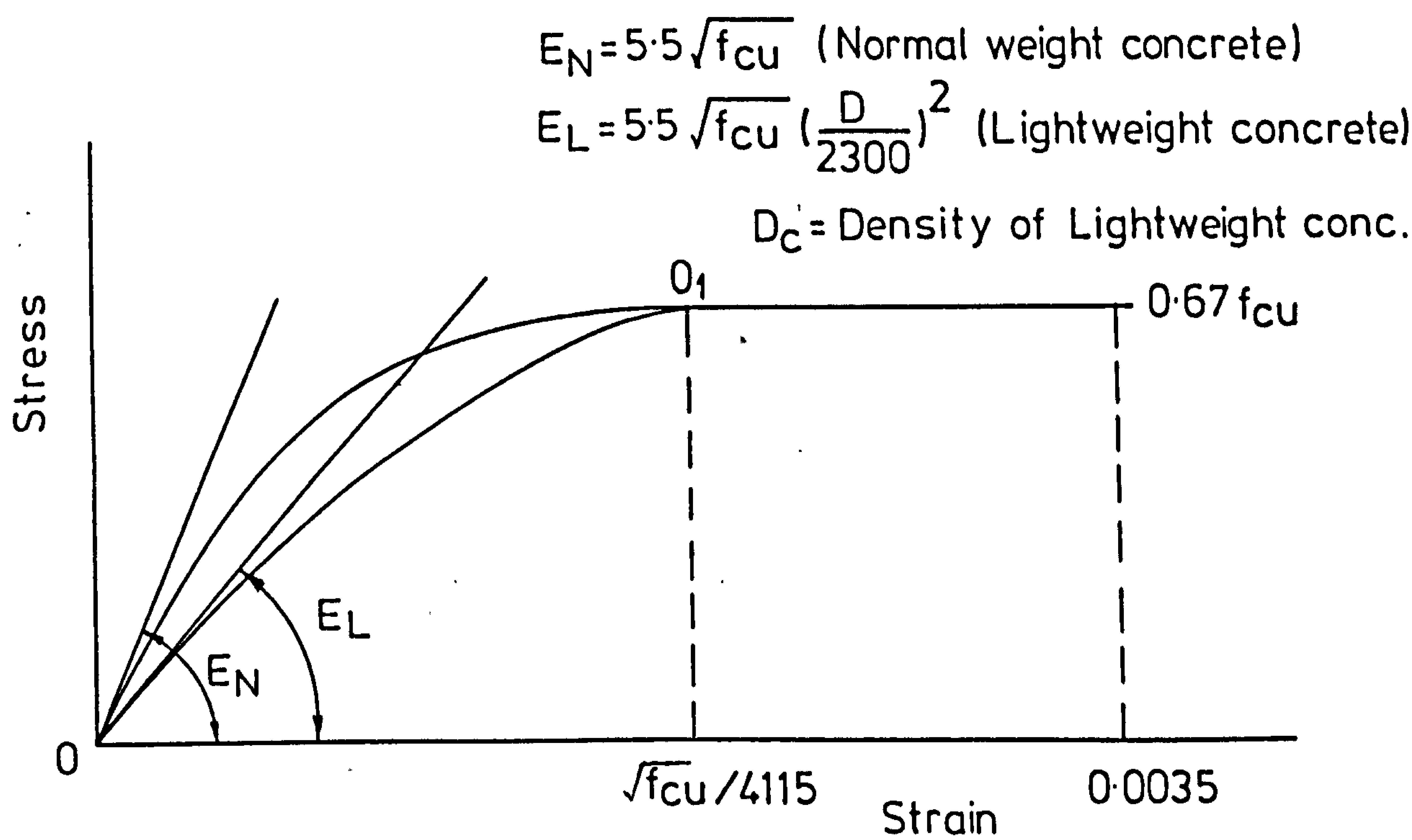

FIG. 7-6 STRESS-STRAIN CURVE OF CONCRETE IN COMPRESSION (CP 110)

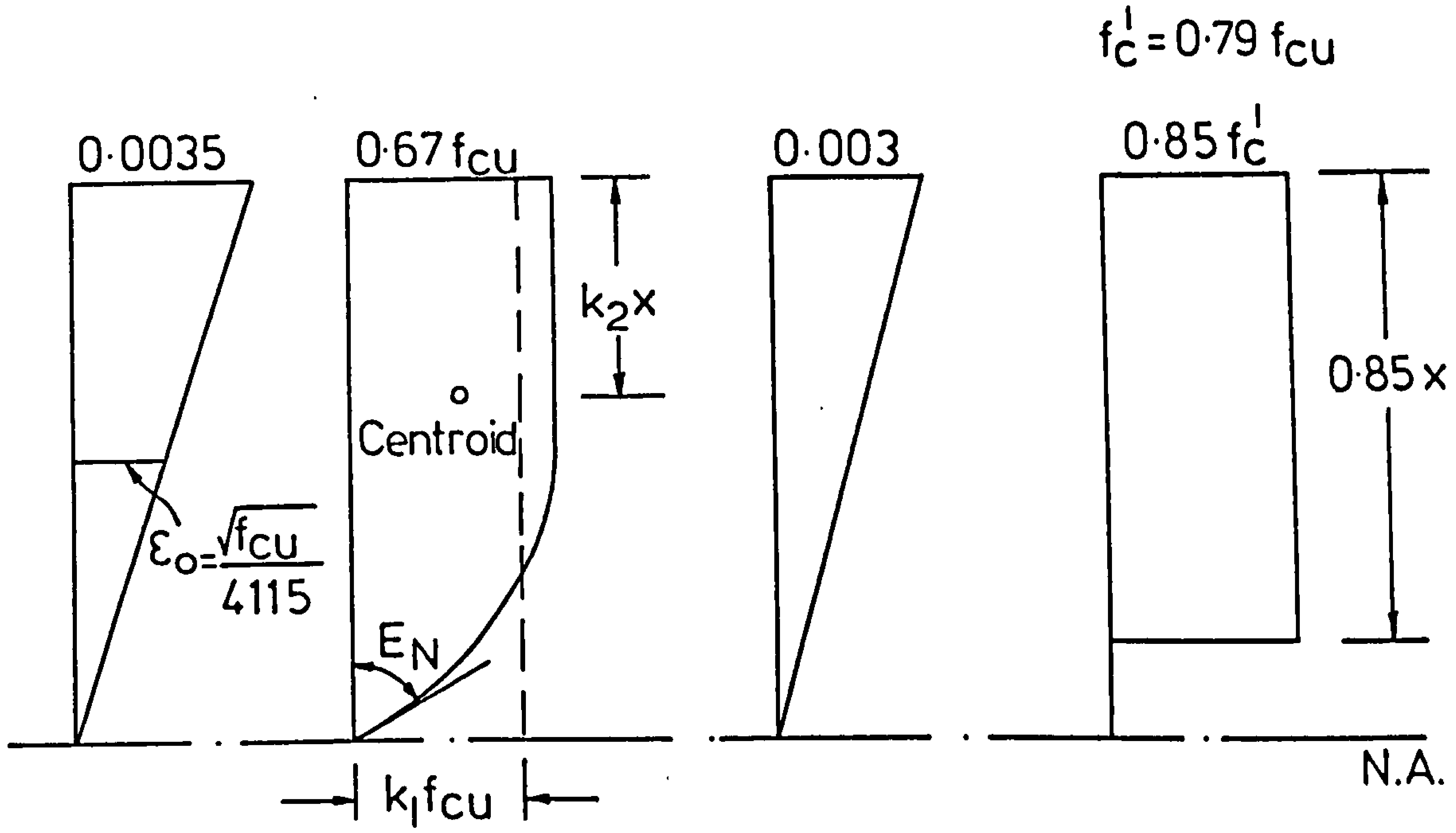

(a) According to CP 110 (b) According to A.C.I.

FIG. 7·7 COMPRESSIVE STRESS BLOCK AND STRAIN DISTRIBUTION ACCORDING TO CP110 AND A.C.I. FOR NORMAL WEIGHT PLAIN CONCRETE

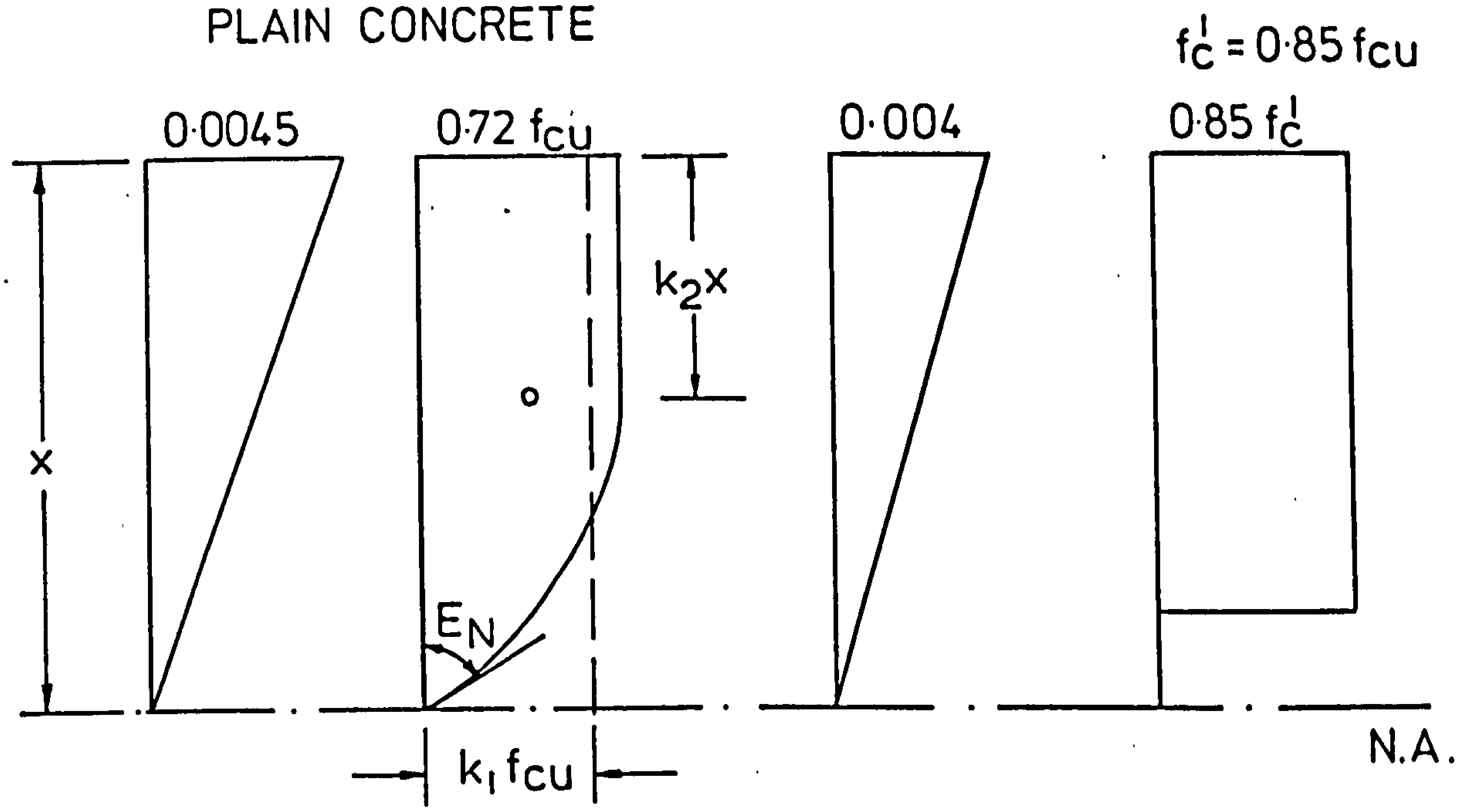

(a) Modified CP110'S (b) Modified A.C.I'S

FIG. 7-8 MODIFIED COMPRESSIVE STRESS BLOCK AND STRAIN DISTRIBUTION FOR NORMAL WEIGHT FIBRE REINFORCED CONCRETE

When these factors apply, the approximate reduction factor of 0.85 for cylinder compressive strength is used (A.C.I.). Based on a cylinder/cube strength ratio of 0.79 the reduction factor recommended by CP110 is 0.85 x 0.79 = 0.67 of the cube compressive strength. For fibre concrete a higher value for the cylinder/cube strength ratio was found by Al Noori (96). The percentage increase in the above ratio with fibres was 5.3 as compared to that of plain concrete. By applying this increase of 5.3% to the cylinder/cube ratio equal to 0.79 for plain concrete proposed by CP110, the resulting cylinder/cube ratio for fibre concrete is about 0.83. For the present analysis a cylinder/cube strength ratio equal to 0.85 is adopted which gives a maximum stress for the compressive stress block in the case of fibre concrete equal to 0.85 x 0.85 = 0.72 f_{cu}. Al-Taan (29) used a maximum stress equal to 0.77 f_{cu} for fibre concrete and found an increase in the calculated flexural load of about 2.5% as compared to that found with a maximum stress equal to 0.67 f_{cu}. Fig.7.7 shows the compressive stress block and strain distribution for plain concrete according to CP110 (69) anc A.C.I. code of practice (67) and Fig.7.8 shows the modified compressive stress blocks and strain distributions used in this analysis for fibre reinforced concrete.

5. To estimate the ultimate flexural strength of a flexural member it is usual to use the yield stress of the tensile reinforcement. In this investigation, however, the stresses in the reinforcement are derived from the appropriate stress-strain curve (Fig.3.3) corresponding to the strain obtained from the compatability of strains and the equilibrium of forces acting in the cross-section.

7.6.2 Analysis.

The CP110 (69) stress block parameters are the following:

$$\varepsilon_o = \sqrt{f_{cu}}/4115 \qquad \ldots\ldots \qquad (7.13)$$

$$K_1 = (\varepsilon_{cu} - \frac{\varepsilon_o}{3}) \frac{K}{\varepsilon_{cu}} \qquad \ldots\ldots \qquad (7.14)$$

$$K_2 = \frac{(2 - \frac{\varepsilon_o}{\varepsilon_{cu}})^2 + 2}{4\ (3 - \frac{\varepsilon_o}{\varepsilon_{cu}})} \qquad \ldots\ldots \qquad (7.15)$$

The above parameters are given by assuming that an equation of the form $y = 1.0xX_1^2$ is assigned to the parabolic part of the stress block. In the case of lightweight concrete an equation of the form $y = AxX_1^2$ must be assigned to the parabolic part of the stress-strain curve to account for the different initial slope (Fig.7.9). The value of constant A at point D (Fig.7.9) must be equal to $1/(D_c/2300)^2 = 1.64$ and at point 0_1 equal to 1.00, and therefore an average value of 1.32 is used for parameter A for the parabolic part of the stress-strain curve in the case of lightweight concrete. Then, the new stress block parameters K_1' and K_2', shown in Fig.7.10, for lightweight concrete become

$$K_1' = (\varepsilon_{cu} = A \frac{\varepsilon_o}{3}) \frac{K}{\varepsilon_{cu}} \qquad \ldots\ldots \qquad (7.16)$$

$$K_2' = \frac{(2-A \frac{\varepsilon_o}{\varepsilon_{cu}})^2+2.0}{4\ (3 - \frac{A\varepsilon_o}{\varepsilon_{cu}})} \qquad A = 1.32 \qquad \ldots\ldots \qquad (7.17)$$

From compatibility of strains (Fig.7.6(a)):

$$\frac{\varepsilon_{cu}}{X} = \frac{\varepsilon'_s}{x-d'} = \frac{\varepsilon_s}{d-x} \qquad \ldots\ldots \qquad (7.18)$$

Hence for ultimate conditions:

$$\varepsilon_s' = \varepsilon_{cu} \frac{x-d'}{x} \qquad \ldots\ldots \qquad (7.19)$$

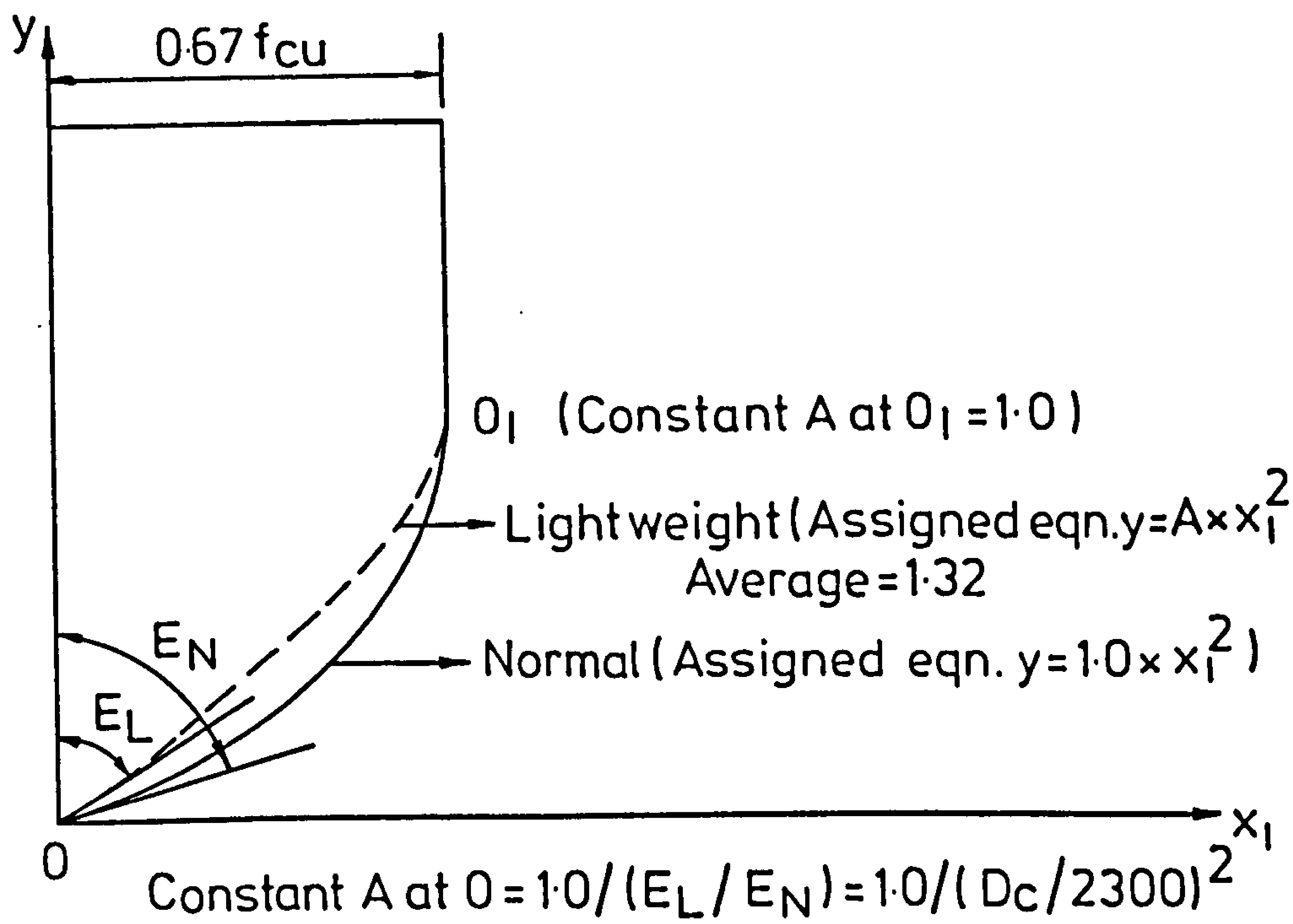

FIG. 7·9 DIFFERENCE IN STRESS BLOCK PARABOLIC PART BETWEEN NORMAL AND LIGHTWEIGHT CONCRETE

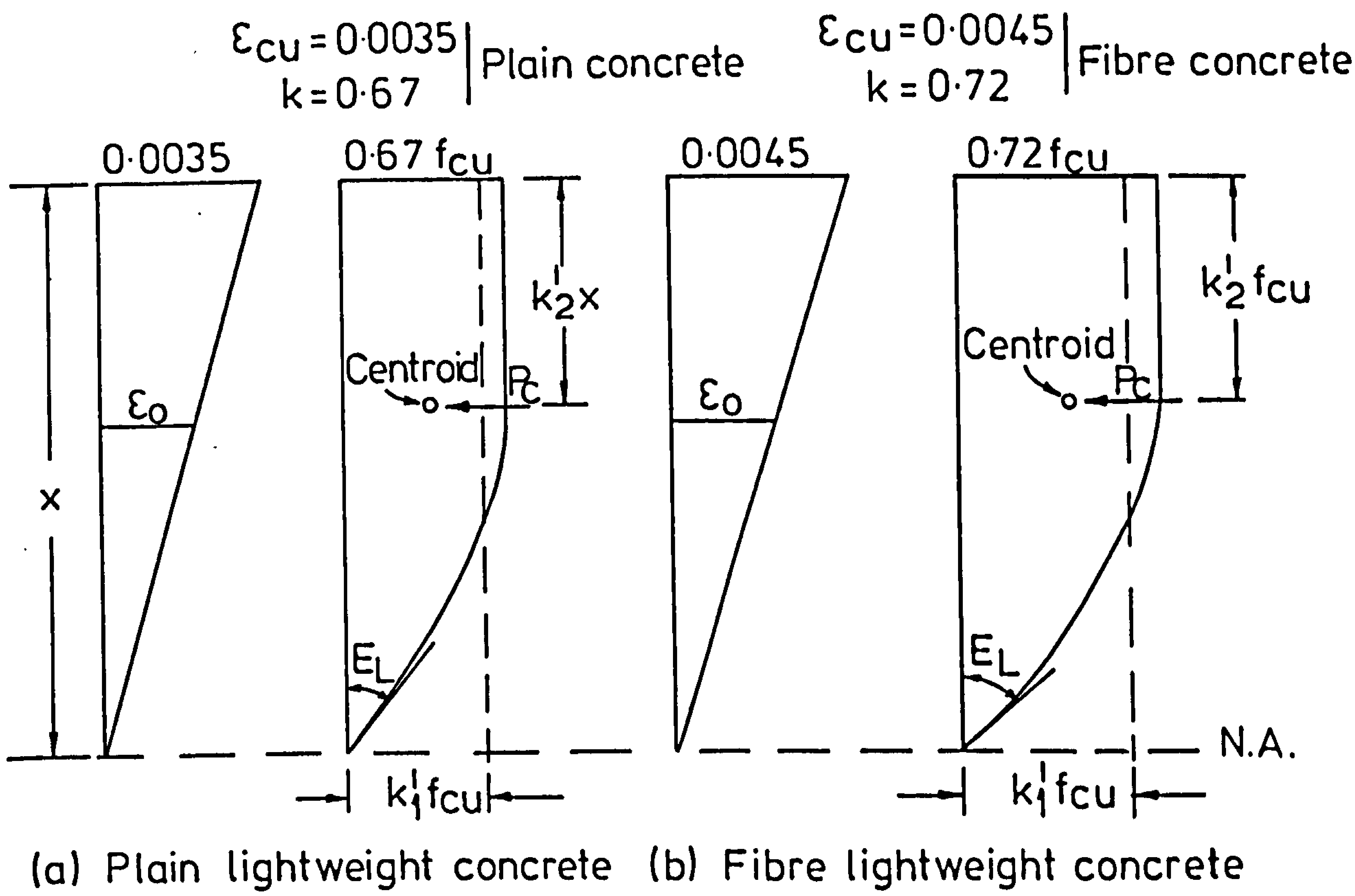

FIG. 7·10 MODIFIED CP 110'S COMPRESSIVE STRESS BLOCK AND STRAIN DISTRIBUTION FOR LIGHTWEIGHT CONCRETE and $$\varepsilon_s = \varepsilon_{cu} \frac{d-x}{x} \quad ..... \quad (7.20)$$

The forces on the cross-section can be expressed in terms of the following characteristics:

1. Concrete compression, $F_c = K_1' f_{cu} b' x$ (Fig.7.10)
2. Concrete tension (contribution of fibres), $F_f = \sigma_{cu} b' (h-x)$
3. Reinforcement compression, $F'_s = A'_s . f'_s$
4. Reinforcement tension, $F_s = A_s f_s$

   where the steel tensile stress is related to the strain ε_s by the corresponding stress-strain curve and $f'_s = E'_s \varepsilon'_s$.

Referring to Fig.7.6(c) the equilibrium equation is:

$$F_c + F'_s = F_f + F_s \qquad \text{or}$$

$$K_1' f_{cu} b' x + A'_s f'_s = \sigma_{cu} b' (h-x) + A_s f_s \quad ..... \quad (7.21)$$

Taking moments about the N.A for each force

1. Concrete compression, $M_1 = K'_1 f_{cu} b' x (x-K'_2 x)$
2. Concrete tension, $M_2 = \sigma_{cu} b' (h-x) \frac{(h-x)}{2}$ ..... (7.22)
3. Reinforcement compression, $M_3 = A'_s f'_s (x-d')$
4. Reinforcement tension, $M_4 = A_s f_s (d-x)$

Considering the value of the width of cross-section, b', as unity, the ultimate moment of resistance per unit width of the cross-section to be used in the yield line theory is given by:

$$M = M_1 + M_2 + M_3 + M_4 \quad ..... \quad (7.23)$$

7.6.3 Evaluation Procedure.

The steps to be followed for the evaluation of the ultimate moment of resistance per unit width of the slab are the following:

1. The value of ε_o is found by substituting for f_{cu} in equation 7.13.

2. The values of stress block parameters are calculated by substituting ε_o in equations 7.14 and 7.15 in the case of normal weight concrete and in equations 7.16 and 7.17 in the case of lightweight concrete. The values of ε_{cu} and K in the above equations are 0.0035 and 0.67, and 0.0045 and 0.72 for plain concrete and fibre concrete respectively.

3. Using an assumed value of neutral axis depth, x, the strain in the tension reinforcement, ε_s, is calculated from Eqn. 7.20 and the strain ε'_s from Eqn. 7.19.

4. The value of f_s corresponding to ε_s is obtained by referring to the steel stress-strain curve in Fig.3.3.

5. Substituting the K_1 or K'_1 and f_s values obtained, in the equilibrium equation 7.21, a quadratic equation in x is obtained and hence a new value of x is calculated.

If the two values of x are equal, then the assumed value of x is the true neutral axis depth. If not, this procedure is repeated from step 3 until two consecutive values of x are found to be close to each other and the final value of x is taken as the average of the last two values.

The ultimate moment of resistance of the cross section is calculated from Equations 7.22 and 7.23.

All the results obtained with the procedure outlined above for the slabs FS-6, FS-7, FS-11 and FS-17, which failed in flexure are tabulated in Table 7.5. From this Table it can be seen that the effect of the fibres is to check the upward movement of the neutral axis (column 5). For example, the neutral axis depth at the ultimate limit in the case of plain concrete sections of the slabs FS-7 (ρ=0.3710%) and FS-11 (ρ=0.5574%) was 11.09 and 15.41 mm respectively, whereas in the case of fibre concrete sections, the neutral axis depth was 15.51 and 19.67 mm for slabs FS-7 and FS-11 respectively. Thus, the increase in the neutral axis depth due to

Table 7.5 Results of ultimate flexural strength analysis according to CP110 modified compressive stress block.

Slab Number	Fibre Type	f_{cu} N/mm^2	σ_{cu} N/mm^2	X mm	ε_c	ε_o	ε_s	ε'_s	M_1^* KN.m/m	M_2^* KN.m/m	M_3^* KN.m/m	M_4^* KN.m/m	M^* KN.m/m
1	2	3	4	5	6	7	8	9	10	11	12	13	14
FS-6	-	45.0	0.0	8.22	0.0035	0.00163	0.03907	-	0.942	0.0	0.0	17.632	18.574
	Crimped	44.6	1.736	14.48	0.0045	0.00162	0.02658	-	3.214	10.602	0.0	16.429	30.245
FS-7	-	45.0	0.0	11.09	0.0035	0.00163	0.02805	0.00376	1.714	0.0	0.799	17.080	19.593
	Crimped	45.8	1.736	15.51	0.0045	0.00164	0.02460	0.00217	3.779	10.406	0.291	16.232	30.708
FS-11	-	45.0	0.0	15.41	0.0035	0.00163	0.01921	0.00172	3.308	0.0	0.545	24.377	28.230
	Crimped	42.8	1.736	19.67	0.0045	0.00159	0.01837	0.00076	5.703	9.629	0.105	23.148	38.586
FS-17	-	57.5	0.0	13.57	0.0035	0.00184	0.02229	0.00243	3.200	0.0	0.957	24.908	29.065
	Paddle	58.56	1.671	16.24	0.0045	0.00185	0.02321	0.00187	5.226	9.877	0.528	24.138	39.769

*Moments are based on 1 m width.

NOTES: 1) 1.0% by volume fibres around the column were used in all four slabs.

2) ρ = 0.3716% for slabs FS-6 and FS-7.
ρ = 0.5574% for slabs FS-11 and FS-17.

addition of fibres was 39.8% for slab FS-7 and 26.8% for slab FS-11.

From Table 7.5 it can be seen that the contribution of the compressive reinforcement (column 12) on the ultimate moment of resistance (column 14) is very small as compared to the contribution of the tension reinforcement (column 13).

By using a value of 1.0 for coefficient A in equations 7.16 and 7.17 i.e. considering no distinction between normal and lightweight concrete in compression zone a higher value of about 0.6% is obtained for the ultimate moment of resistance of the slabs, which is almost negligible.

A unique moment, m, can be found (Appendix A) along a yield line from the two values obtained for each slab corresponding to plain and fibre reinforced sections, to be used in Equation 7.1 or 7.4 for the calculation of the ultimate flexural strength of the slabs.

7.7 Results and Discussion.

The maximum experimental load values of all slabs with steel fibres tested in this investigation and failing in flexure as well as those computed by using the ultimate strength analysis carried out in the previous sections of this chapter are shown in Table 7.6. Values in column 10 are those obtained by using the CP110 modified concrete compressive stress blocks and strain distribution for lightweight and fibre, and those in column 13 obtained by using ACI modified stress blocks and strain distribution. It can be seen that both sets of values are almost of the same magnitude, which is an indication that the difference between the two stress-strain blocks used, is not of great importance. The average of the ratios and standard deviations of calculated to test values of maximum flexural load for slabs FS-6, FS-7, FS-11 and FS-17 are shown in columns 11 and 14, being 0.988 and 0.043, and 0.992 and 0.044 for CP110 and ACI modified stress-strain curves respectively, giving a good support of the proposed theory.

Table 7.6 Comparison of Experimental and Calculated Ultimate Flexural Strength of Slabs (CP110*, ACI*)

Slab No.	Column Size in mm	Reinforcement Distribution	Tension Steel Reinforcement ratio $\rho = \frac{A_s}{bd}$	Steel fibre Location	Experimental Max. Flexural Load in KN	CP110*					ACI*		
						m in KN.m/m	m′ in KN.m/m	$\lambda = \frac{m'}{m}$	$V^F_{U.F}$, $V_{calc.}$ in KN	$\frac{V_{calc.}}{V_{test}}$	m in kN.m/m	$V^F_{U.F}$, $V_{calc.}$ in kN	$\frac{V_{calc.}}{V_{test}}$
1	2	3	4	5	6	7	8	9	10	11	12	13	14
FS-6	150	Equal Spacing	0.003716	Distributed only for 550 mm from centre	174.3	25.773	0.0	0.0	161.936	0.929	25.821	162.238	0.931
FS-7	150	"	0.003716		192.4	26.449	7.179	0.272	195.896	1.018	26.516	196.392	1.021
FS-11	200	"	0.005574		259.8	34.468	13.537	0.393	265.578	1.022	34.613	266.564	1.026
FS-17	150	"	0.005574		268.4	35.669	13.817	0.384	264.184	0.984	35.867	265.651	0.990
			Average of the ratios Standard Deviation							0.988 0.043			0.992 0.044

*Modified stress-strain curves.

Table 7.7 Comparison of experimental and calculated Ultimate Flexural Strength of Slabs ($f_s = f_y$)

Slab No.	Exp. Max. Flexural Load in kN	CP110*						ACI*					
		m in kN.m/m	$V^F_{U.F'}$ $V_{calc.}$ in kN	$V_{calc.}/V_{test}$	m in kN.m/m	$V^F_{U.F'}$ $V_{calc.}$ in kN	$V_{calc.}/V_{test}$	m in kN.m/m	$V^F_{U.F'}$ $V_{calc.}$ in kN	$V_{calc.}/V_{test}$	m in kN.m/m	$V^F_{U.F'}$ $V_{calc.}$ in kN	$V_{calc.}/V_{test}$
1	2	3	4	5	6	7	8	9	10	11	12	13	14
		$f_s = f_y$			$f_s > f_y$			$f_s = f_y$			$f_s > f_y$		
FS-6	174.3	23.863	149.94	0.860	25.773	161.946	0.929	23.905	150.20	0.862	25.821	162.238	0.931
FS-7	192.4	24.641	182.51	0.949	26.449	195.896	1.018	24.697	182.92	0.951	26.516	196.392	1.021
FS-11	259.8	31.867	245.42	0.945	34.485	265.578	1.022	31.984	246.32	0.948	34.613	266.564	1.026
FS-17	268.4	33.002	244.43	0.911	35.669	264.184	0.984	33.187	245.80	0.916	35.867	265.651	0.990
Average ratios Standard Deviation				0.916 0.041			0.988 0.043			0.919 0.041			0.992 0.044

*Modified stress-strain curves.

Table 7.7 shows the calculated values of the maximum flexural load for all the four slabs obtained by using the proposed analysis but as steel stress equal to the yield stress (f_y = 460 N/mm^2). For comparison purpose the same values for values of f_s of about 520 N/mm^2 i.e. greater than f_y are also presented, from Table 7.6. It can again be seen that there is no significant difference between the values obtained by using modified CP110 and ACI code of practice compression stress-strain curves and that the use of steel yield stress in the proposed analysis gives an underestimation of the actual test load of about 8%.

Table 7.8 shows the theoretical increase of the flexural strength of the slabs due to the inclusion of fibres in the entire slabs. The values in columns 3 and 4 are those found in column 14 of the Table 7.5 for plain and fibre concrete respectively. It can be seen that the theoretical percentage increase depends mainly upon the tensile reinforcement ratio being 56.7 (FS-7) and 36.7% (FS-11) for 0.3716 and 0.5574% tensile reinforcement ratio respectively. (Value of stress block of the fibres equal to 1.736 N/mm^2, Table 7.5). Unfortunately, in this investigation there are no plain concrete slabs and corresponding fibre concrete slabs, both failing in flexure, to verify the above calculated theoretical increases. However, Lamoureaux (43) reported experimental percentage increases in flat slabs failing in flexure due to presence of fibres of about 28.8% (fibre stress block equal to 1.236 N/mm^2) to 31.6% (fibres stress block equal to 1.776 N/mm^2) for normal weight concrete and 33% (fibre stress block equal to 0.93 N/mm^2) for lightweight concrete, with a tensile steel reinforcement ratio of 0.5574% equal to this used in slabs FS-11, and FS-17 in Table 7.8. Criswell (77) reported that the above mentioned experimental percentage increase was 27.2% (fibre stress block

Table 7.8 Theoretical effect of fibres on flexural strength (Fibres for the whole slab).

Slab No.	Reinforcement ratio	Ultimate moment, m, in kN. m/m		$\frac{(4)}{(3)}$	Percentage increase (4)/(3)
		Plain	Fibre		
1	2	3	4	5	6
FS-6	0.003716	18.574	30.245	1.628	62.8
FS-7	0.003716	19.593	30.708	1.567	56.7
FS-11	0.005574	28.230	38.586	1.367	36.7
FS-17	0.005574	29.066	39.769	1.368	36.8

Table 7.9 Comparison of experimental and calculated ultimate flexural strengths of slabs from various investigations.

Investigator	Slab No.	Slab size (square) in mm	Slab effective depth in mm	Column size in mm	Reinforcement distribution	Tension steel Rein. ratio %	Type of fibres, percentage	Steel fibre location	Type of Concrete, cube strength in N/mm^2	Steel stress	Fibre stress block in N/mm^2	Exp.Max. Flexural Load V_{test} in KN	$V^F_{U.F}$, $V_{calc.}$ in KN	$\frac{V_{calc.}}{V_{test}}$
	1	2	3	4	5	6	7	8	9	10	11	12	13	14
Ali Sami (78)	S-9	1690	100	150	Reinf. Concentration under column	-	Crimped 0.9	Distribution for only 512.5 mm from centre	normal weight 51.55	$f_y < f_s$	1.838	179.3	163.43	0.911
	S-10	1690	100	150		-	Crimped 0.9		normal 46.50	$f_y < f_s$	1.838	203.0	179.29	0.883
	S-16	1690	100	150		-	Crimped 0.9		normal 38.99	$f_y < f_s$	1.838	213.0	193.31	0.908
		Average of the ratios Standard Deviation												0.901 0.013
												Moment, m KN.m/m		
Lamoureaux (43)	ST-1	2083	101.6	162.1	equal spacing	0.5575	Plain 1.21	entire slab	normal 35.03	$f_y = f_s$	1.236	33.935	31.005	0.914
	ST-2	2083	101.6	162.1	"	0.5574	Plain 1.74	entire slab	normal 32.0	$f_y = f_s$	1.776	34.69	33.814	0.975
	ST-3	2083	101.6	162.1	"	0.5575	Plain 0.91	entire slab	Light weight 43.26	$f_y = f_s$	0.93	30.57	29.547	0.967
		Average of the ratios Standard Deviation												0.952 0.027
Criswell (77)	1	635	38.1	114.3	equal spacing	1.04	Plain 1.0	equal distrib.	normal 52.6	$f_y = f_s$	1.021	63.38	57.28	0.904

Table 7.10 Calculated ultimate flexural strength of slabs failing in punching shear.

Slab No.	Ultimate Punching Strength in KN	CP110*		ACI*	
		Ultimate moment of resistance in kN.m/m	Flexural Strength in kN	Ultimate moment of resistance in kN.m/m	Flexural Strength in kN
1	2	3	4	5	6
FS-1	175.1	28.169	208.64	28.318	209.74
FS-2	225.0	31.523	233.48	31.645	234.38
FS-3	247.4	34.741	257.31	34.872	258.28
FS-4	224.4	34.353	254.44	34.434	255.04
FS-5	198.1	26.965	199.72	27.063	200.44
FS-8	150.3	28.289	201.72	28.447	202.84
FS-9	216.6	34.864	248.60	34.995	249.54
FS-10	191.4	28.226	217.38	28.423	218.90
FS-12	217.5	31.704	234.82	31.813	235.63
FS-13	235.7	34.301	254.05	34.426	254.98
FS-14	239.5	34.453	255.18	34.581	256.13
FS-15	238	33.736	249.87	33.854	250.74
FS-16	227.8	33.467	247.88	33.526	248.32
FS-18	166.0	30.494	225.85	30.536	226.17
FS-19	136.5	20.188	149.52	20.299	150.35
FS-20	211.0	30.226	223.87	30.327	224.62

*Modified stress-strain curves.

equal to 1.021 N/mm^2) for normal weight concrete with a 1.04% tensile steel reinforcement ratio. Ali (78) also reported an experimental percentage increase in ultimate load of flat slabs of 37% (fibre stress block equal to 1.838 N/mm^2 but fibres were distributed only for 512.5 mm from the centre of a 1690 mm square slab).

The proposed method was applied to analyze some fibre reinforcee concrete flat slabs tested by Ali (78), Lamoureaux,and Criswell (77) and the results are shown in Table 7.9. The calculation of the ultimate moment of resistance of the slabs tested by Ali (78) is presented in Appendix B. The average ratios of the calculated flexural load to test flexural loads and the standard deviation obtained give good support of the proposed method.

Table 7.10 shows the ultimate flexural strength of all flat slabs tested in this investigation, that the slabs would have had if premature shear failures had not taken place. It can be seen that the calculated ultimate flexural load for any slab is greater than the experimental ultimate shear punching load.

7.8 Prediction of Flexural Strength of Slabs by Steel fibres Conversion.

In this section the ultimate flexural strength of slabs is calculated by converting the amount of fibres in a slab in equivalent number of steel bars of the same weight.

The equivalent number of steel bars can be found as follows:

1. Volume of concrete where the fibres are dispersed, V,

$$V = 1.1 \times 1.1 \times 0.125 \ m^3 = 0.15125 \ m^3$$

2. Volume of fibres, V_F,

$$V_F = V_f \times V \quad \text{where } V_f = \text{volume fraction of fibres.}$$

$$V_F = 0.01 \times 0.15125 \ m^3 = 0.0015125 \ m^3$$

3. Assuming that the weight of steel fibres is 7800 kg per cubic meter the weight of fibres in a slab is given by:

$$W_F = 7800 \times 0.0015125 \text{ Kg} = 11.80 \text{ Kg}.$$

4. Considering that the weight per meter for 8 mm and 10 mm diameter steel bars is 0.395 Kg/m and 0.617 Kg/m respectively and that the length of each steel bar is 2.0 m, it can easily be found that 6 bars of 10 mm and 6 bars of 8 mm in diameter give a total weight almost equal to 12.14 Kg, which is very close to the weight of fibres.

$$6 \times (0.395 \times 2.0) + 6 \times (0.617 \times 2.0) = 4.74 + 7.40 = 12.14 \text{ Kg}.$$

5. Number of steel bars in each direction:

   3 x 8 mm and 3 x 10 mm

6. Area of steel bars in each direction:

$$A_e = 3 \times 50.3 + 3 \times 78.5 = 150.9 + 235.5 = 386.4 \text{ mm}^2$$

7. The steel reinforcement ratio corresponding to this equivalent area of steel reinforcement is:

$$\rho_e = A_e/b'd = 386.4/1690 \times 100 = 0.002286.$$

The ultimate flexural strength can now be calculated by using yield line theory where for the calculation of the ultimate moment of resistance a new reinforced ratio is used equal to that used in slabs plus the reinforcement ratio ρ_e.

Table 7.11 shows the new calculated ultimate flexural strength of the slabs FS-6, FS-7, FS-11 and FS-17 by using the above described method i.e. by converting the amount of steel fibres into an equivalent number of steel bars of the same weight. It can be seen that the average percentage increase of the flexural strengths is 9.5% against test values (column 9) and 10.9% against calculated values (column 10) using the proposed method (Section 7.6). The higher values of the flexural strengths in the case of

Table 7.11 Calculated flexural strength using fibre conversion method.

Slab No.	Fibre Type, V_f	Steel rein. ratio, ρ	New steel rein. ratio $\rho + \rho_e$	V_{test} in KN	$V_{calc.}$ in KN (column 7 in Table 7.7)	New moment of resistance μ_e in KN.m/m	New flexural strength, $V^N_{calc.}$ in KN	$\frac{V^N_{calc.}}{V_{test}}$ $(\frac{(8)}{(5)})$	$\frac{V^N_{calc.}}{V_{calc.}}$ $(\frac{(8)}{(6)})$
1	2	3	4	5	6	7	8	9	10
FS-6	Crimped 1%	0.003716	0.00600	174.3	161.936	29.142	183.10	1.050	1.131
FS-7	Crimped 1%	0.003716	0.00600	192.4	195.896	29.557	218.92	1.138	1.118
FS-11	Crimped 1%	0.005574	0.00786	259.8	265.578	37.849	291.49	1.122	1.098
FS-17	Paddle 1%	0.005574	0.00786	268.4	264.185	38.823	287.55	1.071	1.088
Average of ratios Standard Deviation								1.095 0.036	1.109 0.017

equivalent number of steel bars could be explained in terms of steel stress; the additional reinforcement is allowed to develop a stress (of about 520 N/mm^2), which is higher than the average fibre stress being 423.3 and 407.4 N/mm^2 for crimped and paddle fibre respectively. (Example of the calculation of the average fibre stress is given in section 7.9).

From what has been discussed above, one could say that for a given weight of steel, the use of steel bars will give a higher ultimate flexural strength than that obtained by using the same weight of steel fibres, if the steel stress is higher than the average fibre stress. However, this does not necessarily mean that the conversion of a given weight of fibres into an equivalent number of steel bars is desirable, because the replacement will increase the flexural strength of the slab but the new slab being a slab without fibres might fail in punching shear. For example, let us consider the two slabs FS-1 and FS-7 tested in this investigation. The slab FS-1 is a plain lightweight concrete slab with a tensile reinforcement ratio of 0.005574, which failed in punching shear at 173.5 kN. The slab FS-7 has a tensile reinforcement ratio of 0.003716 and fibres distributed for 550 mm from the centre and failed in flexure at 192.4 kN. The conversion of fibres gives a slab without fibres with a tensile steel reinforcement ratio of 0.00600, which is a bit higher than that of the slab FS-1. This conversion would theoretically increase the flexural load from 192.4 kN to 218.92 kN but the new slab being a plain concrete slab would fail in punching shear at a load of about 173.5 kN as obtained for slab FS-1.

7.9 A Simple Expression for the Ultimate Moment of Resistance of a Fibre Concrete Section.

The ultimate moment of resistance of a plain concrete section according to ACI code of practice (68) is given by:

$$m = \rho f_y d^2 (1 - 0.59 \frac{\rho f_y}{f_c'}) \quad ..... \quad (7.24)$$

where ρ = tensile steel reinforcement ratio.

f_y = steel yield stress.

d = effective depth.

f_c' = cylinder cube strength ($f_c' = 0.79 f_{cu}$).

In this section a similar simple formula for a fibre concrete section is proposed. The modified ACI rectangular stress block for fibre concrete Fig.7.8(b)) is used instead of CP110 rectangular-parabolic because of its simplicity and since differences of the results obtained by using the two stress blocks are not of great importance as discussed in section 7.7.

Consider a volume of matrix V where a total number of fibres N are randomly dispersed. The volume fraction of fibres is given by:

$$V_f = \frac{N(\pi d_f^2/4)\ \ell_f}{V} \quad ..... \quad (7.25)$$

The average spacing of the centroids of fibres is given by: (19)

$$S = \sqrt[3]{\frac{V}{N}} \quad ..... \quad (7.26)$$

Since only 41% of the fibres are effective in any direction

$$S_e = \sqrt[3]{\frac{V}{0.41\ V_f}} \quad ..... \quad (7.27)$$

and the number of centroids per unit area of any cross-section is

$$N_1 = (\frac{1}{S_e})^2 \quad ..... \quad (7.28)$$

Since usually the fibre length, ℓ_f, is greater than S_e the fibres will extend to cross-sections previously allocated to other fibres. This will create an overlapping leading to an increase of the number of fibres by the factor $\frac{\ell_f}{S_e}$ and hence the number of fibres at a cross-section is given by

$$N_a = (\frac{1}{S_e})^2 \frac{\ell_f}{S_e} = \frac{0.41\ N\ \ell_f}{V} \quad \ldots\ldots \quad (7.29)$$

after combining with equation 7.27.

Combination of equations 7.29 and 7.25 gives

$$N_a = \frac{0.41\ V_f}{\pi d_f^2/4} \quad \ldots\ldots \quad (7.30)$$

and hence, the area of fibres per unit area of cross-section is:

$$\frac{A_{SF}}{\text{unit area}} = N_a \frac{\pi d_f^2}{4} = 0.41\ V_f \quad \ldots\ldots \quad (7.31)$$

This means that

$$\rho_f' = 0.41\ V_f \quad \ldots\ldots \quad (7.32)$$

where ρ_f' = "fibre reinforcement ratio".

It is now assumed that the fibres are replaced by steel reinforcement placed at a distance (h-x)/2 from the bottom of the cross-section having a reinforcement ratio equal to ρ_f', and working at a stress equal to average fibre stress, σ_f^{av}. To transfer the action of the fibres from point A (Fig.7.11(a)) to the centroid of steel reinforcement (point B), but giving the same moment about the neutral axis a coefficient μ_1 is introduced (Fig.7.11(b)) equal to

$$\mu_1 = \frac{(h-x)/2}{d-x} \quad \ldots\ldots \quad (7.33)$$

To use the steel yield stress, f_y, for the equivalent reinforcement a coefficient μ_2 is introduced (Fig.7.11(c)) equal to

$$\mu_2 = \frac{\sigma_f^{av}}{f_y} \quad \ldots\ldots \quad (7.34)$$

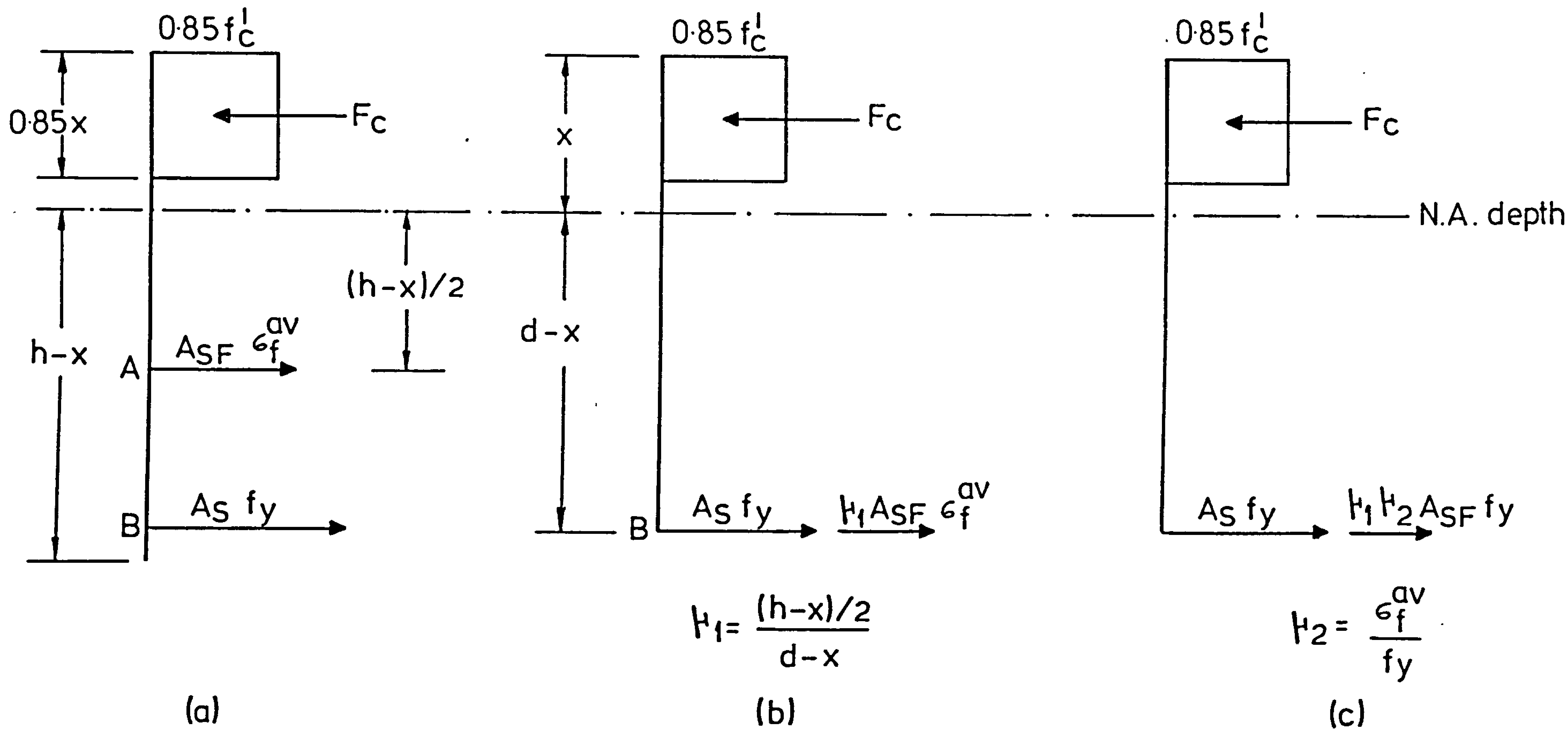

FIG. 7·11 REPLACEMENT OF FIBRES BY STEEL REINFORCEMENT

Using equations 7.32, 7.33 and 7.34 it can be said that the fibres can be replaced by steel reinforcement placed at the level of the reinforcing bars with an equivalent reinforcement ratio equal to:

$$\rho_f = \rho_f' \mu_1 \mu_2 \qquad \ldots\ldots \qquad (7.35)$$

To find coefficient μ_1 from equation 7.33 a value of the neutral axis depth, x, must be assumed. It has been found from the section 7.6.3 (Table 7.5) that the average neutral axis locations for Slabs FS-6, FS-7, FS-11 and FS-17 with fibres, failing in flexure, is 0.867 h from the tension face of the slab. Ali (78) and Lamoureaux (43) found this value at failure 0.804h and 0.849h respectively. Therefore, the choice of a value equal to 0.85h for the location of neutral axis from the tension face seems to be reasonable.

The equation 7.24 can now be modified to give the ultimate moment of resistance for a fibre concrete section

$$m = (\rho + \rho_f)\, f_y\, d^2 \left(1 - 0.59 \frac{(\rho+\rho_f)\, f_y}{f_c'}\right) \qquad \ldots\ldots \qquad (7.36)$$

The steps to be followed for the evaluation of the ultimate moment of resistance for a fibre concrete section are the following:

1. Calculate $\rho_f' = 0.41\, V_f$

2. Calculate σ_f^{av}

   a) for $\ell_f < \ell_c$ $\quad \sigma_f^{av} = \frac{1}{2}\sigma_f = \frac{1}{2}\, 2\tau \frac{\ell_f}{d_f} = \tau \frac{\ell_f}{d_f}$

   where σ_f = maximum fibre stress at which fibre pull-out occurs

   b) for $\ell_f > \ell_c$ $\quad \sigma_f^{av} = (1 - \frac{\ell_c}{2\ell_f})\; \sigma_{fcu}$

3. Calculate $\mu_1 = \dfrac{h-0.15h}{2(d-0.15h)}$

   and $\mu_2 = \dfrac{\sigma_f^{av}}{f_y}$

4. Calculate the equivalent steel reinforcement ratio, ρ_f.

$$\rho_f = \mu_1 \mu_2 \rho_f'$$

5. Calculate the ultimate moment of resistance per unit width from equation 7.3.6. In this equation the effect of compressive reinforcement has been neglected being very small as discussed in Section 7.7.

The evaluation of the ultimate moment of resistance per unit width for slab FS-11 is produced here as an example.

<u>Data</u>: $f_{cu} = 42.8$ N/mm^2, $f_c' = 0.85\text{x}42.8 = 36.38$ N/mm^2

$\ell_f = 50$ mm

$d_f = 0.50$ mm

$\tau = 4.233$ N/mm^2

$\sigma_{fu} = 1920$ N/mm^2

$V_f = 1\%$

$\rho = 0.005574$

$f_y = 460$ N/mm^2

$h = 125$ mm, $d = 100$ mm, $b = 1000$ mm

$\therefore$ 1. $\rho_f' = 0.41\text{x}0.01 = 0.0041$

2. $\sigma_f^{av} = 4.233 \text{ x } \dfrac{50}{0.50} = 423.3$ N/mm^2

3. $\mu_1 = \dfrac{0.85\text{x}125}{2(100-0.15\text{x}125)} = 0.654$

$\mu_2 = \dfrac{423.3}{460} = 0.920$

4. $\rho_f = 0.654\text{x}0.920\text{x}0.0041 = 0.002467$

5. $m = 0.008041\text{x}460\text{x}100^2 \left(1 - 0.59 \dfrac{0.008041\text{x}460}{36.38}\right)$

$= 34.77$ KN.m/m

The value of ultimate moment of resistance for the above fibre concrete section obtained by using the proposed method with steel stress equal to yield stress is 36.094 KN.m/m i.e. 3.8% higher than 34.77 KN.m/m and this small difference can be attributed to the fact that the above outlined procedure neglects the effect of compressive reinforcement and that an approximate value of the neutral axis depth was used to calculate the coefficient μ_1.

Table 7.12

Slab No. 1	Ultimate moment of resistance of a fibre concrete section, m, KN.m/m — Empirical Method 2	Ultimate moment of resistance of a fibre concrete section, m, KN.m/m — Proposed Theor. Method 3	Ratio $\frac{(3)}{(2)}$ 4
FS-6	27.182	28.436	1.046
FS-7	27.215	28.970	1.064
FS-11	34.770	36.094	1.038
FS-17	34.98	37.27	1.065
		Average of ratios	1.053
		standard deviation	0.012

Table 7.12 shows the ultimate moment of resistance for slabs FS-6, FS-7, FS-11, and FS-17 failing in flexure with the procedure outlined above (column 2) and with the proposed theoretical method by using ACI modified compressive stress block and with $f_s = f_y$ (column 3). It can be seen that values of column 3 are only greater than those of column 2 by an average of about 5% for reasons discussed earlier, and therefore it can be said that equation 7.36 is an easy way to calculate the ultimate moment of resistance per unit width of a fibre concrete section. Note that by putting $\rho_f = 0$ in equation 2.36 the equation 7.24 is obtained, which is used for the calculation of the ultimate moment of resistance for plain reinforced concrete sections.

7.10 Conclusions.

Based on the results presented in this chapter the following conclusions can be drawn:

1. The ultimate flexural strength of flat slabs reinforced with steel bars in the two directions and steel fibres may be satisfactorily predicted by using a) the method presented in this chapter to evaluate the ultimate moment of resistance per unit width and b) the yield line theory to calculate the ultimate load.

2. The average of ratios of the calculated to test strengths were 0.988, 0.901 and 0.952 for slabs tested in this investigation, by Ali (78) and by Lamoureaux (43) respectively. The contribution of the compressive steel reinforcement in the flexural strength is almost negligible.

3. The theoretical percentage increase in the flexural strength of a slab due to incorporation of a given volume fraction of fibres depends primarily upon the tensile steel reinforcement ratio; this percentage increase was 56.7 and 36.7 in the slabs FS-7 ($\rho = 0.3716\%$) and FS-11 ($\rho = 0.5574\%$) respectively when 1.0% by volume crimped fibres were used. This theoretical percentage increase is supported only by few test results and further research is needed.

4. The values of ultimate flexural strengths obtained by using the modified compressive stress blocks and strain distributions for fibre concrete sections, of those recommended by CP110 (69) and ACI code of practice (68) for plain concrete sections, are of the same magnitude.

5. The conversion of a given weight of fibres into an equivalent number of steel bars of the same weight increases the ultimate flexural load by an average of about 11%but it is not always desirable because a premature punching shear failure may take place giving eventually a lower load.

6. Equation 7.36 constitutes an easily-applied method for the calculation of the ultimate moment of resistance of a fibre concrete section for design purposes.

7. More research is needed on the application of steel fibres in flat slabs, failing in flexure, using different types of fibres and a wide range in the values of tensile steel reinforcement ratio.

APPENDIX A.

In the slabs tested in this investigation the steel fibres were located within the square ABCD (Fig.A.1) at a distance 550 mm from the slab centre and therefore two different values for ultimate moment of resistance exist along each yield line. The moments M_f and M_p along the yield line JLM corresponding to fibre concrete section and plain concrete section respectively can be calculated according to the proposed method. Once these moments are known unique value of the ultimate of resistance of the yield line and the ultimate load can be evaluated as follows

Section I (EFGH) rotation $\theta_I = \dfrac{2}{\ell-r}$

Section II (EHN) rotation $\theta_{II} = \dfrac{\sqrt{2}}{\ell-x_1-r}$

Corner levers will form permitting the slab corners to lift by rotation about the axes K-K. Assuming a deflection of unity at the column, the principle of virtual work gives

$$V_{flex} = 4\,M_f\,(\ell-2x_1-\ell_2)\,\frac{2}{\ell-r} + 4\,M_p\,\ell_2\,\frac{2}{\ell-r} + 4\,M_f\,c\,\frac{\sqrt{2}}{\ell-x_2-r} + 4\,M_p\,e\,\frac{\sqrt{2}}{\ell-x_1-r} \qquad \text{.....} \qquad (A.1)$$

By geometry

$$\ell_1 = \frac{a}{a+b}(\ell-2x_1) \qquad c = \frac{a}{a+b}\,x_1\sqrt{2}$$
$$\ell_2 = \frac{b}{a+b}(\ell-2x_1) \qquad e = \frac{b}{a+b}\,x_1\sqrt{2} \qquad \text{.....} \qquad (A.2)$$

By substituting equation A.2 into equation A.1

$$V_{flex} = 4\,M_f\,\frac{a}{a+b}(\ell-2x_1)\,\frac{2}{\ell-r} + 4\,M_p\,\frac{b}{a+b}(\ell-2x_1)\,\frac{2}{\ell-r} +$$
$$4\,M_f\,\frac{a}{a+b}\,2\,\frac{x_1}{\ell-x_1-r} + 4\,M_p\,\frac{b}{a+b}\,2\,\frac{x_1}{\ell-x_1-r}$$

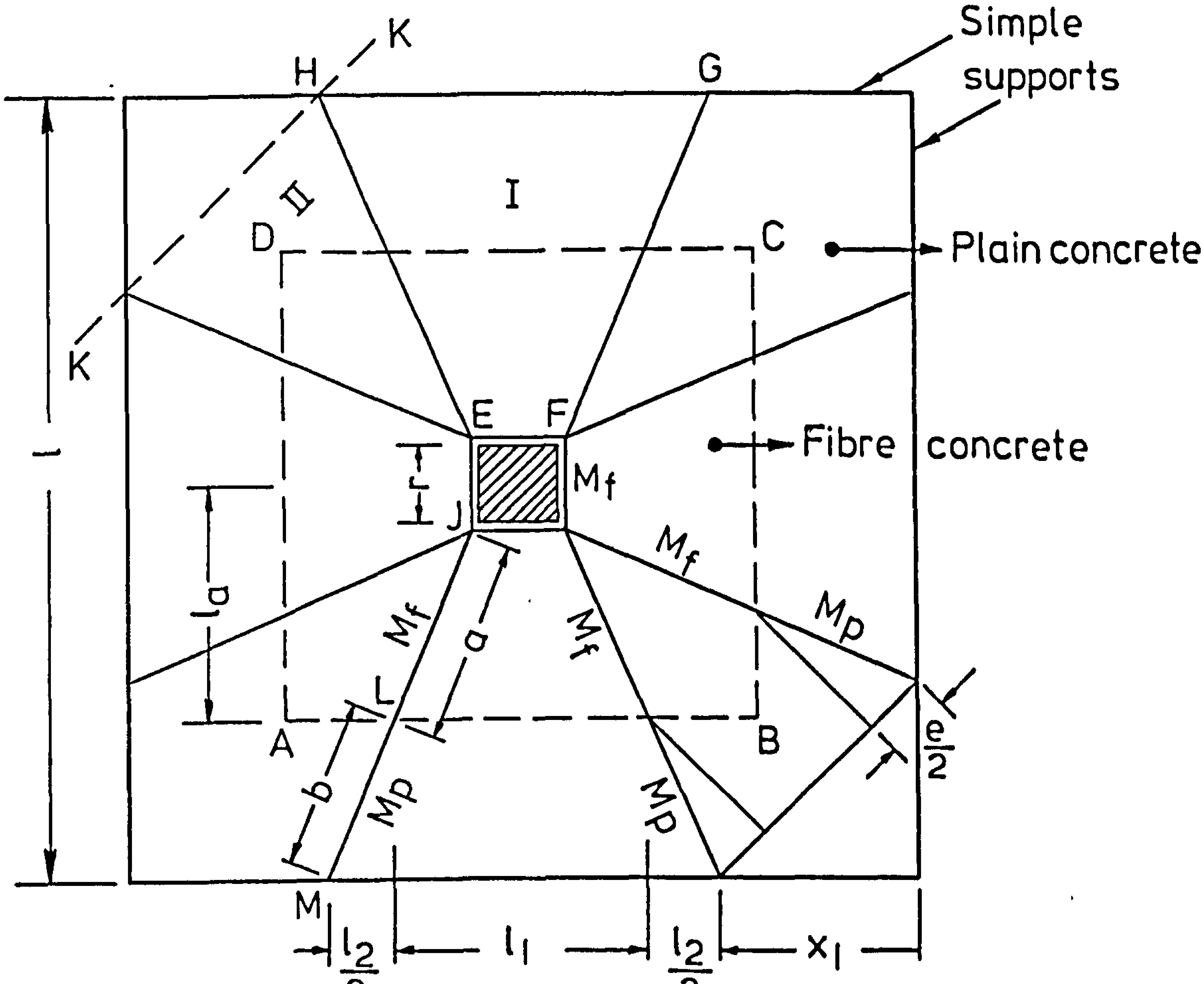

FIG. A1 SQUARE SLAB WITH CORNER LEVERS

or

$$V_{flex} = \frac{8}{\ell-r} \left(\frac{aM_f + bM_p}{a + b}\right) (\ell-2x_1) + 8 \left(\frac{aM_f + bM_p}{a + b}\right) \frac{x_1}{\ell-x_1-r} \quad \ldots \quad (A.3)$$

Putting

$$m = \frac{aM_f + bM_p}{a + b} \quad \ldots\ldots \quad (A.4)$$

$$V_{flex} = \frac{8}{\ell-r}\, m\, (\ell-2x_1) + 8m \frac{x_1}{\ell-x_1-r} \quad \ldots\ldots \quad (A.5)$$

A yield line pattern will develop corresponding to a value of x_1 giving a minimum value of V_{flex}

$$\frac{\partial V_{flex}}{\partial x_1} = 0 \quad \text{gives} \quad x_1 = \left(1 - \frac{\sqrt{2}}{2}\right) (\ell-r) \quad \ldots\ldots \quad (A.6)$$

which substituted into equation A.5 for V_{flex} gives

$$V_{flex} = 8m \left(\frac{1}{1-r/\ell} - 3 + 2\sqrt{2}\right) \quad \ldots\ldots \quad (A.7)$$

where m is now the unique ultimate moment of resistance of the yield line, given by equation A.4.

The evaluation of m for Slab FS-11 is produced here as an example:

M_f = 38.586 KN.m/m

M_p = 28.230 KN.m/m

(From Table 7.5, column 15)

$$m = \frac{a}{a+b} M_f + \frac{b}{a+b} M_p$$

By geometry (Fig.A.1)

$$\frac{a}{a+b} = \frac{\ell_a - r/2}{\frac{\ell-r}{2}} \quad , \quad \frac{b}{a+b} = \frac{\ell/2-\ell_a}{\frac{\ell-r}{2}}.$$

For ℓ_a = 550 mm, ℓ = 1690 mm, r = 200 mm

$$\frac{a}{a+b} = \frac{550-100}{745} = 0.60403 \qquad \frac{b}{a+b} = 0.39597$$

and hence

$$m = 0.60403 \times 38.586 + 0.39597 \times 28.23 =$$

$$= 23.307 + 11.161 = 34.468 \text{ KN.m/m}$$

This is the value of the ultimate moment of resistance for slab FS-11 used in Table 7.6 (column 7).

APPENDIX B.

In the flat slab specimens tested by Ali (78) and failing in flexure there is a concentration of the reinforcement under the column and therefore along the yield line ILM (Fig.B.1) two different values of the ultimate moment of resistance exist. In the square ABCD the moment M_f is the same in the two directions and can be calculated from the contribution of both the band of steel reinforcement and fibres. In the area AEFG there are different values of the moment of resistance in the two directions. Moment M_{1p} can be calculated from the contribution of the band reinforcement in direction x and moment M_{2p} from the steel reinforcement in direction y outside the band reinforcement area (ABCD). The axes of the moments are shown in Fig. B.1.

For the part of the yield line (IL) inside the area ABCD the ultimate moment of resistance is equal to M_f since the moments in the two directions are perpendicular to each other and are of the same magnitude. For the part LM the ultimate moment of resistance is given by:

$$M_p = M_{1p} \operatorname{Cos}^2 \phi_2 + M_{2p} \operatorname{Cos}^2 \phi_1 \qquad \text{or}$$

$$M_p = M_{1p} \operatorname{Sin}^2 \phi_1 + M_{2p} \operatorname{Cos}^2 \phi_1$$

The unique ultimate of resistance of the yield line can now be calculated as in Appendix A.

Table B.1 shows all the relative values for the calculation of ultimate moment of the slabs from Reference (78)

Table B.1

	M_f	M_{1p}	M_{2p}	ϕ_1	M_p	m
S-9	28.943	16.629	12.21	25.344	13.018	22.066
S-10	32.192	20.362	12.21	25.344	13.704	24.207
S-16	35.007	24.050	12.21	25.344	14.379	26.099

where M_f, M_{1p}, M_{2p}, M_p m in kN.m/m
ϕ_1 in degree.

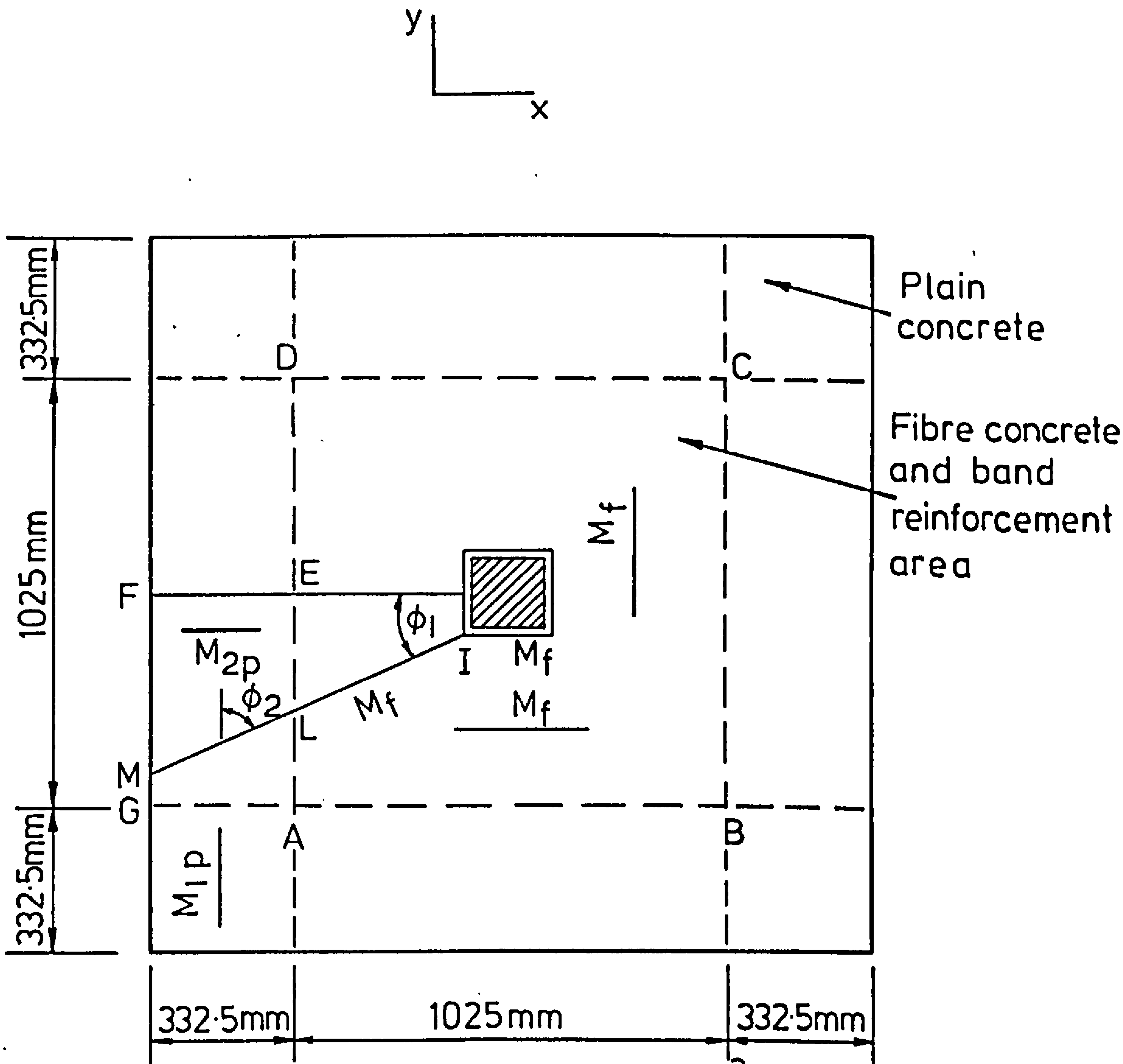

Steel reinforcement mm^2/m

S-9	237·9	306·34	237·9	Ref.(78)
S-10	237·9	382·93	237·9	
S-16	237·9	459·51	237·9	

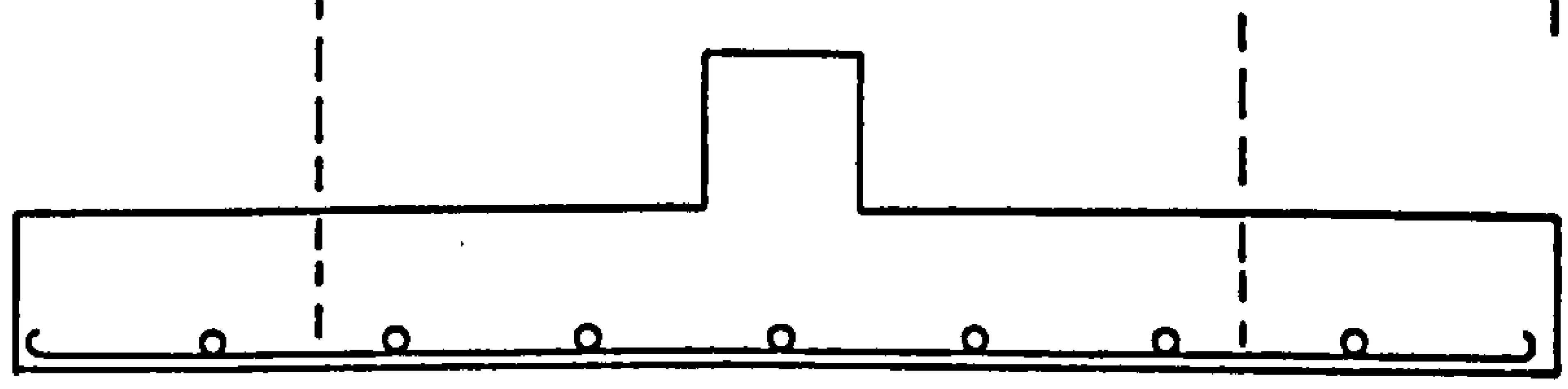

Typical arrangement of steel reinforcement for slab S-16 (Ref. 78)

FIG. B-1 SQUARE SLABS WITH FIBRES FROM REF. 78

CHAPTER 8.

ULTIMATE PUNCHING SHEAR STRENGTH ANALYSIS OF SLABS.

8.1 Introduction.

The ultimate strength of a slab under concentrated load is often determined by shear failure load, smaller than flexural failure load calculated by the yield line theory.

Some variables appear to have a marked effect on the punching shear strength of slabs. These include the concrete strength, the ratio of column size to slab effective depth, the ratio of shear strength to flexural strength, the column shape, the lateral restraints available. At present, the mechanism of shear failure of a reinforced concrete slab remains unsolved. Most research on the shear strength of slabs has been concerned with the generation of experimental data and the development of empirical equations. Few theoretical analyses have been proposed by various investigators (Chapter 2) based on different models. But problems such as stress distribution around column, development of diagonal tension cracks, dowel action effect have been left unsolved, and equations satisfying all conditions have not yet been obtained.

This chapter includes, 1) comparisons between experimental and calculated strengths by applying the existing expressions for predicting the shear strength of a slab, 2) an attempt to develop equations predicting the ultimate punching shear strength of fibre reinforced concrete flat slabs and 3) comparison of strengths obtained by these equations with experimental data from other investigations.

8.2 Ultimate Punching Shear strength of Plain Lightweight Concrete Slabs.

The measured ultimate punching strength of four test slabs without fibre reinforcement (FS-1, FS-8, FS-10 and FS-19) included in this investigation is compared with the capacities given 1) by the three codes of practice, CP110, ACI and CEB-FIP, 2) by the existing expressions for predicting the shear strength of lightweight concrete slabs and 3) by the existing expressions for predicting the shear strength of normal weight concrete slabs.

8.2.1 Comparison of the Test Results with the Methods of CP110, ACI and CEB-FIP Codes.

The calculated shear strengths of all four plain lightweight concrete slabs and of the slab S-1 (78) according to methods of CP110 (69),ACI (67) and CEB-FIP (121) codes as well as the ratios of the calculated to measured strengths are shown in Table 8.1. The average of ratios of the three slabs with ρ = 0.557% according to CP110 design strength is 0.604 with a standard deviation of 0.019. The ratio of slab FS-19 with ρ = 0.3716% is 0.581, which is very close to average of ratios of the slabs with ρ = 0.5574%. The corresponding values according to ACI design method are 0.829 and 1.025 for the slabs FS-1, FS18, FS-10 and FS-19 respectively. The higher value of $V_{u.calc}/V_{test}$ ratio of Slab FS-19 may be attributed to the fact that the ACI code's permissible stresses depend only upon the concrete strength, while CP110takes into account, for the permissible stresses both concrete strength and flexural reinforcement. The calculated design strengths of all four slabs according to CEB-FIP model code (121) (column 10) are very close to those predicted by ACI code (67) (column 8) since the CEB-FIP and ACI code provisions for shear in slabs are very similar. From Table 8.1 it can be seen that CP110's design method underestimates the actual punching strength by about 40% while this underestimation is 12.2% when the ACI design method is used. In the case of normal weight concrete slab S-1 (78) the CP110 and ACI design methods underestimate the actual strength by about 35 and 10% respectively.

The $V_{u.calc}/V_{test}$ ratios according to ACI ultimate strength equation for slabs FS-1 and FS-8 are 0.961 and 0.904 respectively, i.e. less than

Table 8.1 Comparison of experimental and calculated shear strengths of plain concrete slabs according to CP110, ACI and CEB-FIP Code provisions.

					DESIGN STRENGTH						ULTIMATE STRENGTH				
					CP110 (69)		ACI (67)		CEB-FIP (121)		CP110(69)		ACI(67)		
Slab number	Column size, r, in mm	% Tension Reinforcement Ratio, ρ.	Cube Compressive Strength in N/mm^2	Experimental load, V_{test}, in kN	$V_{u.calc}$ in kN	$\frac{V_{u.calc}}{V_{test}}$	$V_{u.calc}$ in kN	$\frac{V_{u.calc}}{V_{test}}$	$V_{u.calc}$ in kN	$\frac{V_{u.calc}}{V_{test}}$	$V_{u.calc}$ in kN	$\frac{V_{u.calc}}{V_{test}}$	$V_{u.calc}$ in kN	$\frac{V_{u.calc}}{V_{test}}$	Ratio of experimental load to V_{flex} yield line theory $\phi_o = \frac{V_{test}}{V_{flex}}$
1	2	3	4	5	6	7	8	9	10	11	12	13	14	15	16
FS-1	150	0.5574	44.20	173.5	103.42	0.596	141.77	0.817	139.20	0.802	155.13	0.894	166.79	0.961	0.955
FS-8	100	0.5574	45.83	150.3	93.81	0.624	115.46	0.768	114.56	0.762	140.72	0.936	135.83	0.904	0.858
FS-10	200	0.5574	45.50	191.4	113.14	0.591	172.62	0.902	170.87	0.893	169.71	0.887	203.08	1.061	1.012
Average of the ratios of the three slabs						0.604 0.019		0.829 0.067		0.819 0.062		0.906 0.020		0.975 0.079	
FS-19	150	0.3716	43.10	136.5	79.35	0.581	140.00	1.025	126.58	0.927	119.03	0.872	164.70	1.206	1.111
Average of the ratios of the four slabs Standard Deviation						0.598 0.019		0.878 0.125		0.846		0.897 0.020		1.033 0.132	
S-1*	150	0.5574	50.68	197.7	129.27	0.654	178.66	0.904	155.10	0.843	210.19	1.063	195.29	0.988	1.082

*Plain normal weight concrete slab from Ref. (78).

unity, while the ratios for slabs, FS-10 and FS-19 are greater than unity (column 15). This is because the slabs FS-1 and FS-8 have a value of ϕ_o (ratio of observed load to calculated according to yield line theory flexural strength) less than unity while the slabs FS-10 and FS-19 have a value of ϕ_o greater than unity (column 16); the ACI code equation was derived to be applicable to a ϕ_o value equal to one. Because of the favourable interaction of shear and flexural strength, the ACI Code equation is less conservative for slabs with a ϕ_o value greater than one, i.e. for slabs with a calculated flexural strength below the shear strength. As can be seen from Table 8.1 (columns 15 and 16) the higher the value of ϕ_o the less conservative the ACI code strength.

Table 8.2 shows the observed unit shear stresses and those calculated by ACI and CP110 codes at ultimate strength by using a critical section located at the column face. All these values are plotted in Fig. 8.1. From Fig. 8.1 it can be seen that the decrease in actual shear stress with increasing r/d values is much higher than that predicted by the ACI code but almost of the same order as that predicted by the CP110 code. The greater values of unit shear stress predicted by ACI code than those found in the tests for $r/d = 2.0$ and $\rho = 0.5574\%$, and for $r/d = 1.5$ and $\rho = 0.3716\%$ can again be explained in terms of the value of ϕ_o.

Both CP110 and ACI Codes take into account the influence of the r/d ratio by using critical sections away from the column face; this implies, for example, that if the column size is doubled the critical section perimeter will not be doubled. ACI code's critical section is at a distance d/2 and CP110's is at a distance 1.5h from the column face. A 100 percent increase in the column perimeter (from 400 mm in slab FS-8 to 800 mm in slab FS-10) increased the slab strength only by 27.34% (191.4/150.3=1.2734). But the corresponding increases in length of critical sections are 50%

Table 8.2 Ultimate unit shear stress at column perimeter.

Slab number	Column size, r, mm	% Reinforcement Ratio	Compressive Strength, f_{cu} N/mm^2	r/d	Ultimate Unit Shear Stress: Test unit stress $v_u = \frac{V_{test}}{4rxd}$ N/mm^2	ACI unit stress* $v_u = 4(1 + \frac{d}{r})\ 0.85 \sqrt{f_c'}$ N/mm^2	CP110 unit stress* $v_u = 1.5\ \xi_s\ v_c\ (1 + \frac{3\pi h}{4r})$ N/mm^2
1	2	3	4	5	6	7	8
8	100	0.5574	45.83	1.0	3.758	3.396	3.518
1	150	0.5574	44.20	1.5	2.892	2.780	2.585
10	200	0.5574	45.50	2.0	2.392	2.539	2.122
19	150	0.3716	43.10	1.5	2.275	2.746	1.983

*The unit stress is equal to ultimate strength given by Code over the column perimeter times the effective depth.

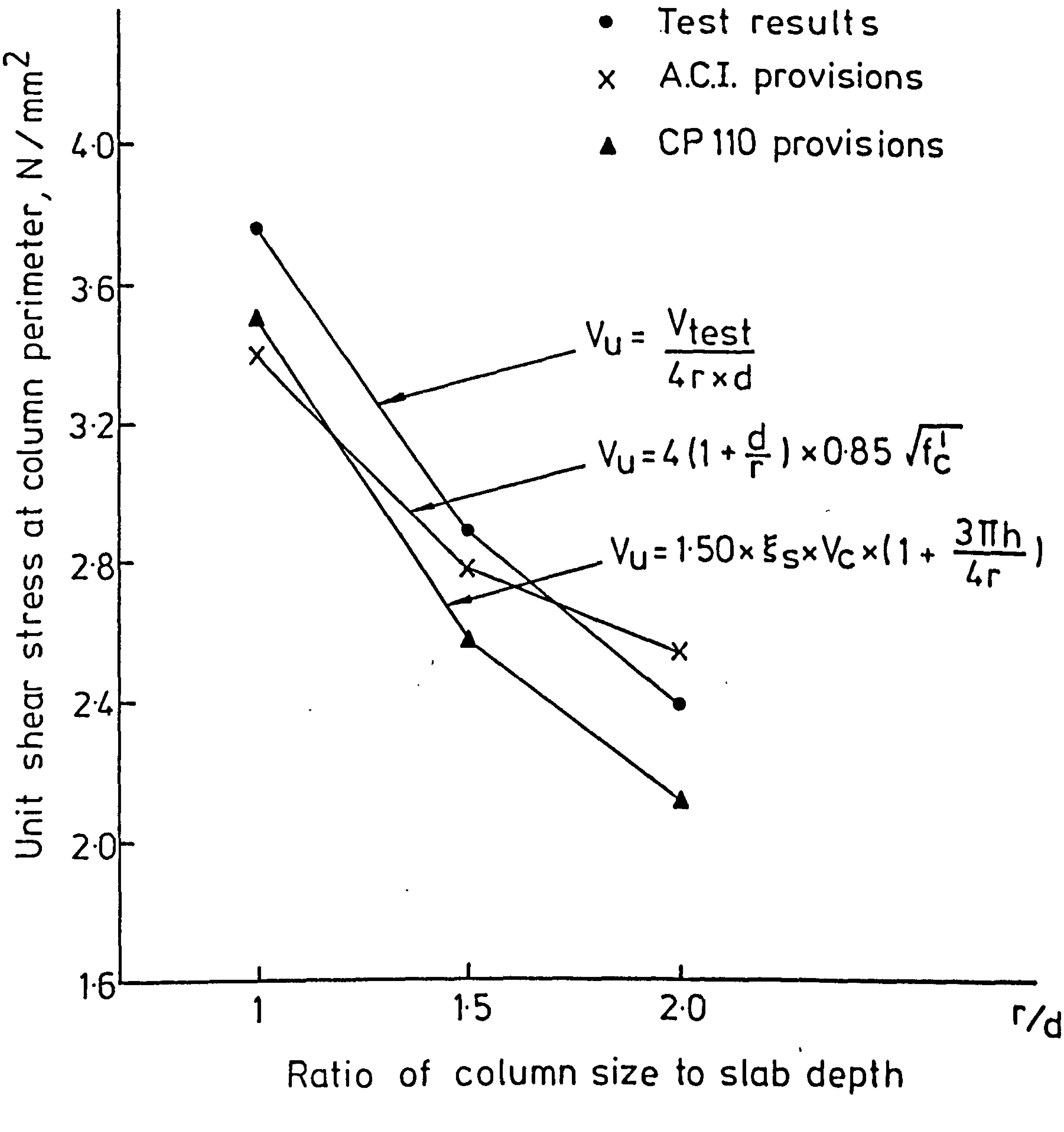

FIG. 8·1 COMPARISON OF A.C.I. AND CP110 CODES PROVISIONS WITH TEST RESULTS

(1200/800 = 1.50) and 25.34% (1978/1578 = 1.2534) for ACI and CP110 respectively. That means that CP110's larger perimeter takes better account of the tendency to a concentration of stresses at the corners of large columns, which reduces the effectiveness of increasing column dimensions.[70]

8.2.2 Comparison of the Test Results with Expressions for Lightweight Concrete.

The calculated shear strengths of all four plain concrete slabs according to Hognestand, et al. (3) and Mower and Vanderbilt (59) expressions for lightweight concrete are shown in Table 8.3. In the case of Hognestand et al. (3) expression the FS-1 and FS-8 slabs give better $V_{u.calc}/V_{test}$ ratios than FS-10 and FS-19 slabs, since their ϕ_o value is less than unity; but even with a ϕ_o less than unity the V_{calc}/V_{test} ratios are greater than unity.

The important point in Table 8.3 is that slab-column connections may fail as a result of punching shear at an average of 85.6% (1.0/1.167 = 0.856) and 65.9% (1.0/1.516 = 0.659) of the shear strengths predicted by Hognestand's (3), and Mower and Vanderbilt's (59) expressions respectively, if extensive flexural yielding occurs as it was observed in all four plain lightweight concrete connections tested in this investigation.

8.2.3 Comparison of the Test Results with Expressions for Normal weight Concrete.

The calculated shear strengths of all four plain concrete slabs according to expressions for normal weight concrete, as well as the V_{calc}/V_{test} ratios are shown in Tables 8.4, 8.5 and 8.6. The strengths obtained by these expressions have been multiplied a) by 0.85, which is the ACI code's factor for sand lightweight concrete and b) by 0.80, which is the CP110's factor for lightweight concrete. Table 8.4 includes the expressions for normal weight concrete dependent primarily on concrete strength and Table 8.5 the expressions dependent primarily on flexure.

Table 8.3 Comparison of experimental and calculated shear strengths according to expressions for lightweight concrete.

Slab number	Column size, r, mm	% Tension Reinforcement Ratio	Experimental Load, V_{test} kN	Hognestand et al. (3) Equation 2.28 $V_{u.calc.}$ kN	$\frac{V_{u.calc}}{V_{test}}$	Mower and Vanderbilt (59) Equation 2.29 $V_{u.calc.}$ kN	$\frac{V_{u.calc}}{V_{test}}$
1	2	3	4	5	6	7	8
FS-1	150	0.5574	173.5	202.16	1.165	258.52	1.490
FS-8	100	0.5574	150.3	162.35	1.080	241.03	1.604
FS-10	200	0.5574	191.4	229.73	1.200	274.46	1.434
Average of the ratios of three slabs Standard Deviation					1.148 0.062		1.509 0.086
FS-19	150	0.3716	136.5	167.16	1.224	209.70	1.536
Average of the ratios of four slabs Standard Deviations					1.167 0.063		1.515 0.073

From Table 8.4 it can be seen that Moe's (52) equation gives better $V_{u.calc.}/V_{test}$ ratios than Herzog's (53) equation, the average $V_{u.calc}/V_{test}$ ratios, in the case of 0.80 factor, being 0.979 and 1.031 respectively. Tasker and Wyatt's equation overestimates the actual punching shear strength by an average of 12.3%. Moe's equation (52) and Herzog's equation (54) became less conservative with increasing r/d ratio while Tasker and Wyatt's equation (53) became more conservative with increasing r/d ratio.

From Table 8.5 it can be seen that from the expressions dependent primarily on flexure only Yitzaki's equation (56) is applicable, especially for the more heavily reinforced slabs (ρ=0.5574%). This equation became less conservative with increasing r/d ratio but in a lesser degree than, for example, Moe's equation as can be seen from the standard deviations of the average ratios of the slabs FS-1, FS-8 and FS-10, being 0.024 (Table 8.5 column 8) and 0.045 (Table 8.5 column 6) respectively, in the case of 0.80 factor. Whitney's (55) and Long's (58) equations underestimate the shear strength by about 30% in the case of 0.85 factor.

Long's equation used in Table 8.5 is that corresponding to flexure mode method since in all four plain concrete slabs tested in this investigation yielding occurred before the concrete failed. The relatively conservative calculated values are probably due to the development of much more extensive yielding than that assumed in the lower bound solution upon which the flexure mode equation is based.

Table 8.6 shows the calculated shear strengths according to Kinnunen and Nylander (61) and Kinnunen (62) methods. These methods are directly applicable only to circular columns and slabs. The values necessary for their equations were determined by assuming a circular column with perimeter equal to column perimeter and a circular slab with 1) perimeter equal to slab perimeter and 2) diameter equal to 1.1 times the slab length (113). The

Table 8.4 Comparison of Experimental and Calculated Shear Strengths according to expressions for normal weight concrete (Expressions dependent primarily on concrete strength).

Slab Number	Column size, mm	% Reinforc. Ratio	Experim. Load kN	Moe* (52) Equation 2.19 $V_{u.calc.}$ kN	$V_{u.calc.}/V_{test}$	Tasker and Wyatt* (53) Equation 2.21 $V_{u.calc.}$ kN	$V_{u.calc.}/V_{test}$	Herzog* (54) Equation 2.23 $V_{u.calc.}$ kN	$V_{u.calc.}/V_{test}$
1	2	3	4	5	6	7	8	9	10
K = 0.85									
FS-1	150	0.5574	173.5	180.95	1.043	203.06	1.170	184.03	1.061
FS-8	100	0.5574	150.3	146.53	0.975	193.0	1.284	149.86	0.997
FS-10	200	0.5574	191.4	204.43	1.068	212.77	1.112	224.06	1.170
Average ratios of three slabs Standard Deviation					1.029 0.048		1.189 0.087		1.076 0.087
FS-19	150	0.3716	136.5	146.75	1.075	164.72	1.207	157.38	1.153
Average ratios of four slabs Standard Deviation					1.046 0.046		1.193 0.072		1.096 0.081
K = 0.80									
FS-1	150	0.5574	173.5	170.31	0.982	191.12	1.101	173.2	0.998
FS-8	100	0.5574	150.3	137.91	0.918	181.65	1.209	141.05	0.938
FS-10	200	0.5574	191.4	192.4	1.005	200.25	1.046	210.88	1.102
Average ratios of three slabs. Standard Deviation					0.968 0.045		1.118 0.083		1.013 0.083
FS-19	150	0.3716	136.5	138.12	1.012	155.04	1.136	148.12	1.085
Average ratios of four slabs Standard Deviation					0.979 0.043		1.123 0.068		1.031 0.077

*The values obtained from each equation are multiplied by factors 0.85 and 0.80, which are values proposed for sand-lightweight concrete by A.C.I. and CP110 respectively.

Table 8.5 Comparison of Experimental and Calculated Shear Strengths according to expressions for normal weight concrete (Expressions dependent primarily on flexural strength).

Slab Number	Column Size, mm	% Reinforc. Ratio	Experim. Load, V_{test}, KN	Whitney (55)* Equation 2.24 $V_{u.calc.}$ KN	$\frac{V_{u.calc.}}{V_{test}}$	Yitzaki (56)* Equation 2.25 $V_{u.calc.}$ KN	$\frac{V_{u.calc.}}{V_{test}}$	Long (58)* Equation 2.27a $V_{u.calc.}$ KN	$\frac{V_{u.calc.}}{V_{test}}$
1	2	3	4	5	6	7	8	9	10
K = 0.85									
FS-1	150	0.5574	173.5	115.02	0.663	166.18	0.958	125.55	0.723
FS-8	100	0.5574	150.3	91.30	0.607	142.63	0.949	117.60	0.782
FS-10	200	0.5574	191.4	139.15	0.727	190.12	0.993	134.66	0.704
Average of ratios of three slabs Standard Deviation					0.666 0.060		0.967 0.025		0.736 0.041
FS-19	150	0.3716	136.5	96.78	0.709	152.16	1.115	84.97	0.622
Average of ratios of four slabs. Standard Deviation					0.676 0.054		1.004 0.078		0.708 0.066
K = 0.80									
FS-1	150	0.5574	173.5	108.26	0.624	156.40	0.901	118.17	0.681
FS-8	100	0.5574	150.3	85.93	0.572	134.24	0.893	110.68	0.736
RS-10	200	0.5574	191.4	130.96	0.684	178.94	0.935	126.74	0.662
Average of ratios of three slabs. Standard Deviation					0.627 0.056		0.909 0.024		0.693 0.038
FS-19	150	0.3716	136.5	91.09	0.667	143.22	1.049	79.98	0.586
Average of ratios of four slabs Standard Deviation					0.634 0.050		0.945 0.074		0.666 0.062

*The values obtained from each equation are multiplied by factors 0.85 and 0.80, which are values proposed for sand-lightweight concrete by A.C.I. and CP110 respectively.

Table 8.6 Comparison of Experimental and Calculated Shear Strengths according to Kinnunen and Nylander, and Kinnunen methods.

Slab Number	Column Size, mm	Equivalent column diameter, mm	Equivalent diameter of 1690 mm square slab mm	Experimental load, V_{test}, KN	Kinnunen and Nylander (61)							Kinnunen (62)						
					y / d	V_u calc for normal conc. KN	$\frac{V_{u.calc.}}{V_{test}}$ $\frac{(7)}{(5)}$	$V_{u.calc.}$ 0.85 x column 7 KN	$\frac{V_{u.calc.}}{V_{test}}$ $\frac{(10)}{(5)}$	$V_{u.calc.}$ 0.8 x column 7 kN	$\frac{V_{u.calc.}}{V_{test}}$ $\frac{(11)}{(5)}$	y / d	$V_{u.calc.}$ for Normal Conc. KN	$\frac{V_{u.calc.}}{V_{test}}$ $\frac{(14)}{(5)}$	$V_{u.calc.}$ 0.85 x column 14 KN	$\frac{V_{u.calc.}}{V_{test}}$ $\frac{(16)}{(5)}$	$V_{u.calc.}$ 0.88 x column 14 KN	$\frac{V_{u.calc.}}{V_{test}}$ $\frac{(18)}{(5)}$
1	2	3	4	5	6	7	8	9	10	11	12	13	14	15	16	17	18	19
FS-1	180	191.0	2152	173.5	0.213	123.9	0.708	105.3	0.607	99.1	0.571	0.207	125.9	0.719	107.0	0.617	100.7	0.581
FS-8	100	127.3	2152	150.3	0.215	113.0	0.752	96.1	0.639	90.4	0.602	0.208	115.7	0.770	98.3	0.654	92.6	0.616
FS-10	200	254.6	2152	191.4	0.202	146.7	0.767	124.7	0.651	117.4	0.613	0.191	145.7	0.761	123.8	0.647	116.6	0.609
FS-19	150	191.0	2152	136.5	0.160	96.6	0.707	82.1	0.602	77.3	0.566	0.155	95.4	0.699	81.1	0.594	76.3	0.559
Average of ratios Standard Deviation							0.733 0.031		0.625 0.024		0.588 0.023			0.737 0.034		0.628 0.027		0.591 0.026
Equivalent diameter of circular slab = 1.1x1690 = 1859 mm																		
FS-6	150	191.0	1859	173.5	0.226	137.6	0.786	117.0	0.674	110.1	0.635	0.199	138.3	0.790	117.5	0.678	110.6	0.638
FS-8	100	127.3	1859	150.3	0.229	125.9	0.838	107.0	0.712	100.7	0.670	0.201	127.2	0.846	108.1	0.719	101.8	0.677
FS-10	200	254.6	1859	191.4	0.214	161.3	0.848	137.1	0.716	129.0	0.674	0.181	158.1	0.826	134.4	0.702	126.5	0.661
FS-19	150	191.0	1859	136.5	0.174	106.3	0.719	90.4	0.662	85.0	0.623	0.147	102.5	0.751	87.1	0.638	82.0	0.600
Average of ratios Standard Deviation							0.812 0.034		0.691 0.027		0.650 0.025			0.803 0.042		0.684 0.035		0.644 0.033

strengths given by the equations of Kinnunen and Nylander (61) were increased 10 percent as recommended for slabs with two-way reinforcement (61).

From Table 8.6 it can be seen that both methods underestimate the shear strength of plain lightweight concrete slabs by about 37.5% in the case of 0.85 factor. The $V_{calc.}/V_{test}$ ratios were improved by about 10% when 1.1x slab length = 1859 mm was used as the diameter of the equivalent circular plate. Even not applying the reduction factors for lightweight concrete, the calculated strengths by both methods are less than experimental ones by about 27% (column 8) in the case of equal perimeter circular slab. The underestimation of the ultimate punching shear strength of the plain lightweight concrete slabs by both methods should be expected since these methods give considerable weight to the flexural strength of the slab. i.e. amount of tension steel.

8.3 Ultimate Punching Shear Strength Analysis - Empirical Method.

In this section an attempt is made to develop a general empirical equation to predict the ultimate shear strength of a fibre reinforced concrete slab failing by punching.

The test results in this investigation and those by Ali (78) indicate that there is an increase in ultimate punching shear strength of a slab-column connection due to inclusion of fibre reinforcement. This increase seems to be dependent upon 1) the volume fraction (V_f) of the fibres and 2) the particular type of fibres used. The effect of each fibre used, could be expressed as a function of its characteristics 1) aspect ratio $\frac{\ell_f}{d_f}$ and 2) its shape (crimped, hooked, enlarged ends etc.), which in turn could be expressed as a function of the bond efficiency factor, η_b. All these three parameters, V_f, ℓ_f/d_f, η_b, are the main parameters, which determine the superior behaviour of fibre concrete to plain concrete with respect to tensile strength.

It can now be written that

$$V^F_{u.p} = V^P_{u.p} \left(1 + A \times \frac{\ell_f}{d_f} \times V_f \times \eta_b\right) \quad \ldots\ldots \quad (8.1)$$

where $V^F_{u.p}$ = ultimate shear strength of a slab with steel fibres.

$V^P_{u.p}$ = ultimate shear strength of plain concrete slab of equal compressive strength.

A = a constant to be adjusted to fit the test results.

An expression of the form $A_1 + A_2 \times \frac{\ell_f}{d_f} \times V_f \times \eta_b$ instead of $A \times \frac{\ell_f}{d_f} \times V_f \times \eta_b$ cannot be used because it would yield a non-zero fibre contribution for $V_f = 0$.

The constant A is found to have a value equal to 0.32 from Fig. 8.2 where the ratio of the ultimate strength for slabs FS-3, Fs-4, FS-12, FS-13, FS-14, FS-15 (with same flexural reinforcement and with 1% steel fibres but different type of fibres) to ultimate strength of the plain concrete slab FS-1 is plotted against the $\frac{\ell_f}{d_f} V_f \eta_b$ values.

Finally the proposed equation is

$$V^F_{u.p} = V^P_{u.p} \left(1 + 0.32 \frac{\ell_f}{d_f} V_f \eta_b\right) \quad \ldots\ldots \quad (8.2)$$

In the equation 8.2 as a value of $V^P_{u.p}$ can be used either the experimental strength of plain concrete slab or that obtained by any expression predicting the ultimate strength of plain concrete slabs. In this section Moe's equation, modified with the correction factor 0.80 for lightweight concrete is used, since this equation gives good $V_{u.calc.}/V_{test}$ ratios for the four plain lightweight concrete slabs tested in this investigation (Table 8.4). Thus, equation (8.2) becomes

$$V^F_{u.p} = 0.80 \frac{15(1-0.075\ r/d)\ bd \sqrt{f_c'}}{1 + 5.25 \frac{bd \sqrt{f_c'}}{V_{flex}}} \left(1+0.32 \frac{\ell_f}{d_f} V_f \eta_b\right) \quad \ldots \quad (8.3)$$

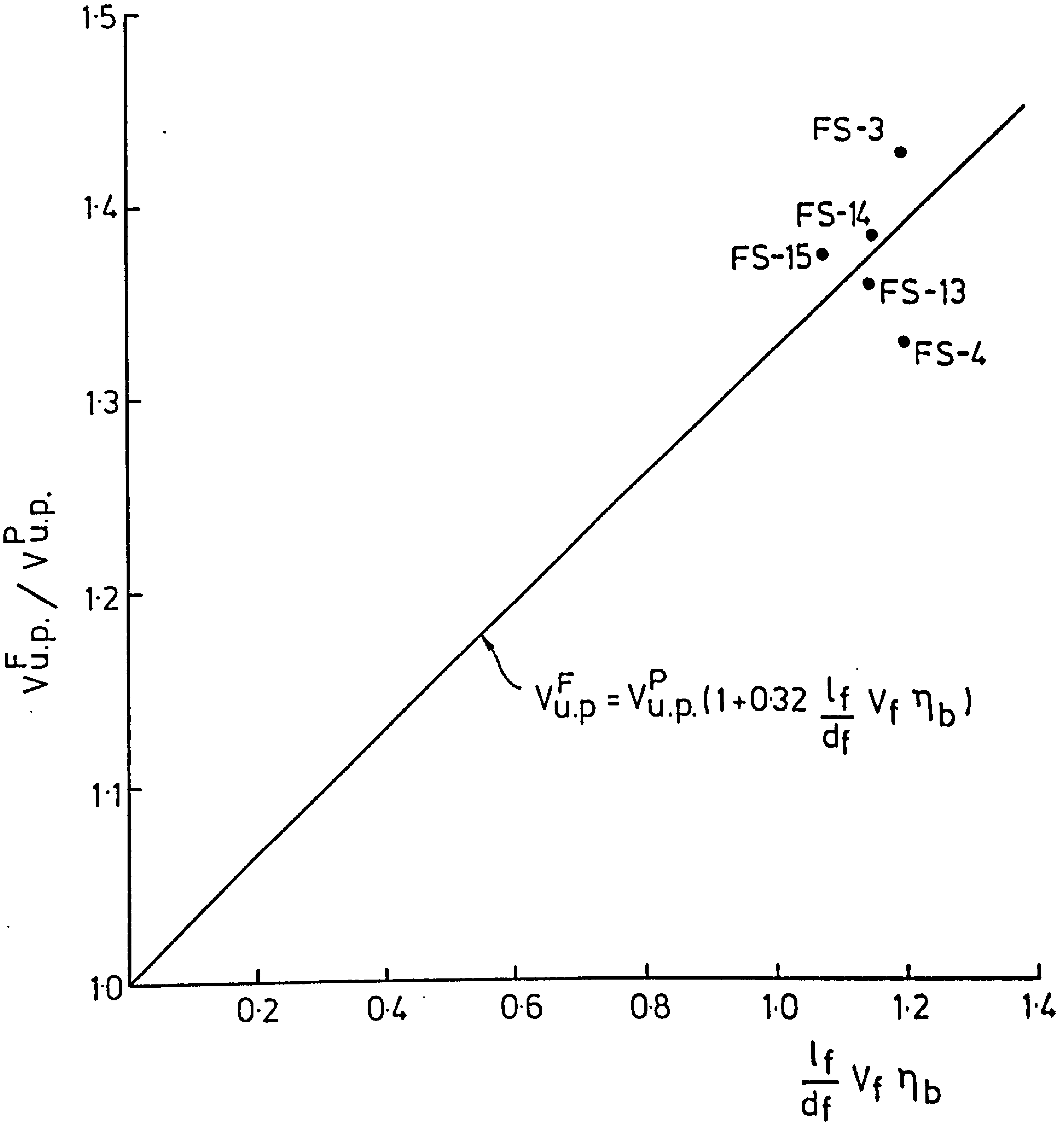

FIG. 8·2 ULTIMATE PUNCHING SHEAR STRENGTH WITH STEEL FIBRES

Table 8.7 Comparison of Experimental and Calculated Ultimate Shear Strengths of L.W. Fibre Reinforced Slabs according to Empirical Proposed Method.

Slab Number	Column size, r, mm	% Reinforcement Ratio	Fibre Type	Fibre Percentage V_f	Fibre Aspect Ratio, $\frac{\ell_f}{d_f}$	Bond Eff. Factor, η_b	Cube Comp. Strength N/mm^2	Experim. Load, V_{test} kN	Moe (52) $V^P_{u.p} = 0.80 \dfrac{15(1-0.075r/d)bd\sqrt{f_c'}}{1 + \dfrac{5.25\ bd\sqrt{f_c'}}{V_{flex}}}$ Light Weight Concrete kN	$V^F_{u.p} = V^P_{u.p}\ (1+0.32 \frac{\ell_f}{d_f} V_f \eta_b)$ ($V_{calc.}$) kN	$\frac{V_{calc.}}{V_{test}}$
1	2	3	4	5	6	7	8	9	10	11	12
FS-2	150	0.5674	Crimped	0.5	100	1.2	42.50	225.0	167.45	199.6	0.887
FS-3	150	0.5574	Crimped	1.0	100	1.2	44.56	247.4	169.79	234.99	0.950
FS-4	150	0.5574	Crimped	1.0	100	1.2	46.67	224.4	172.07	238.15	1.061
FS-5	150	0.3716	Crimped	1.0	100	1.2	47.50	198.1	141.29	195.54	0.987
FS-9	100	0.5574	Crimped	1.0	100	1.2	44.50	216.6	134.74	186.48	0.861
FS-12	150	0.5574	Japanese	1.0	60	1.0	45.10	217.5	170.40	203.12	0.934
FS-13	150	0.5574	Hooked	1.0	100	1.15	41.85	235.7	166.70	228.05	0.967
FS-14	150	0.5574	Paddle	1.0	70	1.65	43.73	239.5	168.86	231.27	0.966
FS-15	150	0.5574	Crimped	1.0	90	1.2	39.05	238.0	163.30	219.73	0.923
FS-16	150	0.5574	Paddle	1.0	70	1.65	34.9	227.8	157.82	216.15	0.949
FS-18	150	0.5574	Paddle	1.0	70	1.65	17.75	166.0	125.89	172.42	1.039
FS-20	150	0.3716	Crimped	1.0	100	1.2	46.30	211.0	140.48	194.42	0.921
									Average of ratios Standard Deviation		0.953 0.048

Table 8.8 Comparison of Experimental and Calculated Ultimate Shear Strengths of Fibre Reinforced Slabs from various investigations (Empirical method).

Investigator	Slab Number	Column Size, mm	% Reinforcement Ratio	Fibre Type	Fibre Percentage	Fibre Aspect Ratio $\frac{\ell_f}{d_f}$	Bond Eff.Factor, η_b	Cube Comp. Strength, N/mm^2	Experim. Load, V_{test} KN	Moe (52) $V^P_{u.p} = 0.90^{\bullet} \dfrac{15(1-0.075\ r/d)bd\sqrt{f_c'}}{1 + \dfrac{5.25\ bd\sqrt{f_c'}}{V_{flex}}}$ Normal Weight Concrete KN	$V^F_{u.p} = V^P_{u.p}\ (1+0.32\ \frac{\ell_f}{d_f}\ V_f \eta_b)$ ($V_{calc.}$) KN	$\frac{V_{calc.}}{V_{test}}$
	1	2	3	4	5	6	7	8	9	10	11	12
Ali Sami (78)	S-1	150	0.5574	-	0.0	-	-	50.68	197.7	198.17	198.17	1.002
	S-2	150	0.5574	Crimped	0.6	100	1.2	48.72	243.6	195.98	241.13	0.990
	S-3	150	0.5574	Crimped	0.9	100	1.2	47.21	262.9	194.22	261.34	0.994
	S-4	150	0.5574	Crimped	1.2	100	1.2	46.09	281.0	192.70	281.50	1.002
	S-5	150	0.5574	Crimped	0.9	100	1.2	47.27	267.2	194.30	261.45	0.978
	S-6	150	0.5574	Crimped	0.9*	100	1.2	47.51	239.0	194.62	226.89	0.949
	S-8	150	0.5574	Crimped	0.9	100	1.2	51.36	255.7	198.91	267.64	1.047
	S-11	150	0.5574	Crimped	0.9	100	1.2	46.43	262	193.22	259.99	0.992
	S-12	150	0.5574	Hooked	0.9	100	1.15	46.01	249	192.79	256.64	1.031
	S-13	150	0.5574	Plain	0.9	83	1.0	49.09	236.7	196.45	243.4	1.028
	Average of ratios excluding the Slab S-1 Standard Deviation											1.001 0.028
Criswell (77)	No.4	114.3	1.88	Plain	1.0	60	1.0	52.26	97.86	80.73**	96.23	0.983

*Fibres located at 60 mm in tension zone.

**Ultimate shear strength of plain concrete Slab.

● Correction factor.

where V_{flex} is calculated from Equations 7.1 and 7.24

$f_c' = 0.79 f_{cu}$

and the characteristics of fibres are taken from Table 7.2.

The equation 8.2 was applied to all slabs with steel fibres tested in this investigation and failing in punching and the calculated strengths are compared with test results as shown in Table 8.7. From this Table it can be seen that the average of the ratios and standard deviation of calculated to test values of ultimate shear strength for fibre reinforced lightweight concrete slabs are 0.953 and 0.048 respectively, giving a good support of the proposed empirical equation.

Equation 8.2 together with Moe's equation (Eqn 2.19) was also applied to fibre normal weight concrete slabs tested by Ali (78) and the calculated strengths are shown in Table 8.8. The correction factor 0.90was used in Moe's equation in order to give $V_{calc.}/V_{test}$ ratio for plain normal weight concrete slab S-1 equal to one (Table 8.8 column 12). From Table 8.8 it can be seen that the average of ratios and standard deviation of calculated to test values of ultimate shear strength for fibre reinforced normal weight concrete slabs are 1.001 and 0.028 respectively, giving again a good support of the proposed empirical equation. Table 8.8 also includes a fibre normal concrete slab tested by Criswell (77); equation 8.2 was again applied but as $V^P_{u.p}$ value, it was used the ultimate shear strength of the corresponding plain normal concrete slab. The $V_{calc.}/V_{test}$ ratio for this fibre concrete slab is 0.983.

8.4 Ultimate Punching Shear Strength Analysis - Approximate Theoretical Analysis.

In this section an approximate theoretical analysis is presented to predict the ultimate punching shear strength of slab-column connections with fibre reinforcement. Failure is assumed to occur in the compression zone above the inclined cracking when the shear stress is equal to the tensile splitting strength of concrete. The method includes the calculation of the depth of the compression zone; dowel action is taken into account by using a critical perimeter larger than the column perimeter. The calculated strengths are compared with the test results of this investigation and test results from other investigations.

8.4.1 Slab-Column Connection Failure Mechanism.

Consider a simply supported slab loaded at the centre by a load transferred to the slab by a column stub. The slab is assumed to be reinforced in such a way that flexural failure does not take place.

The main flexural cracking in the slab is along radial lines and not in the circumferential direction except at the column face. This can be attributed to the fact that tangential moments exceed the radial moments throughout nearly all of the slab, even for the elastic range and thus cracking should be in the radial direction (114). At some stage of loading, inclined cracking develops immediately in the region of the loaded area (column), since the area resisting shear increases with distance from the column. It is likely that inclined cracking develops first in the corners of the column where high stress concentration occurs and then propagates laterally in the plane of slab with increasing load. Since the main flexural cracking of the slab is in the radial direction that implies that the inclined cracking crosses the flexural cracks approximately at right angles. This behaviour is different from that occurring in beams where the development of inclined cracking from flexural cracks is the usual case.

After the opening of inclined cracking in the slab, its propagation is prevented by the compression zone above the top of the crack and by the dowel action of the tension reinforcement acting in a perimeter where its length is greater than that at which crack is initiated. Since the inclined cracking in a slab always forms close to loaded area, the compression zone above the inclined crack is effectively strengthened by the presence of vertical compression imposed by the column and even more by the existence of compressive stresses in the lateral direction. In the favourable combination of these triaxial stresses (two compressive stresses in orthogonal directions due to bending moments and vertical compressive stress due to column load) can be attributed the higher shear stresses in slabs than those obtainable in beams. Thus, in slabs, rather the ultimate strength can be considered as the usable strength than the inclined cracking strength as is the case in beams, especially with long shear spans, where the inclined cracks form at some distance away from the position of the applied load.

Once inclined shear cracking has developed, the load is resisted by the concrete compression zone above the crack, the aggregate interlock force and by the dowel action of flexural reinforcement (Fig. 8.3). Thus, the total shear resistance of a slab without shear reinforcement is

$$V_u = V_c + V_a + V_d \qquad \ldots\ldots \qquad (8.4)$$

where the components V_c, V_a and V_d are due respectively to the concrete compression zone, aggregate interlock and dowel action. The portion of load resisted by the compression zone can be taken to be dependent upon the area of slab at a perimeter close to column and the shear resistance of concrete. The aggregate interlock effect, which happens only after the appearance of the inclined cracking depends upon the concrete properties, including strength and aggregate type, crack width, and the relative displacement between the two faces of crack due to rotation about the head of the crack (115). If it is assumed that the movement across the crack is

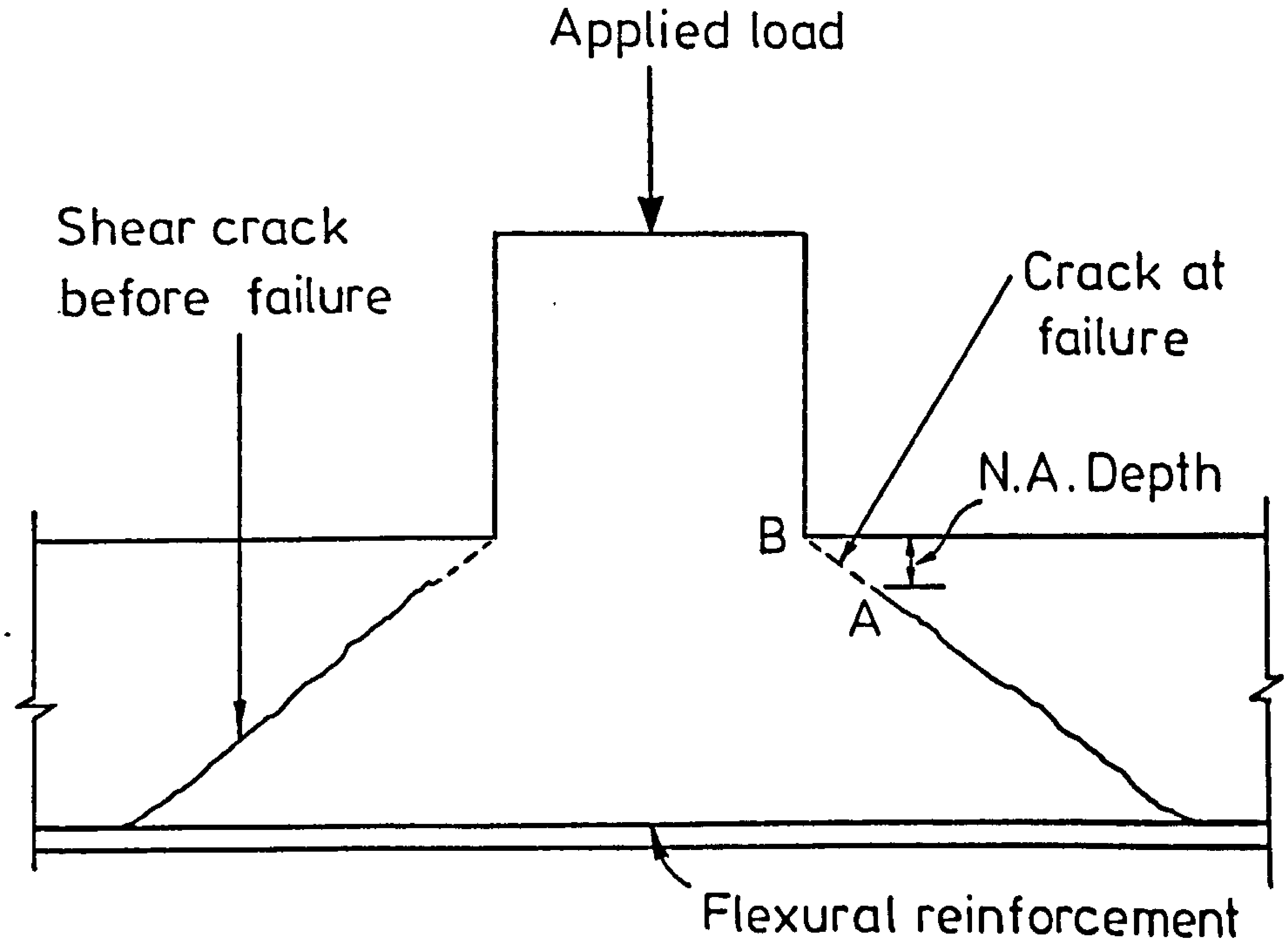

(a)

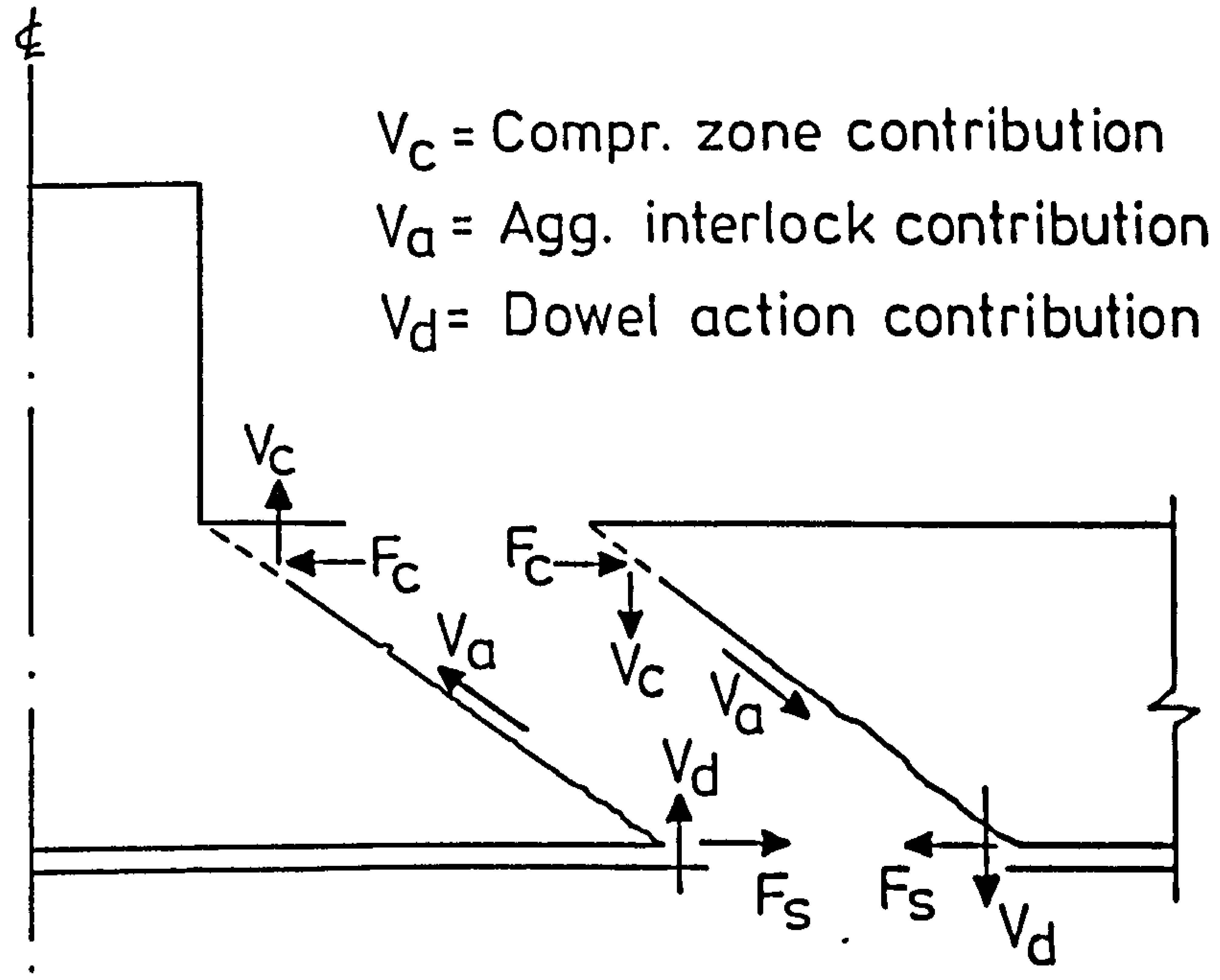

(b)

FIG. 8·3 CONDITIONS AFTER INCLINED CRACKING IN A PLAIN CONCRETE SLAB practically vertical, the interlock forces even in steep cracks tend to produce flatter cracks and then it can be said that residual interlock forces are negligible. The dowel action effect depends upon a number of parameters, reported in Chapter 2 but basically it can be said that it is the combination of two effects, the tensile resistance of the concrete along the splitting plane and the bending resistance of the bar.

8.4.2 Influence of Fibres on V_c, V_a and V_d components.

In Chapter 7 (Table 7.5) it was concluded that the effect of inclusion of fibres was to check the upward movement of the neutral axis. That implies an increase in the area of the compression zone above the inclined cracking and therefore an increase in component V_c. The inclusion of fibres also increases the strength of concrete, which leads to an increase of V_c.

From tests carried out on beams (75) it was concluded that the influence of fibre reinforcement on aggregate interlock force is very limited. This is attributed to the fact that the presence of fibres has two opposite effects on aggregate interlock. The first one is that there is a reduction in crack width and therefore an increase in the contribution of aggregate interlock (115). The second one is that the presence of fibres reduces the rotation about the head of crack and therefore a smaller force will be on interlocking aggregates. The net influence of fibre reinforcement on aggregate interlock force may be rather limited or insignificant.

Fibres in reinforced concrete increase the tensile strength of the composite and improve the stiffness and deformation characteristics of the members including the concrete cover, which assists the bars in resisting the bending due to dowel action, and therefore an increase is expected in the dowel action of the reinforcement due to provision of fibres. The test results of this investigation and from other investigations (75, 77, 78) showed an improvement in dowel action due to inclusion of fibres.

In addition to the above mentioned influence of fibres on the V_c, V_a and V_d components, it can be said that fibres increase the punching resistance of a slab by acting as shear reinforcement because of the ability of fibres of bridging the shear cracks. This new component, V_s, which provides a force perpendicular to the direction of inclined cracking, should be added to the right hand part of equation (8.4) in order to get the ultimate punching strength of fibre reinforced concrete slabs.

A realistic analysis of the problem of punching shear would require an analytical estimation of the compression zone, aggregate interlock, dowel action forces as well as the force due to fibres acting as shear reinforcement. These estimations might be based on results from specialized tests, from which the contribution of each component could be studied. However in a real slab-column connection, the components do not remain isolated quantities but exist together at one stage or another in the loading history of the connection and therefore their contributions are not expected to reach their maximum values at the same stage of loading. This was proved from test on beams with fibres (75) and without fibres (116) where an interaction and a time lag between dowel action and aggregate interlock was suggested at the ultimate stage of loading. The test results of this investigation showed that after punching failure had occurred, the slabs with fibre reinforcement could still support approximately 75% of their total punching load, which is much greater than that supported in the case of a plain concrete slab (Chapter 6). This higher percentage of the remaining strength in the case of fibres could be attributed partly to increased dowel action due to fibres and partly to the fact that at the moment of failure the component V_s has not reached its maximum value.

The failure of slabs with or without fibres takes place in the compression zone i.e. the maximum value of V_c is always reached. Since the values of the other three components at the moment of failure are unknown, the problem of calculating the ultimate punching shear strength of a slab becomes mainly a problem of calculating the ultimate contribution of the compression zone, V_c, above the inclined cracking.

8.4.3 Mode of failure.

In the slabs tested in this investigation either with or without fibre reinforcement it was apparent that the compression zone failed by splitting along the line AB as shown in Fig.8.3(a) and there was not any sign of crushing of concrete. This was also observed in many of the slabs tested by other investigators, both for plain concrete (52) and fibre concrete (78). Thus, it can be said that the punching is a form of shearing. Shear-compression failure is not at issue in slab-column connections, especially when the ultimate moment of resistance is reached in the region of the column since the attainment of a limiting moment around the column is not a criterion of failure for the slab, which can continue to carry increasing load until a full pattern of yield lines is developed (66).

8.4.4 Proposed Approximate Theoretical Method.

8.4.4.1 Plain Concrete Slab-Column Connections.

As was mentioned before, the resistance offered by the concrete compression zone is equal to the area of concrete confined between the plane of slab-column junction and the neutral axis plane multiplied by a critical shear stress, v_{cc}.

Referring to Fig. 8.4 the area of concrete is calculated as follows:

$$\text{Area} = 4 \cdot (A_1B_1) \cdot (EE')$$

$$A_1B_1 = \frac{AB+A'B'}{2}$$

$$EE' = X/\sin\theta$$

where $AB = r$

$A'B' = r+2X\cot\theta$

θ = inclination of the failure surface

X = neutral axis depth

$$\therefore \quad \text{Area} = 4(r + X\cot\theta).X/\sin\theta \qquad \ldots\ldots \qquad (8.5)$$

The equation, which gives the compression zone resistance can now be written as follows:

$$V_c = v_{cc}\, 4(r + X\cot\theta)\, X/\sin\theta \qquad \ldots\ldots \qquad (8.6)$$

Neglecting the aggregate interlock contribution equation (8.4) can be written as follows:

$$V_u = V_c + V_d \qquad \text{or}$$

$$V_u = v_{cc}.4.(r + X\cot\theta)\, X/\sin\theta + V_d \qquad \ldots\ldots \qquad (8.7)$$

As it is known CP110's large perimeter at distance 1.5h from the column face takes into account the dowel action contribution of the slab's flexural reinforcement (70). Since both concrete compression zone and dowel contributions depend on the same parameter, the dowel action effect can be taken into account if the perimeter of the compression zone (equal to $4.(r+X\cot\theta)$) in the equation 8.6 is substituted by the CP110's perimeter. And then equation 8.7 becomes:

$$V^P_{u.p} = v_{cc}\, b_p\, X/\sin\theta \qquad \ldots\ldots \qquad (8.8)$$

where $b_p = 4r + 3\pi h$.

To apply equation 8.8 to find the ultimate punching shear strength of a slab-column connection a knowledge of the three parameters, v_{cc}, X and θ is required.

1. <u>Critical stress, v_{cc}.</u>

Since punching failure is a form of splitting or shearing of the compression zone, the ultimate punching strength will be assumed to be

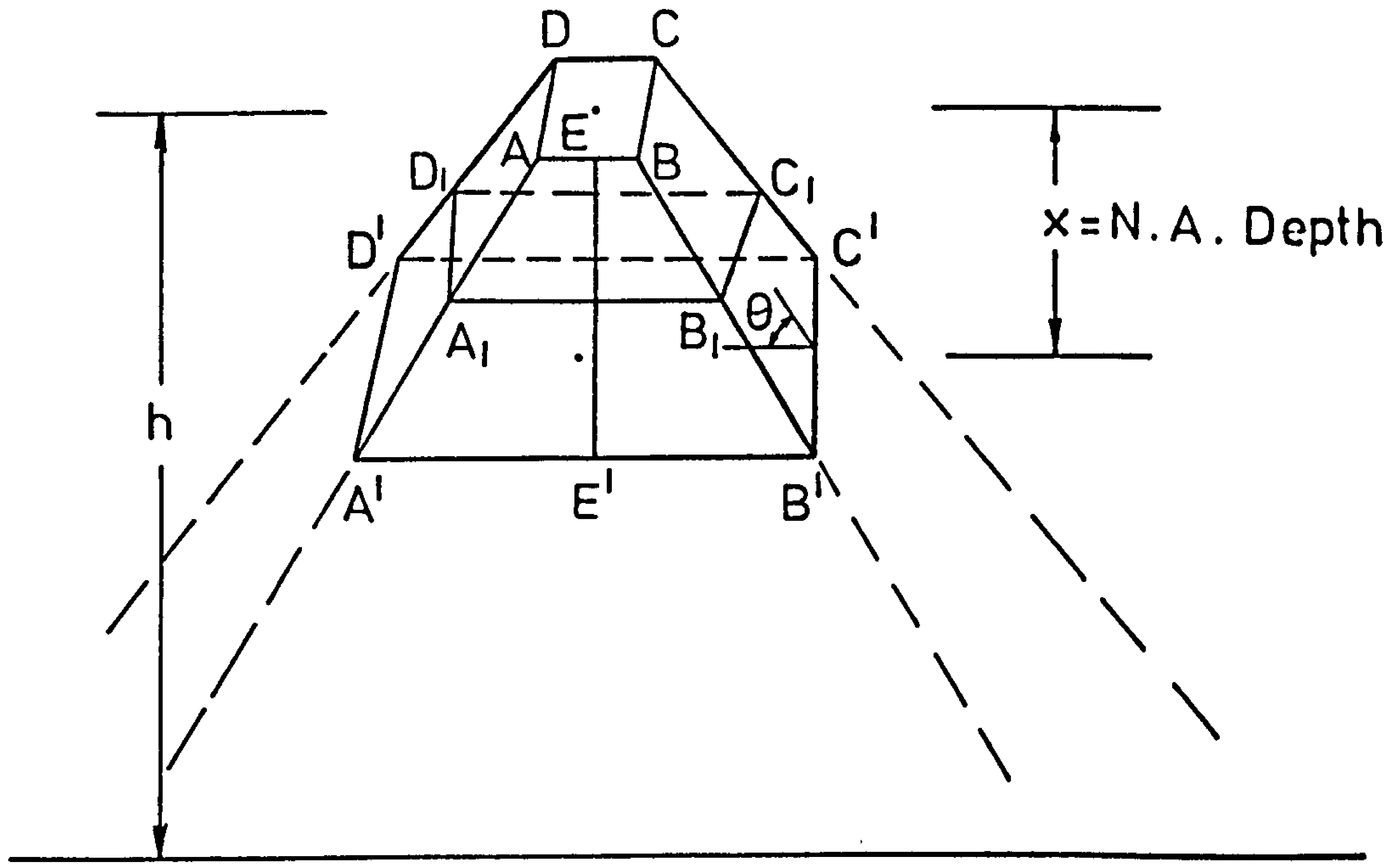

ABCD = Slab-column junction plane

$A^1B^1C^1D^1$ = Neutral axis plane

θ = Angle of failure surface

FIG. 8·4 FAILURE SURFACE ABOVE N.A.

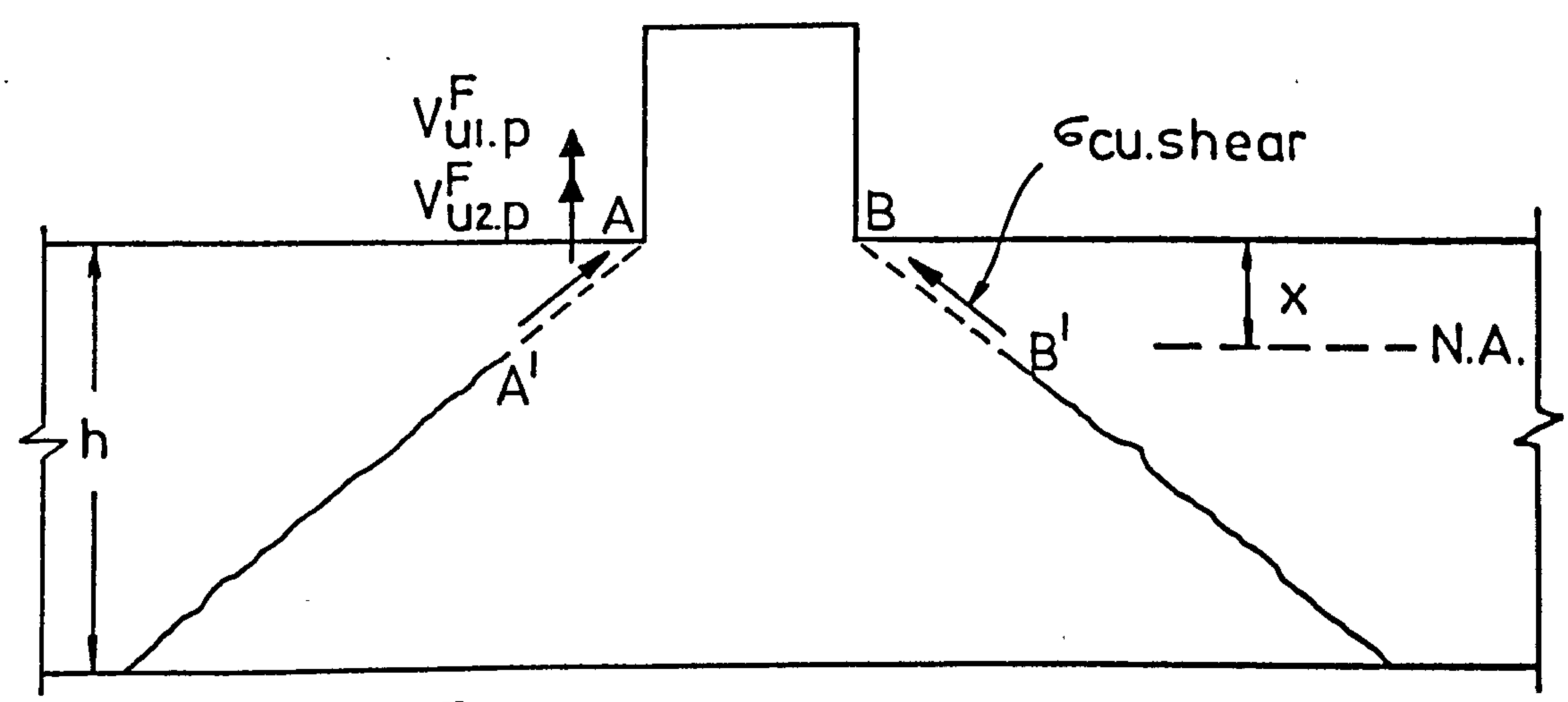

$V^F_{u1.p}$ = Comp. zone contribution

$V^F_{u2.p}$ = Fibre concrete shear resistance (Vert. comp.)

FIG. 8·5 FIBRE CONCRETE SHEAR RESISTANCE ALONG FAILURE SURFACE reached when the average shear stress, v_{cc}, is equal to the tensile splitting strength of concrete. This criterion of failure is also adopted by CEB recommendations for punching shear failure as well as in many empirical formulae where the ultimate strength is assumed to be governed by the tensile splitting strength of concrete, expressed as a function of square root of compressive strength.

The splitting tensile strength cannot be considered as a linear proportion of compressive strength (13) and many investigators have related tensile resistance to the square root of the compressive strength, such as:

$$v_{cc} = f_{ct} = K\sqrt{f_{cu}} \quad \ldots\ldots \quad (8.9)$$

The constant K obtained from four different castings in this investigation had values ranging from 0.4295 to 0.4625 with an average equal to 0.444. This value of constant K is very close to the value of 0.42 found by Bandyopadhyay (11) for Solite lightweight concrete and to the value of 0.47 found by Sittampalam (80) for sand lightweight concrete; it is also within the limits 0.37 and 0.54 for dry and wet all lightweight aggregates respectively given by Teychenne (6). Finally a value of K equal to 0.44 is selected to be used in equation 8.9 for sand-lightweight concrete.

Assuming that the tensile splitting strengths of sand-lightweight and normal weight concrete are related with the coefficient 0.85, then the value of constant K is equal to 0.44/0.85 = 0.5176, which is very close to the value of 0.506 found by Ali (78) for normal weight concrete. Finally a value of K equal to 0.51 is selected to be used in equation 8.9 for normal weight concrete. Thus, equation 8.9 can be written

$$\left.\begin{array}{ll} v_{cc} = f_{ct} = 0.44\sqrt{f_{cu}} & \text{(Sand-Lightweight Con.)} \\ v_{cc} = f_{ct} = 0.51\sqrt{f_{cu}} & \text{(Normal weight Con.)} \end{array}\right\} \quad \ldots\ldots \quad (8.10)$$

The values of tensile splitting strength for normal weight concrete obtained by equation 8.10 are compared with the values of limiting shear stress of the compression zone proposed by Regan (66) and Nielsen (118) as shown in Fig. 8.6

2. Neutral axis depth, X.

In the case of shear failure of a beam, the determination of the depth of compression zone at failure stage is an obstacle to any satisfactory theory for ultimate strength. Regan (66) in his expression for shear resistance of beams and slabs used as depth of neutral axis the value corresponding to yielding of the tension reinforcement. Swamy and Qureshi (117) in their theory for shear resistance of beams assumed that the depth of compression zone at the failure section is related to the depth of the compression zone at flexural failure. In the case of punching shear of slab-column connections with realistic reinforcement percentages it has been observed that the tension reinforcement in the immediate region of the column yields before punching. This implies that the ultimate moment of resistance of the slab has been reached in the region of the column. This was the case in all of the slabs with and without fibres tested in this investigation.

The inclined cracking in a slab always forms close to the loaded area and therefore the failure section at punching is that of the ultimate maximum moment of resistance of the slab. It is therefore reasonable to assume that the depth of the compression zone above the inclined cracking at punching is equal to the depth of the compression zone at flexural failure. Thus the depth of the compression zone can be calculated by following the procedure outlined in Chapter 7 (section 7.6).

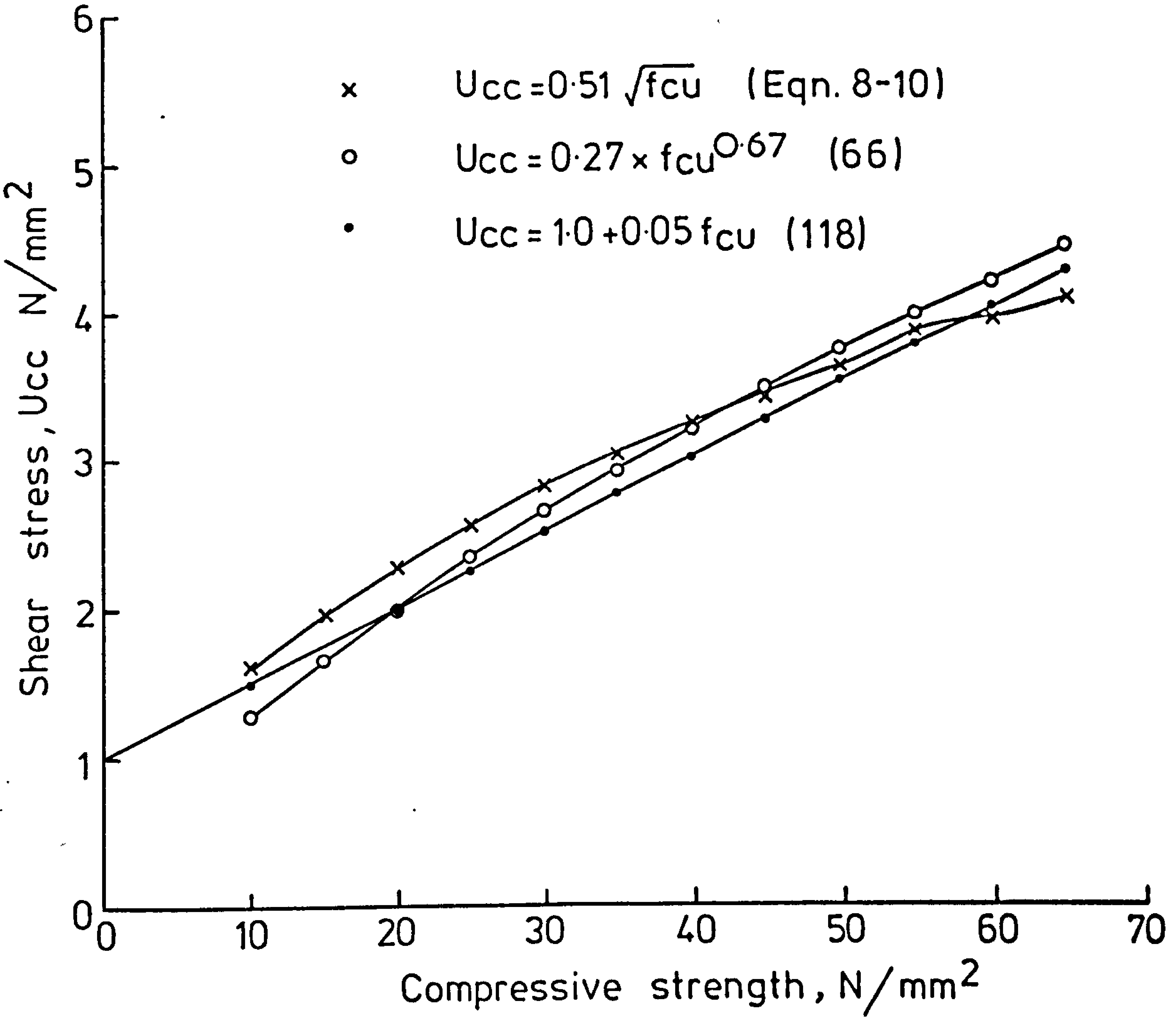

FIG. 8-6 LIMITING SHEAR STRESS OF THE COMPRESSION ZONE

3. Inclination of the failure surface.

The angle of failure surface in the plain concrete slabs tested in this investigation varied from 22^o to 28^o. Moe (52), Aoki and Seki (113), Akatsuka and Seki (82), Kinnunen (61) and Ali (78) reported values of the angle of failure surface 28^o, 30^o, 27^o, 29^o and 24^o respectively. In this analysis a value equal to 29^o is assumed which is in agreement with the value corresponding to the selected perimeter at a distance 1.5 h from column face (θ = arc tan $d/1.5\ h = 0.85h/1.5h = 29.53^o$).

8.4.4.2 Fibre Concrete Slab-Column Connections.

Equation 8.8 could be used to estimate the ultimate punching strength of fibre concrete slabs by 1) using the value of neutral axis depth found with the procedure outlined in section 7.6 for sections with fibre reinforcement and 2) using a new limiting value of v_{cc} corresponding to fibre reinforced concrete. However, the splitting tensile strength of fibre reinforced concrete cannot be related to the compressive strength with an expression having the form of equation (8.9) because the splitting strength of fibre concrete is largely dependent upon the percentage and the characteristics of fibres while compressive strength is almost unaffected.

In this analysis it is assumed that the ultimate punching shear strength of a fibre concrete slab-column connection is given by:

$$V^F_{u.p} = V^F_{u1.p} + V^F_{u2.p} \qquad \ldots\ldots \qquad (8.11)$$

where $V^F_{u1.p}$ is given by equation 8.8, v_{cc} is calculated by equation (8.10) and X is the neutral axis depth found with the procedure outlined in section 7.6 for sections with fibre reinforcement. The term $V^F_{u2.p}$ in equation 8.11 is the shear resistance offered by fibres when the compression zone fails by shearing along the line B'B as shown in Fig. 8.5. This resistance can be taken to be equal to the vertical component of a unit shear resistance of fibre concrete acting in a direction parallel to inclined cracking multiplied by the area of the compression zone given by equation 8.5

$$V^F_{u2.p} = [\sigma_{cu}.\text{shear} \cdot 4\ (rtxcot\theta)X/\sin\theta\ \sin\theta] \quad \text{or}$$

$$V^F_{u2.p} = \sigma_{cu}.\text{shear} \cdot 4\ (r+X\cot\theta)\ X \qquad \ldots\ldots \qquad (8.12)$$

Oakley and Unsworth (119) from tests on glass fibre reinforced concrete found that the shear strength of fibre concrete is approximately equal to the ultimate tensile strength of fibre concrete. This can be explained by considering the mechanism of fibre reinforcement in the composite. Until the first cracking of the matrix the load is largely carried by the matrix. After that the fibres control the crack behaviour until cracking is complete. The ultimate strength of the composite depends upon the characteristics of the fibres, their orientation and the degree of pull out. Once matrix cracking is complete it will not matter whether the cracks of the failure plane run parallel (shear) or perpendicular (tension) to the applied stress - it is the fibres alone that carry the load (119). Thus, the value of unit shear resistance of fibres, $\sigma_{cu.}$ shear, in equation 8.12 can be taken as equal to the tensile strength of fibre concrete, σ_{cu}, used in Chapter 7 (section 7.4.1).

Substitution of equations 8.8 and 8.12 into equation 8.11 gives

$$V^F_{u.p} = v_{cc}\ b_p\ X/\sin\theta + 4\ (r+X\cot\theta)X\ \sigma_{cu} \qquad \ldots\ldots \qquad (8.13)$$

8.4.5 Evaluation Procedure.

The steps to be followed for the evaluation of the ultimate punching shear strength of a given slab with fibre reinforcement are the following:

1. Determine $v_{cc} = K\ \sqrt{f_{cu}}$ from equation 8.10.
2. Calculate the ultimate tensile strength of fibre concrete, σ_{cu}, from section 7.4, Chapter 7.
3. Evaluate the neutral axis depth, X, from section 7.6, Chapter 7.

4. Calculate the ultimate punching shear strength of the fibre concrete slab from equation 8.13.

8.4.6 Results and Discussion.

The ultimate strength of all slabs without and with fibres tested in this investigation and failing in punching has been analyzed by the approximate theoretical method carried out in the previous section of this chapter and the results are presented in Tables 8.9 and 8.10.

Table 8.9 shows close agreement between experimental values and those predicted by the theoretical method, for plain sand-lightweight concrete slabs, the average of $V_{calc.}/V_{test}$ ratios and standard deviation being 0.970 and 0.010 respectively.

Table 8.10 shows close agreement between experimental values and those predicted by the theoretical method, for fibre sand-lightweight concrete slabs, the average of $V_{calc.}/V_{test}$ ratios and standard deviation being 0.940 and 0.064 respectively. In this Table it can be seen that the theoretical method overestimates the actual strength of slab FS-18 by 66%. This high overestimation might be due 1) to the value of σ_{cu}, equal to 1.67 N/mm^2, used in equation (8.13) and in the procedure to find the neutral axis depth and 2) to value of angle of failure surface, θ, used in equation (8.13). Because of the low cube compressive strength (= 17.75 N/mm^2), the value of bond strength, τ, between fibres and matrix equal to 4.15 N/mm^2 on which the estimation of σ_{cu} is based, is rather high. Applying the method of reference (39) to the experimental results of modulus of rupture of slab FS-18, being 3.93 and 2.60 N/mm^2 for fibre and plain concrete respectively, a new value of τ equal to 2.50 N/mm^2 is obtained, which gives σ_{cu} = 1.006 N/mm^2 (section 7.4.1). The value of angle θ used in equation (8.13) was taken as equal to 29^o while the value of θ found from the test was equal to 41^o. Using these

Table 8.9 Comparison of Experimental and Calculated Ultimate Strengths of Plain L.W. Concrete slabs according to approximate theoretical method.

Slab Number	Column Size, r, mm	% Tension Reinforcement Ratio	CP110's perimeter, b_p, mm	Cube Compressive Strength, f_{cu}, N/mm^2	Experim. Load, V_{test} KN	Neutral axis depth, X, mm	Sin θ	$V^P_{u.p}$ ($V_{u.calc.}$) KN Eqn. 8.8	$\frac{V_{u.calc.}}{V_{test}}$
1	2	3	4	5	6	7	8	9	10
FS-1	150	0.5574	1778	44.20	173.5	15.56	0.4848	166.93	0.962
FS-8	100	0.5574	1578	45.83	150.3	15.27	0.4848	147.99	0.984
FS-10	200	0.5574	1978	45.50	191.4	15.32	0.4848	185.51	0.969
FS-19	150	0.3716	1578	43.10	136.5	12.43	0.4848	131.68	0.965
Average of ratios									0.970
Standard Deviation									0.010

Table 8.10 Comparison of Experimental and Calculated Ultimate Shear Strengths of fibre L.W. reinforced Slabs according to approximate theoretical method.

Slab number	Column size, r, mm	% Tension Reinforcement Ratio	Fibre Type	Fibre Percentage	CP110's Perimeter b_p, mm	Cube Compres. Strength f_{cu}, N/mm^2	Experim. Load, V_{test}, KN	σ_{cu} N/mm^2	Neutral axis depth X, mm	$V^F_{u1.p}$	$V^F_{u2.p}$	$V^F_{u.p}$ ($V_{u.calc}$/kN) Equation 8.13	$\frac{V_{u.calc.}}{V_{test}}$
1	2	3	4	5	6	7	8	9	10	11	12	13	14
FS-2	150	0.5574	Crimped	0.5	1778	42.50	225.0	0.868	17.40	183.04	10.96	194.0	0.862
FS-3	150	0.5574	Crimped	1.0	1778	44.56	247.4	1.736	19.21	206.92	24.63	231.55	0.936
FS-4	150	0.5574	Crimped	1.0	1778	46.67	224.4	1.736	17.21	189.72	21.64	211.35	0.942
FS-5	150	0.3716	Crimped	1.0	1778	47.50	198.1	1.736	16.32	181.50	20.34	201.84	1.019
FS-9	100	0.5574	Crimped	1.0	1578	44.50	216.6	1.736	19.22	183.62	17.97	201.59	0.931
FS-12	150	0.5574	Japanese	1.0	1778	45.10	217.5	0.801	16.84	182.49	9.73	192.22	0.883
FS-13	150	0.5574	Hooked	1.0	1778	41.85	235.7	1.665	19.74	206.07	24.40	230.47	0.979
FS-14	150	0.5574	Paddle	1.0	1778	43.73	239.5	1.670	19.25	205.42	23.75	229.17	0.957
FS-15	150	0.5574	Crimped	1.0	1778	39.05	238	1.562	20.27	20440	23.63	228.03	0.958
FS-16	150	0.5574	Paddle	1.0	1778	34.9	227.8	1.670	22.04	210.10	27.94	238.0	1.045
FS-18	150	0.5574	Paddle	1.0	1778	17.75	166	1.670	33.57	228.64	47.22	275.86	1.660
FS-20	150	0.3716	Crimped	1.0	1778	46.30	211	1.736	14.37	157.78	17.55	175.33	0.831
Average of ratios excluding FS-18 slab.													0.940
Standard Deviation													0.064

new values of σ_{cu} and θ in the present method the following results are obtained for Slab FS-18:

$$\text{NA depth} = 29.80 \text{ mm}$$

$$V^F_{u1.p} = 149.73 \text{ kN}$$

$$V^F_{u2.p} = 21.96 \text{ kN}$$

$$V^F_{u.p} = 171.69 \text{ kN}$$

$$V_{calc.}/V_{test} = 171.69/166.0 = 1.034$$

The proposed approximate theoretical method was applied to analyze some fibre normal weight concrete slabs, failing in punching, tested by Ali (78) and Criswell (77) and the results are shown in Table 8.11. The average of the $V_{calc.}/V_{test}$ ratios and standard deviation being 0.972 and 0.040 respectively for slabs tested by Ali (78) give good support of the proposed method. The ratherlow $V_{calc.}/V_{test}$ ratio, equal to 0.765, for the slab tested by Criswell (77) might be due to the fact that the neutral axis depth was found using as steel stress the yield stress of steel (= 390 N/mm^2) while this is not the case for the rest of the slabs of Tables 8.10 and 8.11 where the effect of steel strain hardening was taken into account. Neglecting this effect the punching strengths predicted by the present method are decreased by about 12%.

In Tables 8.12, 8.13 and 8.14 all the fibre sand-lightweight concrete slabs tested in this investigation and those tested by Ali (78) and Criswell (77) are separated into groups, to study the effect of various parameters on punching strength such as fibre percentage and fibre type (Table 8.12), cube compressive strength and reinforcement ratio (Table 8.13) and r/d ratio (Table 8.14). From Table 8.14 it can be seen that although slab FS-11 failed in flexure both empirical and approximate theoretical methods predict

Table 8.11 Comparison of Experimental and Calculated Ultimate Shear Strengths of Fibre Reinforced Slabs from various investigations (Appr. Theoretical Method).

Investigator	Slab Number	Column Size, r, mm	% Tension Reinforcement Ratio	Fibre Type	Fibre Percentage	CP110's Perimeter b_p, mm	Cube Comp. Strength N/mm^2	Experim. Load, V_{test} KN	σ_{cu} N/mm^2	Neutral axis depth X, mm	$V^F_{u1.p}$, KN	$V^F_{u2.p}$, KN	$V^F_{u.p}$ ($V_{u.calc.}$) in KN Equation 8.13	$\frac{V_{u.calc.}}{V_{test}}$
	1	2	3	4	5	6	7	8	9	10	11	12	13	14
Ali S. (78)**	S-1	150	0.5574	-	0.0	1778	50.68	197.7	-	13.67	182.02	-	182.02	0.921
	S-2	150	0.5574	Crimped	0.6	1778	48.72	243.6	1.225	16.27	212.41	14.30	226.71	0.931
	S-3	150	0.5574	Crimped	0.9	1778	47.21	262.9	1.837	18.02	231.58	24.17	255.75	0.973
	S-4	150	0.5574	Crimped	1.2	1778	46.09	281.0	2.45	19.79	251.29	36.02	287.31	1.022
	S-5	150	0.5574	Crimped	0.9	1778	47.27	267.2	1.837	18.00	231.47	24.14	255.61	0.957
	S-6	150	0.5574	Crimped	0.9*	1778	47.51	239.0	1.837	16.90	217.87	-	217.87	0.912
	S-8	150	0.5574	Crimped	0.9	1778	51.36	255.7	1.837	17.11	229.3	22.75	240.6	0.941
	S-11	150	0.5574	Crimped	0.9	1778	46.43	262.0	1.837	18.20	231.95	24.46	256.41	0.979
	S-12	150	0.5574	Hooked	0.9	1778	46.01	249.0	1.761	18.12	229.88	23.32	253.20	1.016
	S-13	140	0.5574	Plain	0.9	1778	49.09	236.7	1.531	16.89	221.34	18.66	240.00	1.014
	Average of ratios excluding S-1 slab Standard Deviation													0.972 0.040
Criswell (77) **	No.4	114.3	1.88	Plain	1.0	935.18	52.26	97.86	1.021	9.76	79.61	5.25	74.85	0.765

*Fibres Located at 60 mm in Tension Zone.
**Normal Weight Concrete.

Table 8.12 Comparison between Experimental and Theoretical Results.

i) Effect of fibre percentage.

Slab Number	Concrete Type	Fibre Type	Fibre Percentage	Empirical Method $V_{u.calc}/V_{test}$ Eqn. 8.2	Approximate Theor. Method $V_{u.calc.}/V_{test}$ Eqn. 8.13
1	2	3	4	5	6
FS-2	L.W.	Crimped	0.5	0.887	0.862
FS-3	L.W.	Crimped	1.0	0.950	0.936
S-2	L.W.	Crimped	0.6	0.990	0.931
S-3	N.W.	Crimped	0.9	0.994	0.973
S-4	N.W.	Crimped	1.2	1.002	1.002
Average of ratios Standard Deviation				0.965 0.048	0.945 0.059

2) Effect of fibre type.

Slab Number	Concrete Type	Fibre Type	Fibre Percentage	Empirical Method $V_{u.calc.}/V_{test}$ Eqn. 8.2	Approximate Theor. Method $V_{u.calc.}/V_{test}$ Eqn. 8.13
FS-3	L.W.	Crimped	1.0	0.950	0.936
FS-12	L.W.	Japanese	1.0	0.934	0.883
FS-13	L.W.	Hooked	1.0	0.967	0.979
FS-14	L.W.	Paddle	1.0	0.966	0.957
FS-15	L.W.	Crimped	1.0	0.923	0.958
S-3	N.W.	Crimped	0.9	0.994	0.973
S-12	N.W.	Hooked	0.9	1.031	1.016
S-13	N.W.	Plain	0.9	1.028	1.014
No.4	N.W.	Plain	1.0	0.983	0.765
Average of ratios Standard Deviation				0.975 0.038	0.942 0.077

Table 8.13 Comparison between Experimental and Theoretical Results.

1) Effect of Compressive strength.

Slab Number	Concrete Type	Cube Compressive Strength N/mm^2	Empirical Method $V_{u.calc}/V_{test}$ Eqn. 8.2	Approximate Theor. Method $V_{u.calc.}/V_{test}$ Eqn. 8.13
1	2	3	4	5
FS-18	L.W.	17.75	1.039	1.034
FS-16	L.W.	34.9	0.949	1.045
FS-15	L.W.	39.05	0.923	0.958
FS-13	L.W.	41.85	0.967	0.979
FS-3	L.W.	44.56	0.950	0.936
S-3	N.W.	47.21	0.994	0.973
S-13	N.W.	49.09	1.028	1.014
S-8	N.W.	51.36	1.047	0.941
Average of ratios Standard Deviation			0.987 0.047	0.985 0.042

2) Effect of tension reinforcement ratio.

Slab Number	Concrete Type	% Reinforce-ment Ratio	Empirical Method $V_{u.calc.}/V_{test}$ Eqn. 8.2	Approximate Theor. Method $V_{u.calc.}/V_{test}$ Eqn. 8.13
FS-5	L.W.	0.3716	0.987	1.019
FS-20	L.W.	0.3716	0.921	0.831
FS-3	L.W.	0.5574	0.950	0.936
S-3	N.W.	0.5574	0.994	0.973
No.4	N.W.	1.83	0.983	0.765
Average of ratios Standard Deviation			0.967 0.031	0.905 0.104

Table 8.14 Comparison Between Experimental and Theoretical Results - Effect of r/d ratio.

Slab Number	Concrete type	r/d ratio	Empirical Method $V_{u.ca.c.}/V_{test}$ Eqn. 8.2	Approximate Theor. Method $V_{u.calc.}/V_{test}$ Eqn. 8.13
1	2	3	4	5
FS-9	L.W.	1.0	0.861	0.931
FS-3	L.W.	1.5	0.950	0.936
FS-11*	L.W.	2.0	1.019	1.013
Average of ratios			0.943	0.96

*Slab FS-11 failed in flexure.

strengths close to the experimental one. Tables 8.12-8.14 show close agreement between the test results and those predicted by both empirical and approximate theoretical methods, for each major parameter that may affect the punching strength of a fibre concrete slab. However, because of the limited number of tested slabs it is appreciated that more tests are required especially with a wider range of compressive strength and reinforcement ratio, to check the validity of the two methods proposed in this section.

8.5 Conclusions.

Based on the results presented in this chapter the following conclusions can be drawn.

1. The design method of CP110 and ACI codes for punching shear underestimate the actual strength of plain sand-lightweight concrete slabs tested in this investigation by about 40 and 12% respectively. CP110's larger critical perimeter as compared to ACI code's perimeter takes better account of the tendency to a concentration of stresses at the corners of large columns.

2. The existing expressions for the ultimate punching strength of lightweight concrete slabs overestimate the actual strength of the plain concrete slabs tested in this investigation by 16.7% (3) and 51.6% (59).

3. From the existing expressions for ultimate punching strength of normal weight concrete slabs only Moe's and Yitzaki's equations give close agreement with the experimental strengths when the reduction coefficient 0.80 for lightweight concrete is introduced.

4. The ultimate punching shear strength of flat slabs reinforced with steel fibres may be satisfactorily predicted by the empirical and approximate theoretical methods presented in this chapter.

5. The average of $V_{calc.}/V_{test}$ ratios were 0.953 and 0.940 by empirical and approximate theoretical methods respectively for the fibre sand-

lightweight concrete slabs tested in this investigation and 1.001 and 0.972 for fibre normal weight concrete slabs tested by Ali (78).

6. More research is needed on the application of steel fibres in slab-column connections failing in punching, using a wide range in values of cube compressive strength and tensile steel reinforcement ratio.

CHAPTER 9.

LIMITATIONS, GENERAL CONCLUSIONS AND RECOMMENDATIONS FOR FUTURE WORK.

9.1 Limitations of the Present Work.

The main object of this investigation was to study the punching shear resistance and deformation characteristics of lightweight concrete slab-column connections with steel fibres.

It is hoped that the present investigation has helped in understanding the structural behaviour of steel fibre reinforced lightweight concrete slabs and the advantages of the inclusion of fibre reinforcement in lightweight concrete. However, this investigation cannot be considered as a complete study of the structural behaviour of slab-column connections with steel fibres due to the limited number of tests carried out and parameters studied. The main limitations of the whole of this investigation can be summarized as follows:

1. Only one lightweight coarse aggregate was used throughout the investigation.

2. Only one mix proportion was used to study the short and long term properties of fibre reinforced lightweight concrete.

3. More slab-column connections with fibre reinforcement should be tested to confirm the already obtained experimental results.

4. More test results with a wider range in steel reinforcement ratios and/or different yield stress steels, cube compressive strengths, column size and shape, and different supporting conditions, would have provided a much better check in correlating the test results with the theoretically derived values.

9.2 Conclusions.

The conclusions presented here are based on and limited by the test conditions and test procedures used in this investigation. The major general conclusions drawn from the test results are as follows:

1. Fly ash replacement of cement can be successfully carried out with lightweight aggregates and such mixes can be designed for any strength range; the one day strength obtained is comparable to that obtained from an all-cement mix. Fibres can be introduced and successfully incorporated in lightweight aggregate concrete mixes.

2. Inclusion of fibres hardly affects the 28-day cube compressive strength of the unreinforced matrix, but it really does the modulus of rupture and the splitting tensile strength. The increase in the modulus of rupture and splitting tensile strength at 28 days ranged from 65.4 to 119.1% and 26.8 to 54.3% respectively when 1.0% by volume fibres of various types were used. This increase seems to be dependent upon the aspect ratio and the shape of the fibres. The corresponding increase in the modulus of elasticity at 28 days ranged from 9-12%.

3. In a split-cylinder test with fibre concrete, the ultimate splitting tensile strength is not governed by the pull-out resistance of the fibres, as in the case of the flexural test, because of the premature failure in compression of the edges of the diameter where the load is applied. The presence of fibre reinforcement changed the brittle mode of failure of the specimen of both modulus of rupture and split-cylinder tests into a ductile one.

4. The increases of cube compressive strength, modulus of rupture, splitting tensile strength and modulus of elasticity of the plain concrete

mix from 28 days to 540 days were of about 16.1, 42.6, 14.6 and 10.6% respectively. In the case of fibre concrete mixes the increases from 28 days to 540 days were about 15% for cube compressive strength, 8-11% for tensile splitting strength, 16-20% for modulus of elasticity; there was little influence in flexural strength from 28 to 540 days for fibre concrete mixes. Fibre reinforcement generally restrains the shrinkage movements of the unreinforced matrix.

5. Steel fibres with length equal to 50 mm such as crimped, hooked and paddle improved generally better the properties of the unreinforced matrix than Japanese fibres of 25 mm length.

6. The presence of fibre reinforcement in slab-column connections delays the formation of first flexural crack as well as the development of tensile cracking. The first crack load improved by 30-45% when 1.0% by volume fibres were used. The ratio of the first crack load to maximum load for both plain and fibre concrete slabs was about 19% and 16% for 0.5574 and 0.3716% tension reinforcement ratios respectively.

7. Cracking in the lateral direction of tested slabs started before that in the diagonal direction at about 20 and 30% of the maximum load respectively. The crack patterns on the tension face were generally observed to be about the same for the fibre concrete slabs which failed in punching as for the plain concrete slabs, except that in the former, the cracks were much finer and more in number than in the corresponding plain concrete slabs. All slabs which failed in punching shear had no cracks at all on the compression surface and the punching lines formed immediately in the vicinity of the column faces.

8. The radial cracks appeared first in the vertical face of slab at about 30-40% of the ultimate load. They were initially almost vertical,

then inclined at an angle 60-70^{o} to horizontal and, in slabs failing in flexure or in punching but at an ultimate load close to flexural strength, they propagated almost horizontally.

9. The fibre reinforcement substantially reduced all the deformations of the plain lightweight concrete slab connection at all stages of loading. The reduction in deformations was more pronounced at higher stages of loading.

The reductions in deflection, rotation, steel strain and compressive concrete strain at service load (CP110) were about 25.5, 23.5, 55 and 26% when 1.0% by volume crimped fibres were used in slab-column connection with ρ = 0.5574%. The reduction in deformations when different fibre types were used was about the same as for crimped fibres; the reduction in deformations when 1.0% by volume crimped fibres were used seems to be independent from the size of the column.

10. Higher reductions in deformations due to addition of fibres were observed in the lightly reinforced concrete slabs (ρ = 0.3716%) than those in the heavily reinforced slabs (ρ = 0.5574%). The effect of compression reinforcement reduction was higher in lightly reinforced slabs than in heavily reinforced slabs. Higher reductions in deformations were observed when the fibres were used in the whole slab specimen instead of using them around the column stub.

11. The presence of fibres in slab-column connections can confine the compression zone in the slab and enable the concrete to reach higher strains than those in the corresponding plain concrete slab connections.

12. The presence of fibre reinforcement increased the service load by 15-40% beyond that of plain concrete slabs depending upon the type of

serviceability criterion used. When fibres were used over the whole slab specimen a higher increase in service load was obtained.

13. The addition of fibres to the plain lightweight concrete slabs reduced all the deformations to values similar to, or less than, those of a comparable plain normal weight concrete slab.

14. The increase in the ultimate punching shear load of reinforced lightweight concrete slabs with steel fibres was significant. The ultimate punching shear strength increased by 29.7% and 42.6 when 0.5 and 1.0% by volume of crimped fibres were used in slabs with a 0.5574% reinforcement ratio. This increase varied from 25.4 to 38% when different fibre types were used depending upon the particular fibre type used. The improvement in ultimate punching strength was about 44% when 1.0% by volume of crimped fibres were used in slabs with a 100 mm column stub. When 1.0% by volume of crimped fibres were used in slabs with a 33% tensile reinforcement reduction the ultimate punching shear strength increased by about 45%. When fibres were used over the whole specimen a 55% increase in punching strength was obtained. It was found that the ultimate punching shear strength of fibre concrete slabs increases with increasing concrete strength.

15. The addition of fibre reinforcement in some slab-column connections changed the mode of failure and enabled the slabs to fail first in flexure and then in punching as the loading continued. The crack patterns in these slabs on both compression and tension surfaces were quite different from those failing in punching. The yield lines were more close to slab corners in the lightly reinforced slabs ($\rho = 0.3716\%$) than in the heavily reinforced slabs ($\rho = 0.5574\%$).

16. The addition of fibre reinforcement in slab-column connections increased about twice the centre deflections at failure, which leads to better

ductilities and energy absorption characteristics. The ultimate ductility was increased by about 125-158% and about 260% when fibre reinforcement was used around the column stub and in the whole slab specimen respectively. The corresponding increases in ultimate energy absorption were about 237 and 270% respectively.

17. The presence of fibres in a slab-column connection delays the formation of the inclined shear cracking; this delay appears to be increased with increasing fibre percentage, decreasing column size and decreasing tension reinforcement. The ratio of the shear cracking load to maximum load varied from about 45 to 62.0%.

18. The presence of fibres increased not only the ultimate punching shear load of the corresponding plain concrete slabs, but also the residual resistance after punching failure and the load at which the reinforcement was displaced from their original position. At 1.0% fibre volume, the residual resistance improved by 200-275% and 400%for slabs with 0.5574 and 0.3716% tensile reinforcement ratios respectively, the corresponding increases in the reinforcement displacement load being 100-150% and around 150% respectively.

19. In the plain lightweight concrete slabs, the punching failure was complete and sudden. The addition of fibres produced a gradual punching failure which sometimes was incomplete. All punching failures resulted in truncated cone shaped surfaces, starting from the column faces at the compression surface of the slab and extended outwards to give sections at the tension surfaces varying from 1.9 to 2.48 h for plain concrete slabs implying angles of the failure surfaces from 22^{o} to 28^{o}. In fibre concrete slabs the punching perimeter was bigger resulting in a decrease in the angle

of failure surface by a maximum of 3^{o}. The failure surfaces in most fibre concrete slabs were quite irregular while in the plain concrete slabs the perimeter at the tension surface tended to be square.

20. The ultimate flexural strength of steel fibres reinforced slabs may be satisfactorily predicted by using 1) the method presented in chapter 7 to evaluate the ultimate moment of resistance per unit width, employing the tensile strength of the concrete in tension, and 2) the yield line theory to calculate the ultimate load. A good correlation between the test results of this investigation as well as by other investigations and the theoretical predictions was obtained.

21. The conversion of a given weight of fibres into an equivalent number of steel bars of the same weight increases the ultimate flexural load of a slab-column connection by an average of about 11% but it is not always desirable because a premature punching shear failure may take place giving eventually a lower load.

22. An easily applied formula was derived to calculate the ultimate moment of resistance per unit width of a fibre concrete section for design purposes.

23. The design methods of CP110 and ACI codes for punching shear underestimate the actual strength of plain lightweight concrete slabs tested in this investigation by about 40 and 12% respectively. The existing expressions for the ultimate punching strength of plain lightweight concrete slabs overestimate the actual strength of tested slabs by 16.7% (3) and 51.6% (59). Among the existing expressions for the ultimate punching strength of normal weight concrete slabs only Moe's and Yitzaki's equations give close agreement with the experimental strengths when the reduction coefficient 0.80 (proposed by CP110) for lightweight concrete is introduced.

24. Empirical and approximate theoretical methods for the ultimate punching shear strength of slab-column connections reinforced with steel fibres were derived. A good correlation between the test results of this investigation and by other investigations, and the theoretical predictions was obtained.

25. The test results reported in this investigation showed that lightweight concrete can be used as a structural material in flat slab-column connections. The use of fibre reinforcement in lightweight concrete slabs as shear reinforcement is very promising as in the case of normal weight concrete (78). The difference between the type of concrete materials is one of magnitude of various load characteristics and not of fundamental difference in behaviour. However, more research is needed on the application of steel fibres in slab column connections and the following recommendations are suggested.

9.3 Recommendations for Future Work.

1. More tests are needed on the application of steel fibres in lightweight concrete slabs with different types of lightweight aggregate.

2. More experimental work must be carried out to investigate the effect of fibre reinforcement on the behaviour of slab-column connections under eccentric load and in slabs with restraint edges.

3. More test data are required to check the validity of the proposed methods predicting the ultimate flexural and punching shear strengths using a wide range in values of cube compressive strength, column size/ effective depth ratio, and tension steel reinforcement ratio.

4. In future work, the influence of fibre reinforcement on the contributions of concrete compression zone and dowel forces should be studied by individual tests.

REFERENCES

1. WASHA, G.W., "Properties of lightweight Aggregates and lightweight Concretes". A.C.I. Proceedings, V. 53, PT.1, No. 4, October 1956, pp.375-381.

2. TEYCHENNE, D.C., "Lightweight Aggregate: their Properties and Uses in Concrete in the United Kingdom". Proceedings of the International Congress on Lightweight Concrete, V.1, May 1968, London, pp.23-37.

3. HOGNESTAD, E., ELSTNER, R.C. and HANSON, J.A., "Shear Strength of Reinforced Structural Lightweight Aggregate Concrete Slabs". A.C.I. Journal, Proceedings, June 1964, pp.643-656.

4. HANNANT, D.J., "Steel fibres and lightweight Beams". Concrete, August 1972, p.39.

5. SHORT, A., "The Use of Lightweight Concrete for Reinforced Concrete Construction". Reinforced Concrete Review, Vol.5, Sept. 1959, pp.141-188.

6. TEYCHENNE, D.C., "Structural Concrete made with Lightweight Aggregate Concrete". Concrete, Vol.1, No. 4, April 1967, pp.111-122.

7. EVANS, R.H., and HARDWICK, T.R., "Lightweight Concrete with Sintered Clay Aggregate". Reinforced Concrete Review, Vol.5, June 1960, pp.369-400.

8. EVANS, R.H., and DONGRE, A.V., "The Suitability of a Lightweight Aggregate (Aglite) for Structural Concrete". Magazine of Concrete Research, Vol.15, No. 44, July 1963, pp.93-100.

9. EVANS, R.H., and ORANGUN, C.O., "Behaviour in Flexure of Reinforced Lightweight Aggregate (Lytag) Concrete Beams". Civil Engineering and Public Works Review, Vol.59, May and June 1964, pp.587-601.

10. IBRAHIM, A.B., "Structural Properties and behaviour of High Early Strength Lightweight Aggregate (Solite) Concrete". Ph.D. thesis, University of Sheffield, 1972.

11. BANDYOPADHYAY, A.K., "Material properties and Structural behaviour of Lightweight (Solite) Concrete". Ph.D. thesis, University of Sheffield, 1974.

12. SWAMY, R.N., et al., "Use of Lightweight Concrete for Structural Applications". International Conference on Concrete Slabs, 3-6 April 1979, Dundee, Scotland.

13. HANSON, J.A., "Tensile Strength and Diagonal Tension Resistance of Structural Lightweight Concrete". A.C.I. Proceedings Vol. 58, July 1961, pp.1-37.

14. IVEY, D.L., and BUTH, E., "Shear Capacity of Lightweight Concrete beams". A.C.I. Proceedings Vol.64, October 1967, pp.634-643.

15. MATTOCK, A.H., LI, W.K., and WANG, T.C., "Shear transfer in Lightweight Reinforced Concrete". PCI Journal, Jun.-Feb. 1976, pp.20-39.

16. SWAMY, R.N., "Fibre Reinforcement of Cement and Concrete". Rilem Materials and Structures, Vol.8, No. 45, May-June 1975.

17. ROMUALDI, J.P., and BATSON, G.B., "Mechanics of Crack arrest in Concrete". J. Engin. Mech. Div. Proceedings of the American Society of Civil Engineers, Vol.89, EM 3, June 1963, pp.147-168.

18. ROMUALDI, J.P., and BATSON, G.B., "Behaviour of Reinforced Concrete beams with closely spaced Reinforcement". A.C.I. Proceedings, Vol.60, No. 6, June 1963, pp.775-789.

19. ROMUALDI, J.P., and HANDEL, J.A., "Tensile strength of concrete affected by uniformly distributed and closely spaced short lengths of wire reinforcement". A.C.I. Proceedings, Vol.61, No. 6, June 1964, pp.657-671.

20. SHAH, S.P., and RANGAN, B.V., "Fibre reinforced concrete properties". A.C.I. proceedings, Vol.68, No. 2, February 1971.

21. SWAMY, R.N., MANGAT, P.S., and RAO, "The mechanics of fibre reinforcement of cement matrices". Inter. Symposium on fibre reinforced concrete. Proceedings, Ottawa, October 1973, A.C.I. SP-44, Detroit 1974, pp.1-28.

22. McKEE, D.C., "The properties of an expansive cement mortar reinforced with random wire fibres". Ph.D. Thesis, University of Illinois, Urbana 1969.

23. KAR, J.N., and PAL, A.K., "Strength of fibre reinforced Concrete". Structural Division of the American Society of Civil Engineering, Proceedings, Vol.98, No. ST5, May 1972, pp. 1053-1068.

24. COX, H.L., "The Elasticity and Strength of paper and other fibrous materialsP. British Journal of Applied Physics, Vol.72, 1952.

25. KRENCHEL, H., "Fibre Reinforcement". Akademisk Forlag, 1964.

26. LAWS, V., "The efficiency of fibrous reinforcement of brittle matrices". Journal of Applied Physics, Vol.4, 1971, pp. 1737-1746.

27. ALLEN, H.B., "Glass-fibre reinforced cement, strength and stiffness". CIRIA Report 55, September 1975.

28. PARAMESWARAN, V.S., and PAJAGOPALAN, K., "Strength of concrete beams with aligned or random steel fibre microreinforcement". Proc. RILEM Symposium on Fibre reinforced cement and concrete, September 1975, London, pp.95-103.

29. AL-TAAN, S.A., "Structural behaviour of conventionally reinforced concrete beams with steel fibres". Ph.D. Thesis, University of Sheffield, 1978.

30. STAVRIDES, H., "Material properties and structural behaviour of fibre reinforced cement composites". Ph.D. Thesis, University of Sheffield, 1978.

31. DE VECEY, R.C., and MAJUMDAR, A.J., "Determining bond strength in fibre reinforced composites", Magazine of Concrete Research, Vol.20, No. 65, December 1968, pp.229-234.

32. TATTERSALL, G.H., and URBANOWICZ, A.D., "Bond strength in steel fibre reinforced concrete". Magazine of Concrete Research, Vol.26, No. 87, June 1974, pp.105-113.

33. HUGHES, B.P., and FATTUHI, N.I., "Fibre bond strength in cement and concrete", Magazine of Concrete Research, Vol.27, No. 92, September 1975, pp.161-166.

34. DEHOUSE, N.M., "Methodes d'essais et caracteristiques mechaniques des betons armes de fibres metalliques". Fibre reinforced cement and concrete, RILEM Symposium September 1975, London, pp.119-136.

35. NAAMAN, A.E., and SHAH, S.P., "Bond studies on oriented and aligned steel fibres". Proc. RILEM Symposium on Fibre reinforced cement and concrete, September 1975, London, pp.171-178.

36. MAAGE, M., "Fibre bond and friction in cement and concrete". Proc. of Symposium on Testing and Test methods of Fibre Cement Composites, Sheffield, 5-7 April, 1978.

37. GRAY, R.J., and JOHNSTON, C.D., "The measurement of fibre-matrix interfacial bond Strength in steel fibre reinforced composites". Proc. of Symposium on Testing and Test methods of Fibre Cement Composities, Sheffield, 5-7 April, 1978.

38. AVESTON, J., MERCER, R.A., and SILLWOOD, J.H., "Bond strength of fibre cement composite". Proceedings Conf. Composites-Standards, Testing and Design, National Physical Laboratory, 1974.

39. SWAMY, R.N., and MANGAT, P.S., "A theory for the flexural strength of steel fibre reinforced concrete". Cement and Concrete Research, Vol.4, January 1974, pp.313-325.

40. EDGINGTON, J., HANNANT, D.J., and WILLIAMS, R.I., "Steel fibre reinforced concrete". Building Research Establishment, Current paper CP69/74, July 1974.

41. SHAH, S.P., and CHANDRA, S., "Critical stress, Volume change and microcracking of concrete". A.C.I. proceedings, Vol.63, No. 9, September 1966, pp.925-930.

42. SWAMY, R.N., and RAO, C.V.S.K., "Toughness and ductility of fibre reinforced concrete composite in flexure". Proc. of conference on Fibre Reinforced Materials: Design and Engineering Applications, 23-24 March 1977, London, pp.87-96.

43. LAMOUREAUX, R.J., "The experimental investigation of fibrous concrete in full scale flat plate - column junctions subjected to cyclic loading". A report presented to Structural Engineering Department at the University of Illinois, U.S.A., September 1973.

44. SWAMY, R.N., and ALI, S.A.R., "Influence of steel fibres reinforcement on the shear strength of slab-column connections". International conference on concrete slabs, proceedings, 3-6 April 1979, Dundee, Scotland.

45. SWAMY, R.N., "The technology of steel fibre reinforced concrete for practical applications". I.C.E. proc., Vol.56, May 1974, pp.143-159.

46. DIXON, J.,and MAYFIELD, B., "Concrete reinforced with fibrous wire". Concrete, Vol.5, March 1971, pp.73-76.

47. COMMITTEE 544, "State-of-the-Art Report on fibre reinforced concrete". Proc. Int. Symposium on fibre reinforced concrete, Ottawa, October 1973, A.C.I. Sp-44.

48. LANKARD, D.R., "Fibre concrete applications". Fibre reinforced cement and concrete, RILEM Symposium, September 1975, London, pp.3-19.

49. HOGNESTAD, E., "Shearing strength of reinforced concrete column footings". A.C.I. Journal, Proceedings, Vol.50, No. 3, November 1953, pp.189-208.

50. RICHART, F.E., "Reinforced concrete wall and column footings". A.C.I. Journal, Proceedings, Vol.45, No. 2 and 3, October and November 1948, pp.97-127 and 237-260.

51. ELSTNER, R.C., and HOGNESTAD, E., "Shearing strength of reinforced concrete slabs". A.C.I. Journal. Proceedings, Vol.53, No. 1, July 1956, pp.29-58.

52. MOE, J. "Shearing strength of reinforced concrete slabs and footings under concentrated loads". Development Department Bulletin D47, Portland Cement Association, April 1961, 130 pp.

53. TASKER, H.E., and WYAT, R.J., "Shear in flat-plate construction under uniform loading". Special report No. 23, October 1963, Australian Commonwealth Experimental Building Station, Sydney, Australia.

54. HERZOG, M., "A new evaluation of earlier punching shear tests". Concrete, Vol.4, No. 12, December 1970, pp.448-450.

55. WHITNEY, C.S., "Ultimate shear strength of reinforced concrete flat slabs, footings, beams and frame members without shear reinforcement". A.C.I. Journal, Proceedings, Vol.54, No. 4, October 1957, pp.265-298.

56. YITZAKI, D., "Punching Strength of reinforced concrete slabs". A.C.I. Journal, Proceedings, Vol.63, May 1966, pp.527-542.

57. BLAKEY, F.A., "A review of some experimental studies of slab-column junctions". Constructional review, Vol.39, No. 8, July 1966, pp.17-24.

58. LONG, E.A., "A two-phase approach to the prediction of the punching strength of slabs". A.C.I. Journal, Proceedings, Vol.72, 1975, pp.37-45.

59. MOWRER, R.D., and VANDERBILT, M.D., "Shear strength of lightweight aggregate reinforced concrete flat plates". A.C.I. Journal, Proceedings, Vol.64, November 1967, pp.722-729.

60. IVY, C.B., IVEY, D.L., and BUTH, E., "Shear capacity of lightweight concrete flat slabs". A.C.I. Journal, Proceedings, Vol.66, No. 6, June 1969, pp.490-494.

61. KINNUNEN, S., and NYLANDER, H., "Punching of concrete slabs without shear reinforcement". Transactions, No. 158, 1960, Royal Institute of Technology, Stockholm, Sweden.

62. KINNUNEN, S., "Punching of concrete slabs with two-way reinforcement with special reference to dowel effect and deviation of reinforcement from polar symmetry". Transactions, No. 198, 1963, Royal Institute of Technology, Stockholm, Sweden.

63. LONG, A.E., and BOND, D., "Punching failure of reinforced concrete slabs". Proceedings, Institution of Civil Engineers, May 1967, pp.109-136.

64. LONG, A.E., "Punching failure of slabs - Transfer of moment and shear". Journal of the structural division A.S.C.E., Vol.99, No. ST4, April 1973, pp.665-685.

65. NIELSEN, M.P., BRAESTRUP, M.W., JENSON, B.C., and BACH, F., "CONCRETE PLASTICITY, Beam shear - Shear in joints - Punching shear". Structural Research Laboratory, Technical University of Denmark, 1978.

66. REGAN, P.E., "Behaviour of reinforced and prestressed concrete, subjected to shear forces". Paper 7441S, proceedings, The Institution of Civil Engineers, Vol.50, December 1971, p.522, Supplement (xvii) pp.337-364.

67. "A.C.I. 318-71", Building Code requirements for reinforced concrete, A.C.I., Redford Station, Detroit.

68. A.C.I. - A.S.C.E. Committee 326, "Shear and diagonal tension, Pt. 3, slabs and footings". Journal A.C.I., March 1972, pp.352-396.

69. "CP110", Code of Practice for the Structural Use of Concrete, 1972, Codes of Practice Committee for Buildings, British Standards Institution, London.

70. REGAN, P.E., "A comparison of British and ACI 318-71 treatments of punching shear". A.C.I. Sp42, Shear in reinforced concrete, Vol.2, 1974, pp.881-904.

71. BATSON, G., JENKINS, E., and SPATNEY, R., "Steel fibres as shear reinforcement in beams". A.C.I. Journal, Proceedings, Vol.69, No. 10, October 1972, pp.640-644.

72. WILLIAMSON, G.R., and KNAB, L.I., "Full scale fibre concrete beam tests". RILEM Symposium on Fibre Reinforced Cement and Concrete", London 1975, Construction Press, pp.209-214.

73. MUHIDIN, N.A., and REGAN, P.E., "Chopped steel fibres as shear reinforcement in concrete beams". Proc. of conference on Fibre Reinforced Materials: Design and Engineering Applications, 23-24 March 1977, London, pp.

74. LAFRAUGH, R.W., and MOYSTAFA, S.E., "Experimental investigation of the use of steel fibres as shear reinforcement". Concrete Technology Associates, Tacoma Washington, January 1975, pp.53.

75. BAHIA, H.M., "Shear transfer in fibre reinforced conctret T.beams". Ph.D. Thesis, University of Sheffield, July 1976.

76. PATEL, S.J., "Effectiveness of steel fibres as shear reinforcement in concrete slabs". MS Thesis, Clarkson College of Technology, New York, U.S.A., August 1970.

77. CRISWELL, M.E., "Shear in fibre reinforced Concrete". Personal Communication, pp.20, 1976.

78. ALI, S.A.R., "Effect of fibre reinforcement on the punching shear of flat plates". Ph.D. Thesis, University of Sheffield, 1979.

79. HANNANT, D.J., "Steel fibres and lightweight beams". Concrete, August 1972, pp.39-40.

80. SITTAMPALAM, K., "Flexural behaviour of limited prestressed lightweight (Lytag) concrete beams with and without fibre reinforcement". M.Eng.Thesis, University of Sheffield, 1979.

81. ANIS, N.N., "Shear strength of reinforced concrete flat slabs without shear reinforcement". Ph.D. Thesis, University of London, 1970.

82. AKATSUKA, Y., and SEKI, H., "Ultimate strength of a reinforced concrete slab with boundary frame subjected to a concentrated load". Second International Symposium on Concrete Bridge Design, SP-26, A.C.I., Detroit, U.S.A., 1971, pp.457-475.

83. SWAMY, R.N. and AL-NOORI, K.A., "Bond strength of steel fibre reinforced concrete". Concrete, Vol.8, No. 8, August 1974, pp.36-37.

84. SWAMY, R.N. and BAHIA, H.M., "Influence of fibre reinforcement on the dowel resistance to shear". A.C.I. Journal, Proceedings, February 1979, pp.327-341.

85. PARK, R., "Tensile membrane behaviour of uniformly loaded rectangular reinforced concrete slabs with fully restrained edges". Magazine of Concrete Research, Vol.16, No. 46, March 1964, pp.39-44.

86. TAYLOR, R., and HAYES, B., "Some tests on the effect of edge restraint on punching shear in reinforced concrete slabs". Magazine of Concrete Research, Vol.17, No. 50, March 1965, pp.39-44.

87. BROTCHIE, J.F., and HOLLEY, M.S., "Membrane action in slabs". A.C.I. publication SP-30, Cracking, Deflection and Ultimate Load of Concrete Slab Systems, pp.345-377.

88. TONG, P.Y. and BATCHELOR, B., "Compressive membrane enhancement in two-way bridge slabs". A.C.I. publication SP-30, Cracking, Deflection and Ultimate Load of Concrete Slab Systems.

89. HAWKINS, N.M. and MITCHELL, D., "Progressive collapse of flat plate structures". A.C.I. Journal, Proceedings, July 1979, pp.775-809.

90. LANDER, M. and SCHAEIDT, W. and GUT, S., "Expeimentelle Untersuchungen an Stahlbeton-Flachdecken". Eidgenössische Materialprüfungs-und Versuchsanstalt, Bericht Nr. 205, Dübendorf 1977.

91. JOHANSEN, K.W., "Yield line theory" Translated from the Danish, Cement and Concrete Association, London 1962.

92. HOGNESTAD, E. "Yield line theory for the Ultimate Strength of reinforced concrete slabs". A.C.I. Journal, Proceddings, March 1953, V.49, pp.637-656.

93. ORANGUN, C.D., "Influence of properties of lightweight aggregate (Lytag) concrete on behaviour of reinforced and prestressed concrete members". Ph.D. Thesis, University of Leeds, 1963.

94. SWAMY, R.N. "Prestressed Lightweight Concrete", in Developments in Prestressed Concrete - I, Ed. F. Sawkd, Applied Science Publishers Ltd., London, pp.149-191 (1978).

95. HUGHES, B.P., and FATTUHI, N.I., "Stress-strain curves for fibre reinforced concrete in compression", Cement and Concrete Research, Vol.7, March 1977, pp.173-183.

96. AL-NOORI, K.A., "Flexural behaviour of Conventionally reinforced fibre concrete beams". Ph.D. Thesis, Sheffield University, July 1974.

97. SHAH, S.P. and RANGAN, B., "Effects of reinforcements on ductility of concrete". Journal of Structural Division, Proceedings of A.S.C.E., Vol.96, ST6, June 1970.

98. PAILLERE, A.M., and SERRANO, J.J., "Use of metal fibres in lightweight aggregate concrete". Laboratoire Central des Ponts et Chaussees, Paris, France.

99. SAVVAS, C.S., "Ultimate strength analysis of conventional R.C. beams with fibre reinforcement". M.Eng. Thesis, University of Sheffield, September 1979.

100. SHAH, S.P. et al. "Complete stress-strain curves for steel fibre reinforced concrete in uniaxial tension and compression". International Symposium on Testing and Test methods of Fibre Cement Composites. Sheffield, April 5-7, 1978.

101. RITCHIE, A.G.B., and AL-KAYYALI, O.A. "The effects of fibre reinforcements on lightweight aggregate concrete". RILEM Symposium on Fibre Reinforced Cement and Concrete. London 1975, pp.247-256.

102. JAMROZY, Z. "Light aggregate concrete after fibre admixture". International Symposium on Testing and Test methods of Fibre Cement Composites. Sheffield, April 5-7, 1978.

103. BRITISH STANDARDS INSTITUTE, "Specification for Portland cement (ordinary and rapid hardening)". B.S.12: 1971.

104. SWAMY, R.N., and STAVRIDES, H., "Some properties of high workability steel fibre concrete". Fibre Reinforced Cement and Concrete, RILEM Symposium, Sept. 1975, pp.197-208.

105. BRITISH STANDARDS INSTITUTE. "P.F.A. for use in Concrete". B.S. 3-92, 1965.

106. BRITISH STANDARDS INSTITUTE, "Specification for aggregates from natural sources for concrete". B.S.882: 1965.

107. BRITISH STANDARDS INSTITUTE, "Specification for lightweight aggregates for concrete". B.S.3997. Part 2: 1976.

108. BRITISH STANDARDS INSTITUTE, "Method of Testing Concrete". B.S. 1881, Parts 4 and 5, 1970.

109. JOJAGHA, A.H., "Workability and Strength characteristics of structural lightweight concrete with and without steel fibres". M.E. Thesis, University of Sheffield, Sept. 1979.

110. SWAMY, R.N. and MANGAT, P.S., "Influence of fibre geometry on the properties of fibre reinforced concrete". Cement and Concrete Research, Vol.4, No. 3, May 1974.

111. SWAMY, R.N. and THEODORAKOPOULOS, D.D. "Flexural creep behaviour of fibre reinforced cement composites". The International Journal of Cement Composites, Vol.1, No. 1, May 1979, pp.37-47.

112. SWAMY, R.N. and STAVRIDES, H., "Some statistical considerations of steel fibre composites". Cement and Concrete Research, Vol.6, March 1976, pp.201-216.

113. AOKI, Y. and SEKI, H., "Shearing Strength and Cracking in two way slabs subjected to concentrated load". ACI publication, SP30, Paper SP30-5, March 1971, pp.103-126.

114. CRISWELL, E.M. "Strength and behaviour of reinforced Concrete slab-column connections subjected to Static and Dynamic Loadings". Technical Report M-70-1, U.S. Army Engineers Waterways Experiment Station, Dec. 1970.

115. TAYLOR, H.P.J., "Investigation of the forces carried across cracks in reinforced concrete beams in shear by interlock of Aggregate". Cement and Concrete Association, Technical Report TRA 42.477, Nov. 1970, pp.22.

116. SWAMY, R.N. and ANDRIOPOULOS, A.D., "Contribution of aggregate interlock and dowel forces to the shear resistance of R.C. beams with web reinforcement", ACI publication Sp-42-6, 1974,pp.129-166.

117. SWAMY, R.N. and QURESHI, S.A. "An ultimate shear strength theory for reinforced concrete T-beams without web reinforcement". Proceedings of Civil Eng. Part 2, Vol.57, March 1974, pp.21-34.

118. NIELSEN, M.P., "Punching shear resistance according to the CEB model code". ACI-CEB-PCI-FIP special publication SP-59-11, 1976, pp.193-210.

119. OAKLEY, D.R. and UNSWORTH, M.A., "Shear strength testing for glass reinforced cement". Proceedings of International Symp. Testing and Test Methods of Fibre Cement Composites, April 1978, University of Sheffield.

120. SWAMY, R.N. and MANGAT, P.S., "The interfacial bond stress in steel fibre cement composites". Cement and Concrete Research, Vol.6, 1976, pp.641-650.

121. "CEB-FIP model code for concrete structures". Vol.I and II, CEB-FIP International Recommendations, 3rd Edition,1978.

122. HANNANT, D.J., "Fibre cements and fibre concretes", John Wiley and Sons Ltd., 1978.